ISBN 0-9698420-6-6
ISSN 1198-273X

PICES SCIENTIFIC REPORT No. 6 1996

Proceedings of the Workshop on the Okhotsk Sea and Adjacent Areas

NORTH PACIFIC MARINE SCIENCE ORGANIZATION

PICES

PICES Scientific Report No. 6
1996

PROCEEDINGS OF THE WORKSHOP ON THE OKHOTSK SEA AND ADJACENT AREAS

Workshop Co-Convenors:
Yutaka Nagata, Vyacheslav B. Lobanov, Lynne D. Talley

September 1996
Secretariat / Publisher
North Pacific Marine Science Organization (PICES)
c/o Institute of Ocean Sciences, P.O. Box 6000, Sidney, B.C., Canada. V8L 4B2
pices@ios.bc.ca

TABLE OF CONTENTS

FOREWORD

This proceedings is from the Workshop on the Okhotsk Sea and Adjacent Areas held in Vladivostok in June 1995. The Workshop was recommended by the Physical Oceanography and Climate Committee to complement the Working Group 1 Report on The Okhotsk Sea and Oyashio Region (PICES Scientific Report No. 2 1995).

The following are to be thanked for their efforts in editing this manuscript: Dr. Olga Temnykh (TINRO), Dr. Konstantin A. Rogachev (POI), Dr. Alexander Rabinovitch (IORAS), and Dr. Robert Lake (IOS).

I. REPORT ON THE PICES WORKSHOP ON THE OKHOTSK SEA AND ADJACENT AREAS

Yutaka Nagata, Vyacheslav B. Lobanov and Lynne D. Talley

(Co-Chairmen of the Scientific Steering Committee for the Workshop)

1. Outline of the Workshop

The PICES Workshop on the Okhotsk Sea and Adjacent Areas was held at the Pacific Academy of Management and Business in Vladivostok, Russia, on June 19-24, 1995. Prof. W.S. Wooster, the Chairman of PICES addressed the meeting at the opening ceremony on July 19. Following the opening ceremony, a keynote lecture on Physical Oceanography of the Okhotsk Sea and Oyashio Region was given by Prof. L.D. Talley, the Chairman of the former PICES Working Group 1. Four more keynote lectures were given: Biota of the Okhotsk sea: Structure of communities, its interannual dynamics and currents by V.P. Shuntov and E.P. Dulepova; Maritime nature use problems by B.V. Preobrazhensky; Northwest Pacific paleohydrography by L.D. Keigwin; and Bank of fishery-biological and oceanographical data by L.N. Bocharov and V.K. Ozerin.

Eight parallel sessions were held under the following titles:

A) Circulation and water mass structure of the Okhotsk Sea and northwestern Pacific
B) Sea ice and its relation to circulation and climate
C) Waves and tides
D) Physical oceanography of the Japan/East Sea
E) Communities of the Okhotsk Sea and adjacent waters: composition, structure and dynamics
F) Abundance, distribution, dynamics of the common fishes of the Okhotsk Sea
G) Salmon of the Okhotsk Sea: biology, abundance and stock identification
H) Biodiversity of island ecosystems and seaside's of the North Pacific

The workshop Scientific Steering Committee (SSC) recognized that many of the items discussed in the biodiversity session would be outside of the present scope of PICES, but gave consent to utilize the occasion if it was beneficial to Russian scientists. 97 oral papers (including sixteen papers by overseas investigators) were presented and 44 were presented in the poster sessions. 144 scientists attended the various sessions. A rapporteur was nominated for each session during the first meeting of the SSC and time was allowed for discussion at the end of each session. Free discussions were held, on a one day excursion on the R/V Academik M.A. Lavrentiev, that proved very useful for creating mutual understanding among participants. A second meetings of SSC was held on the vessel in order to discuss and prepare a draft workshop report for Science Board to review at the Fourth Annual Meeting in Qingdao. Additionally, a special meeting on data management was held.

A plenary session was held to present summary reports of the eight sessions and approve the outline of the workshop report. Finally, Prof. W.S. Wooster provided closing remarks to the workshop.

2. Summary reports from sessions

The summary reports from the workshop sessions given by the rapporteurs are below. Additional recommendations from discussion in the SSC meetings, in the meeting on data management and in the

plenary session are added at the end of each report and at the end of this document in the recommendations of the workshop.

A. Circulation and water mass structure of the Okhotsk Sea and northwestern Pacific
Rapporteur: S.C. Riser (University of Washington, U.S.A.)

From the wide variety of talks and posters presented at this session the following main themes emerged:

a) There is a great deal of research activity taking place in the Okhotsk Sea and its adjacent waters, perhaps more than at any time in recent history. There is interest in the Okhotsk Sea in many of the countries that are members of PICES, due to both local economic and social issues and to questions concerning the impact of the Okhotsk Sea on the larger-scale North Pacific circulation. Included in this research are efforts to synthesize historical data sets into a larger picture of the flow in and around the Okhotsk Sea, such as Talley's large-scale picture of Okhotsk Sea-North Pacific interaction and Luchin's attempts to characterize the tides over a large portion of the Okhotsk Sea.

b) Rapid progress is being made to improve the Okhotsk Sea data bases (i.e., water masses, tides, ice cover, atmospheric parameters). Important zero-order problems remain, such as determining the long-term exchange between the Okhotsk Sea and the North Pacific Ocean.

c) As the data bases continue to improve, more quantitative studies should be initiated. Some models of the Okhotsk Sea circulation are already operational and the improved data bases should help to constrain these models. Quantitative studies of many kinds, including inverse models, box models, and process-oriented models should now begin, and should be compared and contrasted with the new data, in an attempt to fully exploit the observational data base.

Related discussion in the SSC meetings and the plenary session:

a) This workshop was built on past PICES activities, especially the work of WG 1/POC and its issue of the PICES Scientific Report No. 2, 1995 on the Okhotsk Sea and Oyashio Region. This workshop was also very successful not only as it reviewed the recent investigations on physical oceanography in the region but also facilitated information exchanges among nations, agencies, and individual investigators. This is an important step for future international, bilateral and individual investigations.

b) Further understanding of the physical processes in the regions and their impacts on world climate is urgent. Organized international cooperative studies are suggested, such as:

i) the dense water formation in the shelf regions of the northwest Okhotsk Sea,
ii) water exchanges between the Okhotsk Sea and the North Pacific Ocean,
iii) the role of the Soya Current on physical processes in the Okhotsk Sea,
iv) the detailed formation processes of the North Pacific Intermediate Water including water mass modification in the Oyashio and Mixed Water Regions.

Modeling efforts might move in the direction of combining with the larger subarctic region, which influences the circulation and properties of the Okhotsk Sea.

c) There is no reason to maintain a steering committee for studies of the Okhotsk Sea and adjacent areas in POC or in the Science Board after the final report of the meeting is produced. We recommend for POC, however, to maintain interest in this region, and to organize a well focused symposium or a new working group in future. The next

symposium may be held around 1998 on the Okhotsk coast of Hokkaido, Japan (e.g. Nemuro or Mombetsu), or at the time of the PICES Annual Assembly.

d) In order to study the important physical processes, we need much more detailed data, which we hope that TCODE can assist in obtaining. For example, high resolution CTD data of 1 to 2-decibar interval in the Oyashio and Mixed Water Regions are essential to clarify the formation mechanisms of the North Pacific Intermediate Water, but such data are not routinely archived.

B. Sea ice and its relation to circulation and climate
Rapporteur: M. Aota (Hokkaido University, Japan)

There were seven presentations during this session that can be classified into four groups:

a) Characteristics of sea ice in the Okhotsk Sea; Dr. Yakunin provided statistical evidence of the peculiarities of the sea ice in the Okhotsk Sea, and Dr. Polomoshnov reported on the behavior of sea ice off the east coast of Sakhalin from point of view of oil development.

b) Relationship among magnitude of sea ice in the Okhotsk Sea and atmospheric and oceanic conditions; Dr. Sekine suggested that a teleconnection exists among the variations in sea ice areas in the Okhotsk Sea, from the intensity of the subarctic circulation in the North Pacific, and from the air temperature on the Asian continent. Dr. Petrov reported the interaction between the hydrological structure in the active layer and the ice cover in the Okhotsk Sea. Dr. Dashko pointed out that the monthly mean temperature and precipitation over the South Far East Region is linearly connected with atmospheric parameters over the Okhotsk region in summer.

c) Wind waves and surges in the Okhotsk Sea and Kuril Islands region, Dr. Polyakova described the nature of wind waves and surges in the Okhotsk Sea and Kuril Island Region by using synoptic data and,

d) Technical method in studies of sea ice dynamics; Dr. Lebedev reported that acoustic methods are useful for studies of sea ice dynamics.

C. Waves and tides
Rapporteur: Y. Nagata (Mie University, Japan)

Four papers were presented: satellite observation of surface and internal waves, paleo-tsunami investigation by analyzing sediment columns in marshes, and computational techniques of tsunamis and tides. Several papers on forecasting wind waves and storm surges were given in the poster session. In addition, several papers on tides and tidal mixing appeared in session A and one paper on oceanic waves in the session D.

Tidal currents are strong enough to destroy oceanic stratification in the Okhotsk sea Region and to create thick homogeneous layers especially in the shelf and bank regions and in straits of the Kuril Islands. Further investigation is warranted as the mixing plays an important role in water mass modification in the Okhotsk Sea and adjacent areas. It was also pointed out that typhoons and strong cyclones may produce strong vertical mixing in the subarctic oceans where the oceanic stratification is relatively weak.

Importance of nonlinearity and baroclinicity structures has not yet been clarified, thus, there is still a need for more elaborate observational efforts.

Participants agreed that modeling and forecasting of tsunamis is an important subject in the region and PICES should support the activities of the relevant organizations such as ITSU, the IUGG Tsunami Commission.

D. Physical oceanography of the Japan/East Sea
Rapporteur: C.N.K. Mooers (Miami University, U.S.A.)

Two main topics were discussed concerning observations and models:

a) The circulation of the Japan/East Sea; Prof. Kozlov presented a new (quasi-geostrophic) theory for "background currents" (or, mean circulation) for semi-enclosed seas, was applied to the Japan/East Sea. The "background currents" consist of three components: planetary, topographic and "running" (or throughflow). As a result, two-to-three main gyres (and one of the Tsushima branch currents) occur, depending upon an unknown parameter (alpha) for a two-layered regime. This model can assist the interpretation of both observations and numerical simulations.

Dr. Goncharenko (for Drs. Danchenkov, Kim, and Takematsu) summarized the studies of the subpolar front, "chimney" region (off Vladivostok), and of Japan/East Sea Proper Water by the joint Japanese, South Korean and Russian CREAMS Program, including CTD/ADCP cruises and current meter moorings from 1993 to 1995 and for future plans.

Dr. Ro described studies of the East Korean Warm Current (and, especially, of a recurrent anticyclone) by a consortium of (South) Korean universities.

Prof. Mooers presented results on the 10-day spin-up of the high-resolution [about 10 km and 20 sigma (terrain-following) levels], wind-and-inflow-driven Japan/East Sea Princeton Ocean model, noting the barotropic adjustment (including strong subsurface jets and deep flow) due to a strong JEBAR (topography/pressure gradient) interaction associated with the coarse, over-smooth Levitus climatology. The most notable feature is the development of a strong cyclonic circulation poleward of the subpolar front. The fully spun-up model, and then the annual cycle, will be of considerable interest in comparison with observations and other models.

Overall, there is now an improved bases for close coordination between observations and modeling to rapidly increase our understanding of the circulation.

b) The ventilation of the Japan/East Sea; Prof. Yakunin presented his analysis of salt flux as a by-product of ice production in the Tartarski Strait, Dr. Ponomarev presented his analysis of mixing as a by-product of ice production in Peter the Great Bay, and Dr. Goncharenko presented his analysis of the pre-conditioned, cyclonic eddy (and suspected "chimney") region over the seamount near the continental slope and surface front off Vladivostok. Though the chemists estimate about 1% of the deepwater is produced each year, the physicists cannot (yet) account for that much from these three sources.

Overall, there is a lack of observations (temperature, salinity, dissolved oxygen, etc.) in wintertime near the coast, and over the continental shelf and slope in general. It may be necessary to integrate along all the coastal bays (and over the shelf/slope) of the Primorye Coast. Not much addressed yet, is the interannual variability in the ventilation processes.

Discussions:

There was lively discussion, making it clear that there is both great interest and controversy on these topics, which indicates a strong basis for scientific collaboration and rapid progress in the near future.

Recommendations:

a) An international, long-term (about 10 yrs) study is needed of the Japan/East Sea circulation and ventilation processes, including coordinated observational and modeling efforts.

b) A special emphasis is needed on the subpolar front, annual cycle, interannual variability, and coastal ocean processes.

c) Air-sea interaction processes (especially associated with ventilation) need to be addressed on an (atmospheric) synoptic time scale with daily resolution, rather than with monthly averages on events. For example, establishment of a meteorological buoy near 42°N, 132°E would be particularly revealing of ventilation events and help to qualify the rate of deepwater formation.

d) There is a need for observations of jet trapped continental margin and seamount topography as indicated in various numerical models.

e) Deployment of numerous Lagrangian drifters, especially subsurface (RAFOS) floats at intermediate depths and vertically cycling (ALACE) floats (to sample the mass field in the (pycnocline) for two or more years would be very revealing of the general, mesoscale, and transient circulation.

f) There is a need to organize a high-resolution (about 1/4 degree) seasonal ocean climatology to support both observational and modeling studies. For this, an international effort is needed to aggregate and manage both physical and chemical data.

g) It is important for all interested countries and institutions to be involved in both the observational and modeling studies so that model-data and model-model comparisons can be made. In particular, it is important that POI become directly involved in the numerical modeling studies; for this, one or more powerful PCs or (preferably) workstations dedicated to modeling would be needed.

h) Finally, creation of PICES Working Group on the Japan/East Sea circulation and ventilation could facilitate the support and integration of CREAMS and other observational campaigns with several ongoing modeling efforts.

E. Communities of the Okhotsk Sea and adjacent waters: composition, structure and dynamics
Rapporteur: O.S. Temnykh (TINRO, Russia)

Twelve oral presentations were made at this session. The range of interest was very wide and concerned all organisms from microorganisms to whales. However, the main questions, considered were the composition, structure and dynamics of plankton and nekton communities of the Okhotsk Sea and the changes in ecosystems related to climatic-oceanological conditions.

The changes in epipelagic fish communities of the Okhotsk Sea are though to be caused by climatic-oceanological changes. Total abundance of epipelagic fishes in the Okhotsk Sea decreased by about 1.5 times and there is an obvious change in the ratio of the most common species such as walleye pollock and herring.

Significant changes were also noted in nekton communities of the Pacific waters of the Kuril Islands. Biomass of the epipelagic fishes decreased while the share of squids increased. Data on species composition, abundance of the mesopelagic fishes as well as the interannual dynamics of the trophic relations between plankton and mesopelagic nekton were investigated. The decrease of abundance of predominant mesopelagic fish such as deep-sea smelt has been established. Total plankton consumption by nekton also decreased.

Some presentations concerning plankton communities were made at the session:

a) An anomalous oceanological situation in 1993 in comparison with 1991-1992 is assumed to have caused the high phytoplankton abundance in the Sakhalin-Kuril region.
b) No observed changes in plankton and benthic communities in the northeastern Sakhalin shelf, where oil extraction occurs, was found. However, an oil spill appears to have cause a large-scale death of zooplankton.

It was hypothesized that a high bioproductivity in northeastern Okhotsk Sea is conditioned by the high concentration of mercury, which stimulates hydrobionts vitality and prolongs their life. Therefore, current climatic-oceanological changes are presumed to initiate considerable changes in the plankton and nekton communities of the Okhotsk Sea and adjacent water. A mechanism of this influence is not clear and it appears to be a goal of further explorations.

Recommendations:

a) Mesopelagic fishes are very important in the functioning of an ecosystem. We propose to conduct a special workshop "Mesopelagic fishes as the sea communities component"

b) Some fish species are important internationally (herring, pollock, sardine, saury, mackerel, anchovy, salmon). Representatives at this workshop should form a working group to collect and change all information on catch, size and age of these fishes.

c) A lot of information on composition, structure and long-term dynamics of the pelagic and demersal communities has been collected in TINRO over more than ten years. Therefore, we propose to form a editorial board to prepare a review monograph on the biological resources of the Okhotsk Sea (tentative name of this monograph may be "Ecosystems of the Okhotsk Sea and Adjacent Waters")

F. Abundance, distribution, dynamics of the common fishes of the Okhotsk Sea
Rapporteur: T. Nishiyama (Hokkaido Tokai University, Japan)

The eight papers in this session dealt with the commercially important fish species in the Okhotsk Sea. These included walleye pollock, herring, Greenland turbot and many other flatfishes. Most of the papers have analyzed catch, abundance, migration, depth distribution, spawning, and associated biological aspects. These papers were presented by Drs. Fadev, Zolotov, Pushnikova, Dyakov and Nikolenko. Dr. Nishiyama reported Japanese fisheries activities on the Okhotsk Sea side of Hokkaido.

The historical data on several fish species were analyzed, and the long-term fluctuation of abundance and the characteristics of population structures were discussed. The strong yearclass and weak yearclass of fish were pointed out in pollock and herring, and the effects of both natural and human factors were analyzed. The results of presented papers show that the spawning, transport and dispersion of early life stages, depth distribution, and other biological aspects were strongly influenced by the changes in circulation, flow pattern, eddies, water

temperature, and other oceanographic conditions. The studies also suggested some possible ocean-atmosphere causes on the ecosystem dynamics.

Age determination of fish is an essential technique for the analysis of population structure in fish stock assessment and management. Dr. McFarlane raised a question on the validity of the present employed methods. The burnt otolith section method has indicated significant discrepancies in annual count from the scale reading method, otolith surface method, and other methods. Therefore, the necessity of re-examination of the age data previously determined by the traditional methods is emphasized, and implication for pollock population dynamics and environmental influence was addressed.

Walleye pollock is not only a major target species in many fisheries, but also a key species in marine ecosystem. This fish is prey for marine mammals, sea birds and other large predatory fishes. The partitioning of pollock resource to the human use and to the other animals is a serious concern in the Bering Sea. Based on the analyses of biomass abundance, Dr. Wespestad clarified the present status of pollock resources in different regions. The results suggest the appropriate size for the pollock resource, the survival and abundance of the higher trophic animals in the Bering Sea.

Some papers focused mainly on fluctuation in abundance of single species, but the changes in fish community structure in relation to the abundance fluctuation of mixed species are of serious concern. Therefore examining the changes in fish community structure should be encouraged.

The presented papers and discussion in this session came to the following conclusions that future research should be directed towards:

i) conducting comparative research on the causes of year-class variation of walleye pollock around the Pacific rim,
ii) examining possible ocean atmosphere causes and effects on ecosystem dynamics,
iii) examining changes in fish community structure, and
iv) establishing an appropriate age determination method.

Recommendation:

Several papers have shown a common trend in abundance fluctuation of walleye pollock between the Okhotsk and Bering Sea. Specific year-classes were strong and weak in both areas, especially the very strong 1977-78 and 1988-1989 year-classes. Thus, participants in this session believe it would be beneficial to hold a specific workshop on the causes of year-class variation of walleye pollock around the Pacific rim.

G. Salmon of the Okhotsk Sea: biology, abundance and stock identification
Rapporteur: R.J. Beamish (Pacific Biological Station, Canada)

There were six oral presentations relating to salmon in this session. Topics ranged from growth, survival and stock identification to new concepts of the factors affecting the dynamics of pink salmon populations. Kamchatka pink salmon stocks were shown to be separate from Sakhalin-Kuril region pink stocks in the ocean but overlapped during periods of higher abundance. Using stock identification techniques to develop stock composition models, it was observed that a small percentage (~6%) of the juvenile pink salmon in the Sea of Okhotsk originated from Alaska stocks.

Feeding studies of pink, chum and sockeye indicated that feeding was mainly on zooplankton during the day and not at night. Pink salmon fed principally on nekton and decapod larvae, sockeye on hyperiids and chum on pteropods. River lamprey in Canada and Russia were identified as major predators of salmon in some areas of the ocean, indicating that similar but distinct species of salmon predators have common impacts on the marine survival of salmon. The marine survival of hatchery-reared pink and chum salmon fry can be improved by releasing smaller numbers earlier at the end of April and larger numbers in mid-May followed by smaller releases at the end of the release period.

A new approach to forecasting the returns of pink salmon using chaos theory in a basic production model allows for a more realistic way of incorporating the non linearity of the "natural system".

There were no recommendations made after the session but later discussions identified the need for a workshop on the behavior and population dynamics of pink salmon.

Recommendations:

Fish species that are important internationally are salmon and walleye pollock. The management issue related to pollock is the relative importance of fishing and natural changes in abundance. Papers presented at the workshop provided information that pollock stocks may not be overfished, may be overfished in some areas, or may fluctuate with trends in carrying capacity.

a) Representatives at this workshop should form a working group to collate all information on catch, size and age information of pollock in the Sea of Okhotsk.

b) Any future workshop should address the issue of the impact of short-term and long-term changes in the climate/ocean environment on abundance trends of pollock.

   The major issue in salmon was related to factors affecting marine survival and behavior of pink salmon. At the southern part of the range, in the Amur and Fraser Rivers, returns in recent years have been below forecasts; while in the more northerly areas, returns are approximating historic high levels. In addition, there are suggestions by some scientists that pinks may be straying more than in the past.

c) A special workshop (PICES sponsored) would bring together experts to determine what is affecting pink salmon abundance and if the increased straying is real.

H. Biodiversity of island ecosystems and seaside's of the North Pacific
Rapporteur: B.I. Semkin (Pacific Institute of Geography, Russia)

In Vladivostok, the main center of marine, ecological and biological studies is located (Pacific Institute of Oceanography, Pacific Institute of Geography, Institute of Marine Biology, Institute of Biology and Pedology FEB RAS, etc.).

In this session scientists were involved in discussions on various aspects of the biodiversity problem. 20 papers and a keynote lecture (B.V. Preobrazhensky, opened the session) were discussed. The two days session was divided into four parts, and chaired by B.I. Semkin (2), B.V. Preobrazhensky, A.G. Ablajev. Abstracts of twenty nine papers were published.

Scientists from Vladivostok (26), Magadan (3), Khabarovsk (2) and St. Petersburg (2) took part in the workshop.

The main topics presented were:

a) biodiversity of marine, brackish water and terrestrial (coastal) ecosystem (salt marshes, dry coastal ecosystems wetlands, forests, etc.),

b) biodiversity of shelf landscapes and their mapping,

c) biodiversity of terrestrial floras,

d) taxonomic diversity of vascular plants, lichens and fungi of Pacific sea coasts and islands (Kurils, Commander Islands, Okhotsk Sea islands, Peter the Great Bay Islands (Japan/East Sea),

e) application program for biodiversity conservation,

f) productivity forecasts of cultivated marine organisms,

g) vitality assessment of rare and endangered species in the island microrefuges,

h) flora and vegetation of Pacific islands,

i) natural ecological framework for territories and aquatories,

j) halophytic plants of the Northwest Pacific coast: chromosomes, ecology and protection,

k) taxonomic diversity and relationships in major and important groups of plants in the Northwest Pacific area,

l) rare plant species in the Russian Far East and their protection,

m) Pacific basin biodiversity protection,

n) plant communities diversity in wildlife areas of the Russian Far East,

o) mathematical methods of comparative study and assessment of biodiversity, and

p) databases of biodiversity components.

Proposals:

a) The biodiversity problem is of a great importance and must be placed among priorities in the framework of PICES.

b) Coastal ecosystems determine bioproductivity of marine ecosystems, but there is a lack of information about them, because terrestrial and marine ecosystems have, for a long time, been investigated separately. We stress that studies on biodiversity of island and coastal ecosystems are growing in importance.

c) Nature use and nature conservancy problems are the most urgent in coastal ecosystems.

Future actions and recommendations

The participants of the workshop are grateful to PICES for providing the opportunity to present and discuss their work. Many participants hope consideration will be given to have the proceedings as the workshop published. The workshop asked for a volunteer group of Russian scientists (contact person: V. Lobanov) to plan to publish the proceedings, with the cooperation of PICES Secretariat. The proceeding would be a good supplement to the PICES Scientific Report No.2, 1995 on the Okhotsk Sea and Oyashio Region, which does not fully include recent Russian work.

As the PICES Scientific Report No. 2 focuses on physical oceanographic items, another report on biological and fisheries aspects of the Okhotsk Sea region would be desirable. In addition, translation of Russian monograph, Hydrometeorological Conditions of the Okhotsk Sea, Gidrometeoizdatt, St. Petersburg, 1995 the Okhotsk Sea (in press) would be useful for us, and we hope that the book will be published as soon as possible. After it is published, we suggest that PICES support translation into English and publish its English version.

3. Recommendations of the Workshop

a). PICES publish the workshop proceedings. PICES should also take the initiative to publish the other reports mentioned above.

b). POC should take the lead on research in this region and assists to create relevant international cooperative studies to solve the urgent problems. POC should hold another more focused workshop on the Okhotsk Sea Region in the near future.

c). POC should organize a Working Group on the circulation and ventilation of the Japan/East Sea. The Working Group should further discuss the recommendation items given in the session D summary above.

d). BIO and/or FIS should focus on the biological and fisheries aspects of the Okhotsk Sea and adjacent areas, through the medium of a report or workshop.

e). FIS should discuss recommendations proposed in the sessions E, F and G above and take the appropriate action.

f). The workshop recommends that PICES member countries bordering the Okhotsk Sea facilitate access to investigators to cooperate on scientific research in the region. PICES should endorse and support international research programs such as CREAMS in the Japan/East Sea and the Soya/La Perouse Project.

g). The workshop recommends that CCCC Implementation Group coordinate an international cooperative project on the Okhotsk Sea area as one of its key projects.

h). TCODE should consider amassing the data necessary for the special process oriented studies. Complete data inventories from relevant institutions and individuals need to be identified. It is recommended that TCODE takes an initiative to solve these problems.

i). POC should takes the initiative to prepare for publication a complete list of nomenclature of bays, straits, currents in all languages of PICES member countries.

4. Acknowledgments

On behalf of all those who attended the Workshop, the Scientific Steering Committee would like to express their thanks to the Local Organizing Committee, Workshop Secretariat, conveners of the paper sessions and the PICES Secretariat for their tremendous efforts in making the workshop a success. We also express thanks to the Russian government agencies for their supported.

II. SCIENTIFIC PAPERS SUBMITTED FROM SESSIONS

1. Physical Oceanography Sessions

A. Circulation and water mass structure of the Okhotsk Sea and Northwestern Pacific
B. Sea ice and its relation to circulation and climate
C. Waves and tides
D. Physical oceanography of the Japan Sea / East Sea

Seasonal Variability of the Pycnocline in La Perouse Strait and Aniva Gulf

Valentina D. BUDAEVA[1] and Vyacheslav G. MAKAROV[2]

[1] Far Eastern Regional Hydrometeorological Research Institute, Vladivostok, Russia
[2] Pacific Oceanological Institute, Russian Academy of Sciences, Vladivostok, Russia

The properties of the pycnocline reflect a number of processes (i.e., atmosphere-ocean heat exchange, vertical and horizontal motions, etc.) which influence the water structure (Vinogradov et al., 1984; Lebedev and Aizatulin, 1984; Ozmidov, 1986; Zyryanov, 1980; Trotsenko et al., 1992). Investigation of the temporal-spatial pycnocline variability plays an important role for fishery and ecology of the productive shelf regions within the Far Eastern Marginal Seas.

The most difficult problem in evaluating the pycnocline characteristics is to find the point of inflection based on discrete density estimations at the standard horizons assuming, in advance, continuous vertical assignment of the density function *r(z)*. Layer by layer calculations are unacceptable since such way permits one to define the layer of the maximal density change, but not the inflection point. In order to eliminate the uncertainty, as a rule, the spline approximation is used (Ahlberg et al., 1967). This approach allows restoration of the curve of vertical distribution *r(z)* in the preliminary searched layer of the maximum density change with the help of a polynomial of the third order and then to determine the position of the inflection.

An algorithm to define the pycnocline characteristics is given below. Firstly, the layer $[z_i, z_{i+1}]$ of the maximum density change *r(z)* was found from discrete experimental data. In the cases when the maximal change *r(z)* covered more that one layer their combination was considered as the layer $[z_i, z_{i+1}]$. Within this layer distribution of *r(z)* was approximated by the cubic spline:

$$\rho(z) = a_0 z^3 + a_1 z^2 + a_2 z + a_3 \qquad (1)$$

In order to find the coefficients a_i (i = 0-3) the following boundary condition have been applied:

$$\rho(z)\big|_{z=z_i} = \rho_i \; ; \quad \rho(z)\big|_{z=z_i+1} = \rho_{i+1} \; ;$$

$$\left.\frac{\partial\rho}{\partial z}\right|_{z=z_i} = \begin{cases} 0, & z_i = 0 \\ D_i = \left[\rho(z_i) - \rho(z_{i-1})\right]/(z_i - z_{i-1}), & z_i > 0 ; \end{cases}$$

$$\left.\frac{\partial\rho}{\partial z}\right|_{z=z_{i+1}} = \begin{cases} D_{i+1} = \left[\rho(z_{i+2}) - \rho(z_{i+1})\right]/(z_{i+2} - z_{i+1}), & z_{i+1} < H \; ; \\ 0, & z_{i+1} = H \end{cases}$$

As a result the system of four algebraic equations was obtained and solved using the standard approach.

By equating to zero the second derivative of the function *r(z)*:

$$d^2\rho/dz^2 = 6a_0 z_p + 2a_1 = 0, \qquad (2)$$

the point of $r(z)$ inflection z_p was computed:

$$z_p = -a_1 / 3a_0 .$$

The first derivative of the function $r(z)$ gives the density gradient. By substituting the equation (2) in (1), the expression for calculation of the pycnocline intensity at the depth z_p , i.e., the maximum vertical density gradient G_{max} in the fixed point was received.

$$G_{max} = \left.\frac{d\rho}{dz}\right|_{z=z_p} = a_2 - \frac{a_1^2}{3a_0} . \qquad (3)$$

The analytical equations to determine coefficients a_i have been obtained from the boundary conditions:

$$a_0 = -2\left[\frac{(\rho_i - \rho_{i+1})}{(z_i - z_{i+1})^3} - 0{,}5\frac{(D_i + D_{i+1})}{\left((z_i - z_{i+1})^2\right)}\right];$$

$$a_1 = \frac{(D_i - D_{i+1}) - 3a_0\left(z_i^2 - z_{i+1}^2\right)}{2(z_i - z_{i+1})};$$

$$a_2 = (1/2)\cdot\left[(D_i + D_{i+1}) - 3a_0\left(z_i^2 - z_{i+1}^2\right) - 2a_1(z_i + z_{i+1})\right]$$

Based on the given algorithm the charts of the maximum vertical density gradients (G_{max}) and the depths of their location (z_p) in spring, summer, and fall have been prepared and used to reveal the spatial pycnocline structure and its annual transformation in La Perouse Strait and Gulf of Aniva (Fig. 1). The multi-year means of the seasonal density fields, being restored in the nodes of regular net by the standard graphic packages, have been applied for our calculations.

The charts clearly demonstrate that the pycnocline shape is a result of the water dynamic in the region. Thus, the Soya Current meandering leads to the vorticity strengthening in the current field and as a consequence, to the rising or deepening of the pycnocline.. For example, the Soya Current cyclonic meander south-eastward off the Cape of Krilion is responsible for the pycnocline movement upward to a depth of 10 m (Fig. 1a) and an increase of the intensity up to 0.06-0.07 sda/m (specific density anomaly per meter) (Fig.1d). The Soya current anticyclonic meander in the La Perouse Strait, on the contrary, forms an intensive downwelling zone where the pycnocline deepens to a depth of 30-35 m (Fig. 1c).

The pycnocline properties are influenced by the intrusion of external water in the region. The Gulf of Aniva is characterized by the intense river runoff which in summer period causes the increased persistence of two-layer vertical water stratification and the high (more than 0.1 sda/m) pycnocline intensity in the upper layer (Fig. 1e). The sources of external water for the La Perouse Strait are the streams or mesoscale vortexes of the East-Sakhalin Current (Fig. 1b).

The spatial heterogeneity in the depth distribution of the pycnocline location is most vividly expressed in spring and fall (Fig. 1a-c). In addition to the dynamic reasons, the spatial heterogenity could be correspondingly explained by the radiation heating and the fall-winter convection in spring and fall,. During the transitional seasons, the horizontal field structure of z_p is represented by the

combination of closed isolines considered as the local dynamic formations. Within these formations the depth of the pycnocline location changes abruptly, and the sharp density variations are observed similar to those for other regions of the World Ocean, in particular, for the Sea of Scotia (Lebedev and Aizatulin, 1984) and the Gulf of Aden (Trotsenko et al., 1992).

In the summer period, within the Gulf of Aniva, the large area of sinking waters is formed due to the prevailing of anticyclonic current. As a result the pycnocline deepens and reaches the depth of 20 m (Fig. 1b). The pycnocline rises slightly northward and in the nearshore zone of upwelling it becomes thin and shows significant gradients (Fig. 1e).

Significant seasonal variations of the maximum vertical density gradients are revealed in the La Perouse Strait and Gulf of Aniva. The lowest G_{max} values of 0.02-0.05 sda/m are found in spring and fall (Fig. 1d, 1f) and the highest G_{max} values of 0.14-0.18 sda/m are displayed in summer (Fig. 1e). As a whole, summer is characterised by a more homogeneous distribution of z_p and by the general increase of G_{max} values, approximately by an order. During this season, a decrease of vertical density gradient location to 15-20 m is also observed everywhere. These essential differences in the vertical density stratification are related, mainly, to the annual insolation variation and seasonal transformation of the current fields.

Our results show that the pycnocline within the shelf zone in the La Perouse Strait and Gulf of Aniva is characterized by the strong seasonal variability with preserved mosaic G_{max}. distribution during all seasons. This is evidence that the area under study is a region with a complex climatic regime of dynamic and thermohaline water structure formation. In perspective the properties and interannual variability of the pycnocline in other regions within the Sakhalin Shelf have to be evaluated.

REFERENCES

Ahlberg, J.H., E.N. Nilson, and J.L. Walsh. 1967. Theory of splines and their applications. N.Y., Academic Press. 316 p.

Lebedev, V.L., and T.A. Aizatulin. 1984. The classification of the oceanological attributes of increased biological productivity of the marine waters. Voprosy Geografii No 125. Oceany i Gizn:160-172. (in Russian).

Ozmidov, R.S. 1986. The inter-layers of hydrophysical parameters and its role in formation of hydrochemical and hydrobiological fields in the ocean. Issledovaniya ekosistemy pelagiali Chernogo morya. M., Nauka. p. 9-18. (in Russian).

Trotsenko, B.G., S.P. Klimenko, V.V. Dronov, and G.P. Korshunova. 1992. The seasonal pycnocline variability of the Bay of Aden. Okeanologiya. 32(4):647-653. (in Russian).

Vinogradov, M.E., A.A. Elizarov, and P.A. Moiseev. 1984. The biological efficiency of dynamically active zones in the open ocean. Proc. III Congress of Soviet Oceanologists. M., Nauka. p.107-127. (in Russian).

Zyryanov, V.N. 1980. The water dynamics in the south-western Atlantic and features of pycnocline locations. Okeanograficheskie Issledovaniya Promyslovyh Raionov Mirovogo Okeana. M., Pishevaya promyshlennost. p. 50-64. (in Russian).

FIGURES

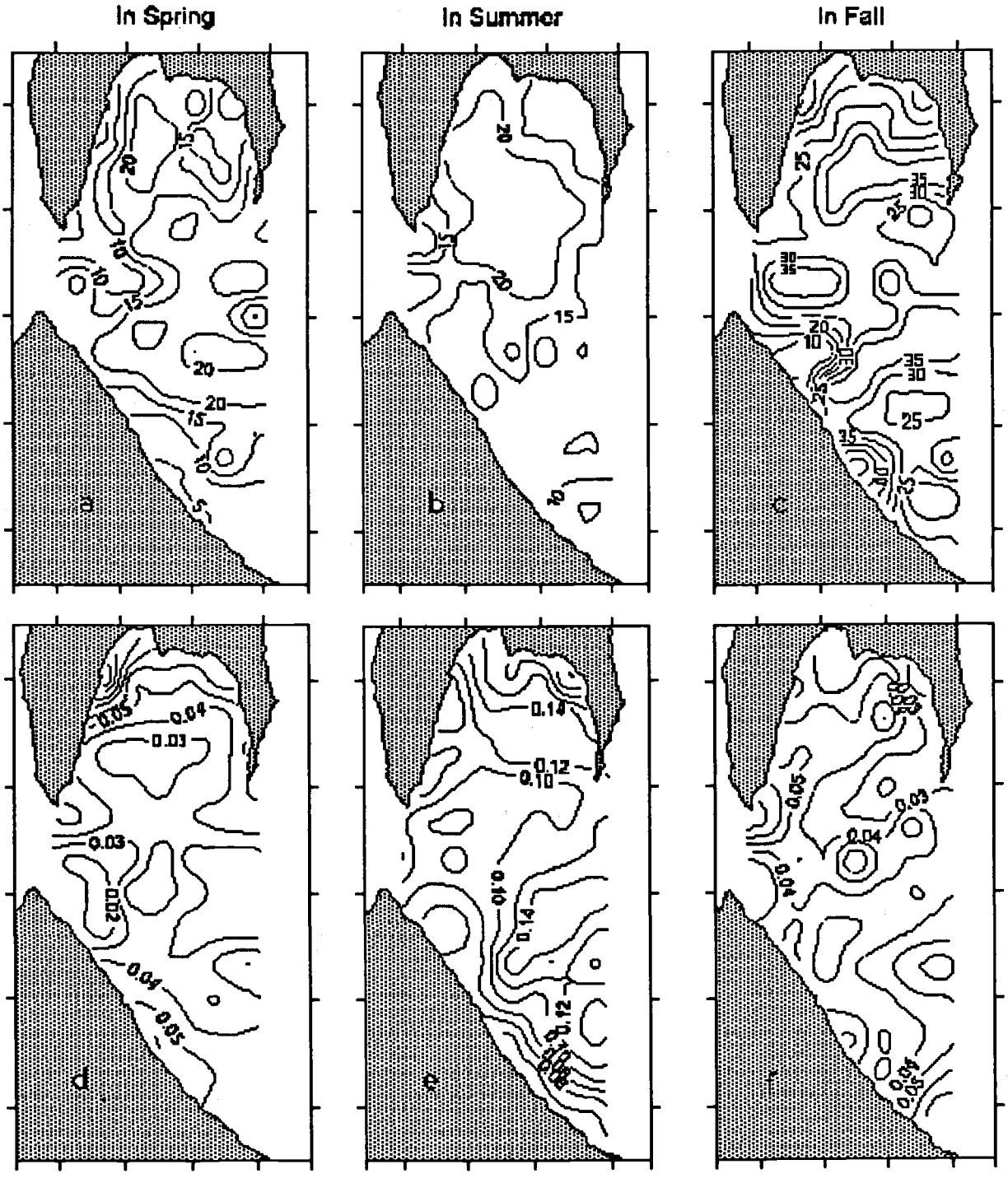

Fig. 1. Multi-year means of the maximum vertical density gradients and depths of their location in the Gulf of Aniva and La Perouse Strait in spring (a, d), summer (b, e) and fall (c, f).

Modeling of the Typical Water Circulations in the La Perouse Strait and Aniva Gulf Region

Valentina D. BUDAEVA[1] and Vyacheslav G. MAKAROV[2]

[1] Far Eastern Regional Hydrometeorological Research Institute, Vladivostok, Russia
[2] Pacific Oceanological Institute, Russian Academy of Sciences, Vladivostok, Russia

INTRODUCTION

The Aniva and La Perouse Region is characterized by a quite complex spatial water circulation structure. It was shown that the circulation patterns are determined by the sea level gradient of the northern Japan Sea and southwestern Okhotsk Sea parts (Aota, 1970; 1975; 1982; 1988), but there is not general agreement on the gradient's nature. In some works the supposition has been stated that the sea level gradient is due to a difference in the sea water density between the Japan and Okhotsk Seas, whereas other papers considered such factors as atmospheric circulation and tidal currents (Leonov, 1960; Shelegova, 1960).

The Japan Sea water discharge through the La Perouse Strait, under the influence of the sea level gradient, has essential fluctuations within the range of the interannual, seasonal and synoptic scales. Data on the diurnal mean transport through the La Perouse Strait are extremely limited. Regarding the seasonal variability of discharge, it is known (Aota, 1988) that in the warm period (July - October) the eastward (east or south-east) transport with velocities of about 50-80 cm/sec prevails. In the early winter, the resulting vector of the flow reverses and has a northwestward direction; at that time the current velocity, as a rule, does not exceed 10-15 cm/sec.

In the warm period, the diurnal currents are dominant in the Aniva and La Perouse Region, and the main axis directions for diurnal and semidiurnal currents correspond to the direction of the mean flow. In the early winter, the diurnal and semidiurnal currents become significantly weaker (Aota, 1988).

Due to the shallow waters (the maximal depth is about 130-140 m) and the funnel-shaped configuration of the shoreline in the Aniva and La Perouse areas, the water circulation in this region is under the great influence of the relatively strong monsoon type local winds. Under some baric conditions, these winds can transform the sea level gradient and the current structure on the southern Sakhalin shelf. Therefore, to understand the water circulation variability it is crucial to reveal atypical characteristics of the background currents resulting from these transformations.

The goal of this paper is to construct the typical water circulation schemes for the La Perouse and Aniva Region taking into account the different types of the regional baric field applying numerical modelling. Such an approach was successfully used previously for the Chukchi Sea (Kulakov, 1993).

MODEL DESCRIPTION

An improved version of the 3D diagnostic model (Budaeva et al., 1980) worked out for the coastal Sakhalin waters was applied to estimate water circulation in the La Perouse Strait and Aniva Gulf Region. Diagnostic calculations of water circulation and the three-dimensional field of the

currents have been performed for the different regional baric situations (Atlas, 1977; Atlas, 1979). The grid used approximated the area with the steps of 10'x12'. The number of grid nodes was 72 and the maximal calculated level was 125 m. The numerical modeling was conducted in the frames of linear equations for shallow waters under the condition of free flowing liquid boundaries and a discharge through the La Perouse Strait. In accordance with the our previous results (Budaeva et al., 1980) the sea water baroclinity was considered.

RESULTS

Figs. 1a and 1b present schemes of the integral circulation and surface currents corresponding to the type (I) of the regional baric situation. This type is characterized by the southward winds (southwestern and southern) that induce a significant sea level elevation in the eastern part of the Aniva Gulf and a sea level depression along the Okhotsk Sea coast of Hokkaido Island. Under the effect of the winds water circulation in the La Perouse Strait and Aniva Gulf region becomes anticyclonic and, as a rule, vertically homogeneous. As a consequence of circulation intensification, an increased inflow of the relatively warm Japan Sea waters is observed in the western and central parts of the Aniva Gulf and their transport along the Okhotsk Sea coast of Hokkaido. The anticyclonic mesoscale eddy generated in the offshore area of the La Perouse Strait is the major element of such a type of water circulation. It should be noted that the maximal development of the eddy is found under the influence of the southwestern winds and within the area of 45°30' and 46°00'N with a transport about 0.3 Sv. The highest surface current velocities (greater than 50 cm/sec) are revealed at the entrance to La Perouse Strait near the Capes of Krilion and Aniva and on the northern periphery of the mesoscale anticyclonic eddy.

A similar type of the water circulation, that could be generally considered as type (I), is observed when the western winds prevail (Fig. 1c). The only difference from the type (I) is found in the structure of the surface currents along the Okhotsk Sea coast of Hokkaido where a sea level depression is manifested less clearly and the scheme of currents is closer to the climatic circulation.

Figs. 1d and 1e demonstrate schemes of the integral water circulation and surface currents corresponding to the regional baric situation of the type (II). It is characterized by the northern and northwestern winds that generate low sea level in the northern shallow part of the Aniva Gulf and a sea level elevation along the Okhotsk Sea coast of Hokkaido. Changes in water circulation are observed, mainly, in the formation of the mesoscale cyclonic eddy-meander on the western periphery of the Soya current and in the water rising in the northern shallow part of the Aniva Gulf. The cyclonic current active, mainly, in the surface layer (up to 50 m) is observed from the western side of this meander, whereas a non-persistent anticyclonic current is noted eastward off the main flow. When this type of regime exists, an increase of compensative near bottom inflow of the transformed Japan Sea waters is revealed in the central and east part of the Aniva Gulf, from which point, being under the effect of the eastern and southeastern flows, it follows to the southwestern part of the Okhotsk Sea.

Figs. 1f - 1h illustrate the schemes of the integral circulation and the surface currents associated with the type (III) of the regional baric situation. This circulation is formed when the northeastern, eastern and southeastern winds occur and create a "counter current" in the La Perouse Strait for the eastward transport of the Japan Sea waters. Prevailing winds cause a sea level elevation in the northern (southeastern winds) or western (northeastern and eastern winds) parts of the La Perouse Strait and Aniva Gulf region. This decreases the sea level gradient between the Japan and Okhotsk Seas and can even change the sign of the gradient in the La Perouse Strait and favor the western flow in the Strait. In this case the currents has a vividly pronounced two-layer vertical structure. In the surface layer (above 15-20 m) the main current flows westward/southwestward and, as a result, the

Soya current is blocked along the Okhotsk Sea coast of the Hokkaido. According to our estimations the maximum velocities at the surface can reach 50-80 cm/sec in the La Perouse Strait, and 20-30 cm/sec in the Aniva Gulf. The current has the right rotation but at the depth of 25-30 m it reverses, and the velocities observed are 2-4 times lower as compared with the surface velocities. The water circulation, corresponding to the type (III) of the regional baric situation, has the most anomalous character and leads to non-regular intraseasonal disturbances of the hydrological water structure along the southwestern coast of Sakhalin Island (Shelegova, 1960).

The model calculations show that in the La Perouse Strait and Aniva Gulf region the current fields are essentially dynamic and demonstrate the strong dependence on the type of regional baric situation. In such cases the current structure has a number of peculiarities. Generally, during prevailing northeastern, northern or eastern, northwestern (southeastern) winds the two-layer vertical structure of currents is found and with southwestern, western (southern) winds it has, mostly, one direction. The major activity of the mesoscale cyclonic eddies is observed when the persistent types III (eastern,, northeastern and southeastern winds) and II (northern and northwestern winds) of the regional baric situation occur, and the anticyclonic eddy exists under the influence of the southern southwestern and western winds (the baric situation of type I).

The proposed method of standardization and dialogue computer program for the typical circulation calculations generated by the wind in the La Perouse Strait and Aniva Gulf region are useful for the diagnostic aims of the present climate and providing the navigation service with the available information.

REFERENCES

Aota, M. 1970. Study of the variation of oceanographic condition North-East of Hokkaido in the Sea of Okhotsk. Low Temp. Sci. Ser. A. 28:261-279.

Aota, M. 1975. Studies on the Soya warm current. Low Temp. Sci. Ser. A. 33:151-172.

Aota, M. 1982. On oceanic structure of a frontal region of Soya warm current. Low. Temp. Sci. Ser. A. 4:207-215.

Aota, M., M. Ishikawa, and T. Yamada. 1988. Dynamic of flow in the Soya Strait. Low Temp. Sci. Ser. A. 47:147-160.

Atlas of typical wind fields in the Okhotsk Sea. Yugno-Sakhalinsk. 1977. 110 p. (in Russian)

Atlas of typical fields of zone of continental shelf around Sakhalin. Yugno-Sakhalinsk. 1979. 113 p. (in Russian)

Budaeva, V.D., V.G. Makarov, and I. Yu Melnikova. 1980. The diagnostic calculations of stationary currents in the Aniva Gulf and La Perouse Strait. Trudy DVNIGMI. 87:66-78. (in Russian)

Kulakov, Yu.M. 1993. The simulation of typical circulation of waters of Chukchi Sea. Trudy AANII. 429:76-85. (in Russian)

Leonov, A.K. 1960. Okhotsk Sea. Regional oceanography.Part.1. L.: Gidrometeoizdat. p. 186-290. (in Russian)

Shelegova, E.K. 1960. The cases of sharp cooling of the waters in summer period at southwestern coast of Sakhalin. Izvestiya. TINRO. 46:249-251. (in Russian)

FIGURES

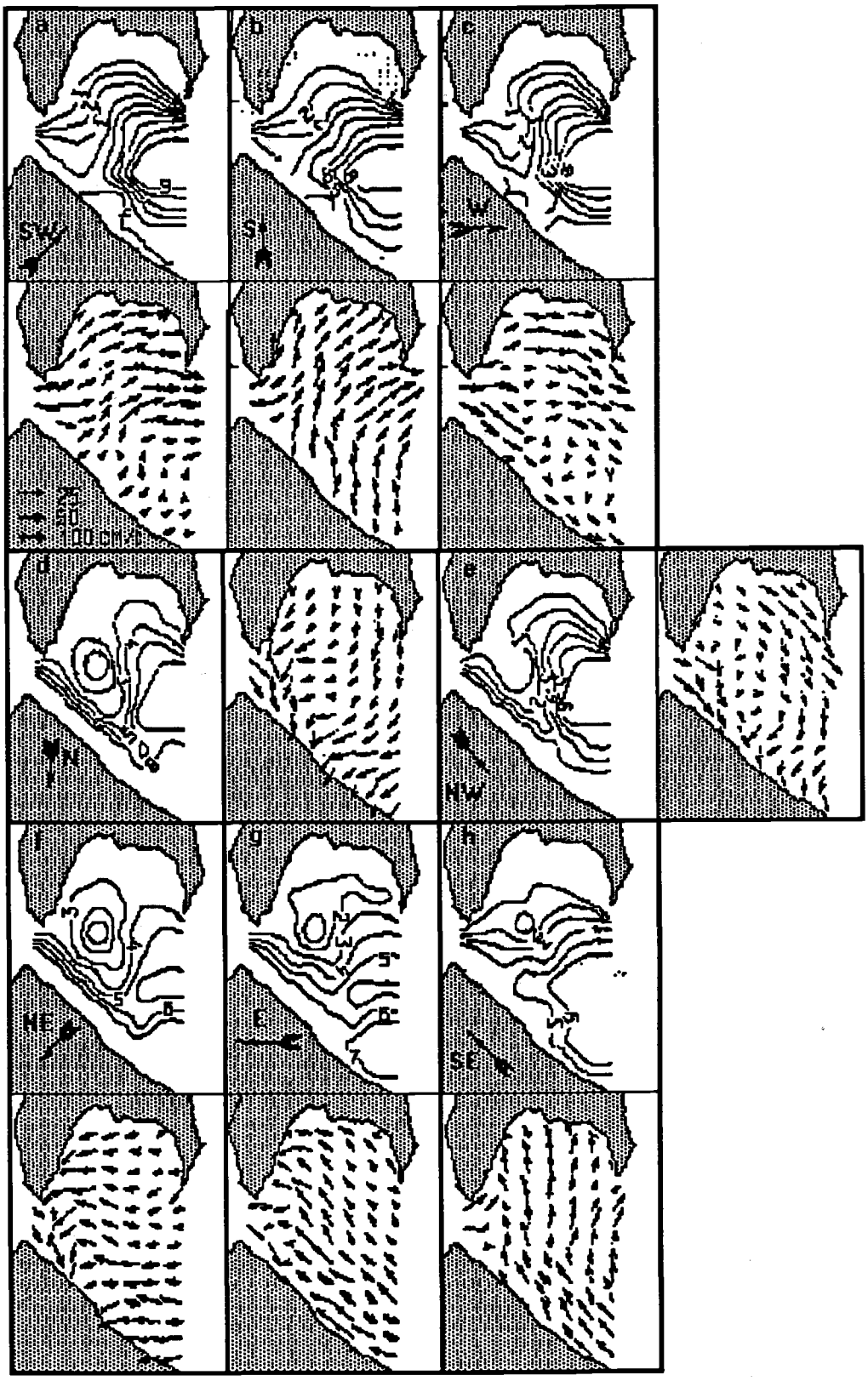

Fig. 1. Schemes of the integral circulation and surface currents in the La Perouse Strait and Aniva Gulf region for the different regional basic situations:
Type I - prevailing of SW (a), S (b) and W (c) winds;
Type II - prevailing of N (d) and NW (e) winds;
Type III -prevailing of NE (f), E (g) and SE (h) winds.

Anticyclogenesis over the Okhotsk Sea and its Influence on Weather

Nina A. DASHKO[1], Sergey M. VARLAMOV[2], Young-Ho HAN[3] and Young-Seup KIM[3]

[1] Far-Eastern State University, Vladivostok, Russia
[2] Far-Eastern Regional Hydrometeorological Research Institute, Vladivostok, Russia
[3] National Fisheries University of Pusan, Pusan, Republic of Korea

The anticyclonic activity over the Far Eastern Seas is one of the reasons for the weather anomalies over the adjacent territories. The anticyclogenesis over the Okhotsk Sea, most developed in May-July, contributes significantly to the synoptic processes in summer. In the years of active anticyclogenesis the air temperature over Primorye, Sakhalin and the Western Kamchatka coast is mostly below normal. Precipitations over Sakhalin and Kamchatka are also below normal, whereas over Primorye, on the contrary, they are above average.

At the beginning of summer, especially at the end of May and June, the intensification of the anticyclone occurs over the Okhotsk Ridge and moves towards the Japan Sea, across the periphery to the south of Primorye. The maritime air mass appearance is accompanied by the southern or south-eastern winds reaching sometimes about 15-20 m/sec, as well as by rain, drizzle or fogs. Such situations can continue for 5-7 days and lead to a decrease of the daily mean air temperature in Vladivostok up to 9-10°C, while the daily mean air temperatures in June from the multi-year observations is 12.8°C (Manual of the Short-term.., 1965; Dashko and Teslenko, 1991).

June in South Primorye is a transition period from spring to summer, and thus, a month of weather contrasts. It is a central month in the first half of the summer monsoon which provides the coast of Primorye with a continuous drizzle, thick fogs and strong, primarily, southern winds (Manual of the Long-term.., 1968; Dashko and Teslenko, 1991).

Fig. 1 demonstrates that the temperature regime in June in Vladivostok is distinctly different from the temperature regime of Nice and Rome located at the same latitude. The monthly mean air temperature in Vladivostok from April till July is the same as in Stockholm situated at 59°N (Fig. 1).

The duration of day light increases from 14 hours 32 minutes in May to 15 hours 12 minutes in June. The duration of sun radiance, on the contrary, decreases from 170 hours in May to 130 hours in June, on average. The ratio of the actual to the possible sun radiance duration is 41% in May and only 32 % in June.

The monthly mean temperature in June is 12-13°C. This is slightly lower than in September and can be compared with the mean air temperature in the first half of October. The air temperature shows significant variations during the month: the minimal temperature of 4.4°C and the maximal of 32°C were recorded (Soviet Union's Climatic Reference Book, 1966-1970). It should be noted that moving off the coast, the continental climatic features prevail and June becomes the typical warm summer month.

The comparison of the summer weather characteristics over the Primorye edge of Russia and Korean Peninsula, based on a 50 year data set from observations at meteorological stations, demonstrated that the air temperature field distribution depends, to a great extent, on the circulation peculiarities and thermal state of the Okhotsk Sea.

For more detailed analysis, the correlation matrices were constructed for the monthly mean air temperature at stations of Primorye and Korean Peninsula and the monthly mean meteorological parameters (pressure, air temperature, surface geopotential at 500 gPa), their derivatives ($\partial S / \partial x$, $\partial S / \partial y$, $\partial^2 S / \partial x \partial y$, $\partial^2 S / \partial x^2$, $\partial^2 S / \partial y^2$) and Laplacians ΔS at 30 points over the Okhotsk Sea and adjacent regions. The correlation coefficients of 0.7 were found between the monthly mean air temperature and air pressure over the Okhotsk Sea and the monthly mean air temperature at stations of Primorye and Korean Peninsula (Fig. 2). The significant correlation coefficients were also revealed between the monthly mean air temperature and the first $\partial S / \partial y$ and second $\partial^2 S / \partial y^2$ derivatives, and Laplacians for the air pressure field at sea level (P_o) and the geopotential at standard pressure level 500 mbar and their relative topography (Fig. 3).

The cold subsurface (dichothermal) layer of the Okhotsk Sea creates the favorable conditions for the intensification and stability of the anticyclonic atmospheric fields in the region. On climatic maps for the summer months (from the beginning of May and sometimes even from the end of April) the pressure fields over the Okhotsk Sea are revealed as the ridge of the North Pacific anticyclone.

The permanent North Pacific (Honolulu, Hawaii) anticyclone is an enormous high warm baric formation developed over the warm oceanic surface within the high pressure band of the Pacific subtropical and tropical zones (20-40°N) with a center located to the north of the Hawaiian Islands. The appearance of the North Pacific anticyclone results from dynamic factors and is supported by migration of Arctic and Asiatic continent anticyclones into the system.

The summer thermal conditions over the oceanic surface lead to the ridge propagation from the source towards the Far Eastern Seas, in particular, to the Okhotsk Sea. Under the favorable tropospheric thermodynamic conditions in the Maritime Polar Air Mass over the Okhotsk Sea the original anticyclone generates a cold baric formation with the relatively low height extension.

Generally, from May till July, in the period of the most intensive anticyclogenesis, the high pressure fields over the Okhotsk Sea were observed from 27 up to 60 days or, on average, in a half of all cases (47%) with an increase in June up to 55% (Table 1). The ridge was detected two times more often than the anticyclone centre. The essential variations in the yearly mean distribution of the high pressure fields over the Okhotsk Sea were revealed. For example, in June the ridge or anticyclone centre was fixed from 6 up to 24 days. The summary duration of the whereabouts over the Sea was 10-14 days for the anticyclone and 15-19 days for the ridge.

The lowest air temperatures were recorded in the period of the most intensive anticyclogenesis. A weakening of the anticyclone induced an enhancement of the air temperature in Vladivostok, Magadan and at other stations.

The same conclusions were made based on the analysis of the air temperature variations at the station of the Korean Peninsula (Pyongyang and Seoul) (Fig. 4).

Thus, the Okhotsk maritime anticyclogenesis is a result of the atmospheric processes not over the temperate zone but their interaction with the ocean and the processes over the Tropical and Arctic zones in the Northern Hemisphere. The role of the anticyclonic activity in the Far Eastern weather formation is not doubted and complex.

REFERENCES

Dashko, N.A., and E.I. Teslenko. 1991. Study of Thermal Regime in June over the South Primorye. Obninsk Informormation Centre of All Union Hydrometeorological Research Institute. WDC. 1090:gm-91. (in Russian).

Manual of the Long-term (3-10 days) Weather Forecast. 1968. L., Gidrometeoizdat. (in Russian).

Manual of the Short-term Weather Forecast. 1965. L., Gidrometeoizdat. (in Russian).

Soviet Union's Climatic Reference Book (Solar radiation, air temperature). 1966-1970. L., Gidrometeoizdat. (in Russian).

TABLES AND FIGURES

Table 1. Frequency (days, %) of anticyclonic and cyclonic baric fields over the Okhotsk Sea

Characteristics		Month			In all of the period
		May	June	July	
		Anticyclonic field			
Ridge of	min (days)	1	4	3	16
high pressure	max (days)	16	16	18	39
Average	(days)	7.5	9.8	10.4	27.4
	%	24.2	32.7	33.5	29.8
Centre of	min (days)	0	1	2	6
high pressure	max (days)	13	10	19	27
Average	(days)	4.5	5.8	5.4	15.8
	%	14.5	19.3	17.4	17.2
In all	min (days)	3	6	8	27
	max (days)	24	24	26	60
Average	(days)	12	15.6	15.7	43
	%	38.7	52	50.6	47
		Cyclonic field			
In all	min (days)	7	6	5	32
	max (days)	28	24	23	65
Average	(days)	19	14.4	15.3	49
	%	62.3	48	49.4	53

FIGURES

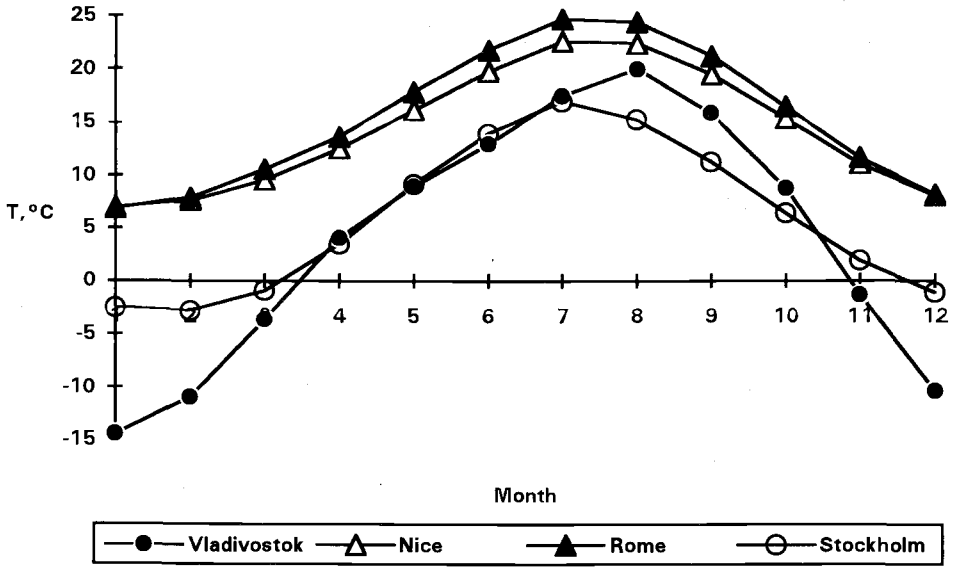

Fig. 1. The monthly (January - December) mean air temperature in Vladivostok, Nice, Rome and Stockholm.

a)

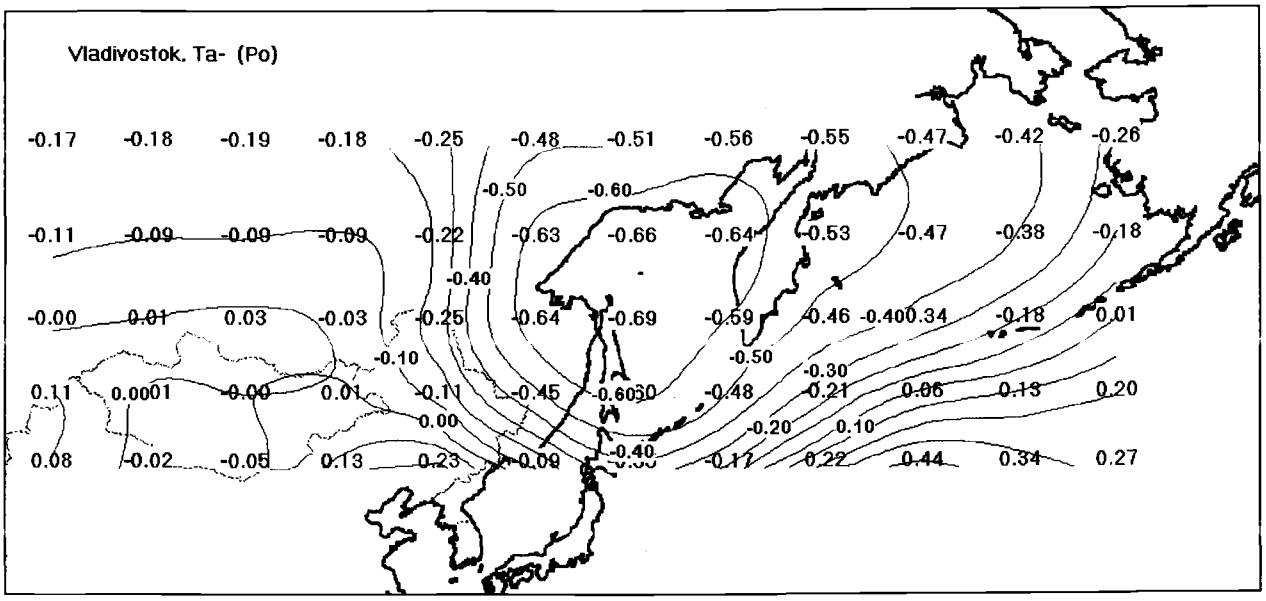

b)

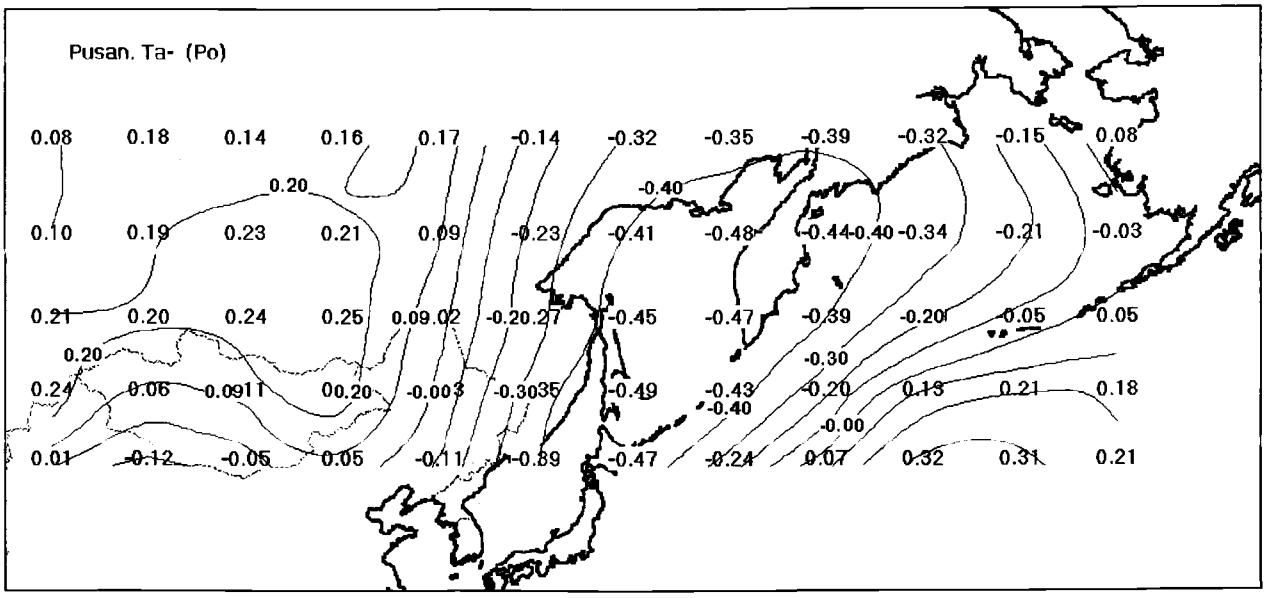

Fig. 2. Cross-correlation of the average monthly air temperature at stations Vladivostok (a) and Pusan (b) with air pressure over the Okhotsk Sea in June.

a)

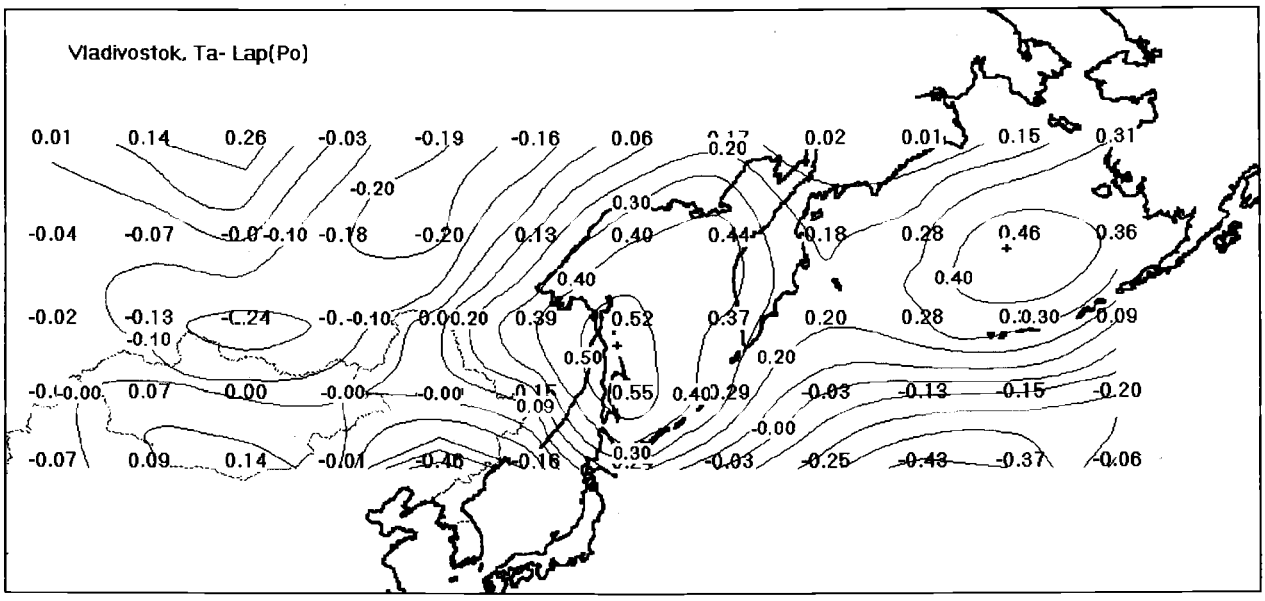

b)

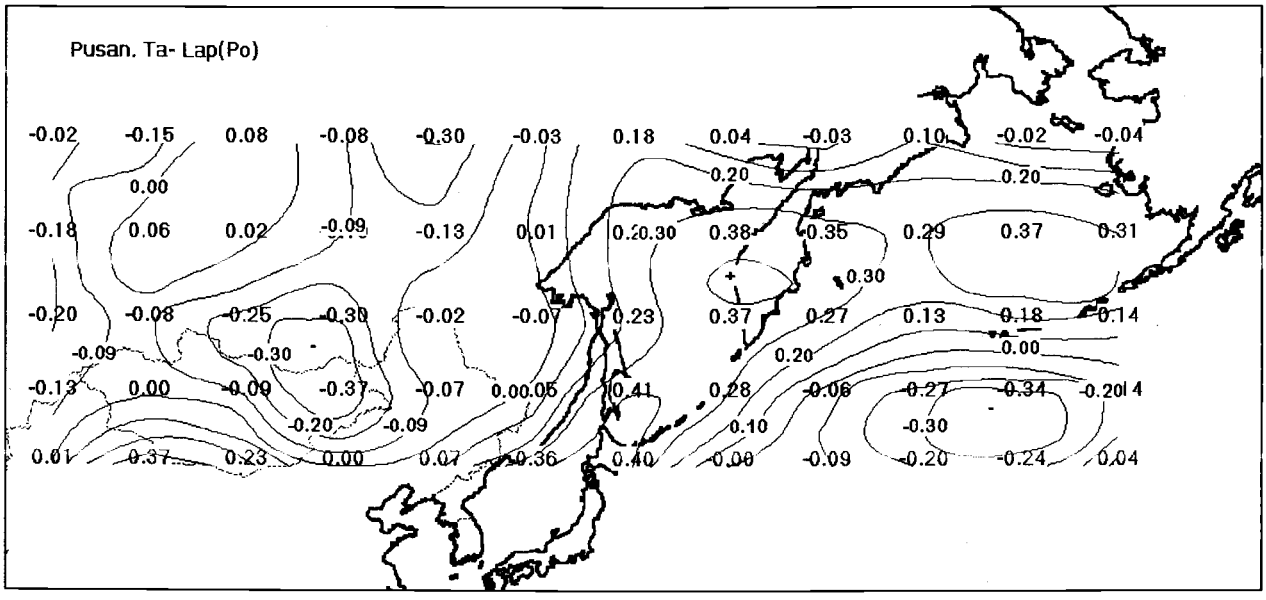

Fig. 3. Cross-correlation of the average monthly air temperature at stations Vladivostok (a) and Pusan (b) with the air pressure derivatives over the Okhotsk Sea in June.

a)

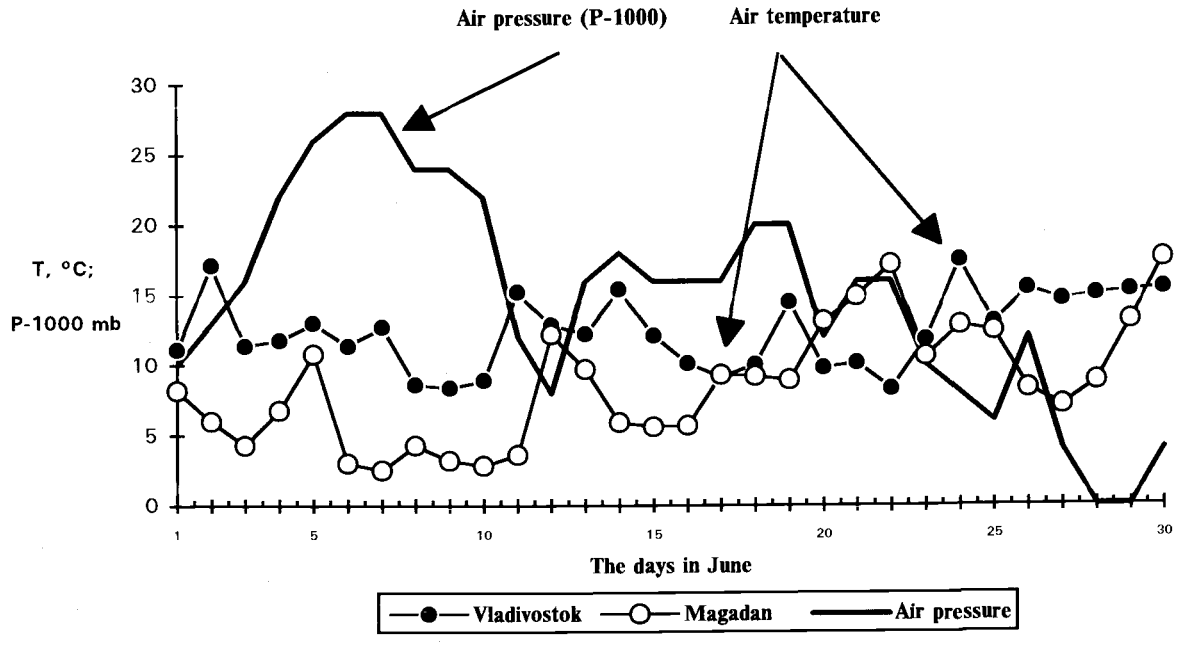

b)

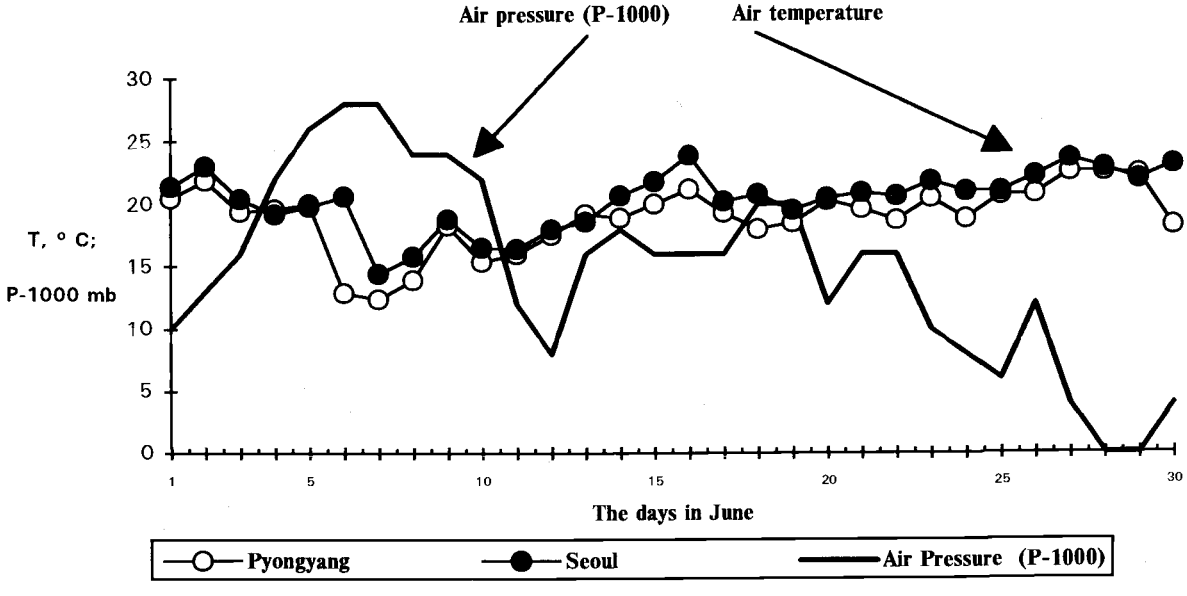

Fig. 4. The daily mean air temperature in June 1992 at the meteorological stations of Primorye (a) and Korean Peninsula (b) and mean air pressure over the Okhotsk Sea.

Research of Water Structure and Dynamics in the Okhotsk Sea and Adjacent Pacific

Boris S. DYAKOV, Alexander A. NIKITIN and Vadim P. PAVLYCHEV

Pacific Research Institute of Fisheries and Oceanography (TINRO-centre)

Vladivostok, Russia.

Water structure and dynamics of the Okhotsk Sea and adjacent Pacific have been studied based on satellite information and CTD data from the section carried out aboard the *R/V Academik Nesmeyanov* in September 3-12 1993. Spatial variability of geostrophic currents and hydrological conditions in the layer of 1,000 m have been investigated. It was established that the most complex dynamic zone was situated near the Kuril Islands.

The international expedition organized by the Pacific Oceanological Institute (Vladivostok, Russia) and the Institute of Ocean Sciences (Sidney, Canada) was performed in September 3-12 of 1993 aboard the *R/V Academik Alexander Nesmeyanov*. The oceanographic section along the WOCE P1W line has been carried out. A total of 30 stations, separated nominally by 30 nautical miles, were occupied.. The section started in the Pacific at 44°00'N and 153°30'E and ended on the northern Okhotsk shelf at 58°30'N and 141°48'E. On the way section passed through the Bussol Strait and crossed the basin and the shelf region of the Okhotsk Sea. A total length of the section was 870 miles (Fig. 1).

CTD data from this section and satellite information were used to investigated the water structure and dynamics of the Okhotsk Sea and adjacent Pacific. Velocities and volume transport of the geostrophic currents in the layer of 1,000 m were calculated applying the standard procedure (Zubov, 1979).

In September the cyclonic activity in the Okhotsk Sea and adjacent are of the Pacific strengthed. Also, the intrusion of water from the Pacific through the Bussol and Fourth Kuril Straits in the Okhotsk Sea increased (Luchin and Darnitsky, 1993; Luchin, 1987). Satellite images indicated the complex horizontal water structure near the Kuril Islands and on the northwestern shelf of the Sea (Fig. 1). The main features of this structure are: thermal front, currents, eddies of different scales and rotations (cyclonic and anticyclonic). Within the Kuril Islands area the intrastructure of the Kuril front and seasonal and synoptical secondary fronts have been revealed (Gladyshev, 1994). The cold Kuril current was observed along the Kuril Islands, and the warm Soya current was detected near the northern coast of Hokkaido. Six anticyclonic eddies were found in the region, five (A1-A5) in the Okhotsk Sea and one (A6) in the Pacific. The transverse streamers branched from topographical upwelling near the Central Kuril Islands (Darnitsky and Bulatov, 1995). The formation of Okhotsk sea eddies and streamers is a result of the interaction of large-scale tidal currents with the bottom topography (Gladyshev, 1994; Darnitsky and Bulatov, 1995).

The anticyclonic eddy A6 was found to the southeast from the Bussol Strait at 45°00'N and 152°00'E. The eddy was not stationary but was a type of eddy usually observed in the area of current convergence or divergence (Bulatov and Lobanov, 1983). The main formation mechanism of this eddy is the displacement of currents (Ginzburg, 1992). At the same time Lobanov (1993) considered all Kuril anticyclones as old Kuroshio rings. He suggested that in result of water transformation the warm core of these rings was destroyed and the cold core was formed.

The oceanographic section crossed the northeastern periphery of the eddy A6 (Fig. 1). In the layer of 50-350 m (stations 1-5) the cold water core with temperature less than 2°C was found (Fig. 2). During the survey more eddies were established in the Okhotsk Sea as compared with the adjacent Pacific, similar to that was observed in 1991 and 1994 (Darnitsky and Bulatov, 1995). Eddy formation is connected to general water circulation of the Okhotsk Sea and the water exchange between the Sea and the Pacific (Gladyshev, 1994). Analysis of the satellite information demonstrated the entry of the Pacific waters through the Bussol Strait in the Okhotsk Sea (Fig. 1).

Some structural zones were revealed on the section "Pacific Ocean-Okhotsk Sea". The most complex dynamic zone was situated near the Kuril Islands. The cold Kuril current of 100 miles width moved along Simushir Island (Fig. 3). In the center of this current (20-300 m) geostrophic velocity was 18.0-19.8 cm/s. The discharge of the Kuril current ws equal to 10.2×10^6 m^3/s (near normal), but in July 1993 the discharge was 6×10^6 m^3/s.

The speed on the periphery of the eddy A6 was 5.2-8.9 cm/s and increased to the center to 12.8-15.9 cm/s (Fig. 3). The diameter of eddy A6 was equal to about 70 miles and the discharge changed from 6.8 up to 8.4×10^6 m^3/s which compared with the intensity of the Kuril current. The Kuril current and anticyclone A6 spreaded approximately up to 700 m (depth of speed isoline of 5 cm/s).

To the northwest from the Kuril current the Northeastern current (stations 8-12) of 140 miles width and speed in the center 6.3-7.5 cm/s was traced (Fig. 3). The discharge of this flow was 7×10^6 m^3/s and water temperature in the upper layer of 20 m was 10-12°C (Fig. 2). In central deep water part of the Okhotsk Sea a calm halistatical zone was found where the current velocity of different directions did not exceed 2.5 cm/s in the upper 50 m layer and the volume transport in the layer of 1,000 m between separate stations fluctuated from 0.1 to 0.7×10^6 m^3/s. Water temperature of the upper homogeneous 20 m layer was 12°C (Fig.2).

The increase in the current velocity to 5.5-11.7 cm/s is observed in the north near the continental slope and at Iona Island (Fig. 1). Close to the southwestern part of the Kashevarova bank (stations 23-25) the cyclonic rotation with speeds 9.1-11.7 cm/s was found. The eddy led to the powerful upwelling of the intermediate waters (Chernavsky et al., 1993) (Fig. 2). Near the northwestern shores of the Okhotsk Sea, the Northern Okhotsk current to the west had a speed of 4.5 cm/s (Fig. 1). The more southern current with speed 5.5 cm/s was opposite in direction (Northern Okhotsk counter current). These two currents formed the cyclonic gyre.

The oceanographic section crossed the region of the subarctic hydrological water masses. Typical T, S curves of a variety of subarctic water structures are presented in Fig. 4. For example, T, S curve from station 3 was characteristic for waters from the Pacific (Pacific variety). The region near the Kuril Islands was characterized by T, S curves from stations 6,7,9 (Kuril variety). The subarctic hydrological structure of the deep water part of the Okhotsk Sea was reflected on T, S curves from stations 12, 16, 20, 2, 24. The water structure on the Okhotsk sea shelf was presented by T, S curves from stations 26, 28, 30.

Acknowledgements

The authors would like to express sincere gratitude to Drs. Alexander S. Bychkov and Gennady I. Yurasov (Pacific Oceanological Institute, Far-Eastern Branch of Russian Academy of Sciences, Vladivostok, Russia) and Drs. Howard J. Freeland and Frank A. Whitney (Institute of Ocean Sciences, Department of Fisheries and Oceans, Sidney, B.C., Canada) for providing data from the WOCE Section P1W.

References

Bulatov, N.V., and V.B. Lobanov. 1983. Investigation of mesoscale eddies to the east of the Kuril Islands on the base of meteorological satellites data. Earth Research from Space. 3:40-47 (in Russian).

Chernyvsky, V.I., I.A. Zhigalov, and V.I. Matveev. 1993. Oceanological bases of high biological productivity zone formation in the Okhotsk Sea. Hydrology and Hydrochemistry of Seas. St.-Petersburg. 9(2):157-160 (in Russian).

Darnitsky, V.B., and N.V. Bulatov. 1995. The Okhotsk Sea eddies of the Kuril nearshore area. Vladivostok, POI. (in press).

Ginzburg, A.I. 1992. Non-stationary vertical motions in the ocean. Oceanology. 32(6):997-1004 (in Russian).

Gladyshev, S.V. 1994. Thermohaline fronts near the Kuril Islands. Oceanology. 34(4):504-512 (in Russian).

Lobanov, V.B. 1993. Investigation of synoptical eddies in the Kuroshio-Oyashio region based on satellite and vessel information. Ph.D. Thesis. Vladivostok. POI. 24 p. (in Russian).

Luchin, V.A. 1987. Water circulation of Okhotsk Sea and its specific interannual variability as a result of diagnostic calculations. Trudy DVNIGMI. 36:3-13 (in Russian).

Luchin, V.A., and V.B. Darnitsky. 1993. Climatic eddies current structure of the Okhotsk sea in autumn (part 2). Proc. 9-th conference on catching oceanology. Moscow. p. 219-222 (in Russian).

Zubov, N.I. 1929. Calculation of sea current elements according to information of hydrological section. Morskoy Nauchny Institute. 69 p. (in Russian).

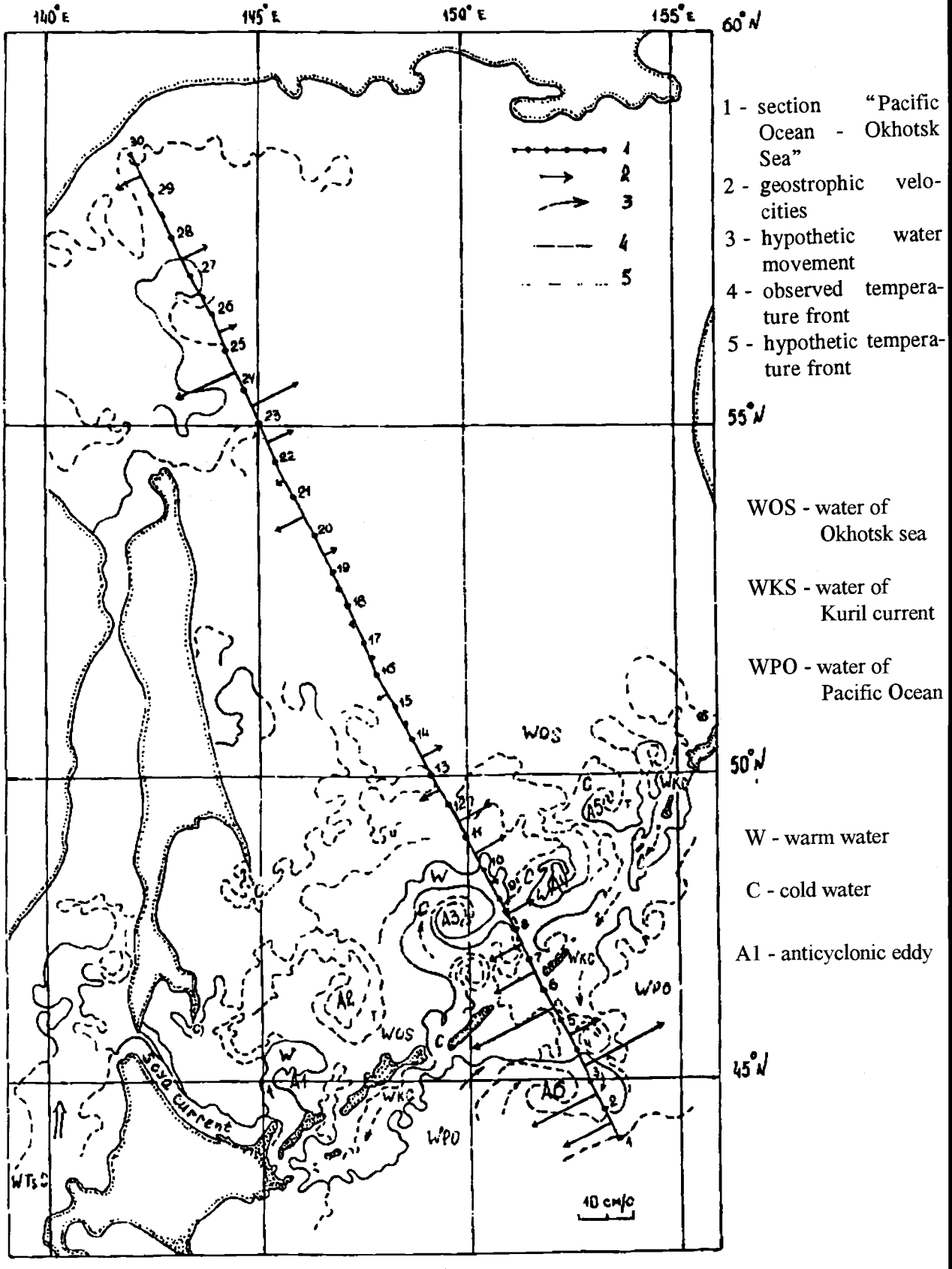

Fig. 1. Oceanographic stations occupied and the Okhotsk Sea water structure (according to satellite data) in September 1993.

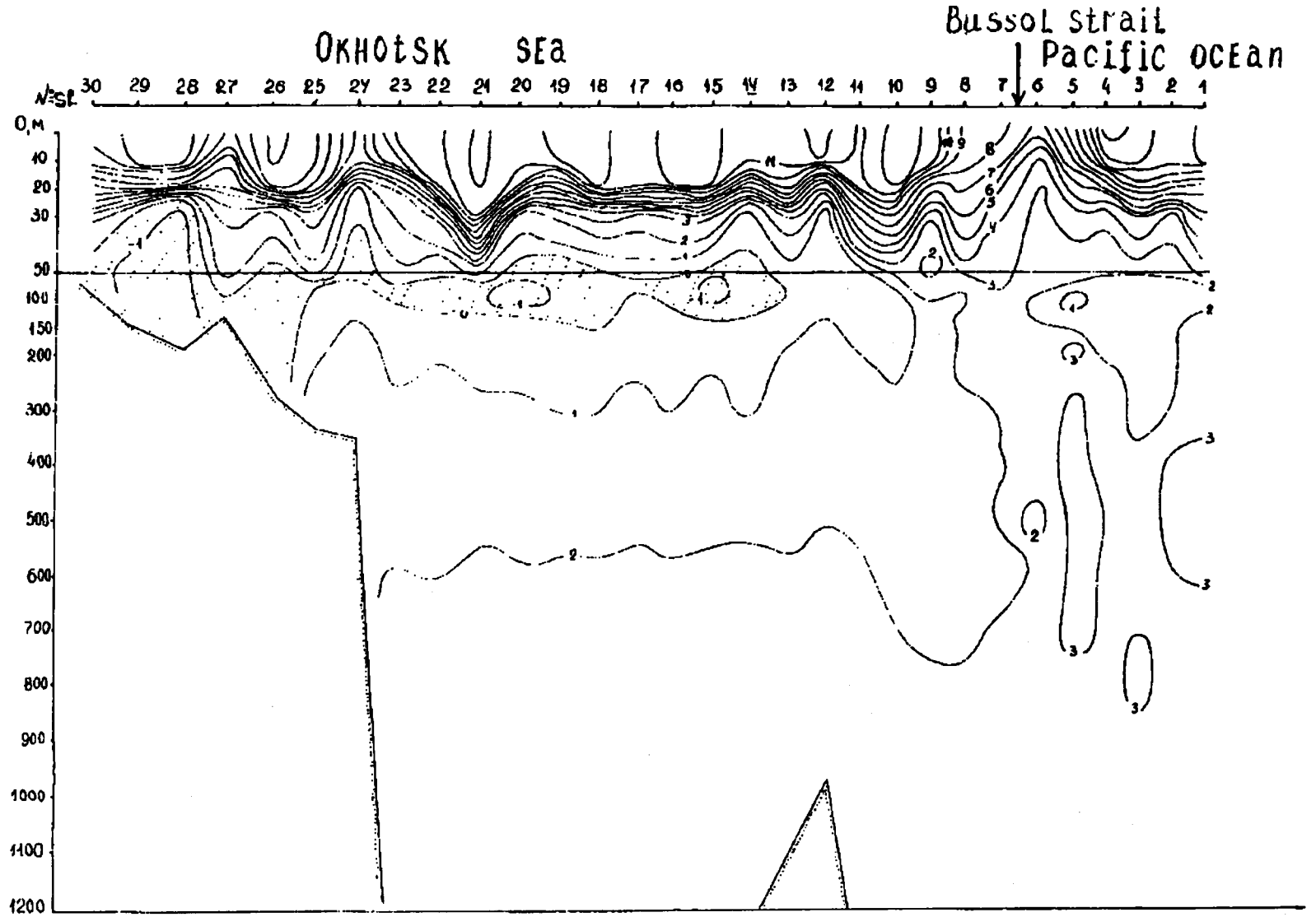

Fig. 2. Temperature distribution along the section "Pacific Ocean - Okhotsk Sea" through the Bussol' Strait in September 1993.

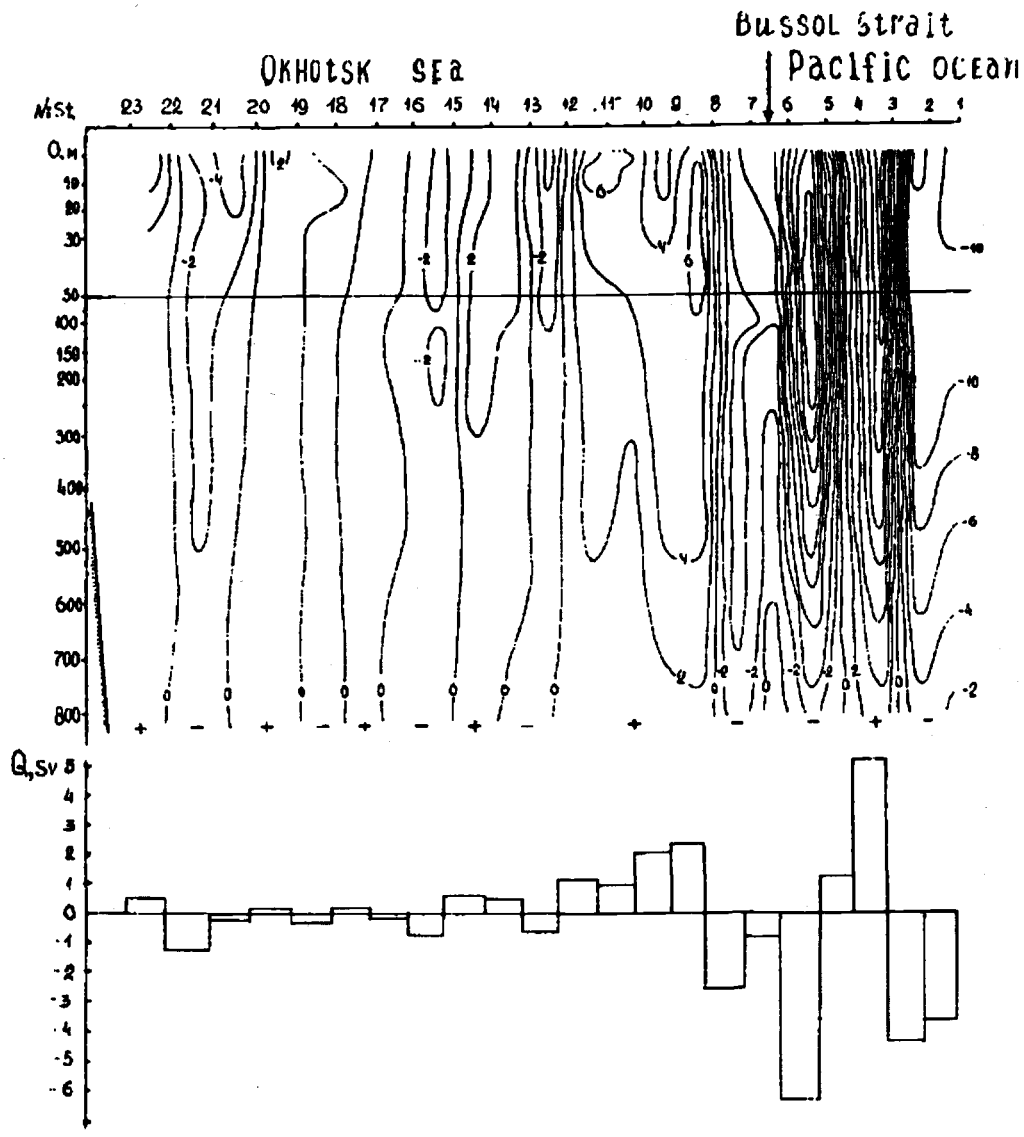

Fig. 3. Geostrophic velocities and water transport along the section "Pacific Ocean - Okhotsk Sea" through the Bussol' Strait in September 1993.

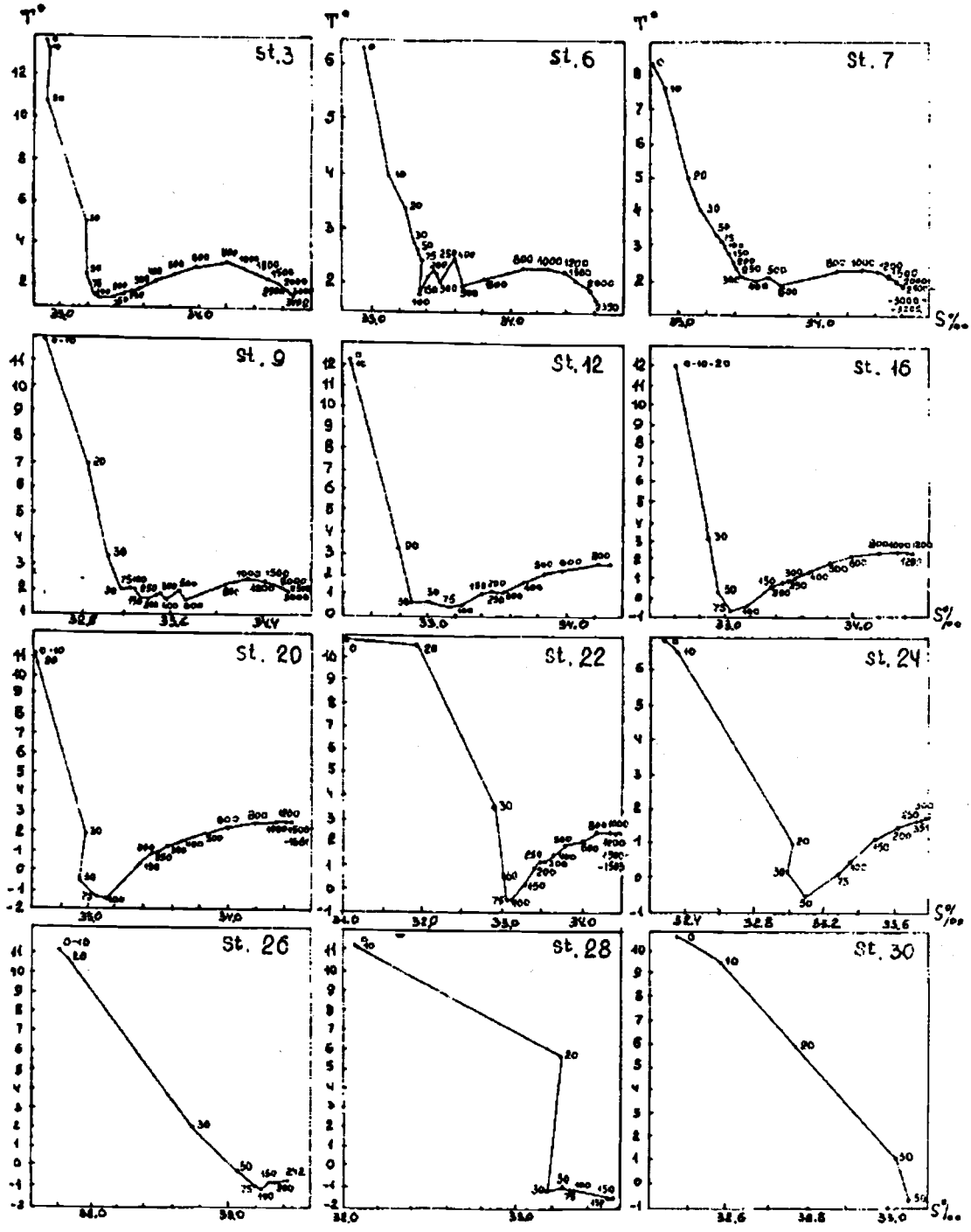

Fig. 4. T, S - curves for selected stations along the section "Pacific Ocean - Okhotsk Sea" through the Bussol' Strait in September 1993.

The Okhotsk Sea Component of Pacific Intermediate Water

Howard J. FREELAND[1], Alexander S. BYCHKOV[2], C.S. WONG[1], Frank A. WHITNEY[1] and Gennady I. YURASOV[2]

[1] Institute of Ocean Sciences, Department of Fisheries and Oceans, Sidney, B.C., Canada
[2] Pacific Oceanological Institute, Far Eastern Branch, Russian Academy of Sciences, Vladivostok, Russia

INTRODUCTION

In the fall of 1993 an opportunity arose to conduct a CTD and hydrographic survey along a line of stations through the Okhotsk Sea. This line of observations was conducted to *WOCE* (World Ocean Circulation Experiment) specifications for the accuracy of sampling and the nominal spacing (30 nautical miles) of stations. The observations were acquired as a joint project involving scientists from Canada and Russia to execute the westernmost leg of the *WOCE* line P1, hereinafter referred to as P1W, from the research vessel *Akademik Nesmeyanov* operated by the Pacific Oceanological Institute in Vladivostok, Russia.

Fig. 1 displays a map of the station locations. A total of 35 stations were occupied to the bottom or 3,500 metres, whichever is shallower. However, for the purposes of this paper only the first 30 stations will be discussed as they included all variables sampled and specifically constitutes the line of observations known as P1W. These are the stations identified with triangles and circles on Fig. 1.

It is well known (Talley, 1991) that the salinity distribution in the top 1,000 metres of the N.E. Pacific is dominated by a salinity minimum tongue. The salinity minimum dominates the salinity distribution between latitudes 45°N to 25°N and is still detectable as far south as 10°N. Talley (1991) reviews some of the history concerning speculation about the possible origin of the NPIW, and some of that material bears repeating here. The Okhotsk Sea does have lower salinity (33.45 psu) and higher oxygen (170 μM/kg) at σ_θ = 26.8 than is encountered in the North Pacific. Typical values along the 165°W section presented in Fig. 2 being 34 psu and 120 μM/kg, respectively. Furthermore, the density of water at the sill in the Bussol' Strait is high (σ_θ = 27.7) suggesting that it could be a source of dense water in the North Pacific. These ideas were pursued by Wüst (1930) who concluded, based on very little information, that the Okhotsk Sea likely was the source of NPIW. Reid (1965, 1973) concluded otherwise. In particular, Reid felt that the Okhotsk Sea could never supply the volume of water required. Favorite et al (1976) disagreed with Reid and actually attributed the sources of both the Oyashio and the East Kamchatka Currents to water formed within the Okhotsk Sea. Kitani (1973) suggested that water mass modification on the Okhotsk Sea shelf could produce water at densities up to 27.05 σ_θ which might subsequently flow into the northwest Pacific. Finally, Talley (1991) concurs with the opinions of Kitani, though is unable to estimate the volume of NPIW that might be formed within the Okhotsk Sea. This paper will demonstrate evidence in support of Kitani's conjecture.

In this paper we will present results from a single section completed from the open Pacific, through the Bussol' Strait and continuing through the Sea of Okhotsk to the coast of Siberia. The data will be described in section 2 and discussion of the implications for the formation of the NPIW mass will be presented in section 3. We will conclude that we have observed the Okhotsk Sea component of

the NPIW water, but that only part of that water mass is formed by direct ventilation from surface processes.

DATA DESCRIPTION

The observations discussed in this paper were completed as part of the cruise designated P1W (western leg of line P1) by the WOCE Hydrographic Program office, 9316 by the Institute of Ocean Sciences (which took a major part in the program), and AN25 by the Pacific Oceanological Institute, Vladivostok, which operates the vessel, the *R/V Akademik A. Nesmeyanov*. In all that follows it will be cited by the WOCE designation, P1W. This survey was a joint endeavour completed by scientists from the Institute of Ocean Sciences (Canada), the Pacific Oceanological Institute (Russia) and the Woods Hole Oceanographic Institution (U.S.A.). The cruise began on the 30th August and was completed on the 21st September, 1993. The Woods Hole interest was in sedimentary processes within the Okhotsk Sea, and none of those observations will be presented or discussed here.

Fig. 2 displays profiles of the primary variables. The indicated bottom is determined from the bottom of each CTD cast. This is reliable as a bottom determination as the CTD was lowered to within a few tens of metres of the bottom with the aid of a pinger suspended below the rosette sampler.

Potential temperature and density are computed relative to the surface. A notable feature is the presence of two lenses of very cold water lying entirely within the Okhotsk Sea. The dichothermal layer, centred at a depth of about 100 metres was contoured in the open water between stations 13 and 24 (Fig. 2a). It is characterized by low salinities 33.0-33.2 psu (Fig. 2b) and densities 26.4-26.6 σ_θ (Fig. 2c) and is supersaturated (up to 360 μmol/kg) by oxygen (Fig. 2d). The latter indicates that winter convection reaches to the depth of the dichothermal layer and that surface heating covers the layer in summer. Temperatures within this sub-zero water mass are as low as -1.1°C near station 20 and represents the temperature of the winter surface mixed layer (Moroshkin, 1966; Talley and Nagata, 1995). The "saline" (about 33.48 psu) water with temperature near the freezing point (-1.71°C), density of 26.85-26.90 σ_θ and oxygen concentration of 250-260 μmol/kg was found just above the bottom on the northwestern shelf on stations 28 and 29 (Figs. 2a-d). This is the so-called Kitani Water originated due to brine rejection during active sea-ice formation (Kitani, 1973; Alfultis and Martin, 1987). We should also mention that in the temperature field there is evident of a discontinuity in properties on opposite sides of the Bussol' Sill. This could suggest either that exchange between the Okhotsk Sea and the open Pacific is restricted at depths from 1,000 m to as shallow as 100 metres, or that the area of the Bussol' Strait is a region where water masses are being modified rapidly, perhaps by tidal mixing.

The potential density structure through the Bussol' Strait and into the Pacific Ocean is interesting (Fig. 2c). Isopycnals at all depths shoal as they are followed from the Okhotsk Sea towards the Pacific. Between stations 5 and 3 they then deepen and then rise between stations 3 and 1. This indicates the presence of a very energetic eddy. In fact there are persistent reports of the presence of a semi-permanent anticyclonic eddy directly outside the Bussol' Strait, and has been named 'The Bussol Eddy' by Russian Scientists. Descriptions of the Bussol' Eddy can be found in papers by: Saitoh, Kosaka and Iisaka (1986); Rogachev and Goryachev (1991) and Rogachev et al (1995). Over the central Okhotsk Sea a general doming of isopycnals is evident, suggestive of a general cyclonic circulation pattern. All of these features are also reflected in the salinity distributions shown in Fig. 2. Between stations 11 and 24 contours of all variables are fairly flat, suggesting little dynamics taking place at the time of the survey. A doming of isopycnals near station 24 may be indicative of a recirculation over the Kashevarov Bank which was close to line P1W.

The dissolved oxygen concentrations in the deep water within the Kuril Basin are more homogeneous than those at similar depths in the open Pacific (Fig. 2d). Oxygen levels throughout the Kuril Basin are similar to values in the Pacific at sill depth. This fits the distribution of other properties, where in all cases the profiles below sill depth inside the Kuril Basin are different from those outside. This suggests that some exchange is occurring in the very deep waters replacing water in the Kuril Basin. But we see little evidence of exchange at other depths. We will return to this point in more detail later in the paper. We see a water mass at the bottom of the Deryugin Basin which is very low in dissolved oxygen, and is also (see Fig. 2) extremely rich in dissolved silicate. This has all of the marks of a very old water mass that is rarely replaced and so sets this basin apart from the Kuril Basin. Water this low in dissolved oxygen is actually found at stations 1 to 4 outside of the Okhotsk Sea where the dissolved oxygen profiles show typical for the northern N. Pacific minimum near a depth of 1,000 metres. However, there can never have been any actual connection between these two water masses as the dissolved silicates are substantially different

The distributions of the nutrients, reveal patterns that are largely reflected in the other, dynamic variables. The notable exception being the presence of very high silicate levels within the Deryugin Basin. The absence of extremely high silicate levels near the bottom of the Kuril Basin suggests that water within that basin is freely exchanged with water in the open north Pacific. The other nutrients (phosphate and nitrate) do not show elevated values in the Deryugin Basin.

Fig. 3 demonstrates details of the potential density distribution around the sill in the Bussol' Strait computed from data at the first 11 stations (shown by the triangle symbols of Fig. 1). This clearly shows that water at a depth of 3,000 metres near the bottom of the Kuril Basin can be exchanged freely with water at a depth of only 2,000 metres in the open Pacific. Examination of other properties indicate that these waters have identical silicate and oxygen profiles, and we will see later that these also have identical θ-S relationships. We presume, therefore, that the properties of the seawater in the open Pacific at 2,000 metres and near bottom in the Kuril Basin are identical, and that deep water is freely exchanged across the Bussol' Sill. Indeed, it appears from Fig. 3 that the survey actually caught a deep water replacement event in the act, so to speak.

The density structure shown in Fig. 3 suggests that the Bussol' Eddy penetrates very deeply. If the eddy intensifies its circulation then the dip in deep isopycnals centred on station #3 must become more pronounced and either isopycnals will rise at stations 1 and 5, or fall at station 3, or both. This suggests that the density of water appearing at the Bussol' Sill from the Pacific Ocean may be determined by the strength of the eddy. In other words, the probability of a deep water replacement event in the Kuril Basin may well be pre-conditioned, or possibly even determined, by the strength of the Bussol' Eddy.

NORTH PACIFIC INTERMEDIATE WATER

Fig. 4 shows θ-S curves for all data collected along the major line of 30 stations indicated in Fig. 1. At the far right of the diagram all curves converge to a single water mass. This is expected from the detailed structure around the Bussol' Sill shown in Fig. 3. The θ-S curves separate into two distinct curves in the σ_θ range of 26.9 to 27.3. The upper branch contains θ-S curves from stations 1 to 5, inclusive, i.e., stations from the open Pacific to the sill in the Bussol' Strait, but no further. The lower branch contains profiles from all the other stations 6 to 30 within the Okhotsk Sea.

A region of θ-S space has been marked with a square. This identifies the profiles that are typical of the Okhotsk Sea, but having θ-S properties (at the same sigma-theta values) distinctly different from water in the open Pacific. Ohtani (1989) identifies this water as the Sea of Okhotsk

component of the North Pacific Intermediate Water mass (NPIW), and Watanabe et al (1991) agree with this conclusion. In the remainder of this paper we will refer to the Sea of Okhotsk component of NPIW as Sea of Okhotsk Intermediate Water, or SOIW. Let us assign an SOIW concentration of 1.0 to the θ-S values that occupy the centre of that rectangle. Allow this concentration to fall linearly to zero at the boundary of the box, and remain zero for any θ-S value outside of the box. We can then search the distributions of θ and S and use this concentration to examine the spatial distribution of the SOIW which is illustrated in Fig. 5. The highest concentrations of this water mass occur between depths of 700 to 800 metres. The water does not penetrate to the bottom in the deepest part of the Deryugin Basin and appears to be cut off very abruptly in the approaches to the Bussol' Strait. We see no evidence of exchange of water through the Bussol' Strait within this water mass. The dashed line superimposed on the contour chart is the path of the contour $\sigma_\theta = 27.05$, discussed above. This, as expected, delineates the upper surface of the SOIW distribution.

If a water mass is formed at the surface and then ventilates a deeper basin, then some properties of this water mass will be carried from the surface and maintained. McDowell et al (1982) point out that for quasi-geostrophic ocean dynamics the horizontal velocity is nearly non-divergent and so at scales larger than the Rossby radius of deformation the relative vorticity is much smaller than the stretching term and so potential vorticity can be estimated from hydrographic measurements alone as:-

$$\bar{q} = \frac{f}{\rho_0}\frac{\partial \rho}{\partial z}.$$

The quantity q is conserved as water sinks below the surface and has been used by Talley and McCartney (1982) to track the penetration of Labrador Sea Water into the deep waters of the north Atlantic by tracking the locations of a tongue of potential vorticity minimum. A ventilated water mass will show up as a minimum in q because a convectively renewed water mass should show excessive vertical homogeneity relative to the water above and below it.

The potential vorticity q is presented on Fig. 6. The contour interval is variable because q has a very large dynamic range. In this plot we have shaded the region of q less than 100×10^{-14} and greater than 50×10^{-14} $cm^{-1}s^{-1}$. Also, the bold dashed lines show σ_θ values of 26.85 and 27.05. The potential vorticity at stations 1 through 4 (in the open Pacific) decreases monotonically from the surface to the deep water and so show no evidence of any recent ventilation. However, the vorticity separates the water masses within the Okhotsk Sea into 4 distinct regions. Starting from the top we find the high potential vorticity region, above 200 metres. Extending from 200 m to a depth of perhaps 450 m we find a region of low potential vorticity. The line $\sigma_\theta = 26.85$ lies down the centre of this potential vorticity minimum. Below this value of σ_θ the potential vorticity increases to a maximum value at a mean σ_θ of 27.05 (region 3) and thereafter decreases steadily to the bottom (region 4). This diagram suggests that a recent convection event has occurred that has ventilated the Okhotsk Sea at a mean density of $\sigma_\theta = 26.85$. The region of ventilation extends to greater densities, perhaps as great as $\sigma_\theta = 27.05$, the maximum density possible indicated by *Kitani*, but certainly no deeper. Thus we have observed ventilation of the Okhotsk Sea essentially to the top surface of the water mass identified as the SOIW, and possibly a short distance into that water mass.

DISCUSSION

What this paper has shown is that if the water mass identified here, and by others, as the SOIW then we have a problem. The calculations of Kitani and the observations here indicate that only

the upper levels of this water mass are ventilated. If we are to move some of this water to higher densities then it is necessary to invoke some form of mixing process that will move water properties selectively downwards. Talley (private communication) has suggested that cabelling might be a significant process. Certainly, if two water masses of equal density are mixed, then cabelling will always increase the density of the mixture so leading to steady sinking. However, the density changes that can be effected by cabelling are rather small compared with the increases of density that we require here, of order 0.2 to 0.3 σ_θ units. Another possibility might be mixing by bottom generated turbulence originating from the very strong tidal flows known to run through the Bussol' Strait. We recommend that the Okhotsk Sea should be subjected to much greater scrutiny than has hitherto been the case. In particular future surveys should have as one object a determination of the role of sub-thermocline mixing processes and the role that these may play in the determination of the properties of the Okhotsk component of the North Pacific Intermediate Water mass.

REFERENCES

Alfultis, M.A., and S. Martin. 1987. Satellite passive microwave studies of the Sea of Okhotsk ice cover and its relation to oceanic processes, 1978-1982. J. Geophys. Res. 92:13013-13028.

Favorite, F., A.J. Dodimead and K. Nasu. 1976. Oceanography of the Subarctic Pacific region, 1960-71. International North Pacific Fisheries Commission. 33, 187p.

Kitani, K. 1973. An oceanographic study of the Sea of Okhotsk - Particularly in regard to cold waters. Bull. Far Seas Fish. Res. Lab. 9:45-77.

Moroshkin, K.V. 1966. Water masses of the Sea of Okhotsk. US Dept. of Commerce, Joint publication service 43.942, 98p. Translation of Vodnye Massy Okhotskogo Morya. Nauka Publ. House, Moscow, 65p., 1965

McDowell, S., P.B. Rhines, and T. Keffer. 1982. North Atlantic potential vorticity and its relation to the general circulation. J. Phys. Oceanogr. 12:1417-1436.

Ohtani, K. 1989. The role of the Sea of Okhotsk on the formation of Oyashio Water. Sea and Sky. 65:63-83 (in Japanese).

Reid, J.L. 1965. Intermediate waters of the Pacific Ocean. Johns Hopkins Press, Baltimore, MD, U.S.A. 85p.

Reid, J.L. 1973. Northwest Pacific Ocean waters in winter. Johns Hopkins Press, Baltimore, MD, U.S.A. 96p.

Talley, L.D., and M.S. McCartney. 1982. Distribution and circulation of Labrador Sea Water. J. Phys. Oceanogr. 12:1189-1197.

Talley, L.D. 1991. An Sea of Okhotsk water anomaly: implications for ventilation in the North Pacific. Deep-Sea Res. 38:S171-S190.

Talley, L.D., and Y.Nagata (Eds.). 1995. The Okhotsk Sea and Oyashio Region. PICES Scientific Report No 2, 227p.

Watanabe, Y.W., S. Watanabe, and S. Tsunogai. 1991. Tritium in the northwestern North Pacific. Journal of the Oceanographical Society of Japan. 47:80-93.

Wüst, G. 1930. Meridionale Schichtung und Tiefenzirkulation in der Westhalften der drei Ozeane. Journal du Conseil, Conseil Internationale pour l'Exploration de la Mer. 5:21p..

FIGURES

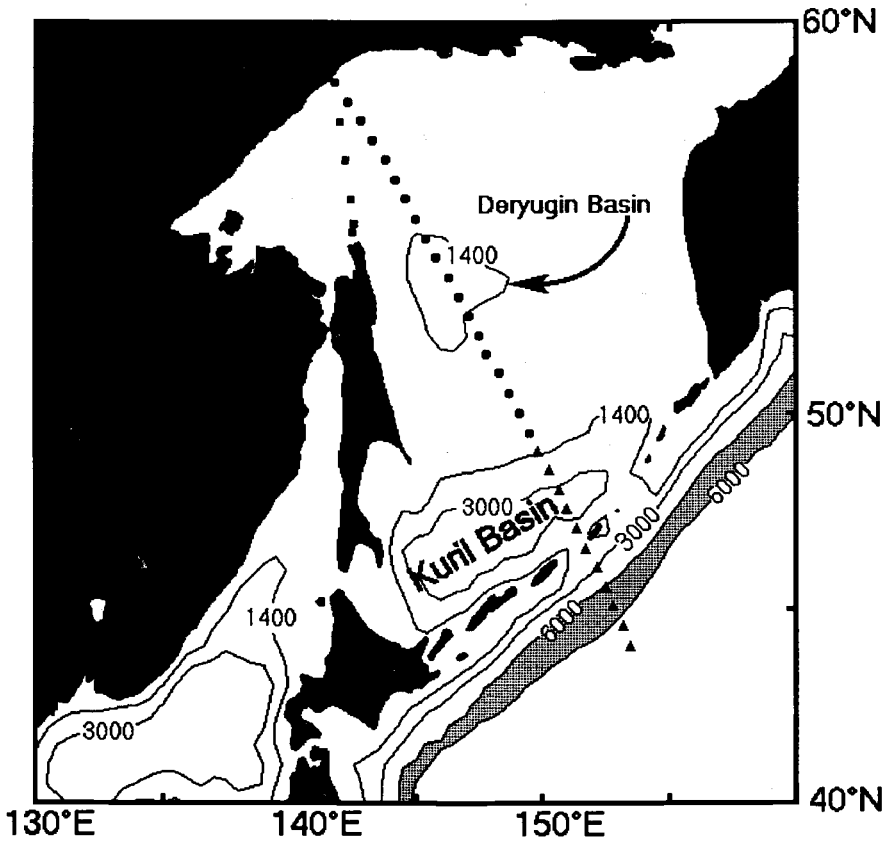

Fig. 1. Map of the station locations.

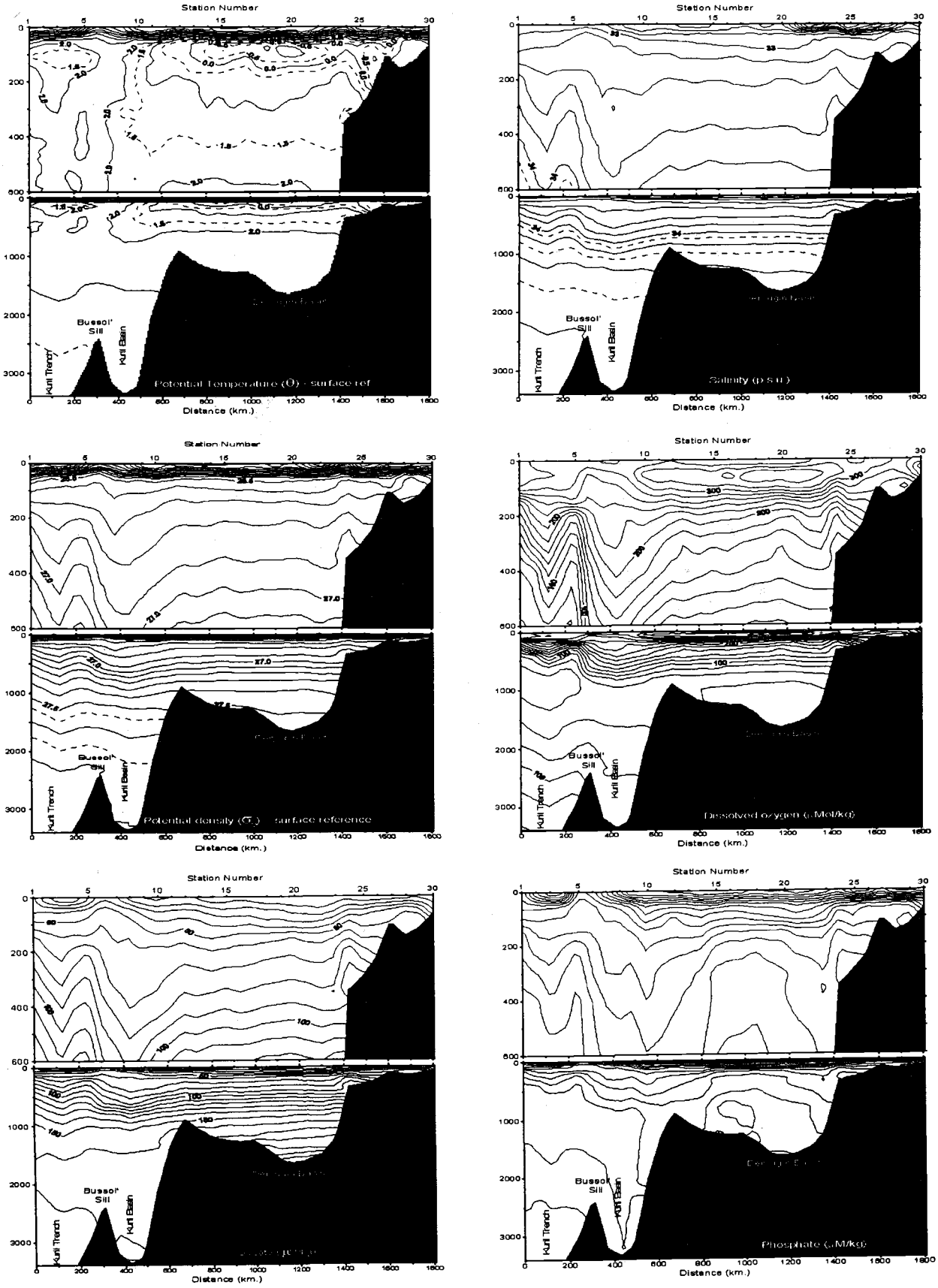

Fig. 2. The distribution of potential temperature, salinity, density dissolved oxygen, silicate and phosphate along line P1W. The upper panel of each plot shows properties in the top 600 metres of the water column.

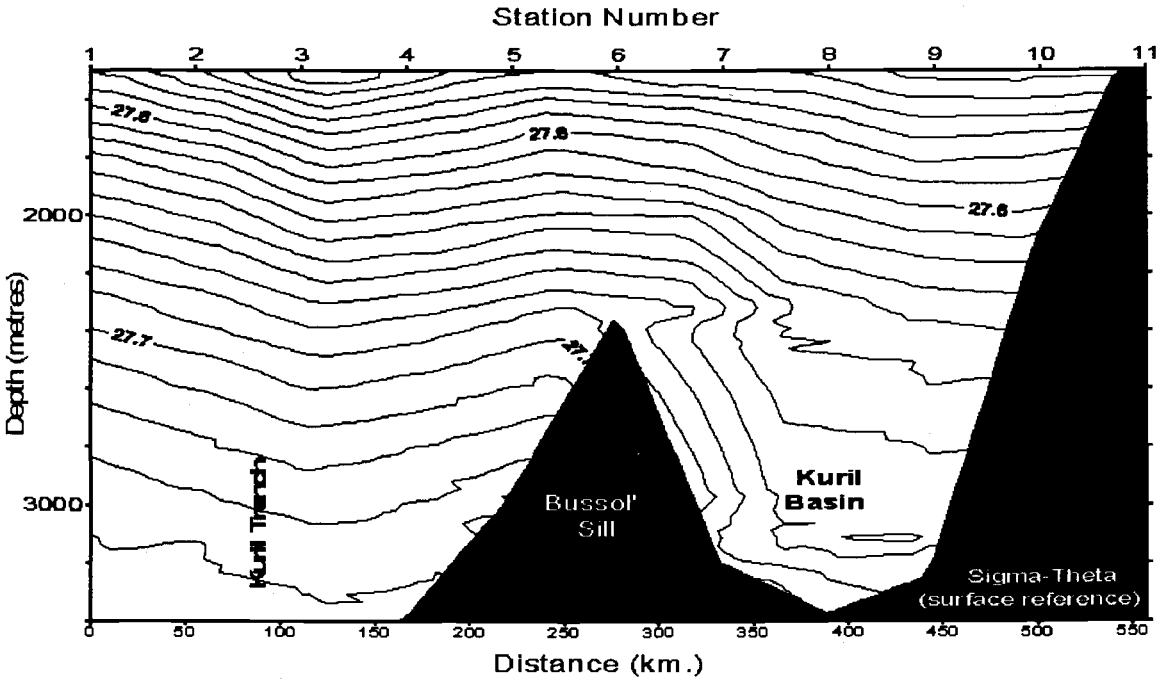

Fig. 3. The distribution of potential density in deep water near the Bussol' Sill.

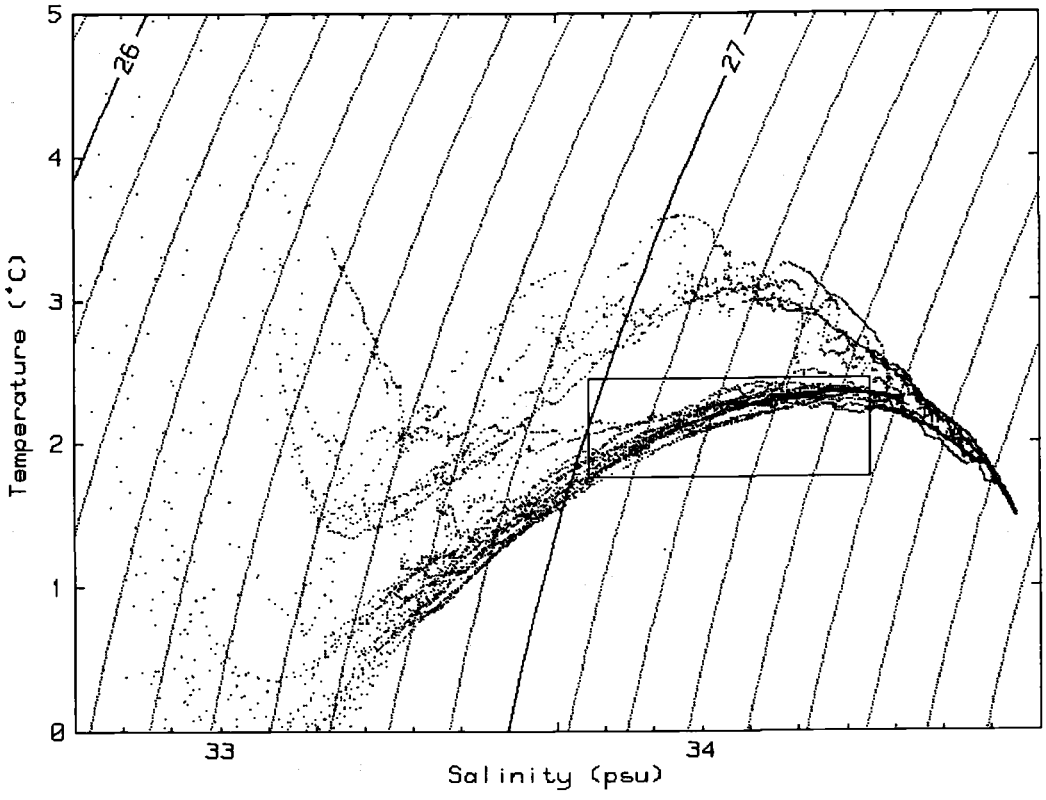

Fig. 4. θ-S curves for the first 30 stations.

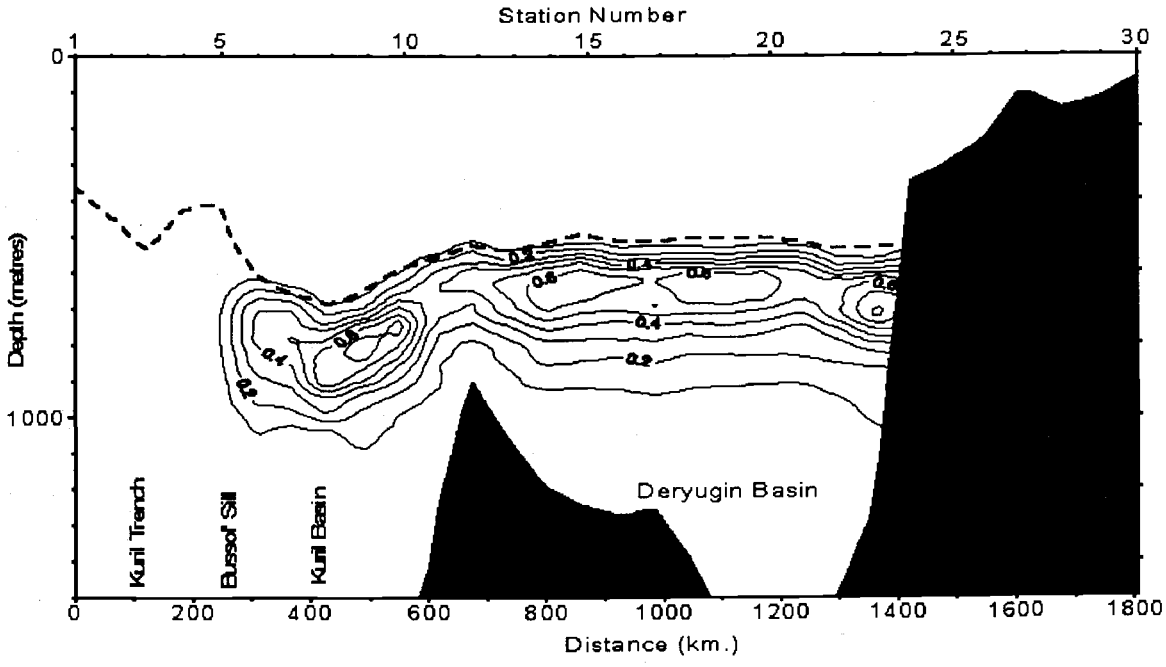

Fig. 5. The distribution of the Sea of Okhotsk Intermediate Water as defined by the box on Fig. 4. The dashed line indicates a potential density of 27.05 σ_θ.

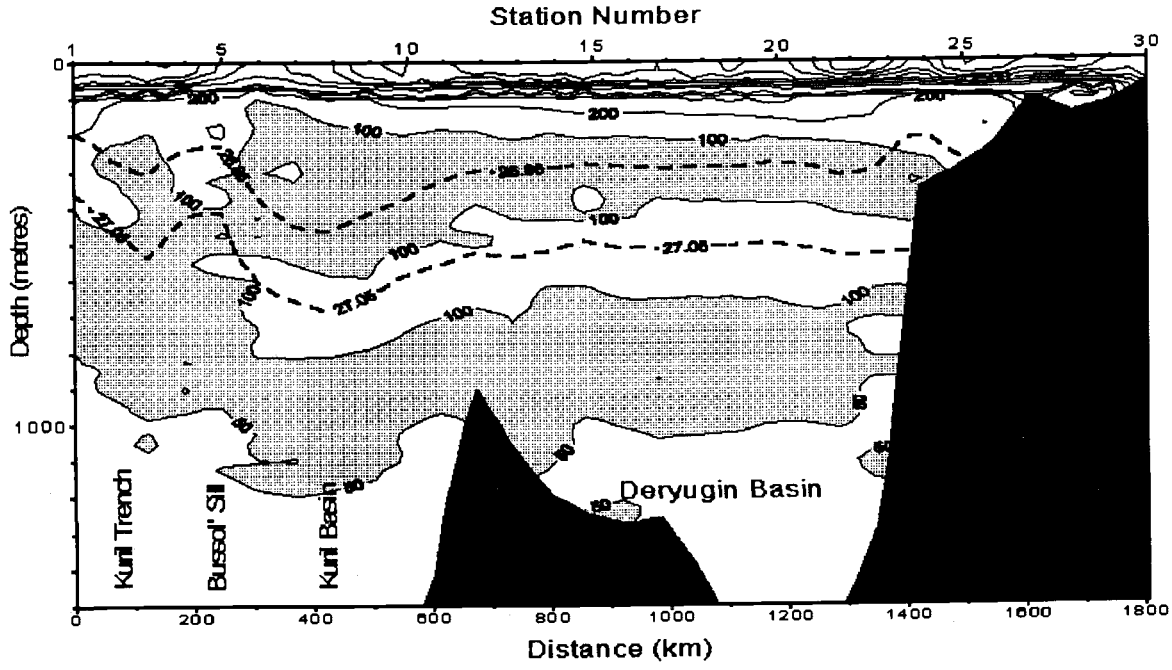

Fig. 6. The distribution of potential vorticity along line P1W. The dashed lines indicate potential densities of 26.85 and 27.05 σ_θ.

Some Experience of the Satellite Environmental Support of Marine Expeditions at the Far East Seas

Emil E. HERBECK, Anatoly I. ALEXANIN, Igor A. GONTCHARENKO, Igor I. GORIN, Yury V. NAUMKIN and Yury G. PROSHJANTS

Institute of Automation and Control Processes, Far-Eastern Branch,
Russian Academy of Sciences, Vladivostok, Russia

1. INTRODUCTION

Geophysical satellite monitoring of the environment becomes a necessary tool for investigation the of seas and atmosphere, especially for such a hard-to-research area as the Okhotsk Sea. It seems that the most interesting results in studies of variable natural objects could be obtained by combining satellite and *in-situ* data. Using the regular satellite information, it is possible to control the *in-situ* data acquisition according to location and development of the object investigated, and thus to increase the productivity and cost-effectiveness of marine expeditions. These are the considerations that determine the direction of our work as well as the objects of interest and methods of data processing. At present moment, we are developing the technology that may be specified as *Regional Environmental Satellite Monitoring* (RESM). The technology includes:

- regular capture of high-resolution multi-channel satellite data,
- extracting of geophysical parameters from the data,
- reconstruction of geophysical fields,
- location and tracing of natural and human-made objects and phenomena at sea surface and atmosphere (eddies, cyclones, frontal zones, currents and its meanders, ice fields, pollution, etc.),
- evaluation of spatial and temporal variability of the fields, objects and phenomena.

Because of high variability of our objects, the data processing should be performed in the quasi-real-time mode and the results should be transmitted to the vessel immediately.

Since 1993, we performed the RESM support for several cruises in the Japan and Okhotsk Seas. The following paragraphs are brief description of our RESM Data System, technology and methods we used, as well as some problems we have met.

2. THE RESM DATA SYSTEM: GENERAL DESCRIPTION

The RESM technology is based on daily capture and processing of data transmitted by meteorological NOAA (HRPT mode) and GMS (digitized LRFAX mode) satellites.

To achieve the goal, the Data System consisting of a 1.7 GHz Receiving Ground Station and local network of five IBM PC compatible computers was built. One of the computers executes a data receiving and antenna control functions; another one (the most powerful) is proposed for the data processing and packing. The rest of the computers are used for both data processing and software development. Being located in Vladivostok our System covers a wide area: from 17 to 62°N and up to 160°E. This area includes the Okhotsk, Japan, Yellow and East China Seas, and some areas of Western Pacific.

At the moment a major part of our work is dealing with sea surface temperature (SST) fields, thermal structures (SSTS), currents (SSC), and ice location and movement. For the last two objects, as well as to provide the fine cloudy filtering and atmosphere correction, both the single images and their series are processed. In the nearest future we plan to work with some atmosphere phenomena, especially typhoons. To research these objects, the System should be upgraded to receive the S-VISSR data from the new geostationary satellite GMS-5.

Main RESM output products include:

a. calibrated IR images, transformed into Mercator projection, both instantaneous and composed (in the last case a cloudy filtering may be performed);
b. SST charts and/or grid information of various resolutions, both instantaneous and composed;
c. SSTS charts;
d. charts of ice cover margins and ice movement;
e. surface current vectors and circulation maps.

3. THE RESM SUPPORT OF MARITIME STUDIES

It is extremely importance to obtain the information regularly during marine expeditions. As a rule, our support was carrying out according to the following scheme:

- day-to-day receipt and pre-processing of the NOAA/HRPT data (2-3 satellites, 4-6 times a day);
- packing the raw and pre-processed data onto a streamer tape;
- processing of the data as described above;
- making of the 5-10 day composed SST, SSTS, and SSC charts;
- transmitting of the charts to the expedition vessels by radio-facsimile channel;
- post-expedition processing of the data collected.

This approach has been used already to support five scientific and fishing cruises to the Okhotsk and Japan Seas.

Apart from the evident advantages, this way has some serious limitation, such as:

- the impossibility of supporting expeditions outside the area covered (e.g., in the central part of the Bering Sea);
- low noise-immunity of the radio-channel used does not allow recognition of small details on the charts;
- low channel capacity hinders transmission of such informative products as images;
- the time of satellite information transmission from the coastal System to a vessel is relatively long, so efficiency may be lost.

But the most significant limitation is that researchers do not have immediate access to the data processing system. As a result, they cannot control (or specify) the satellite data processing according to their observations or changed needs. On the other hand, the absence of *in-situ* information during the satellite data handling decreases the quality of RESM products.

Installation of the RESM System onboard the research vessel eliminates all the difficulties providing the best combination of remote and *in-situ* observations. This was done aboard the *SHIRASE* (Japan) and *POLARSTERN* (Germany) research vessels in the mid-80's. We have a similar experience, where our first RESM System was installed onboard the r/v *AKADEMIK KOROLEV* and took part in several cruises in 1988-1990 (Herbeck et al., 1992). Of course, it was a very difficult and expensive device at that time, because of the high cost of satellite ground stations and due to the

necessity of placing the antenna drive onto a gyro-stabalized platform. But at the present time, both stations and computers have become reasonably priced. Besides, due to the increase of computer capacity it is possible to compensate the vessel motion by using a computer controlled antenna drive over a wide range.

4. THE DATA PROCESSING

Several details and problems of satellite data processing we have met during the RESM support of cruises mentioned above are briefly discussed here.

4.1. Sea Surface Temperature (SST) Fields

Within the framework of our SST field retrieval technology (Goncharenko and Kazansky, 1992) the main output products are SST charts which might be classified according to time-averaging as follows:

- *type A*: averaged SST charts over a period of 5-10 days and 50-100 km resolution (Fig. 1a);
- *type B*: composite charts of 2-3 days / 10-20 km averaging (Fig. 1b);
- *type C*: high resolution charts of 5 km averaging from a single image (Fig. 1c).

In addition SST fields are presented as cartographic Mercator projections of 1 km resolution. These products of digital processing are single images under cloud-free conditions or composite images under partially cloudy conditions (Fig. 1d). The data may be presented both as a picture and as digital grid field information.

A major problem in using satellite measurements for ocean flow visualization is cloud cover. During an expedition, only a few of images can yield usable data (cloud-free images). The Okhotsk Sea region has the most cloudy conditions for satellite surveying. Therefore, it is necessary to make a average or composite map to represent the full SST distribution over the Japan or Okhotsk Seas.

It should be mentioned that SST *type A* fields are used for hierarchical control while products *(B)* and *(C)* are processed. *(A)* is successfully applied to fine cloud filtering of every individual image from the sequence and to normalize images for *(B)* composition. The last procedure is required to avoid artificial defects associated with errors from an atmospheric correction and false thermal front appearances.

The operative linear atmospheric correction MCSST recommended by NOAA/NESDIS for NOAA-11/12/14 satellites was used to make a preliminary SST retrieval. The technique provided an accuracy for SST determination of about 0.5°C. Corrected measurements were filtered to detect obvious cloudy elements and averaged inside 50 km squares to obtain a preliminary SST field *(A)*. Both filtration and correction procedures were based only on satellite data from AVHRR channels 2 (0.9 mkm), 4 (11 mkm) and 5 (12 mkm) without any *in-situ* measurements. The SST field provided test temperature values when the time sequence of all infra-red images was iteratively filtered to eliminate residual cloud contamination. To retrieve the field *(B)*, relevant images must be additionally normalized by *(A)* and averaged inside 10 km squares. Hence, temperature values of *(B)* depend on the time-overlapped 'climatic' field *(A)*. Note, that the accuracy of SST determination is not a limiting factor when a spatially detailed picture is required.

It is advisable to provide the maximal spatial resolution for a SST map obtained from a single image, so AVHRR data were corrected and averaged inside 5 km squares. To retrieve surface current fields from satellite data, the navigated images from the AVHRR band of 10.8 mkm were used. To avoid noise, these images were not corrected pixel-by-pixel.

Fig. 2 illustrates the results of applying of our cloudy filtering technique. There were very hard cloudy conditions as one can see from the images Fig. 2a and Fig. 2b. After the processing of a 7-days imagery sequence, the composed SST fields have been built (Fig. 2c) which are in a good agreement with the momentary SST fields (Fig. 2d) obtained through 4 days (when cloudiness is dissipated).

4.2. Sea Surface Velocity

4.2.1. Methods And Their Accuracy

Two methods were applied to prepare the sea surface velocities charts:

- feature tracing on sequential satellite images (FT);
- maximum cross-correlation technique (MCC) .

The FT procedure was based on a displacement estimation of water submesoscale inhomogeneity (ΔX) and velocity vector calculation (V):

$$V=\Delta X/\Delta T,$$

where ΔT is time interval between two images. The positions of an object are pointed out manually.

The MCC is an automatic method for velocity estimation. The essence of the method is the identification of the maximum cross correlation between search (second image) and template (first image) windows, as the end points of displacement vectors from the window center. Statistical significance of the cross-correlation maxima was used to refuse vectors with a low level of significance.

Instrumental accuracy of velocity estimation was in the range of 2-6 cm/c. It depended on space resolution of satellite images and time interval ΔT. The final accuracy was usually achieved by comparison with another kind of velocity measurements, as a rule with *in-situ* ones.

It should be mentioned that *in-situ* and satellite velocity measurements have different mining. The first are measurements at specific points, while a tracing feature on a satellite image has spatial size of tens to hundreds of square kilometers. Obviously, the short-scale and short-time velocity components are absent in its satellite evaluations, and thus satellite velocity estimations are usually underestimated. The time interval ΔT is comparable with the tide periods and from this reason the satellite velocity measurements should be interpreted correctly.

To consider the accuracy of the satellite technique as a technique for velocity displacement of large-scale water mass, we have to compare satellite and ship measurements (1) for flows with negligible short-scale and short-time velocity components and (2) when the space-time discrepancy between measurements compared is less than the space-time variability of flow.

Some estimation of the FT technique accuracy on the Kuroshio extension flow data has been done:

1. 12 velocities calculated by satellite APT-images (year 1984) have been compared with dynamic method estimations by Alexanin, 1991. The accuracy of comparing scheme was 30 cm/s. Velocities range was 80-160 cm/s and the average difference between two fields was :

   $$\Delta V = [\varsigma(V_i-U_i)]/N = 6.3 \text{ cm/s},$$

   that was less then instrumental accuracy. V_i and U_i are projections of satellite and *in-situ* velocity measurements on the flow direction, N - the number of measurements.

2. The dynamic overfall across Kurosio extension on 142°E has been calculated as 90 cm by satellite HRPT-images of 1990 (Alexanin and Kazansky, 1994) whereas according to Japanese data this value on 144°E was near 100 cm. Such difference could be explained by natural factors.

3. Two sea surface velocities, 124 cm/s and 45 cm/s, were measured in the same region and time aboard R/V KOFU MARU (Japan). The differences between ship and satellite velocity measurements were 26 cm/s and 3 cm/s and the scheme accuracy was about 10 cm/s.

As we can see, the satellite velocity estimations differ from other ones in the limits of the scheme accuracy (not worse then 20% of value).

As a rule, the FT technique was used because this method gives more information about circulation as compared with MCC when measurement accuracy is severe. The MCC method was usually applied for ice velocity calculations.

4.2.2. Observation Conditions And Data Volumes Received

The ability to create sea surface velocity charts is based on the existence of sea regions without cloudiness and mist during 6 hours or more. The results (number of velocity vectors) received naturally depend on the weather conditions (Table 1). For this reason the most difficult place in the Far East region is the central and southeast parts of the Okhotsk Sea in summer. Two expeditions in the region have been supported. Circulation charts were built in operative mode and sent to the ships. The weather conditions during these cruises were difficult (Table 2), nevertheless the detailed charts for the most interesting regions and water objects were built 2-3 times a month using data processing from 3-4 polar NOAA satellites. The longest time interval during which we could not make a chart was 3 weeks. But for the last expedition we could not prepare any chart for the North-Kuril region (approximately 3*3 degrees).

4.2.3. Chart Samples

Fig. 3a displays a chart fragment of the sea surface circulation during April 3-6, 1995. Dynamic topography overfall of the eddy presented in the right and lower corner has been estimated as 45 cm and velocity profile across the eddy was developed. The highest velocity revealed was 70 cm/s.

Fig. 3b presents a chart calculated during the CREAMS expedition, whose main goal was to investigate circulation in the north part of the Japan Sea. Large-scale charts were extracted from the velocity estimations received during August 28-31, 1993. The circulation was in a good agreement with direct *in-situ* measurements.

REFERENCES

Alexanin, A.I. 1991. Geostrophic surface current velocities: comparison of satellite and ship-borne measurements. Soviet J. Remote sensing. 6:55-61 (in Russian).

Alexanin, A.I. and A.V. Kazansky. 1994. Development of a synoptic approach for monitoring oceanic circulation. Proc. OCEANS-'94 OSATES, 13-16 Sept. 1994, Brest, France. 2:II,412-II,417.

Goncharenko, I.A., and A.V. Kazansky. 1992. A hybrid system for monitoring of the sea surface mesoscale features from satellite IR-imagery. Proc. of IEEE International Conference. on Ocean (OCEANS'92). Newport, RI, 26-29 Oct. 1992. Newport, Rhode Island. Vol.1.

Herbeck, E., A. Kazansky, Ju. Proshjants, et al. 1992. Shipboard Complex for Satellite Monitoring of Mesoscale Ocean Variability. Proc. of IEEE International Conference on Ocean (OCEANS'92). Newport, RI, 26-29 Oct. 1992. Newport, Rhode Island. Vol.1.

TABLES AND FIGURES

Table 1. Number of velocity vectors obtained during different expeditions

EXPEDITIONS	NUMBER OF VECTORS
April-May 1995	1551
June-August 1994	2018

Table 2. Example of weather conditions in the Okhotsk Sea during summer period

WEATHER:	CLEAR SKY DAYS (cloudiness 0-3)	CLOUDY DAYS (cloudiness 7-10)	MIST DAYS
MAY	10-20%	70-80%	15-20%
AUGUST	10-20%	70-80%	20-35%

FIGURES

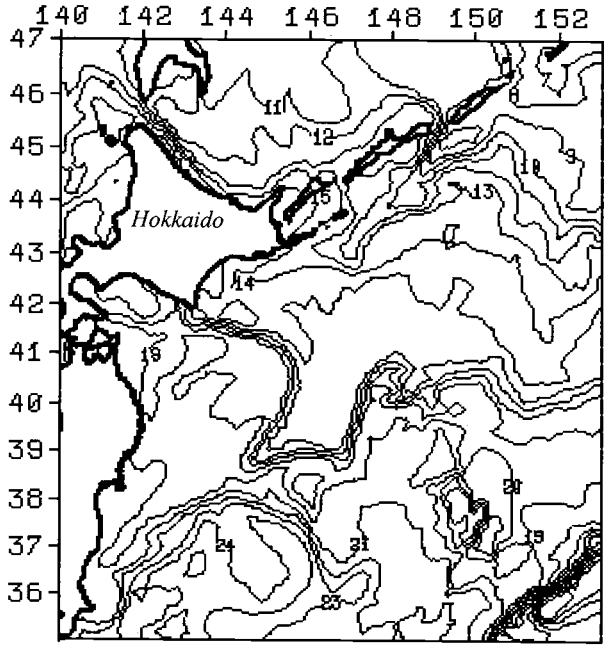

a) 8-day averaged SST chart (8-15 Oct, 1995)

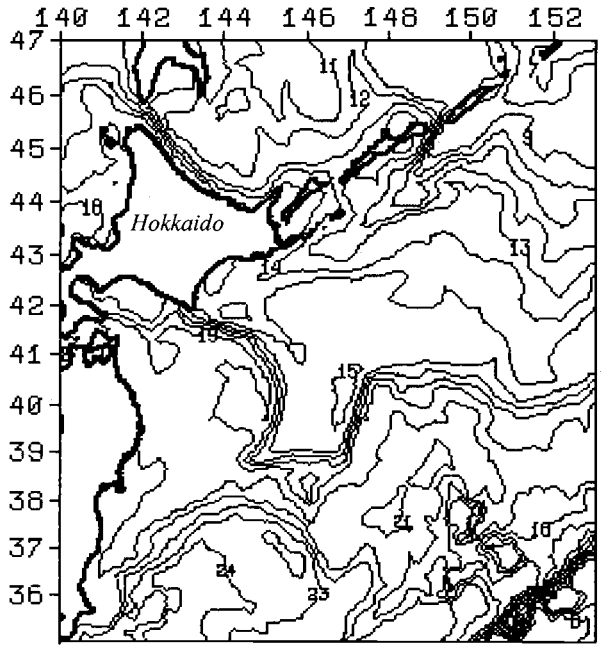

b) 4-day composite SST chart (12-15 Oct, 1995)

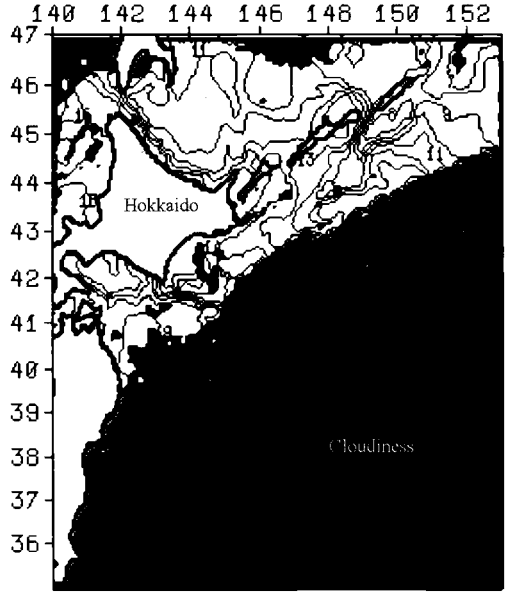

c) momentary SST chart (10 Oct., 1995)

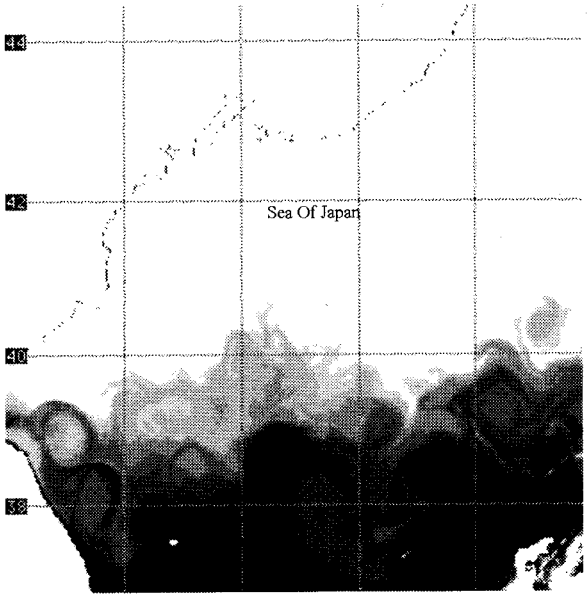

d) SST fields (composite image, 7-9 May, 1994)

Fig. 1. Examples of RESM (Regional Environmental Satellite Monitoring) of SST output products.

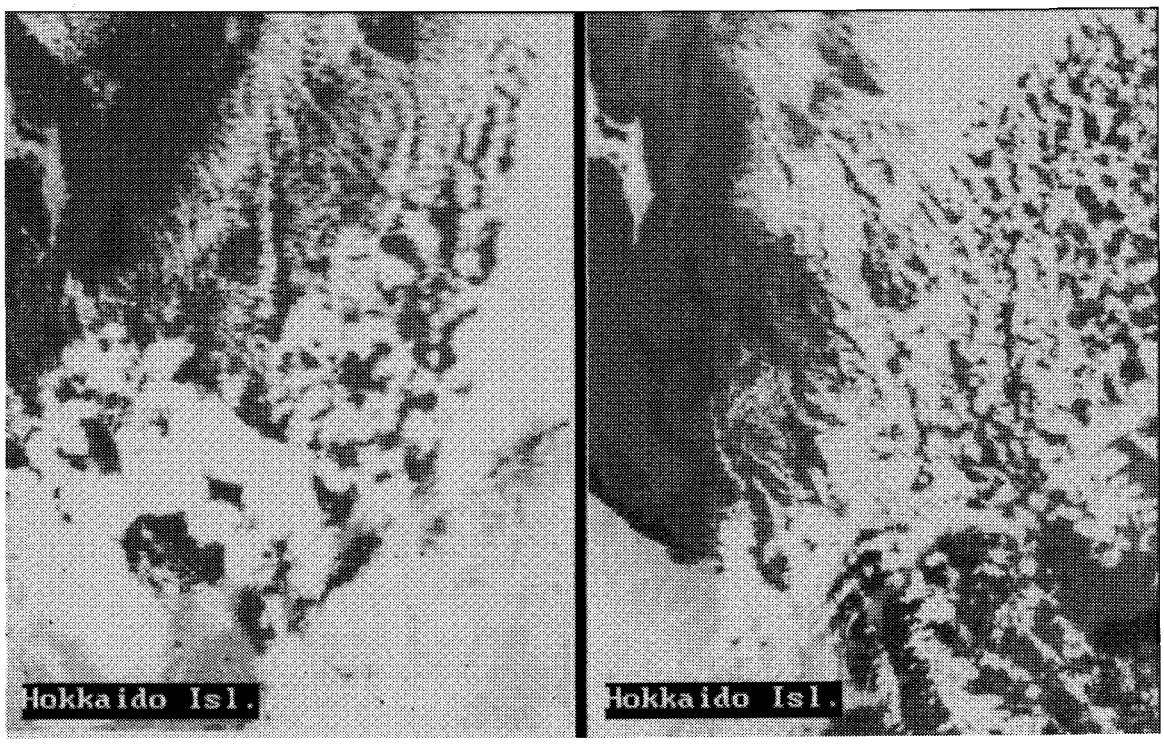

a) b)

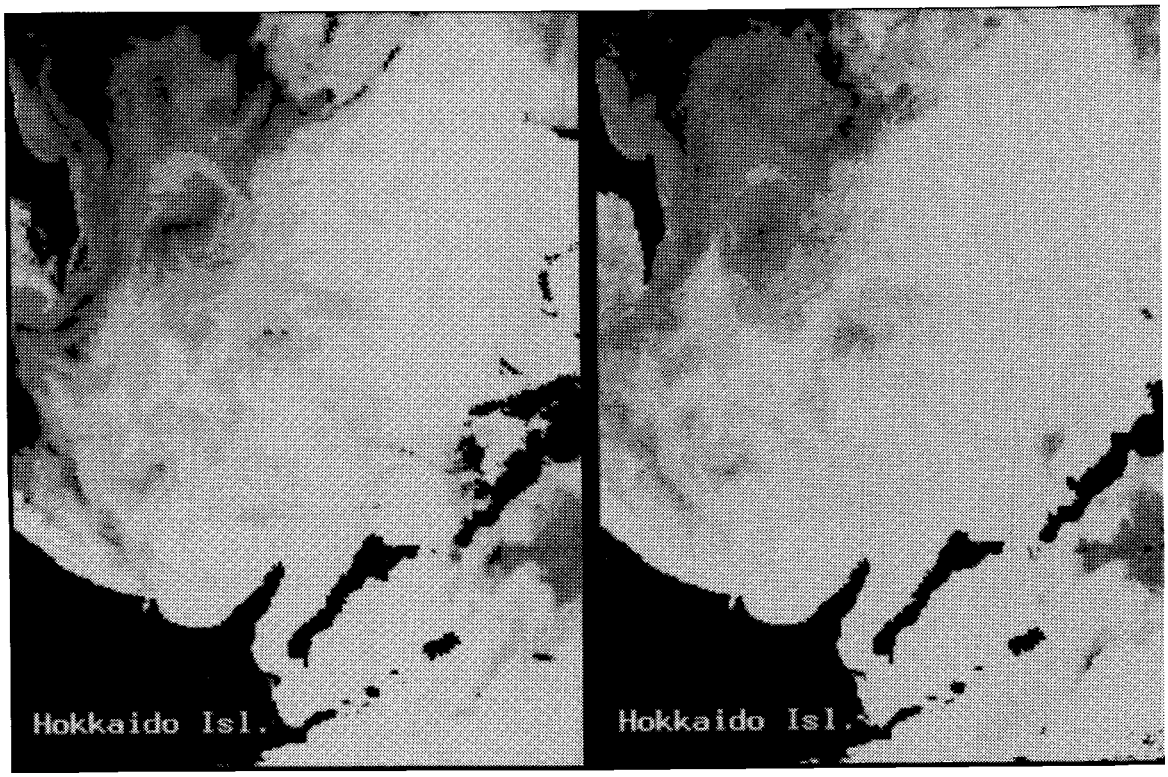

c) d)

Fig. 2. Examples of RESM cloudy filtering technique application.

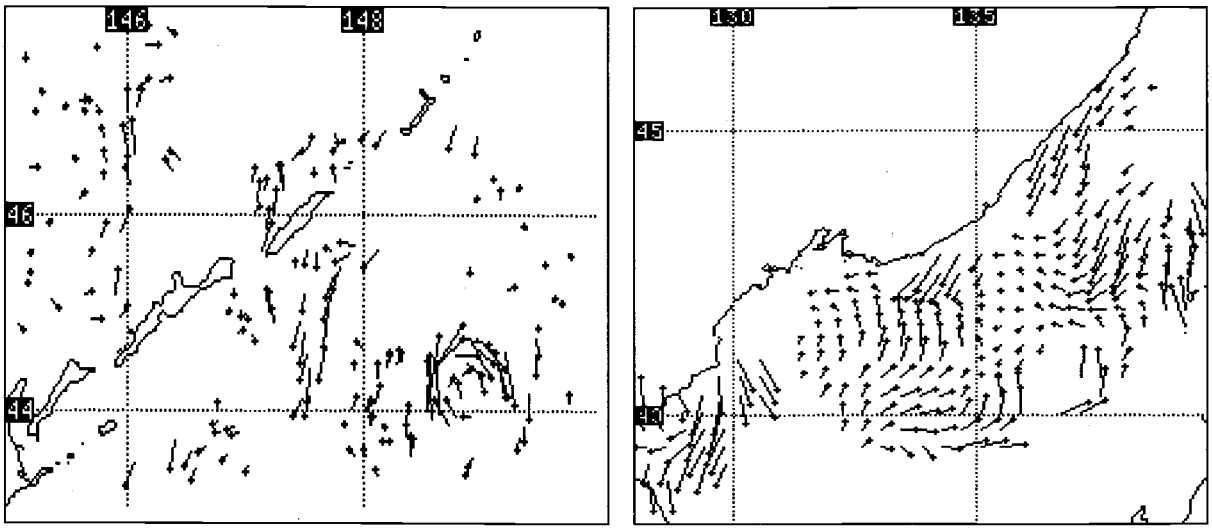

(a) (b)

Fig. 3. Examples of RESM sea surface circulation charts.

The Tidal Influence on the Sakhalin Shelf Hydrology

Alexander A. KARNAUKHOV

Pacific Oceanological Institute, Far Eastern Branch, Russian academy of Sciences, Vladivostok, Russia.

The international ecological expedition aboard the *R/V Academik M. Lavrentjev* was performed on the eastern Sakhalin shelf in October-November of 1994. The character of hydrological observations was determined by small site sizes and the general situation in the studied areas. Sites "C" and "D" were situated in the zone of the influence the East-Sakhalin Current, on the western periphery of the Okhotsk Sea cyclonic circulation (Fig. 1). Water masses, moved by the current, have been formed under the influence of the Amur River drainage in the areas of the Sakhalin Gulf and Nevel'skoy Passage. The gradual salinity increase of these waters is observed southward

All observations were carried out in the beginning of autumn - winter convection characterized by cooling of surface waters and subsequent intermixing. The thickening of the upper homogeneous layer, observed at this time, is accompanied by simultaneous decline of the seasonal layer of abrupt temperature and salinity changes. The process is supported by the wind activity typical for this season. These are the basic conditions forming the thermohaline structures of the East Sakhalin shelf region.

The small-scale spatial - temporal variability is caused basically by two factors: (1) the strong influence of the East Sakhalin Current executed by wind and (2) the influence of tidal motions. The prevailing western winds force the removal of the deep stream current from the shore and the subsequent active upwelling. During our study the wind field was quasi-stationary relative to the period of survey (less than two days) and only tides could determine the dynamics of hydrophysical fields.

Therefore, the full tidal cycle observations are necessary to examine the nature of temperature and salinity variability in the area. Unfortunately, only two day measurements were performed at each site and the actual observational period was only from 8 AM till 10 PM. The corresponding data set makes the interpretation of results more difficult as it does not overlap the tidal cycle. The tidal regime off the east Sakhalin coast is rather complicated. The semidiurnal tides prevail in the southern part of the investigated area, whereas the diurnal tides are dominant in the region of Chaivo.

Observations at sites "C" and "D" demonstrate the significant influence of tidal waves on the temperature and salinity distribution. Based on surface T-S diagrams all stations of site "D" could be divided into two classes with average values equal to 5.15°C - 27.4 psu and to 5°C - 30.0 psu (Fig. 2a.). The average time (ship time) of sampling was approximately 9:30 AM for the first class and 4:30 PM for the second class. A similar situation was observed at site "C"; here all the stations are concentrated in two areas of the T, S plane: 5.0°C - 29.6 psu and to 4.65°C - 31.0 psu (Fig. 2b). The lesser contrast of mean T, S characteristics on site "C" in comparison with site "D", apparently, could be explained by the distant location of the former from the main stream of the East Sakhalin Current. In this area the average time of sampling was about 11 AM for the first and 3 PM for the second group of stations. It should be noted, that the periodicity of measurements of 7 and 4 hours does not adequately reflect the temporal structure of tidal processes, since the time of observations corresponded only to certain tidal phases and does not overlap the tidal cycle. In other words, if the time of

observation is symmetric to the phase of high or low waters, the shorter periodicity will be recorded. If a fewer number of stations is sampled during the ebb phase and more during the high water, the longer periodicity will be fixed. This process plays an important role in the distortion of the tide wave form at a shoal where variations of the sea level become comparable with depth. In this case the crest moves faster than the trough and the forward slope of a wave becomes steeper.

The coincidence of cotidal lines and isohalines (Fig. 3) reflects the significant temporal variability in the region. The subarctic waters (the Okhotsk Sea water belongs to this water type) are characterized by the dominant influence of salinity on water stability and stratification. Therefore the spatial distribution of isohalines is the most representative for comparative purposes. It is remarkable, that for both sites, the variability picture is qualitatively preserved at all horizons (Fig. 3a and 3b). That corresponds to the present conception of current structure in the long progressive waves in the shallow sea, where the reversal fluctuations in longitudinal (horizontal) direction prevail at all depths. Thus, the influence of tides is reflected in horizontal shifting of the whole thermohaline water structure. As it was mentioned, sites "C" and "D" are situated in the area of two spatially homogeneous water masses, which can occupy the region under study in different time periods. During this process the entire replacement of one water type by another occurs. Taking into account the size of the sites "C" and "D" (approximately 6x6 miles), it seems that the amplitude of horizontal transformation of the whole water column exceeds 3 miles. One of the mentioned water structures is under the direct influence of the East Sakhalin Current which provides a salinity contrast forcing the observed variability.

Assuming the tidal nature of T-S variability on the Sakhalin shelf we can conclude that the spatial temperature and salinity distributions on sites "C" and "D" in fact represent the temporal variability of these properties. At 9 AM site "D" was occupied by the water mass of East Sakhalin Current that was reflected in the freshening of the upper homogeneous layer. Hereafter, the shifting of this water structure occurred, and before 4 PM it was completely replaced by a practically non-stratified water mass (Figs. 4a and 4b; St. 23 and 15), conditionally called "background water". The temperature inversions (Fig. 4, St. 15) indicate the active horizontal transformation of water masses. A similar situation was observed at site "C". However, the "background" conditions here were different and were determined by the larger offshore distance and, possibly, by another character of the large-scale circulation. At site "C" the East Sakhalin Current water mass was observed about 11 AM (Fig. 4c, St. 34). The water mass transformation was completed closer to 3 PM and resulted in an increase of salinity of the surface layer and in the deepening of the thermocline from 50-60 to 70-80 meters (Fig. 4d, St. 32).

Investigations of the hydrophysical fields on the East Sakhalin shelf should be planned taking into account the tidal processes in this zone. In future, we have to coordinate the continuous measurements at daily stations with site surveys executed during definite tidal phases. Despite the limited number of representative data, this study expands our understanding of dynamic processes in this region.

REFERENCES

The Atlas of Oceans: The Pacific Ocean. 1974. Moscow, Head Administration of Navigation and Oceanography XIV, 302p. (in Russian)

The Ocean Dynamics (Ed. Yu. P. Doronin). 1980. Leningrad, Gidrometeoizdat, 303p. (in Russian)

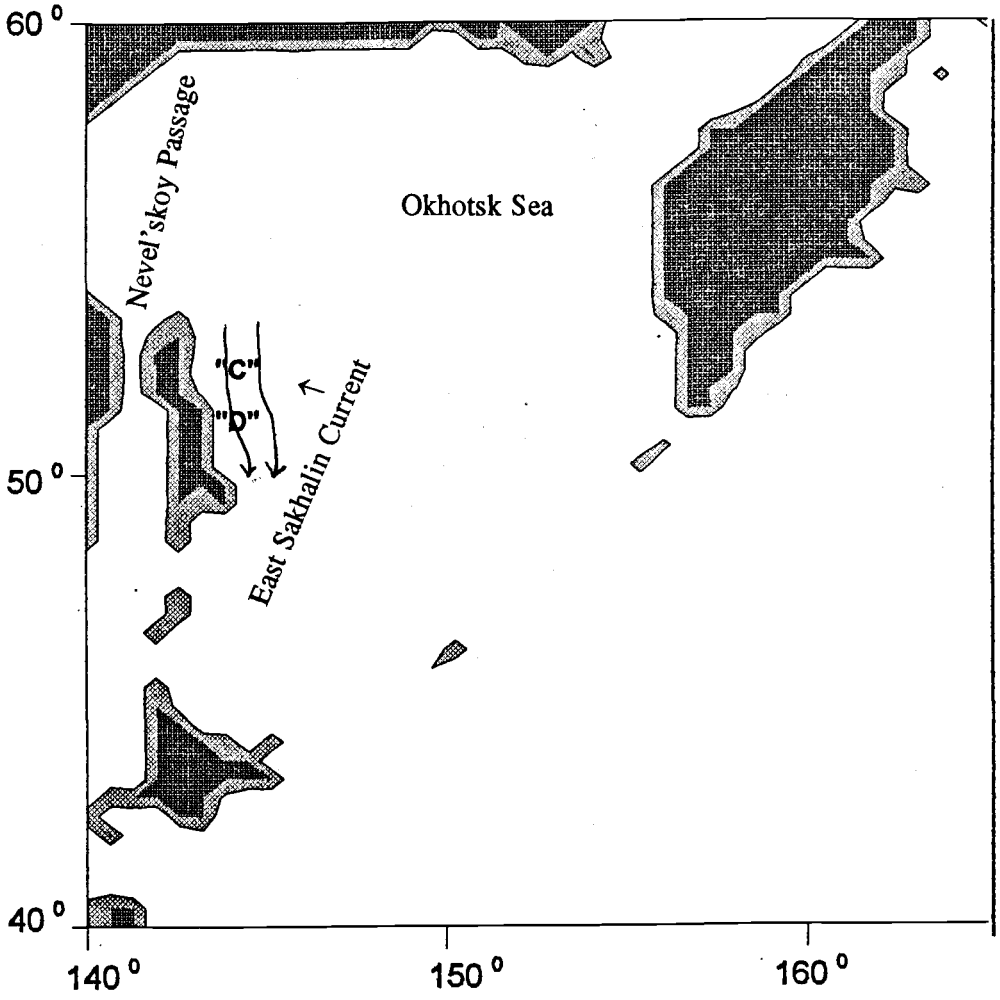

Fig. 1. The observational sites "C" and "D" in the zone of the East Sakhalin Current in October-November 1994.

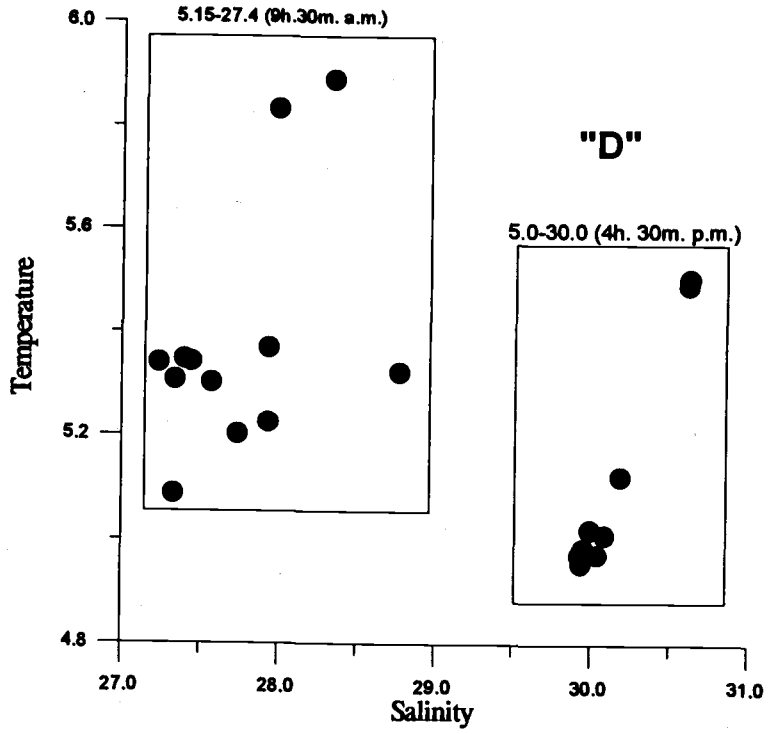

(a)

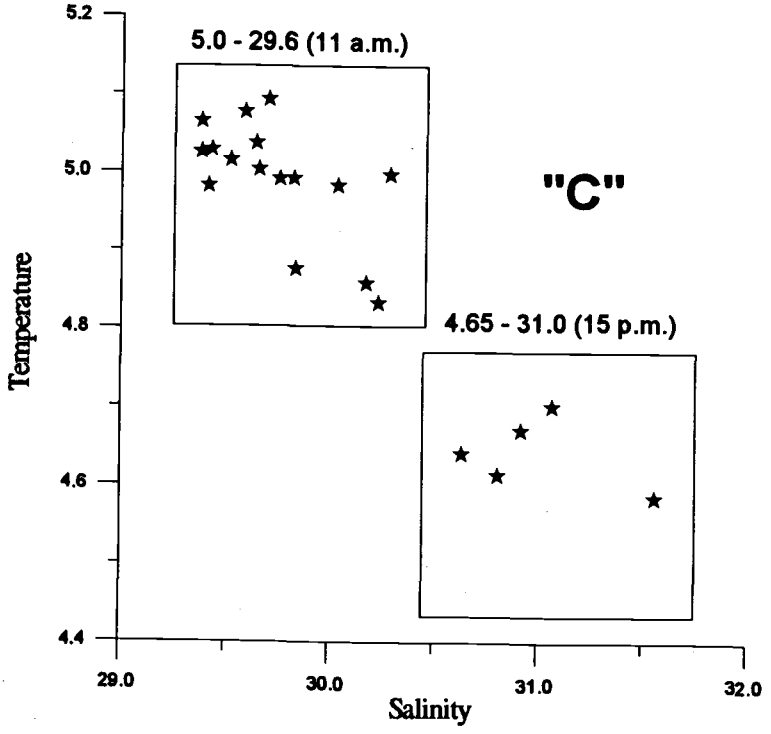

(b)

Fig. 2. Surface T, S - diagrams for sites "D" and "C".

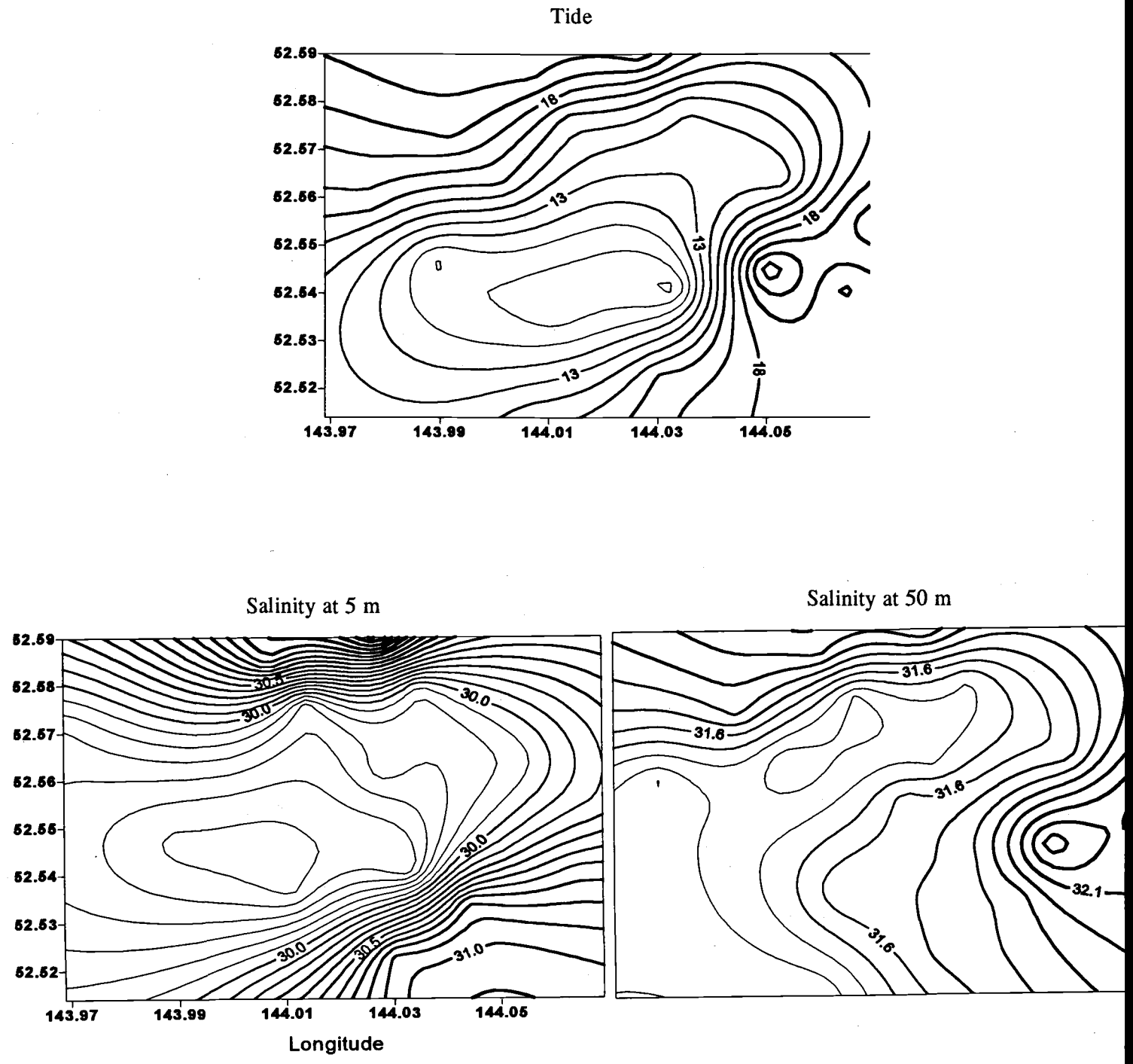

Fig. 3a. Plots of spatial distribution of tides and salinity demonstrating the coincidence of cotidal lines and isohalines for site "C".

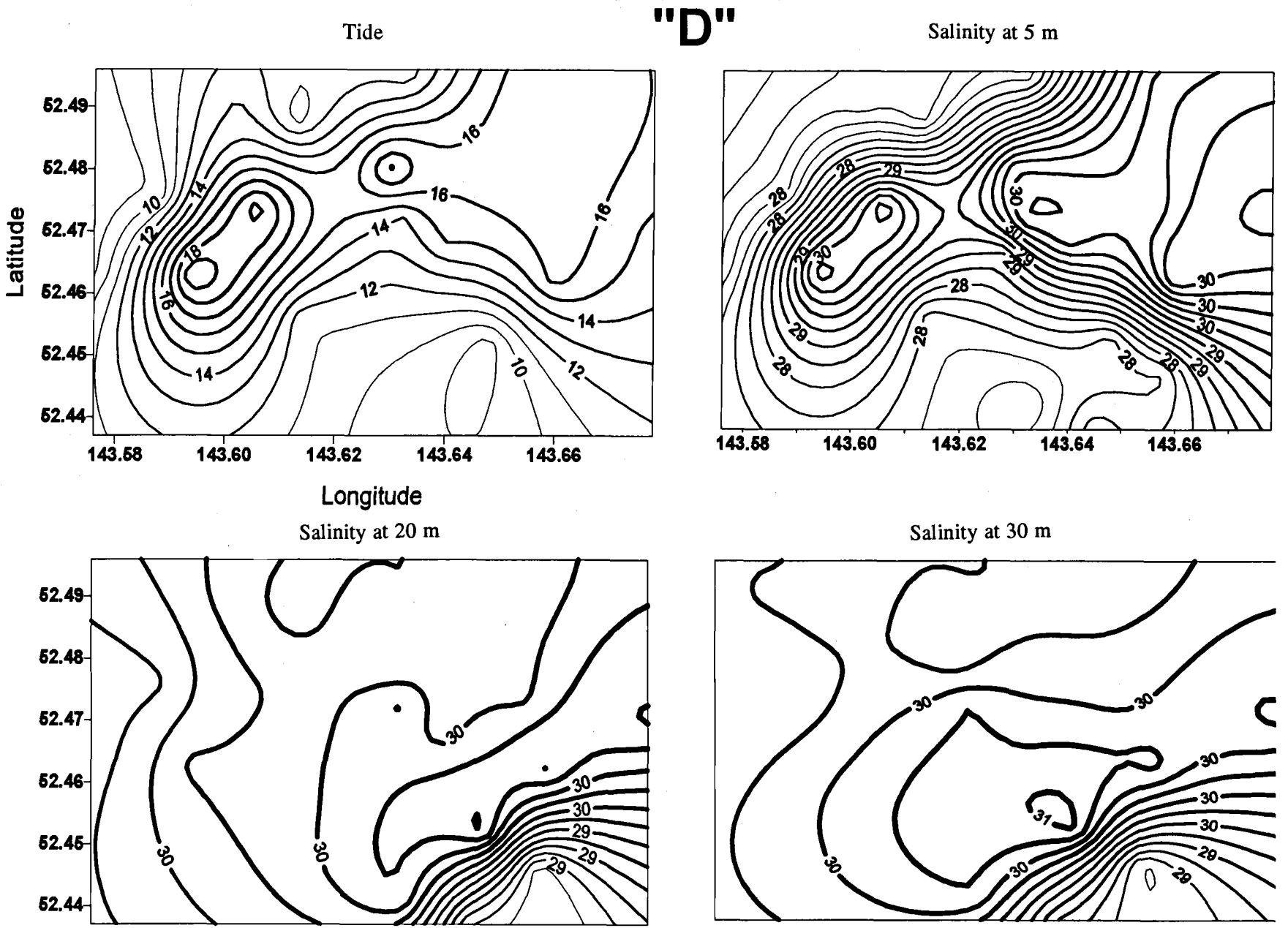

Fig. 3b. Plots of spatial distribution of tides and salinity demonstrating the coincidence of cotidal lines and isohalines for site "D".

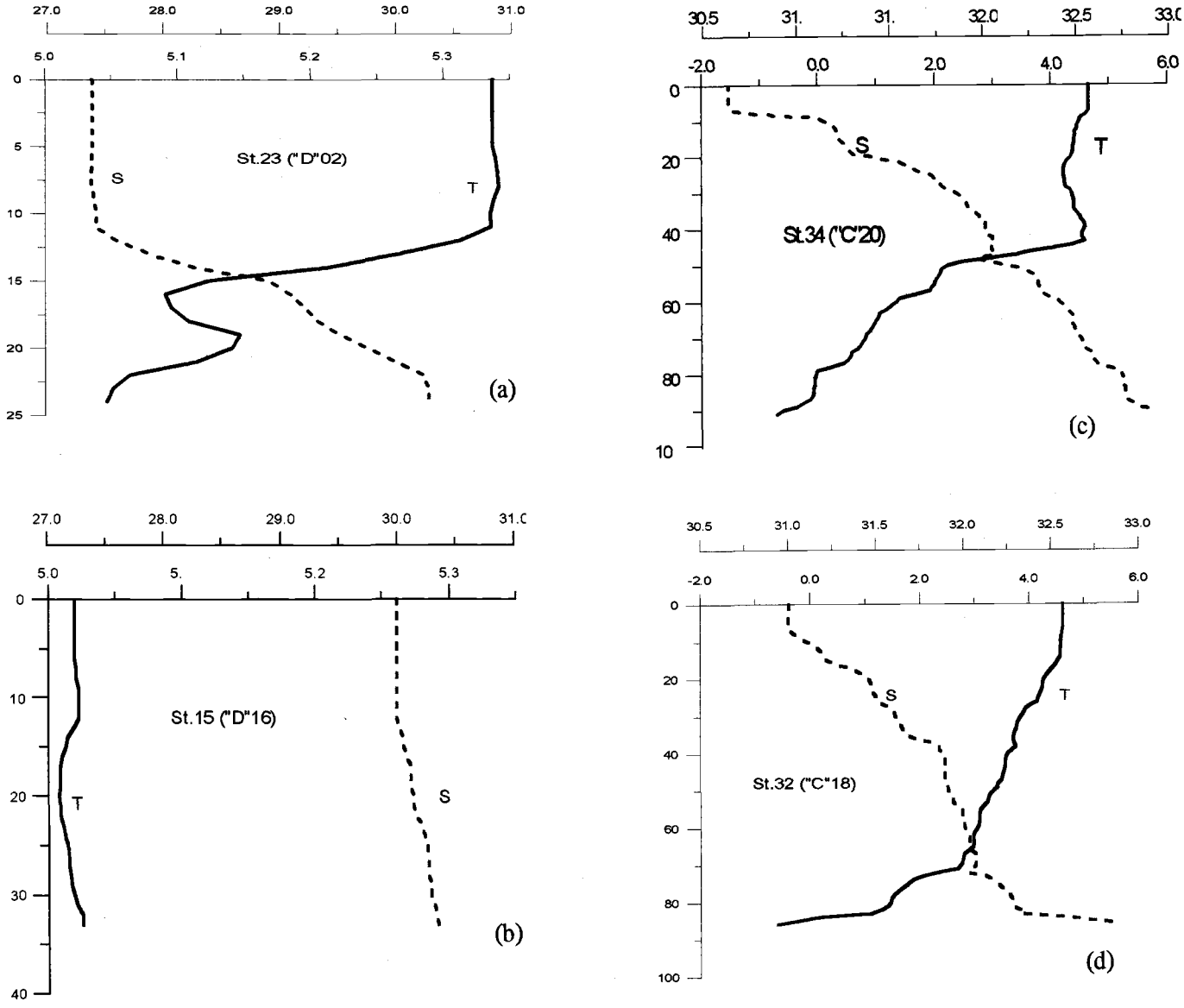

Fig. 4. Temperature and salinity profiles at sites "D" (a - 9 AM; b - 4 PM) and "C" (c - 11 AM; d - 3 PM).

On the Formation Process of the Subsurface Mixed Water Around the Central Kuril Islands

Yasuhiro KAWASAKI

Hokkaido National Fisheries Research Institute, Kushiro, Hokkaido, 085 Japan

The formation of the Oyashio Water (Oy) seems to be related to the mixing of two Subarctic waters: the Okhotsk Sea Water (OW) and the East Kamchatka Current Water (EKCW). On the other hand, near the Central Kuril Islands, a relatively warm and saline Mixed Water was surveyed on the shallow isopycnals lighter than 26.7 sigma-theta (Kawasaki and Kono, 1994). This water shows the vertically homogeneous temperature profile from 2 to 3°C, contrary to the dichothermal (inter-cooled) structure with temperature lower than 2°C revealed for both Subarctic Waters. The surface layer of the Mixed Water has peculiar characteristics: it is cold, saline, dense and rich in nutrient. This suggests that the Mixed Water originates from the deeper layer.

Surface silicate distribution within the study area during the period from late August to early September 1993 is shown in Fig. 1a. High silicate concentrations were found over the bank (hereafter called Bank A) to the east of the Kruzenshtern Strait and to the south of the Bussol' Strait. Sections of potential temperature (deg-C) and salinity (psu) as a function of potential density (kg/m^3 in sigma-theta, cl/ton in thermosteric anomaly) through the Kruzenshtern Strait are given in Fig. 2. The origin of the Mixed Water was observed at the Bank A (Stn. MU5) as isolated warm water with salinity higher than 33.3 psu on the isopycnal layer 26.5-26.6 sigma-theta. This suggests that the effect of bottom topography is an important factor for the formation of the Mixed Water. In the present paper vertical nutrient profiles will be used to discuss the mechanism of the Mixed Water formation.

We assumed that the horizontal supply of subtropical waters, like a warm-core ring (WCR) or Soya Warm Current waters, cause the appearance of saline and warm Mixed Water on the isopycnals lighter than 26.7 sigma-theta. However, this is in contradiction with the nutrient data: the silicate concentration of Subtropical Water is lower than 5 μmol/l. Also, the formation of the Mixed Water cannot be explained by horizontal isopycnal mixing of two Subarctic Waters as they have a dichothermal layer with temperature below 2°C. Therefore, saline and nutrient-rich water has to be supplied from the deeper layer.

During the 1994 summer cruise, CTD and nutrient bottle sampling were carried out concurrently within the Bussol' Strait area. The observation line through the Bussol' Strait and surface silicate distribution are shown in Fig. 1b. Silicate concentrations higher than 40 μmol/l were revealed in the Strait. Sections of potential temperature (deg-C), salinity (psu) and silicate (μmol/l) as a function of potential density (sigma-theta and thermosteric anomaly) through the Bussol' Strait during the period from late August to early September 1994 are presented in Figs. 3a-3c. The warm, saline and nutrient rich Mixed Water is observed in the Strait (Stn. NU1) at density levels less than 26.8 sigma-theta. Stations NU'1, NU1, NU5 and NU9 were selected to compare the characteristics of each water type, i.e. OW, Mixed Water, EKCW, and Subtropical Water, respectively. Silicate and potential density relationships for the different waters are given in Fig. 4. Numerals on the shoulder of each symbol indicate sampling depths in hecto-meters. It should be mentioned that the upper 50 m layer of the Mixed Water is nutrient rich and its silicate - potential density relationship is similar to

that of EKCW. On the other hand, OW is characterized by lower nutrient concentrations at the same density level as compared with other Subarctic waters such as EKCW.

Vertical profiles of silicate (open symbols) and phosphate (closed symbols) for each station on the section through the Bussol' Strait are displayed in Fig. 5. Nutrient concentrations for the Okhotsk Sea Water (Stn. NU'1) do not exceed those within the upper 600 m of the Mixed Water. These data suggest that the Mixed Water can not be produced by vertical mixing of OW itself. Additionally, vertical mixing within the upper 200 m of EKCW can not lead to the Mixed Water formation, as the mean silicate concentration in the 200 m layer of EKCW is about 43 μmol/l, whereas mean silicate concentration in the upper Mixed Water is about 56 μmol/l.

If vertical mixing of EKCW induced by tidal current over the continental shelf is predominant, the upper Mixed Water becomes more warm, fresh, and poor in nutrients. To consider the vertical supply of saline and nutrient-rich water from the deeper layer, relationships between salinity and silicate for selected station are shown as in Fig. 6. Characteristics of the Mixed Water shallower than 200 m coincide with subsurface 100-150 m layer of EKCW. Assuming silicate and salinity are more conservative than a water property such as temperature, the dichothermal layer of EKCW (33.1-33.4 psu in salinity) might be a possible source of the upper Mixed Water. However, in this case a heating process should follow the upwelling. In order to heat up the 30-40 m of water column (see Fig. 4) to about 0.5-2°C, what kind of process should occur?

We presumed that vertical mixing induced by tidal current occurs only over the continental shelf, however, the sill depths for the straits of the Central Kuril Islands are about 400-500 m. Recalculated mean silicate concentration over 400 m water column, EKCW (68 μmol/l) exceeds the mean concentration for the Mixed Water (63 μmol/l). Thus, if tidal currents around the Central Kuril Islands are strong enough to mix the entire water column, vertical mixing of EKCW is another possible forcing mechanism to produce the Mixed Water.

SUMMARY

Around the Central Kuril Islands, a peculiar warm, saline and nutrient rich upper Mixed Water was found on the isopycnals lighter than 26.7 sigma-theta near the Bank A. It seems to be responsible for high primary production of the Oyashio. However, isopycnal mixing of two Subarctic Waters and horizontal transport of the Subtropical Water can not produce the upper Mixed Water.

Vertical transport of the Okhotsk Sea Water is also disregarded as the source of the upper Mixed Water formation based on the nutrient and salinity relationships, whereas upwelling of the subsurface East Kamchatka Current Water appears to be a cause of the upper Mixed Water formation, though the heating process after upwelling remains unknown. The entirely vertical mixing of the upper 400-600m of EKCW is another possibility for the production of the upper Mixed Water.

In future, we have to analyze the water formation process using time resolution tracers or properties and also to carry out model experiments combined with direct current measurements around the Bank A and within the continental shelves near the Central Kuril Islands.

REFERENCES

Kawasaki, Y. and T. Kono. 1994. Distribution and transport of Subarctic Waters around the middle of Kuril Islands. Umi to Sora. 70(2):71-84.

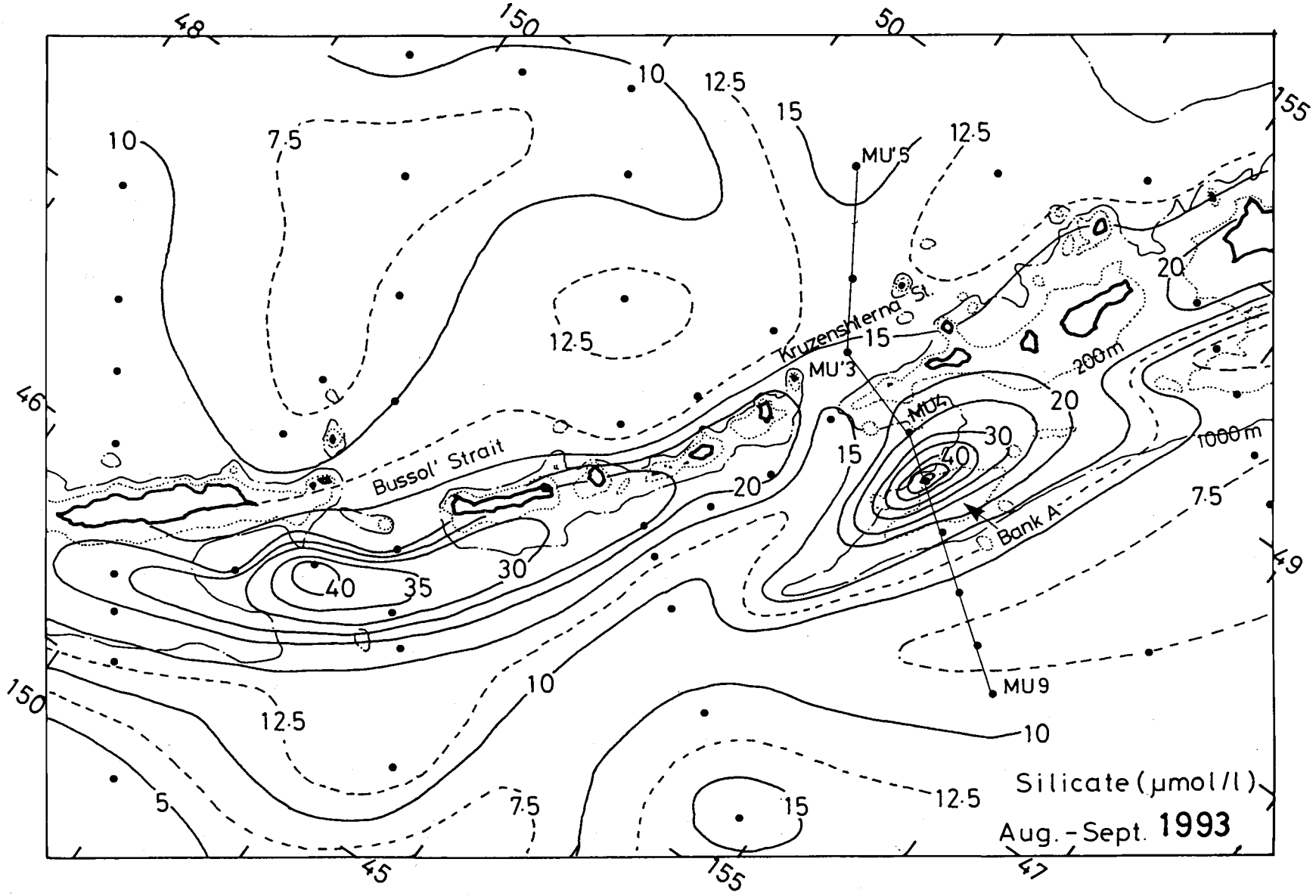

Fig. 1a. Surface silicate distribution (μmol/l) during the period from late August to early September 1993 (a) and 1994 (b). Observational sections through the Kruzenshtern (a) and Bussol' (b) Straits are shown. Study area presented in Fig. 1a is displayed as the dashed rectangular in Fig. 1b.

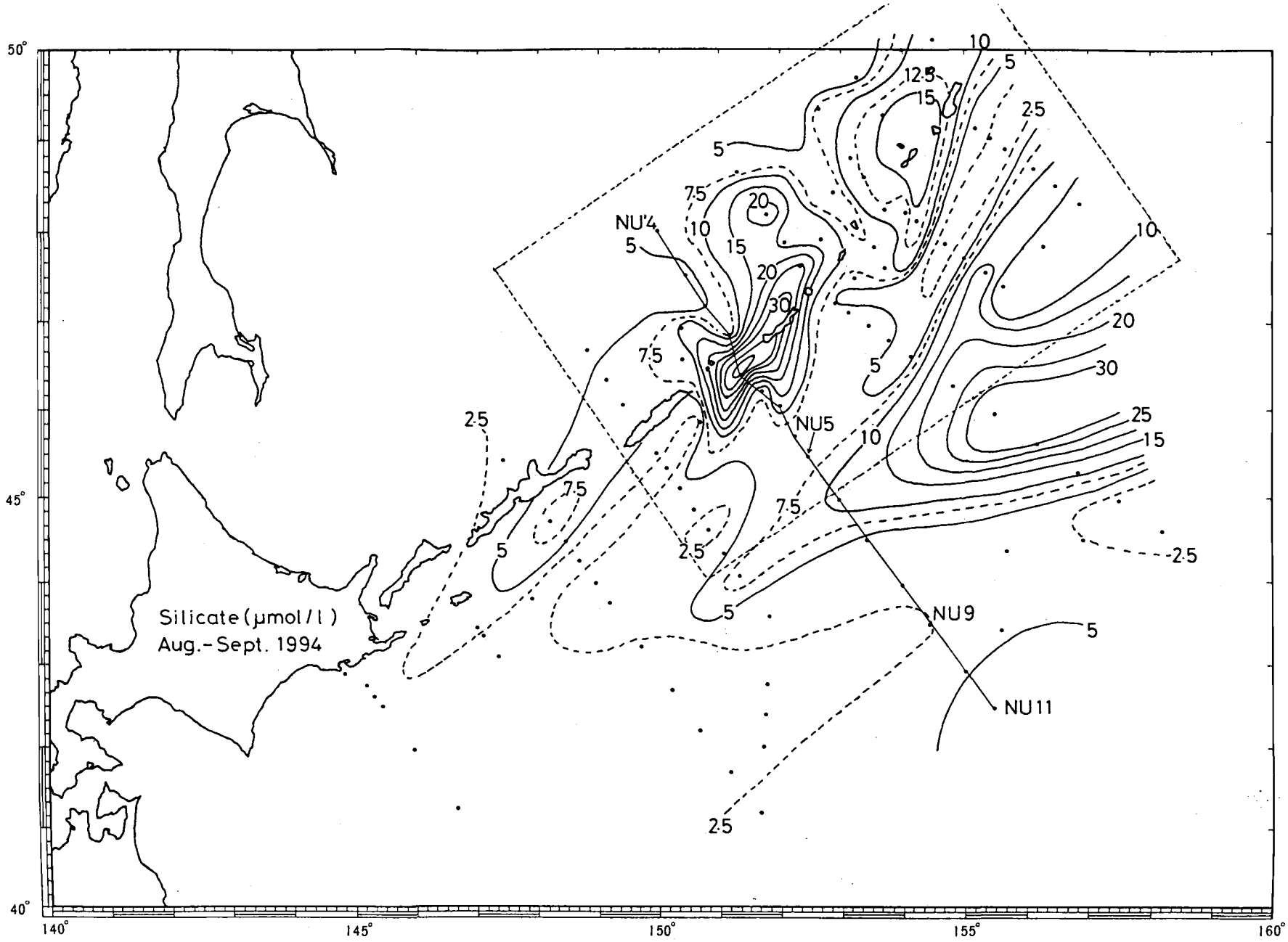
50°
45°
40°
140°
145°
150°
155°
160°
Silicate (μmol/l)
Aug.-Sept. 1994
NU'4
NU5
NU9
NU11
2.5
5
7.5
10
12.5
15
20
25
30

Fig. 1b.

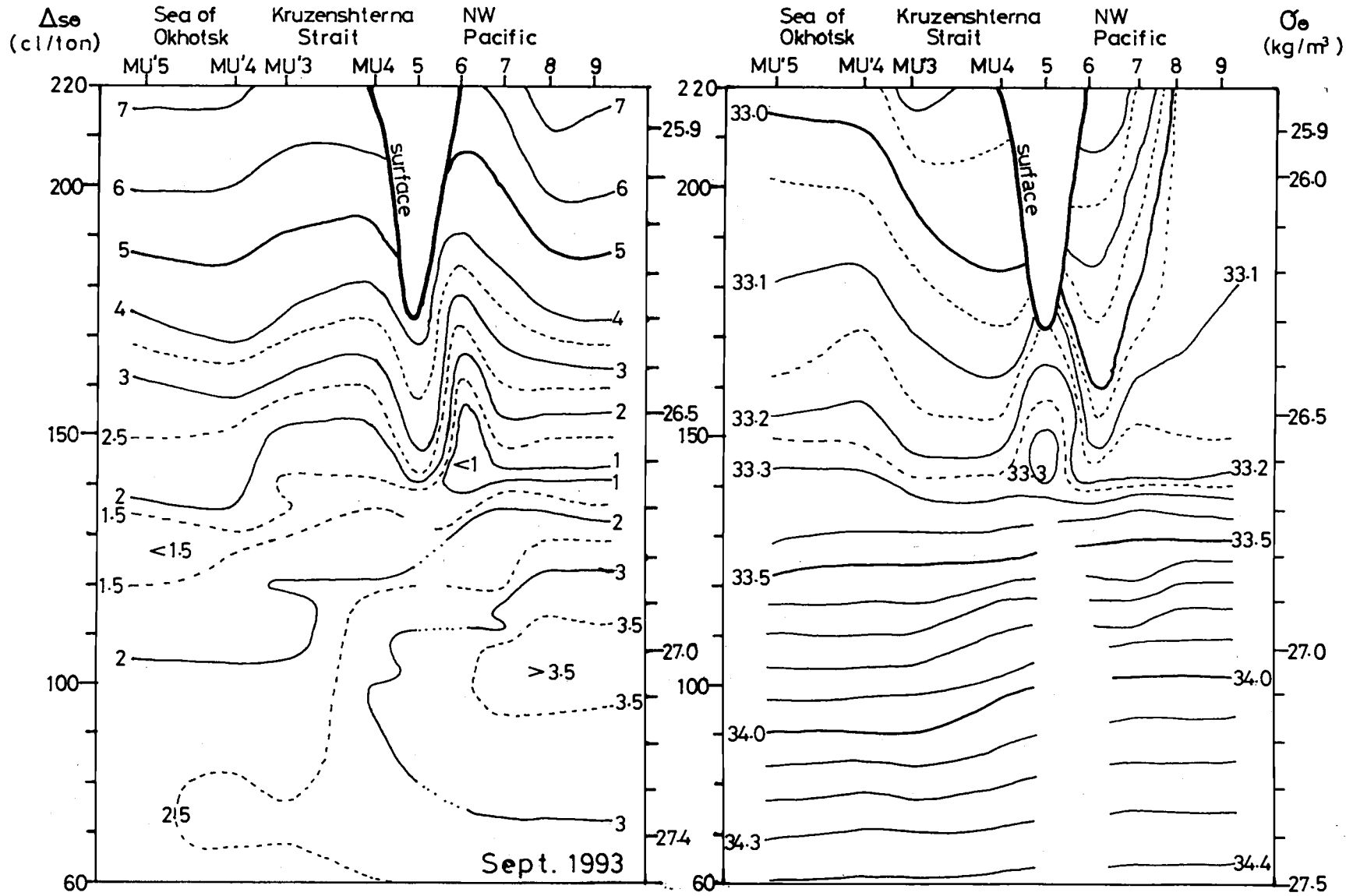

Fig. 2. Sections of potential temperature (deg-C, left) and salinity (psu, right) as a function of potential density (sigma-theta, thermosteric anomaly) through the Kruzenshtern Strait in September, 1993.

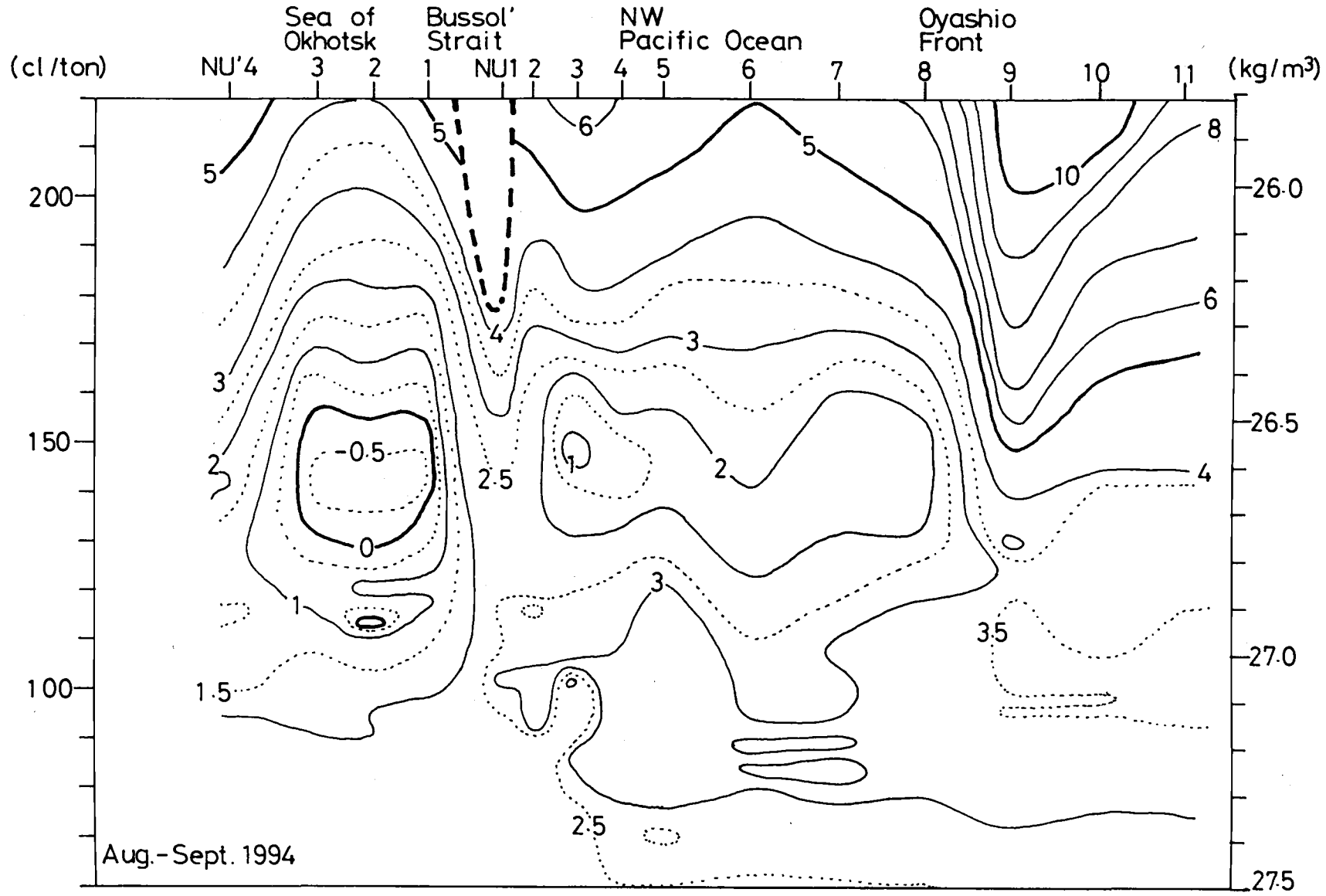

Fig. 3a.

Fig. 3. Sections of (a) potential temperature (deg-C), (b) salinity (psu) and (c) silicate (μmol/l) as a function of potential density (sigma-theta, thermosteric anomaly) through the Bussol' Strait during the period from late August to early September, 1994. Stations NU'1-NU'4 represent the Okhotsk Sea, and stations NU1-NU11 represent the North Pacific. The Bussol' Strait is located between NU'1 and NU1.

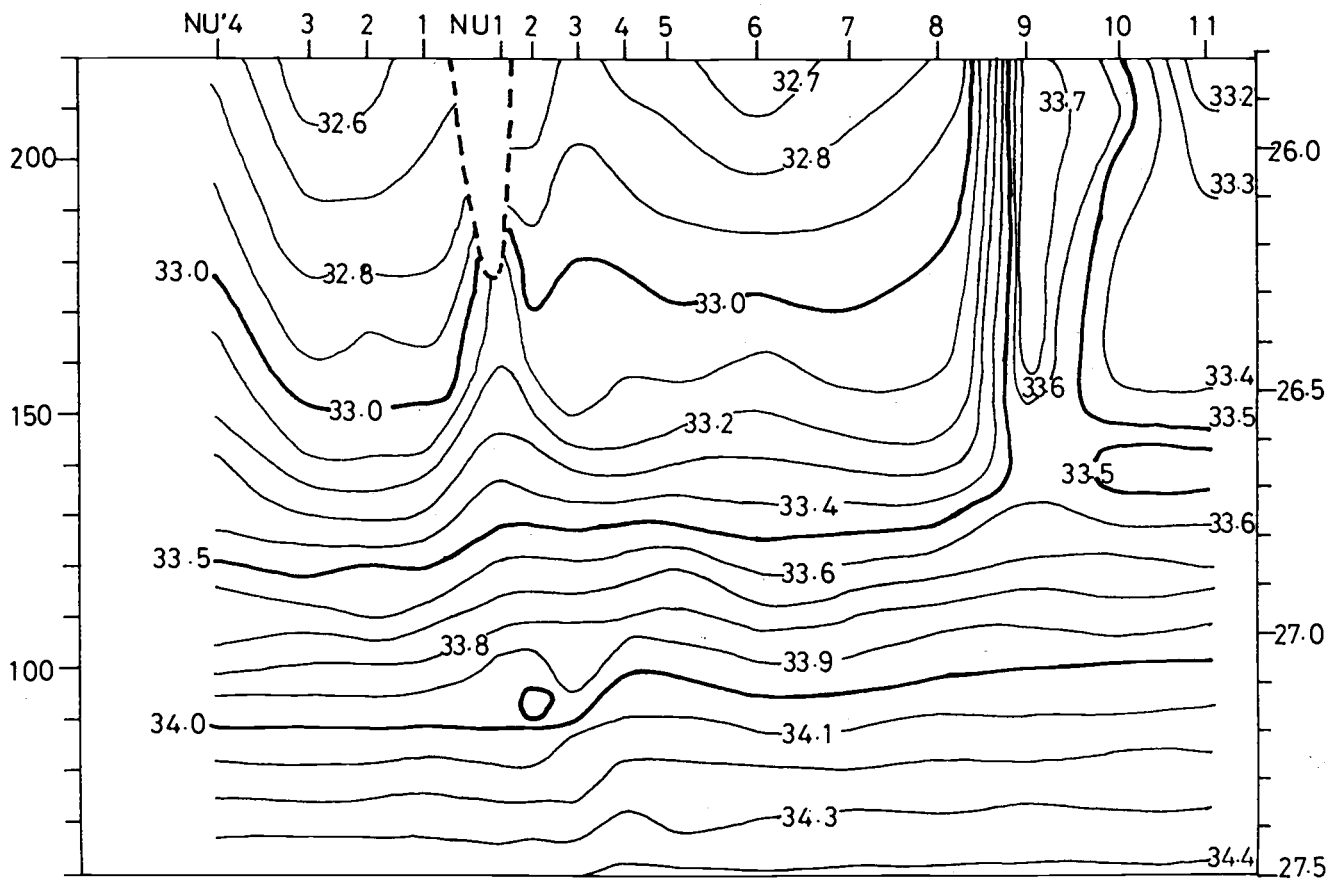

Fig. 3b. (psu)

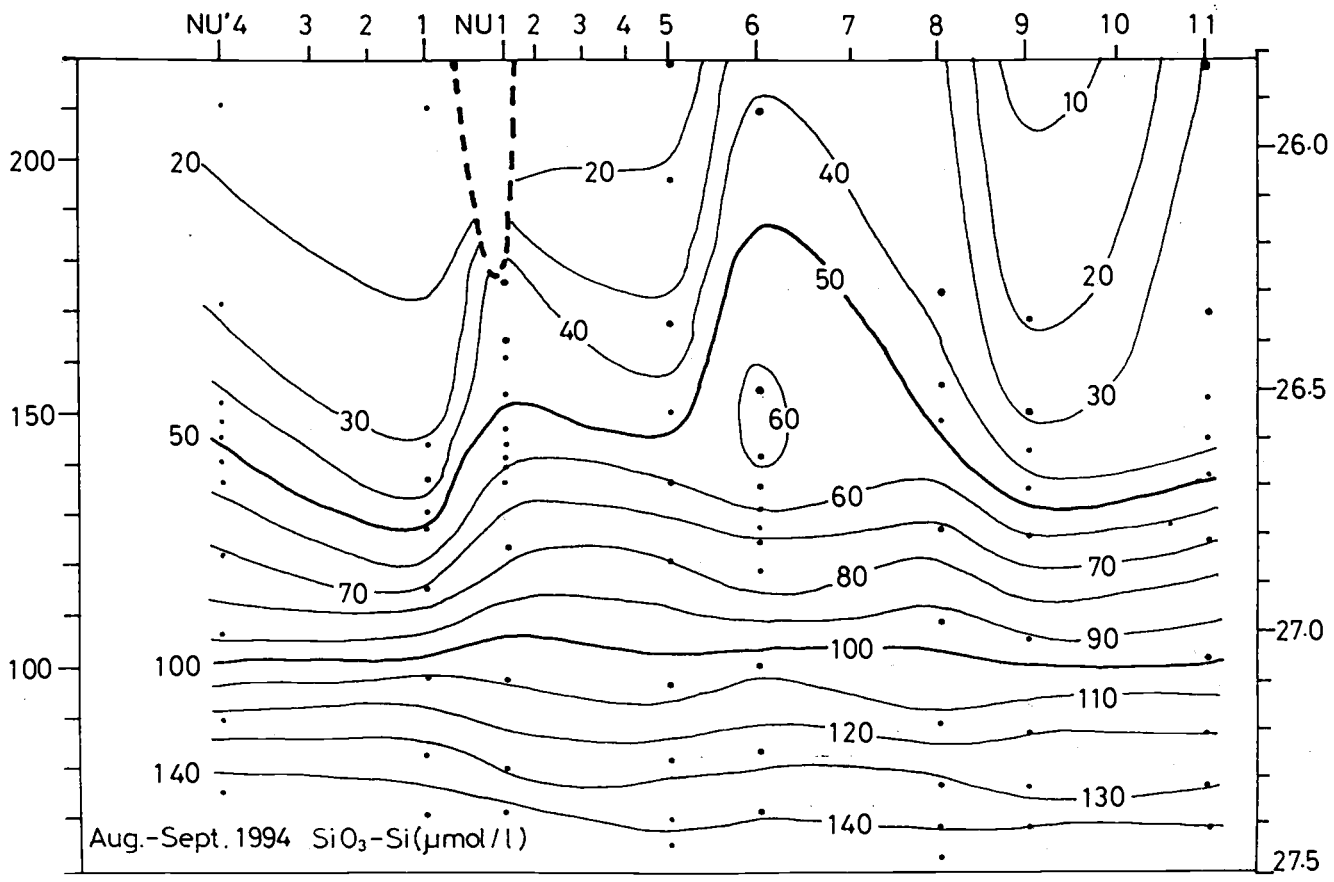

Fig. 3c. (μmol/l)

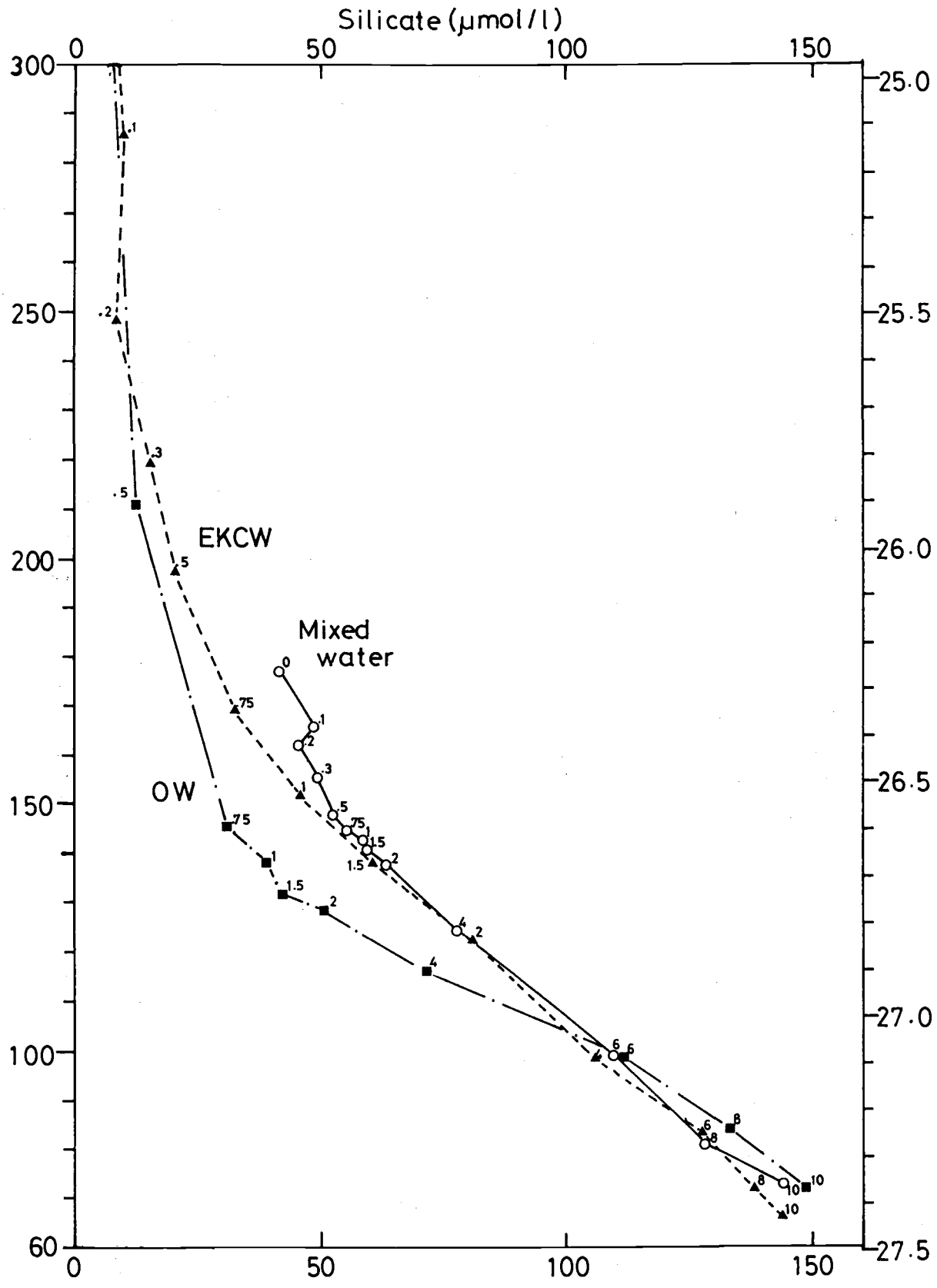

Fig. 4. Plot of silicate concentration (µmol/l) versus potential density (kg/m^3 in sigma-theta, cl/ton in thermosteric anomaly) for OW (closed squares), EKCW (closed triangles) and Mixed Water (open circles) in late August - early September, 1994. Numerals on the shoulder of each symbol indicate the sampling depths in hecto-meters.

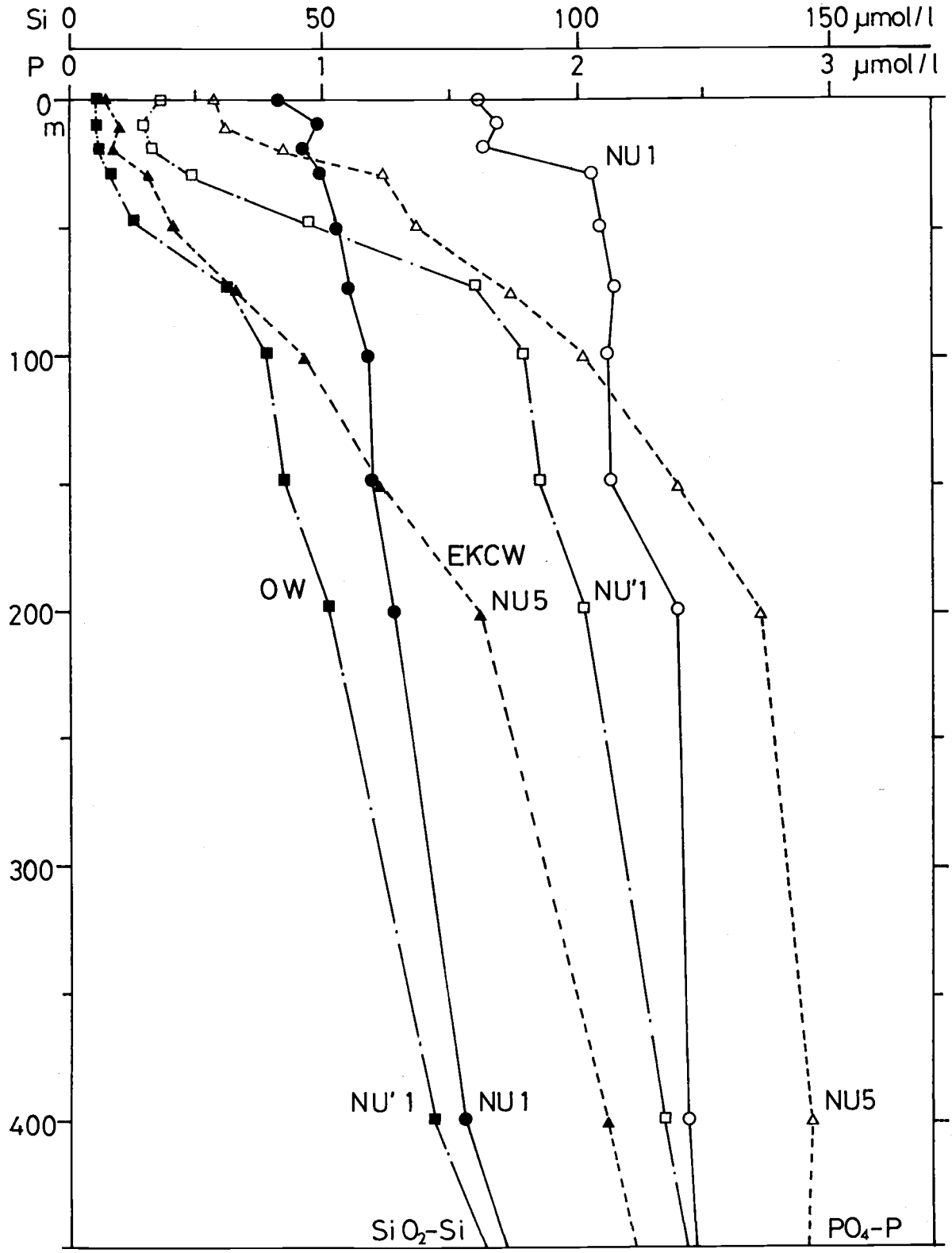

Fig. 5. Vertical distributions of silicate (closed symbols) and phosphate (open symbols) for stations NU'1 (OW, squares), NU1 (Mixed Water, circles) and NU5 (EKCW, triangles) on the section through the Bussol' Strait during the period from late August to early September, 1994.

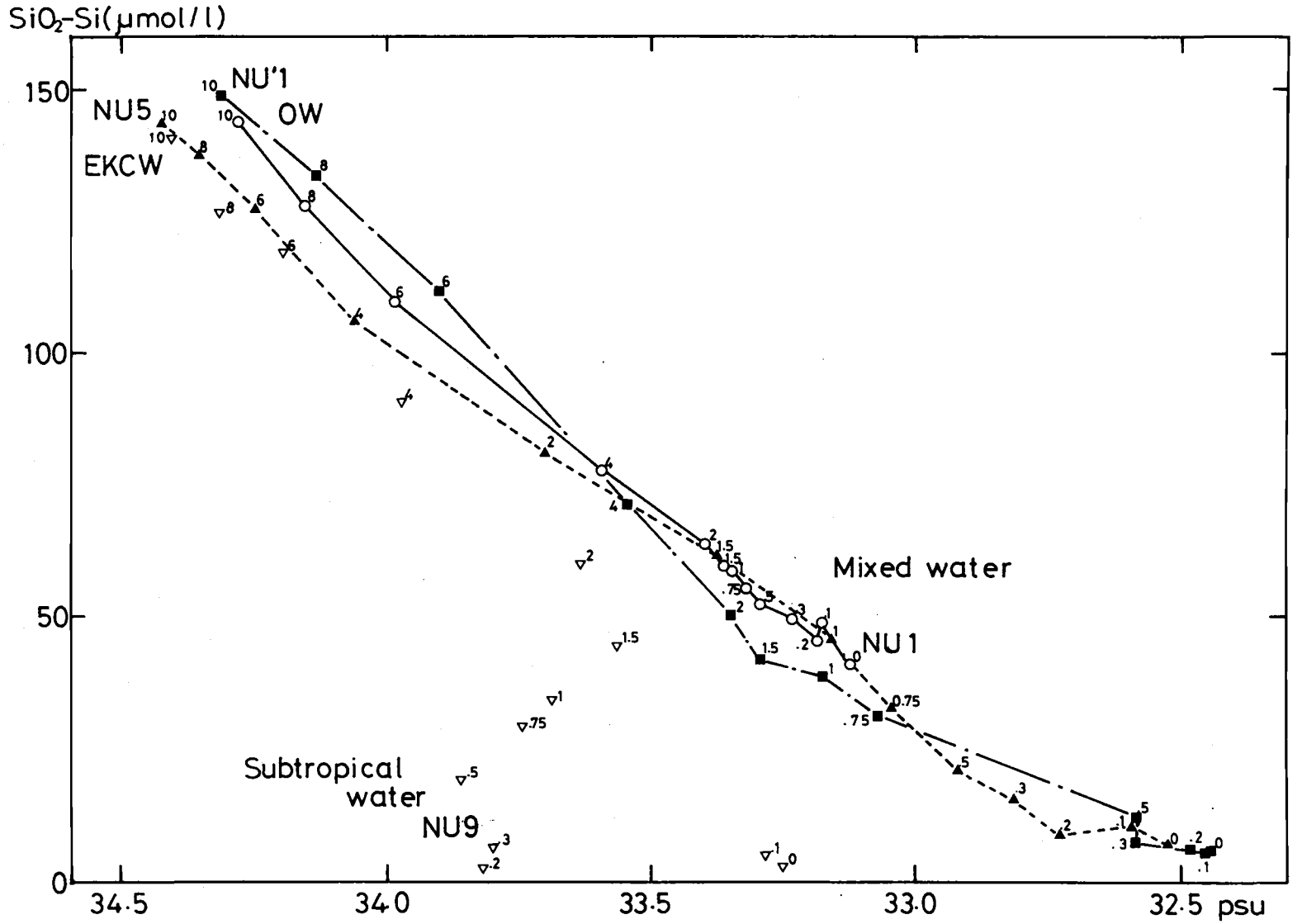

Fig. 6. Plot of silicate concentration (μmol/l) versus salinity (psu) from the surface to the depth of 1000 m for stations NU'1 (OW, closed squares), NU1 (Mixed Water, open circles) and NU5 (EKCW, closed triangles), NU9 (Subtropical Water, open triangles) on the section through the Bussol' Strait during the period from late August to early September, 1994.

Northwest Pacific Paleohydrography

Lloyd D. KEIGWIN

Woods Hole Oceanographic Institution, Woods Hole, MA 02543, U.S.A.

It is important to document carefully glacial-interglacial changes in North Pacific circulation and hydrography in order to understand changes in atmospheric pCO_2 because the Pacific Ocean is the end-member of the modern circulation regime. The modern circulation pattern tends to accumulate CO_2 in the deep Pacific, yet there has been considerable speculation that there may have been a young deep water mass produced in the Pacific during glacial times (Mammerickx, 1985; Keigwin, 1987; Keigwin et al., 1992; Zahn et al. 1991). In addition, it is thought that the marginal seas of the North Pacific contribute to the ventilation of that basin at intermediate depths (for example, Reid, 1973; Talley, 1991). Elsewhere in the world ocean it has been shown that the intermediate depth waters were better ventilated during glaciation, at the expense of the deep ocean (Boyle and Keigwin, 1987; Kallel et al., 1988; Oppo and Lehman, 1993). Could the processes which generate Pacific Intermediate Water in today's ocean have been extended to produce Pacific Deep Water 15,000 years ago?

To answer this and other critical questions about the history of northwestern Pacific circulation, I have been involved in several cruises in the region onboard American and Russian ships to collect new sediment cores and conduct hydrographic investigations. Paleontological and geochemical results from numerous cores on the northern Emperor Seamounts (Fig. 1) support our previous observations based on a single core (Keigwin et al., 1992). For example, the diatomaceous facies centered on deglaciation is found to be widespread (see also Sancetta, 1992) and many new Accelerator Mass Spectrometer (AMS) ^{14}C determinations show that sedimentation rates peaked at that time. The oxygen isotope events in deglacial benthic foraminifera have been confirmed, as has been the evidence for a low salinity event in surface waters. Recently, we have calibrated the $\delta^{13}C$ of the benthic foraminifera *Cibicidoides* against the $\delta^{13}C$ of the total CO_2 in nearby seawater samples, finding that *Cibicidoides* $\delta^{13}C$ is an excellent proxy for the seawater nutrient content in the northwestern Pacific Ocean (McCorkle and Keigwin, 1994). Carbon isotope measurements on *Cibicidoides* of glacial age are uniformly low in the depth range 2,300 m to 4,000 m, supporting the contention that deep ventilation has been low for at least the past 20,000 years. However, the lack of hemipelagic sediment sequences from $<2,300$ m on the Emperor Seamounts denies us a window on the past for shallower depths.

Previous work indicates that the Okhotsk Sea contains appropriate sediment for reconstructing paleoclimate and paleohydrography (Gorbarenko et al., 1988; Morley et al., 1991). Many new cores from that basin reveal that the hemipelagic deposition rates are very high and that, at least during glacial maximum conditions, the benthic fauna contained enough *Cibicidoides* to reconstruct intermediate depth hydrography (for example, Fig. 2). Cores of quality similar to Vulkanolog 34-91 have been recovered at ~100 m spacing in the Kuril Basin along the seaward margin of Akademia Nauk Rise between 1,000 and 3,200 m.

My goal is to combine data from the Okhotsk Sea cores with comparable data from the Emperor Seamounts to produce a composite paleohydrographic profile for the far northwestern Pacific. The two regions are shown schematically in Fig. 3. Various data from hydrocasts in the these regions,

including T, S, $[PO_4]$, $\delta^{13}C$ and $[O_2]$, indicate that water in the Okhotsk Sea between 2,300 m and 1,000 m is in full communication with open Pacific water. This is consistent with modern views of the intermediate depth circulation which show inflow of water to the Okhotsk Sea through Kruzenshtern Strait (sill = 1,600 m) and outflow through Bussol' Strait (sill = 2,300 m) (Figs. 1 and 3).

I suppose that there was no barrier to this circulation pattern during glacial maximum conditions. In addition, because of the general absence of this genus from the modern Okhotsk Sea, it must also be assumed that *Cibicidoides* are as good a proxy for nutrient content of intermediate depth water as they are for deep water. Using the $\delta^{18}O$ of the benthic foram *Uvigerina* to mark the glacial maximum level in our core collection, we have taken additional samples where necessary to extract enough *Cibicidoides* for $\delta^{13}C$ analysis and plotted all those results vs. water depth (Fig. 4).

In Fig. 4, data points connected by the bold solid line are the $\delta^{13}C$ of total CO_2 from the Emperor Seamounts, and the data connected by the fine line are those from the Okhotsk Sea. As noted above, the two hydrocast data sets are indistinguishable between 2,300 m and 1,000 m. It is seen that where the *Cibicidoides* are abundant in modern sediments their $\delta^{13}C$ (open circles) lies close to the water column data. So far, we have found *Cibicidoides* abundant in only one coretop from the Okhotsk Sea, near a depth of 1,000 m off the coast of Sakhalin (BC-32 in Fig. 1).

During glacial times, *Cibicidoides* are present throughout the region. In the open sea the glacial $\delta^{13}C$ data (solid circles) are systematically offset from the coretop data by an amount roughly equivalent to the secular change in seawater chemistry (0.3-0.4 ‰). Those data argue against any major change in deep ocean ventilation, although Cd/Ca data in benthic foraminifera are contradictory (Boyle, 1992). Above 2,300 m, on the other hand, Okhotsk Sea $\delta^{13}C$ data indicate relatively increased ventilation, consistent with results from other locations worldwide. If the glacial data were adjusted by +0.3 to 0.4 ‰ to account for the secular change in world ocean carbon isotope composition, then it would be seen that the change in ventilation begins at the depth of the sill at Bussol' Strait. These results suggest that the Okhotsk Sea was an important source of more oxygenated intermediate waters in the glacial North Pacific Ocean. The influence of this better ventilation may be evident as far downstream as the Gulf of California. There, in Guaymas Basin which is anoxic today at Pacific Intermediate Water depths, glacial bottom waters contained enough oxygen to support an active benthos (Keigwin and Jones, 1990).

REFERENCES

Boyle, E.A. 1992. Oceanic chemical distributions during the stage 2 glacial maximum: Cadmium and $\delta^{13}C$ evidence compared. Annual Reviews of Earth Planet. Sci. 20:245-287.

Boyle, E.A., and L.D. Keigwin. 1987. North Atlantic thermohaline circulation during the past 20,000 years linked to high-latitude surface temperature. Nature. 330:35-40.

Gorbarenko, S.A., N.N. Kobaliuch, et. al. 1988. Okhotsk Sea upper Quaternary sediment and reconstruction of paleoceanographic conditions. Pacific Ocean Geology. 2:25-34.

Kallel, N., L.D. Labeyrie, A. Juillet-Leclerc, and J.-C. Duplessy. 1988. A deep hydrological front between intermediate and deep water masses in the glacial Indian Ocean. Nature. 333:651-655.

Keigwin, L.D. 1987. North Pacific deep water formation during the latest glaciation. Nature. 330:362-364.

Keigwin, L.D., and G.A. Jones. 1990. Deglacial climatic oscillations in the Gulf of California. Paleoceanography. 5:1009-1023.

Keigwin, L.D., G.A. Jones, and P.N. Froelich. 1992. A 15,000 year paleoenvironmental record from Meiji Seamount, far northwestern Pacific. Earth Planet. Sci. Lett. 111:425-440.

Mammerickx, J. 1985. A deep-sea thermohaline flow path in the Northwest Pacific. Marine Geology. 65:1-19.

McCorkle, D.C., and L.D. Keigwin. 1994. depth profiles of $\delta^{13}C$ in bottom water and core top C. *wuellerstorfi* on the Ontong Java Plateau and Emperor Seamounts. Paleoceanography. 9:197-208.

Morley, J.J., L.E. Heusser, and N.J. Shackleton. 1991. Late Pleistocene/Holocene radiolarian and pollen records from sediments in the Sea of Okhotsk. Paleoceanography. 6:121-131.

Oppo, D.W., and S.J. Lehman. 1993. Mid-depth circulation of the subpolar North Atlantic during the last glacial maximum. Science. 259:1148-1152.

Reid, J.L., Jr. 1973. North Pacific Ocean waters in winter. The Johns Hopkins Oceanographic Studies. 5:96 p.

Sancetta, C. 1992. Primary production in the glacial North Atlantic and North Pacific Oceans. Nature. 360:249-251.

Talley, L.D. 1991. An Okhotsk Sea water anomaly: implications for ventilation in the North Pacific. Deep-Sea Res. 38:S171-S190.

Zahn, R., T.F. Pedersen, B.D. Bornhold, and A.C. Mix. 1991. Water mass conversion in the glacial Subarctic Pacific (54N, 148W): Physical constraints and the benthic-planktonic stable isotope record. Paleoceanography. 6:543-560.

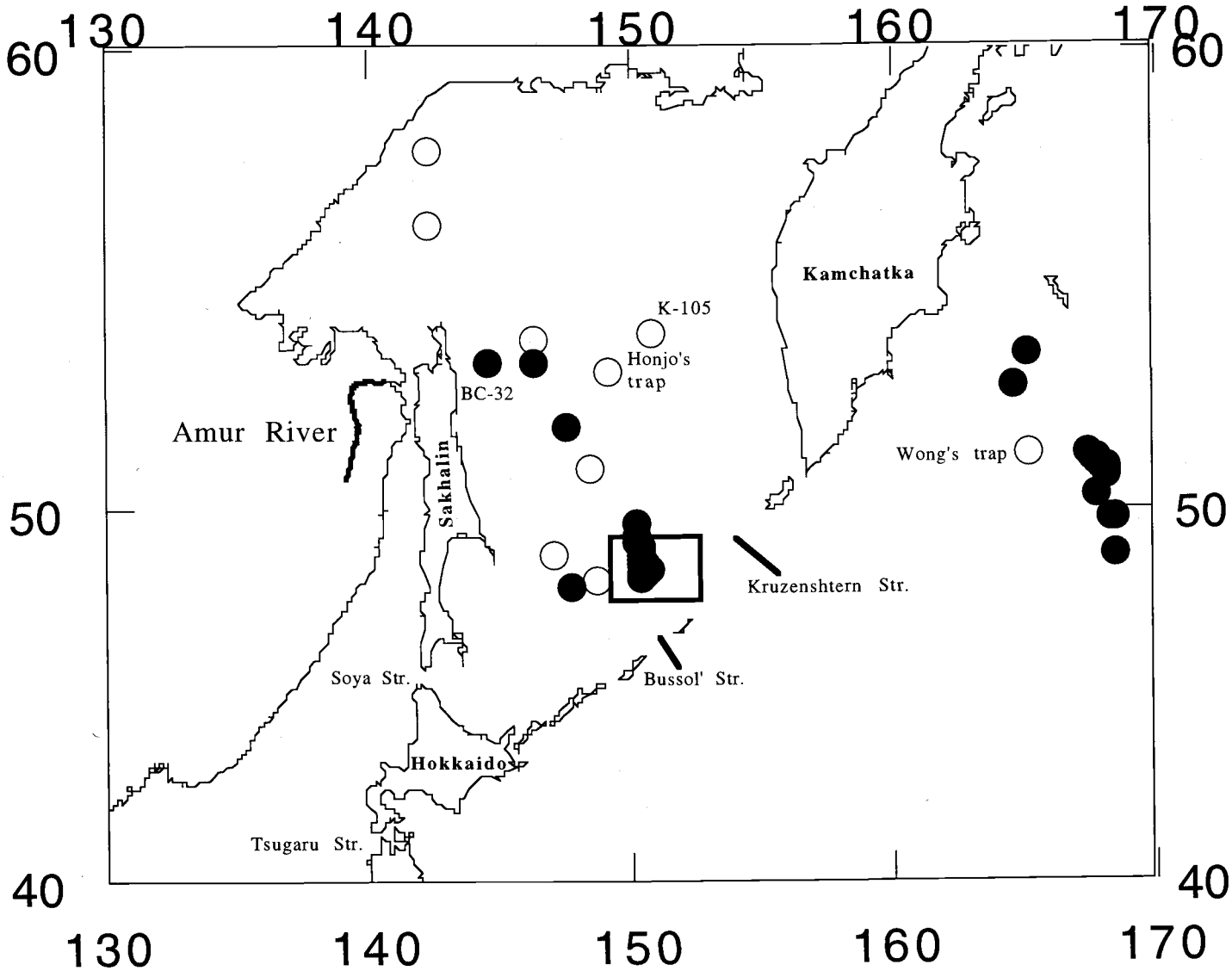

Fig. 1. Some core and sediment trap locations in the far northwestern Pacific Ocean. Solid symbols mark sediment cores in the Woods Hole collection. The box shows the positions of about 20 cores at ~100m depth spacing on the seaward flank of Akademia Nauk Rise in the Kuril Basin.

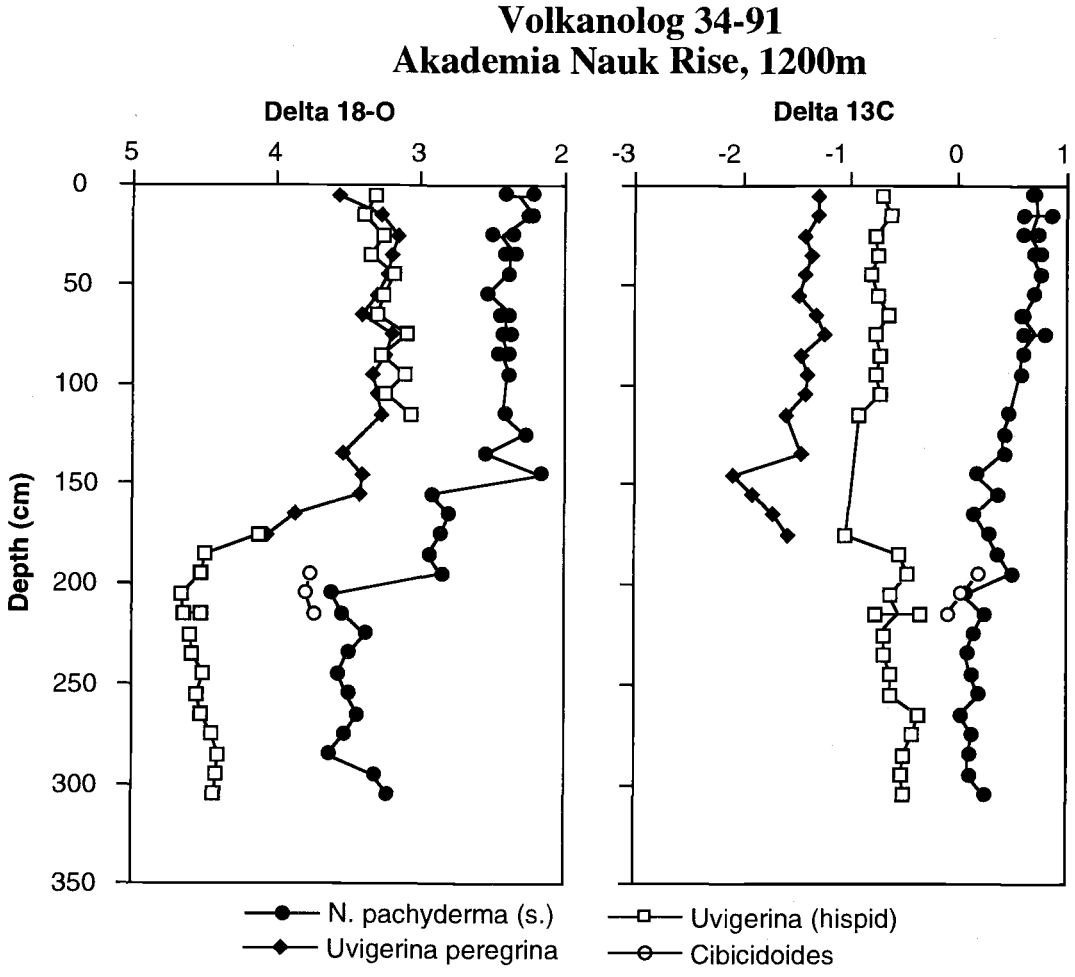

Fig. 2. Stable isotope record from core Volkanolog 34-91 at ~1,200 m water depth on Akademia Nauk Rise. Oxygen isotope results on the benthic foram Uvigerina and the planktonic N. pachyderma (s.) show that there is about 150 cm of Holocene section, with glacial maximum conditions deeper than ~200 cm. Carbon isotope analyses of Cibicidoides from the glacial maximum level at this and many other locations are used in making the paleohydrographic section shown in Fig. 4.

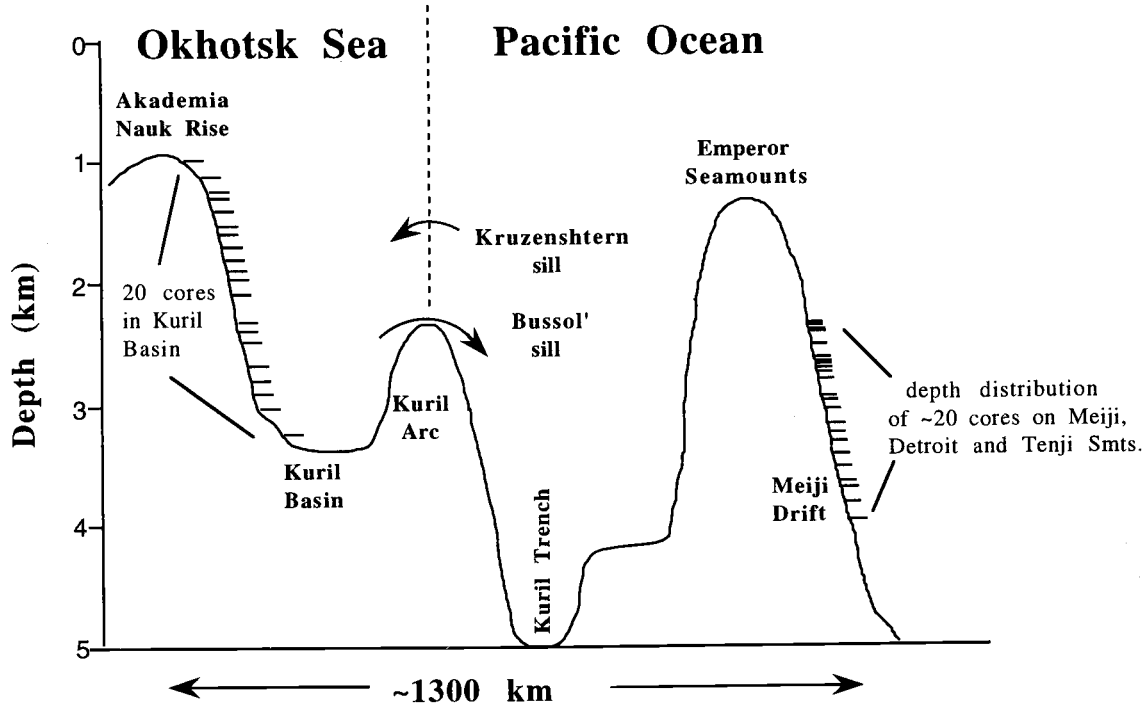

Fig. 3. A schematic diagram illustrating the physiography, circulation and distribution of some sediment cores in the Okhotsk Sea and on the northern Emperor Seamounts in the open Pacific Ocean.

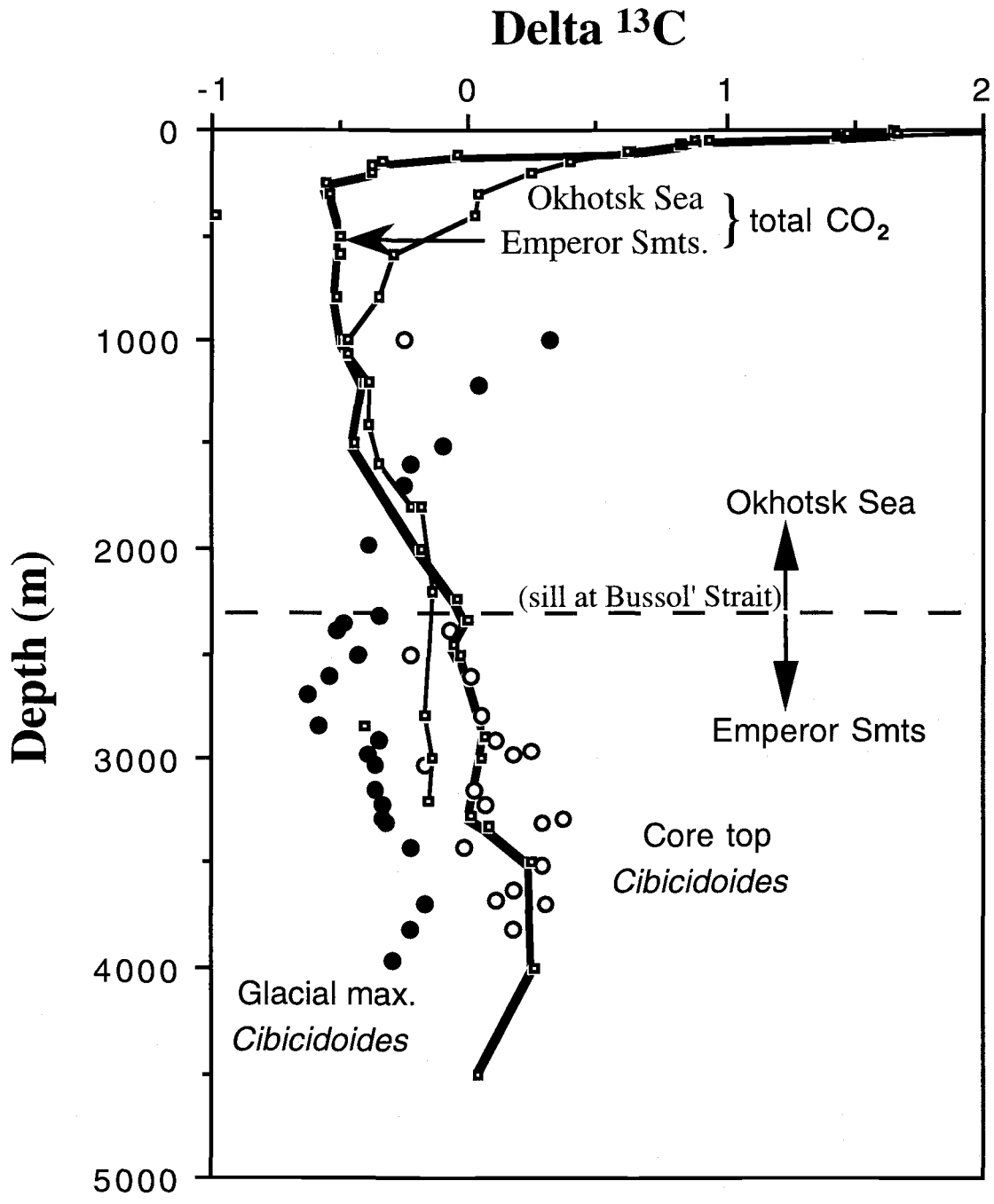

Fig. 4. Modern water column hydrography ($\delta^{13}C$ of total CO_2) in the Okhotsk Sea (thin line) and the open northwestern Pacific (thick line), compared to $\delta^{13}C$ of Holocene Cibicidoides (open circles) and glacial maximum Cibicidoides (filled circles). The paleohydrographic data depart from the modern circulation pattern above ~2,300 m, where $\delta^{13}C$ increases indicating better ventilation. The fact that this change occurs at about the sill depth of the Okhotsk Sea suggests that that sea may have been the source region.

Physical Mechanisms for the North Pacific Intermediate Water Formation

Talgat R. KILMATOV

Pacific Oceanological Institute, Far-Eastern Branch, Russian Academy of Sciences,
Vladivostok, Russia

1. The surface and subsurface fresh water sources for the North Pacific Intermediate Water (NPIW) formation are disposed in the Mixed Water Region between the Kuroshio and Oyashio Currents, especially at the Subarctic Front (SF). The analysis of the salinity fields across this region shows that the connection of the NPIW with surface waters occurs in the SF and this front is the southern border of the subarctic low salinity water distribution. This water moves to the southeast and downward to the intermediate depth in the subtropical part of the North Pacific.

The surface of the North Pacific subtropical zone loses about 40 cm of pure water every year as the result of evaporation. Assuming the low salinity water from the Subarctic Gyre compensates the superfluity of salt in the subtropical zone, the minimum fresh water transport is .5 S_v (10^6 m^3/s) to form the NPIW. The direct estimations of this transport give values of about 6 S_v (Talley and Nagata, 1995). The total volume of the NPIW is approximately $2*10^{6-7}$ km^3 (Kuksa, 1968), and thus its renewal time is 10-100 years. Based on the isotopic measurements the intermediate water longevity is about 10 years. These data clearly demonstrate that the NPIW is an important factor influencing the climatic change of the North Pacific on the time scales of 10-100 years.

The formation of the NPIW is due to the downwelling process. The Subarctic Front is a distinct downwelling zone where dynamic equilibrium keeps the climatic thermohaline front as a sharp border in temperature and salinity fields. In this work we will review several possible physical mechanisms of downwelling at the SF.

2. The Subarctic Front can be roughly described as the axis of the convergence. If the SF is regarded as the longitudinally-uniform thermohaline front, the density ratio ($\alpha\Delta T/\beta\Delta S$) is about 1 and the cross velocity on the convergence axis equals zero. The vertical component of the planetary vortex is the Coriolis parameter $f = 2\omega \sin\varphi = 0.43*10^{-4}\ s^{-1}$, ($\varphi \approx 40°N$), the horizontal component of the planetary vortex is $m = 2\omega \cos\varphi = 0.59*10^{-4}\ s^{-1}$. If the inertial and vorticity forces are balanced along the convergence axis, the following equation is correct (Pedlosky, 1979):

$$u(du/dx) + mw = 0$$

This equation shows that the planetary vortex produces the vertical motion on the convergence axis, and thus, turns the inertial velocity along the SF downward. The estimation of vertical velocity gives

$$w \approx u^2/(m \times L) \approx 10^2\, cm^2 s^{-2}/(5.9 \times 10^{-4}\, s^{-1} \times 10^3\, km) \approx 10^{-4}\, ms^{-1}$$

Besides, there is a link between the latitude advection and the convergence intensity at the climatic thermohaline front.

3. The thermohaline SF is the place of the intensive cabbeling process (Kilmatov and Kuzmin, 1990, 1991). The necessary condition of the downwelling due to the cabelling is $\alpha\ \Delta T/\beta\Delta S = 1$. The

changes in temperature and salinity in the upper layer across the Subarctic Front are $\Delta T \sim 4 \div 10°C$ and $\Delta S \sim 0.5 \div 1.5$ psu. The value of the cabelling can be estimated by the next formula:

$$\delta\rho \approx -0.125 * d^2\rho/dT^2 * \Delta T^2 \approx 0.125 * 10^{-5} g\ cm^{-3}\ °C^{-2} * 10^2\ °C \approx 10^{-4} g\ cm^{-3}.$$

As an example, distribution of basic hydrographic characteristics across the SF at the end of the cooling period is presented in Table 1. The maximum of water density is emphasized.

Cabelling reaches its maximum value in winter due to the favorable conditions (Kilmatov and Kuzmin, 1990). Thus, in the cooling period downwelling occurs at the front to some intermediate depth, where densities of the sinking and surrounding waters become equal. Hence, the cabelling effect in the upper ocean layer at the SF has an annual periodicity with the maximum during the winter. At that time the maximum convergence is observed at the front and its kinetic energy is transformed from the available potential energy of the cabelling process. The vertical velocity produced by the cabelling can be evaluated from the mechanical energy balance equation:

$$w \sim h_M L_M^{-1} (g\ h\ \delta\rho/\rho)^{0.5} \sim 10^2\ m\ (10^5\ m)^{-1} (10\ ms^{-2} * 10\ m * 10^{-4})^{0.5} \sim 10^{-4}\ ms^{-1}$$

4. The cyclic sinking of the ordinary portion of the upper water layer at the SF during winter due to the cabbeling assumes the "spotted" structure of waters in a horizontal direction at intermediate depths. Although the NPIW in the Mixed Water Region of the Kuroshio-Oyashio is characterized by complicated dynamic and thermohaline structure: the horizontal periodicity in values of salinity, temperature and dissolved oxygen at depth about 300 m is observed. The "spotted" structure in the core of the intermediate water mass with decreased salinity at a depth of 600-800 m is also found in the subtropical part of the North Pacific. The observations show that the core of NPIW in the horizontal direction consists of zones with closed isolines alternating at almost equal intervals of about 100-200 miles. Within these zones the decreased salt content takes place. The horizontal and vertical scales of zones are $\Delta L \sim 100$ km, $\Delta h \sim 100$ m, respectively.

Note, that the mechanism of formation of these zones does not exclude such elements as the synoptical deformation fields. In particular, storms, winter convection, ocean rings at the Mixed Water Region of Kuroshio - Oyashio lead to an increase of water exchange between the upper and intermediate waters. But the cabelling process occurs only at the Subarctic Front and it produces the downwelling.

REFERENCES

Kilmatov, T.R., and V.A. Kuzmin. 1990. The Pacific Subarctic Frontal Zone. Vladivostok, FEB RAS. 114 p. (in Russian).

Kilmatov, T.R., and V.A. Kuzmin. 1991. The Effect of Cabbeling and its Season Variations in the Subarctic Front. Izv. Akad. Nauk SSSR (ser. fiz. atm. i okeana). 27:883-887 (in Russian).

Kuksa, V.I. 1968. The Intermediate Waters in the World Ocean. Leningrad, Gidrometeoizdat, 271p. (in Russian).

Pedlosky, J. 1979. Geophysical Fluid Dynamics. N.Y., Springer-Verlag, 624p.

Talley, L.D. 1993. Distribution and Formation of North Pacific Intermediate Water. J. Phys. Oceanogr. 23:517-537.

Talley, L.D., Y. Nagata et al. 1995. North Pacific Intermediate Water in Kuroshio/Oyashio Mixed Water Region. J. Phys. Oceanogr. 25:475-501.

TABLES AND FIGURES

Table 1. Temperature, salinity and conditional density of seawater in the upper (0-5 m) ocean layer across the Subarctic Front along 152°E (April, 1980, R/V "Stepan Malygin").

φ^0 N	θ^0C	S $^0/_{00}$	σ_t	
43°52'	0,9	32,71	26,21	
43 41	0,8	32,66	26,18	
43 05	1,3	32,64	26,13	
42 30	1,8	32,65	26,11	
42 00	6,4	33,66	**26,45**	< SF
41 28	7,6	33,78	26,39	
40 30	9,0	34,04	26,39	
39 28	9,9	34,06	26,26	

Water Masses in the Okhotsk Sea

Vladimir A. LUCHIN

Far Eastern Regional Hydrometeorological Research Institute, Vladivostok, Russia

INTRODUCTION

The cold intermediate layer in the Okhotsk Sea was firstly distinguished by Makarov (1884). The water masses in this marginal sea has been described in details by Kitani (1986), Leonov (1960) and Moroshkin (1966). These surveys contain many illustrations and sufficient analysis of the previous studies. The water structure of the southern Okhotsk Sea has been discussed by Takizawa (1982) and Vakao and Kodzima (1962). The number of papers are devoted to the substantial contribution of the Kuril Straits in modification of the Okhotsk Sea water (Bogdanov, 1968; Bruevich et al., 1960; Leonov 1960; Moroshkin, 1966) and to the considerable influence of the Okhotsk Sea hydrological processes on the North Pacific water structure (Favorite et al., 1976; Kajiura, 1949; Kitani, 1986; Reid 1965; Tally, 1991; Wakatsuchi and Martin, 1991; Yasuoka, 1967).

DATA AND METHOD

The hydrographic (temperature and salinity) data collected at 51,607 stations during the period from 1930 to 1988 were analyzed and classified in times (by months) and in space (trapezia of 1 degree). To distinquish the Okhotsk Sea water masses the TS analysis method was applied and T-S curves were created for each 1 degree square.

RESULTS

The Okhotsk Sea water structure is formed under the influence of the Pacific water advection, fall-winter cooling, river run-off, water mixing in the regions of intensive dynamics, solar radiation as well as the system of the occurring currents. Fig. 1 strictly demonstrates four different water masses in the Okhotsk Sea: the surface layer, the cold intermediate layer, the deep Pacific water mass and near-bottom water mass of the southern (Kuril) basin.

The surface layer is distinquishable only in the warm period. In winter the boundary between the surface and cold intermediate water masses disappears. The influence of the Pacific water is clearly observed within the temperature field: due to the intensive tidal water mixing in the Kuril Straits the Pacific waters are the warmest in winter and the coldest in summer (Figs. 2a, b). The same effect takes place for the low temperature formations in summer near the Shantar Islands and at the entrance to Shelikhov Bay. The temperature anomaly over the Kashevarov Bank is the result of the water rising from below. The warm Soya current in the southern Okhotsk Sea is well pronounced in the summer season.

During the whole year the more saline Pacific waters penetrate into the Okhotsk Sea and fill in its southern and eastern parts. At the same time the coastal dilution is distinctly expressed in summer in the western part of sea: for instance, the influence of Amur river is observed for 100-150 miles from the northern tip of Sakhalin Island (Figs. 2c, d).

In the warm period the cold intermediate water mass can be revealed in the Okhotsk Sea. The distribution of basic temperature and salinity features are preserved in this layer during spring and summer, but the depth of the core location increases by 20-30 m in summer as compared with spring. The deepening of the upper boudary and core of the cold intermediate water mass continues in autumn. Fig. 3 demonstrates characteristics of the summer modification of the cold intermediate water mass. Temperature distribution in the core (Fig. 3c) indicates that the cold waters are transported southward in the western part of the sea. The water flow from the Cape of Terpenie to the southern tip of Kamchatka Peninsula is also distinquished. The intensive dynamic processes at the entrance to Shelikhov Bay promote formation of the positive temperature values here. The salinity isolines show the Pacific water inflow northward in the eastern part of the sea (Fig. 3d).

Fig. 4 presents properties of the deep Pacific water mass. The temperature maximum ($>2°C$) is observed in this water. The T-S distribution in the core suggests that the Pacific water moves from the Kuril Straits towards the Kashevarov Bank. The temperature within the core of the near-bottom water mass of the southern (Kuril) basin does not exceed 1.8-1.9°C and salinity varies from 34.6 to 34.7 psu.

The density (sigma-t) distributions in the cores of the Okhotsk Sea water masses are displayed in Fig.5. In accordance with our estimations density in the cold intermediate water mass varies from 26.0 to 26.75 sigma-t (near the Kuril Straits from 26.3 up to 26.75). In the deep Pacific water mass the density changes from 27.0 up to 27.4 sigma-t and maximum values are observed within the Central Kuril Straits. During the last decades the Okhotsk Sea region has been considered as one of the sources for the North Pacific Intermediate Water formation. Taking into account the water mass parameters (Figs. 2-5) together with the Okhotsk Sea current system (f.e., Luchin, 1995) we can conclude that on the way to the Pacific Ocean the cold intermediate waters from the northern Okhotsk sea (with density of 26.0-26.75 sigma-t) are blocked and transformed at least twice: first, in the anticyclonic circulation system over the southern basin and then within the Kuril Straits Region.

REFERENCES

Bogdanov, K.T. 1968. Hydrological conditions in the Freez Strait in summer period. Oceanological studies. 19:95-104.

Bruevich, S.V., A.N. Bogoyavlensky, and V.A. Mokievskaya. 1960. Chemical characteristics of the Okhotsk Sea. Trudy of Institute of Oceanology of USSR Academy of Sciences. 42:125-198 (in Russian).

Favorite, F., A.J. Dodimead, and K. Nasu. 1976. Oceanography of the Subarctic Pacific region, 1960-1971. Bull. Int. North Pacific Comm. 33:1-187.

Kajiura, K. 1949. On the hydrography of the Okhotsk Sea in summer. J. Oceanogr. Soc. Japan. 5:19-26 (in Japanese).

Kitani, K. 1986. Water mass structure in the Okhotsk Sea. Kaiyo Monthly. 18:93-98 (in Japanese).

Leonov, A.K. 1960. Regional Oceanography. Gidrometeoizdat, Leningrad. 766 p. (in Russian).

Luchin, V.A. 1995. System of currents and peculiarities of temperature distribution in the Okhotsk Sea. The Okhotsk Sea and Oyashio Region. PICES Scientific Report No. 2:211-227.

Makarov, S.O. 1894. R/V "Vityaz" and the Pacific Ocean. St.Petersburg. 505 p. (in Russian).

Moroshkin, K.V. 1966. Water masses of the Sea of Okhotsk. Nauka, Moscow. 65 p. (in Russian).

Reid, J.L. 1965. Intermediate Waters of the Pacific Ocean. Johns Hopkins Oceanogr. Studies. 2: 1-85.

Takizawa, T. 1982. Characteristics of the Soya Warm Current in the Okhotsk Sea. J. Oceanogr. Soc. Japan. 38:281-292.

Talley, L.D. 1991. An Okhotsk Sea water anomaly: implications for ventilation in the North Pacific. Deep-Sea Res. 38 (Supp. 1):S171-S190.

Wakao, M., and I. Kojima. 1962. On the oceanographical conditions in the southwestern region of the Okhotsk Sea. J. Hokkaido Fish. Exp. Sta. 18:1-25 (in Japanese).

Wakatsuchi, M., and S. Martin. 1991. Water ciculation of the Kuril Basin of the Okhotsk Sea and its relation to eddy formation. J. Oceanogr. Soc. Japan. 47:152-168.

Yasuoka, T. 1967. Hydrography in the Okhotsk Sea. Oceanogr. Mag. 19:61-72.

FIGURES

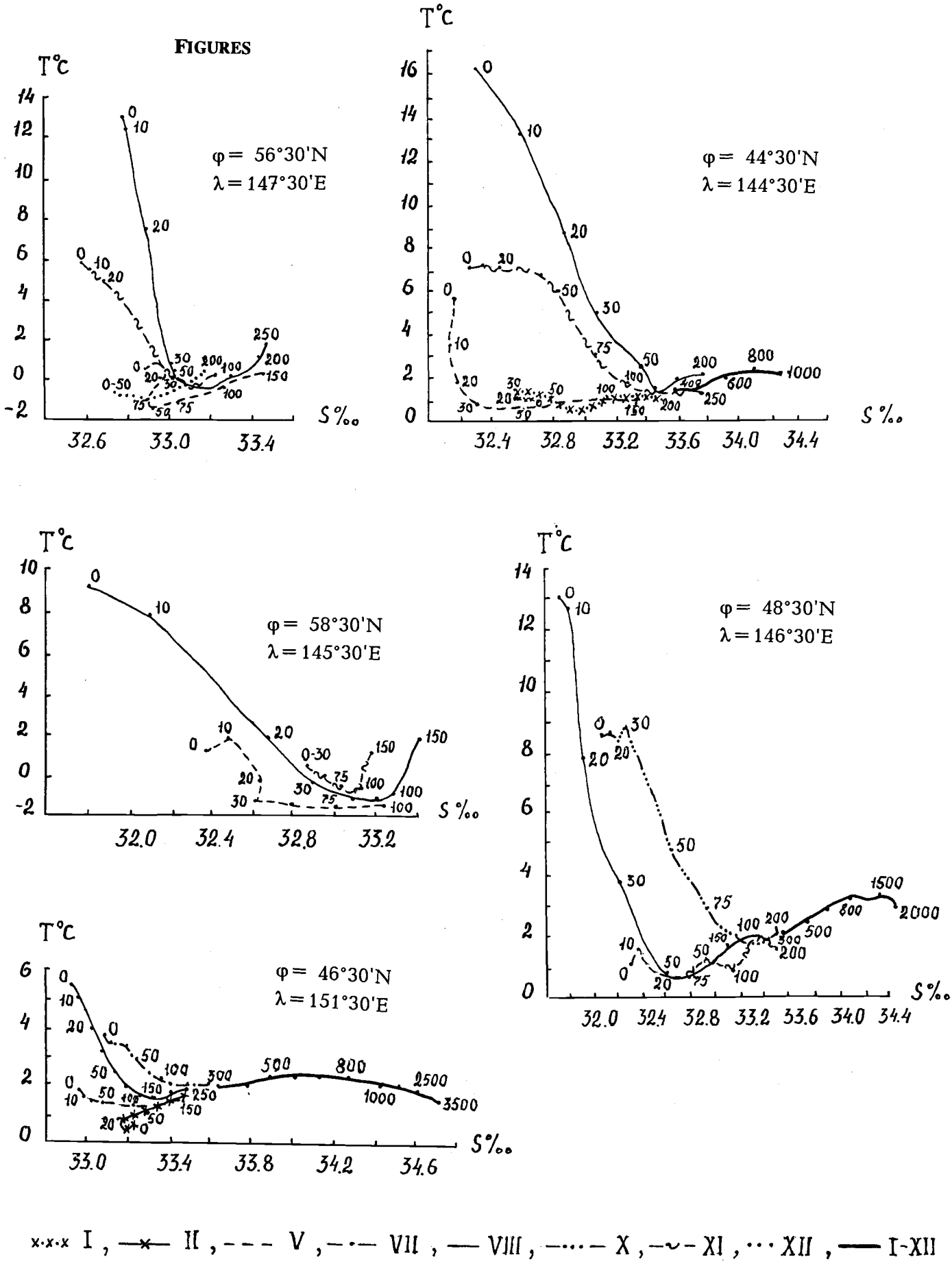

Fig. 1. Typical T-S curves for the Okhotsk Sea.

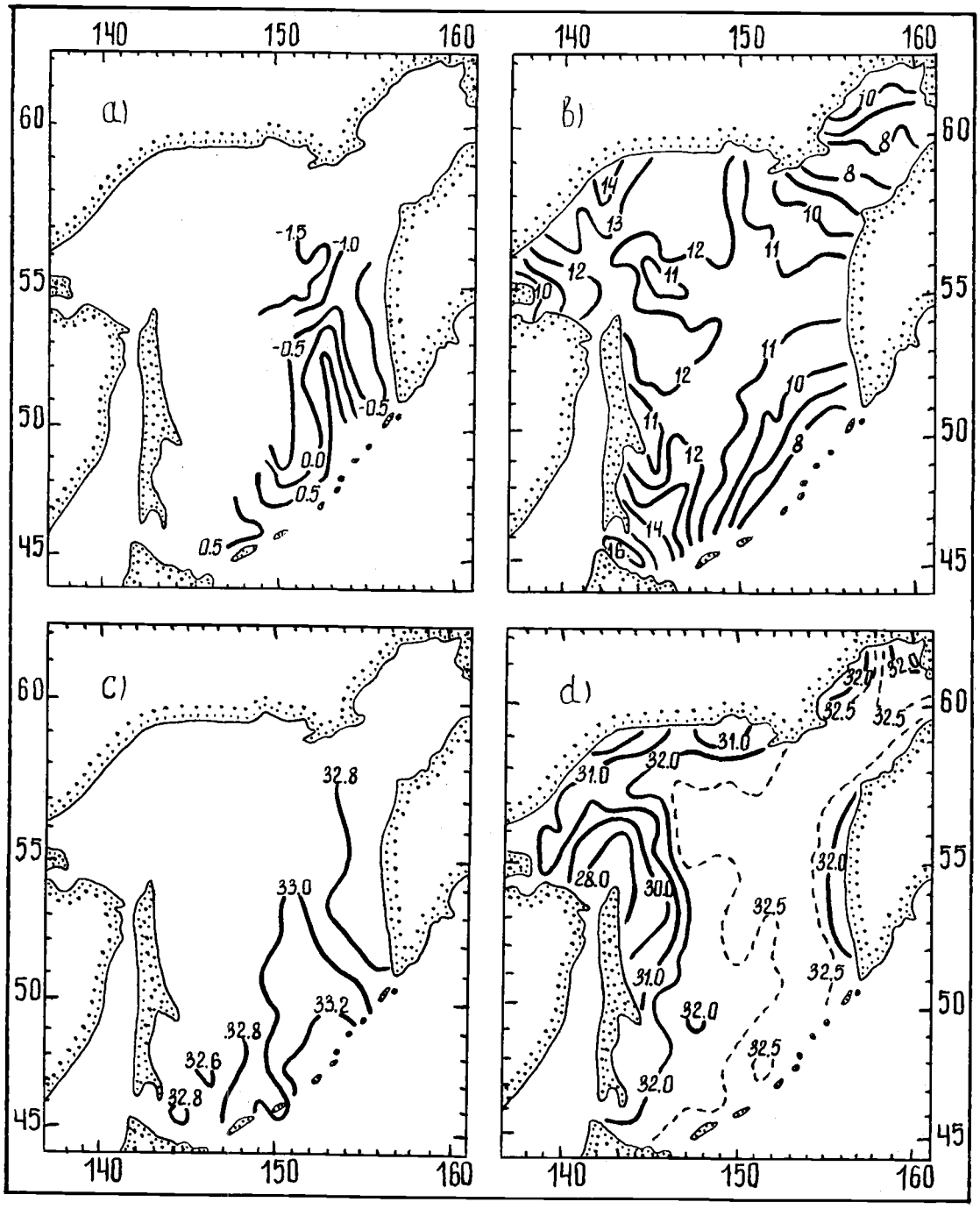

Fig. 2. Surface distribution of temperature (°C) (a - February; b - August) and salinity (psu) (c - February; d - August) in the Okhotsk Sea.

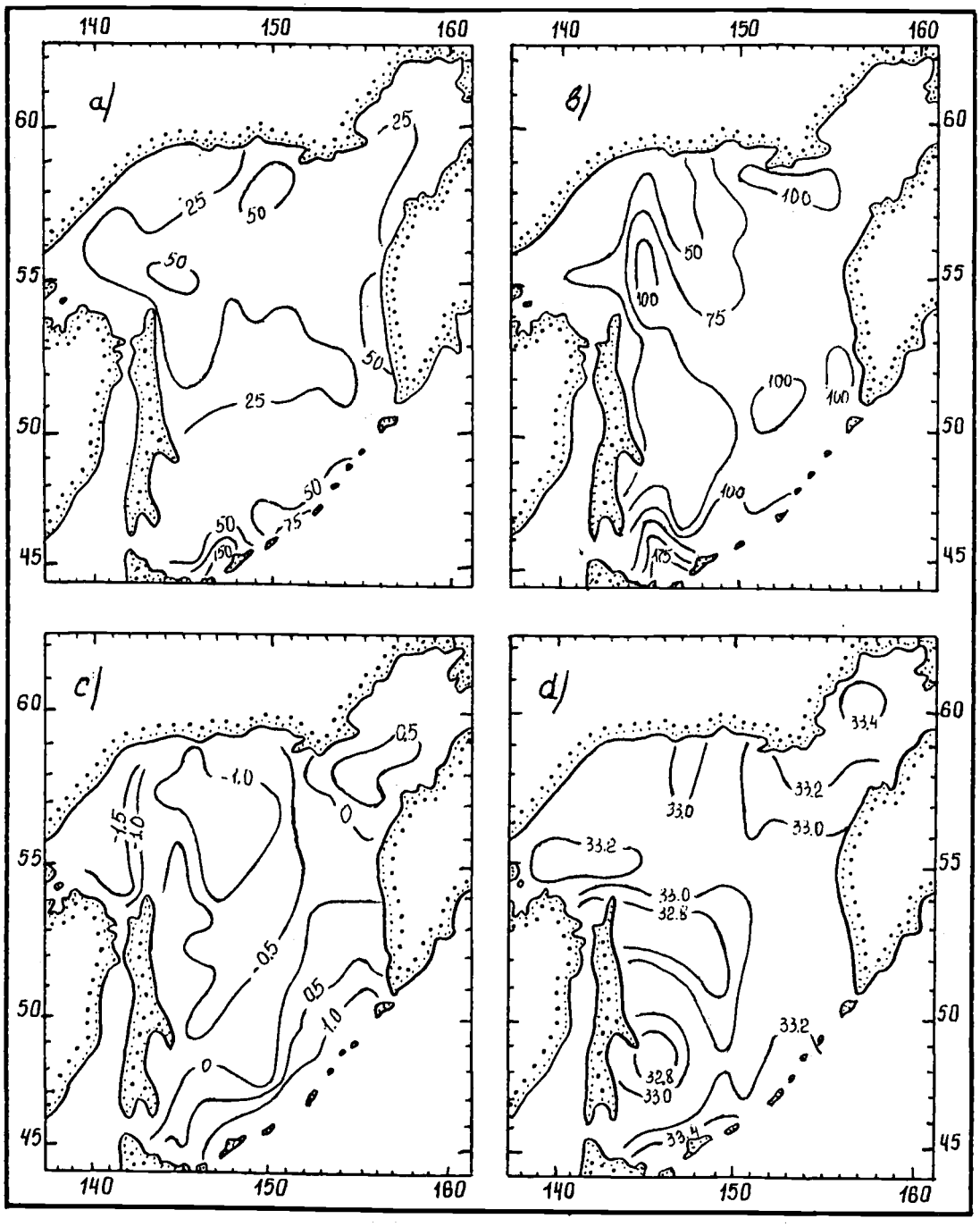

Fig. 3. Characteristics of the intermediate cold water mass (summer modification) in the Okhotsk Sea: a - depth of the upper boundary (m); b - depth of core location (m); c - core temperature (°C); d - core salinity (psu)

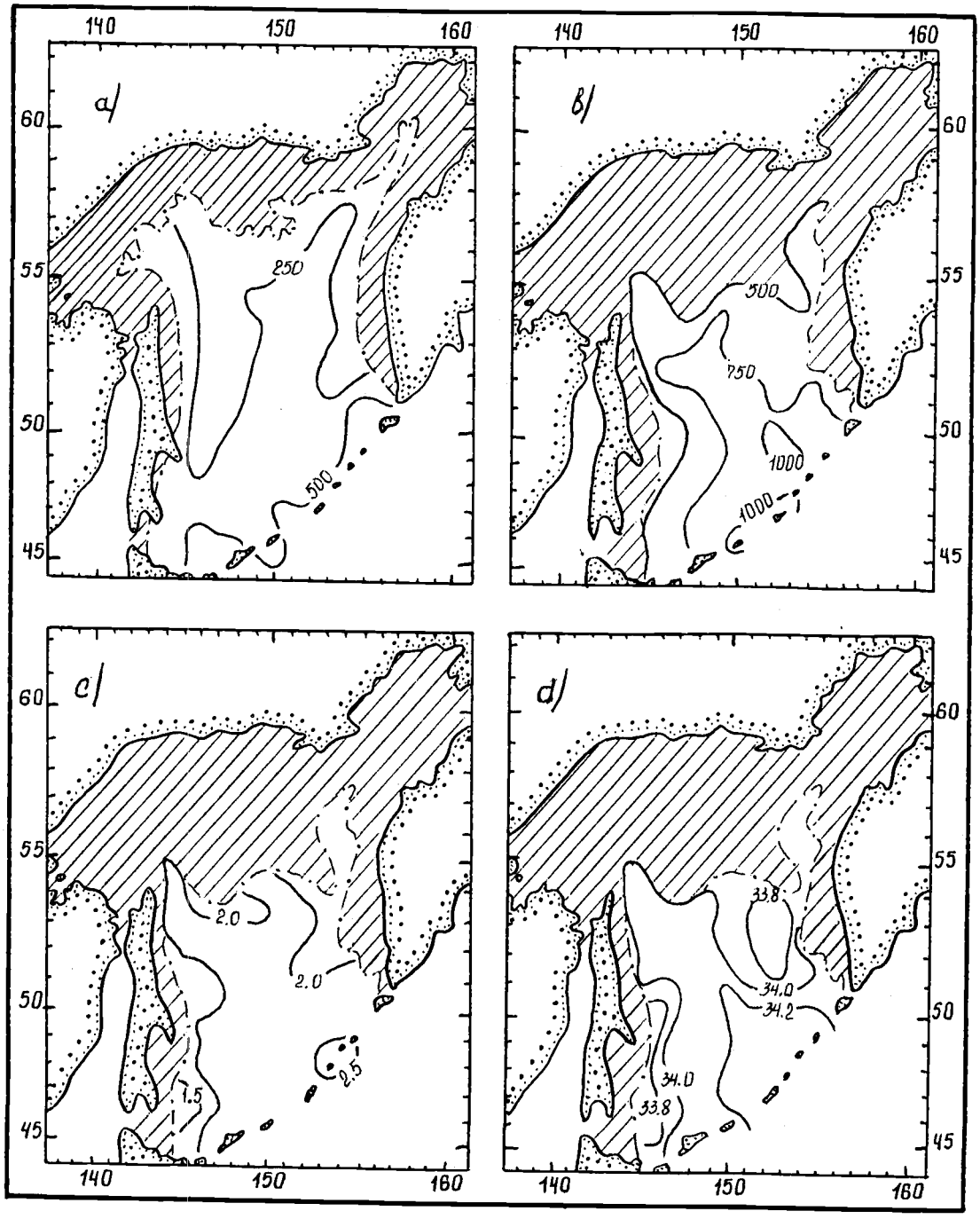

Fig. 4. Characteristics of the deep Pacific water mass in the Okhotsk Sea:
a - depth of the upper boundary (m); b - depth of core location (m);
c - core temperature (°C); d - core salinity (psu)

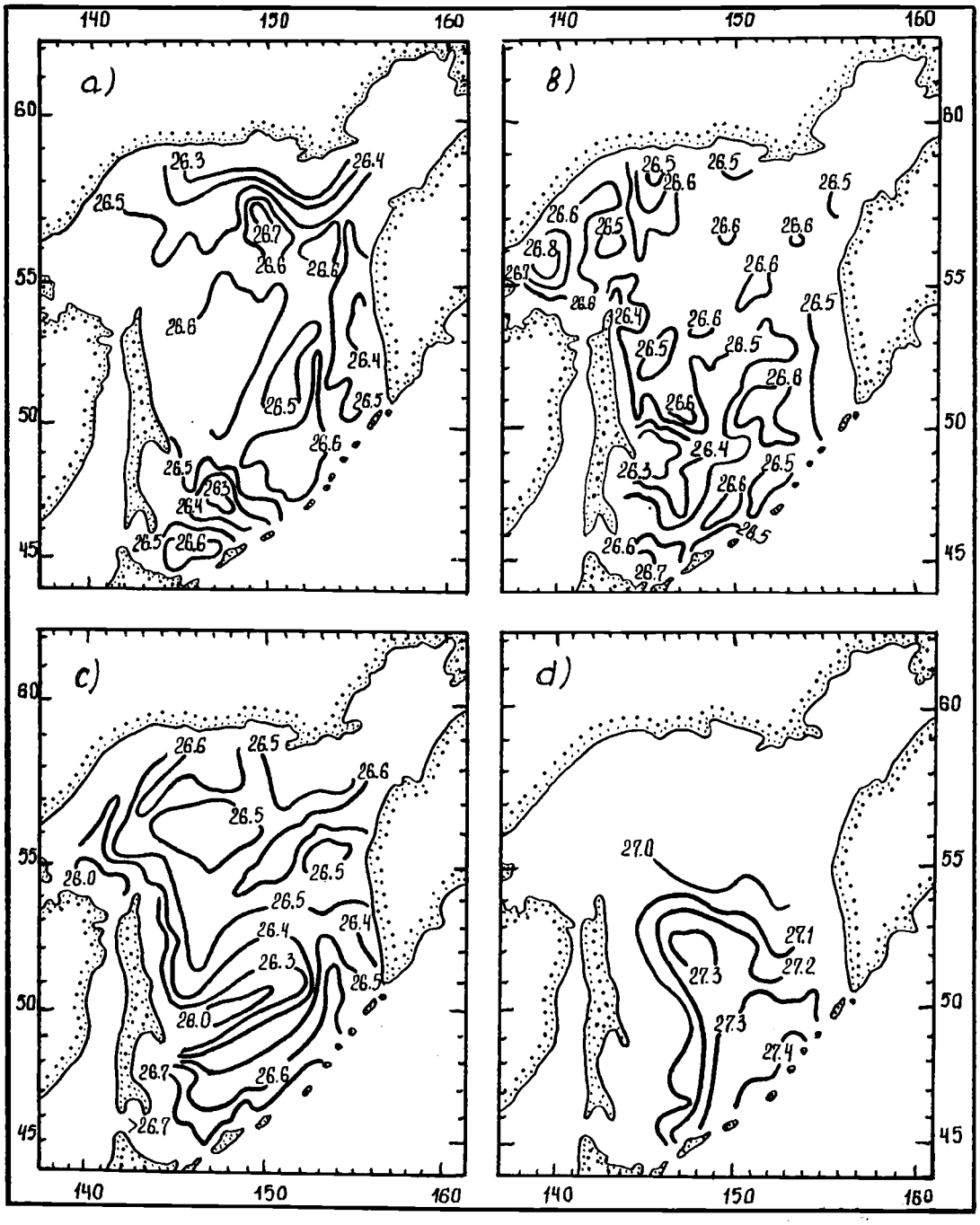

Fig. 5. Distribution of sigma-t in the cores of water masses in the Okhotsk Sea:
a, b, c - the intermediate cold water mass in spring, summer and fall respectively;
d - the deep Pacific water mass.

Numerical Experiments with Finite Element Model of the Okhotsk Sea Circulation

Andrey V. MARTYNOV, Elena N. GOLUBEVA and Victor I. KUZIN

Computing Center, Siberian Branch, Russian Academy of Sciences, Novosibirsk, Russia

INTRODUCTION

In the recent years the coastal areas and marginal seas of the World ocean attract the attention of oceanographers. This interest derives from the fact that these regions are of exceptional importance for the earth's climate and from the point of view that the overwhelming majority of nations' marine activities are performed within 200 mile Exclusive Economical Zones. This special interest did not exclude scientists working in the numerical modeling of oceanic processes. Some well known general ocean circulation models were used as regional models to investigate the circulation of the Greenland and Norwegian Seas (Legutke, 1991), the South China Sea (Shaw and Chao, 1994), the Japan Sea (Holloway et al., 1995), etc. The Okhotsk Sea is the object of the present study.

The general circulation of the Okhotsk Sea consists of a large cyclonic gyre which begins with surface and subsurface northward flow of the North Pacific water through the Kruzenshtern Strait along the Kamchatka Peninsula (the West Kamchatka current), then curves to the northern part of the Okhotsk Sea and flows south along the Sakhalin Island as the Eastern Sakhalin current. The existence of counter currents with the same names one is mentioned for both cases in some recent references (e.g., Zhigalov and Figurkin, 1994). Main features of the current system are the Oyashio inflow through the northern straits and its outflow through the central straits. The warm Soya current inflows through the Soya strait in the southern part of the Okhotsk Sea, comes along the Hokkaido Island and outflows through the Kunashiri strait (Leonov, 1960; Luchin, 1987).

The air circulation above the Okhotsk Sea has a monsoon character which is controlled by the interconnection of the main high and low pressure centers above the mainland and adjacent sea regions during winter and summer. Strong northerly geostrophic winds dominate during the winter monsoon and weak winds from the opposite direction are more typical for the summer monsoon. Investigation of the Okhotsk Sea water circulation response to the seasonal variability of the wind stress in the region is the primary goal of the present study. Analogous numerical experiments were performed by Sekine (1990). The main distinctions of that study from the above mentioned work are connected with some differences in the model formulation. We used different bottom topography as well as wind stress data.

The 3-D ocean general circulation model of the Novosibirsk Computing Center (1986) is adapted to the Okhotsk Sea. This model was earlier applied for the Kuroshio region (Kuzin et al., 1992). The bottom topography used in the model is presented in Fig. 1. The horizontal grid size is 0.25°. The study region covered the entire Okhotsk Sea with the exception of the shelf region with depths less than 30 m.

WIND STRESS DATA

Wind stress is one of the major factors determining the strength of the surface currents. The model was forced using both the monthly climatological wind stress data of Wright (1988) and the seasonal wind stress data prepared based on the same source. These data are sparse and their coverage implies some uncertainty, nevertheless, they were used to increase the wind stress influence because of their higher values in comparison with the analogous data of Hellerman and Rosenstein (1983)(HR):

Source of wind stress data	WINTER		SPRING		SUMMER		AUTUMN	
	Vmax	Vmean	Vmax	Vmean	Vmax	Vmean	Vmax	Vmean
HR, 1983	1.76	1.23	0.38	0.18	0.32	0.18	1.29	0.90
Wright, 1988	2.63	0.92	1.30	0.41	1.32	0.75	2.91	1.65

* All values are in dyne/cm^2.

Numerical experiments were carried out for selected seasons and 12 months separately. The definition of seasons has no rigid "calendar" in this region where the first sea ice forms in November and covers up to 97% of the sea surface in March-April (Wakatsuchi and Martin, 1990). So, the winter period can continue in the Okhotsk Sea for 5-6 months.

The following approach was applied to select the seasonal wind stresses: winter and summer fields were estimated by averaging the monthly mean data of December, January, February, and June, July, August, respectively; spring and autumn fields were estimated by averaging the monthly mean data of April and May, and October and November, respectively. The selected averaging periods were used in order to correctly consider the impact of winds. According to the available wind stress data the winter monsoon begins in October and relatively stable strong northern and western winds are conserved during October and November (Fig. 2d). With the development of a high-pressure center over Siberia a wind stress field is reconstructed and northern winds prevail. The sea ice cover initially forms in northern bays and along the continental shelf. The position of the sea ice edge spreads southward under the influence of cold air coming from the north and due to transportation by the northerly wind. This wind is rather stable for three months but its influence on water circulation is less remarkable compared to the autumn because of the gradual decrease in the open water zone (Fig. 2a). The maximum area of ice is observed in March when transformation of the wind stress field to the summer monsoon begins and the western winds prevail. The influence of the sea ice cover is essentially during the whole spring season including May (Fig. 2b). To specify this influence in numerical experiments, no wind stress was imposed above the ice covered regions for both winter and spring. The mean location of the ice edge was defined from the Pacific Ocean Atlas (1974). A relatively stable southern wind is dominant during June, July and August (Fig. 2c). Mean and maximum (Fig. 2) estimates of the wind stress show that wind strength is higher in the autumn and winter periods, and it is weaker in spring and summer.

GENERAL DESCRIPTION OF THE MODEL

The governing equations of the model are primitive, written for the sphere of radius a in spherical coordinates (λ, θ, z) (z is directed from the surface to the bottom):

$$\frac{du}{dt} - (f-\gamma)v = -\frac{m}{\rho_0}\frac{\partial p}{\partial \lambda} + \frac{\partial}{\partial z}(k\frac{\partial u}{\partial z}) + F^{\lambda},$$

$$\frac{dv}{dt} + (f-\gamma)u = -\frac{n}{\rho_0}\frac{\partial p}{\partial \theta} + \frac{\partial}{\partial z}(k\frac{\partial v}{\partial z}) + F^{\theta},$$

$$\frac{\partial p}{\partial z} = g\rho,$$

$$m\left(\frac{\partial u}{\partial \lambda} + \frac{\partial}{\partial \theta}(v\frac{n}{m})\right) + \frac{\partial w}{\partial z} = 0,$$

$$\frac{dT}{dt} = \frac{\partial}{\partial z}(k_T\frac{\partial T}{\partial z}) + F^{T},$$

$$\frac{dS}{dt} = \frac{\partial}{\partial z}(k_S\frac{\partial S}{\partial z}) + F^{S},$$

$$\rho = r(T,S).$$

Initial and boundary conditions are:

t = 0: $\quad u = u^0, \quad v = v^0, \quad T = T^0, \quad S = S^0;$

at the ocean surface $z = 0$:

$$T = T_0, \quad S = S_0, \quad -\rho k\frac{\partial \vec{U}}{\partial z} = \vec{\tau}, \quad w = 0;$$

at the ocean bottom $z = H(\lambda,\theta)$:

$$\frac{\partial T}{\partial z} = \frac{\partial S}{\partial z} = 0, \quad k\frac{\partial \vec{U}}{\partial z} = -R_H\bar{\vec{U}}, \quad w = mu\frac{\partial H}{\partial \lambda} + nv\frac{\partial H}{\partial \theta};$$

at the solid boundary (all passages are closed in the current version of the model):

$$\frac{\partial T}{\partial \vec{N}} = 0, \quad \frac{\partial S}{\partial \vec{N}} = 0, \quad \vec{U}\bullet\vec{N} = 0, \quad \frac{\partial \vec{U}\cdot\vec{K}}{\partial \vec{N}} = 0;$$

where $\vec{N}$ and $\vec{K}$ are normal and tangential unit vectors to the surface G, respectively.

$$\vec{U}=(u,v), \qquad H\bar{\vec{U}} = \int_0^H \vec{U}dz,$$

The following notations are used in the above equations: t - time, H- depth; u,v,w - the velocity components by λ,θ and z, respectively; $n = 1/a$, $m = 1/(a\cdot\sin\theta)$, a - radius of the earth, $f = -2\omega\cos\theta$, $\gamma = m\cos\theta$, ω - angular velocity of the earth rotation, p - pressure, ρ - density deviation from the mean ρ_0 = const, R_H - drag coefficient; k,μ- coefficients of horizontal viscosity and turbulent diffusion, respectively, $\vec{\tau}$ -wind stress vector, $r(T,S)$ is a sea water function, T-

temperature, S - salinity, F^{λ} and F^{θ} - are the forms parameterizing subgrid turbulent momentum exchange:

$$F^{T,S} = m\left(\frac{\partial}{\partial\lambda}[\mu m\frac{\partial(T,S)}{\partial\lambda}]+\frac{\partial}{\partial\theta}[\mu\frac{n^2}{m}\frac{\partial(T,S)}{\partial\theta}]\right).$$

In system (1) the common notation is used for the time derivative:

$$\frac{d}{dt}=\frac{\partial}{\partial t}+mu\frac{\partial}{\partial\lambda}+nv\frac{\partial}{\partial\theta}+w\frac{\partial}{\partial z}.$$

The governing equations of the model were transformed by separations of the external and internal modes. Equations for the external mode were reduced by the rotor operation to the vorticity equation. This equation in terms of the stream function ψ was solved as a separate 2-D model during barotropic experiments.

$$(\frac{\partial}{\partial t}+R)m\Delta_{\mathrm{H}}\psi - rot((\zeta+f/\mathrm{H})\Delta\psi) = \mu(\Delta\mathrm{H}\zeta+2n^2\mathrm{H}\zeta)+F,$$

in which H is the depth of the sea and F is the wind stress source.

NUMERICAL EXPERIMENTS WITH BAROTROPIC MODEL

The simulation of seasonal situations for the general water circulation clearly shows the presence of cyclonic circulation in autumn (Fig. 3d) which corresponds the most known references listed in PICES report No.2 (1995). Simultaneously, the anticyclonic gyre is formed within the Kuril Basin. The cyclonic circulation is also revealed in winter, but only at the central part of the Sea (Fig. 3a). At the same time, two anticyclonic gyres appear to the north and south of the cyclonic one. Spring and summer distribution of the stream function (Fig. 3b and c) is smoother and does not represent the analogous large-scale formations with the exception of the small cyclonic gyre west off Kamchatka and anticyclonic circulation in the southern part of the Okhotsk Sea during the summer season.

The results of numerical experiments for 12 monthly mean wind stress fields (not presented in figures) suggest that the cyclonic circulation is formed under the influence of steady northern and north-western winds as a main feature of the Okhotsk Sea from October till April. This circulation is replaced by the anticyclonic one from April till September, but its intensity is several times weaker. The Eastern Sakhalin current is expressed best of all in December.

Some other characteristic quasi-stationary features were obtained in the northwestern part of the Okhotsk Sea, west off the Kamchatka Peninsula and north off Hokkaido. In particular, the last two circulations are very important because of their significant influence on the strength of the West Kamchatka and the Soya Currents. The change in rotation is observed during the annual cycle for both cases. The first medium scale circulation is formed near the entrance to Shelikhov Bay. There is the cyclonic eddy at this location which enhances the West Kamchatka Current for June, July and August. The anticyclonic rotation is typical for an eddy situated at the same location from December till May. As a result the intensification of the counter current with the opposite direction (from north to south) is observed west of Kamchatka. In the southern part of the Okhotsk Sea the cyclonic eddy induces the enhancement of the warm Soya current from November till March. The existence of similar cyclonic eddies north off Hokkaido coast has been reported on the basis of the radar imagery data collected during 1969-1988 (Wakatsuchi and Ohshima, 1990). The anticyclonic eddy occurring near the same

location promotes the weakening of the Soya current and decreases the intensity of the western boundary circulation during the period from April till October.

NUMERICAL EXPERIMENTS WITH 3-D MODEL

At the next stage of the study the density stratification was included in the model which has 21 vertical levels. Shelihova Bay was excluded from the domain as temperature/salinity data for this region are not available. The climatological temperature and salinity distributions for summer were used in the initial conditions. These data were prepared on the basis of all observations accessible at the Far Eastern Regional Hydrometeorological Institute, Vladivostok, Russia (V. Luchin, personal communication). The model was spun up by the summer wind stress field prepared on the basis of the monthly mean stresses of Wright (1988). At the diagnostic stage the numerical integration was made with a 15 minute time step. According to the control of the total kinetic energy the equilibrium state was attained after 20 days of model time. The adaptation calculations with the whole system of equations were carried out for another 30 days. Some preliminary results are presented below.

The Ekman drift dominates the flow in the upper layer from the surface to about 30 m. There is no obvious cyclonic circulation on the whole. Although the structure of currents is very complex, some main features of the Okhotsk Sea general circulation are revealed. The north periphery of the anticyclonic gyre above the Kuril Basin is well-developed but the gyre is divided into several cyclonic and anticyclonic eddies. The Eastern Sakhalin current begins to appear below 50 m, it spreads southward to about 50°N, the West Kamchatka current flows north of about 55°N, and strong anticyclonic eddy extends from the upper layers to the bottom near the Kashevarov Bank north of Sakhalin Island. An intense stream in the southern part of the Okhotsk Sea is artificial. The appearance of this simulated stream is connected, probably, with extrapolation of initial data to the southern part of the domain and can not be recognized as the Soya Current directly. Also the formation of two eddies, exactly in the central part of the Sea, is induced by data discrepancy in this region (initial temperature/salinity fields did not smooth to test the model sensitivity for different instabilities).

DISCUSSION

The obvious dependence of the general Okhotsk Sea water circulation on the wind stress field is considered in the present investigation. The reconstruction of atmospheric conditions from the winter monsoon to the summer monsoon induces the essential changes of the whole current system in the region. But this alteration embraces only thin the upper 20-30 meters layer. Some characteristic features of the general circulation and its variability in the annual cycle are obtained in this layer during numerical experiments with the barotropic model. At the second stage of our research some interesting features of the vertical structure of the Okhotsk Sea current system are simulated. For example, the Eastern Sakhalin current is well-developed in the subsurface layer (50-200 m). This current can transport the water generated in the northern part of the Okhotsk Sea far to the south.

Preliminary presentation of in-flow and out-flow through the passages is proposed at the next stage of this study. Winter observations are very sparse even in the open water regions, but during future experiments we hope to prepare some climatic winter fields for comparison with the summer season.

ACKNOWLEDGMENTS

This study was started during Dr. A. Martynov's stay as a visiting scientist at the Institute of Ocean Sciences (Sidney, B.C., Canada). We appreciate the continuous support by Dr. Falconer Henry, Dr. Eddy Carmack and Dr. Mike Foreman. This work was partly supported by grant 93-05-8993 of the Russian Foundation for Basic Research.

REFERENCES

Hellerman, S., and M. Rosenstein. 1983. Normal monthly wind stress over the World ocean with error estimates. J. Phys. Oceanogr. 13:1093-1104.

Holloway, G., T. Sou, and M. Eby. 1995. Dynamics of circulation of the Japan Sea. J. Mar. Res. 53:539-569.

Kuzin, V.I., and E.N. Golubeva. 1986. Numerical modelling of the temperature and currents in the World ocean using finite element method, p. 137-150. *In* Numerical modelling of the World ocean climate. Computer Center Press. Novosibirsk. (in Russian).

Kuzin, V.I., E.N. Golubeva, and A.V. Martynov. 1992. Model of Kuroshio region circulation. Proc. of the Int. Symp. PORSEC-92, Okinawa, Japan. p.1281-1287.

Legutke, S. 1991. A numerical investigation of the circulation in the Greenland and Norwegian seas. J. Phys. Oceanogr. 21:118-148.

Leonov, A.K. 1960. The Sea of Okhotsk, NTIS AD 639 585. Natl. Tech. Inf., Spring-field, Va. 95 p.

Luchin, V.A.. 1987. Water circulation in the Okhotsk Sea and some features of its interannual variability on the base of the diagnostic calculations, in Oceanographic problems of the Far Eastern Seas. 36:3-13 (in Russian).

Pacific Ocean. 1974. Atlas of oceans.

Sekine, Y. 1990. A barotropic numerical model for the wind-driven circulation in the Okhotsk Sea. Bull. Fac. Bioresources, Mie Univ. 3:25-39.

Shaw, P.-T., and S.-Y. Chao. 1994. Surface circulation in the South China Sea. Deep-Sea Res. I. 41:1663-1683.

Talley L.D., and Y. Nagata [ed.] 1995. The Okhotsk Sea and Oyashio Region. PICES Scientific Rep. No. 2. 227 p.

Wakatsuchi, M., and S. Martin. 1990. Satellite observation of the ice cover of the Kuril Basin region of the Okhotsk Sea and its relation to the regional oceanography. J. Geophys. Res. 95(C8):13393-13410.

Wakatsuchi, M., and K.I. Ohshima. 1990. Observations of Ice-Ocean Eddy Streets in the Sea of Okhotsk off the Hokkaido coast using radar images. J. Phys. Oceanogr. 20:585-594.

Wright, P. 1988. An Atlas based on the 'COADS' data set: Fields of mean wind, cloudiness and humidity at the surface of the global ocean. Max-Plank-Institute for Meteorology/ Hamburg, Report 14.

Zhigalov, I.A., and A.L. Figurkin. 1994. Interannual variability of water dynamics in the Okhotsk Sea, p.75. Abstracts of the Third Annual Meeting of PICES in Nemuro, Japan.

FIGURES

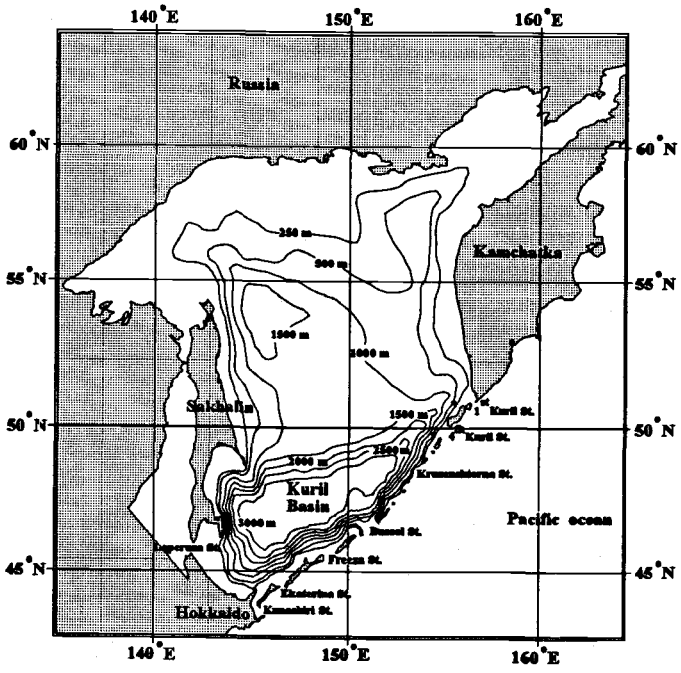

Fig. 1. A map of the Okhotsk Sea with bottom topography contours (in meters).

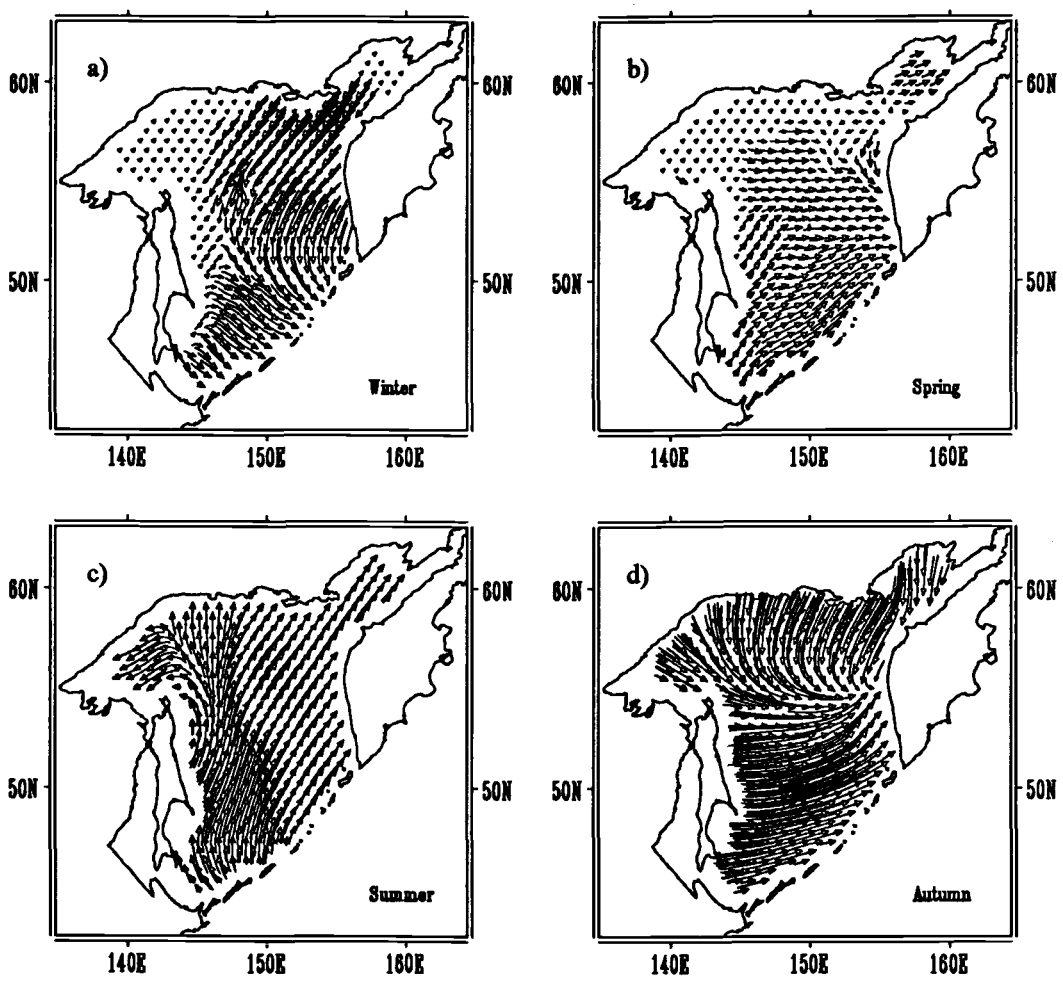

Fig. 2. Wind stress fields for: winter (a), spring (b), summer (c) and autumn (d).

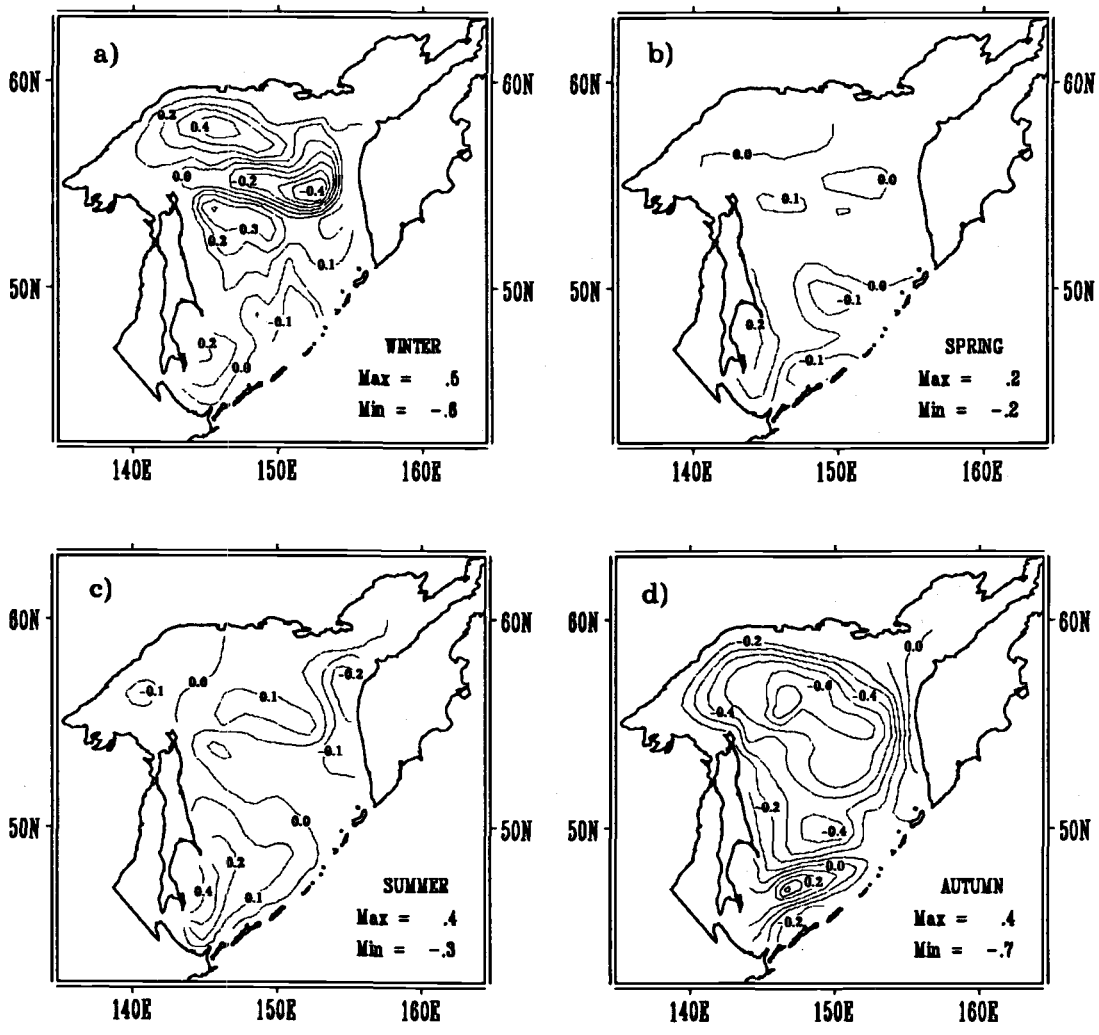

Fig. 3. Volume transport streamlines for winter (a), spring (b), summer (c) and autumn (d) Contour interval is 0.1 Sv (Sv: Sverdrup = $10^6 m^3 s^{-1}$). Real bottom topography.

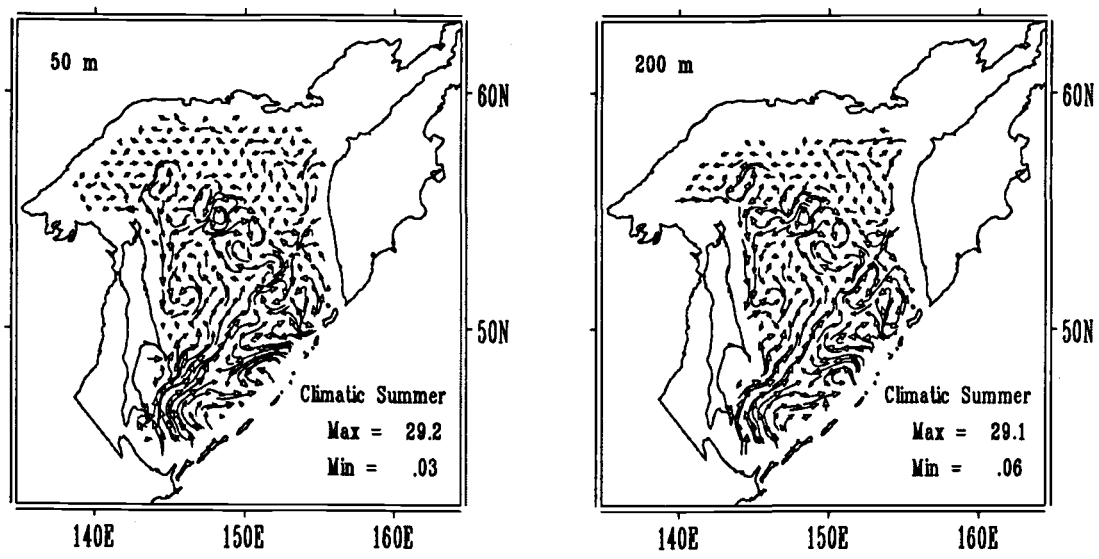

Fig. 4. Current velocity fields at 50 and 200 m after the adaptation. Real bottom topography.

Structure of Intermediate Water Layer in the Northwest Pacific

Nikolay A. MAXIMENKO, Anatoly I. KHARLAMOV and Raissa I. GOUSKINA

Institute of Oceanology, Russian Academy of Sciences, Moscow, Russia

Data collected during Japanese surveys in the northwestern Pacific (Fig. 1) were used to investigate the spatial structure and seasonal variability of the North Pacific Intermediate Water (NPIW) (Talley, 1993). The corresponding information for about 1,300 hydrographic stations in the area contoured by 30-50°N and 140-155°E was published in "The Results of Marine Meteorological and Oceanographic Observations" in 1970-80's. We revealed that although the depth of the salinity minimum and water properties at that depth express significant temporal variations (connected, probably, with eddies activity) their spatial structure is quite stable. The NPIW layer outcrops around 40-42°N where salinity, temperature, potential density and oxygen content are equal to 33.3 psu, 5°C, 26.5 sigma theta and 6.9 ml/l, respectively.

Two principal results were obtained from the general analysis of these data:

1. Spatial variability along the latitude of 41°N did not exceed the accuracy of measurements as well as no reliable difference has been found between sections along 144°E, 148°E and 150°E.
2. Seasonal variability beneath the depth of 100 m was not identified (it was also below the data accuracy).

In the meridional direction the NPIW layer deepens southward to a depth of 800 m at 30°N where the salinity, temperature and potential density reach 34.1 psu, 6.2°C and 26.95 sigma-theta, respectively, but concentration of dissolved oxygen drops to 3.0 ml/l. Typical standard deviations of those parameters are equal to 30 m, 0.03psu, 0.2°C, 0.03 sigma-theta and 0.3 ml/l. Thus, within the NPIW all characteristics are variable and, hence, the layer cannot be traced by any fixed iso-surface (e.g., isohaline or isopycnal). The only distinct tracer of the NPIW is a salinity minimum at an intermediate depth.

The following features of the NPIW layer structure have been determined from the detailed analysis of data along 155°E between 45°N and the equator (Fig. 1):

a) The NPIW outcrops again at 7-8°N around the Subtropical Front (Fig. 2a);
b) At the southern edge of the NPIW layer salinity and temperature increase (Figs. 2b and c), whereas the content of dissolved oxygen and potential density (Figs. 2d and e) decrease southward;
c) Curvatures of vertical salinity (Fig. 2f) and temperature (Fig. 2g) profiles are positive everywhere and express the highest values at the southern and northern edges of the NPIW layer, while the curvature of the dissolved oxygen profile (Fig. 2h) is much noisier and at any latitude it has readings of both signs.

These data were also used to investigate kinematic and dynamic properties of the NPIW layer. Important for our consideration is the fact that the stationary solution of the diffusion equation for salinity may not contain internal extremes without intrusions of "new" water from the boundaries. Since the salinity vertical profile has a minimum in the middle of the layer, the value of this minimum grows towards the equator and the curvature is positive everywhere, we anticipate southward water flow along 155°E.

Mathematically this can be expressed in the following way. Using the above conclusions 1 and 2 (stationary and weak spatial variability of the NPIW layer structure), full equations of salinity, temperature and dissolved oxygen evolution may be presented as

$$V \times S_Y = k_S \times S_{ZZ} \,, \tag{1}$$

$$V \times T_Y = k_T \times T_{ZZ} \,, \tag{2}$$

$$V \times O_Y = k_O \times O_{ZZ} - q, \tag{3}$$

where y- and z-axis are parallel and normal, respectively, to the NPIW layer (traced as a salinity minimum), V is velocity component along y-axis, k_i is corresponding diffusion coefficient, expected to be positive (below we will suggest that effective mixing processes in the NPIW are governed by turbulence and all the k-coefficients are of the same magnitude), q is dissolved oxygen dissipation rate due to biological and chemical processes (also expected to be positive). Thus (1-3) may be rewritten as

$$V / k = S_{ZZ} / S_Y = T_{ZZ} / T_Y = O_{ZZ} / O_Y - q / O_Y \tag{4}$$

and the two last equations of (4) may be checked from the data. A good correspondence between S_{ZZ} / S_Y and T_{ZZ} / T_y and significant difference between S_{ZZ} / S_Y and O_{ZZ} / O_Y were revealed (Fig. 3), that can be explained by a large positive q. Roughly Fig. 3 provides an estimate for meridional velocities

$$V \approx -1 cm^{-1} \times k \tag{5}$$

that gives 1 cm/s for typical value of $k =$ 1 cm^2/s and should be directed everywhere towards the equator.

Thus, we may conclude that the source of a "new" NPIW is located at the southern edge of the layer. The NPIW has a tendency to shift equatorward and must outcrop and "die" at the Subtropical Front. This event was observed by Bingham and Lukas (1994), but the mechanism is not clear yet. Of course, meridional motion should be superimposed on the general large-scale circulation in the North Pacific, however some results suggest that this effect is not so strong (Kilmatov and Kuzmin, 1991).

Our attempts to investigate physical mechanisms of the NPIW formation and dynamics (Maximenko et al., 1995) revealed that the local geostrophic balance can be disturbed by vertical (diapycnal) mixing that in the case of tilted isopycnals will push water particles quasi-isopycnally up or down towards a new geostrophic equilibrium. From traditional 2D dynamic equations we can derive for meridional velocity

$$V = -g \times \tan\Theta \times \rho_t / (\rho_o \times f^2) \tag{6}$$

where g is the gravitational constant, Θ is tilt of isopycnals, f is the Coriolis parameter, ρ_o is seawater density and ρ_t is evolution rate in time. Depending on sign of ρ_t water should sink or rise, what we really observe in the NPIW layer.

Values of ρ_t for the section along 155°E (calculated as a local evolution of ρ_o due to vertical mixing of temperature and salinity) were found to be in good correlation with Figs. 2a and 2e: ρ_t has the same sign as the tilt of isopycnals. Again if k is estimated as 1cm^2/s, V is equal about 1 cm/s and is directed towards the equator.

Quite unexpected results have been obtained from our investigation of the cabbeling effect on NPIW dynamics. We developed an original formal mathematical description of cabbeling rate that for the salinity minimum layer can be written as

$$\rho_t^{cabb} = -\rho_{TT}(T_z)^2 \quad (7)$$

We found that the cabbeling effect is significant everywhere in the NPIW layer and its contribution to local density evolution reaches 30%. That means that analysis of the NPIW should be based on the exact nonlinear equation of state.

ACKNOWLEDGMENTS

This study was supported by grant NDY000 of the International Science Foundation, grant 95-05-14907 of the Russian Foundation for Basic Research, grant NDY300 of the International Science Foundation and the Russian Government, and is a part of the International Research Project "Drifter Investigation of the North-Western Pacific Surface Circulation" supported by the Ministry of Science of the Russian Federation.

REFERENCES

Bingham, F., and R. Lukas. 1994. The southward intrusion of North Pacific Intermediate Water along the Mindanao coast. J.Phys.Oceanogr. 24:141-154.

Kilmatov, T.R., and V.A. Kuzmin. 1991. Cabbeling effect under mixing of seawaters and its seasonal appearance at the North Pacific Subarctic Front. Izvestia Acad. Sciences of USSR (Physics of Atmosphere and Ocean). 27:883-887 (in Russian).

Maximenko, N.A., T. Yamagata, and K. Okuda. 1995. Frontal convection in the Kuroshio and Subarctic Front. Oceanologia. (in Russian, accepted).

Talley, L.D. 1993. Distribution and formation of North Pacific Intermediate Water. J. Phys. Oceanogr. 23:517-537.

FIGURES

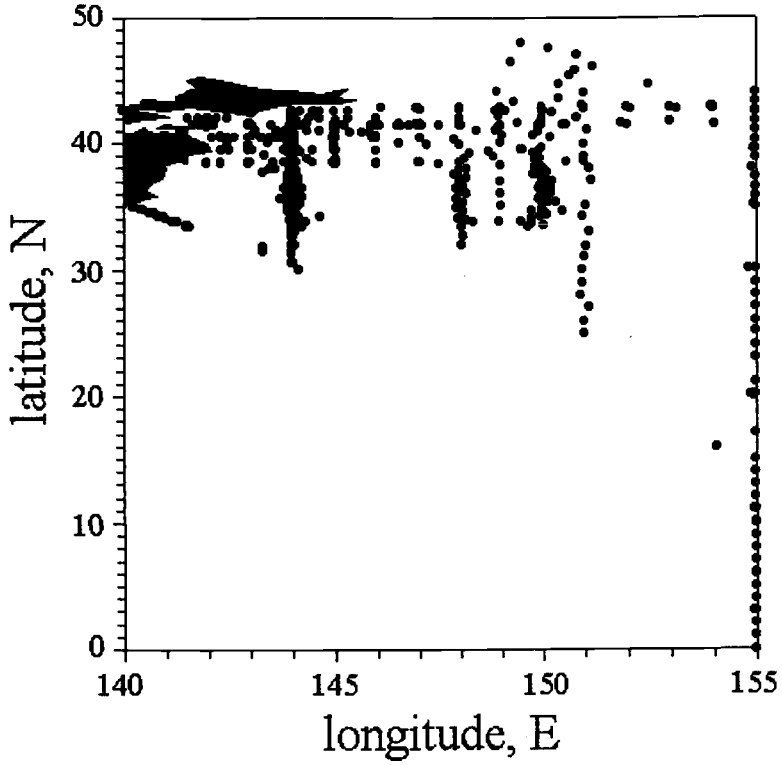

Fig. 1. Location of hydrographic stations used for analysis.

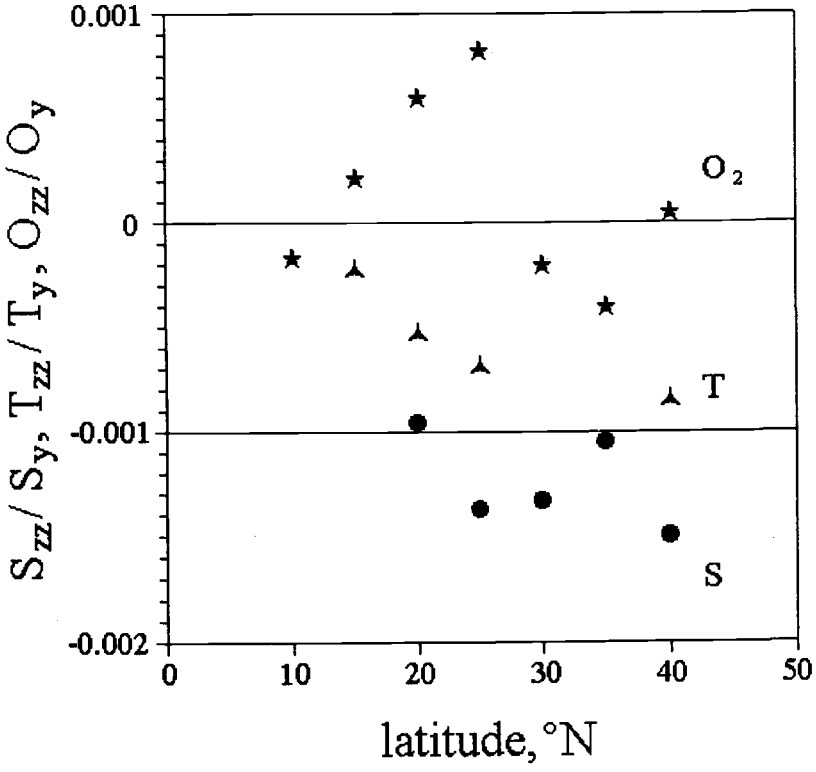

Fig. 3. Meridional distribution of S_{zz}/S_y, T_{zz}/T_y and O_{zz}/O_y calculated from hydrographic data along 155° E.

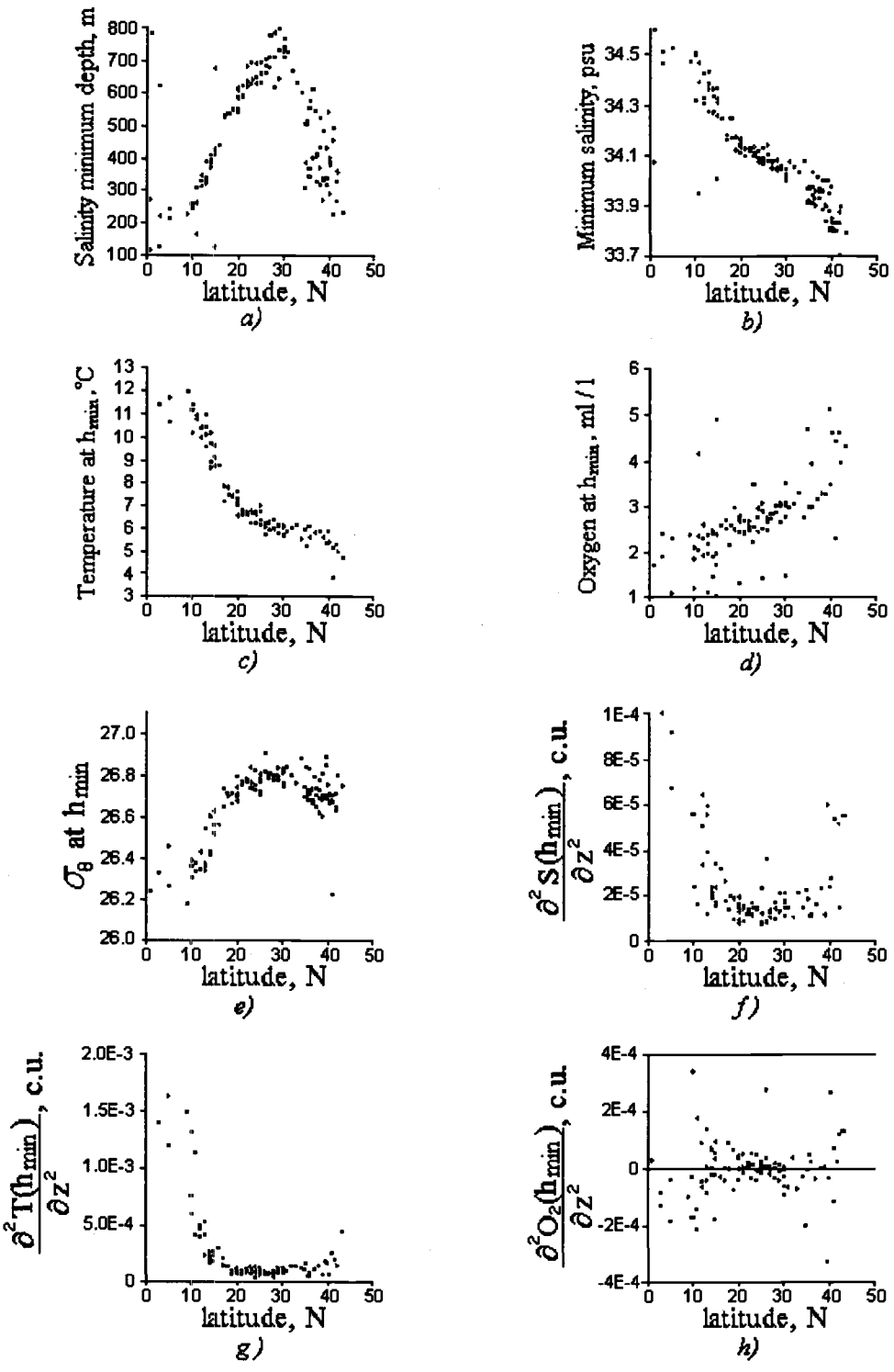

Fig. 2. Distribution of the depth of salinity minimum in the NPIW layer (a), minimum salinity (b), and temperature (c), dissolved oxygen content (d), potential density (e) and corresponding second vertical derivatives (f - h) at the depth of salinity minimum along 155°E .

Fine-structure of the North Pacific Intermediate Water Layer

Nikolay A. MAXIMENKO and Andrey Yu. SHCHERBINA

Institute of Oceanology, Russian Academy of Sciences, Moscow, Russia

INTRODUCTION

The North Pacific Intermediate Water (NPIW), characterized by an obvious salinity minimum and slight increase of dissolved oxygen concentration, is observed within the latitude range 10-40°N (Yang and Nagata, 1992). This layer outcrops at its border contouring the area of the Subtropical water mass distribution. In the north the NPIW is limited by the Subarctic Front (SF). The concept of the NPIW formation by waters of the Okhotsk and Japanese Seas (Yang and Nagata, 1992) coexists with the hypothesis of its role as an interface between the Subtropical and Subarctic water masses (Burkov, 1972). The search for a possible physical processes governing the NPIW formation and evolution is under way.

Role of cabbeling in the frontal zone has been investigated by Kilmatov and Kuzmin (1991). In accordance with Talley (1993), at a narrow front cabbeling breaks the pre-existing geostrophic equilibrium and forces the layer to slip down isopycnically to recover the balance. The proposed mechanism is expected to be the most efficient in the upper ocean at sharp fronts. Data collected from the section along 155°E demonstrated that the dynamics of the NPIW layer in the central and southern parts is determined by the diapycnal (vertical) heat and salt mixing and resulted in an equatorward drift of the layer, superimposed on a subtropic gyre (Maximenko et al., 1995).

DATA

We analyzed numerous CTD data of the "Megapolygon" experiment conducted in the summer-fall period of 1987 in the 500 x 500 km area centered at 40°N and 155°E (Ivanov, 1992). To decrease the effect of the probe calibration, as well as to exclude mesoscale variability of various fields, our primary attention was paid to long longitudinal sections carried out by the same vessel. The section along 152°E, carried out by *R/V "Vityaz"* in October 1987 with 20 miles resolution, is a good example and is discussed below.

RESULTS AND CONCLUSIONS

At least three sub-mesoscale objects are disclosed within the NPIW layer which is clearly seen as a salinity minimum (Fig. 1). These objects are characterized by negative salinity and temperature anomalies of 0.1 psu and 0.6°C, respectively. The horizontal (in the meridian direction) diameter of the anomalies does not exceed 40 miles occupying depths of 200-400 m. Analysis of vertical profiles of 1 m resolution revealed well developed fine-structure inside the mesoscale anomalies mentioned above. Temperature and salinity pulsations are as much as 5-10 times higher than in surrounding waters (Fig. 1). Vertical profiles of water properties at one specific station are shown in Fig. 2. Note, that pulsations of T and S, reaching 0.1 psu and 0.6°C, respectively, do not influence the stability of

stratification, which can be explained by their good inter-correlation (Fig. 3). The vertical scale of the pulsations varies from 1 to 60 meters.

We have discovered that in the horizontal plane the anomalies look like isolated intra-thermocline lenses. Within the "Megapolygon" area we observed simultaneously 3 to 5 such lenses associated with negative temperature and salinity anomalies, each being 40 miles or less in diameter. The actual number of the anomalies could be even greater as not all of them were resolved by the sampling grid. The typical scale of horizontal coherence of T and S pulsations was close to the distance between the stations (20 miles).

Fig. 4 displays the Cox numbers (< > sign shows averaging over the 200 m layer centered at the salinity minimum depth) calculated along the Section as

$$C_T = \frac{< (\nabla T')^2 >}{< \nabla T >^2}, \quad C_S = \frac{< (\nabla S')^2 >}{< \nabla S >^2} \tag{1}$$

C_T exceeds C_S by 1.4 times almost everywhere in the NPIW. Assuming that molecular diffusion plays the leading role at the finest resolved scale and that the mixing process at the larger scale is governed by developed turbulence, we can estimate the turbulent diffusion coefficients as $K_T = k_T \cdot C_T^2 = 2 \cdot 10^{-2}$ cm²/s and $K_S = k_S \cdot C_S^2 = 6 \cdot 10^{-4}$ cm²/s, where k_T and k_S are corresponding coefficients of molecular diffusion. Although this evaluation is very rough, the difference between the coefficients as well as their small values prove the pulsations to be a feature of fossil turbulence rather than of a developed one. The time of dissipation of anomalies with a vertical scale of h = 30m

$$t = h^2 / K \tag{2}$$

is equal to $5 \cdot 10^8$ s » 15 years for the temperature and $2 \cdot 10^{10}$ s » 500 years for the salinity. This means that our lenses may have a long pre-history and still preserve the footprints of the processes which formed the lenses.

Another possible source of the pulsations is the isopycnal intrusions, which are frequently observed on narrow fronts and on the periphery of mesoscale intra-thermocline lenses. Calculations of potential temperature and salinity on the surfaces of constant potential density show that corresponding isopycnal gradients are too weak to provide high values of pulsations. Moreover, water properties viewed in the lenses can be found nowhere except for the vicinity of the Subarctic Front where high mean gradients coexist with high small-scale pulsations of temperature and salinity.

Thus, from both approaches we may conclude:

- the fine-structure of the anomalies revealed contains water relevant to that observed around the SF;
- both the temperature and salinity pulsations are generated by intensive local mixing at the SF, rather than by local dynamics of the sub-mesoscale anomalies;
- those sub mesoscale anomalies represent a "new" intermediate water, which ventilates the layer.

It should be noted, that all three lenses on the section described above (Fig. 1) are located inside the large warm anticyclonic eddy, which is, apparently, a separated Kuroshio meander shifted about 300 km north from the Kuroshio Extension. Such an eddy can create a local narrow high-contrast front essential for effective mixing and cabbeling.

ACKNOWLEDGMENTS

This study was supported by grant NDY000 of the International Science Foundation, grant 95-05-14907 of the Russian Foundation for Basic Research, grant NDY300 of the ISF and the Russian Government, and is a part of the International Research Project "Drifter Investigation of the North-Western Pacific Surface Circulation" supported by the Ministry of Science of the Russian Federation.

REFERENCES

Burkov, V.A. 1972. General circulation of the Pacific ocean waters. Moscow, Nauka. 195 p. (in Russian).

Ivanov, Yu. A. [ed.] 1992. Experiment "Megapolygon", Moscow, Nauka. 415 p. (in Russian).

Kilmatov, T.R., and V.A. Kuzmin. 1991. Cabbeling effect under mixing of seawaters and its seasonal appearance at the North Pacific Subarctic Front. Izvestia Acad.Sciences of USSR. Physics of atmos. and ocean. 27:883-887 .(in Russian).

Maximenko, N.A., R.I. Gouskina, A.I. Kharlamov, and A. Yu. Shcherbina. 1995. Spatial structure and dynamics of intermediate water in the North Western Pacific. Oceanologia. (in Russian, in press).

Maximenko, N.A., T. Yamagata, and K. Okuda. 1995. Frontal convection in the Kuroshio and Subarctic Front. Oceanologia. (in Russian, in press).

Talley, L.D. 1993. Distribution and formation of North Pacific intermediate water. Phys. Oceanogr. 23:517-537.

Yang, S.-K., and Y. Nagata. 1992. North Pacific Intermediate Water in the seas adjacent to Japan. Preprint.

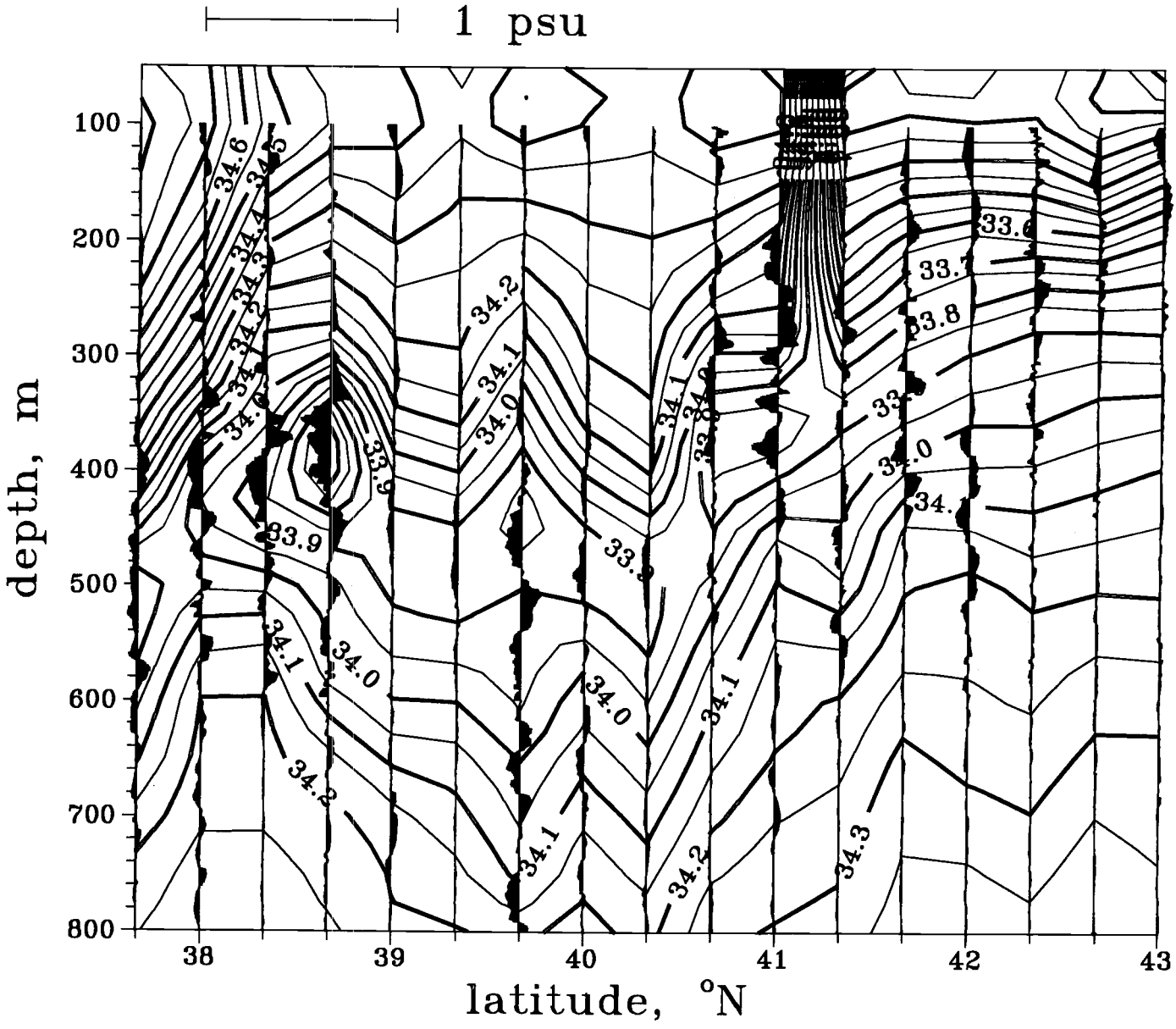

Fig. 1. Salinity distribution and vertical profiles of salinity pulsations of scale less than 100 m. along 152°E in October 1987.

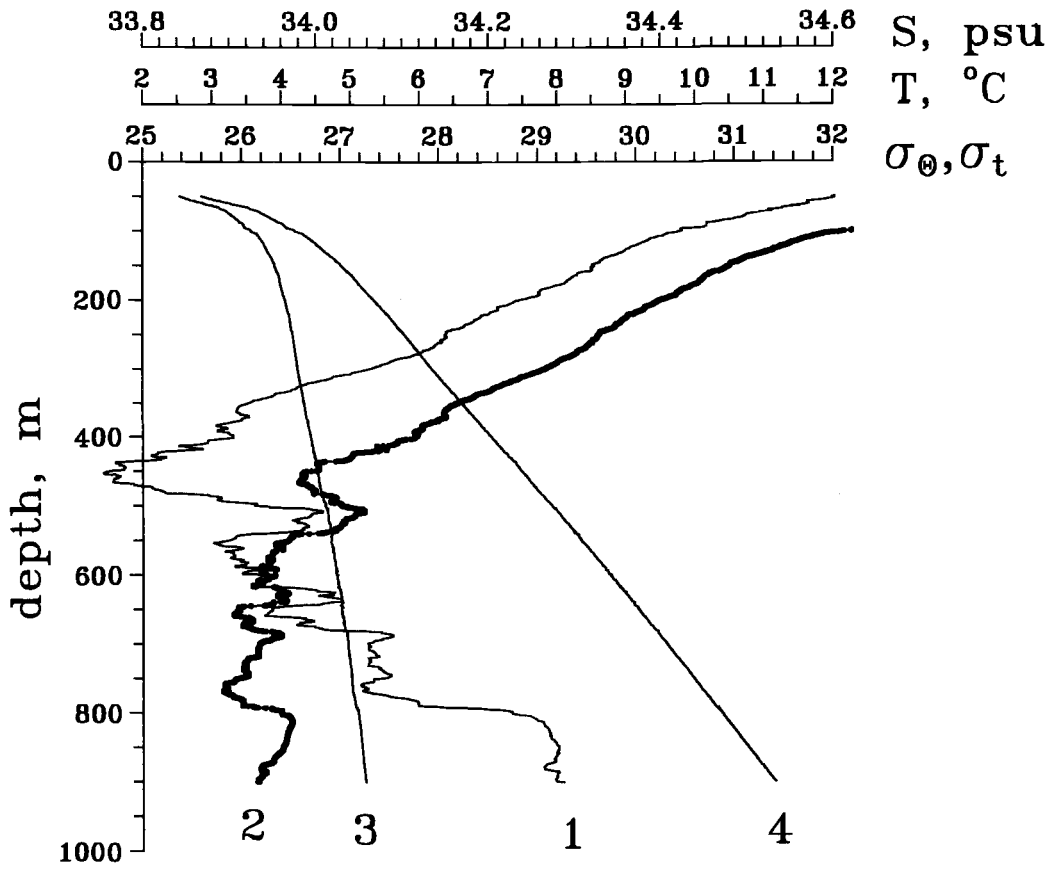

Fig. 2. Vertical profiles of (1) salinity, S; (2) temperature, T; (3) potential density, σ_θ and (4) density σ_t at 39°40'N, 152°E.

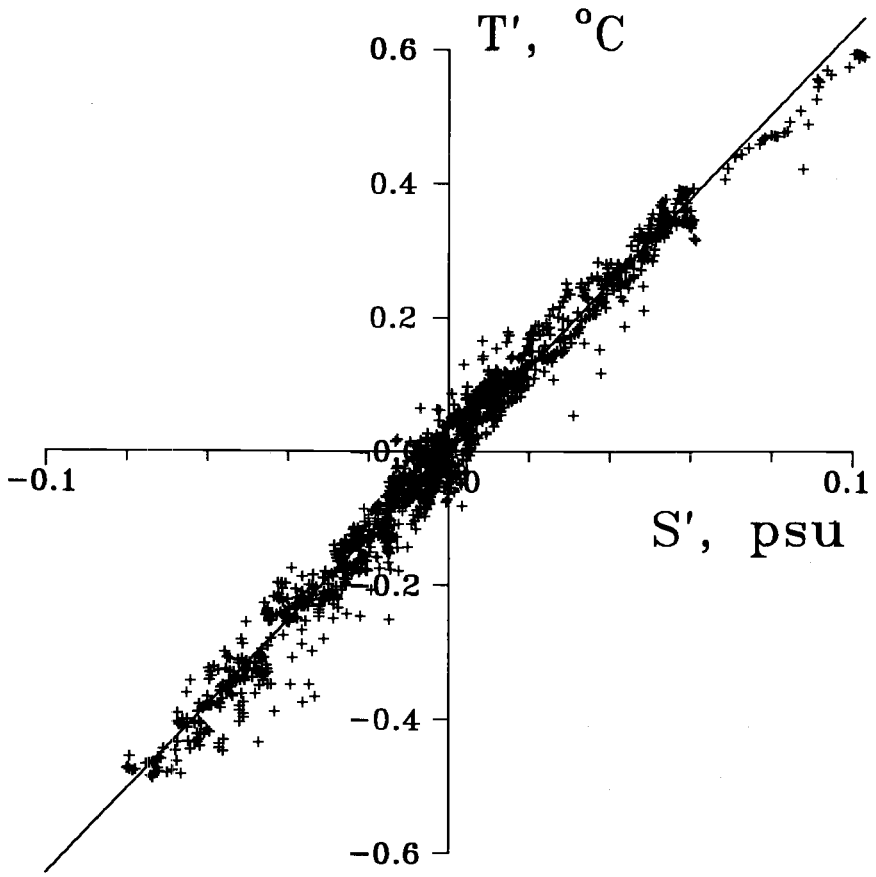

Fig. 3. Relation between T and S pulsations shown in Fig. 2.

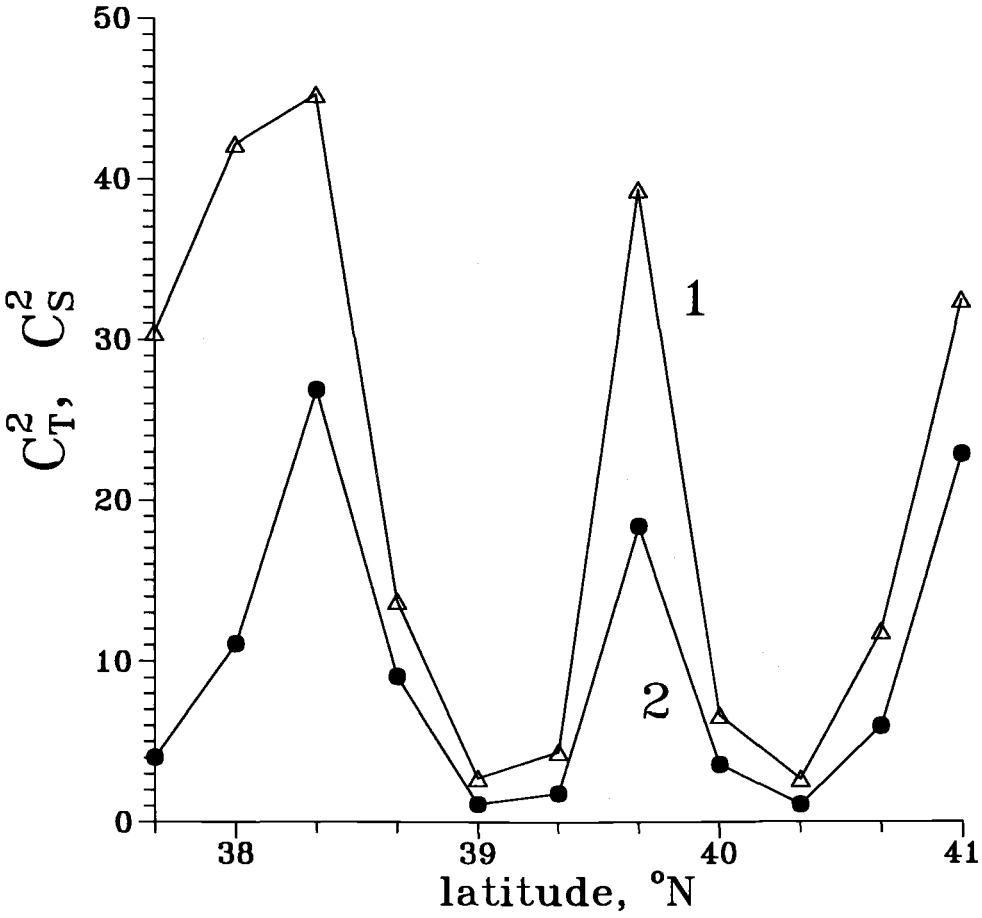

Fig. 4. Meridional distribution of Cox numbers C_T (1) and C_S (2), calculated from (1).

An Experimental Study of Water Transport through the Straits of Okhotsk Sea by Electromagnetic Method

Renat D. MEDJITOV and Boris I. REZNIKOV

Pacific Oceanological Institute, Far Eastern Branch, Russian Academy of Sciences, Vladivostok, Russia

Studies of water dynamics and transport through straits require rapid and accurate observations of water velocities over large spatial scales. Application of standard oceanographic technique is complicated due to hydrometeorological conditions of the area. Significant new information about steady and variable ocean transport can be extracted from the measurements of motion induced electric fields being made with submarine cables and towed electrode systems. Such experiments were performed in the Nevelskoy Strait with the aid of a bottom mounted electrode system that detected the horizontal electric fields at several points of the Strait. Information about lateral and temporal structure of water exchange between the Japan Sea and the Okhotsk Sea was obtained. From these results it is evident that the data were dominated by diurnal and semidiurnal tidal elements. Geomagnetic electro kinetograph (GEK) profiling of the Kuril Straits was realized using towed electrodes to demonstrate the possibilities of this method for future oceanographic investigations.

INTRODUCTION

The depth integral of horizontal water velocity (the transport) in the straits is one of the fundamental characteristics of general water circulation in the Sea. Only two conventional tools to measure barotropic currents are now available. Long-term observations of the velocity fields can be carried out directly with a set of current meters, but this method is usually costly, especially if good resolution is desired. The second method is based on calculations of the bottom pressure records.

An unconventional technology measuring the motion induced electric field is also available for direct observation of transport, but it remains almost unclaimed. This technique detects signals which arise from the motion of sea water through the Earth's magnetic field and contain information about local and regional water velocities. The method of towed electrode pairs or geomagnetic electro kinetograph (GEK) and the utilization of submarine cables are two principal examples of the electromagnetic approach to measuring sea flows. Only a few of that kind of results in straits are known at present, in particular, measurements carried out by Teramoto (1971) in the Sugaru Strait, by Larsen and Sanford (1985) in the Florida current and by Bowden, (1961) near England. This is quite an abnormal situation, since the induced electric fields can yield information on both the spatial and temporal variability of transport in real time scale by using simple, reliable and very cheap tools. This paper presents examples of electromagnetic measurements that have been made in the Straits of Okhotsk Sea.

METHOD AND INSTRUMENTS

The theory of motional electromagnetic induction in the ocean has been refined over the last few decades. In the case where temporal magnetic fluctuations can be neglected, the electric field E

and electric current density J arising from interaction of moving water with Earth's magnetic field F are related by the Ome's law for moving conducting media:

$$E = \nabla f = V \cdot F - J / s \tag{1}$$

where f is the electric potential, V is the velocity vector and s is the electric conductivity.

To define the vector velocity field V, in general case we need to accomplish the simultaneous measurements of F and J at the same points or to determine only one of these parameters and use an adequate theoretical model of induction process based of Maxwell's equations. Usually it is a rather difficult and complex problem, but in some specific situations it can be simplified. Namely, in the low frequency limit when the effect of self induction is weak, the vertical velocity may be neglected by comparison with the horizontal components. Further assuming that the ocean bottom is flat, it can be shown that in the stationary reference frame the induced horizontal electric field is related to the horizontal velocity field by (Sanford, 1971)

$$E_H = C \cdot F_Z \cdot <V_H>^* \tag{2}$$

where C is a constant, F_Z is the known local vertical component of the geomagnetic field, $<V_H>^*$ is the vertically-averaged sea water conductivity - weighted horizontal water velocity determined by

$$<V_H>^* = \frac{\int_0^H V_H(z) \cdot \sigma(z) \cdot dz}{\int_0^H \sigma(z) \cdot dz} \tag{3}$$

and H is the depth.

Due to the cross-product relationship in equations (1) - (2), the north electric field is proportional to the west component of $<V_H>^*$, and the east electric field is proportional to the north component of $<V_H>^*$.

Oceanographic interpretation of equations (2) and (3) depends on the specific effects of the scale factor C and sea water conductivity weighting in (3). The first of these values is principally a function of the local sea floor electrical conductivity structure, and is a measure of the extent to which electric currents induced in the ocean are shorted out by underlying rock. Theoretical predictions suggest that C should lie between 0.9 and 1, and observations give actual values of 0.91-0.94 (Sanford, 1971).

For many oceanic regions, i.e., such as shallow wide straits, it can be shown that the quantity, specified by equation (3) is nearly equivalent to the simple vertically-averaged horizontal water velocity, also called the transport T [m^3/sec], so the expression (2) can be reduced to the following form

$$\Delta f = F_Z \cdot T / H \tag{4}$$

From the other hand, in a reference frame attached to a water element moving at the velocity V, an observer would measure the so-called apparent electric field E_A

$$E_A = J / s = B_Z \cdot (V_H - <V_H>^*) = k \cdot F_Z \cdot V_H \tag{5}$$

where V_H is the local velocity at the depth of measurement, and "k-factor" is an empirical parameter defined as

$$k = |V_H| / |V_H - \langle V_H \rangle^*|$$

So, the GEK data should be interpreted as a vector difference between the surface and vertically averaged velocities (Sanford, 1971).

The surface drift generated by wind and waves generally effects only a very shallow surface layer h in such a way, that h is often small compared to H

$$k = (1 - h/H)^{-1} \sim 1, \tag{6}$$

and therefore, GEK is a very suitable tool to study a shallow surface drifts in a deep sea.

RESULTS AND CONCLUSIONS

The long-term observations of the velocity field were performed in the Nevelskoy Strait with the aid of bottom deployed electrode system that measured the horizontal electric fields at several points of the Strait. This Strait separates the Sakhalin Island from the Main Land and is the place where the water exchange between the Japan Sea and Okhotsk Sea occurs.

The bottom topography with the disposition of electrodes is shown on Fig. 1. Five electrodes in contact with sea water were connected to the measuring circuit by an insulated cable at a distance of 0.2 km, 0.75 km, 2 km, 3 km and 5 km from the shore. This method can be operated to examine the lateral structure of the horizontal electric field, and hence the structure of transport in the Strait. We used the silver-silver chloride electrodes selected in such a way that any pair difference in electrode potential was hundred of times smaller than would be observed in the Strait.

Fig. 2 displays the data (a one-day section) registered by different pairs of the electrodes (curves 1 - 4). Curve 5 shows the potential difference over the whole section (electrodes 1 - 5), while curve 6 represents the sum of the results on separate elements of antenna (curves 1 - 4). It is evident that results of measurements are dominated by irregular diurnal and semidiurnal tidal elements with velocity and transport amplitudes up to 80 cm/sec and $4 \cdot 10^4$ m^3/sec, respectively, and with approximately zero average transport. It should be noted that the presented data were obtained during quiet weather. Under other weather conditions with a strong north wind the southward water transport was found in the Strait. An excellent coincidence of the curves 5 and 6 demonstrates experimental evidence of the theoretical prediction, and thus we can use only two electrodes to measure the total transport through the Strait.

A horizontal GEK-profiling along the Kuril Straits was conducted in August 1983. The results are presented in Fig. 3, where one component of the surface velocity normal to the vessel's course is drawn (k- factor in equation 5 was found being equal to 0.8 from the hydrological soundings).

It is evident from the data, that currents were not uniform, but consisted of a set of individual narrow streams frequently with opposite directions. Besides, this velocity structure is not an instantaneous picture, as it took about two days to cross all these straits and, certainly, the surface currents depend upon the spatial and temporal structure of wind. So, we naturally see that these data do not constitute a considerable global oceanological result, but are presented here only to demonstrate the possibilities of electromagnetic methods for the sea current measurements.

REFERENCES

Bowden, K.F. 1956. The flow of water through the Straits of Dover related to wind and difference in sea level. Phil. Trans. Roy. Soc. London. A, 248 (953):517-551.

Larsen, J.C., and T.B. Sanford. 1985. Florida current volume transport from voltage measurements. Science. 227:302-304.

Sanford, T.B. 1971. Motionally induced electric and magnetic fields in the Sea. J. Geophys. Res. 76:3476-3492.

Teramoto, T. 1971. Estimation of Sea - Bed Conductivity and its Influence upon Velocity Measurements with Towed Electrodes. J. Oceanograph. Soc. Japan. 27:7-19.

FIGURES

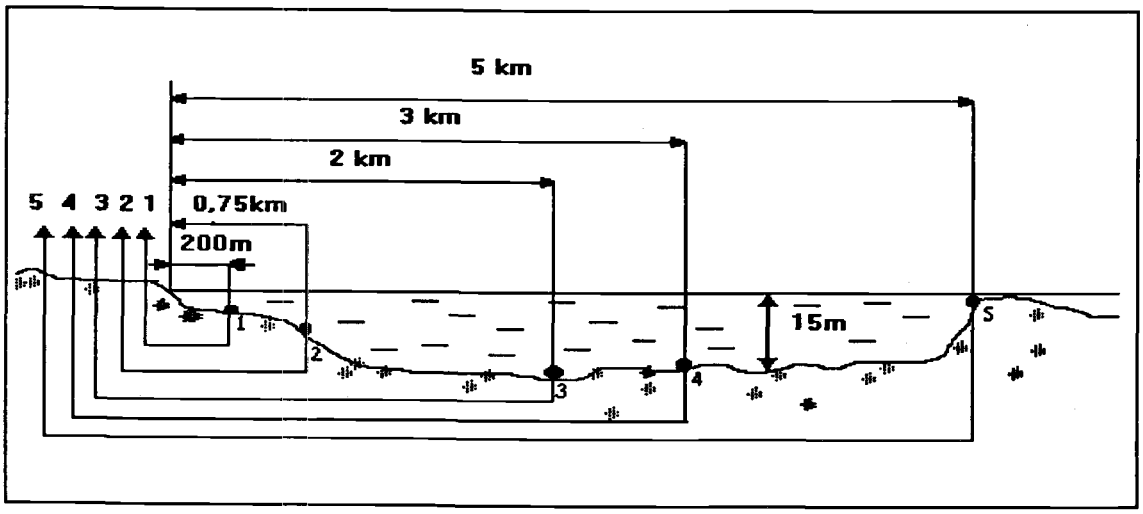

Fig. 1. The topography of bottom with the disposition of electrodes.

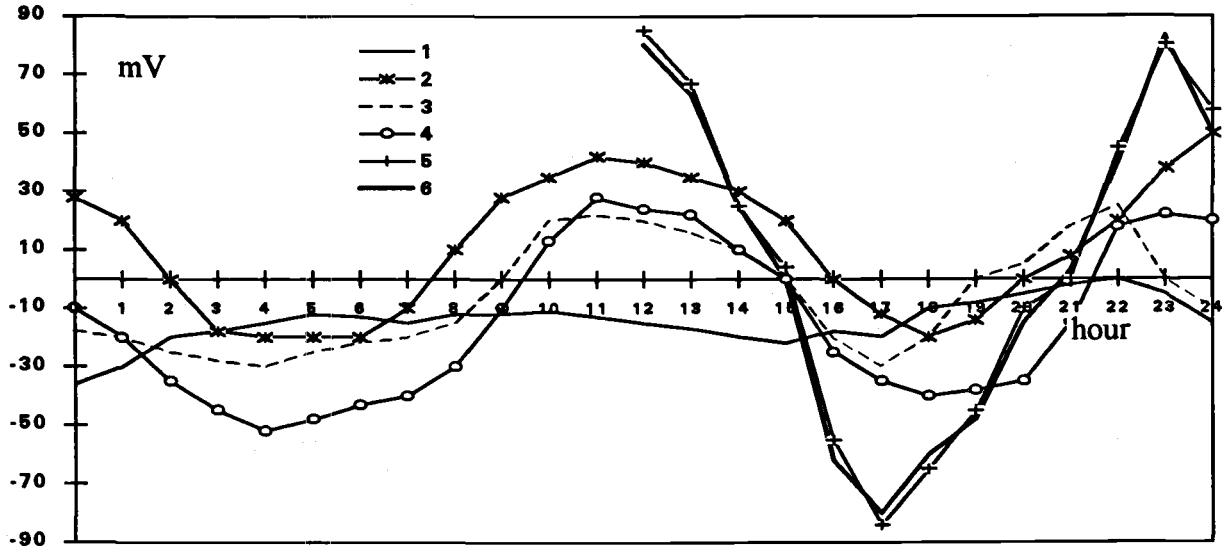

Fig. 2. Data (selected daily section) registered by different pairs of electrodes shown on Fig. 1. See text for details.

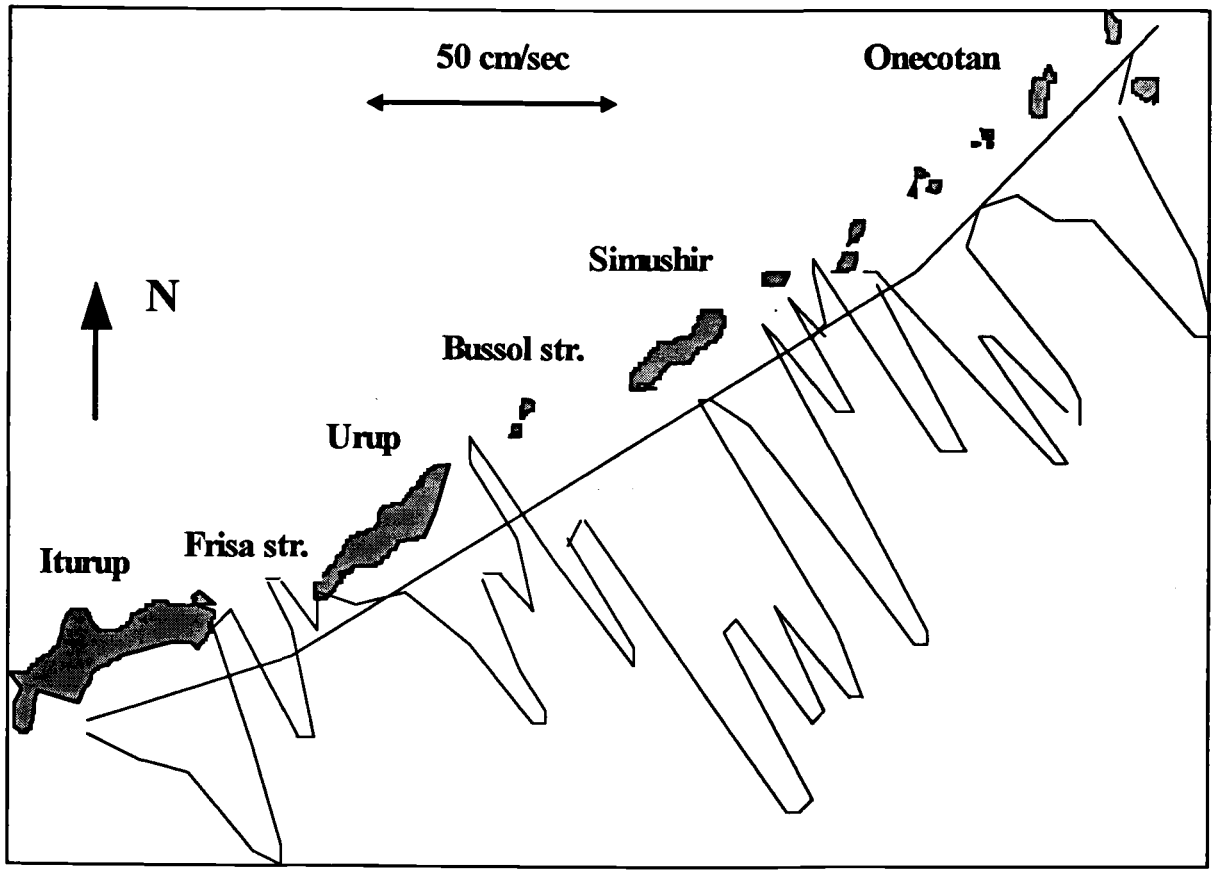

Fig. 3. Normal component of the surface velocity from horizontal GEK-profiling along the Kuril Straits conducted in August 1983.

Oceanological Zoning of the Kuril Islands Area in the Spring-Summer Period

Valentina V. MOROZ

Pacific Oceanological Institute, Far Eastern Branch, Russian Academy of Sciences,
Vladivostok, Russia

In the present paper we provide the regional classification of water adjacent to the Kuril Islands (within a 120-mile zone) in both the Okhotsk Sea and Pacific Ocean for the spring-summer period.

The following materials were considered during this study:

1. Expeditions of the Pacific Oceanological Institute of Far-Eastern Branch of Russian Academy of Siences to the Kuril Straits in the spring-summer period of 1989-1991,
2. Expeditions of the Pacific Research Institute of Fisheries and Oceanography to the South Kuril Islands region in the spring-summer period of 1980-1988,
3. Japanese expeditions to the Kuril Islands area in the spring-summer period of 1963-1972.

Based on systematization of temperature and salinity data and results of T-S analysis, five different thermohaline structures were revealed in the region:

1. Pacific type (Oyashio water)
2. Okhotsk Sea type
3. South Okhotsk Sea type (Soya current zone)
4. Deep straits zone type (Kuril Straits variety of subarctic structure)
5. Islands shelf zone type (homogenized).

Distribution of these water types is shown in Fig.1, while thermohaline indexes of the corresponding water masses are given in Table 1.

It was shown that the water structures displayed above are separated by frontal zones of various intensity, namely by:

1. Oyashio front
2. Okhotsk Sea Kuril front
3. Soya current front
4. Kuril straits fronts
5. Shallow zone fronts.

It was also found, that peculiarities of formation and distribution of different water structure types are not constant and are conditioned by the variable intensity of the current system in the area.

TABLES AND FIGURES

Table 1. Thermohaline structure of Kuril islands area.

Water mass	Spring (April - June)			Summer (July - September)		
	H, m	T, °C	S ‰	H, m	T, °C	S ‰
Pacific type						
Surface	0-30	2.5-4.0	32.4-33.2	0-50	7.0-12.0	32.8-33.0
Cold Intermediate	30-200 core 75-100	min 0-0.5	33.3-33.6	50-200 core 75-100	min 0.5-1.0	33.2-33.3
Warm Intermediate	200-900 core 250-350	**max 3.3-3.5**	33.8-34.0	200-900 core 250-350	**max 3.3-3.5**	33.8-34.0
Deep	900-3000	2.5	34.5	900-3000	2.5	34.5
Bottom	> 3000	1.5	34.7	>3000	1.5	34.5
Okhotsk Sea type						
Surface	0-30	2.0-3.0	32.5-32.8	0-50	6.0-12.0	32.5-32.8
Cold Intermediate	30-150 core 75-100	**min -1.5-0**	32.9-33.0	50-150 core 75-100	**min -1.3-0**	32.9-330
Okhotsk Sea Intermediate	150-600	1.5	33.75	150-600	1.5	33.75
Warm Intermediate	600-1300 core 500	max 2.4	34.3	600-1300 core 500	max 2.4	34.3
Deep	> 1300	1.8	34.7	>1300	1.8	34.7
South Okhotsk Sea type						
Surface	0-30	**5.0-10.0**	33.8-33.9	0-50	**13.0-16.0**	33.8-34.3
Cold Intermediate	30-300 core 75-150	min -0.5-0	33.2-33.3	50-300 core 75-150	min-0.5-0.5	33.2-33.3
Warm Intermediate	300-1200 core 600	max 2.0	34.0	300-1200 core 600	max 2.0	34.0
Deep	>1200	1.5	34.3	>1200	1.5	34.3
Deep straits zone type						
Surface:						
Fourth Kuril	0-20	1.9-2.5	32.7-33.3	0-30	5-8	32.5-33-2
Kruzenshtern	0-20	1.7-2.0	32.5-33.2	0-30	4-8	32.5-33.2
Bussol	0-10	1.5-2.0	33.1-33.4	0-30	3-5	33.1-33.4
Friza	0-20	1.0-2.0	33.0-33.2	0-30	4-14	33.2-33.7
Cold Interm.						
Fourth Kuril	20-600 core 75-200	**0.9-1.3**	33.2-33.5	30-600 core 80-200	**1.1-2.0**	33.7-33.8
Kruzenshtern	30-400 core 75-150	**1.5-2.0**	33.5	30-400 core 75-150	**1.5-2.0**	33.5
Bussol	10-600 core 100-150	**1.0-1.2**	33.5	20-600 core 100-200	**1.4-1.5**	33.8
Friza	20-500 core 75-200	**0.9-1.3**	33.7	30-500 core 100-200	**1.7-1.8**	33.7-34.0
Warm Interm.						
Fourth Kuril	600-bottom	1.3-2.0	33.7-33.8	600-bottom	1.3-2.0	33.7-33.8
Kruzenshtern	400-650 core 500	3.0	33.8-34.0	400-650 core 500	3.0	33.8-34.0
Bussol	600-1200 core 1000	2.3	34.2	650-1200 core 1000	2.1	34.2
Friza	500-bottom	2.2-2.4	34.3	500-bottom	2.2-2.4	34.3
Deep						
Kruzenshtern	> 650	2.5	34.2	> 650	2.5	34.2
Bussol	> 1200	2.0	34.5	> 1200	2.0	34.5
Islands shelf zone type						
Homogenized	0-150	1.0-2.0	33.2-33.5	0-150	3.0-4.0	33.2-33.5

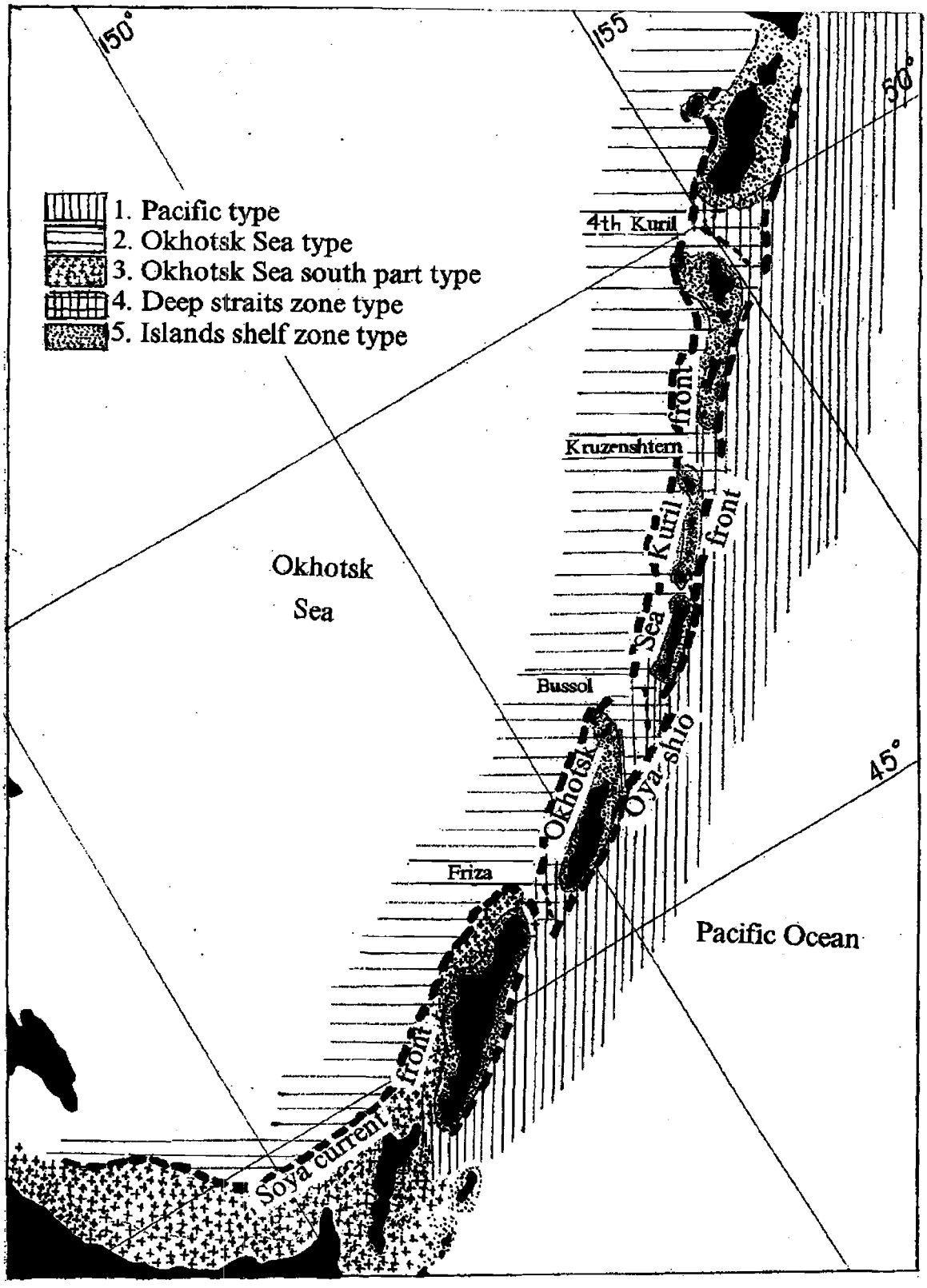

Fig. 1. Distribution of different water structures.

Note on the salinity balance in the Okhotsk Sea

Yutaka NAGATA

Faculty of Bioresources, Mie University, Tsu, Mie-ken, Japan

The source water of the North Pacific Intermediate Water (NPIW) is believed to be generated in the shelf region of the northwestern Okhotsk Sea (e.g. Talley and Nagata, 1995: the figures used in the following discussion will be referred by figure numbers in this report). Sea ice formation occurs actively in the coastal polynya just off the Siberian coast throughout winter season, and the annual rate of the dense water formation is estimated to be about 0.5 Sv by Alfultis and Martin (1987). They urge that the volume of the formed dense water is large enough to maintain NPIW, as it is doubled by horizontal mixing before it flows out into the North Pacific Ocean and reaches to the formation area of NPIW. We shall discuss whether such a formation process of the dense water is physically feasible by considering salinity balance.

Characteristics of the waters and oceanic currents which would affect the salinity balance in the Okhotsk Sea are:

1. The temperature of the dense shelf bottom water is almost at freezing point - 1.8°C, and the salinity is between 33.3 and 33.6 psu (Kitani 1973: Fig.2.3.29). We assume the typical salinity value here as 33.5 psu.
2. The salinity of the surface water in the shelf region is 32.5 psu in summer and between 32.7 and 33.2 psu in winter. Its temperature in winter is -1.8°C (Kitani, 1973 and Reid, 1965). We assume the typical salinity value as 32.5 psu.
3. As to the salinity of the East Kamchatka Current Water near the northern straits of the Kuril Islands, 33.1 psu is selected as the typical value from the figures of Ohtani (1989) (Fig. 2.5.4).
4. The salinity at the temperature minimum (almost at freezing point) in the central part of the Okhotsk Sea is from 32.9 psu (sigma-t 26.5) to 33.1 psu (sigma-t 26.7). We select 33.0 psu as the typical value (Kitani, 1973: Fig.2.3.29).
5. The salinity of the Soya Current Water is about 34.0 psu, and the averaged flow rate is 0.7 Sv (Aota and Ishikawa, 1991).
6. The fresh water supply from Amur River into the region under consideration is of the order of 0.01 Sv (Aota and Ishikawa, 1991).
7. The volume transport from the Pacific Ocean to the Okhotsk Sea through the northern straits of the Kuril Islands is not clear, but is estimated to be 13.2 Sv by Kurashina et al. (1967). The averaged salinity value in the upper 1,900 m layer is about 34.1 psu. The transport from the Okhotsk Sea to the North Pacific through the southern straits of the Kuril Islands is 16.7 Sv (Kurashina et al., 1967). The averaged salinity of the upper 1,900 m is about 33.9 psu. We use these values tentatively.

If we assume the formation rate of the dense water in the shelf region is 0.5 Sv as estimated by Alfultis and Martin (1987), the resulting salinity loss of the surface layer due to ice formation is:

$$(33.5 - 32.5) \times 10^{-3}\ \mathrm{Kg/m^3} \times 0.5 \times 10^{6}\ \mathrm{m^3/s} = 0.5 \times 10^{3}\ \mathrm{Kg/s} \qquad (1)$$

If the salinity loss is balanced with the horizontal transport in the surface layer from the East Kamchatka Current Water, the required transport U is:

$$(33.1 - 32.5) \times 10^{-3}\ \mathrm{Kg/m^3} \times U = 0.5 \times 10^{3}\ \mathrm{Kg/s}, \quad \text{and} \quad U = 1.1\ \mathrm{Sv}. \qquad (2)$$

This value would be considerably underestimated because the distance between the East Kamchatka Current and the shelf regions is about 1,000 km, and because the effective horizontal salinity difference may be one order of magnitude smaller than that used in the above estimation. So, the surface current in the order of 10 Sv is required to be flowing into the region. This is not realistic as we find no eminent current there.

One of the curious behaviors of the dense shelf water is that it looses its high-salinity before it flows out into the central part of the Okhotsk Sea (Kitani, 1973: Fig. 23.2.8-9), though its temperature remains almost at freezing point. This indicates that the water is mixed with low-salinity cold water, which may be found in the surface layer in late winter or in early spring. If we assume its salinity is equal to the typical value (32.5 psu) in the surface layer in the shelf region, the mixing ratio R of the dense shelf water with the cold surface water can be given:

$$32.5\ R + 33.5 \times (1-R) = 33.0, \quad \text{and} \quad R = 0.5. \qquad (3)$$

Namely, the dense water is mixed with the surface water in the ratio of 1:1. This would be reasonable as we find vertically homogeneous water over the Kashevarova Bank which is thought to be generated by strong tidal mixing there (Kitani and Shimazaki, 1971: Figs. 2.3.22 through 2.3.24). This means that half the amount (0.25×10^3 Kg/s) of the salt, which has been given for the shelf bottom layer due to the ice formation, is carried back to the surface layer due to the mechanical mixing in the sea adjacent to the bank.

If net water transport from the surface to the bottom layer due to ice formation is negligible, the dense shelf water would flow out into the central Okhotsk Sea at the rate of 0.5 Sv, and the relatively less saline water would flow into the shelf bottom layer at the same rate. The salinity loss in the shelf bottom layer is given by

$$(33.5 - 33.0) \times 10^{-3}\ \mathrm{Kg/m^3} \times 0.5 \times 10^{6}\ \mathrm{m^3/s} = 0.25 \times 10^{3}\ \mathrm{Kg/s}. \qquad (4)$$

Thus, a half of the salt gain of the bottom layer due to ice formation is carried back to the surface layer, and another half is just carried out from the shelf bottom layer to the intermediate layer of the central Okhotsk Sea.

However, it would be reasonable to assume that some amount of net water mass is transported from the surface to the bottom layer in the process of dense water formation. This would result in the net outflow from the shelf bottom region to the central Okhotsk Sea. If we denote this transport with V, the amount of the salt carried out into the central Okhotsk Sea is 33.5×10^{-3} Kg/m^3 x V. Even if the net water flux is 1/1,000 of the generation rate of the dense water formation rate (0.005 Sv), the resulting salt flux is 0.16×10^3 Kg/s, and of the same order of magnitude as the salt fluxes in the above discussion. This indicates that the accuracy of the present discussion is very limited, and further elaborated investigations would be needed.

The salinity balance in the surface layer of the shelf region is much more complicated as we need to consider the fresh water supply from Amur River. This salinity loss may be estimated as:

$$(33.5 - 0.0) \times 10^{-3}\ \mathrm{Kg/m^3} \times 0.01 \times 10^{6}\ \mathrm{m^3/s} = 0.34 \times 10^{3}\ \mathrm{Kg/s}. \qquad (5)$$

This amount is almost the same order of magnitude as the salinity loss due to the ice formation (0.5 x 10^3 Kg/s). However, the same amount of the water mass in the surface layer should flow out from the shelf region to the central Okhotsk Sea. If the salinity of the out flow is that of the surface shelf water, there would be no net salinity gain or loss. However, most of the Amur River fresh water may spread out over the entire Okhotsk Sea, and additional fresh water would be carried out from the shelf region in the form of drifting ice due to strong westerly winter winds.

It should also be noted that Alfultis and Martin's estimation is based on satellite observation of the coastal polynya, and may include significant error. They assumed that the volume of the dense water would be doubled by horizontal mixing with the surrounding waters before it reaches the Oyashio region, and be enough to maintain NPIW. Recent investigations (see Talley and Nagata, 1995), however, indicate the intermediate Oyashio Water will be modified by horizontal mixing with the old and saline NPIW which is carried by the Kuroshio into the Mixed Water Region (Fujimura and Nagata, 1992). The volume of water is again doubled before it reaches to the formation area of NPIW. The rate of the dense water formation in the shelf region of the Okhotsk Sea, which is required to maintain NPIW, might be much smaller than that estimated by Alfultis and Martin (1987).

If we take the typical salinity values of the Soya Current Water and of the Okhotsk interior water as 34.0 and 33.0 psu, respectively, the effective salt flux carried into the Okhotsk Sea by the Soya Current is:

$$(34.0 - 33.0) \times 10^{-3}\ \mathrm{Kg/m^3} \times 0.7 \times 10^6\ \mathrm{m^3/s} = 0.7 \times 10^3\ \mathrm{Kg/s}. \qquad (6)$$

It should be noted that this effective flux is just in the same order as that produced by ice formation in the shelf region. The Soya Current Water sinks easily by winter cooling due to its high-salinity nature (Talley and Nagata, 1995), and appears to influence directly the nature of the water in the intermediate layers of the Okhotsk Sea.

However, the effective salinity fluxes from and to the North Pacific Ocean through the northern and southern straits of the Kuril Islands are:

$$34.1 \times 10^{-3}\ \mathrm{Kg/m^3} \times 13.2 \times 10^6\ \mathrm{m^3/s} = 450 \times 10^3\ \mathrm{Kg/s} \qquad (7a)$$

and

$$33.9 \times 10^{-3}\ \mathrm{Kg/m^3} \times 16.9 \times 10^6\ \mathrm{m^3/s} = 556 \times 10^3\ \mathrm{Kg/s}, \qquad (7b)$$

respectively. The net flux flows out from the Okhotsk Sea to the North Pacific is of order of 100 10^3 Kg/s, and two orders of magnitude larger than the fluxes discussed above. This means that the salinity fluxes discussed above do not significantly affect the salinity balance in the whole Okhotsk Sea, although they are essential for the formation mechanisms of NPIW.

The accuracy of the present discussion would be very limited, but we may conclude:

1. There would be some efficient mechanisms to maintain the salinity value of the surface water in the shelf region of the north-western Okhotsk Sea. This is essential for the formation of the dense shelf water which is considered as the source water of NPIW.
2. The vertical tidal mixing in vicinity of the Kashevarova Bank plays an important role to carry back salt from the shelf bottom layer to the surface layer.
3. The net water mass transport is a very effective way to carry salt, and so we need to estimate accurately the volume transport of the downwelling associated with the sinking of brine generated by ice formation.

4. The fresh water transport by drifting ice would be important in the salinity balance in the surface layer of the shelf region.

5. The further discussion on salinity balances in various scales is needed: for the northwestern shelf region, for the Soya Current Region and the intermediate layers, and for the whole Okhotsk Sea region.

REFERENCES

Alfultis, M.A., and S. Martin. 1987. Satellite passive microwave studies of the Sea of Okhotsk ice cover and its relation to oceanic processes, 1978-1982. J. Geophys. Res. 92 (C12):13013-13028.

Aota, M., and M. Ishikawa. 1991. Fresh water supply to the Sea of Okhotsk and volume transport of Soya Warm Current. Bull. Hokkaido Nat. Fish. Res. Inst. 55:109-113 (in Japanese).

Fujimura, M., and Y. Nagata. 1992. Mixing process in the Mixed Water and Kuroshio Extension Regions and modification of the intermediate Kuroshio Water. Oceanogr. Magazine. 42:1-20.

Kitani, K., and K. Shimazaki. 1971. On the hydrography of the northern part of the Okhotsk Sea in Summer. Bull. Fac. Fish. Hokkaido Univ. 12:231-242.

Kitani, K. 1973. An oceanographic study of the Okhotsk Sea - Particularly in regard to cold waters. Bull. Far Seas Fish. Res. Lab. 9:45-76.

Kurashina, S., K. Nishida, and S. Nakabayashi. 1967. On the open water in the southeastern part of the frozen Okhotsk Sea and the current through the Kuril Islands. J. Oceanogr. Soc. Japan. 23:57-62 (in Japanese).

Ohtani, K. 1989. The role of the Sea of Okhotsk on the formation of the Oyashio Water. Umi to Sora. 65:63-83 (in Japanese).

Reid, J.L. 1965. Intermediate waters of the Pacific Ocean. Johns Hopkins Oceanogr. Studies. 2:1-85.

Talley, L.D., and Y. Nagata [ed.]. 1995. The Okhotsk Sea and Oyashio Region. PICES Scientific Report No.2, 227p.

Variability of the Kuroshio Front in 1965-1991

Alexander D. NELEZIN

Pacific Oceanological Institute, Far Eastern Branch, Russian Academy of Sciences,
Vladivostok, Russia

The northwestern part of the Pacific ocean is characterized by contact of the cold subarctic and warm subtropical water zones. The Subarctic front, related to the Kuroshio Current, is distinguished by the enhanced bioproductivity and is one of the fishery regions. Doubtless, the fisheries' interest promoted the investigation of the front position and properties (Uda, 1938).

The oceanic fronts are revealed by the enhanced horizontal gradients of the characteristics. The basic frontal zones, or the climatological fronts, are the boundaries of the natural zones in the ocean. They are identified by the multi-year mean (climatic) charts of the oceanographic characteristics distribution. By constructing the climatic fields, the relatively wide frontal zone is charted as a result of the data averaging. This is the region of probable front position fluctuations.

At the present moment only the sea surface temperature data are widely available for the study of fronts (Gulev et al., 1988; Rassadnikov et al., 1987), but deep-sea observations should be performed to analyze the vertical water structure and interannual variability of the front position.

The vertical temperature sections crossing the Subarctic front were constructed along the section of 145°E based on multi-year oceanographic data collected in February and August (Fig. 1). The figure shows that the frontal zone transforms significantly from winter to summer in the upper oceanic layer of 150 m. Moreover, it is difficult to define the front position in August in the upper layer, but it is well distinguished in the layer of 150-300 m.

In order to study variability within the annual climatic period, the monthly charts of multi-year temperature and salinity means were prepared at the standard horizons in the upper layer of 300 m. The front position was marked on each longitude from 140 to 150°E, and then the value corresponding to the average front position eastward from the Honshu Island was calculated. To improve the accuracy of our calculations the characteristic isotherm (isohaline) in zone of maximal gradients was assumed as a criteria of the front.

The preliminary analysis suggested that the isotherm of 13°C and isohaline of 34.6 % at the level of 200 m, located in the Kuroshio current zone, are the most informative for the Subarctic front within the region of 140-150°E. Therefore, for further investigations the term Kuroshio front was used appropriate to the chosen criteria. The Subarctic front concept is broader as it includes the Kuroshio and Oyashio Currents and the Mixed Water Region.

The annual variability of the front position (Fig. 1c) is characterized by the northeast displacement in December and by the southeast displacement in April. During the cold period (December - April) the rapid front displacement southward is observed and then the relatively smooth fluctuation of its northward movement occurs. Perhaps, it can be explained by some changes in the variability of the hydrological parameters within the subarctic and subtropical waters. Southward from the front the semiannual harmonic with maximums in August and

February is distinguished, whereas northward the annual harmonic with maximum in December and minimum in July is revealed.

Interannual front position variations is one of the basic indicators of the ocean thermodynamic regime, but the shortage of information regarding this problem is obvious. The opportunity to solve the above problem appeared as a consequence of the Cooperative Study of Kuroshio (CSK) (The Kuroshio ..., 1972) and the program "Sections" devoted to the monitoring of the energy active zone of the Kuroshio (Expeditional ..., 1989).

To investigate the multi-year Kuroshio front variability, the mean front position (within the region of 140-150°E) and standard deviations were calculated using the seasonal mean temperatures at the level of 200 m from observational data collected in 1965-1991 (Fig. 2). The isotherm of 13°C was also assumed as a criteria of the front. To perform the analysis of the interannual variations the smoothing of the temporary data set was carried out applying the seasonal variation model. To estimate the long-term component the trends were calculated with the help of the parabolic model. The trends with the opposite tendencies in variations of the mean front position and standard deviations were interpreted as meandering of the Kuroshio front.

In 1965-1977 a tendency for the front to move northward from 35.5 to 37°N was observed, then in 1978-1986 the front shifted southward (to 35.2°N) and in the latter period the inverse shearing to 36.4°N (in 1991) occurred. The Kuroshio front was located in the extreme north and south positions in the autumn of 1977 (37.6° N) and in the summer of 1986 (34.7°N), respectively (Fig. 3b). The front meandering decreased in 1965-1977 and increased in 1978-1985.

The front meandering is a wave of the current track deviation (bending) with a consequent eddy detachment, and is considered as one of the basic reasons for the spatial front position variability. Apparently, it is under the influence of quasi-stationary meanders and the Rossby waves, associated with the non-stationary Kuroshio. The quasi-stationary meanders were well distinguished by the averaged spatial front positions for all four seasons for the period of study (Fig. 3a). The greatest meander amplitude was observed in winter, while in the warm period the front shear became more sloping. The temporal variation analysis suggested the presence of non-regular processes in the interannual Kuroshio front position variations caused by transfrontal heat and mass transport, as the stationary frontal divisions play the role of barrier for the sea waters located on the opposite sides of the front.

To investigate the Kuroshio front position fluctuations the spectral analysis of the temporal sets along with a preliminary exclusion of the trends was applied. The initial temporal set, including 105 realizations, was approximated by the model of "piece-wise linear trend" and divided on three specified sections of the predominant tendencies. After removal of the trend components the spectra of the residual set were calculated (Fig. 4). The significant interannual fluctuation periodicity of 5-6 years (at the level of 90%) was obtained for the residual smooth set of the average front position. It should be noted that previously the temperature anomaly in the system of the North Pacific circulation with the period of 6 years has been considered and related to the Polar front shear or the Kuroshio Current axis movement (Kort, 1970). Spectrum based on the initial set of standard deviations after separating of the trend component had two maximums corresponding to the periods of 2-3 seasons and about 2 years, respectively.

Multi-year variability of the average front position is under the influence of the water circulation intensity on the western periphery of the subtropic Pacific gyre. Fig. 4a illustrates the results of water transport calculations for the North Trade Current and the Kuroshio along the section of 137°E in 1972-1991. The trends approximated by the parabolic model showed

unidirectional tendencies for the currents associated with the long-period variations of the Kuroshio front position. The running means of the current discharges have been obtained with an averaging interval of 7 seasons (3, 5 years). Fig. 4b demonstrates the residual curves after the trend component is separated. As it was noted, in the Kuroshio front variability the extreme north and south positions were recorded in the autumn of 1977 and in the summer of 1986. This coincides with the enhanced current intensity in the first mentioned period and weakening of the current intensity during the second period. The abrupt increase of the current discharges in 1975 -1977 was due to the rapid front shear northward, while the relatively slow decrease of water transport in 1979-1985 could be explained by a comparatively smooth front shift southward. Thus, the Kuroshio front movements, to a great extent, are related to the multi-year fluctuations of the current intensity within the Subtropical gyre.

REFERENCES

Gulev, S., D. Kadaev, and I. Yashaev. 1988. Synoptic variability of sea water temperature in the Gulf Stream and the North Atlantic currents. Oceanology. 28(5):721-727 (in Russian).

Expeditional investigation results in the Kuroshio energy active zone in accordance with the program "Sections". 1989. Summary of Science and Technology. Ser. Atmosphere, Ocean, Space - program "Sections". 12, 187 p. (in Russian).

Kort, V. 1970. The large-scale ocean-atmosphere interaction (the North Pacific). Oceanology. 10(2):222-240 (in Russian).

Rassadnikov, Y., and A. Nikitin. 1987. Variability of generalized ocean thermodynamic characteristics in the Kuroshio Energy active zone. Summary of science and technology. Ser. Atmosphere, Ocean, Space - program "Sections". 7:288-295 (in Russian).

The Kuroshio and adjacent Pacific regions. 1972. Trudy GOIN. 106: 209 p. (in Russian).

Uda M. 1938. Researches on "Siome" or current rip in the seas and oceans. Geoph. Mag. 2(4):306-372.

FIGURES

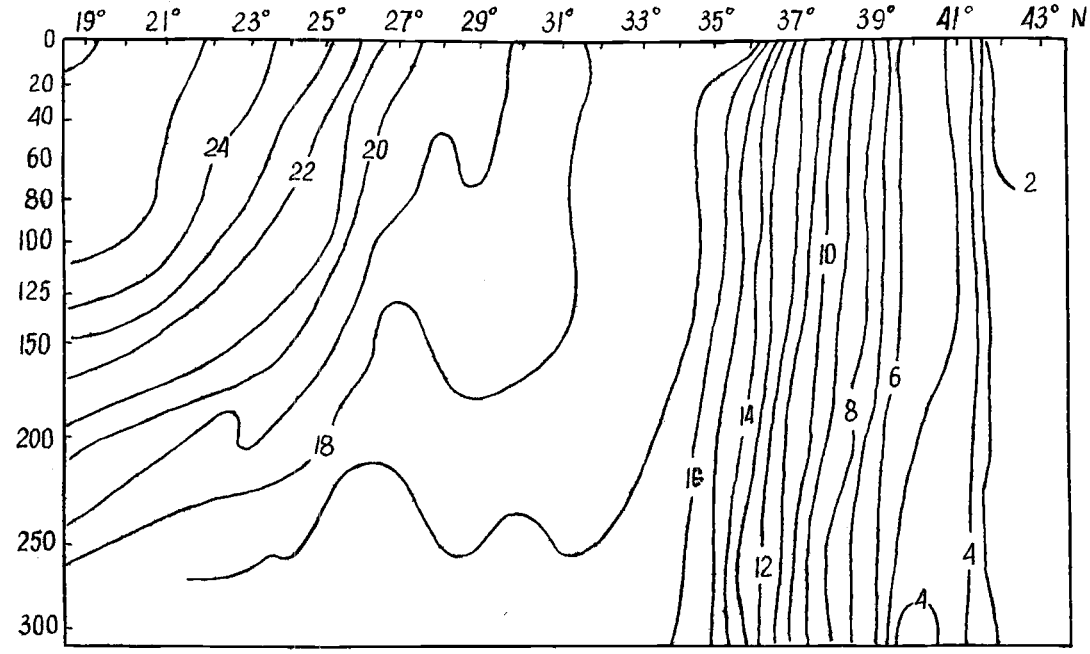

(a)

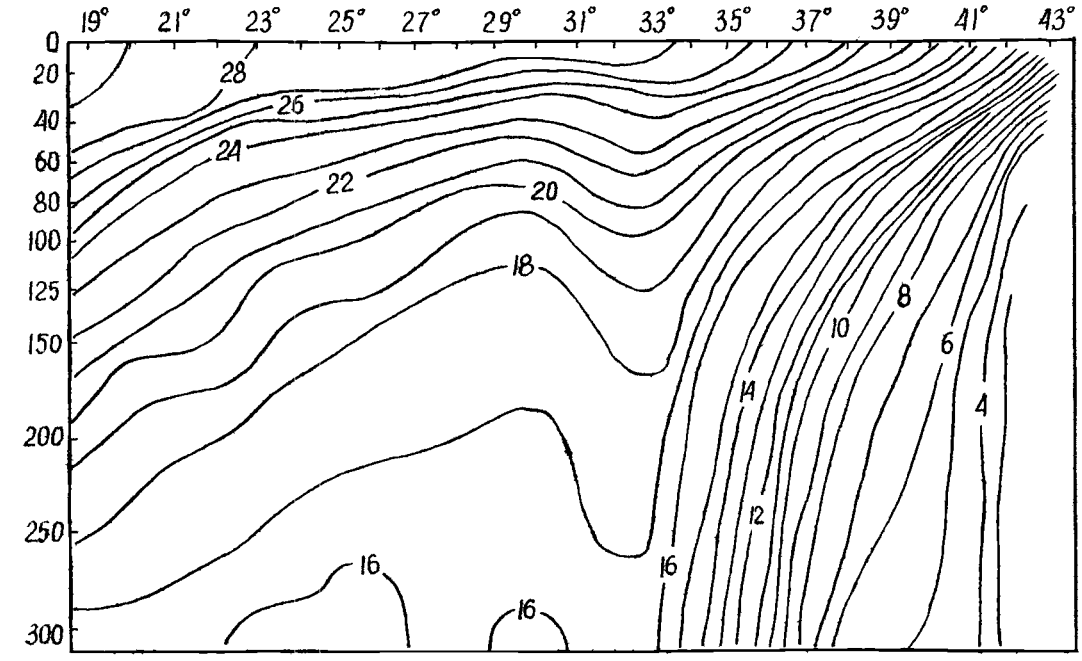

(b)

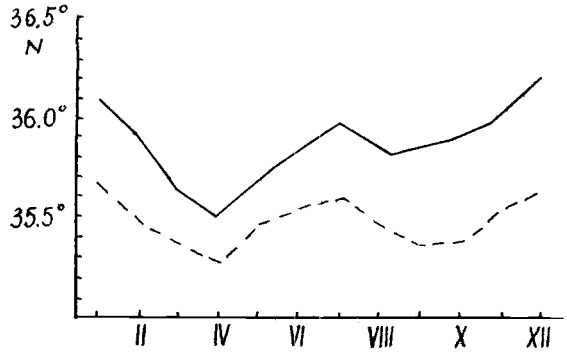

(c)

Fig. 1. Distribution of the multi-year temperature means (°C) along the section of 145°E in February (a) and August (b), and annual variability of mean temperature and salinity (dotted line) front position based on multi-year observations within the region of 140-150°E (c).

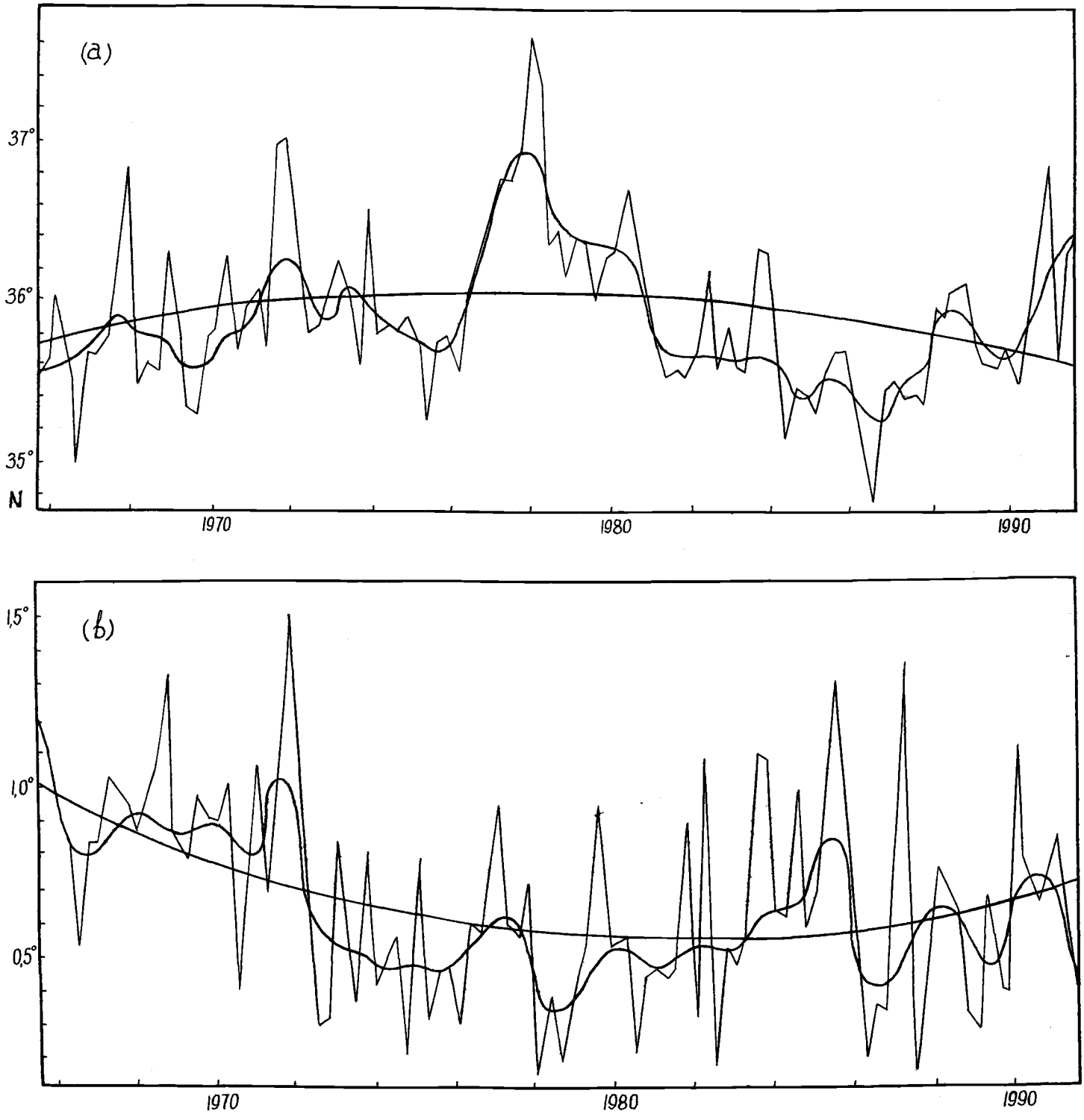

Fig. 2. Temporal variability of the seasonal values for the mean front position (a) and its standard deviation (b) in 1965-1991; components were smoothed by using the seasonal variability and parabolic trend models.

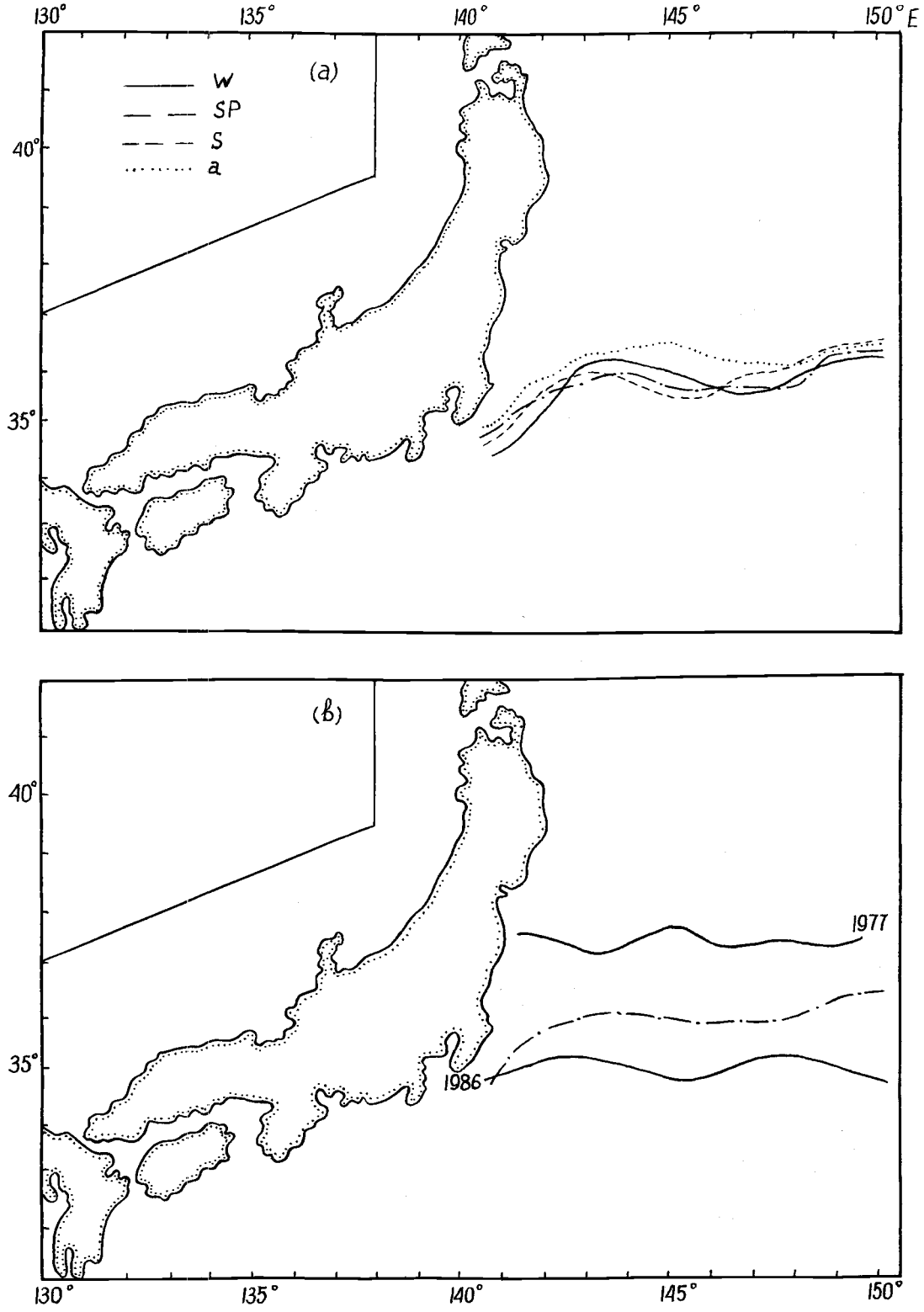

Fig. 3. Spatial seasonal means of the Kuroshio front position in winter, spring, summer, autumn (a); mean and extreme front positions in 1977 and 1986 (b) from 1965-1991 data.

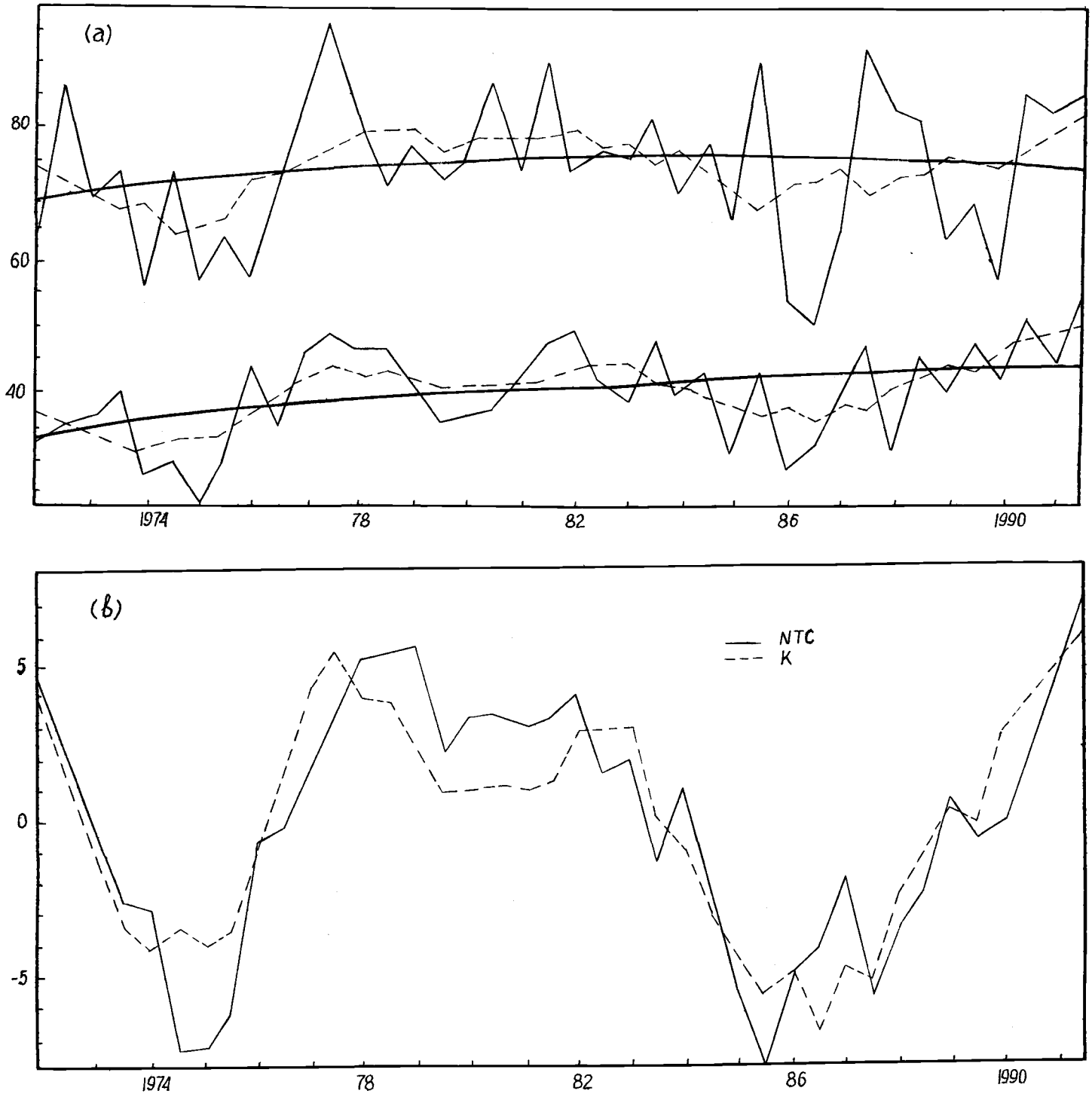

Fig. 4. Temporal variability of the North Trade Current (NTC) and Kuroshio (K) discharges (10^6 m^3/s) along the section of 137°E in the 0-1,000 m layer (a) and residual curves of discharges after filtration and trend component separation (b).

An Experimental Study of Currents in the Near-Kuril Region of the Pacific Ocean and in the Okhotsk Sea

Vladimir I. PONOMAREV, Evgeny P. VARLATY and Mikhail Yu. CHERANYEV

Pacific Oceanological Institute, Far Eastern Branch, Russian Academy of Sciences, Vladivostok, Russia

INTRODUCTION

Direct current measurements in the main pycnocline of the Pacific and the Okhotsk Sea waters adjacent to the Kuril Islands are presented and compared with observations of temperature, salinity, density and dissolved oxygen. These data were collected in July 1993 aboard of *R/V Academik Aleksandr Nesmeyanov* during the joint expedition organized by the Russian Federal Research Institute of Fisheries and Oceanography (VNIRO), the Pacific Research Institute of Fisheries and Oceanography (TINRO) and the Pacific Oceanological Institute (POI) and supported by the Fisheries Committee of Russian Federation. Direct current measurements were carried out by Dr. E.P .Varlaty, Mrs. M.Y. Cheranyev and G.P. Shvetsov from POI.

MEASUREMENTS

Current velocity was determined by the acoustic equipment (complex) designed at the Pacific Oceanological Institute. The equipment and method of measurements were described in details by Varlaty and Tihomirov (1980), and Varlaty and Ozmidav (1981). Current speed and direction were detected synchronically by sinking of the acoustic complex from a drifting vessel. The technique used to measure absolute current parameters included relative velocity sounding and ship drift determination by any available satellite navigation system. Accuracy of velocity, current direction and depth were estimated as 0.5 cm/sec, 3° and 0.25%, respectively. Temperature, conductivity, pressure and oxygen concentration were obtained using Neil Brown MK3 CTD Probe.

A total of 120 stations in the Kuril Islands adjacent areas and the Okhotsk Sea were sampled during the cruise. On the shelf and over the continental slope CTD and current measurements, as well as Rosette sampling, were carried out mostly to the near-bottom. Oceanographic stations in deep areas were taken to a depth of 800-1,000 m

RESULTS

The major patterns of the obtained velocity fields are in agreement with known general circulation of the Okhotsk Sea and the Pacific Subarctic western boundary area in summer, in particular, with the current velocity in August (Fig. 1) estimated by geostrophic balance referenced to 2,000 dbar in deep area and to the bottom on the shelf (Moroshkin, 1964). The Kuril (Oyashio) Current of the Pacific, the Eastern Sakhalin and the Western Kamchatka Currents over the Okhotsk Sea continental slope associated with cyclonic gyre in the central part of the Sea were displayed from the observations.

However, the detailed distribution of current velocity demonstrated some specific features and differences. According to our survey, in July 1993, the jets of the Oyashio Current were situated over the steep continental slope near the shelf break and in the deeper area over the western slope of the Kuril Trench. Meandering, branching and eddy generation off the Boussole and Vriez Straits were typical for the Oyashio Current in summer. The main branch of this Current was located off the Kuril Islands and deep Straits, that was also characteristic of summer situation. The current velocity module of the Oyashio decreased from the northeast (0.7-0.8 m/s) to the southwest (0.3-0.4 m/s) due to disturbances and water exchange through the Straits. In the southwest region the Oyashio turned to the south-southeast off the Small Southern Kuril Islands (Fig. 2).

At all Pacific stations adjacent to the Kruzenshtern, Boussole and Vriez Straits, streams in the layer of 0-800 m possessed a major component directed from the Pacific to the Straits (Fig. 2). The current velocity in this area was 0.4 - 0.8 m/s and its direction demonstrated a good link with bottom topography. At the same time the total flow in the relatively thick upper layer of the Straits (0-800 m) was directed to the Okhotsk Sea only in the Kruzenshtern Strait and in the deep channel of the Boussole Strait adjacent to the Simushir Island shelf slope. The average speed in the Straits was about 0.3-0.4 m/s. In the Okhotsk Sea, along the Kuril Ridge, the current was directed from the northeast to the southwest (or from Kruzenshtern to Vriez Strait). The major inflow to the Sea of Okhotsk through the Vriez Strait occured mainly below the depth of 400-500 m in the deep strait channel and gentle outflow dominated in the upper layer of the Strait.

The dynamic topography (Fig. 3) based on CTD data provided by Verkhunov and Maslennikov (1993) and Moroshkin's geostrophic currents (Fig. 1) revealed the surface inflow stream through the Kruzenshtern Strait and surface outflow current through the southwestern part of the Boussole and Vriez Straits. The current speed in the whole layer of 0-700 m reached maximal values 0.7-0.8 m/s in the area adjacent to Kruzenshtern Strait. The dominated inflow of the Pacific waters to the Okhotsk Sea through the Kruzenshtern Strait was confirmed by both direct current measurements (Fig. 2) and the dynamic topography (Fig. 3), that is in agreement with Leonov (1960) and Moroshkin (1964). The features described above were characteristic for the summer of 1993 and might be typical for summer climate in general.

Regularities of the vertical current velocity distribution were also disclosed for the areas with different water structure, bottom topography and depth. It was shown that the stream current over the shelf break border on the steep continental slope was at maximum speed in the undersurface layer of the pycnocline between 200-300 m. This situation was revealed at stations 276 (Fig. 4c), 283 and 287 in the current over the shelf break of the Small Southern Kuril ridge area. A local velocity minimum was observed in this layer of pycnocline when we move away from the shelf break to the deep offshore area (station 275, Fig. 4a). The velocity maximum shifted to the surface layer at station 275. This phenomenon is related to the vertical and horizontal oscillations of current velocity over the continental slope and also with jet generation and vertical circulation over the shelf break (Johnson and Manja, 1979, 1982).

The main feature of the vertical current velocity distribution on the northern Okhotsk Sea shelf was the two layer structure associated with a two layer density profile. Two current velocity maxima over and under the density interface are typical on the Okhotsk Sea shelf under strong and temperate wind conditions. In this case the current vector turned right with depth from sea surface to the upper maximum and left below this maximum towards the density interface, just as in the surface and bottom planetary boundary layers. In the lower layer the current vector turned in a similar way.

CONCLUDING REMARKS

Thus the important features of the horizontal and vertical current velocity distribution in the main pycnocline of the Kuril adjacent Pacific and in certain areas of the Okhotsk Sea were revealed by direct current measurements. The acoustic measuring complex of POI could be useful in future investigations of currents and eddy dynamics.

ACKNOWLEDGMENTS

We gratefully acknowledge the assistance of Gennady Shvetsov in current measurements and Anatoly Saluk for drawing some figures.

REFERENCES

Johnson, J.A., and B.A. Manja. 1979. Shear layers above a break in bottom topography Geophys. and Astrophys. Fl. Dynam. 14:45.

Johnson, J.A., and B.A. Manja. 1982. Longshore current over the shelf break. Rapp. P.-v. Reun. Cons. Int. Explor. Mer. 180:73-74.

Leonov, A.K. 1960. The Japan Sea. *In* Regional oceanography, Part 1. Leningrad, Gydrometeoizdat. 291-463 (in Russian).

Moroshkin, K.B. 1964. A new surface current map in the Okhotsk Sea. Oceanologia. 4:614-643 (in Russian).

Varlaty, E.P., and V.P. Tihomirov. 1980. Acoustic measuring complex for studying microstructure hydrophysical fields in the ocean. Proc. Symp. "Fine structure and synoptic variability of the seas.", Tallinn, 1980: 48-52 (in Russian).

Varlaty, E.P., and R.V. Ozmidov. 1981. On the values of the local Richardson number in the ocean. Okeanologiya, 21(2):211-216 (in Russian).

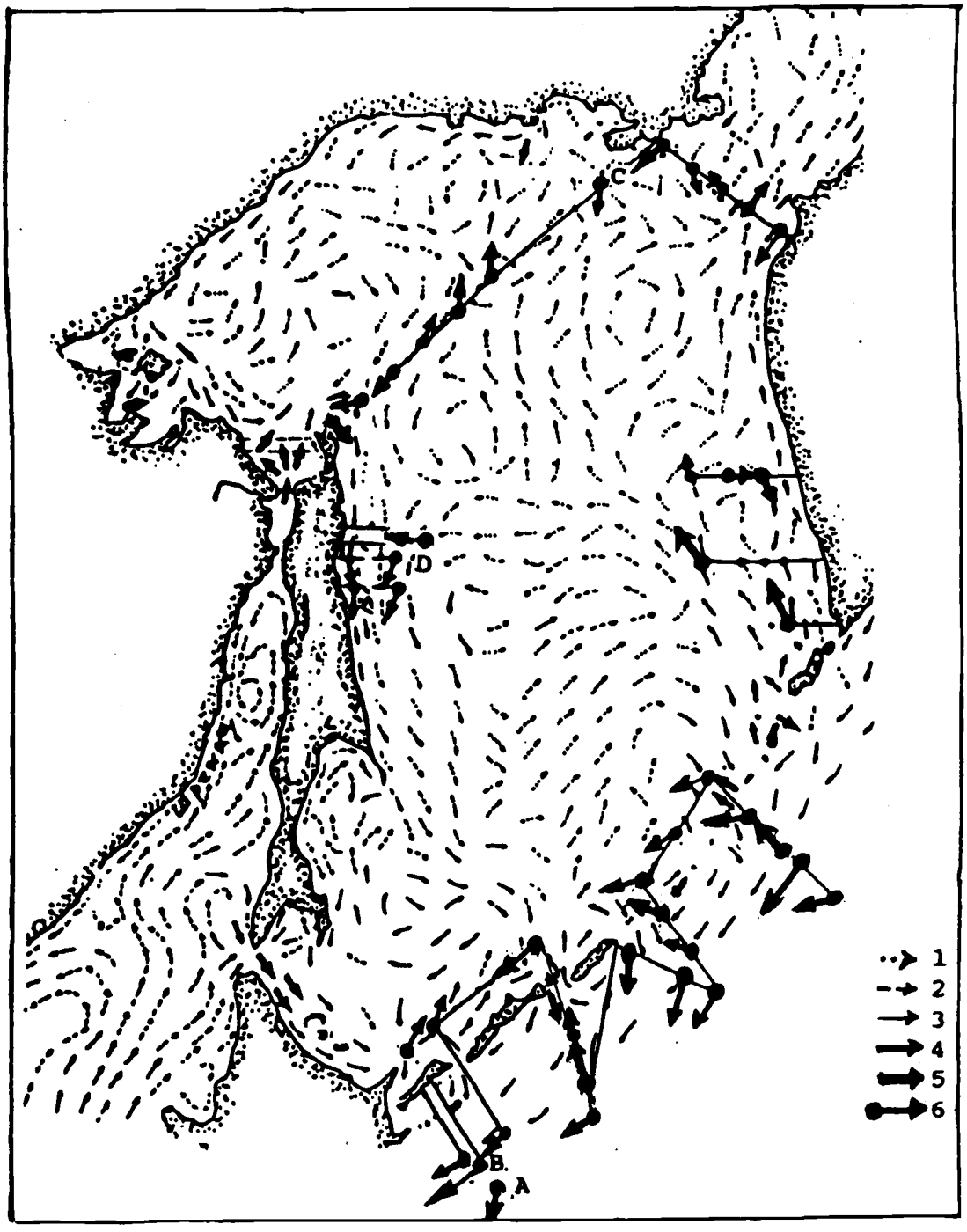

Fig. 1. Surface current velocity in August estimated by geostrophic balance referred to 2,000 db in deep area and to the sea bottom on the shelf (Moroshkin, 1964):
1 - < 5 cm/s; 2 - 5-10 cm/s; 3 - 10-20 cm/s;
4 - 20-30 cm/s; 5 - >30 cm/s;
6 - current velocity measured at 300 m in July 1993.

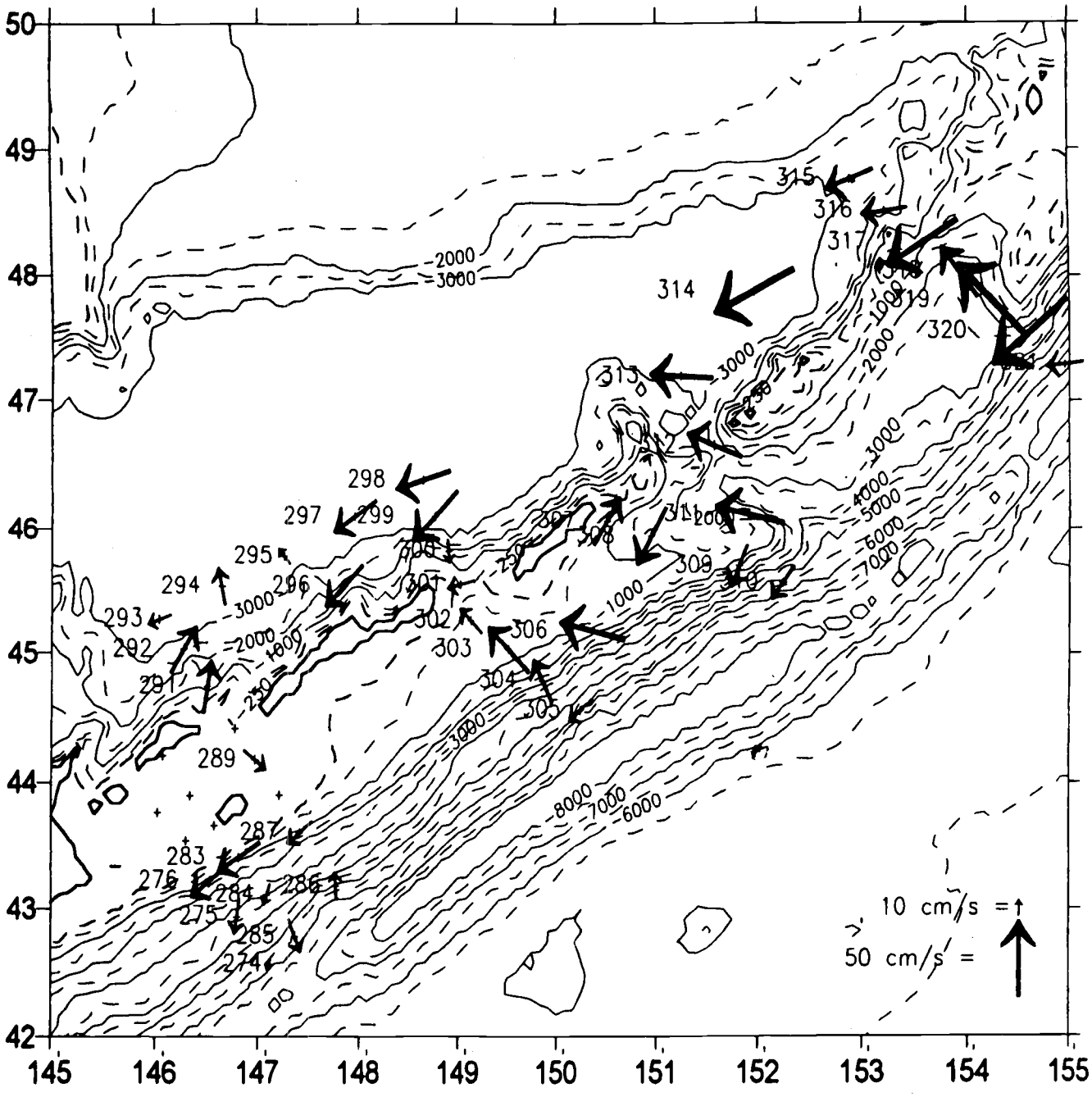

Fig. 2. Experimental currents at 200 m depth.

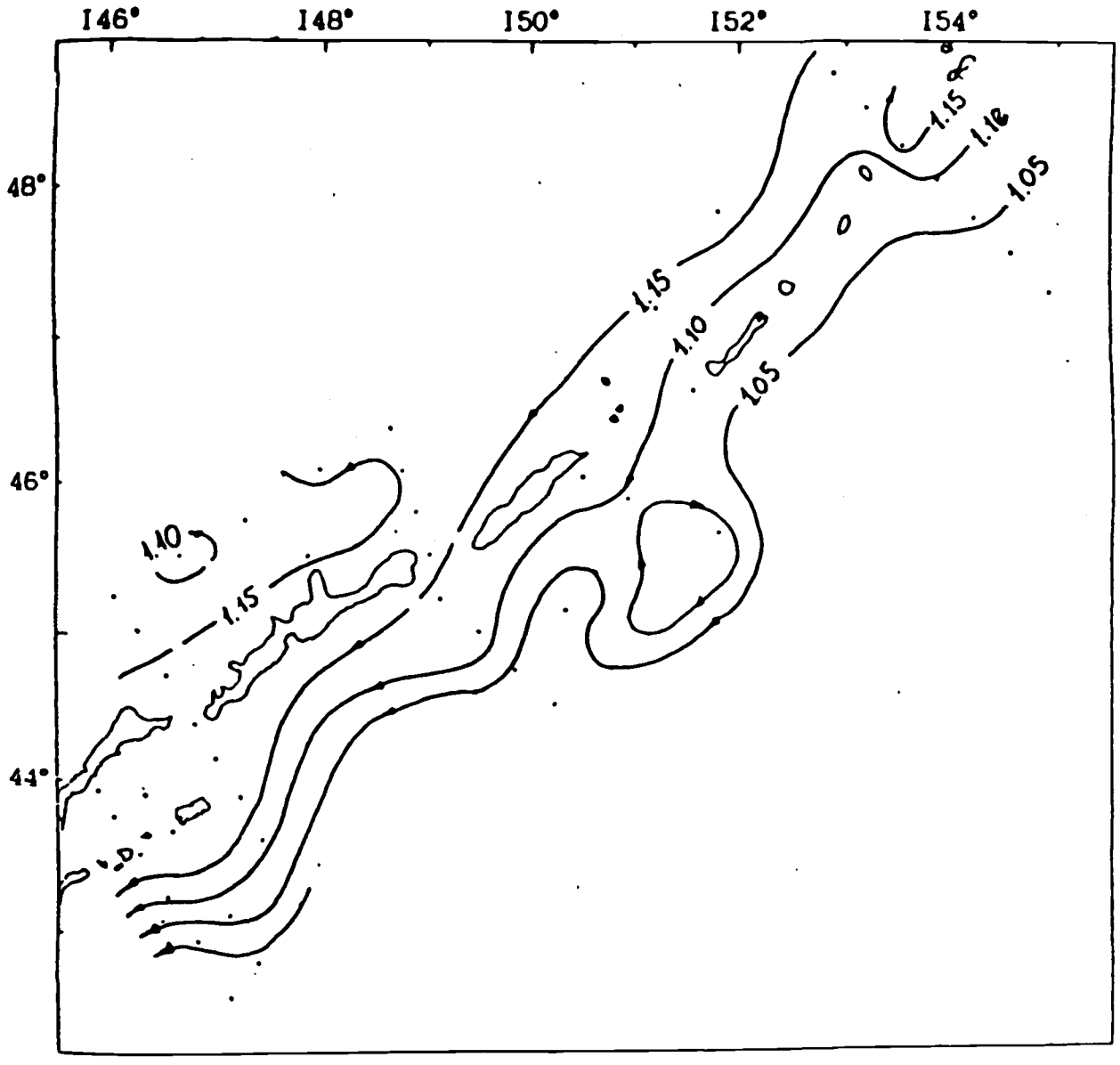

Fig. 3. Surface dynamic topography (in dynamic meters) in July 1993 estimated by geostrophic balance referred to 1,000 dbar.

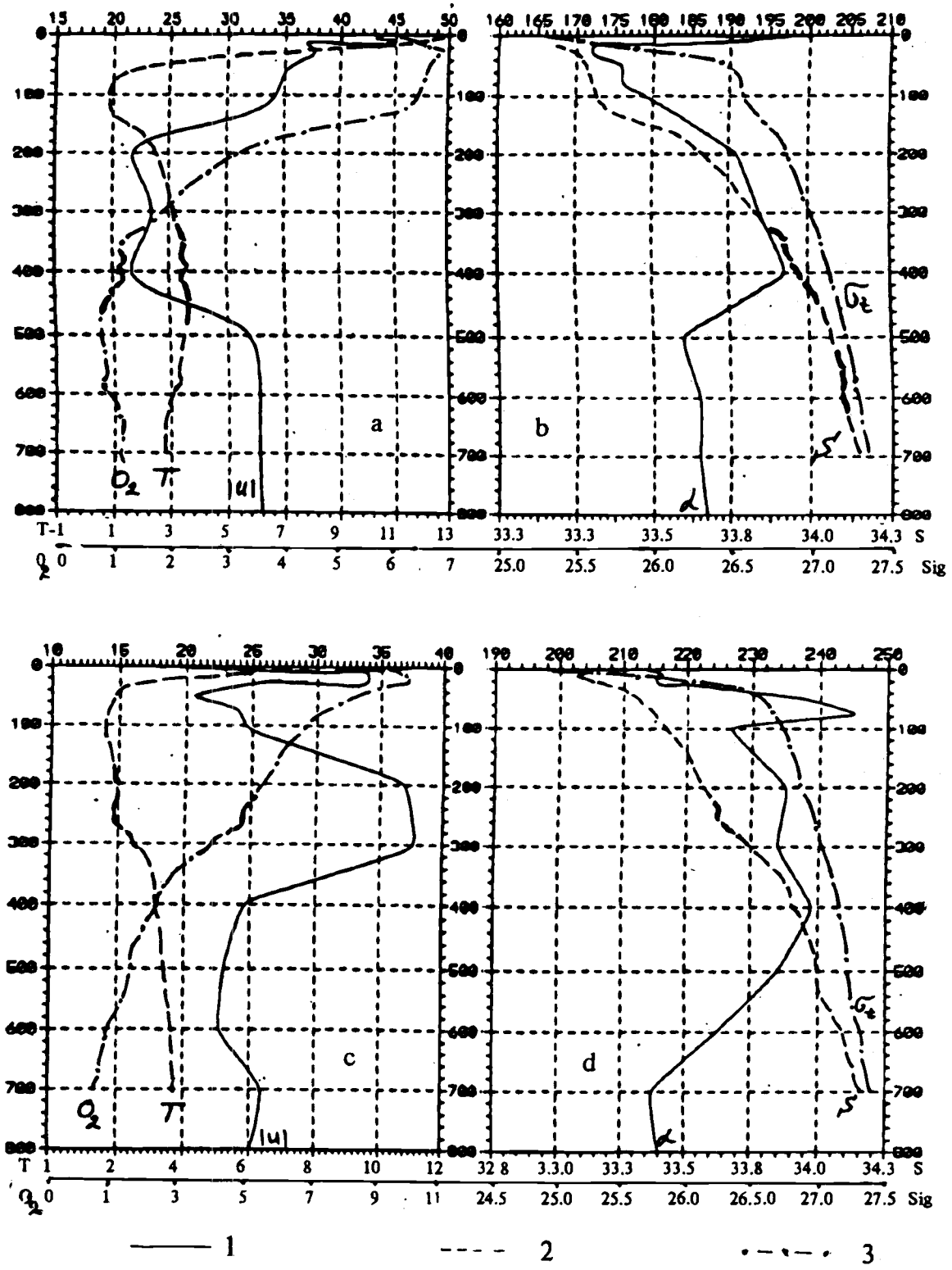

Fig. 4. Vertical profiles of water properties: current velocity (cm/s) - curve 1, temperature (°C) - curve 2, and dissolved oxygen (ml/l) - curve 3 (a, c); current direction - curve 1, salinity (ppt) - curve 2, and density anomaly - curve 3 (b, d) at stations 275 (a, b) and 276 (c, d), points A and B respectively in Fig. 1.

Hydrographic and Tracer Measurements of the Water Mass Structure and Transport in the Okhotsk Sea in Early Spring

Stephen C. RISER[1], Gennady I. YURASOV[2] and Mark J. WARNER[1]

[1] School of Oceanography, University of Washington, Seattle, U.S.A
[2] Pacific Oceanological Institute, Russian Academy of Sciences, Vladivostok, Russia

In April and May of 1995 a detailed survey of the most important portions of the Okhotsk Sea, including the Kuril Straits, the Kuril Basin, and northern part of the Okhotsk Sea was undertaken in a joint USA-Russian expedition aboard the Russian research vessel *Akademik Lavrentjev*. Observations were collected at over 160 stations in the Okhotsk Sea, using both CTD and Niskin bottle methods, with all measurements made over the entire water column. The parameters measured included temperature, salinity, dissolved oxygen, nutrients, chlorofluorocarbons, carbonate chemistry, and tritium and helium-3. A map of the expedition location is given in Fig. 1. Many of the data were collected close to the ice-edge or in regions where ice had been present only a few days or weeks before. The resulting data set represents one of the most complete modern surveys of the Okhotsk Sea in late winter/early spring conditions.

When plotted on a potential temperature-salinity (θ/S) diagram, the CTD data from these 160 stations are suggestive of the regional differences in the character of the water masses of the Okhotsk Sea, as shown in Fig. 2 (note that these are preliminary data, and some editing is obviously required). There are several branches to the main θ/S manifold in the region $1.0°C < \theta < 3.4°C$ and $33.0 < S < 34.6$. At the lowest temperatures in this region lies the main water of the upper 500 m of the Okhotsk Sea; at the highest temperature lies the water of the North Pacific Ocean, just outside Bussol' and Kruzenshtern Straits. Between these curves lie data from a number of stations that suggest the complexity of the mixing between the Okhotsk Sea and North Pacific. It appears that a third water mass, at potential temperatures somewhere between the general Okhotsk Sea and the North Pacific, lies between these extremes and exists as a result of mixing between these two endpoints. Similar properties can be seen in many of the chemical tracers collected on the expedition. It is suggested that the main mechanism responsible for this third curve is tidal mixing through the Kuril Straits.

At the highest densities in the Okhotsk Sea the water mass characteristics are asymptotically similar to the deep water of the North Pacific Ocean. This is due to the fact that the deepest entrance to the Okhotsk Sea is through Bussol' Strait, at a depth of 2,200 m. At depths greater than this within the Okhotsk Sea, in the Kuril Basin, there is no other apparent source of water. Stated differently, although the surface waters of the Okhotsk Sea in winter are among the coldest anywhere in the world ocean, there is no evidence of the occurrence of deep convection within the Okhotsk Sea. The dissolved oxygen concentrations and chlorofluorocarbon ratios in the deepest portions of the Kuril Basin (not shown) appears to preclude this possibility. The chlorofluorocarbon measurements suggest that the deepest waters of the Kuril Basin have not been exposed to the sea surface for 30-50 years, although waters above 1,000 m in the Sea appear to have been ventilated in the past 15 years. In general, the vertical distribution of these variables inside the Okhotsk Sea is quite different from the North Pacific, suggesting that vertical mixing is much stronger inside the Okhotsk Sea, perhaps again due to enhanced tidal activity.

At the lowest potential temperatures in the Okhotsk Sea ($\theta < 0°C$) two main masses of water appear to be present, both formed near the sea surface during the winter, both having some expression close to the freezing point of seawater. At the lowest salinities (< 32.7) and densities ($\sigma_\theta < 26.4$), the remnants of melting ice can be seen. At somewhat higher salinities (> 33.0) and densities ($\sigma_\theta > 26.5$) a second general water mass appears at these cold temperatures. This is the water discussed by Dr. Kitani that is formed by brine rejection under ice shelves. Almost all of this type of water was observed in the northwest Okhotsk Sea, off the northern coast of Sakhalin Island. Taken together, these measurements allow us to make better estimates of the water mass characteristics of the Okhotsk Sea, the residence time of water in the Sea, and the mechanisms that lead to the distributions of these water masses.

A central goal of this expedition was to examine the nature of the flow through the main passages between the Kuriles and the North Pacific, Bussol' Strait and Kruzenshtern Strait. A CTD section across Bussol' Strait was carried out twice over a 3-day period, and a section across Kruzenshtern Strait was run three times over a 2-day period. The repeat times of these sections were chosen to attempt to minimize effects of tidal aliasing. Potential temperature sections across Bussol' Strait are shown in Fig. 3; from the data it can clearly be seen that there is a great deal of change in the subsurface temperature field in Bussol' Strait over time scales of a day or two. Note especially the apparent warming in the western portion of the strait between section 1 and section 2 and the apparent cooling near the central portion of the strait, near the major topographic feature, also between section 1 and section 2. These changes suggest that there is a great deal of tidal energy present at the straits and that the flow near the straits changes on quite short time scales. With this in mind, it is suggested that it will in general be quite difficult to determine the low-frequency (i.e., geostrophic) flow through these straits with any acceptable degree of accuracy in the absence of a dedicated program to carry out direct measurements of currents in the straits for times of a few years or more.

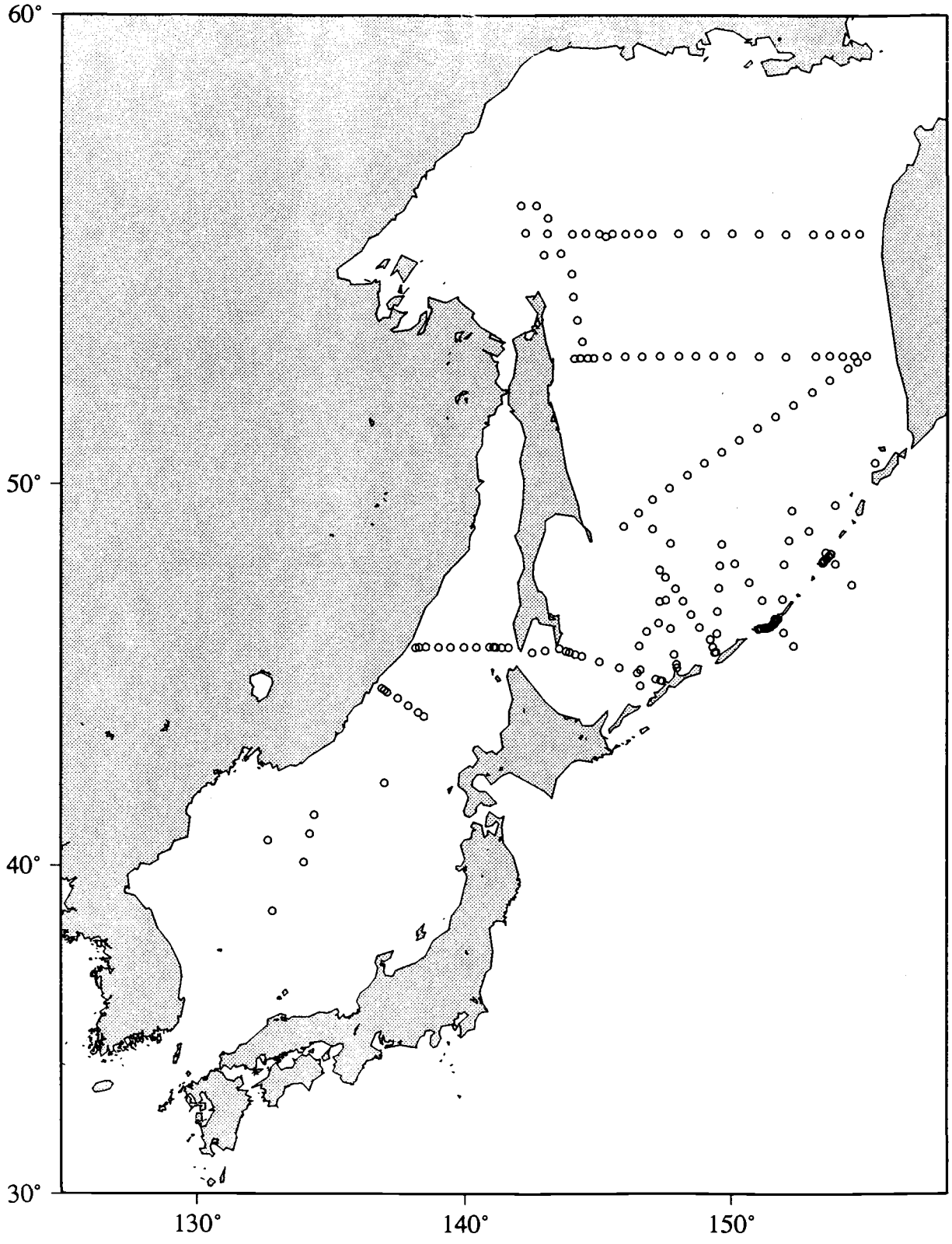

Fig. 1. Map of the expdeition location (R/V Akademik Lavrentjev, April-May 1995).

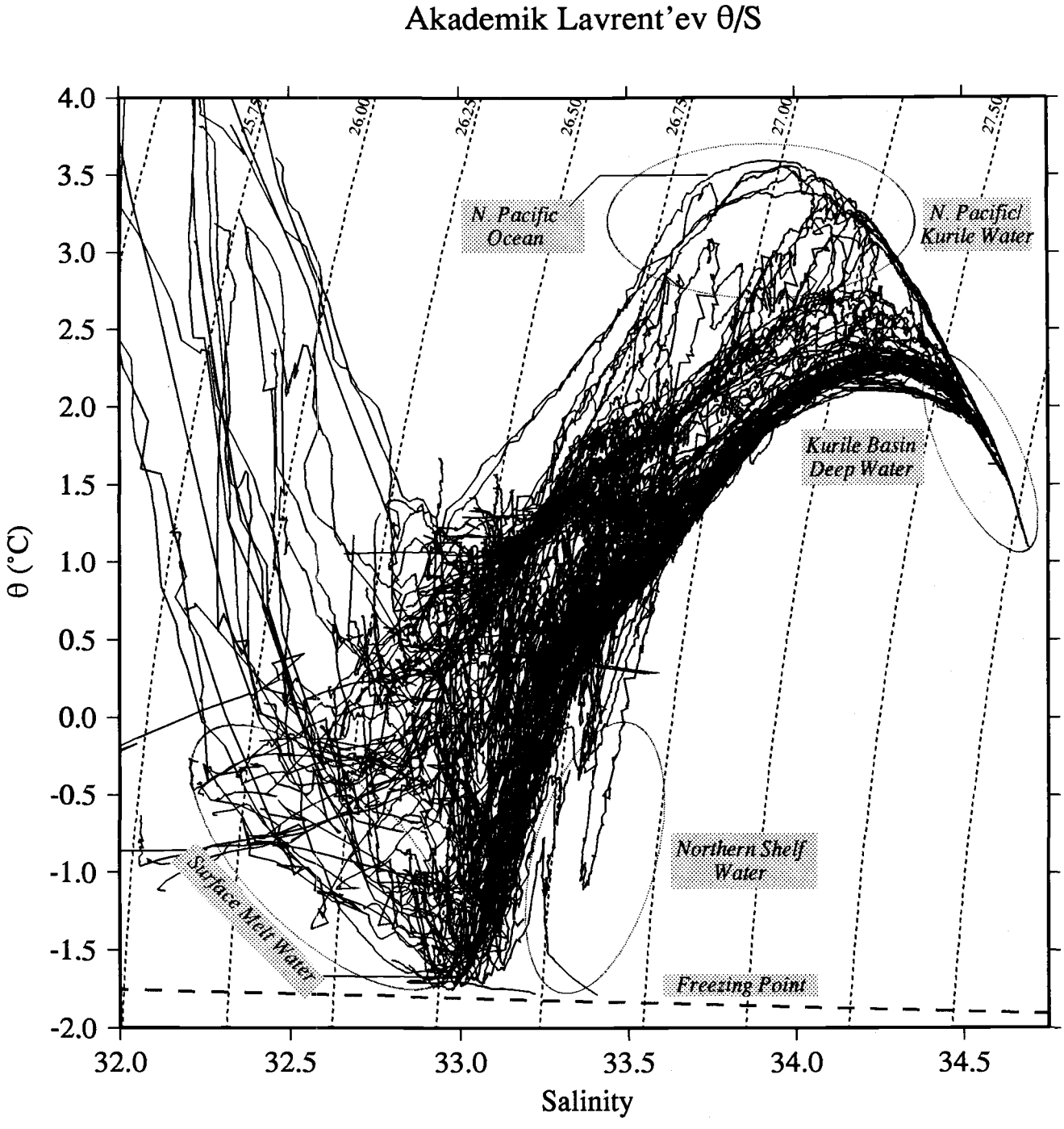

Fig. 2. Potential temperature - salinity diagrams for 160 CTD stations within the Okhotsk Sea in April-May 1995.

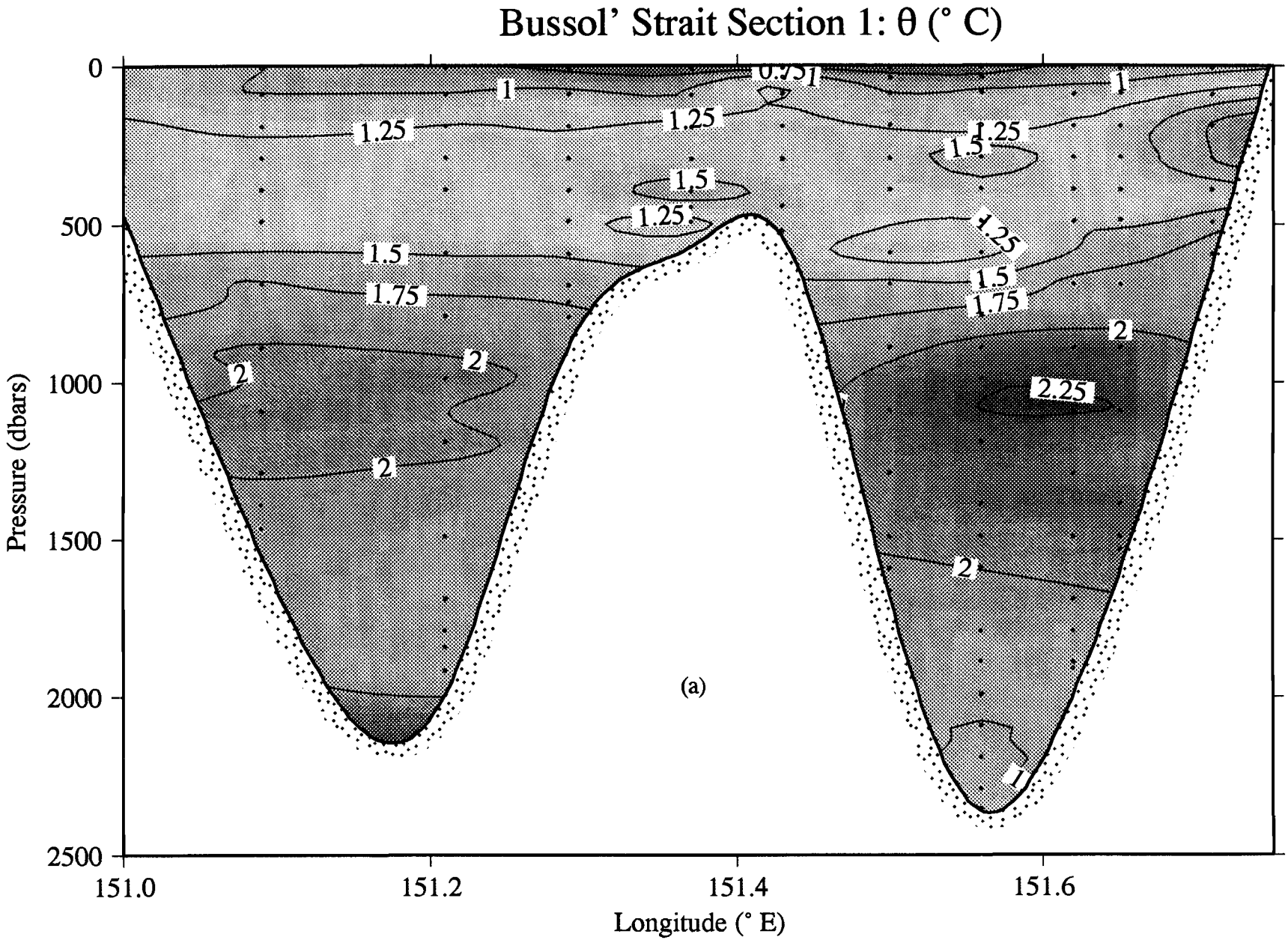

Fig. 3. Potential temperature sections across Bussol' Strait carried out over a 3-day period: (a) section 1; (b) section 2.

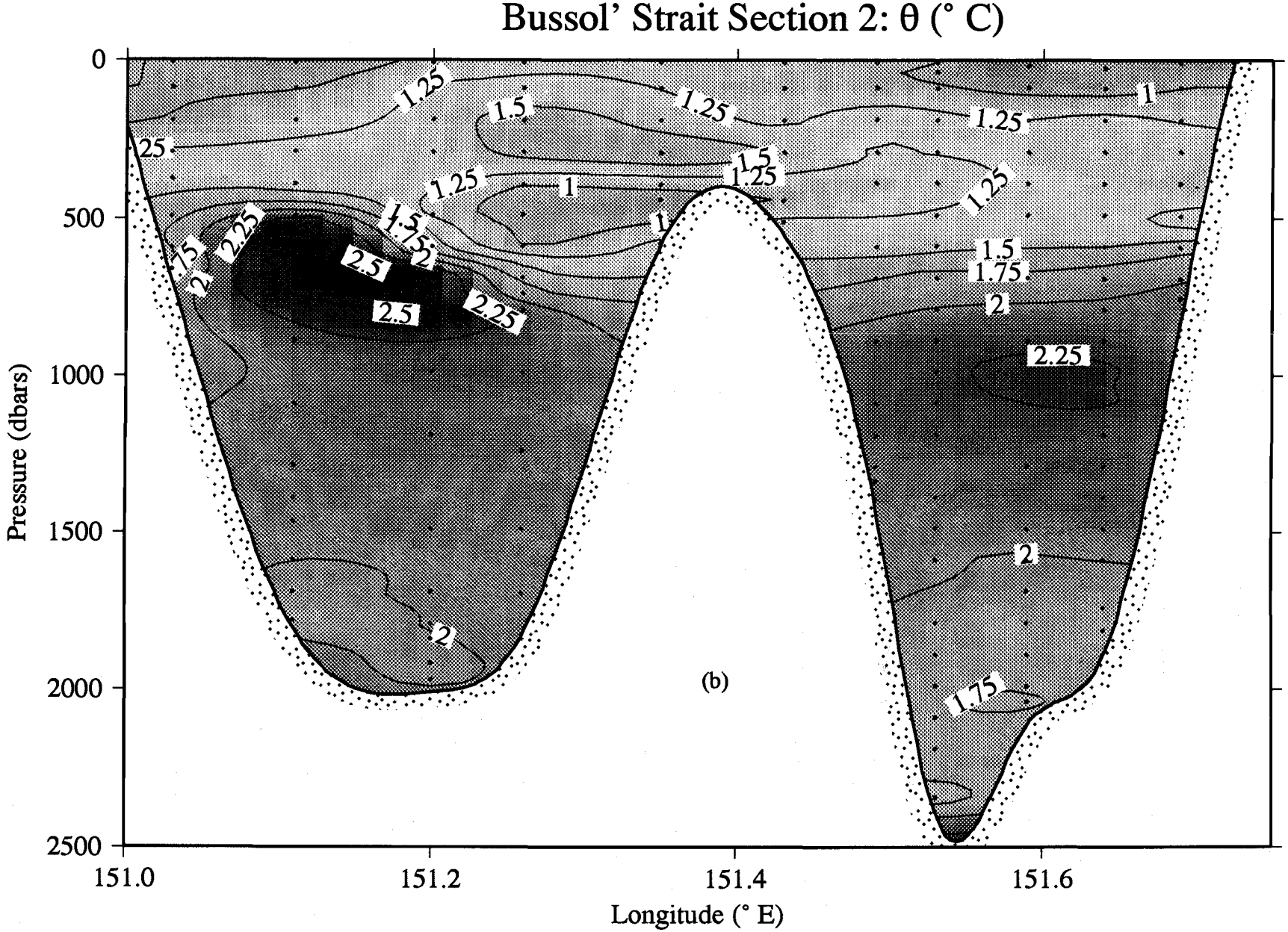

Fig. 3b. Section 2.

Circulation and Water Mass Structure in the Southern Okhotsk Sea, as Observed in Summer, 1994

Konstantin A. ROGACHEV[1] and Andrey V. VERKHUNOV[2]

[1] Pacific Oceanological Institute, Far Eastern Branch, Russian Academy of Sciences, Vladivostok, Russia
[2] Russian Federal Research Institute of Fisheries and Oceanography, Moscow, Russia

INTRODUCTION

Significant transformation of the subarctic water from the northern part of the Okhotsk Sea occurs in the Kuril Basin. Using satellite and a few CTD observations Alfultis and Martin (1987) and Wakatsuchi and Martin (1991) disclosed the anticyclonic circulation in the Kuril Basin in contrast with the large cyclonic Okhotsk Sea gyre by which cold northern shelf waters propagate to the Basin. The detailed synoptic structure of the Kuril Basin is studied insufficiently due to very sparse surveys.

In the present work we describe observations obtained in August 1994 during the cruise of the *RV "Akademik M.A. Lavrentyev"* and demonstrate that anticyclonic circulation in the Kuril Basin constitutes the chain of three anticyclonic eddies with their centers located along the axis of the Basin. Significant water mass transformation and mixing were revealed inside these eddies. Strong inflow of the Pacific warm intermediate waters to the Okhotsk Sea has been detected above 500 dbar (with geostrophic transport through the Boussole Strait of $9.8 \cdot 10^6$ m^3/s), while outflow from the Okhotsk Sea has been found at pressure below 750 dbar.

METHOD OF OBSERVATIONS

CTD survey has been conducted in the period from July 26 to August 26, 1994, using *NBMK3* instrumentation. *Guildline model 8737* probe provided by the Institute of Ocean Sciences (Sidney, B.C., Canada) and calibrated at IOS just before the cruise was used for inter-comparison of the data.

RESULTS

Fig. 1 shows the geopotential anomaly and geostrophic currents at 200 dbar relative to 1,000 dbar for the Kuril Basin area. Three anticyclonic eddies with diameters of 125-300 km in the Okhotsk Sea and one off Boussole Strait are clearly seen. The position of the eddy centers coincide with the Kuril Basin axis, similar to the Kuril Islands anticyclonic rings, which axis lies along the Kuril-Kamchatka trench. The Okhotsk Sea eddies of the Kuril Basin separate cold intermediate waters from the northwest Okhotsk Sea and warm intermediate waters penetrating through the Boussole Strait. The dynamic heights for the Kuril Basin anticyclonic eddies are higher than those in the center of the Boussole ring and have maximum value for the western ring of 12.5 J/kg. The lower boundary of the cold intermediate layer changes from 150 m within the Oyashio to 950 m in the center of the western anticyclone, the biggest eddy of the survey (Fig.2).

Geostrophic transport to the Okhotsk Sea

Recently, Stabeno and Reed (1994) evaluated geostrophic transport through the Aleutian Straits. A similar approach was used in the present work to calculate geostrophic transport (relative to 1,000 dbar) for the Kuril Straits area. We found that transport by the First Oyashio Branch (southward transport to the west of the Boussole ring) was $9.2 \cdot 10^6$ m^3/s, while total transport through the section across the Oyashio First Branch and anticyclonic eddy was $10.4 \cdot 10^6$ m^3/s. The transport through the Boussole Strait to the Okhotsk Sea has been computed as $9.8 \cdot 10^6$ m^3/s. These data contradict the earlier estimations of geostrophic outflow through the Boussole Strait (Reid, 1973). However, despite the uncertainties of geostrophic transport calculations for the Strait area, we assume that the direction of flow reflects the propagation of warm intermediate waters to the Okhotsk Sea. This penetration is clearly seen in the temperature and salinity profiles (Fig. 3).

Penetration of warm intermediate layer to the Okhotsk Sea

A warm intermediate layer to the east of the Kuril Islands was observed at 200-700 dbar. Its maximum temperature was 3.55°C at 300 dbar on station 86. Warm layer with temperature of 3.54°C was also found at 500 dbar on station 82 in the canyon of the Boussole Strait. Simultaneously, water with temperature from 2.6 to 2.68°C was revealed at the other side of the Boussole Strait in the Okhotsk Sea on stations 94 and 95 at 650 dbar. It was the highest temperature of the intermediate waters in the Okhotsk Sea in the area of study. Salinity in the warm core continuously decreased from 33.983 psu (station 86 at 300 dbar) and 33.987 psu (station 82 at 500 dbar) to 33.840 psu (station 94 at 650 dbar) and 33.903 psu (station 95 at 650 dbar). It appears that warm intermediate water penetrates through the Strait deepening gradually from 300 dbar to 650 dbar between station 86 and stations 94-95. Abrupt changes which lead to the temperature and salinity decrease were detected within the Boussole Strait.

Okhotsk water outflow through the Boussole Strait

Our observations in the Boussole Strait canyon (station 82) strictly demonstrated a four-layer vertical water structure (Fig. 4): the surface warm layer (at pressure less than 100 dbar); the cold intermediate layer (typical for summer) with the core at 100 dbar; the warm intermediate subarctic layer (with distinct boundaries at pressures of 450 and 780 dbar) characterized by temperature higher than 3.2°C and salinity over 34.0 psu. However, the most interesting feature of the vertical structure is the lower layer of water which is relatively cold (< 2.3°C), fresh and rich in oxygen. A very sharp dropping of salinity and temperature, as well as an increasing of oxygen concentration take place at a pressure of 780 dbar. Comparison of TS diagrams for stations 82 and 94-97 shows that water of this layer originates from the Okhotsk Sea, i.e. below the warm intermediate layer the TS diagram of station 82 coincides with those in the Okhotsk Sea. Note, that Okhotsk Sea waters in TS diagrams are obviously separated from the Oyashio and Kamchatka current waters with its lower temperature and higher salinity at maximum temperature. Hence, the gap between TS-curves for ocean and Okhotsk Sea stations is evident. Similar signs of the Okhotsk Sea outflow were observed at station 85, however, at station 82 they were more pronounced. The reason could be that this particular station is located exactly in the Boussole Strait canyon.

The CTD results are confirmed by the oxygen bottle data. The Okhotsk Sea water is characterized by high oxygen saturation (up to 15% at pressure of 1,000 dbar) and the absence of an oxygen minimum within the Boussole Strait at pressures less than 1,000 dbar. Meanwhile, oxygen minimum with saturation below 10% and absolute values less than 0.7 ml/l (station 80) exists in the

ocean to the east of the Strait at pressures of 700-850 dbar. Therefore, oxygen concentration of 1.32-1.69 ml/l and saturation of 17-22% at 800-1000 dbar detected at station 82 clearly prove that these waters have originated from the Okhotsk Sea.

Two stations were taken in the Boussole Strait canyon in April 1995, during the joint Russian-USA expedition to the Okhotsk Sea on board of the *RV "Akademik M.A. Lavretyev"*, in which the first co-author participated. These results (not shown here and kindly provided by Dr. S. Riser from the University of Washington and Dr. G. Yurasov from the Pacific Oceanological Institute) definitely indicate the gap between TS-curves for stations at the opposite sides of the Boussole Strait, similar with 1994 data. In particular, vertical structure at station 23 in the Boussole Strait canyon was similar to station 82 (August 1994): cold and relatively fresh layer with high oxygen concentration was found below the warm intermediate layer at pressure 800 dbar. Thickness of this layer was greater than 400 dbar and its thermohaline characteristics coincide with the Okhotsk Sea waters.

Talley (1991) described unusually cold, fresh and rich-oxygen water with sigma-theta of 27.4 at pressure of 800 dbar, observed off the Boussole Strait in August 1985. Isopycnal maps allow the conclusion that this water has an Okhotsk Sea origin. The only station considered by Talley (1991) shows an anomaly of temperature, salinity and oxygen in the layer of 100 m thickness, which is much less than during our survey. It can be explained by the greater distance of this station from the Strait, as compared with our station 82 in August 1994. Moreover, anomalies of temperature and salinity with respect to neighboring waters reached 0.2-0.5°C and 0.07 psu in 1985, whereas anomalies of 0.84°C, 0.08 and 1 ml/l for temperature, salinity and oxygen were revealed in 1994.

Therefore, these observations permit the assumption of the regular outflow from the Okhotsk Sea through the Boussole Strait at pressure below 800 dbar and inflow of warm subarctic waters through this Strait at 300-700 dbar.

ACKNOWLEDGMENTS

We deeply appreciate the efforts of scientific and ship's personnel of the *RV Akademik M.A. Lavrentyev*. We are especially grateful to Drs. Stephen Riser and Gennady Yurasov who provided additional data for the Boussole Strait area mentioned above.

REFERENCES

Alfultis, M.A. 1987. Martin S. Satellite passive microwave studies of the sea of Okhotsk ice cover and its relation to oceanic processes, 1978-82. J. Geophys. Res. 92(C12):13013-13028.

Reid, J.L. 1973. Northwest Pacific Ocean waters in winter. John Hopkins Oceanogr. Studies. 5:1-96.

Stabeno, P.J., and R.K. Reed. 1992. A major circulation anomaly in the western Bering Sea. Geophys. Res. Lett. 19:1671-1674.

Talley, L.D. 1991. An Okhotsk sea water anomaly: Implication for ventilation in the North Pacific. Deep-Sea Res. 38:S171-S190.

Wakatsuchi, M., and S. Martin. 1990. Satellite observations of the ice cover over the Kuril Basin region of the Okhotsk sea and its relation to the regional oceanography. J. Geophys. Res. 95(C8):13393-13410.

FIGURES

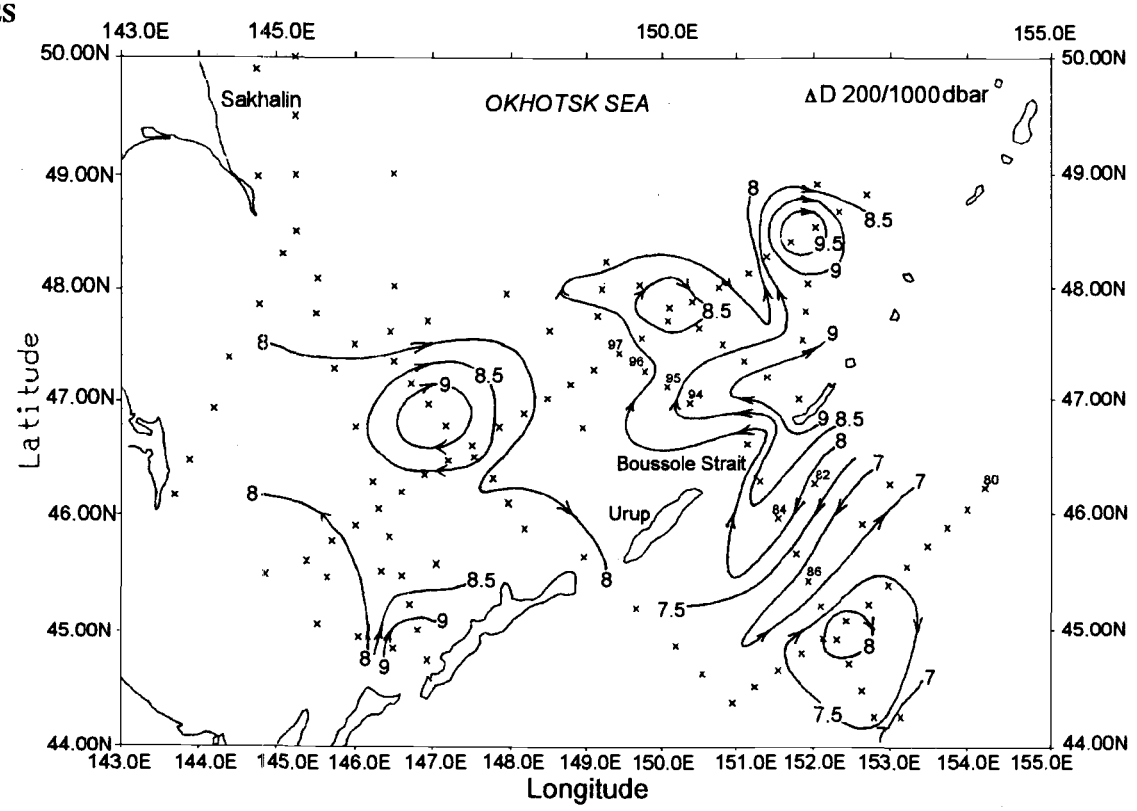

Fig. 1. Geopotential anomaly (J/kg) at 200 dbar, relative to 1,000 dbar, observed in August, 1994.

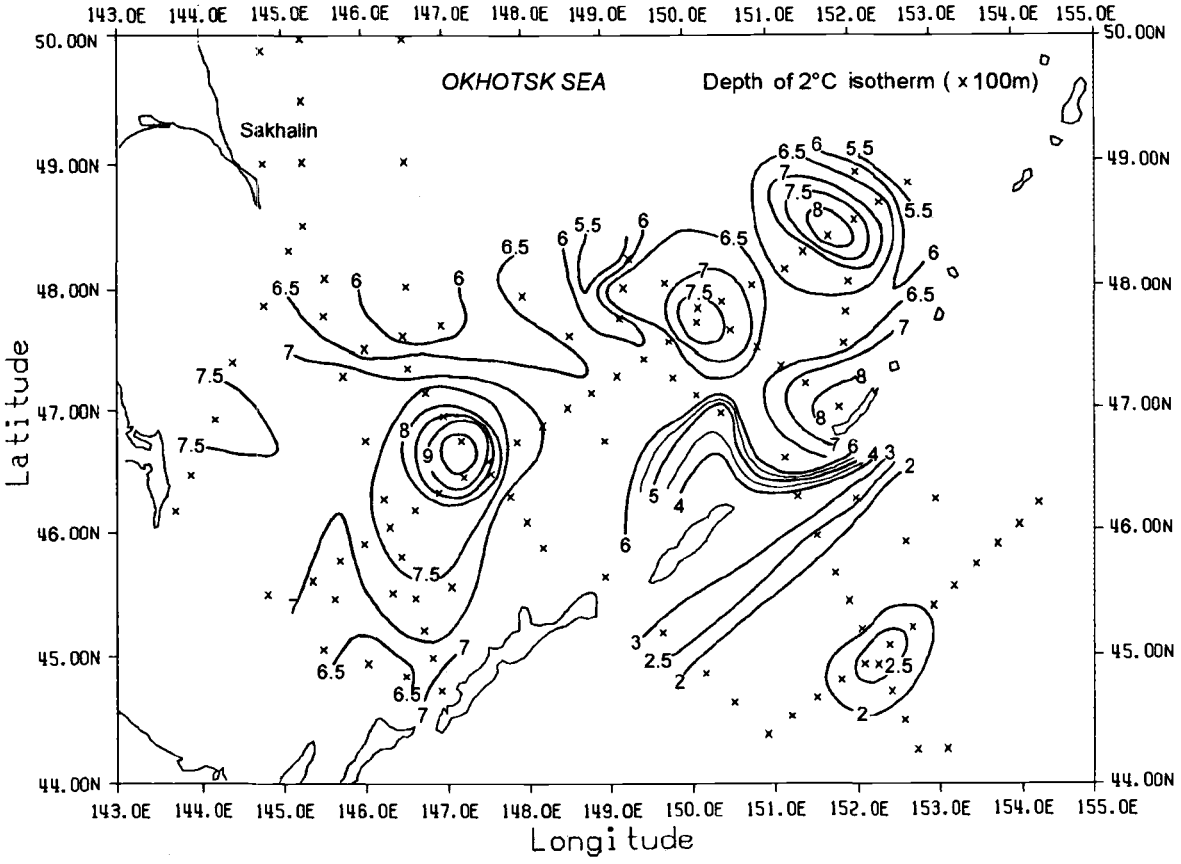

Fig. 2. Depth of 2°C isotherm (x 100m), observed in August, 1994.

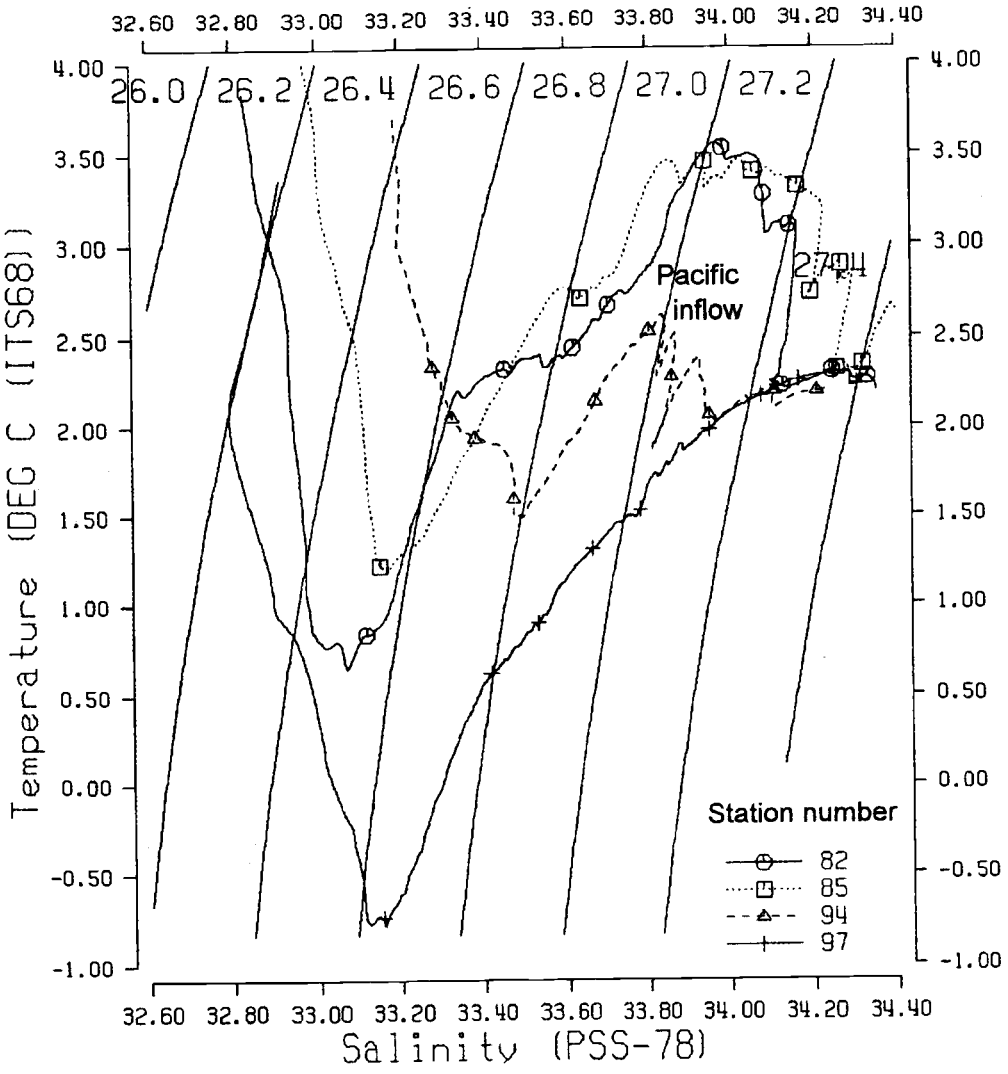

Fig. 3. TS - diagrams for selected stations near the Boussole Strait.

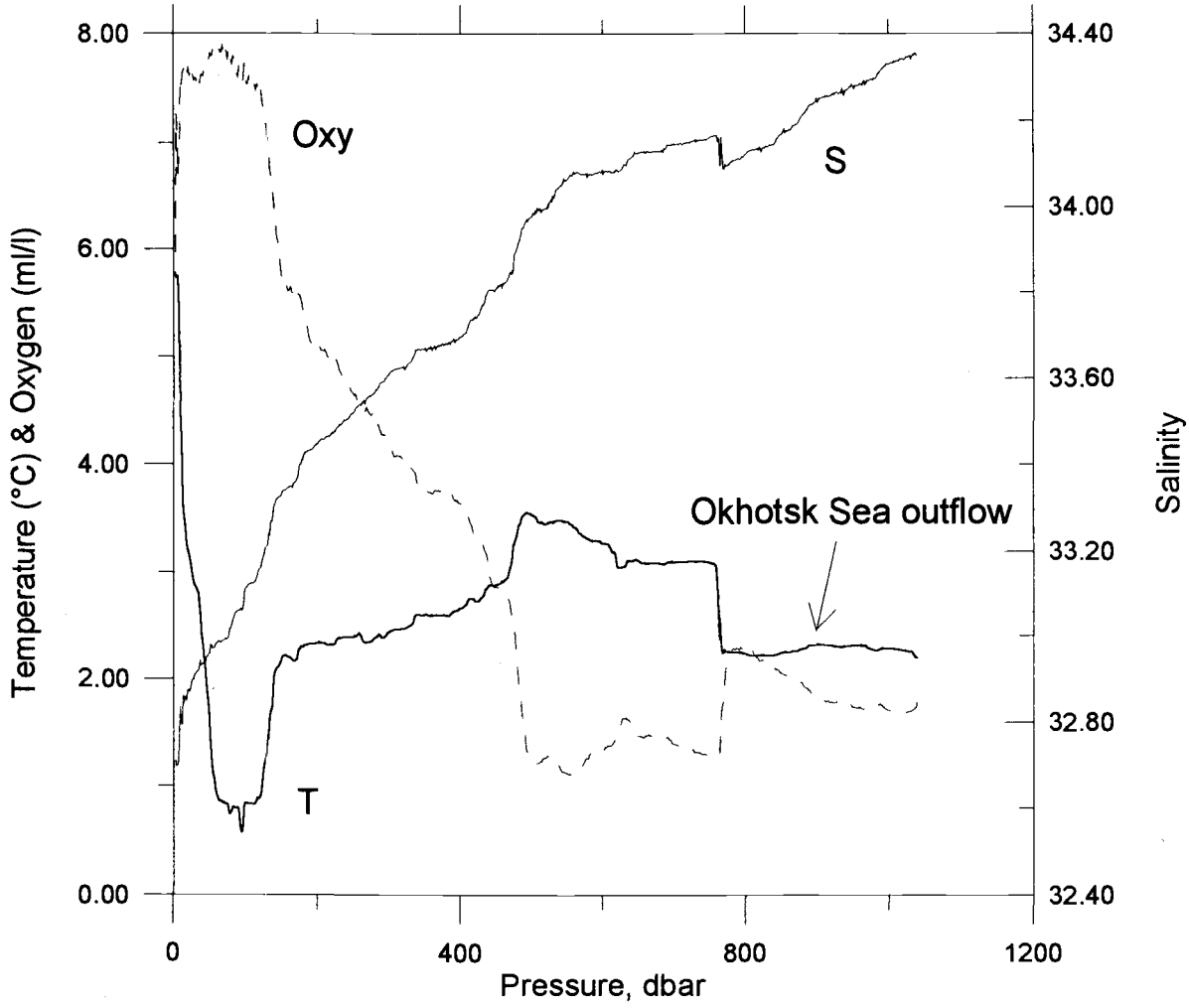

Fig. 4. Vertical profiles of temperature (T), salinity (S) and dissolved oxygen (Oxy) at station 82 near the Boussole Strait. Okhotsk Sea outflow is observed deeper than 780 dbar.

North Pacific Intermediate Water Formation and the Role of the Okhotsk Sea

Lynne D. TALLEY

Scripps Institution of Oceanography, University of California, San Diego, U.S.A.

The following is an extended abstract of a talk which was presented on NPIW, with emphasis on how the salinity minimum forms in the Mixed Water Region. A more general talk, which included more emphasis on the role of the Okhotsk Sea, was presented separately. Because this is an extended abstract, the references are greatly truncated and include primarily my own work. More complete references can be found in those publications.

LARGE-SCALE PROPERTIES OF NORTH PACIFIC INTERMEDIATE WATER

North Pacific Intermediate Water (NPIW) can be defined as either the salinity minimum of the subtropical gyre of the North Pacific, at a potential density of 26.7 to 26.8 sigma-theta, or as the subtropical layer which is freshened by subpolar water with a potential density range of about 26.65 to 27.6. The subtropical gyre's salinity minimum is evident in any vertical section of salinity which crosses it.

The NPIW salinity minimum should be carefully differentiated from the shallower salinity minima which are found in the eastern and tropical North Pacific, and from the Antarctic Intermediate Water (AAIW) found in the tropical Pacific, because their sources differ from that of NPIW. The shallower salinity minima, arrayed around the eastern subtropical gyre, arise from subduction of surface waters as they move southward and encounter less dense surface waters (Talley, 1983; Yuan and Talley, 1992). Antarctic Intermediate Water comes from the south and is found up to the southern boundary of the subtropical gyre, although there is some controversy about whether the salinity minimum in the North Pacific's tropical region really derives more from NPIW than from AAIW.

The NPIW salinity minimum is found only in the subtropical gyre (Sverdrup et al., 1942; Talley, 1993) although isopycnal properties show that its low salinity clearly arises in the subpolar region (Reid, 1965; Talley, 1993). Its northern and southern boundaries are well-defined and coincide respectively with a deep expression of the Subarctic Front and the southern side of the subtropical circulation, which is relatively far to the north at the NPIW depth. Its eastern boundary is less easy to define, but the eastern Pacific's California Current is a region of multiple or missing salinity minima, and it appears that intact NPIW does not extend into this region (Talley, 1993).

The NPIW's salinity minimum has a density of 26.7 to 26.9 sigma-theta in the subtropical Pacific (Fig. 1 from Talley, 1993). Where a portion of the NPIW protrudes southward along the western boundary in the Mindanao Current, it appears to be truncated from below and its density can be lower (Bingham and Lukas, 1994). In the Mixed Water Region (MWR) between the separated Kuroshio and Oyashio, NPIW salinity minima are found in this full range of densities; the denser minima have higher salinity and lower oxygen and are apparently old NPIW which has entered the MWR from the Kuroshio. The lighter minima are considered here and in Talley et al. (1995) to be the newest NPIW.

If low salinity and high oxygen are considered to indicate the most recently-ventilated NPIW, then the region of newest NPIW is the northwestern subtropical gyre, in the MWR, based on salinity and oxygen distribution at the NPIW salinity minimum (Talley, 1993). Away from this location of new NPIW, salinity increases, probably due to vertical diffusion and possibly horizontal diffusion along the eastern and southern sides of the gyre; oxygen decreases due to consumption and diffusion. The highest NPIW salinity is found in the southwestern subtropical gyre and in the Kuroshio and Mindanao Currents. Lowest oxygen is found in these regions as well.

CIRCULATION AND TRANSFORMATION IN THE OKHOTSK SEA

In the wintertime, surface densities in the open North Pacific do not exceed approximately 26.65 sigma-theta except in very localized coastal regions. Even these small regions around Hokkaido and northern Honshu do not ventilate water much denser than 26.7 sigma-theta. What is the source of fresh, oxygenated water at densities greater than 26.65 sigma-theta? It appears that the source is the Okhotsk Sea, and results from direct ventilation of densities 26.6 to 27.2 sigma-theta. On isopycnals which intersect the NPIW salinity minimum, it is clear that the highest oxygen and lowest salinity are found in the Okhotsk Sea (Talley, 1991; hints of this in Reid, 1965, 1972). In fact, the highest oxygen, suggestive of the most recent ventilation are found in the Okhotsk Sea for all densities from 26.7 to 27.6 sigma-theta, which is the density at the greatest sill depth separating the Okhotsk Sea and the NW Pacific. The lowest salinities for this density range and even lower are also found in the Okhotsk Sea. Thus one concludes that the Okhotsk Sea is the site for the densest ventilation impacting isopycnals in the open North Pacific. (While deep water is formed in the Japan Sea, its dense waters do not connect with the open North Pacific.)

Most of the Okhotsk Sea ventilation occurs under sea ice in winter. Winter surface density in open water in the Okhotsk Sea does not appear to much exceed 26.7 sigma-theta, even though waters are clearly ventilated to much greater densities. Brine rejection is a very effective mechanism for increasing the density of near-freezing surface water. Dense, cold water has been observed on the shelves of the northern and western Okhotsk Sea (Kitani, 1973). Based on water properties in the western Okhotsk Sea, it appears that the brine rejection mechanism might be operative to a maximum density of about 27.2 sigma-theta (Talley, 1991). Because this mechanism deposits a very cold water on denser isopycnals, this water is also the freshest on those isopycnals, although there is a net flux of salt downward.

The Okhotsk Sea also contains the North Pacific's freshest, most oxygenated water at densities greater than 27.2 sigma-theta. Based on isopycnal salinity and oxygen distributions, Talley (1991) hypothesized that the principal mechanism for this "ventilation" is vertical mixing primarily within the Okhotsk Sea, and operating most vigorously close to Bussol' Strait. Bussol' Strait is the deepest passage through the Kuril Islands, with a sill depth of 2300 meters, and sill density of about 27.6 sigma-theta. This argument is a refinement of Reid's (1965) argument that vertical diffusion in the North Pacific carries the low salinity surface signature downward - the refinement is to suggest that much of the vertical diffusion is localized. Moroshkin (1966) concluded that there is a great deal of mixing in the Kuril Straits. The primary mechanism for mixing might be tidal flows, which are on the order of 4-5 knots near the surface through the various straits.

In the following few paragraphs the circulation and transformation in the Okhotsk Sea are reviewed; a much more complete review can be found in the PICES Scientific Report on the Okhotsk Sea (Talley and Nagata, 1995).

The Okhotsk Sea is the northwesternmost region of the subpolar gyre (Fig. 2). Much of it is ice-covered in winter, although the ice melts away completely each summer. It is connected to the open North Pacific through the Kuril Island chain, and so the subpolar circulation which enters the Okhotsk Sea must do so through island passages. The two most important passages are Bussol' and Kruzenshtern Straits. Part of the East Kamchatka Current, flowing southward out of the Bering Sea, enters the Okhotsk Sea, and part remains outside. Some of the western boundary current might also enter at Bussol' Strait which is also the primary site of the denser outflow. The outflow turns southwestward and becomes the Oyashio. The net exchange between the open North Pacific and the Okhotsk Sea is on the order of 3-5 Sv, although a very good estimate is not possible using available data.

Within the Okhotsk Sea, the flow is basically cyclonic, but eddy activity is prominent, as are local gyres. In this sense it resembles the Bering Sea, which is also separated by an island chain from the open Pacific. Local circulation features in the Okhotsk Sea which appear to be important for water mass transformation are the northern shelf region where coastal polynyas are often found, Kashevarov Bank around which there is commonly intensified cyclonic flow and above which there is upwelling, the East Sakhalin Current which transports dense, ventilated waters southward from the northern shelf region, the Soya Current which transports saline Japan Sea water into the Okhotsk Sea, and an anticyclonic gyre and anticyclonic eddy field in the Kuril Basin which spreads the saline Soya Current waters into the Okhotsk Sea.

Two important physical elements for dense water formation in the Okhotsk Sea are the input of saline water in the Soya Current, which preconditions the Okhotsk Sea to forming denser water, and sea ice formation which produces dense shelf water through brine rejection. Sea ice forms along the northwestern boundary in December and eventually covers most of the northern and western parts of the sea. A coastal polynya appears in mid-winter along the northwestern side; observations of the densest, saline waters have been along this shelf. Kitani (1973) observed shelf water at nearly 27.05 sigma-theta, and showed that the very coldest waters in the summer temperature minimum, indicative of freezing in winter, were located in the northwestern Okhotsk Sea. The exception is above Kashevarov Bank, where strong tides mix the warmer deep water upwards; a polynya is usually found in this location in winter. Since the surface waters in the coastal polynya are probably near freezing, it is more likely to produce the densest water than would the Kashevarov polynya, whose waters are relatively warm.

The dense waters formed in the northern Okhotsk Sea are advected southwards in the East Sakhalin Current and then over towards Bussol' Strait, based on isopycnic properties (Talley, 1991). Strong tides are found around the Kuril Islands, including in Bussol' Strait. These produce a mixed water around the islands (Kawasaki, these proceedings; Kawasaki and Kono, 1993) which includes components of waters from outside the Kurils and which is also vertically mixed, so that the water which leaves the Okhotsk Sea is not pure Okhotsk Sea water. The newly-ventilated and mixed Okhotsk Sea waters join waters from the East Kamchatka Current and flow southwestward towards Hokkaido.

FORMATION OF THE NPIW SALINITY MINIMUM IN THE MIXED WATER REGION

The ventilated water from the Okhotsk Sea exits primarily through Bussol' Strait and joins the southward flow of the Oyashio towards Hokkaido. The Oyashio separates from the western boundary at the southern end of Hokkaido and flows eastward. It typically meanders at least twice, in well-known locations, after it separates (e.g. Kawai, 1972). Some of the Oyashio water separates off and remains in the MWR while the remainder circulates eastward as part of the subpolar gyre circulation.

The MWR occupies an interesting dynamical niche in the North Pacific's gyre circulations. First, it is bounded to the north and south by vigorous, meandering separated boundary currents, which spawn "rings" or "intrusions" into the MWR, so it is a mixing region between Oyashio and Kuroshio waters. (A third source of water for the region is flow from the Japan Sea through Tsugaru Strait, which affects the uppermost density layers, and introduces extra salinity which preconditions the MWR to have higher winter surface densities, on the order of 26.65 sigma-theta [Talley, 1991].) Second, the MWR is part of the subtropical gyre in terms of Sverdrup transport but it is also a region of Ekman upwelling; these can coexist because of the southwest-northeast tilt of the zero of Ekman pumping over the whole North Pacific (Yuan and Talley, 1992).

The complexity of the MWR is evident in any depiction of water properties in the region. Analyses of temperature at 100 meters are produced monthly by the Japan Meteorological Association; an example during April, 1989 (selected because it was the period chosen for Talley et al.'s [1995] CTD analysis) shows an intrusion of cold water of Oyashio origin down the coast of Honshu, a patch of warm water east of Hokkaido at the usual location between the first two Oyashio "intrusion" or meanders and warm water originating from Tsugaru Strait. CTD sections are occupied regularly along 144°E and show the wall of the Kuroshio, often a warm core ring to its north, and the more density-compensated signature of the Oyashio (e.g. Talley et al., 1995). NPIW is found as a salinity minimum south of the Oyashio front; on the sections which we analyzed it was in almost pure form in the Kuroshio warm core ring.

Temperature / salinity profiles in the MWR away from the near-coastal regions can be classified in four to five relatively well-defined categories (Talley et al., 1995): Kuroshio (subtropical) water, Oyashio (subpolar) water, Tsugaru Water, and one or two classes of mixed water (subtropical and subpolar transitional water), in which the upper part of the T/S relation is dominated by Kuroshio water, the middle by the mixture of Oyashio and Kuroshio water, and the lower by either Kuroshio or Oyashio water. A salinity minimum occurs in all but Oyashio water. The subtropical transitional water is considered to contain the "new" NPIW. A map of the MWR in April, 1989 plus earlier sections at 152°E shows new NPIW in patches through the MWR west of 144°E and completely dominating the MWR by 152°E. Using the definition of the subtropical transitional water as the new NPIW, and assuming primarily isopycnal processes on a large scale, we find that new NPIW is composed of about 45% Oyashio water and 55% Kuroshio water (Talley et al., 1995). This ratio breaks down at densities lower than 26.65 sigma-theta, suggesting that much less Oyashio water is available at lower densities.

New NPIW is therefore formed when the ventilated, freshened Oyashio waters encounter the older, more saline waters of the Kuroshio; their mixture creates a salinity minimum. What sets the density of the actual minimum? The density of new NPIW is slightly greater than 26.7 sigma-theta. The surface density in winter in most of the Oyashio and northern Mixed Water Region achieves 26.65 regularly, implying a steady and large source of newly ventilated water at this density. At a few small coastal patches density greater than 26.7 is achieved but they do not seem to produce enough water to influence the density of the NPIW. A density of 26.7 sigma-theta is also clearly denser than most surface water even in the open Okhotsk Sea in winter.

The robustness of the NPIW density after formation, and its nearness to the Oyashio winter surface density suggests that winter surface density is important, but there must also be a density-increasing mechanism. The obvious candidates are cabbeling and double diffusion. Cabbeling is obviously most effective when the source waters are very different, as they are in the MWR. It is easy to show that a mixture of Oyashio and Kuroshio waters of approximately 45%:55% can produce a density increase of about 0.06 sigma-theta, which is clearly enough to increase the density of the Oyashio's winter surface water to greater than 26.7 sigma-theta after it mixes with Kuroshio water

(Fig. 1). Therefore our hypothesis is that the NPIW salinity minimum density is set by: (1) intrusion of Oyashio waters into Kuroshio waters, with the largest volume of Oyashio water near the surface being at its winter mixed layer density, and (2) mixing/cabbeling of these waters.

How much NPIW is formed? In order to answer this, the question needs to be better posed. It can mean either how much ventilation occurs in the NPIW density range (i.e., how much surface water is converted to water in some specified density range each year), or it can mean how water of this density range enters the subtropical gyre from the subpolar gyre each year? In Talley et al. (1995) we answered the latter question, using a density range of 26.65-27.4 sigma-theta. Subsequent calculations have modified the estimates published in that paper. We used two ways to estimate the exchange of Oyashio water into the subtropical gyre: (1) calculating the eastward transport of new NPIW and the amount of pure Oyashio water included in the new NPIW across 152°E south of the subarctic front, and (2) estimating the amount of Kuroshio water which enters the MWR based on the average number of warm core rings formed each year. Using transports across 152°E (and also 165°E and 175°E), we found that 6.1Sv of new NPIW were moving eastward between the subarctic front and the Kuroshio; thus there were 2.7Sv of Oyashio water included in this.

NORTHWEST PACIFIC TRANSPORT BALANCES

A much better-posed question than the formation rate of "new NPIW" is: what is the total transport of Oyashio water into the subtropical gyre. Since the Kuroshio itself begins to incorporate the new NPIW immediately after it separates from Honshu, and the freshening then begins to spread into the Kuroshio recirculation to the south, a complete estimate of the total of new NPIW must include the Kuroshio and its recirculation. At this point it becomes difficult to define "new NPIW" since various mixtures of old and new are involved. Using the same 152°E sections as in Talley et al. (1995), a new estimate of the total amount of Oyashio water being transported eastward south of the subarctic front is 4-5 Sv.

The total Oyashio transport east of Hokkaido is on the order of 10-15 Sv in the upper 1,000 meters. Therefore 5-10 Sv remain in the subarctic gyre while 4-5 Sv cross into the subtropical gyre. A schematic of upper layer transports through the northwestern Pacific, including exchanges with and transformations in the Okhotsk Sea, and the transport of Oyashio water into the subtropical gyre is shown in Fig. 2. Various estimates of the East Kamchatka Current transport in the upper 1,000 meters yield 15-25 Sv (Talley and Nagata, 1995). Approximately 3-5 Sv enter and circulate through the Okhotsk Sea, in which approximately 1 Sv of surface water is transformed into water in the NPIW density range. The Oyashio carries about 10-15 Sv southward. Thus approximately 1/4 of the Oyashio transport is cycled through the Okhotsk Sea, and of this about 1/4 is new dense water. The ventilation time scale for the subpolar gyre, based on the 1 Sv transformation in the Okhotsk Sea, is on the order of several decades. This seems rather long, and hence the total ventilation rate is probably underestimated. Study of these balances is continuing.

REFERENCES

Bingham, F. M., and R. Lukas. 1994. The southward intrusion of North Pacific Intermediate Water along the Mindanao coast. J. Phys. Oceanogr. 24:141-154.

Kawai, H. 1972. Hydrography of the Kuroshio extension. *In* H. Stommel and K. Yoshida [ed.] Kuroshio: physical aspects of the Japan Current.

Kawasaki, Y., and T. Kono. 1993. Water exchange between the Okhotsk Sea and the North Pacific. Abstract of PICES Nemuro Workshop on western subarctic circulation '93.

Kitani, K. 1973. An oceanographic study of the Okhotsk Sea - particularly in regard to cold waters. Bull. Far Seas Fish. Res. Lab. 9:45-76.

Moroshkin, K.V. 1966. Water masses of the Sea of Okhotsk. U.S. Department of Commerce; Clearinghouse for Federal Scientific and Technical Information, Joint Publication Research service 43, 942, 98 p. Translation of Vodnyye massy Okhostkogo Morya, Nauka publishing house, Moscow. 66 p.

Reid, J.L. 1965. Intermediate waters of the Pacific Ocean. Johns Hopkins Oceanogr. Studies. 2:1-85.

Talley, L.D. 1983. Ventilation of the subtropical North Pacific: the shallow salinity minimum. J. Phys. Oceanogr. 15:633-649.

Talley, L.D. 1991. An Okhotsk Sea Water anomaly: implications for ventilation in the North Pacific. Deep-Sea Res. 38:S171-S190.

Talley, L.D. 1993. Distribution and formation of North Pacific Intermediate Water. J. Phys. Oceanogr. 23:517-537.

Talley, L.D., Y. Nagata, M. Fujimura, T. Iwao, T. Kono, D. Inagake, M. Hirai, and K. Okuda. 1995. North Pacific intermediate water in the Kuroshio/Oyashio mixed water region. J. Phys. Oceanogr. 25:475-501.

Talley, L.D., and Y. Nagata. 1995. The Okhotsk Sea and Oyashio Region. PICES Scientific Report No. 2, North Pacific Marine Science Organization (PICES), Institute of Ocean Sciences, Sidney, BC, Canada. 227 p.

Yuan, and L.D. Talley. 1992. Shallow salinity minima in the North Pacific. J. Phys. Oceanogr. 22:1302-1316.

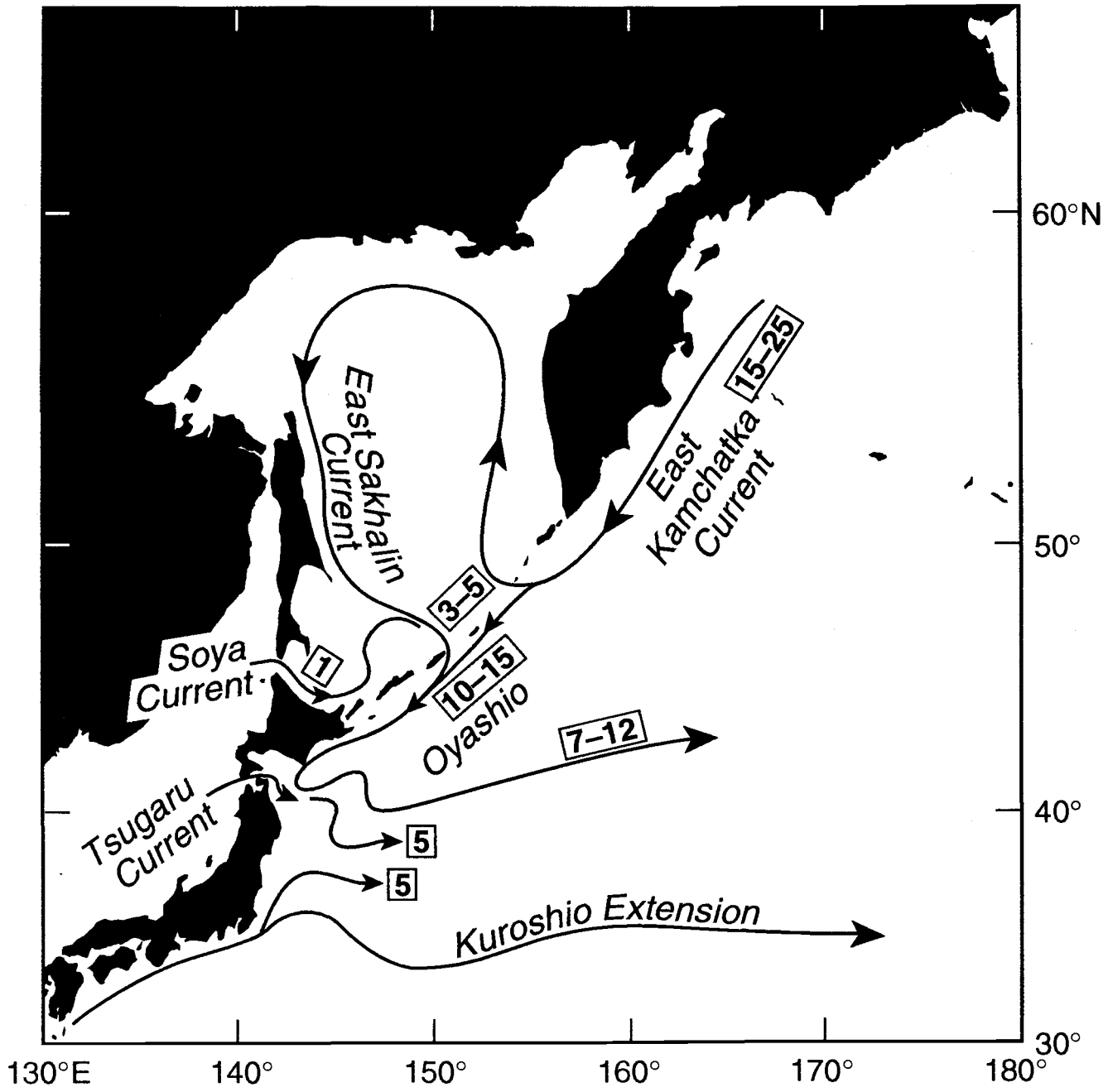

Fig. 1. The influence of cabbeling on the final density of the mixture of Oyashio and Kuroshio water in the Mixed Water Region. Mixing is along straight lines on the potential temperature/salinity diagram. Oyashio water is the cold, fresh curve, based on an average of CTD profiles from a number of stations east of Hokkaido. Kuroshio water is the warm, saline curve, based on an average of a number of profiles within the Kuroshio just east of its separation point. The final mixture is composed of approximately 45% Oyashio water and so obtains nearly the maximum density increase possible.

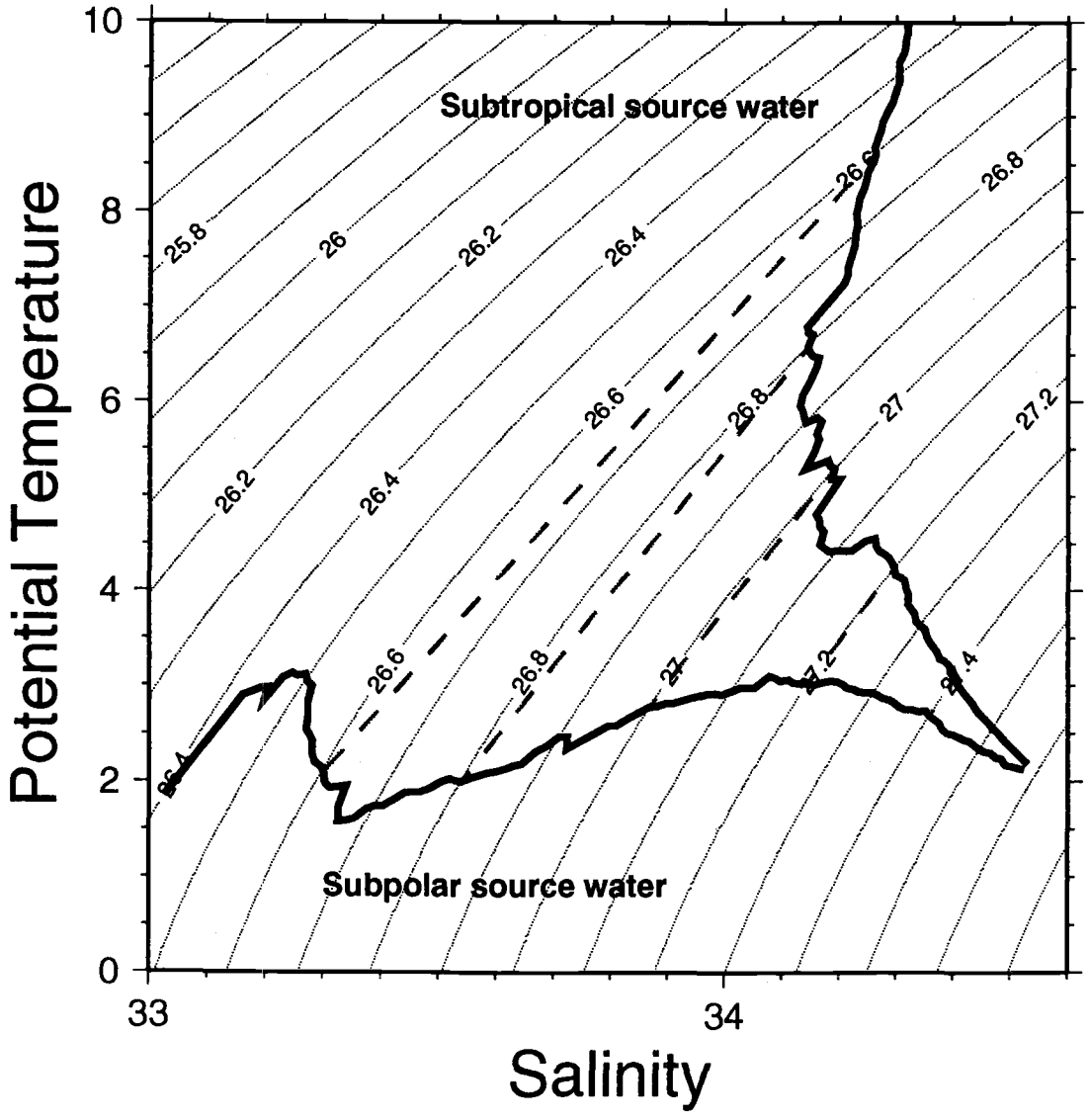

Fig. 2. Schematic of transports and transformations in the upper 1,000 meters in the northwestern Pacific.

Seasonal Variability of Integral Water Circulation in the Okhotsk Sea

Anatoly S. VASILIEV and Fedor F. KHRAPCHENKOV

Pacific Oceanological Institute, Far-Eastern Branch, Russian Academy of Sciences, Vladivostok, Russia

INTRODUCTION

The Okhotsk Sea represents the marginal sea and is separated from the Pacific Ocean by the Kuril Islands and Kamchatka Peninsula, and from the Japan Sea by Sakhalin and Hokkaido Islands. Out of all Far-Eastern Seas the Okhotsk Sea extends farthest into the continent and thus is more influenced by continental conditions. Characteristic morphometric peculiarity of the Sea is the vast shelf which occupies more than 40% of its area. The water exchange between the Okhotsk Sea and the Pacific Ocean is determined by the sizes and depths of the Kuril Islands straits. In the Kuril Islands Ridge there are more than 30 straits with total width about 500 km. The widest and deepest straits are those of Bussol' (the sill depth is 2,318 m and 43.3% of the total width), Kruzenshtern (1,920 m and 24.4%), Freez (900 m and 9.2%) and the Fourth Kuril Strait (600 m and 8.1%). Although the straits are rather deep, even the Bussol' Strait is 1.5 km shallower than the Kuril Basin. The deep water exchange with the ocean is thus restricted. The Okhotsk Sea is connected with the Japan Sea through the shallow strait of La Perouse (the sill depth of 75 m and width of 44 km) and the passage of Nevel'skoy (the sill depth of 14 m and width of 7 km).

Thermochaline structure of the Okhotsk Sea waters is conditioned on the one hand by the intensive water exchange with the Pacific Ocean and, on the other hand, by the strong convective mixing and ice formation during autumn-winter period of the year.

Investigation of the Okhotsk Sea currents started some time ago (Luchin, 1987; Moroshkin, 1966). Most of the known water circulation schemes has been obtained either by the dynamic method with the limited array of the initial data (Moroshkin, 1966) or as a result of diagnostic calculations based on the linear diagnostic model of Sarkisyan (1977) using available water density information and atmospheric pressure fields (Luchin, 1982, 1987). In addition, numerical simulations of currents have been executed applying the simplified baroclinic or barotropic models (Kozlov, 1972; Sekine, 1990).

To investigate the synoptic variability of the Okhotsk Sea currents numerical experiments were performed based on meteorological and CTD observations, and *in situ* current velocity measurements aboard the *R/V Akademik Alexander Nesmeyanov* in September 1993 (Vasiliev and Khrapshenkov, 1994). Seasonal variability of currents has been studied using both the diagnostic Sarkisyan's model for the warm period of the year (Luchin, 1987) and the model of the Novosibirsk Computer Center which takes account of the density stratification (Martynov et al., 1995).

MODEL DESCRIPTION AND INITIAL DATA

The quasigeostrophic model based on principles of self-similarity of the second order was used to reconstruct the sea water circulation by months. It considered spatial distribution of water density, atmospheric effect, bottom topography and coastline, water exchange through the straits, and

b - effect.

The sea water density was taken as the function possessing the natural self-similarity (similarity of the vertical distribution):

$$\rho(x,y,z,t)=\xi(x,y,t)[\sigma(z,t)+\alpha_1 a(x,y,t)(z-h_a^{\vartheta})]+\rho^0(x,y,t), \quad (1)$$

$$where\ \alpha_1=\begin{cases} 0\ at\ z\le h_a^{\vartheta}, & a(x,y,t)=-\dfrac{\partial\sigma(z,t)}{\partial z}\Big|z=H; \\ 1\ at\ z>h_a^{\vartheta}, & \dfrac{\partial(x,y,t)}{\partial x}=\dfrac{\partial(x,y,t)}{\partial y}=0; \end{cases}$$

Here, $\rho\ (x, y, z, t)$ is spatial-temporal distribution of the sea water density; $\rho^0(x, y, t)$ is known sea surface density; $\sigma(z, t)$ is stratification function; $a(x, y, t)$ is discrete-constant function regulating zero flux through the bottom; h_a^{ϑ}- is depth of the near-bottom layer of Ekman friction; $\xi(x, y, t)$ is self-similarity function; x, y, z are coordinates, corresponding to the axes directed eastward, northward or vertically down; t is time, and R is an index related to a characteristic station of the studied region, corresponding to the average vertical distribution of the sea water density.

In a quasistationary statement, computation of currents and density distribution from the tangential stress of wind and surface density leads to the equation for the transport stream function Ψ:

$$-\frac{\partial\Psi}{\partial\nu}+\Delta\Psi=F(T,\rho^0,f);\quad \Psi^L=\Psi^K \quad (2)$$

where L is basin contour; T is tangential stress of the wind; ρ^0 sea surface density; ν is relaxation parameter; f is the errors function related to some additional conditions on surface current velocities (Vasiliev, 1993).

Bringing in the additional conditions on surface current velocities allows calculation of the vertical distribution of currents and components of net fluxes both inside the area and on the liquid margin. Moreover, it permits derivation of the errors function resulting from the need to satisfy the discontinuity equation and water balance in the region. Equation (2) is solved by the method of minimal errors (Marchuk, 1974) by way of reaching a steady state in the time interval corresponding to the period of averaging marginal and surface conditions. The explicit solution of the equation provides the gradients of self-similarity function, the self-similarity function itself, sea water density, level inclinations, and horizontal and vertical distribution of currents.

A more detailed mathematical statement of the problem and the model description are given in (Vasiliev, 1993, 1994; Vasiliev and Dudka, 1994; Vasiliev and Khrapchenkov, 1994). The model has been used for the numerical experiments on dynamic studies in the Northwestern Pacific (Vasiliev, 1993, 1994; Vasiliev and Dudka, 1994; Vasiliev and Khrapchenkov, 1994).

The input data to calculate the integral circulation of the Okhotsk Sea included the real atmospheric pressure fields corresponding to the monthly predominant type of the atmospheric processes (Polyakova, 1994), the average monthly fields of temperature and seasonal surface salinity fields, as well as the monthly averaged stratification function in a characteristic point of the Sea. A uniform mesh with a width of 30' in latitude and longitude, and standard vertical horizons was used for calculations. The ice formation was considered in winter season, but the direct effect of wind was not taken into account for the ice covered area.. Current velocities were determined by the explicit formula, after solving the problem relative to the flow function. Characteristics of the atmospheric influence on the sea surface were computed based on the half-empirical ratios. Discharges in the

straits were either given according to the estimates available (Kozlov, 1972; Luchin, 1982, 1987; Zyryanov, 1974, 1977) or determined from the net fluxes normal to the liquid boundaries of the area, considered while using the given stratification function and the influence function obtained in the solution. The water exchange through the Tartar Strait was not considered. Numerical realization of the model was performed using the method of minimal errors (Marchuk, 1974).

RESULTS

Results of the numerical experiments by months are given in Fig. 1. The cyclonic character of waters circulation, pointed out by many authors studying the Okhotsk Sea currents, was confirmed only for the northern part of the Sea and only for the warm period of the year. A series of not unidirectional gyres which change their sizes and relative location in time was revealed in the southern part of the Sea.

One of the most stable currents of the Okhotsk Sea, namely the East Sakhalin Current, was observed near the eastern coast of Sakhalin Island. Its characteristics, conditioned by the seasonal variability of the atmospheric circulation over the Sea, demonstrated essential temporal changes. During the autumn-winter period (August to May) the current was traced everywhere along the Sakhalin coast. The discharge and velocities were maximal for this season, and reached 1-1.5 S_v and more than 35 cm/s in October. In June-July the current was detected only in the southern part of the Sakhalin coast. Similar changes occurred in the Counter Current, a part of which together with the East-Sakhalin Current forms a cyclonic gyre to the east of Sakhalin Island, and the other part forms the anticyclonic gyre in the central part of the Okhotsk Sea. This dipole structure was well expressed on the maps from October to May, and practically was unobserved in December and June-September, while forming the more complex structures of different vorticity. The maximal discharges and current velocities (more than 2 S_v and 40 cm/s correspondingly) were found in the Counter Current and in the anticyclonic gyre in October.

The North Okhotsk Current of small speed was traced during the warm season and practically vanished for the cold half of the year. This is related probably to generation of the ice cover.

The Kamchatka Current was revealed from January to September, and its core moved gradually (from winter to summer) to the western coast of the Kamchatka Peninsula. For some months we observed the current bifurcation into the northern branch passing to Penzhinsky Gulf and the western branch taking part in the cyclonic gyre to the west of the south-western coast of Kamchatka. The maximal velocities of the Kamchatka Current (exceeded 20 cm/s at 52°N) occurred in November-December. The compensating current near the western coast of Kamchatka was not seen, as it passed on the shelf with water depths less than 100 m. Only in November and December weak flow (with velocities not more than 5 cm/s) directed southward was found near the coast on the section along 52°N.

The Soya Current, with varying level of intensity, was observed during the whole year. In winter it fell into two and sometimes three branches, one of which moved along the coast of Hokkaido Island, the second turned to the north-east, and the last one passed to the east. Both eastward branches were involved into the anticyclonic gyre which shifted to the southern part of the sea in January-February. From June to December, the Soya Current was well manifested as the flow passing along the Hokkaido coast, whereas in July-August and December it turned to the north (not reaching Siretoko Cape) and propagated between two gyres of different vorticity up to the Strait of Freez. In September-November, the main Soya Current branch extended from Siretoko Cape along Kunashir Island as far as the Strait of Freez where it divided into two branches: one of them passed to the

Pacific Ocean through the Strait, another one moved to the north while participating in the anticyclonic gyre.

A series of gyres characterized by different signs of vorticity was observed in the southern part of the Okhotsk Sea during the whole year. From month to month they changed both their sizes and relative location. The Kuril Islands area within the Sea of Okhotsk can be conventionally separated into the northern and southern parts. In January the whole southern part of the Sea was occupied by the anticyclonic gyre with two centers extending along the Kuril Islands up to 48°N. To the north of this structure, a cyclonic vortex of considerably smaller size was located. Together with the anticyclonic gyre it formed a dipole with a meridionally oriented axis. In February the cyclonic gyre was shifted southward to the Islands, while driving back the main anticyclone to the south-west. Their sizes became equal, and the dipole axis extended along the Kuril Islands. At the same time, a cyclonic gyre originated near the southern terminal of Sakhalin Island. In March it displaced the anticyclone from the southern part of the Sea and thus shifted the dipole to the northeast. Such a situation was still preserved in April-May.

In June the anticyclonic gyre moved to the south. It was composed by two centers, one of them was situated to the northwest of the Bussol' Strait, and another to the northwest of the Ekaterina Strait. A cyclonic gyre occurred near the coast of Sakhalin Island and stretched out in the northeastern direction while merging with the cyclone situated to the north of the anticyclonic gyre in the previous months. The similar situation was manifested in July-August when both the anticyclone and cyclone were extended along the Islands to the north-east. Starting from August the cyclonic gyre increased in size from the north to the south and in September it occupied the whole southern part of the Okhotsk Sea up to 49°N and 148°E. Horizontal sizes of the anticyclone grew essentially smaller, and the dipole axis was again oriented to the northwest.

In October the double center cyclonic gyre increased in size, mainly eastward, up to 150°E, and the anticyclone moved to the northeast along the Islands while decreasing in size and stretching out along the meridian. An approximately similar picture was preserved in November-December, but the anticyclone gradually extended along the Islands up to the Strait of Ekaterina.

The cyclonic gyre located near the Kruzenshtern and Forth Kuril Straits was observed during the whole year and its horizontal size was not changed notably. However, during some months, while growing stronger, it merged with the cyclone which moved from the south.

The structure of the main Okhotsk Sea currents, as well as the system of gyres with different vorticity in its southern part, changed considerably from season to season. To the great extent the temporal variability is related to the reconstruction of the atmospheric processes. This allows amplification of existing notions on water dynamics and their seasonal variability, especially in the southern part of the sea.

Based on our calculations it is possible to estimate the integral discharge through the Straits. In practically all the Straits the flows of different orientation were revealed: in the northern straits the Pacific waters inflow being predominant, whereas in the southern straits the outflow of the Okhotsk Sea waters was observed. The total water discharge through the Kuril Straits varied from 0 to -1.0 S_v and was approximately equal to the water discharge through the La Perouse Strait. Table 1 presents the integral discharge of waters through the Kuril Straits for August and December (sign "+" denotes the Pacific waters penetration into the Okhotsk Sea).

Comparison of our numerical calculations with results presented elsewhere (Bobkov, 1992; Luchin, 1982, 1987; Moroshkin, 1966; Sekine, 1990; Zyryanov, 1974, 1977) shows a satisfactory correspondence with the main elements of the Okhotsk Sea circulation schemes. But it should be noted

that the cyclonic character of waters circulation stated by many authors, was confirmed for the northern part of the Sea only. In the southern part the complicated dipole structures changing their sizes and location were observed.

REFERENCES

Bobkov, A.A. 1992. Evolution of notions on water circulation in the southern part of the Sea of Okhotsk. Izvestiya PGO. 124(5):461-470 (in Russian).

Kozlov, V.F. 1972. Calculation of the level surface in the Sea of Okhotsk. Trudy DVNIIGMI. 37:37-43 .(in Russian).

Luchin, V.A. 1982. Diagnostic calculation of water circulation in the Sea of Okhotsk in summer. Trudy DVNIIGMI. 96:69-76 (in Russian).

Luchin, V.A. 1987. Waters circulation in the Sea of Okhotsk and peculiarities of its interannual variability by results of diagnostic calculations. Trudy DVNIIGMI. 36:3-13 (in Russian).

Marchuk, G.I. 1974. Numerical Solution of the Problem on Dynamics of the Atmosphere and the Ocean Using Method of Splitting. L., Gidrometeoizdat. 303 p. (in Russian).

Moroshkin, K.V. 1966. Water masses of the Sea of Okhotsk. U.S. Department of Commerce; Clearinghouse for Federal Scientific and Technical Information, Joint Publication Research service 43, 942, 98 p. (Translation of Vodnyye massy Okhostkogo Morya. Moscow, Nauka, 66 p.)

Martynov, A.V., E.N. Golubeva, and Luchin V.A. 1995. Numerical modelling of the Okhotsk Sea general circulation with the density stratification inclusion. Proc. PICES Workshop on the Okhotsk Sea and Adjacent Areas. Vladivostok.

Oceanographic encyclopedia. 1974. M., Gidrometeoizdat, 631 p. (in Russian).

Polyakova, A.M. 1994 Permanent variations in atmospheric circulation pattern over the Northern Pacific with regard to non-stationarity. Pacific Annual (Part 1). Vladivostok, Far-Eastern Branch of USSR Academy of Sciences.

Sekine, Y. 1990. A barotropic numerical model for wind-driven circulation in the Okhotsk Sea. Bull Fac. Bioresources, Mie Univ. 3:25-39.

Vasiliev, A.S. 1993. Self-similarity of the second order in monitoring of main physical fields of the ocean. Doklady Akademii Nauk. 328(5):613-618 (in Russian).

Vasiliev, A.S. 1994. Application of self-similarity parametrization of thermochaline fields in marine ecological studies. Morskoi Gidrofizicheskii Zhurnal.2:84-88 (in Russian).

Vasiliev, A.S., and K.V. Dudka. 1994. On water exchange of the Sea of Okhotsk and the Sea of Japan with the Pacific Ocean. Meteorologiya i Gidrologiya. 8:64-70 (in Russian).

Vasiliev, A.S., and F.F. Khrapchenkov. 1994. Planning of the oceanological experiment (on the example of the Sea of Okhotsk). Meteorologiya i Gidrologiya. 8:64-70 (in Russian).

Zyryanov, V.N. 1974. To the question on water exchange through the Northern Kuril Straits. Okeanologiya. 14:16-21 (in Russian).

Zyryanov, V.N. 1977. Numerical calculation of stable currents in the Sea of Okhotsk (prognostic model). Trudy VNIRO. 119:24-30 (in Russian).

TABLES AND FIGURES

Table 1. The integral water discharge through the Kuril Straits.

Strait	Discharge in Sv		Width of strait, km	Sill depth, m
	August	December		
Ekaterina	-0.01	-0.01	20	300
Freez	+0.48 -0.99	+0.5 -1.02	40	809
Urup	+0.1	+1.8	24	126
Bussol'	-0.9	-1.8	60	2300
Diana	0	0	18	241
Ricord	0	0	22	450
Nadezhda	-2.0	-2.55	40	500
Kruzenshtern	-0.2	0	72	1945
Severgin	+2.6	+2.65	40	69
4th Kuril	-0.5	-0.7	56	500
1st Kuril	+0.44	+0.5	12	23

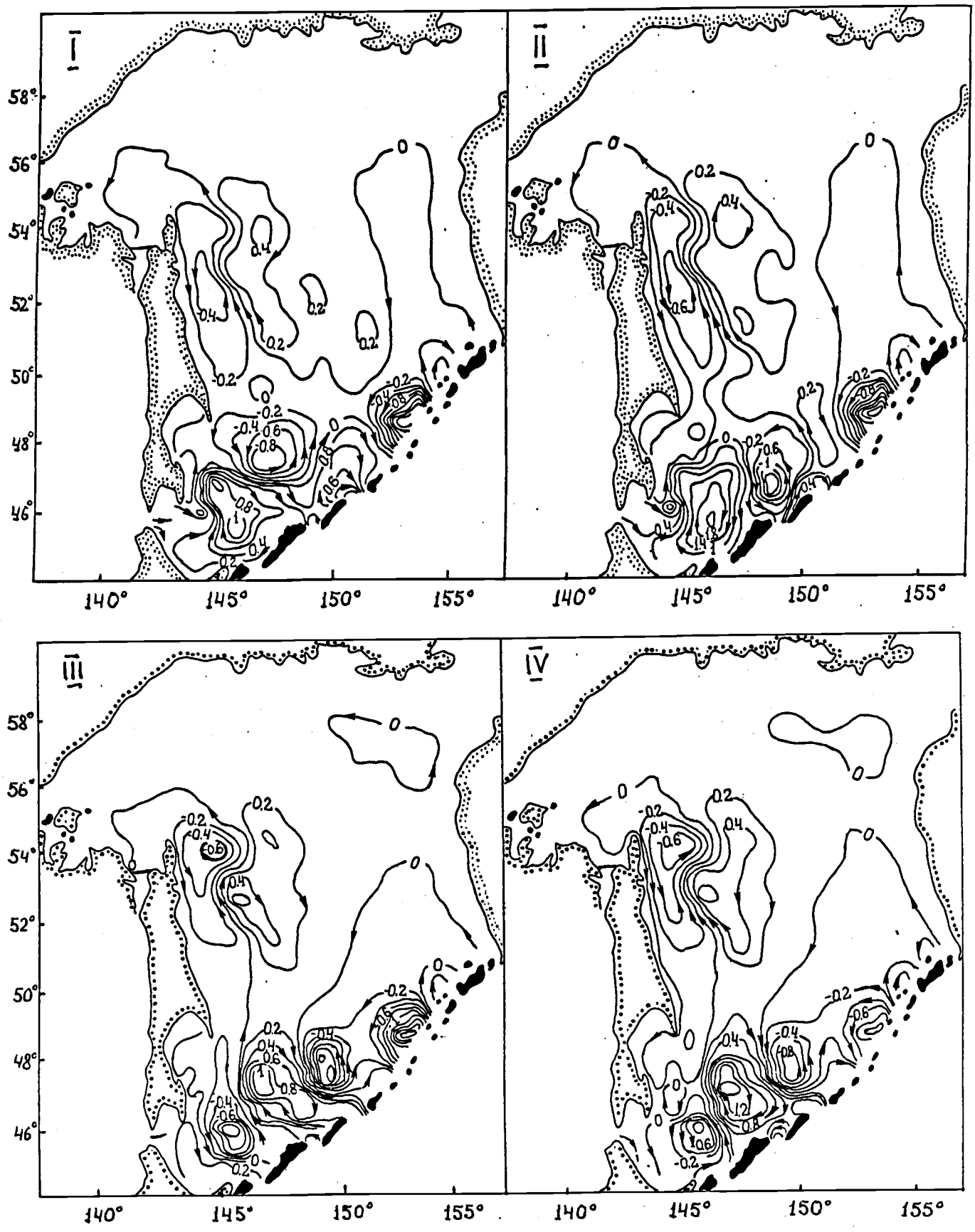

Fig. 1. The monthly transport stream functions (S_v) from the surface to the bottom in the Okhotsk Sea (12 panels).

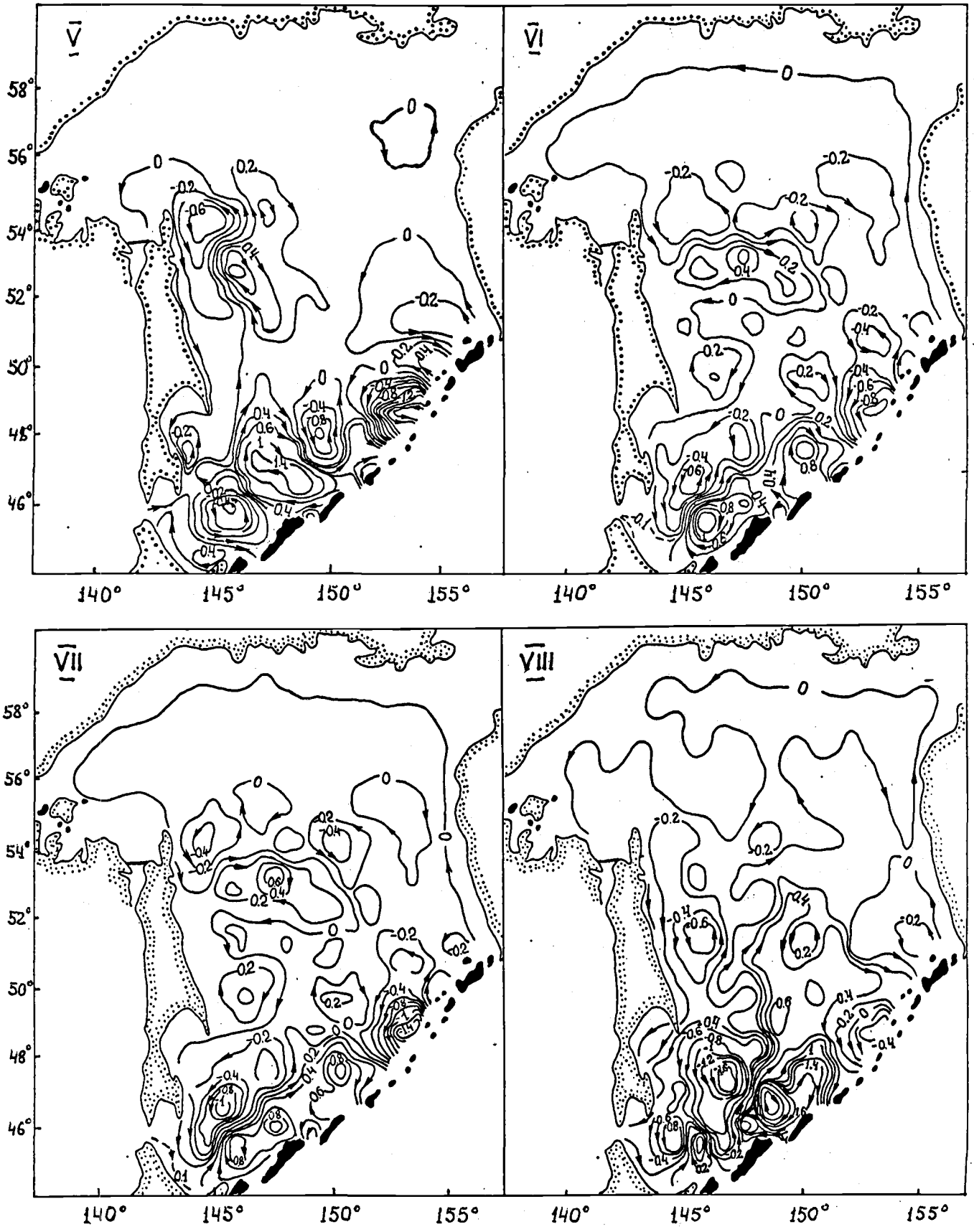
V
VI
VII
VIII
58°
56°
54°
52°
50°
48°
46°
140°
145°
150°
155°

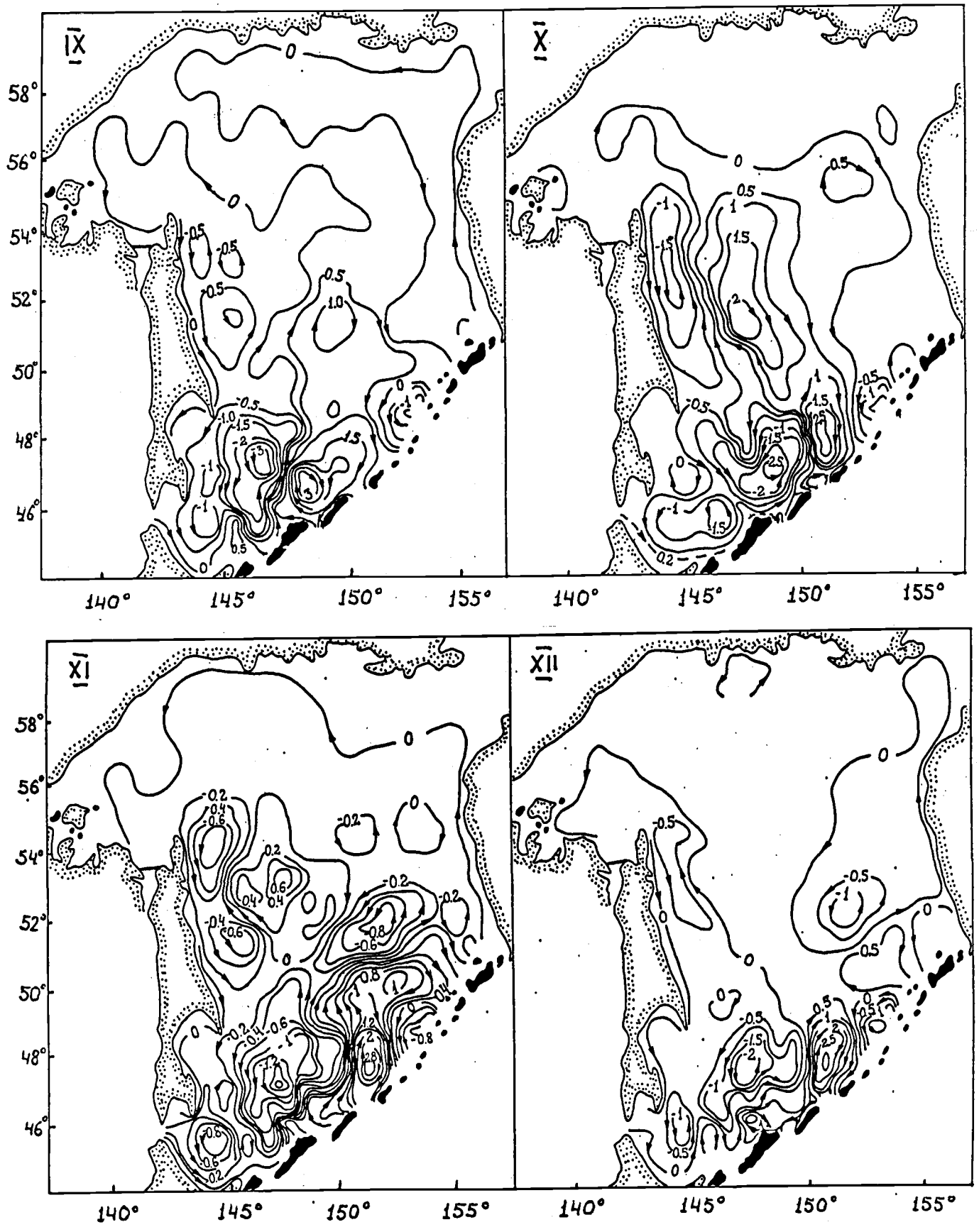
IX
X
XI
XII
58°
56°
54°
52°
50°
48°
46°
140°
145°
150°
155°

Acoustic Methods in Sea Ice Dynamics Studies

V.P. Gavrilo, G.A. Lebedev, A.P. Polyakov

The State Science Center of the Russian Federation
The Arctic and Antarctic Research Institute, St. Petersburg, Russia

The interaction of engineering structures with ice in the regions with fast or drifting ice cover is significant. The most difficult problem is to describe floe interaction, because an ice cover drift depends on external forces acting at some points as well as on the state of ice cover in adjacent areas.

The ice dynamics is determined by hydrometeorological processes. The equation of strength balance on a specific ice surface is based on hydrodynamic theory of ice cover drift:

$$\rho h \frac{\partial V}{\partial t} = \tau_a + \tau_w + C + G + R$$

where V is drift velocity factor; ρ is ice density; τ_a is tangent air pressure on the ice surface caused by wind; τ_w is strength of friction between ice and water; C is the Coriolis force; G is projection of gravity on the sea surface; R is internal resistance caused by interaction between ice flows.

Unfortunately, there are no suitable methods for evaluation of the last parameter R. To overcome this difficulty the following equations were used (Volkov et al., 1971) to describe a spatial irregularity of the ice drift:

$$div\ V = dv/dy + du/dx$$
$$rot\ V = dv/dx - du/dy$$
$$def_1\ V = dv/dx + du/dy$$
$$def_2\ V = dv/dy - du/dx$$

where u and v are projections of vector V on axes x and y correspondingly.

The first equation (divergence) characterizes the intensity of ice cover extension (compacting) at a given point, whereas the second equation (rotation) illustrates the velocity of the turn. It should be noted that both equations are invariant in coordinate axes. The two last equations represent the rate change of ice cover element formation or deformation. So, the third equation gives angular deformation (i.e. the change of angle between the sides of the originally square area) and the fourth shows irregularity of linear deformation along two perpendicular axes. Thus, to solve the problem of the study of sea ice dynamics it is necessary to carry out frequent and accurate measurements of spatial deformation characteristics of the ice cover.

ACTIVE ACOUSTIC METHOD

Two approaches are used to study the ice dynamics. The first is based on the continuous measurements of buoy coordinates installed on different floes. These measurements are performed by a space system designed for observations and radio communication. The second method is based on observations of ice formation characteristics with active and passive sensors from the artificial Earth satellites. Both methods are mainly used to determine the large scale movements of ice cover. To

study the middle scale ice deformations the radiohydroacoustic method was developed in the Arctic and Antarctic Research Institute (Bogorodsky et al., 1975). It is based on measuring (with necessary accuracy) the difference among time intervals corresponding to the propagation of a sound impulse in a water body between several marked drifting flows situated within the distance of one wavelength of acoustic ray propagation.

The change in distance from point A to B for the period between successive observations can be calculated using the sound impulses propagation time:

$$\Delta r = r - r_i = c_w(t - t_i)$$

where t and t_i are the times of sound propagation between A and B, c_w is the sound velocity in sea water. The main limitation of this method is the temporal fluctuations of the vertical sound velocity distribution which can lead to distortions of the refraction sound picture if ray approximation is used.

The relative accuracy of distance evaluation is:

$$\Delta r / r = \Delta t / t + \Delta c_w / c_w$$

The $\Delta t/t$ is the accuracy of sound propagation time registration and $\Delta c_w/c_w$ is the accuracy of known sound velocity. The first parameter is systematic and can be not taken into account. Thus, the accuracy of the $\Delta r/r$ measurement is caused only by $\Delta c_w/c_w$. and is about 0.02% of the measured distance, if Weelson's empirical formula is used to calculate the sound velocity from experimental data (Stashkevich, 1966).

In addition to the seasonal variations of sound velocity, the short period internal waves have an influence on the acoustic signal propagation time. Internal waves are sometimes formed in the zone of the upper thermocline and can induce the distortion of the refraction sound picture. To consider this effect continuous temperature and salinity measurements were carried out in the layer where the main changes of water physical parameters occur.

One of the numerous *in-situ* measurements is presented in Fig. 1, as an example. Here, each point on the experimental curve represents an average r-value determined within the 30-min interval of observation while each marking off was taken every 30 sec. In addition, the results of estimated ice cover linear deformation was obtained with the help of repeated large scale air-photo surveys. Analysis of the independent observations shows their sufficient coincidence as evidence of the high efficiency of the radiohydroacoustic method for the middle scale ice deformation studies. This conclusion justifies the elaboration of a multi-channel radiohydroacoustic automatic station designed for the collection and transmission of information on the strain stress state of the ice cover. Installation of such devices directly on engineering structures will permit exploitation with reduce risk in the regions with fast or pack ice.

PASSIVE ACOUSTIC METHOD

The method is based on the relationship between the energetic and frequency characteristics of ambient noise made during the ice destruction caused by stress state change (which can be explained by the variability of the hydrometeorological processes). Parameters of elastic oscillation (amplitude, frequency spectrum, wave length, sound and vibration velocities, duration of acoustic impulses, sound energy density) can be independent criteria for determination of the ice state before, during and after the moment of ice break up. In particular, the wide spectral maximum at the 50-300 Hz frequency range and 10-12 dB/octave fall of noise level in the direction of high frequency are distinctive characteristics of the noise connected with ice destruction.

The following multi-correlation equation is the result of analysis of the correlation relationships for statistical dependencies linking sound pressure in the water (P), wind velocity (V_w), drift ice velocity (V_i), air temperature (t_a), deformation, divergence and other parameters and their derivatives:

$$P = a*\text{div } V + b*\text{def } C + c*V_w + d*t_a + P_o$$

The coefficients a, b, c and d are functions of the partial coefficients of correlation, dispersion and mean values of the equation parameters, V is the vector of drift velocity. In different seasons some terms of the equation can be neglected (i.e. in winter $P = b*\text{def } C + d*t_a + P_o$). In such cases the reverse task can be solved and def V or div V can be found. These values will characterize the stress state of ice cover in the areas within the radius of spatial correlation.

The practical solution of the task for the Arctic ocean has demonstrated that the proposed method is quite suitable for the estimation of the ice extension or compression intensity. Fig.2 shows fragments of these investigations. The curves 1 (measured) and 2 (calculated) represent temporal changes of noise levels in 20-100 Hz frequency band. The calculated curves 3 and 4 (smoothed) display the deformation of ice cover.

Observations of ice break-up processes, including ice drift at Yenisey, Angara and Daugava rivers also illustrate applicability of acoustic methods for remote studies of ice cover state (Bogorodsky and Gavrilo, 1976). Investigations of ice formation physics during ice destruction performed both in laboratory and *in-situ* have allowed one to obtain the spectrum and energetic characteristics of noise generated at the different stages of ice stress state and during the process of ice drift. Spectral energy characteristics (pressure of underwater ambient noise in the 1 Hz frequency band relative to the zero level $2\ 10^5$ Pa) from the delta region of the Yenisey river are presented in Fig. 3. It clearly shows that extreme dynamic process during the ice drift causes an essential (up to 40 dB) increase of noise level by comparison with the corresponding characteristics for the unmoving ice cover (complete freezing) or for the ice-free river surface (complete ice clearance). Besides, the non-stationary acoustic noise for the river ice break-up differs from the quasi-stationary noise while unmoving ice cover exists on the river. The represented spectra also demonstrate that the wide maximum, caused by the rupturing and crushing of ice, takes place in the frequency band from 0.4 up to 3.0 kHz. The maximum can be widened up to 4.0-5.0 kHz due to friction between snowy ice flows.

The acoustic noise features mentioned above could be the basis for elaboration of methods to control the ice dynamic state at the local river regions in order to improve the ice jam forecast.

REFERENCES

Bogorovsky, V.V., and V.P. Gavrilo. 1976. Possibilities and perspectives of use of acoustic metods in the study of river ice cover. Proc. Coordination Workshop on Hydrotechnik. Moscow, Energoatomizdat. p. 189-193.

Bogorovsky, V.V., V.P. Gavrilo, and A.P. Polyakov. 1975. Radiohydroacoustic method for study of middle scale characteristics of sea ice dynamics. Trudy AARI. 326:219-228 (in Russian).

Stashkevich, A.P. 1966. Acoustic of Sea. Leningrad, Sudostroenie. 363 p. (in Russian).

Volkov, N.A., Z.M. Gudkovich, and D.D. Uglev. 1971. To study of drift irregularity in the Arctic basin. Trudy AARI. 303:76-88 (in Russian).

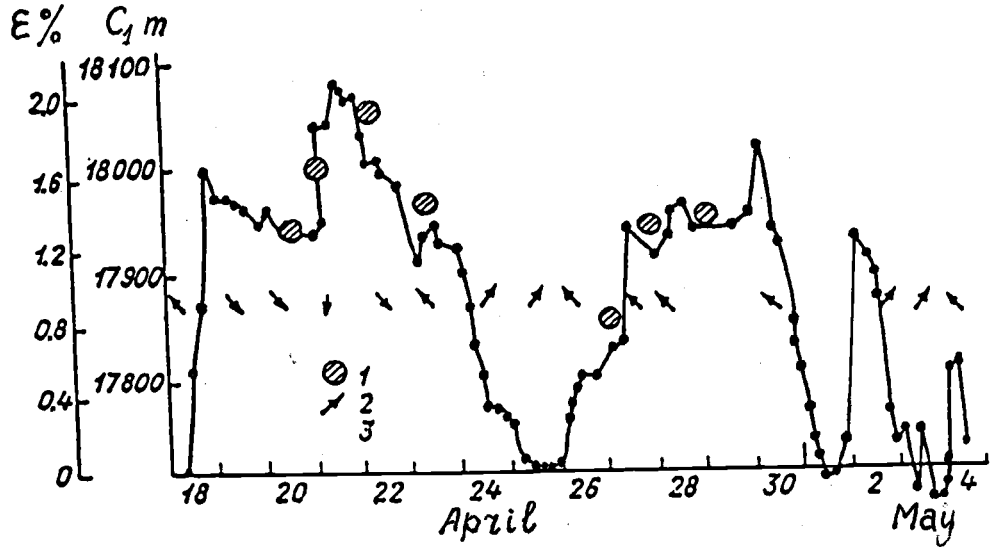

Fig. 1. Time dependence of the distance change (r, m) and linear ice deformation (ε, %) between points A and B:

1 - results from repeated air-photo surveys;
2 - ice drift direction;
3 - results of radiohydroacoustic observations.

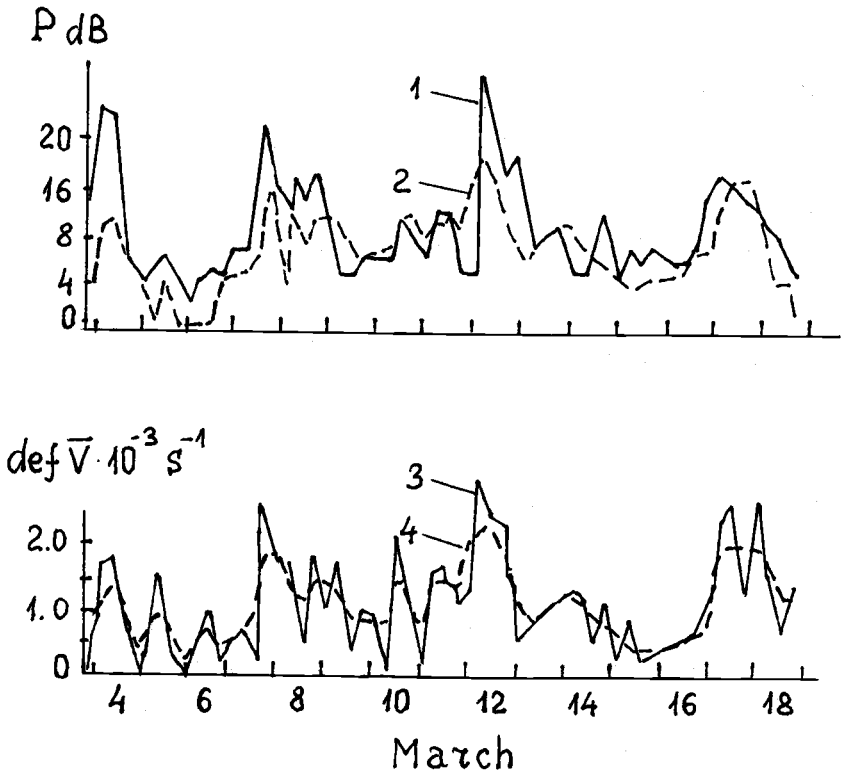

Fig. 2. Temporal changes of the underice noise level in 20-100 Hz frequency band (P, dB) and the ice cover deformation (def $\overline{V}$, S^{-1}) in the Arctic Ocean:
1 - the facts; 2, 3 - calculated curves; 4 - calculated smoothed curve.

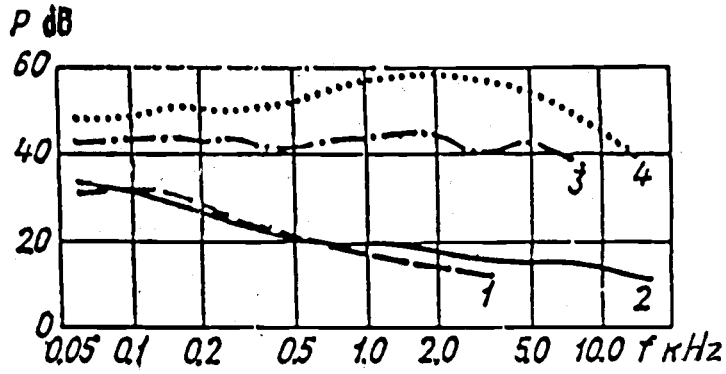

Fig. 3. Spectral characteristics of noise at the different stages of ice stress stage (the delta of Yenisey river, May 20 - June 6).
1 - complete ice clearance; 2 - complete freezing;
3 - ice break-up; 4 - ice drift.

The Role of the Far-East Atmospheric Circulation in the Formation of the Ice Cover in the Okhotsk Sea

Nina M. PESTEREVA and Larissa A. STARODUBTSEVA

Department of Meteorology, Far Eastern State University, Vladivostok, Russia

INTRODUCTION

One of the major characteristics of the intensity of ice formation is the ratio of the ice covered sea area to the whole sea area. In this study we consider a long-term variability of this ratio for the Okhotsk Sea.

The ice cover has a pronounced annual variability explained by natural and, especially during last years, by anthropogenic peculiarities. Natural features include hydrologic factors and the atmospheric circulation in the second natural synoptic region enveloping the area from 80°E up to 160°W.

METHOD AND DATA

Data on the Okhotsk Sea ice cover for the period from 1957 to 1990 have been provided by chiefs of the Sea Forecasting Laboratories of the Primorsky Department on Hydrometeorology and Environment Monitoring. Based on this information the time period was divided on three classes:

(1) years with heavy ice cover;
(2) years with light ice cover;
(3) all other years or years when ice cover of the Okhotsk Sea was normal or near normal.

The years: 1958-59, 1966-67, 1968-69, 1972-73, 1977-78, 1978-79, 1986-87 were regarded as the first class or heavy ice-covered years (Table 1). The second class or light ice-covered years were determined as follows: 1963-64, 1973-74, 1975-76, 1983-84, 1984-85, 1987-88 (Table 2). Features of atmospheric circulation for the second natural synoptic region were analyzed for different year classes.

Snow, as well as ice, are very sensitive elements of the Sun - Earth - atmosphere system and considerably influence both micro- and mesoclimate, weather and atmospheric circulation. Conversely, the atmospheric circulation effects on ice-formation for various classes.

The troposphere circulation anomalies cannot be explained only by the interrelation processes between the troposphere and underlying surface. The stratospheric circulation and its interaction with troposphere also play a key role in the formation of a certain weather regime. The circumpolar gyre is a major synoptic stratospheric phenomenon defining the weather of the northern hemisphere for moderate latitudes. Fluctuations of the intensity and location, to a considerable extent, influence the weather regime in different regions. A detailed description of this approach was given in publications by the distinguished Russian meteorologist Pedya (1976).

The circumpolar gyre trajectories are rather complicated. The cyclonic gyre propagates after the stratospheric cold site, which appears as a result of air cooling during the polar night. Thus, at the first stage we considered the circumpolar gyre intensity and features during the cold period from

November till March for heavy and light ice years using positions of the gyre center and monthly mean data for the geopotential at 100 mbar. In cases where the gyre had two or more centers, we took into account the center located in the Asian sector of the Arctic, or that situated above the Asian continent, and calculated mean values for the first and second year classes.

To reveal the tropospheric circulation features, the data on the Ilyinsky circulation forms were used.

RESULTS

For heavy ice cover years in the Okhotsk Sea, in 60% of cases the circumpolar gyre center shifted to the Asian continent southward of 70°N (e.g. Fig. 1) and the Far Eastern trough stretched to the Khabarovsky Region. The center of the circumpolar gyre was located to the southeast of the usual long-term position in 72% of cases for the period from November till March. Monthly mean distribution of the geopotential at 100 mbar for November 1977 and March 1978 is given on Fig. 1. This map shows that meridional and particularly, western circulation prevailed during this season (it was above normal in 3-11% cases for different years). The planetary high altitude frontal zone was located further to the south in comparison with the long-term mean, which is normally near 40°N. The cyclones moved the southern trajectories. The arctic air mass advection was observed on the western edge of the high-altitude Far-Eastern trough in these circumstances, and negative air temperature anomalies were formed above the southern Far-East, Japanese Islands and Okhotsk Sea. These thermal and dynamic factors contributed to an intensive process of ice formation and maintenance of a severe ice regime in the Okhotsk Sea.

For light ice years in the Okhotsk Sea, the circumpolar gyre shifted to the northwest in comparison with its normal position (Fig. 2). The high altitude Far Eastern trough was weak and an intensive zonal movement was noticed above the region. Meridional processes were below normal up to 5-10% and latitudinal circulation occurred more often in comparison with the normal years. The high-altitude frontal zone stretched to the north from Lake Baikal, to the Amur river and further to the south of the Okhotsk Sea. Simultaneously, with the cyclones movement along the high altitude frontal zone, the drift over of warm air masses towards the Okhotsk Sea was seen. Over the larger part of the Far East, the positive air temperature anomalies at the surface are present followed by less than normal ice cover in the Okhotsk Sea.

Thus, the atmospheric processes in the troposphere and lower stratosphere during fall and the first half of winter are important factors influencing the ice formation in the Okhotsk Sea.

REFERENCE

Pedya, D.A. 1976. O vliyanii kolebaniy circumpolyarnogo vichrya na formirovanie usloviy pogody. Trudy GMC SSSR. 173:45-57 (in Russian).

TABLES AND FIGURES

Table 1. Heavy ice years in the Okhotsk Sea (ice covered area of the Sea, %)

Year/month	1958-1959	1966-1967	1968-1969	1972-1973	1977-1978	1978-1979	1986-1987
December	**30**	**18**	**19**	**26**	**25**	**25**	**28**
March	**85**	**97**	**88**	**94**	**92**	**94**	**90**

Table 2. Light ice years in the Okhotsk Sea (ice covered area of the Sea, %)

Year/month	1963-1964	1973-1974	1975-1976	1983-1984	1985-1986	1987-1988
December	**8**	**16**	**29**	**23**	**11**	**19**
March	**77**	**71**	**66**	**57**	**75**	**63**

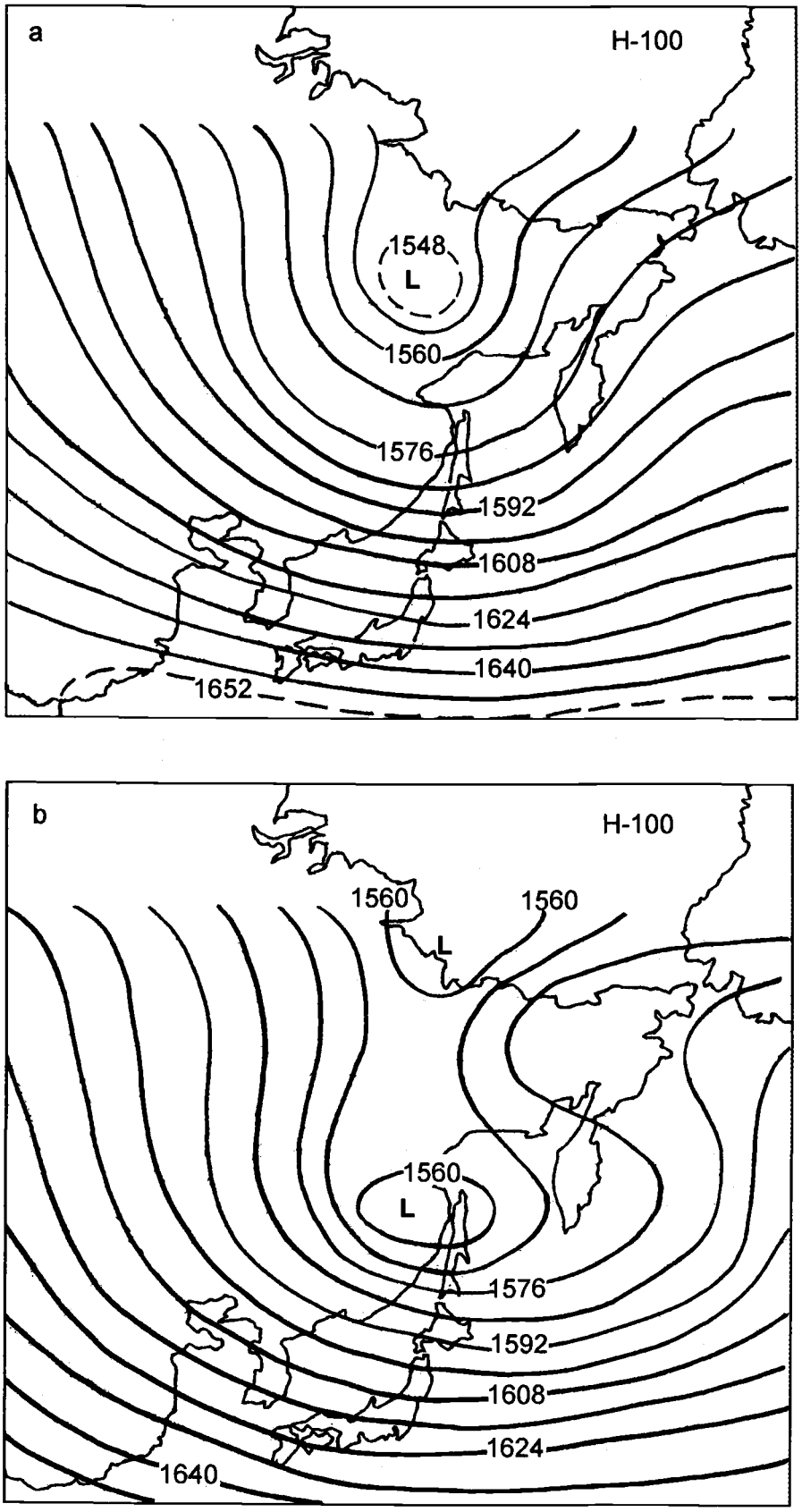

Fig. 1. Monthly mean distribution of geopotential at 100 dbar (x 10m) for November 1977 (a) and March 1978 (b). Heavy ice cover years.

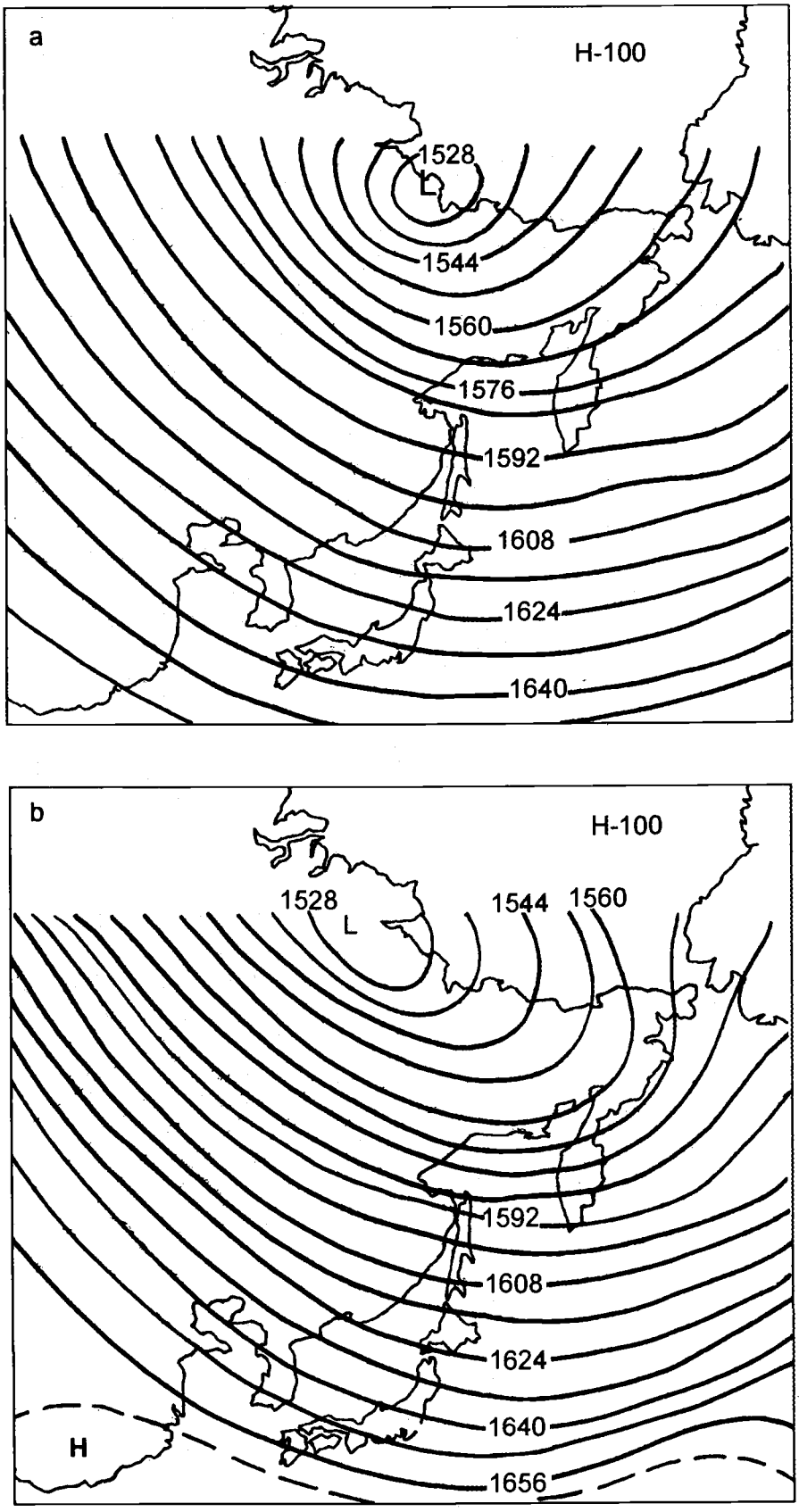

Fig. 2. Monthly mean distribution of geopotential at 100 dbar (x 10m) for November 1984 (a) and March 1985 (b). Light ice cover years.

Anomalous Oyashio Intrusion and its Teleconnection with Subarctic North Pacific Circulation, Sea Ice of the Okhotsk Sea and Air Temperature of the Northern Asian Continent

Yoshihiko SEKINE

Faculty of Bioresources, Mie University, Tsu, Mie-ken, Japan

INTRODUCTION

The subarctic water (known as the First Branch of the Oyashio) extends southward in the surface layer along the coast of Honshu, Japan. Sometimes the Oyashio Water reaches off the Boso peninsula, and then it is often called the Anomalous Oyashio Intrusion. The water near the southern tip of the extended area is considerably modified by horizontal mixing with surrounding waters, but keeps the cold and less saline characteristics of subarctic waters. The Anomalous Oyashio Intrusion usually causes the abnormally cold summer in the northern areas of Honshu, Japan, and influences the coastal fisheries.

The southernmost latitude of the 5°C isotherm at a depth of 100 m is frequently used as an index of this southward Oyashio extension strength. The variation of this latitude is shown in Fig. 1 (the bottom curve). For the period from 1970 to 1988 the eminent Anomalous Oyashio Intrusion occurred in 1973-74, 1981, 1984 and 1986. Charts of the sea surface temperature anomalies in April 1981 and April 1984 taken from the Ten-day Marine Report published by Japan Meteorological Agency are presented on Fig. 2. It can be seen that the Anomalous Oyashio Intrusion is not a local phenomenon, and the low temperature anomalies are widely observed within the subarctic and subtropical waters of the western North Pacific.

In the present work the occurrence of the Anomalous Oyashio Intrusion and its relationship with several oceanographic and meteorological phenomena will be discussed.

THE OCCURRENCE OF THE ANOMALOUS OYASHIO INTRUSION AND WIND CONDITIONS OVER THE NORTH PACIFIC

Based on the wind stress data by Kutsuwada and Teramoto (1987), Sekine (1988a) suggested that the latitude of no wind stress curl is observed in mid-winter just before the occurrence of the Anomalous Oyashio Intrusion. Using a numerical modelling (homogenous ocean model), he also demonstrated (Sekine, 1998b) that change in the wind stress field over the North Pacific Ocean causes the subsequent change in the subarctic circulation pattern: the southward shift of the no wind stress curl is usually accompanied by an increase of the wind stress over the North Pacific. The volume transport of the subarctic circulation is enhanced, and its position at the southern margin is shifted southward. This influences the occurrence of the Anomalous Oyashio Intrusion. In the present paper, only the averaged winter wind stress data just before the Anomalous Oyashio Intrusion (namely the average over late autumns and winters of 1973-4, 1980-81 and 1983-84), and that for the other years are considered.

Here, we numerically examine the year-to-year variations of the subarctic circulation in the North Pacific by using a two-layer ocean model on a beta plane. For simplicity, we consider an ocean

with simplified geometry and bottom topography as shown in Fig. 3a and 3b. The hydrostatic, rigid lid and Boussinesqu approximations are adopted. The governing equations are the same as used by Sekine and Kutsuwada (1994). The grid interval is 1 degree both in the west-east and the south-north directions. The coefficient of horizontal eddy viscosity is set to be 5×10^6 cm^2 s^{-1} in this analysis.

Teramoto and Kutsuwada (1987) compiled monthly mean wind stress fields over the North Pacific Ocean for the period from April 1961 to March 1984. The monthly mean wind stress fields from April 1984 to December 1987 were obtained using the same approach and the wind velocity data supplied by the Japan Meteorological Agency. These monthly mean fields are assumed to represent the field at the middle of the corresponding month, and the daily fields are calculated by interpolating these monthly values. The obtained wind stress data from January 1961 to December 1987 are applied in our model. However, as the ocean is presumed initially at rest and as the time scale of the baroclinic response is several years in our model, baroclinic adjustment may not be completed before 1970. In the later analysis, the comparison with the change of the Oyashio Intrusion strength would be made mainly for the period after 1971.

The distribution of the total volume transport function is displayed in Fig. 4 for January of each year. The western boundary currents are formed even during the first year (January 1961), indicating that such gross features are created through barotropic responses. The portions of anti-clockwise circulation (the subarctic circulation) are shaded in each figure. The area of the subarctic circulation and its strength (the density of the transport function in the shaded area) are characterized by noticeable temporal variability. It can be seen that the area and the strength have a tendency to increase in the years of the Anomalous Oyashio Intrusion: namely, in 1974, 1981, 1984, and 1986.

The southernmost latitudes of the calculated subarctic circulation were obtained for three longitudinal ranges:

1. 142°E - 170°W (the wider domain),
2. 142°E - 170°E (the domain west of the Emperor Sea Mounts) and
3. 142°E - 150°E (the Oyashio region).

Temporal variations of these latitudes for the period from 1971 to 1987 are shown in the upper-top, the upper-middle, and the upper-lower curves of Fig. 1, respectively. The seasonal variation is distinctive for all of three curves, except the period 1972-75 for the wider domain. The southern boundary of the subarctic circulation shifts southward generally in winter and northward in summer-autumn for almost all longitudes under consideration. However, the southernmost latitudes or the strengths of the southward winter shift are very changeable from year to year: the strengths are high in 1974, 1977-1978, 1980-1984, and 1986.

The temporal variation of the Oyashio Intrusion strength (the southern most latitude of the 5°C isotherm at 100 m depth) is also shown in the lower curve of Fig. 1 for the period from 1971 to 1987. The seasonal variability of this curve is not so significant, and variations having longer periods appear to be dominant. As discussed before, the southern shift of the latitude is distinguished in 1974, 1981, 1984 and 1986, and we assume that the Anomalous Oyashio Intrusion occurred for these years. From the same curve, we may conclude that the Anomalous Oyashio Intrusion took place also in 1977, 1978, 1982 and 1983, though its magnitude was somewhat smaller. It should be noted that these years just coincide with the years of the strong southward shift of the southern boundary of the subarctic circulation.

The correlation coefficient between the Oyashio Intrusion strength (the lower curve in Fig. 1) and the latitude of the southern boundary of the subarctic circulation is 0.35 if we chose the Oyashio Region (142°E-150°E: the upper-lower curve in Fig. 1) or 0.38 if we chose the domain west of the

Emperor Sea Mounts (142°-170°: the upper-middle curve in Fig. 1). The latter coefficient is increased to 0.40 if we apply one month lag for the curve of the Oyashio Intrusion strength.

The correlation coefficient between the Oyashio Intrusion strength and the latitude of the no wind stress curl is also calculated for the same period, and the coefficient is 0.31 without lag and 0.40 with one month lag. Though the Anomalous Oyashio Intrusion is a rather local phenomenon along the Pacific coast of the northern part of Honshu, it is strongly suggested that Anomalous Oyashio Intrusion has a close relation to the strength and the position of the global subarctic circulation in the North Pacific and to the position of the no wind stress curl of the wind system over the North Pacific.

OCEANIC AND ATMOSPHERIC PHENOMENA RELATED TO THE ANOMALOUS OYASHIO INTRUSION

Examples of the distribution of the 500 hPa height anomaly over the northern hemisphere are presented in Fig. 5 at the time of the Anomalous Oyashio Intrusion. In these figures, a prominently low pressure area is seen over the North Pacific and high pressure areas over the north Asian Continent (the Siberian High) and over North America. These distributions correspond to the so called PNA pattern, which relates to the ENSO phenomenon or abnormal high sea surface temperatures in the equatorial Pacific (Horel and Wallace, 1981; Shukla and Wallace, 1983). It strongly suggests that the occurrence of the Anomalous Oyashio Intrusion would have a teleconnection with the ENSO phenomenon.

The air temperature anomalies averaged over the nine stations shown in Fig. 6 for the years of the Anomalous Oyashio Intrusion (1974, 1981, 1984, and 1986) were calculated. The anomalies in December and January are positive, and equal to 1.57°C and 1.73°C, respectively. The winter air temperature at the stations surrounding the Okhotsk Sea and in the northern Asian Continent appears to be relatively warmer at the time of the occurrence of the Anomalous Oyashio Intrusion. The similar correlation between the Anomalous Oyashio Intrusion and the sea ice cover of the Okhotsk Sea can be seen: the area of sea ice cover of the Okhotsk Sea were calculated for each month from December to May separately for the years of the Anomalous Oyashio Intrusion and for the years of no Anomalous Oyashio Intrusion (all years from 1970 to 1988 except for 1974, 1981, 1984 and 1986). The obtained results are shown in Table 1. The sea ice cover is clearly larger for the years of no Anomalous Oyashio Intrusion: averaged ice cover area for the whole period analyzed is 61.5×10^4 km^2 for the years of the Anomalous Oyashio Intrusion and 77.1×10^4 km^2 for the other years.

Bhanu Kumar (1988) estimated the area of monthly snow cover of the Eurasian Continent for the period from 1970 to 1986. A significant positive correlation between this snow cover and the Okhotsk sea ice cover areas can be seen for both January data and three months data averaged from December to February (Figs. 7a and 7b). As Yasunari (1990) pointed out the close relationship between the strength of the Asian Monsoon and the occurrence of ENSO phenomena, there is much evidence suggesting the relationship among various oceanic and atmospheric phenomena. Though the Anomalous Oyashio Intrusion is a rather local phenomenon off the Pacific coast of the northern part of Honshu, Japan, but it should be noted that its occurrence is closely related with various large scale phenomena such as the subarctic North Pacific circulation, the wind stress distribution over the North Pacific, the atmospheric pressure pattern like the PNA pattern, the sea ice coverage of the Okhotsk Sea, the snow coverage over the Eurasian Continent, the ENSO phenomenon, and etc. Further investigations are necessary to explain the physical mechanisms of these teleconnections.

ACKNOWLEDGMENTS

I would like to thank professors Y. Nagata of Mie University and K. Ohtani of Hokkaido University for their valuable comments and advice. Thanks are also due to Dr. Kutsuwada of Tokai University and the staff of Japan Meteorological Agency for kind supplying the necessary data. I thank also Mr. F. Yamada of Mie University for his help in data analysis.

REFERENCES

Bhanu Kumar, O.S.R.U. 1988. Interaction between winter snow cover and location of the ridge at the 500 hPa level along 70°E. J. Meteor. Soc. Japan. 66:509-514.

Horel, J. M. and J. M. Wallace. 1981. Planetary scale atmospheric phenomena associated with the southern oscillation. Mon. Wea. Rev., 109, 813-829. Japan Meteorological Agency (1981, 1984): The ten-day Marine Report, nos. 1245 and 1354. (in Japanese) Japan Meteorological Agency (1987): Report on recent climatic change in the world (IV). pp.443.

Kutsuwada, K., and T. Teramoto. 1987. Monthly maps of the surface wind stress fields over the north Pacific during 1951-1984. Bull. Ocean Res. Inst. Univ. Tokyo. 24:1-100.

Sekine, Y. 1988a. Anomalous southward intrusion of the Oyashio east of Japan 1. Influence of the interannual and seasonal variations in the wind stress over the north Pacific. J. Geophys. Res. 93:2247-2277.

Sekine, Y. 1988b. A numerical experiment on the anomalous southward intrusion of the Oyashio east of Japan. Part 1: Barotropic model. J. Oceanogr. Soc. Japan. 44:60-67.

Sekine, Y., and K. Kutsuwada. 1994. Seasonal variation in volume transport of the Kuroshio south of Japan. J. Phys. Oceanogr. 24:261-272.

Shukla, J., and J. M. Wallace. 1983. A numerical simulation of the atmospheric response to equatorial Pacific sea surface temperature anomalies. J. Atmosph. Sci. 40:1613-1630.

Yasunari, T. 1990. Impact of Indian monsoon on the coupled atmosphere/ocean system in the tropical Pacific. Meteor. Atmosph. Phys. 44:29-41.

TABLES AND FIGURES

Table 1. Mean area of sea ice cover (in 10^4 km^2) of the Okhotsk Sea for the years of Anomalous Oyashio Intrusion (1974, 1981, 1984 and 1986: the left column) and for the years of no Anomalous Oyashio Intrusion (the other years: the right column). The standard deviations are also shown.

Month	Anomalous intrusion years	Weak intrusion years
Dec.	27.6 ± 6.7	36.2 ± 8.5
Jan.	69.0 ± 13.2	89.6 ± 12.6
Feb.	98.9 ± 18.4	117.1 ± 11.8
Mar.	94.9 ± 18.8	114.1 ± 16.6
Apr.	60.4 ± 14.8	78.8 ± 16.2
May	17.9 ± 2.9	26.9 ±8.8

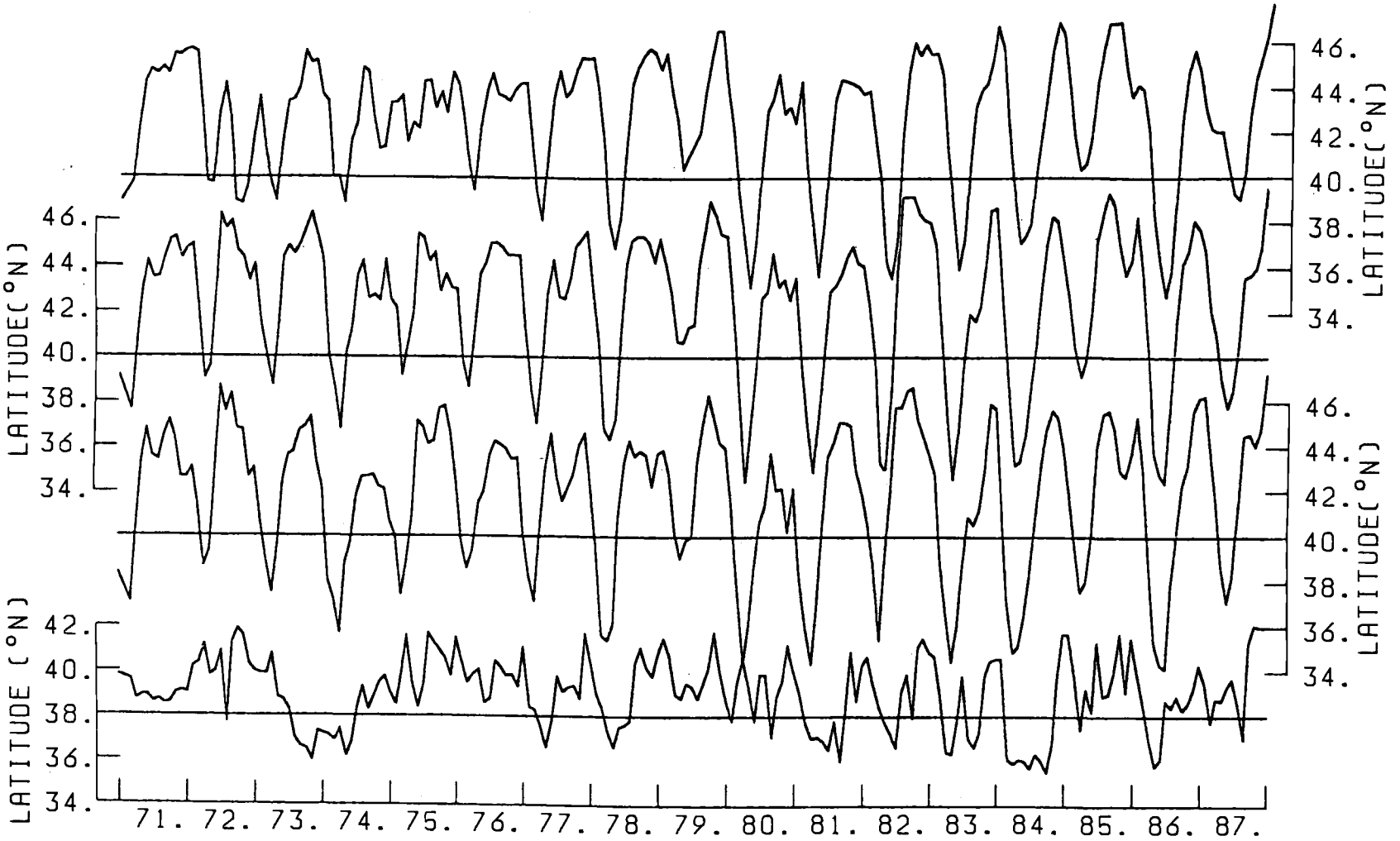

Fig. 1. Temporal variations of the southernmost latitude of the 5°C isotherm at the depth of 100 m (the bottom curve). This latitude is usually used as an index of the Oyashio Intrusion strength. Three other curves demonstrate temporal variations of the latitude of the southern boundary of the calculated subarctic North Pacific Circulation: the upper-top curve indicates that in the longitudinal range between 142°E and 170°W, the upper-middle curve that between 142°E and 170°E (west of the Emperor Sea Mounts), and the upper-lower curve that between 142°E and 150°E (the Oyashio region), respectively.

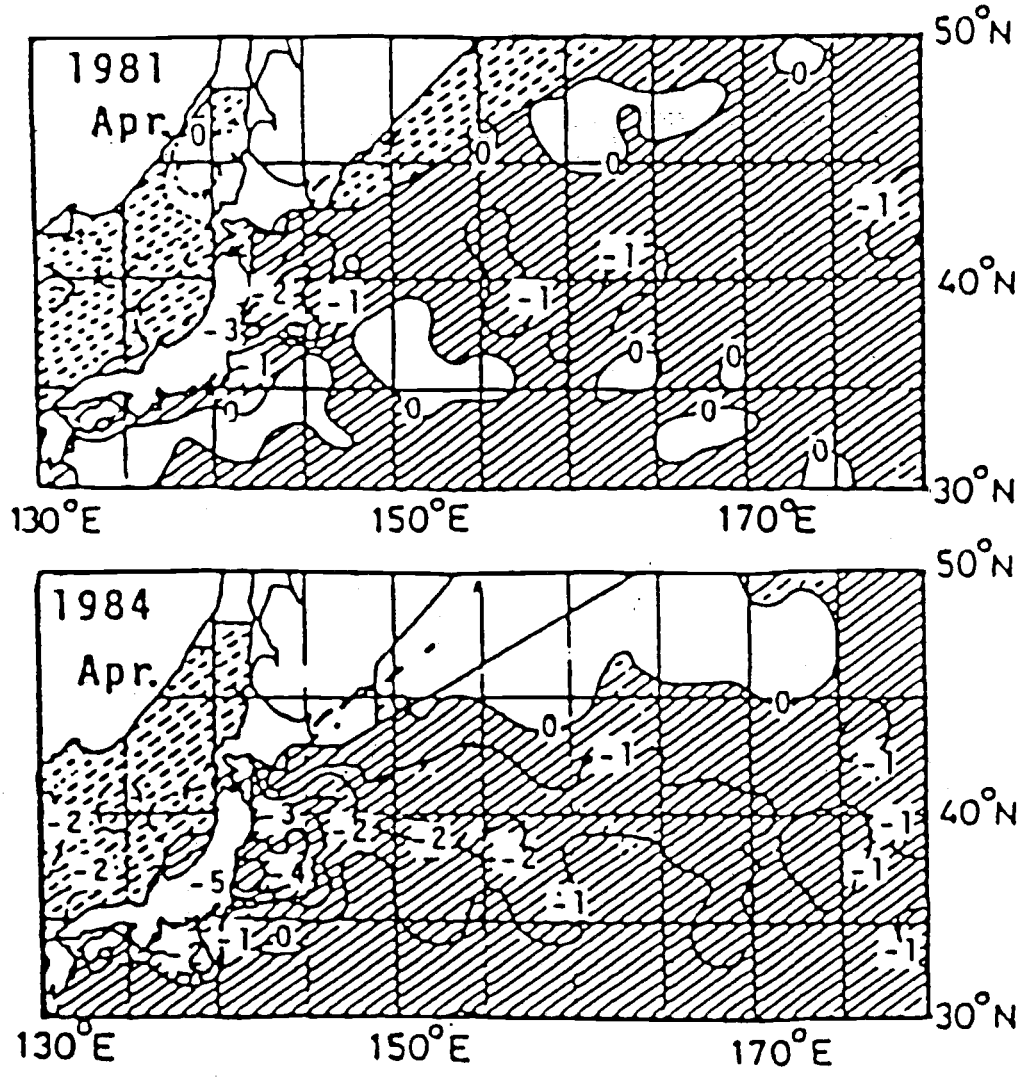

Fig. 2. Sea surface temperature anomalies in April 1981 (upper panel) and April 1984 (lower panel). Conspicuous Anomalous Oyashio Intrusions were observed in these years. The low temperature anomalies (hatched area) are widely seen in the western North Pacific area.

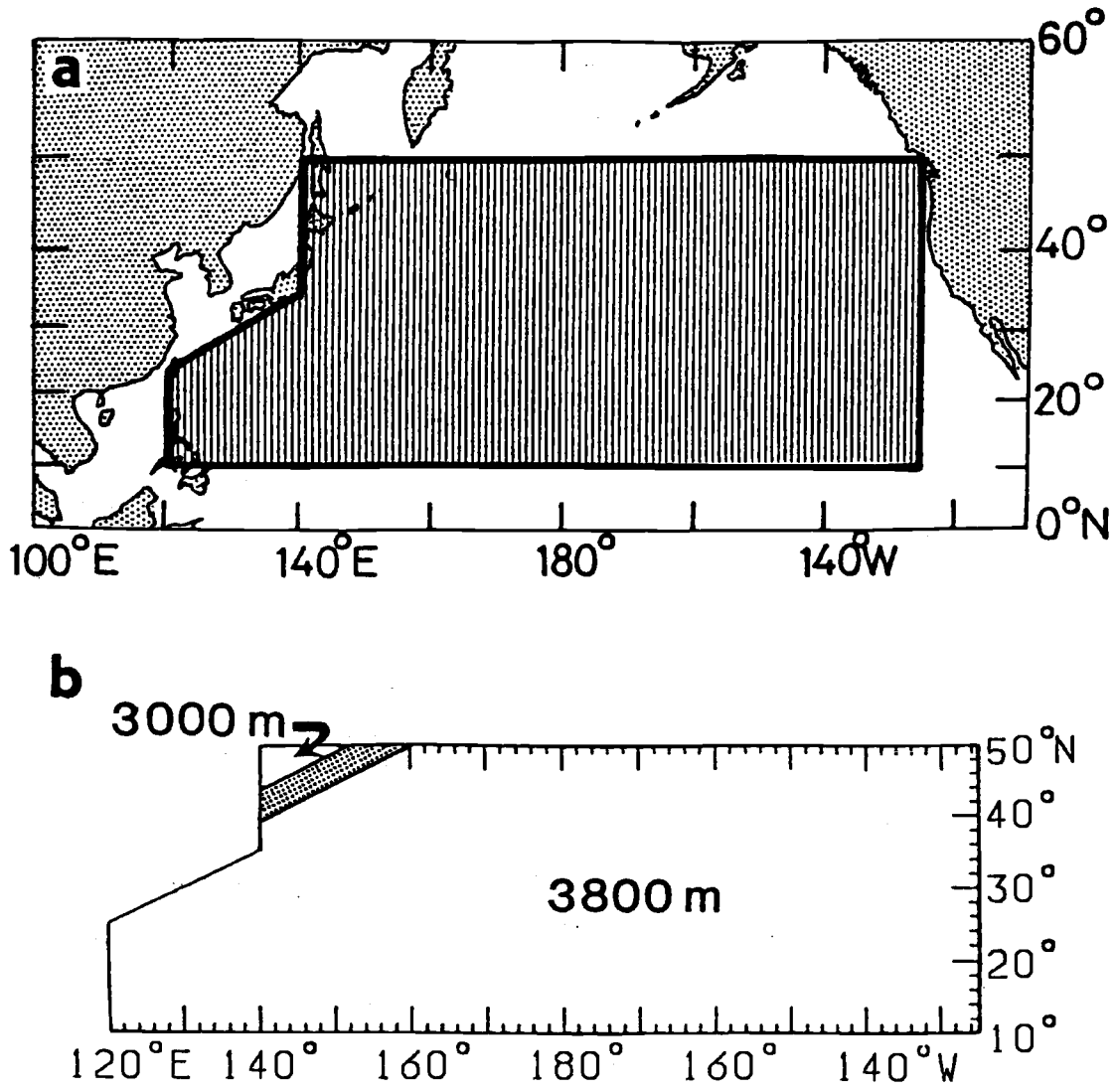

Fig. 3. Geometry of the ocean domain (a) and assumed bottom topography (b) used in the model.

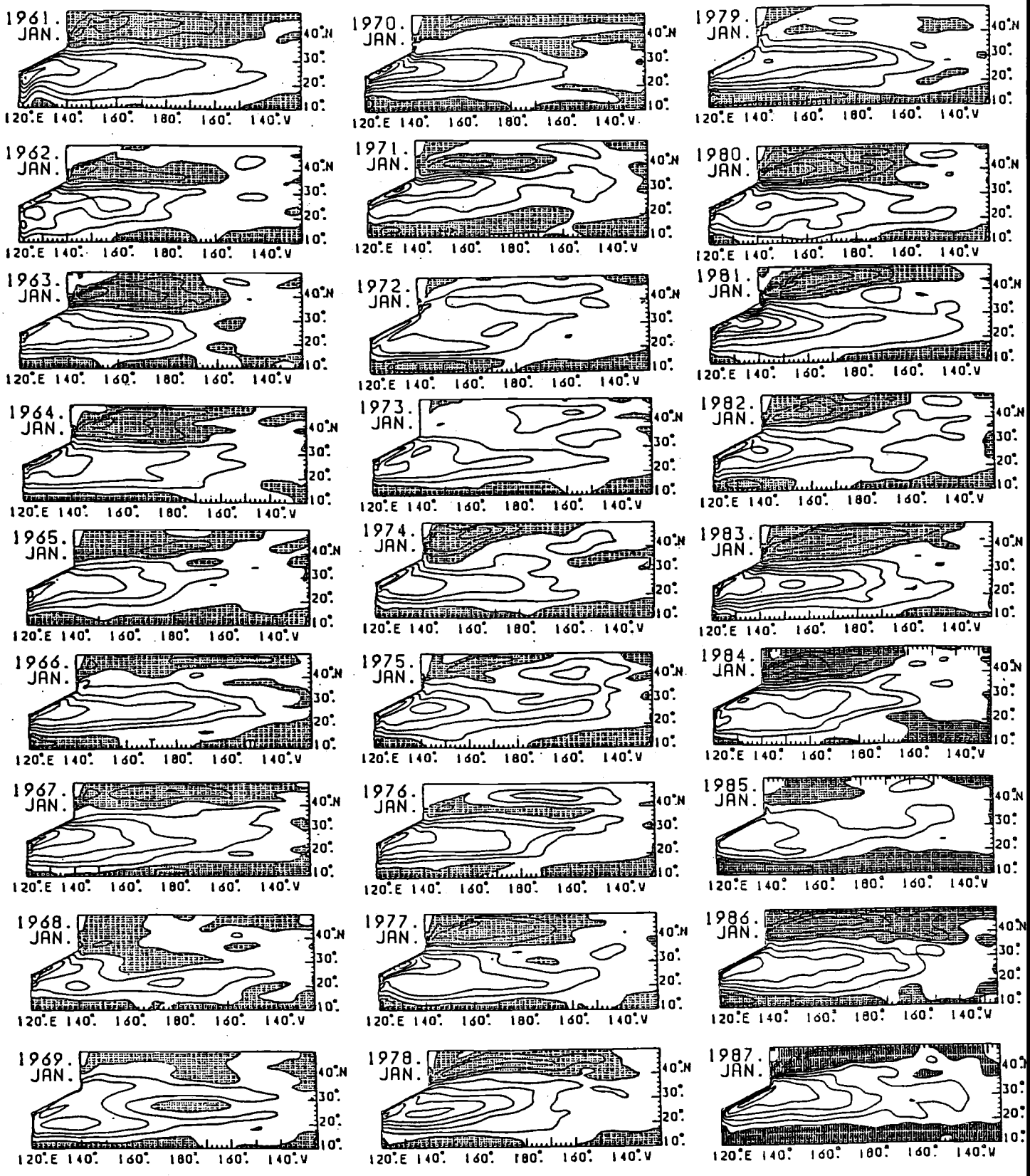

Fig. 4. The calculated total volume transport function at the middle of January of each year. Contour interval is 10 Sv. The shaded area indicate the portion of anti-clockwise circulation.

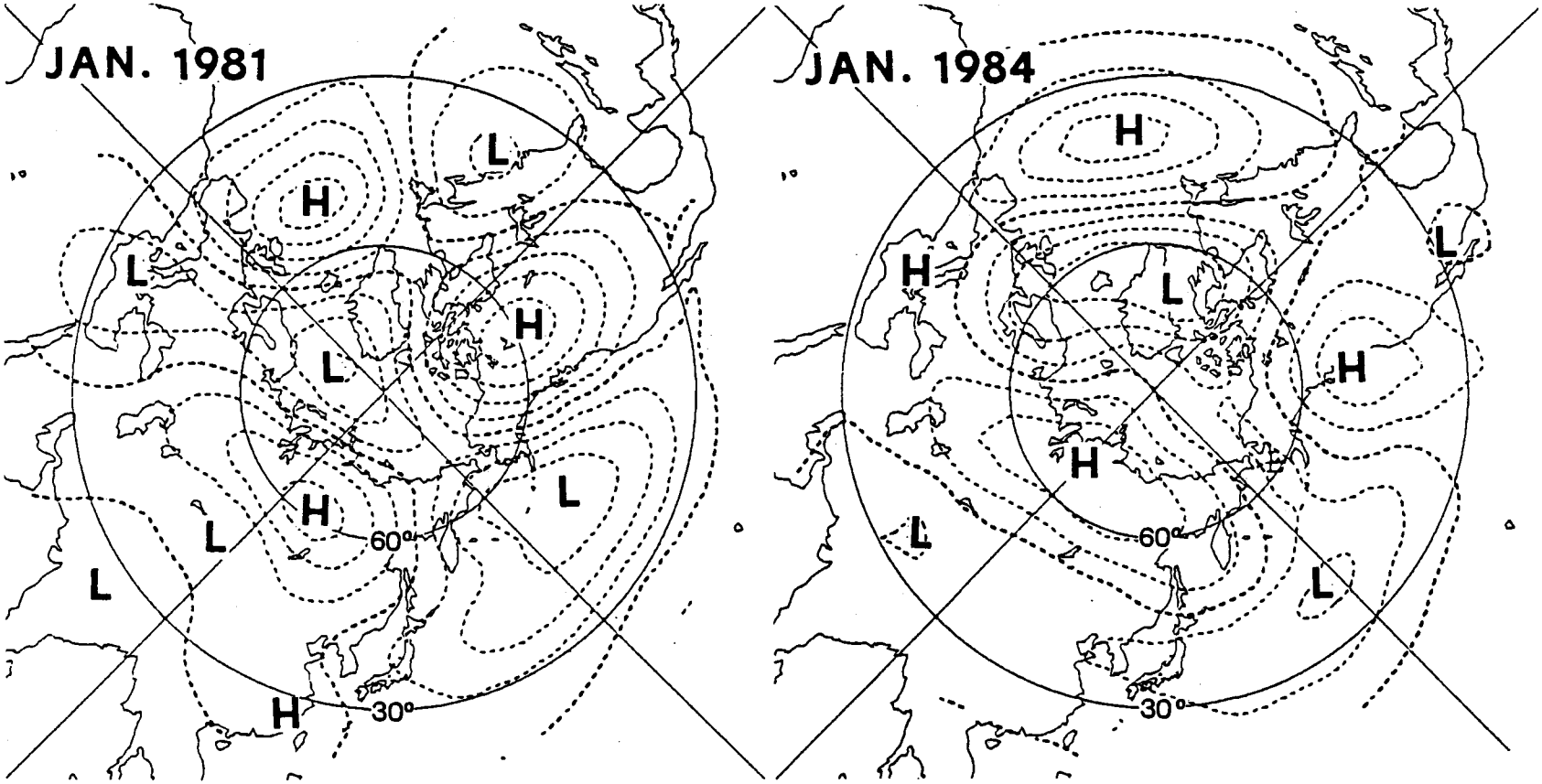

Fig. 5. Examples of the 500 hPa height anomaly distributions over the northern hemisphere at the time of the Anomalous Oyashio Intrusion: January 1981 (left) and January 1984 (right). Contour interval is 50 m.

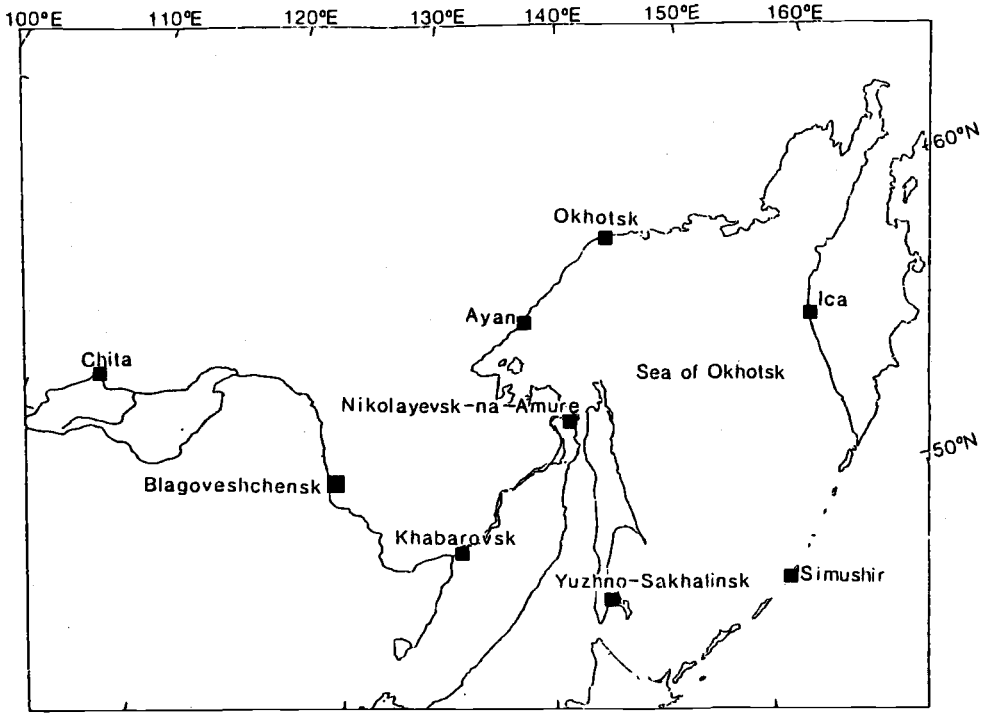

Fig. 6. Meteorological stations used for the air temperature anomalies analysis.

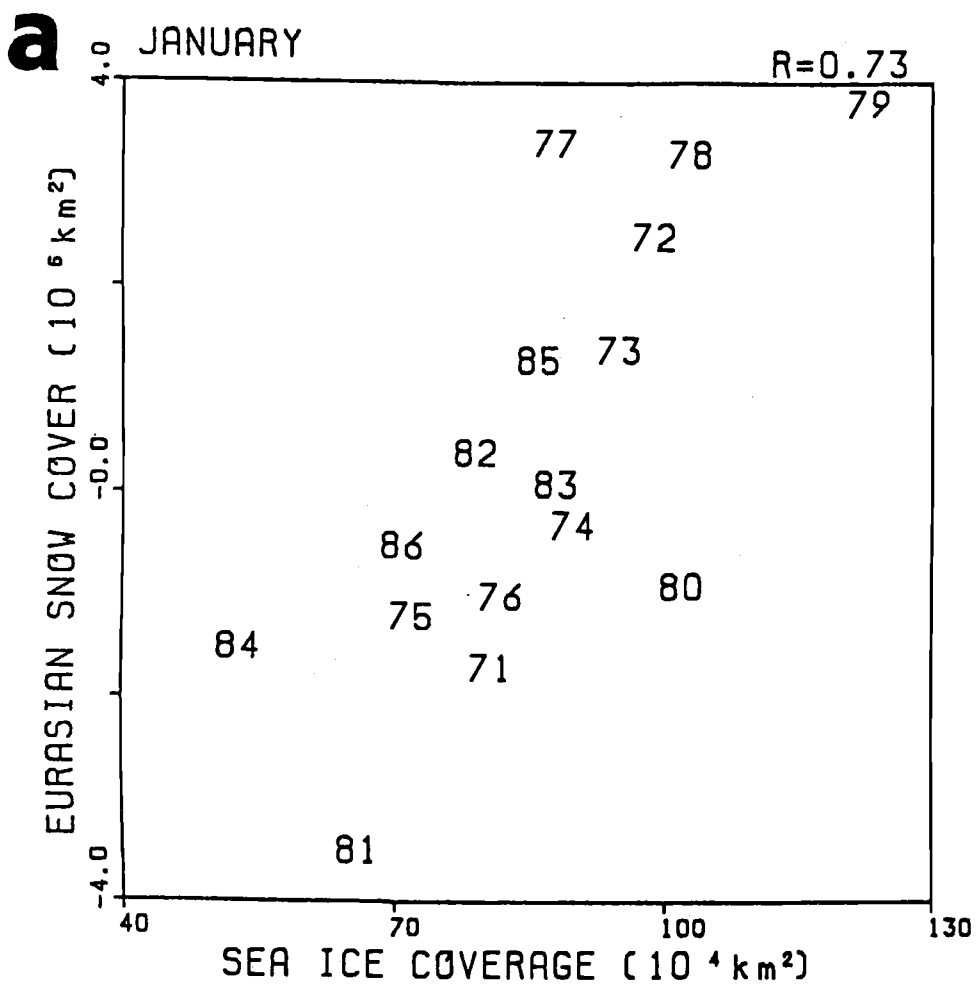

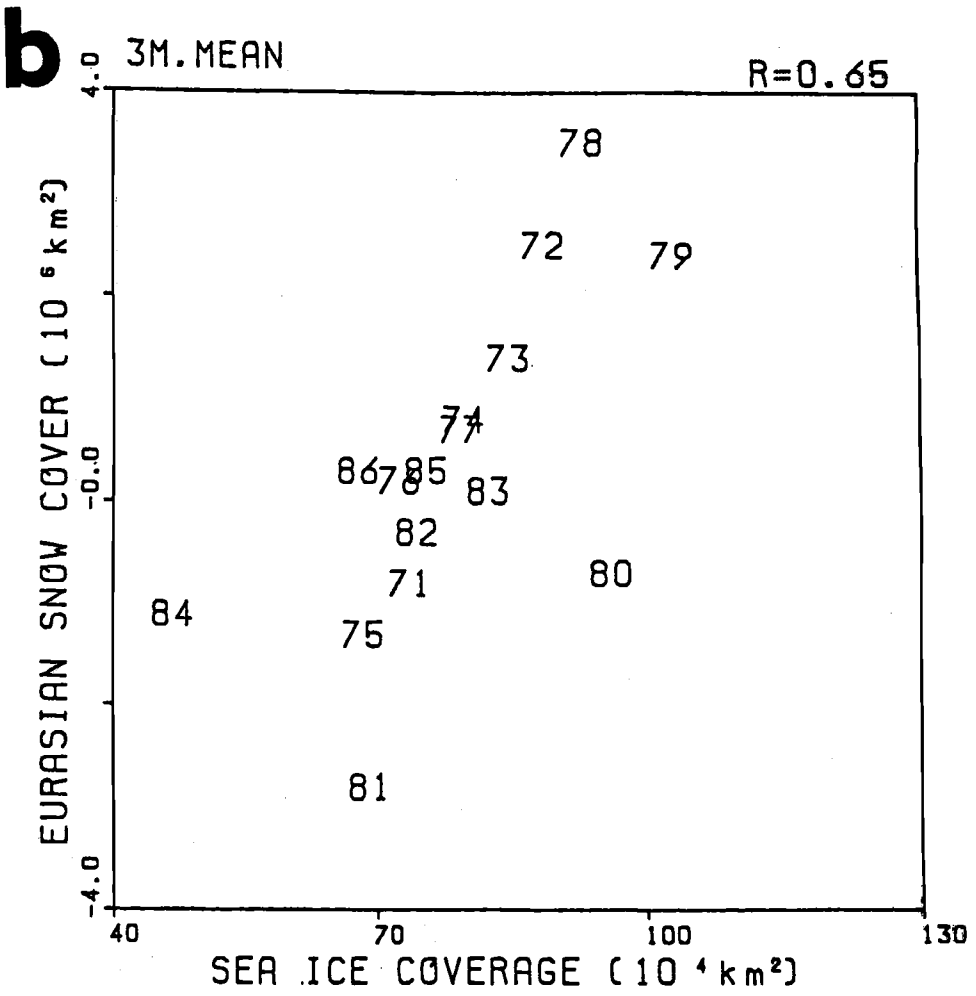

Fig. 7. Correlation between the areas of the Okhotsk Sea ice cover and the Eurasian Continent snow cover: for January data (a) and for three months data averaged from December to February (b). Numbers indicate the corresponding years.

Characteristics of the Tidal Motions in the Kuril Straits

Vladimir A. LUCHIN

Far Eastern Regional Hydrometeorological Research Institute, Vladivostok, Russia

INTRODUCTION

The tidal currents increase considerably their velocity in the Kuril Straits and create favorable conditions for intensive vertical and lateral water mixing leading to a decrease of the vertical gradients of the water properties observed in the region.

Results from previous investigations and data collected from 66 buoy stations within the Kuril Island area were recently examined by Luchin (1995). Tidal constants from 20 island positions were used to calculate yearly sea level fluctuations. All data obtained demonstrate that the main part of the Kuril region is characterized by predominant diurnal tidal currents and sea level fluctuations. These tides and sea levels are in phase: during the low water time it is clearly seen that observed differences in the onset time of tidal extrema do not exceed 1-2 hours and depend mostly on the geographical position and local bottom topography of sea level observational points. The diurnal tidal sea level fluctuations are dominant during both summer and winter and the maximum tidal amplitudes are detected in these seasons. Semidiurnal sea level fluctuations are the most pronounced in March and September.

The major ellipse axes of tidal currents are directed mainly along isobaths, whereas in the straits they are oriented along the troughs. In narrow straits, under specific astronomic conditions, maximum tidal currents can reach 5-8 knots.

DATA AND METHOD

The instrumental current measurements were collected from 516 stations in the Kuril region. Unfortunately, their duration at 450 stations did not exceed 1 day and was from 3 to 15 days only at 66 buoy stations (38 of which have been located in the narrows of straits). Sea level fluctuations along the Kuril Islands have been considered at 20 coastal stations. The hourly sea level heights were calculated using tidal constants for 8 main constituents.

RESULTS

Analysis of available observations show that vertical structure of tidal currents in the Kuril Straits is quite homogeneous (Fig. 1). Variations of current parameters with depth are insignificant and demonstrate that the barotropic component dominates in tidal flow. Certain variations in the current directions at specific depths are probably related to the topographic peculiarities within the straits. The weakest tidal current velocities are observed in the Bussol Strait. Therefore, water structure here is less transformed and the effect of non-periodic and baroclinic disturbances increases in the tidal flow.

Simultaneous current measurements were also performed at several points spatially divided up to 26 miles. These data show that spatial variations of tidal flow (in the absence of abrupt topographic changes) are insignificant.

The sea level temporal variations and tidal current features demonstrate the existence of a certain interaction between them. Temporal sea level fluctuations simultaneous with current observations were calculated using tidal constants from the nearest sea level station and the following results were obtained. In the Bussol Strait (sill depth 2,318 m) tides have a progressive wave character. The maximum tidal currents penetrating into the Pacific occur in the period of low water or about 1 hour before.

Standing fluctuations are observed in the deep part of the Kruzenshtern Strait (sill depth 1,920 m). The maximum currents occur 1-3 hours before low water (Fig. 2). The standing fluctuations dominate also in the shallow straits and over the shallow parts of the deep straits. For instance, the tidal currents move into the Okhotsk Sea over the shallow part of the Kruzenshtern Strait as sea level rises and reverse into the Pacific Ocean as sea level falls (Fig. 3).

The anomaly relation between sea level and the currents is observed in the deep trough of the 4th Kuril Strait. Standing fluctuations are dominant in this case, but the maximum currents into the Okhotsk Sea occur 6-8 hours after the low water (Fig. 4). Further investigations under different astronomic conditions are required for this region.

Thus, in the straits with complicated morphometry different contributions of progressive and standing wave components were observed. It can lead to generation of eddy disturbances within the tidal flow. This event should also be expected in the regions of abrupt depth changes.

RECOMMENDATIONS FOR FIELD OBSERVATIONS

1. Current measurements in the main Kuril Straits should be conducted simultaneously and duration of observations has to be not less than 15 days. Sea level fluctuations should be recorded nearby at the same time.
2. Tidal observations in straits with complicated topography should be simultaneously assessed in both troughs and shallow water regions.
3. Observations have to be carried out in the periods of prevailing diurnal currents as well as when semidiurnal currents are dominant.

REFERENCES

Luchin, V. A. 1995. System of currents and peculiarities of temperature distribution in the Okhotsk Sea. The Okhotsk Sea and Oyashio Region. PICES Scientific Report No. 2:211-227.

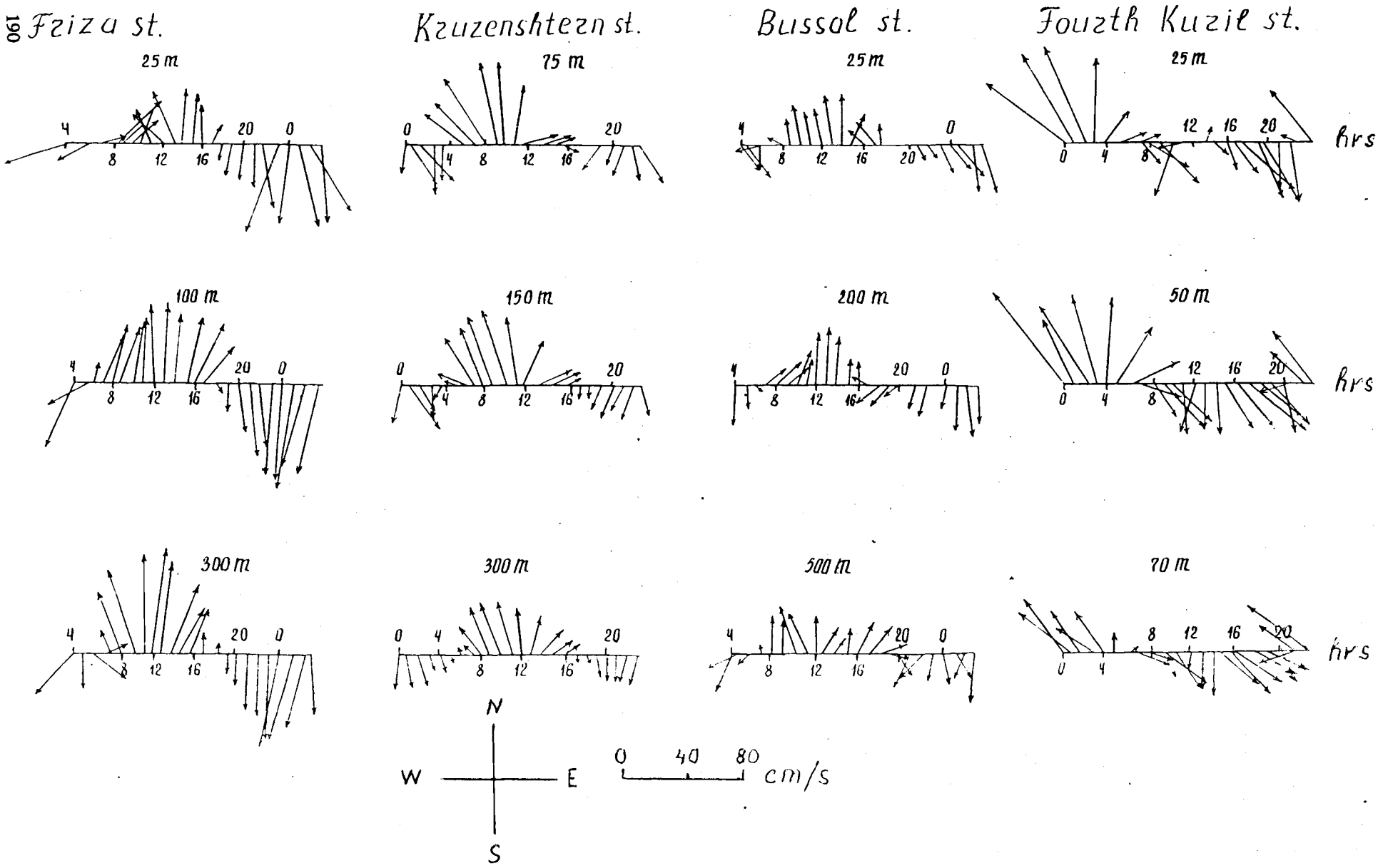

Fig. 1. Temporal variations of tidal current velocities at various depths in the Kuril Straits.

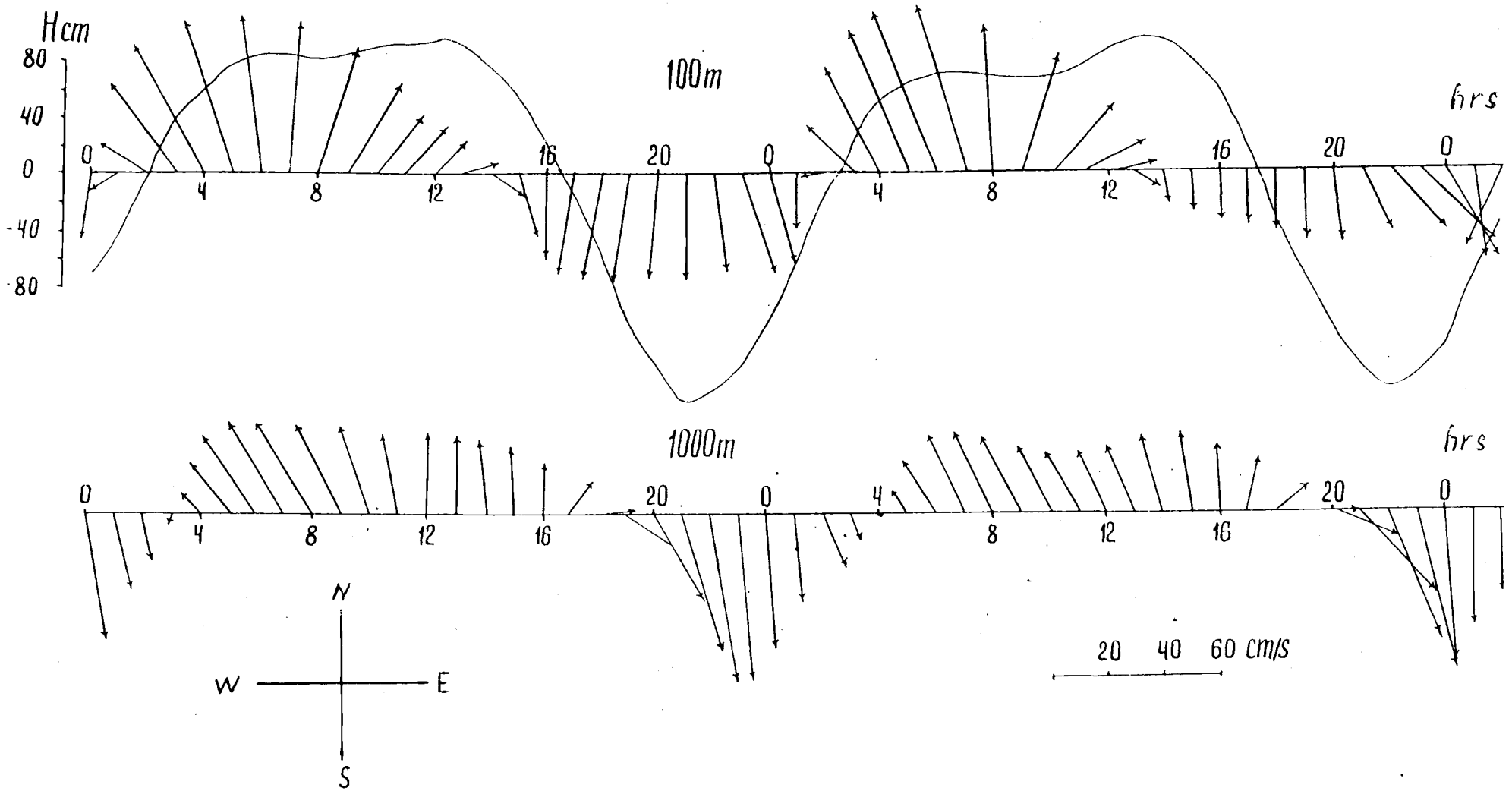

Fig. 2. Temporal variations of tidal current velocities and sea level fluctuations in the deep part of the Kruzenshtern Strait.

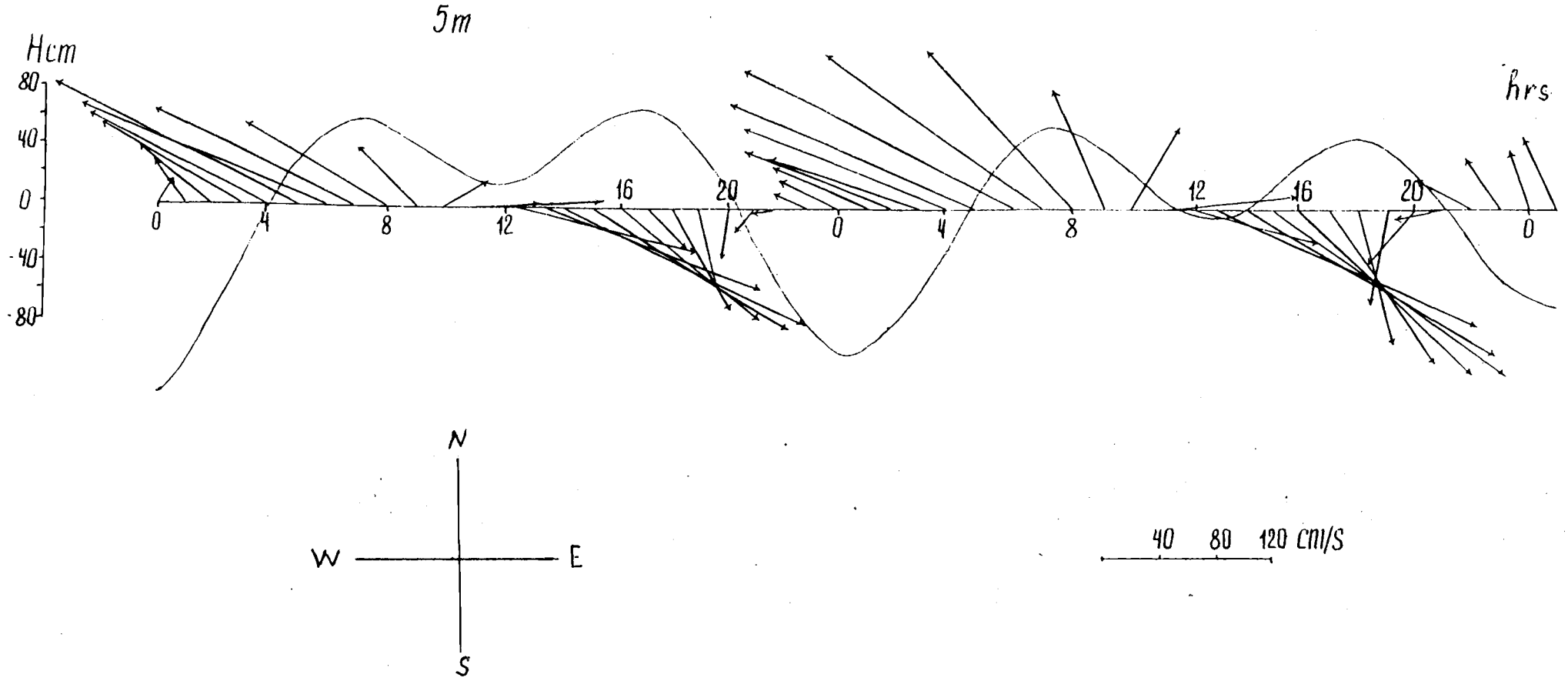

Fig. 3. Temporal variations of tidal current velocities and sea level fluctuations in the shallow part of the Kruzenshtern Strait.

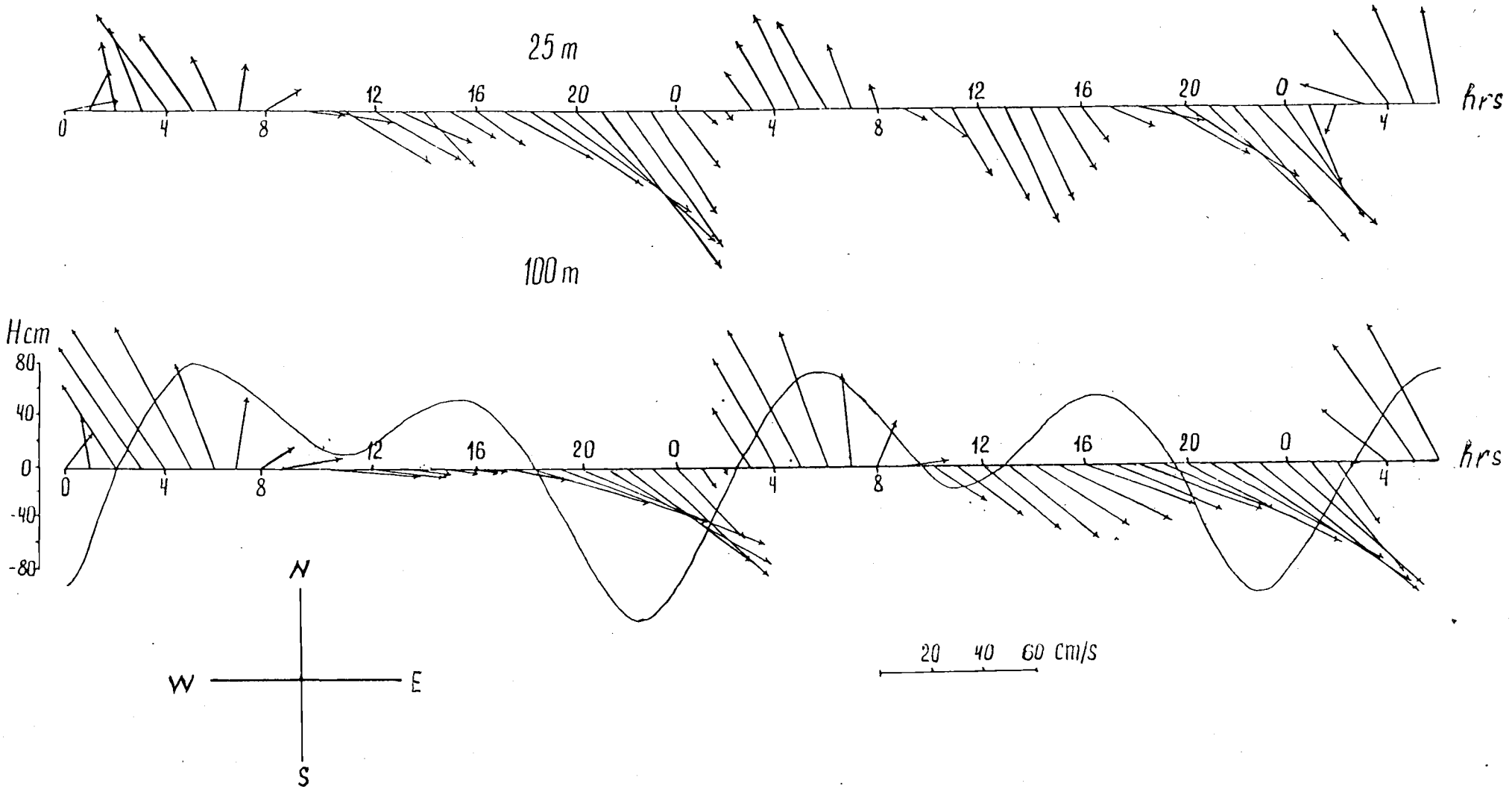

Fig. 4. Temporal variations of tidal current velocities and sea level fluctuations in the 4th Kuril Strait.

On Seasonal Variability of Tidal Constants in the Northwestern Part of the Okhotsk Sea

George V. SHEVCHENKO

Institute of Marine Geology and Geophysics, Far Eastern Branch,
Russian Academy of Sciences, Yuzhno-Sakhalinsk, Russia

INTRODUCTION

The main problem of tidal regime research could normally be reduced to the determination of tidal constants (amplitude h and phase g) from the available sea level observational series. Tidal sea levels and currents for any moment of time can be predicted using these constants. In most cases a monthly observational series is enough for reliable estimation of h and g, and as a rule, a corresponding long-term forecast can be made with sufficiently high accuracy, satisfying practical requirements for hydrology surveys, port activities, coastal engineering, etc.

However, in some ocean regions this method does not work properly for various reasons, such as, change in water circulation, bottom friction, influence of ice, outflow of energy into internal waves, etc. As a result, temporal variability of tidal constants is observed (Pugh and Vassie, 1976; Sgibneva, 1981) and prediction of tides turns into a more difficult problem.

A correct prediction of tidal currents and sea levels is highly important for the northwestern part of the Okhotsk Sea because of planned development of the oil and natural gas industry in this area. In the present work the seasonal variability of tidal constants is studied based on hourly sea level data at three stations: Nabil Bay (Katangli), Okhotsk and Moskalvo. Seven year average tidal constants were used to calculate the amplitude and phase "systematic corrections" for each month.

DATA ANALYSIS

Hourly sea level data from tide gauges in the Okhotsk Sea [Korsakov (1977-1990), Poronaisk (1977-1988), Kurilsk (1977-1985), Magadan (1977-1988), Okhotsk (1982-1988), Moskalvo (1965-1966, January-May) and Katangli (1987-1993)] were analyzed. Tidal sea level constituents were determined by least square method for all years. Significant difference between observed and predicted sea level series has been found at three stations in the northwestern part of the Okhotsk Sea (Okhotsk, Moskalvo, Katangli) where spectra of residual sea levels had prominent peaks at tidal frequency bands). For these stations, tidal constituents were determined for each month separately as in Pugh and Vassie (1976). Since for monthly series some tidal constituents (such as K_1 and P_1 or S_2 and K_2) could not be separated, they were estimated using values obtained from the whole year. Our results (Figs. 1 and 2) clearly demonstrate that the amplitude and phase of main constituents change from month to month.

Similar phenomenon was also revealed in some other Okhotsk Sea regions, in particular for Penzhinskaya Guba (Sgibneva, 1981) and in Amursky Liman (Lyubitsky, 1989).

SEASONAL VARIABILITY OF TIDAL CONSTANTS

Seasonal variability of tidal constants at Okhotsk and Moskalvo stations is very strong. For the principal semidiurnal constituent M_2 variances in amplitude and phase are over 30% and 25°, respectively. Maximum amplitudes are observed in March and April and maximum phases are found in September and October when amplitudes are small. The diurnal tides have maximum amplitudes and minimum phases in January, whereas minimum amplitudes are observed in August and maximum phases in October. Thus, seasonal variability of tidal amplitudes and phases of the main constituents is almost in counter-phase.

Variability of tidal constants on the northeastern coast of Sakhalin Island is not evident. Although the maximum amplitudes (in April and December) mainly correspond to minimum phases, but maximum phases (in September for diurnal tides and in July for M_2) do not coincide with minimum amplitudes observed in June for diurnal tides or in January - February for M_2. It should be noted that variability of tidal constants at Katangli station is not so significant and clearly emphatic as at the Okhotsk station where it has almost periodic character.

"SYSTEMATIC CORRECTIONS" OF TIDAL CONSTANTS

Seven year average tidal constants for Okhotsk and Katangli stations were used to calculate "*systematic monthly corrections*". The amplitude corrections have been estimated as a ratio of the average monthly values to the whole year value, while the phase correction was computed as a difference between monthly and the whole year values. These corrections may be used in analysis of relatively short off-shore measurements of currents and sea levels, and also for more accurate tidal predictions.

To characterize the importance of "systematic corrections" three variances and corresponding ratios (%) have been calculated for each tidal constituent (Table 1):

1. *Factoral (or intergroup) variance* (D_f) related to deviations of the mean monthly values from the mean yearly value;
2. *Average group variance* (D_g) associated with deviations of mean monthly values for every year from the average (over 7 years) monthly values caused by various reasons, considered as casual;
3. *Total variance* (D_t) equals to the sum of two previous.

The relative contribution of the intergroup variances demonstrates the importance of regular events in comparison with the casual elements caused by fluctuations inside the groups. It is also evident, that in the Okhotsk region seasonal fluctuations of tidal constants are the most essential, and casual deviations are insignificant compared to "systematic monthly corrections".

CONCLUSIONS

1. Significant seasonal variability of tidal constants in the northwestern part of the Okhotsk Sea has been revealed based on analysis of tide gauge data.
2. Seasonal variability is high and steady in the Okhotsk region and rather less on the northeastern coast of Sakhalin Island.
3. Use of "*systematic monthly amplitude and phase corrections*", calculated from seven year average tidal constants, reduces errors of sea level prediction up to 0.5 m in the Okhotsk region and up to 0.2 m at Katangli station.

4. Obtained results could be used for more accurate forecast of tidal sea levels and currents in the northwestern part of the Okhotsk Sea.

REFERENCES

Lyubitsky, Yu.V. 1989. Sea level at the river mouth. Trudy DVNIGMI, Vladivostok. 38:69-104 (in Russian).

Pugh, D.T., and J.M. Vassie. 1976. Tide and surge propagation off-shore in the Dowsing region of the North Sea. Deutsche Hydrographiche Zeitschrift. 29:163-213.

Sgibneva, L.A. 1981. Variability of tidal constants as consequence of non-linear effects. Trudy GOIN, Moscow. 156:33-40 (in Russian).

TABLES AND FIGURES

Table 1. Total (D_t), factoral (D_f) and average (D_g) group variances of 7-year average monthly tidal constants (corresponding ratios D_f/D_t and D_g/D_t are given in brackets).

		VARIANCES (Deg^2, cm^2)	
STATION/CONSTITUENTS	*FACTORAL*, D_f	*AVERAGE GROUP*, D_g	*TOTAL*, D_t
KATANGLI			
M_2 (phase)	21.8 (61%)	14.4 (39%)	36.2
M_2 (amplitude)	0.8 (53%)	0.7 (47%)	1.5
K_1 (phase)	10.3 (65%)	5.5 (35%)	15.8
K_1 (amplitude	2.9 (43%)	3.8 (57%)	6.7
OKHOTSK			
M_2 (phase)	59.0 (93.8%)	3.9 (6.2%)	62.9
M_2 (amplitude)	49.4 (84.7%)	8.9 (15.3%)	58.3
K_1 (phase)	15.7 (86.7%)	2.4 (13.3%)	18.1
K_1 (amplitude	6.2 (87.3%)	0.9 (12.7%)	7.1

FIGURES

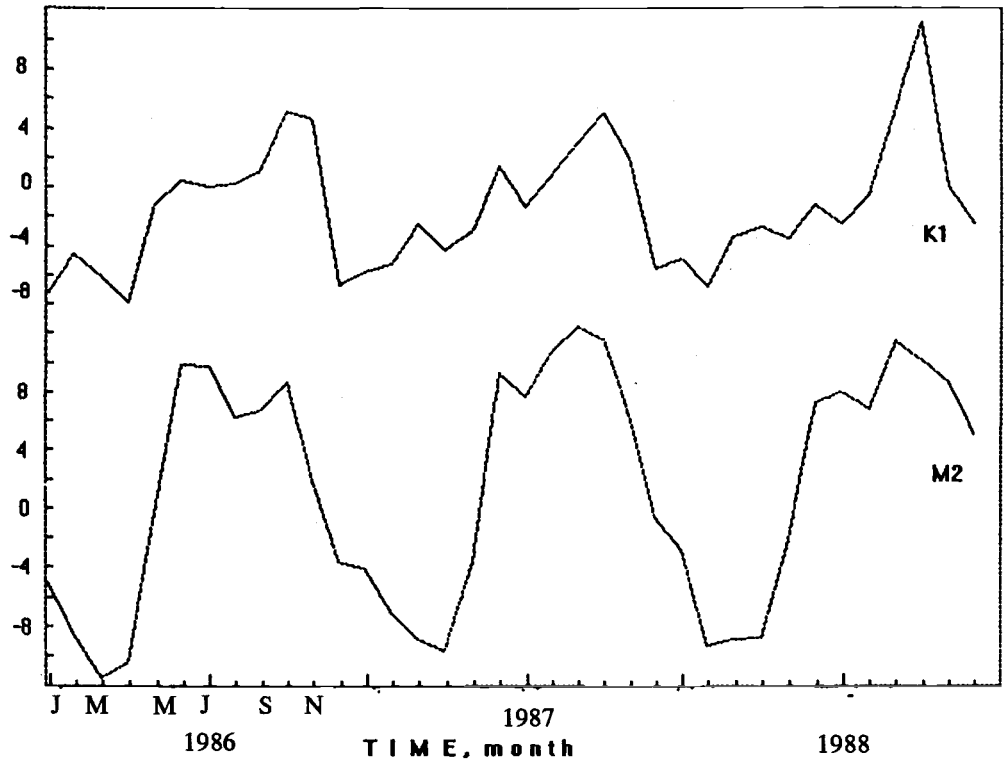

Fig. 1. Phases of the main diurnal and semi-diurnal constituents determined for each month separately (difference between monthly and whole year values). Okhotsk, 1986-1988.

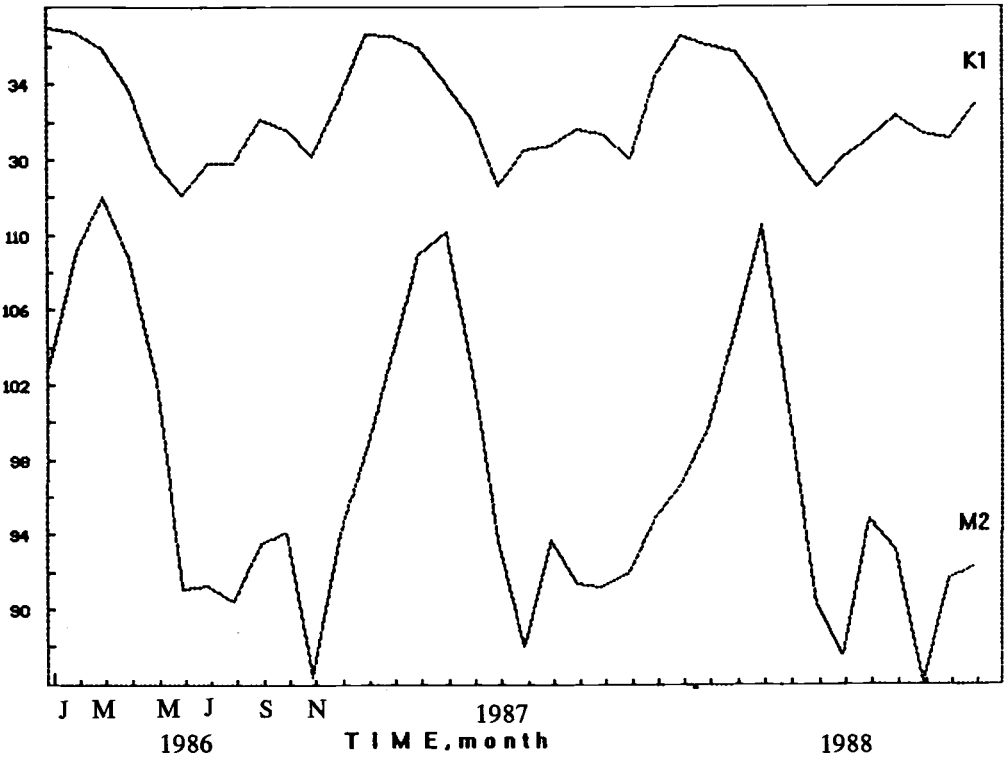

Fig. 2. Tidal amplitudes of main diurnal and semi-diurnal constituents determined for each month separately (in percentage, related to M2 amplitude obtained for whole year). Okhotsk, 1986-1988.

A "Chimney" of Cold Salt Waters near Vladivostok

Mikhail A. DANCHENKOV[1], Kuh KIM[2], Igor A. GONCHARENKO[1] and Young-Gyu KIM[2]

[1] Far Eastern Regional Hydrometeorological Research Institute, Vladivostok, Russia
[2] Research Institute of Oceanography Seoul National University, Seoul, Republic of Korea

INTRODUCTION

It is generally believed that the Japan Sea Proper Water (JSPW) is formed in the northwestern part of the Japan Sea. Nevertheless, this area was investigated very poorly in comparison with the southern part of the Sea. Almost twenty five years ago Nitani (1972) noted that the winter situation in the northwestern Japan Sea is unknown and suggested a survey in Peter the Great Bay just before and during the period of ice formation. None the less, after fifteen years, Gamo et al. (1986) mentioned a lack of information about the spatial and temporal variations of water properties in the northern Japan Sea regarded as a regional source of the bottom water and emphasized the need to research the northern and northwestern Japan Basin, especially in the winter season. According to Sudo (1986), the most probable source of the JSPW formation is the region north of 41°N between 132°E and 134°E. This statement was amplified by Senju and Sudo (1993) who advised that the upper portion of the JSPW is formed by winter convection, likely off the Siberian coast west of 136°E between 40°N and 43°N.

Now the opportunity arose to discuss the process of water formation in the northwestern part of the Japan Sea based on new temperature and salinity data collected during two consecutive winters in 1994 and 1995.

DATA

During the winter of 1994 research vessels of Far Eastern Regional Hydrometeorological Research Institute repeated temperature and salinity measurements nine times on the section along 132°E from Vladivostok to 36.5°N. In March 1995 seven one-time sections were performed from the coast to 41.0°N between 131.5°E and 133.6°E. The total number of stations sampled was 116.

Note the interesting feature of bottom relief in the area of investigation: just south of Vladivostok between 41.5°N and 42.5°N there is a bottom rise with a minimum depth less than 1,000 m contoured by a 2,500 m isobath.

VERTICAL DISTRIBUTION OF WATER CHARACTERISTICS IN 1994 AND 1995

The "chimney" - area of homogenous vertical water properties near the bottom rise - was revealed for the first time in March 1994 along 132°E between 41.5°N and 42.5°N. In March 1995 during the winter CREAMS cruise the meridional boundaries were determined as 131.8°E and 133.2°E. The "chimney" was bordered from the south and west by the Subarctic (Polar) thermal front, from the north by a coastal saline front and from the east by a coastal thermal front.

In March 1994 the temperature in the "chimney" changed from -0.7°C to 0.7°C and was lower than in neighboring waters. Salinity in this area varied between 34.02 and 34.19 psu and was lower than in the northern part of Peter the Great Bay, but higher than in surrounding waters by 0.03-0.10 psu. Density (sigma-t) in the "chimney" was in the range 27.30-27.44, almost uniform in vertical direction and also differed from density of adjacent waters. Seawater homogeneity was observed from the surface down to 1,500 m (the lowest horizon of observations).

In March 1995 measurements at section along 132.3°E were performed with better accuracy and just above the bottom rise, and the characteristics of seawater were found in a good agreement with our previous survey (Table 1). Depth of salinity maximum was situated at 300-500 m and depth of temperature minimum at 1,700-1,900 m.

At 132°E (western border of the "chimney" area) and at 133°E (its eastern edge) the sigma-theta surface of 27.32 was located at depth above 100 m. In the center of the "chimney" near surface sigma-t was higher than 27.32 (Fig. 1). Between the surface and 1,000 m water temperature changed from 0.5°C to 1.0°C and salinity from 34.05 to 34.07 psu. Even during summer, sigma-t of 27.3 was closer to the sea surface than anywhere else in the Japan Sea.

HORIZONTAL WATER STRUCTURE

At the sea surface in winter the "chimney" area was bordered from the south and west by the Subarctic (Polar) front and from the north by the coastal Primorye front. The Subarctic front was best revealed by temperature distribution and the coastal front by salinity distribution. According to satellite images (e.g., November 28, 1983) water of in the "chimney" was colder than surrounding waters, and that cold pool is detected in the area every winter. It should also be mentioned that extremely high salinity (more than 34.15 psu) was observed in the pool at the end of 1994.

CONCLUSION

The "chimney", an area of homogeneous vertical temperature and salinity distribution, was found in winter above the bottom rise near Vladivostok. The "chimney" water is characterized by temperature 0.5°C - 1.0°C, salinity - 34.05-34.07, and density (sigma-t) higher than 27.3.

REFERENCES

Gamo, T., Y. Nozaki, H. Sakai, T. Nakai, and H. Tsubota. 1986. Spatial and temporal variations of water characteristics in the Japan Sea bottom layer. J. Marine Res. 44:781-793.

Nitani, H. 1972. On the deep and bottom waters in the Japan Sea, p.151-201. *In* D. Shoji [ed.] Researches in hydrography and oceanography. Tokyo Hydr. Dept. of Japan.

Senjyu, T., and H. Sudo. 1993. Water characteristics and circulation of the upper portion of the Japan Sea Proper Water. J. Marine Systems. 4:349-362.

Sudo, H. 1986. A note of the Japan Sea Proper Water. Progr. Oceanogr. 17:313-336.

TABLES AND FIGURES

Table 1. Temperature (°C), salinity (PSU) and depth of 27.32 sigma-t (Zs-t) above bottom rise in winters of 1994 and 1995.

Time	Coordinates	Temperature and salinity					Zs-t
		0m	200m	400m	1,000m	2,000m	
22.03.94	42.2°N, 132.0°E	0.89	0.61	0.35	0.18	-	60 m
		34.046	34.066	34.063	34.060	-	
	41.8°N, 132.0°E	0.75	0.58	0.44	0.22	-	100m
		34.046	34.069	34.065	34.061	-	
03.03.95	42.0°N, 132.3°E	0.66	0.67	0.62	0.24	0.19	0m
		34.060	34.068	34.071	34.063	34.063	
	41.8°N, 132.3°E	0.90	0.63	0.53	0.23	-	50m
		34.049	34.066	34.070	34.063	-	

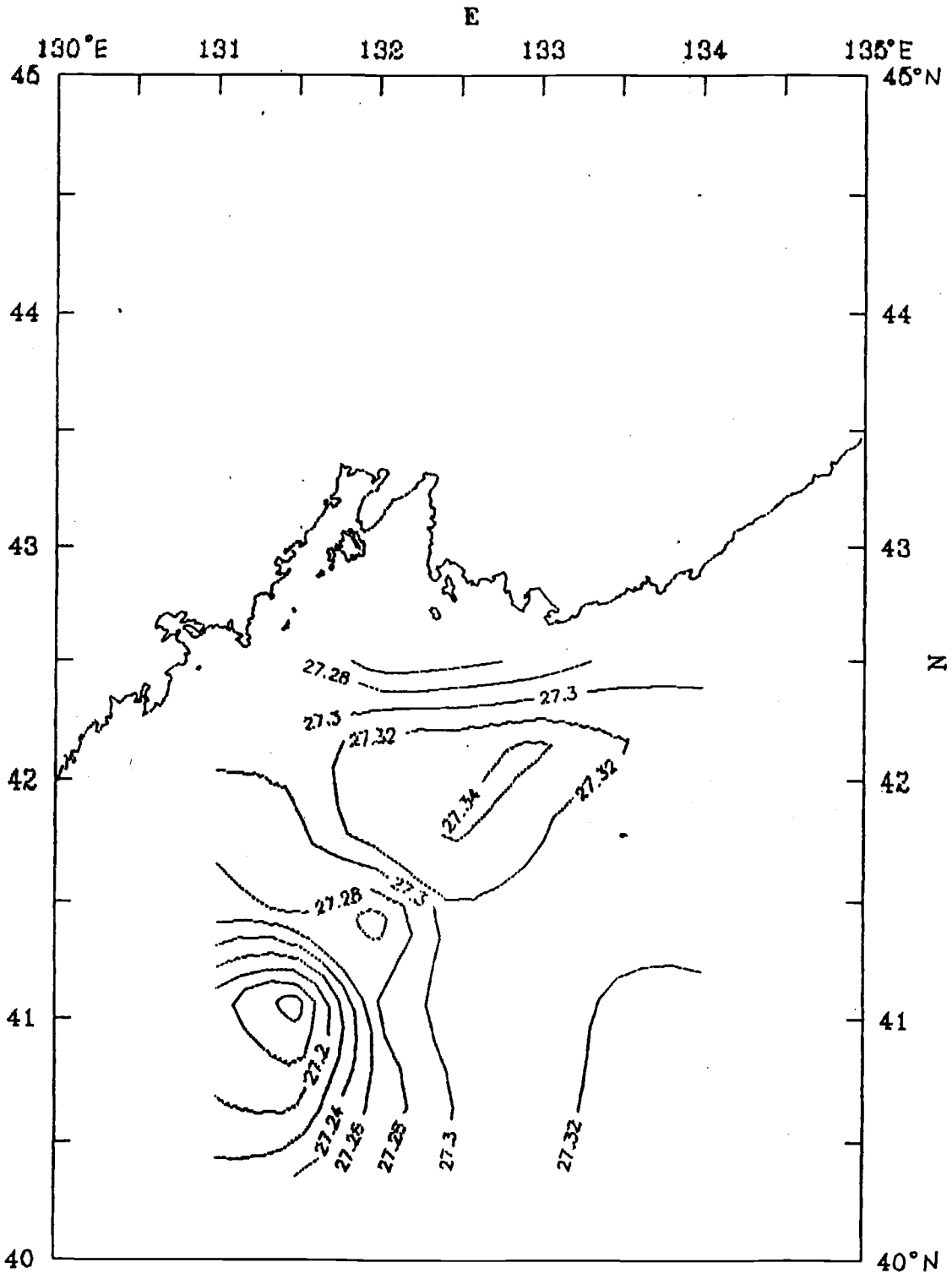

Fig. 1. Distribution of sigma-t at 200 m depth during March 1-8, 1995.

Preliminary Results from a Numerical Circulation Model of the Japan Sea

Christopher N.K. MOOERS and Hee Sook KANG

Ocean Prediction Experimental Laboratory (OPEL), Rosenstiel School of Marine and Atmospheric Science, University of Miami, Miami, FL 33149, U.S.A.

INTRODUCTION

The circulation of the Japan Sea is dominated by the throughflow of the Tsushima Current, which enters through the Korean Straits, branches along the Korean and Japanese coasts, and exits through the Tsugaru and Soya Straits. It is also strongly influenced by atmospheric forcing and river runoff, plus ice formation and tidal circulation, especially in the northern reaches of the Tatarsky Strait. The instantaneous circulation is characterized by intense mesoscale variability; i.e., meandering jets, eddies, and fronts. The upper few hundred meters of the southern half of the basin are much more stratified than the northern half of the basin; the two halves are separated by the subpolar front and jet. The lower few kilometers of the water column are filled with the relatively homogeneous Japan Sea Proper Water, which, however, has fine structure associated with interannual variations in wintertime deep convection.

Major open questions exist concerning the deep convection process, which has at least three candidate source regions: north of the subpolar front off Vladivostok, various shallow sites along the Primorsky Coast (especially Peter the Great Bay), and the Tatarsky Strait in association with ice formation. So far, the physical estimates of deep water formation rates are substantially less than those inferred from geochemical properties. Other open questions include the role of mesoscale variability in the evolution of the general circulation (including deep water formation), the seasonal evolution of the circulation and stratification, the response to Siberian cold air outbreaks and subtropical cyclones, and to seasonal and interannual variability of the inflows. In general, there is presently a strong interest in understanding the circulation of semi-enclosed seas, with the Japan Sea representing a different part of parameter space compared to the Gulf of Mexico/Caribbean Sea and the Okhotsk Sea, for example. Several numerical simulations for the Japan Sea circulation have been undertaken in recent years; for example, Seung and Kim (1993), Kim and Yoon (1994), and Holloway, et al. (1995), with considerable success. However, they have all lacked various elements of realism, and it is desirable to attempt further progress.

Thus, a numerical simulation has been undertaken with an advanced, primitive equation model [Princeton Ocean Model: POM; Blumberg and Mellor (1987)] which can treat realistic bottom topography, atmospheric forcing, free sea surface (for tides and storm surge), and thermohaline processes. The model computes the three-dimensional currents, sea surface height, temperature, salinity, and turbulent exchange variables. POM has been implemented in the Japan Sea (and is called SOJ-POM) with marginal mesoscale eddy-resolution. Thus, it should be capable of treating most (if not all) of the key circulation processes enumerated above. Here, results from the beginning of a long-term campaign are described; namely, some of the properties of the initial spin-up are discussed.

THE JAPAN SEA MODEL

SOJ-POM uses realistic bottom topography from DBDB5 (extending to 20 m at the coastline), a rectangular grid with 10 km resolution in the south and 7.5 km resolution in the north, sigma (terrain-following) coordinates with 15 vertical levels, and Levitus (1982) climatological annual mean temperature and salinity fields. Thus, it has marginal mesoscale eddy-resolution, because the Rossby baroclinic radius of deformation varies from about 17 km in the south to about 8 km in the north. Geostophically-balanced, climatological mean inflow of 2.8 Sv (plus temperature and salinity) through the Korean Straits is specified, and outflows of 2.24 Sv and 0.56 Sv through Tsugaru and Soya Straits, respectively (where a radiation boundary condition is also applied) are designated. For the initial simulation, climatological mean wind stress from Hellerman and Rosenstein (1983) has been applied, and the sea surface temperature and salinity have been clamped to the Levitus climatology. The Mellor-Yamada (1982) level-2½ vertical turbulence closure and Smagorinsky (1963) lateral turbulence closure [with adjustable proportionality constant (HORCON) equal to 0.1] schemes have been utilized. The horizontal integration is on the Arakawa C-grid, vertical time-integration is implicit, and the horizontal time-integration is explicit, split-mode, with a barotropic mode time step of 10 sec. and a baroclinic mode time step of 5 min. The integrations are being carried out on a DEC-Alpha workstation and have been run for 190 days. Early results are also presented from a prognostic 100-day run with a 100-day relaxation of surface temperature and salinity to the Levitus climatology.

INITIAL SPIN-UP OF SOJ-POM

It is of interest to compare the simulation after 190 days of spin-up with the initial condition. Based on the total and eddy kinetic energy (averaged over the volume) versus time (Fig. 1), the model spun-up to statistical equilibrium in about 80 days and undergoes oscillations (due to instabilities) on a timescale of about a month. The surface dynamic height relative to 1,500 m (not shown) from the Levitus climatology (used to initialize SOJ-POM) indicates a broad, weak northeastward surface geostrophic flow from the Korean Coast to the Japanese Coast, which is, of course, consistent with the general circulation; however, the pattern is devoid of the boundary currents and subpolar jet is expected from observations. In contrast, the sea surface height at Day 190 in the prognostic calculation (Fig. 2a) indicates a strong East Korean Warm Current, Nearshore Branch (along Japanese Coast), Middle Branch, and two meandering subpolar jets associated with the bifurcation of the East Korean Warm Current, to be discussed below. There are also several mesoscale eddies or gyres. The surface dynamic height relative to 1,500m (proportional to the approximate baroclinic stream function), computed from the prognostic mass field at Day 190, has an overall pattern and magnitude similar to the sea surface height (Fig. 2b). Compared to a dynamic height difference of about 30 cm across the basin, the difference (barotropic geostrophic) field (Fig. 2c) between sea surface height and surface dynamic height is characterized by anomalies (due to mesoscale eddies and gyres) of typically up to 6 to 8 cm, indicative of the importance of the deep flow and its interaction with bottom topography. The depth-integrated (barotropic) stream function (not shown; similar in pattern to Fig. 2c) is dominated by strong anticyclonic and cyclonic gyres over the deep basin north of 40N. Somewhat weaker cyclonic gyres occurred over basins (Ulleung, Yamato, and southwestern Japan Basins, respectively) off the Korean, Japanese, and southern Primorsky Coasts, plus a mid-basin anticyclonic gyre centered at 39N, 134E over the Yamato Rise and other anticyclonic gyres, generally over rises, are secondary features. The throughflow follows the Japanese Coast. Further details on the basin-scale circulation are given in Mooers and Kang (1995); here other aspects are emphasized: circulation near the inflow and outflow ports, time series and vertical profiles of velocity, etc. at key locations, and a few comparisons of the effects of surface clamping versus 100-day surface relaxation.

The surface currents for in the inflow (Fig. 3) and outflow (Fig. 4) subdomains undergo substantial adjustment from the initial condition (10 day diagnostic run) to 10 days and 190 days of the prognostic run. The inflow is split by Tsushima Island and flows mainly along the Japanese Coast as the Nearshore Branch at Day 10 in the diagnostic run, which is the initial condition for the prognostic run. The East Korean Warm Current and Nearshore Branch developed by Day 10 in the prognostic run. A strong cyclonic meander in the East Korean Warm Current developed just downstream of Tsushima Straits by Day 190 in the prognostic run. For the outflow subdomain, equatorward coastal flow feeds the outflow through both Tsugaru and Soya Straits by Day 10 in the diagnostic run. The equatorward coastal flow intensifies and becomes connected to the offshore flow by Day 10 in the prognostic run. A large anticyclonic meander of the subpolar jet feeds the outflow through Tsugaru Strait by Day 190 in the prognostic run. Obviously, there are strong, complex, and variable cross-isobath flows in the vicinity of the inflow and outflow ports, and it would be useful to understand them.

For several selected levels, time series of currents (Fig. 5) at two grid points (S4 and S5) near CREAMS current meter moorings demonstrate the magnitude and nature of the flow, which varies on a time scale of ca. 1 month. In the upper layer (above 22 m) at S4, the speed is often at least 0.2 ms^{-1}, while in the interior (between 480 and 1,920 m) the speed is generally less than 0.2 ms^{-1}. In contrast, in the upper layer (above 25m) at S5, the speed is generally less than 0.2 ms^{-1}, while in the interior (between 540 and 2,160 m) the speed is often at least 0.2 ms^{-1}. At both S4 and S5 the interior flow is highly (visually) coherent, but the upper layer and deepest level flows are only partially coherent with the interior flow. Thus, there is strong barotropic and shallow baroclinic mesoscale variability, plus variability apparently localized to the surface and bottom layers.

At Day 190, the vertical profiles of velocity (Fig. 6) at S4 and S5 have quite different characteristics. For example, at S4, the zonal velocity is westwards (at about 0.1ms^{-1}) in the upper half of the water column, with a linear shear in the lower half that leads to a reversal to eastward below 2,500 m, and the meridional and vertical velocities are very weak. In contrast, at S5, the zonal velocity decreases from about 0.03ms^{-1} eastward near surface to nearly zero below 500 to 1,700 m, where it increases to about 0.1ms^{-1} near bottom. The meridional velocity is poleward at 0.02 to 0.08ms^{-1} between 200 m below the surface and above the bottom; and the vertical velocity (which is normal to the sigma surfaces) has a downward maximum of 0.2ms^{-1} at 3,000 m (and requires more analysis). At both S4 and S5, the thermocline is largely confined to the upper 400 m and the halocline to the upper 100 m.

A few results at Days 30 and 100 (Figs. 7 and 8, respectively) from a prognostic case in progress with a 100-day relaxation time-scale (*vice* clamping) of the surface thermohaline forcing, illustrate the emerging character of what is expected to be a superior simulation. (This case spun-up to statistical equilibrium in ca. 50 days and at an eddy kinetic energy level about one-half that of the clamped case.) For example, the sea surface height (Figs. 7b and 8b; to be compared with the evolution of the clamped case in Figs. 7a and 8a) has a single subolar jet that separates at 38°N and meanders (gently at Day 30 and vigorously at Day 100) to exit through Tsugaru Straits. There are cyclonic and anticyclonic circulation gyres over the Japan Basin, and there is a cyclonic gyre over the Ulleung (but not the Yamato) Basin. However, comparing Day 100 with Day 30, considerable mesoscale evolution is probably still in progress at mesoscale Day 100.

SUMMARY

Many of the major features of the general circulation of the Japan Sea are revealed in the simulations, and it is clear that flow interaction with bottom topography (JEBAR effect) is an important

factor. However, there are number of improvements to be expected, such as, full separation of the East Korean Warm Current at a lower latitude (ca. 38° to 41°N), as now appears to be emerging in the case of surface relaxation (*vice* clamping).

Improvements are anticipated when the model is run with seasonally-varying wind stress [possibly with the improved climatology provided by Na (1992)] and surface heat and moisture fluxes. It may also be necessary to increase the horizontal resolution, and possibly the vertical resolution and positioning of sigma levels, to account better for the mesoscale variability, especially the smaller (shallow and transient) mesoscale eddies and fronts, and to minimize the effects of spurious horizontal pressure gradients over steep bottom topography.

Another level of improvement can be expected when the model is forced with synoptic wind stress and heat and moisture fluxes, and with river runoff. Then it will be possible to explore the very important wintertime deep convection process, perform energetics calculations for eddy-mean flow interactions, and compare the model output with observations from the CREAMS Program. At that point, the stage will be set for data assimilation (with satellite radar altimetric sea surface heights, etc.), and for development of a nowcast/forecast system.

ACKNOWLEDGMENT

This research has been sponsored by the U.S. Office of Naval Research. The collegiality and friendship of Academician Guri I. Marchuk, Prof. Victor I. Kuzin, Prof. Gennady I. Yurasov, Prof. Masaki Takematsu, and Prof. Kuh Kim (plus other Russian, Japanese, Korean, and American colleagues) were instrumental in motivating this research as the beginning to a long-term collaboration for the International Study of the Circulation of the Japan Sea.

REFERENCES

Blumberg, A.F. and G.L. Mellor. 1987. A description of a three-dimensional coastal ocean circulation model. *In* N.S. Heaps [ed.] Three-Dimensional Coastal Ocean Models, and Coastal Estuarine Sci. 4:1-16. AGU, Washington, D.C.

Hellerman, S. and M. Rosenstein. 1983. Normal monthly windstress over the world ocean with error estimates. J. Phys. Oceanogr. 13:1093-1104.

Holloway, G., T. Sou, and M.. Eby. 1995. Dynamics of circulation of the Japan Sea. J. Mar. Res. 53:539-569.

Kim, C.-H., and J.-H. Yoon. 1994. A numerical study on the seasonal variation of the Tsushima Warm Current along the coast of Japan. Proceedings of the Third CREAMS Workshop, Seoul, Korea, p.73-79.

Levitus, S. 1982. Climatological atlas of the world ocean. NOAA Professional Paper 13, U.S. Dept. of Commerce, NOAA, Rockville, MD.

Mellor, G.L., and T. Yamada. 1982. Development of a turbulence closure model for geophysical fluid problems. Rev. Geophys. Space Phys. 20:851-875.

Mooers, C.N.K., and H.S. Kang. Initial Spin-Up of a Sea of Japan Numerical Circulation Model. AMCA95 Proceedings. (in press)

Na, J.-Y., J.-W. Seo, and S.-K. Han. 1992. Monthly-mean sea surface winds over the adjacent seas of the Korean Peninsula. J. Oceanolog. Soc. Korea. 27:1-10.

Seung, Y.H., and K. Kim. 1993. A Numerical Modelling of the East Sea Circulation. J. Oceanolog. Soc. Korea. 28:292-304.

Smagorinsky, J. 1963. General circulation experiments with the primitive equations, I. The basic experiment. Mon. Weather Rev. 91:99-164.

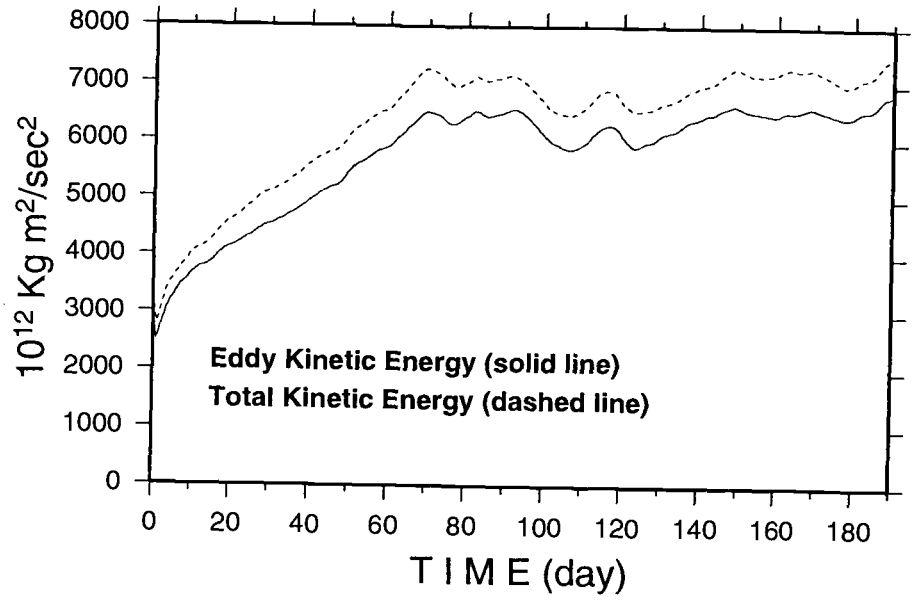

Fig. 1. Volume-integrated total and eddy kinetic energy versus time.

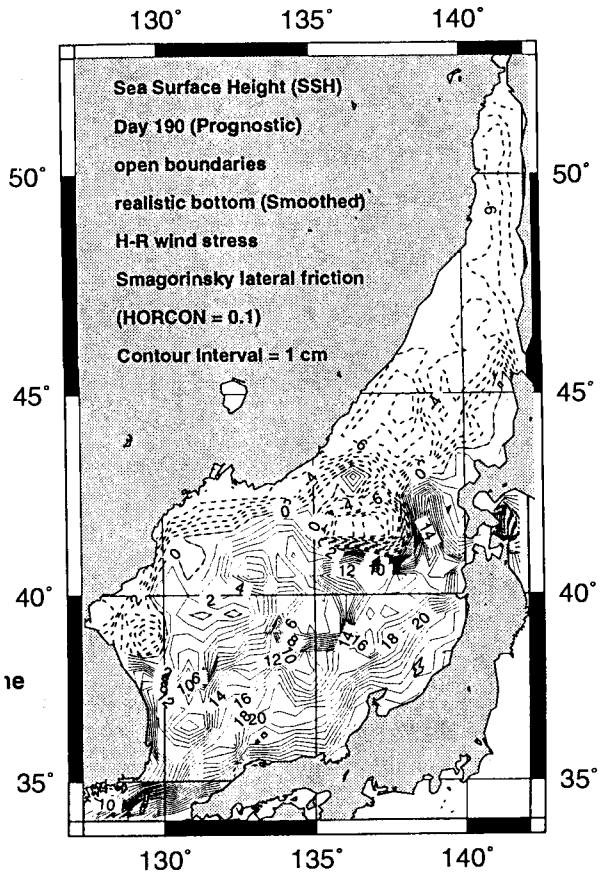

Fig. 2a. Sea Surface - Sea surface height (cm) at Day 190 of prognostic run.

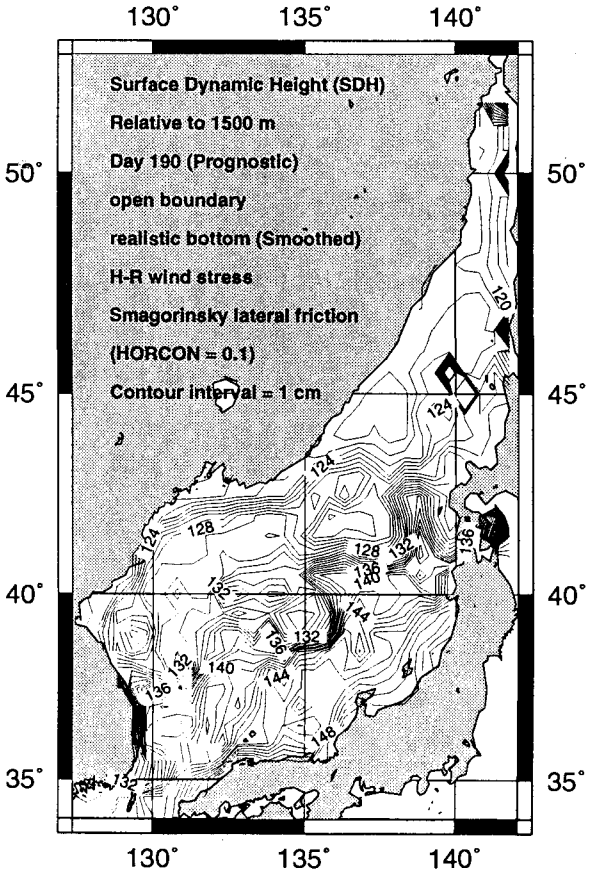

Fig. 2b. Sea Surface - Surface dynamic height (cm) relative to 1500 m at Day 190 based on the prognostic temperature and salinity fields.

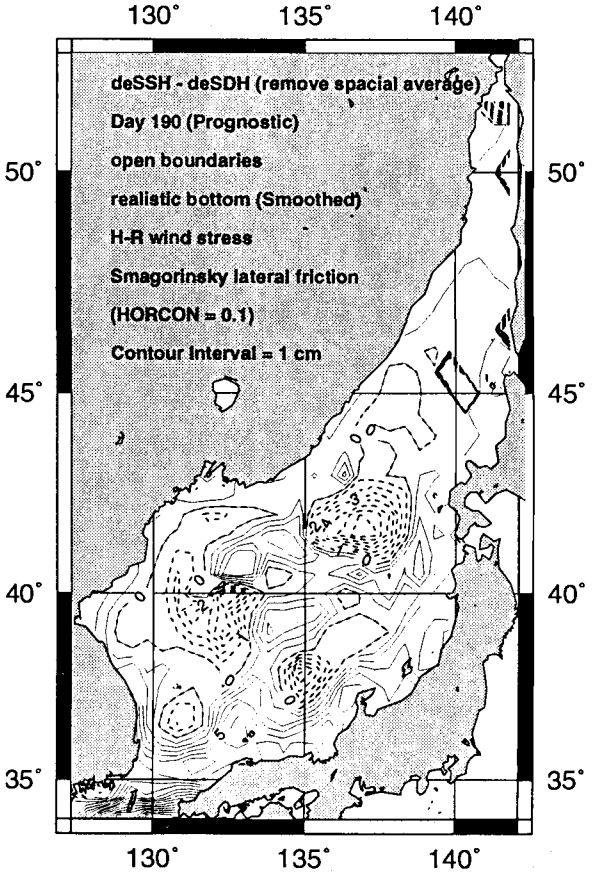

Fig. 2c. Sea Surface - Difference field (cm) (i.e., Fig. 2a-2b).

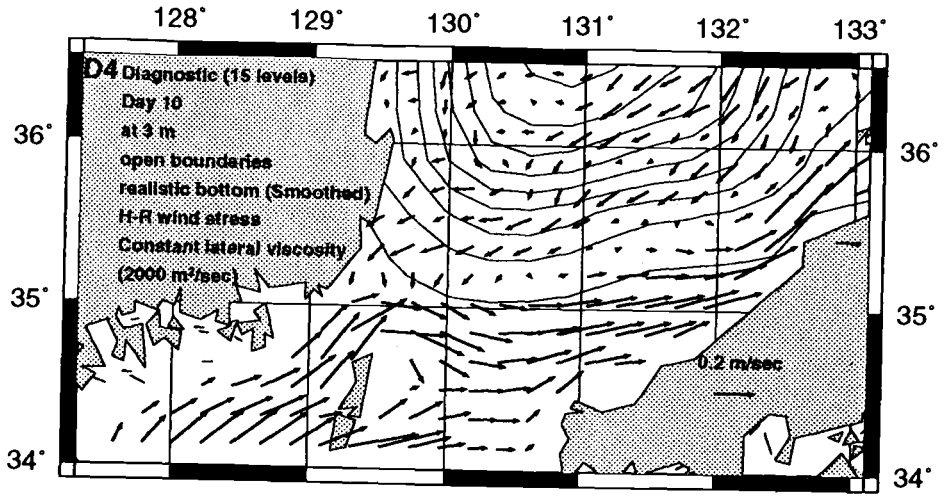

Fig. 3a. Surface currents for inflow subdomain - Day 10 of diagnostic run (initial field for prognostic run).

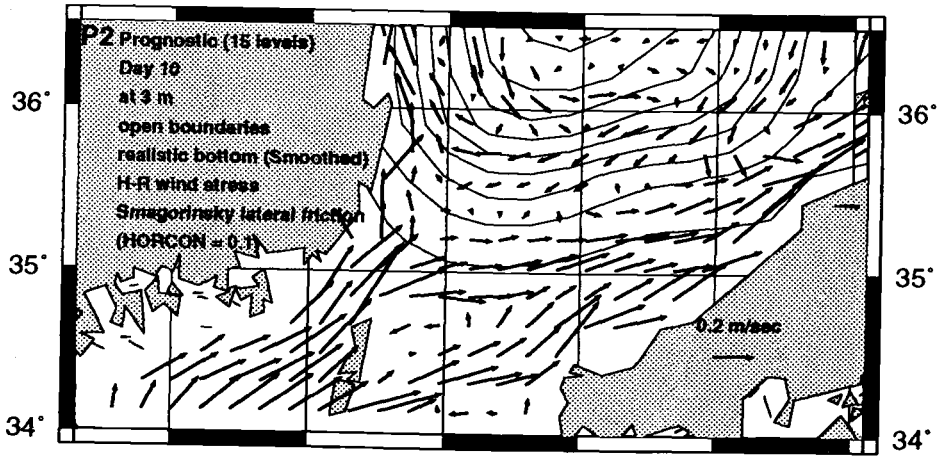

Fig. 3b. Surface currents for inflow subdomain - Day 10 of prognostic run.

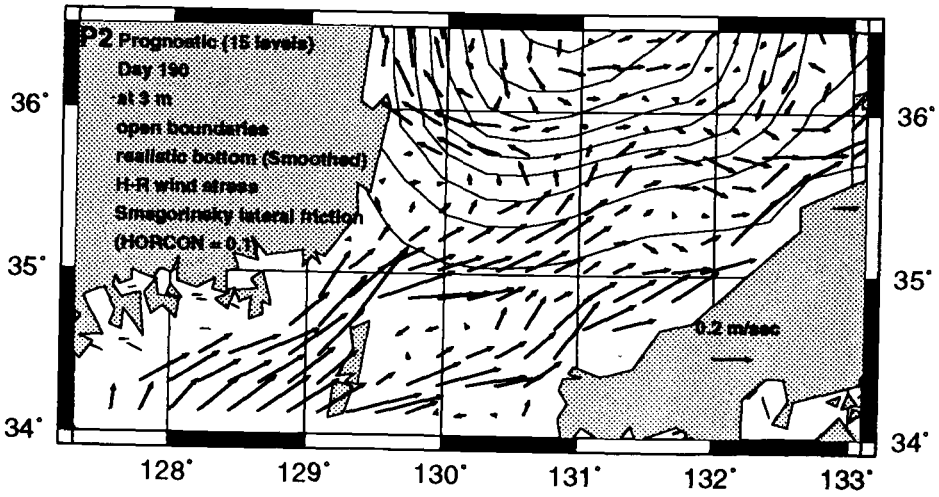

Fig. 3c. Surface currents for inflow subdomain - Day 190 of prognostic run. Contour interval = 200m.

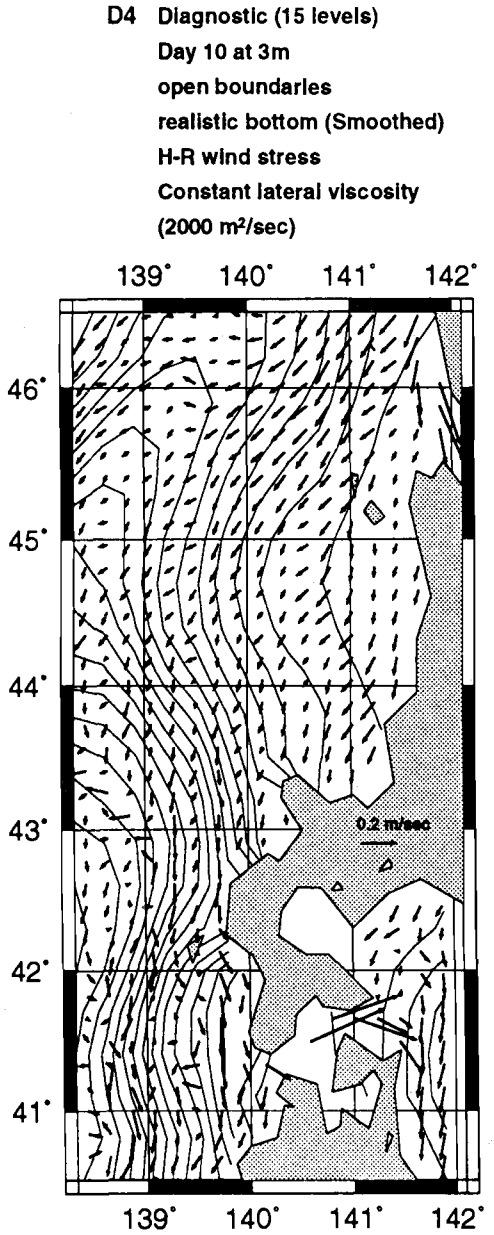

Fig. 4a. Surface currents for outflow subdomain - Day 10 of diagnostic run (initial field for prognostic run).

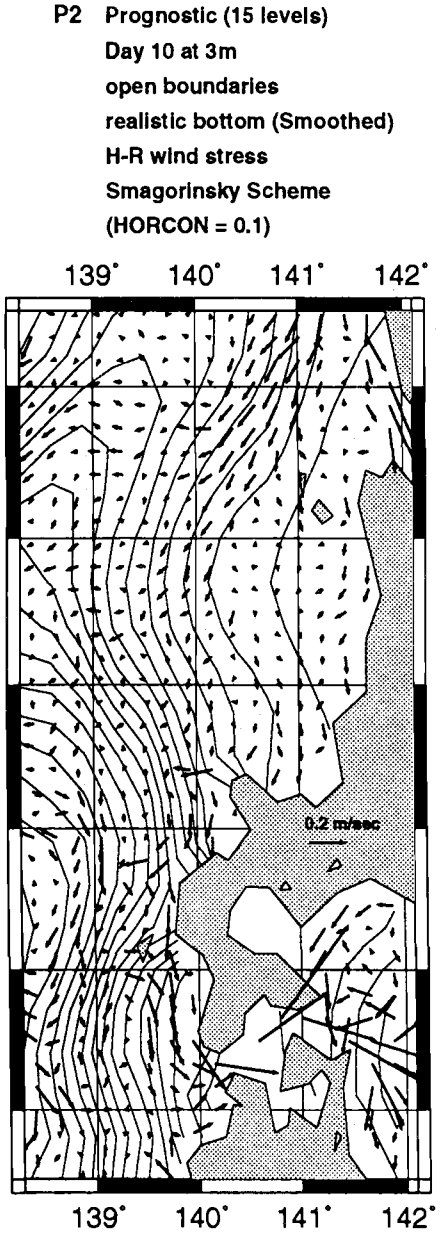

Fig. 4b. Surface currents for outflow subdomain - Day 10 of prognostic run..

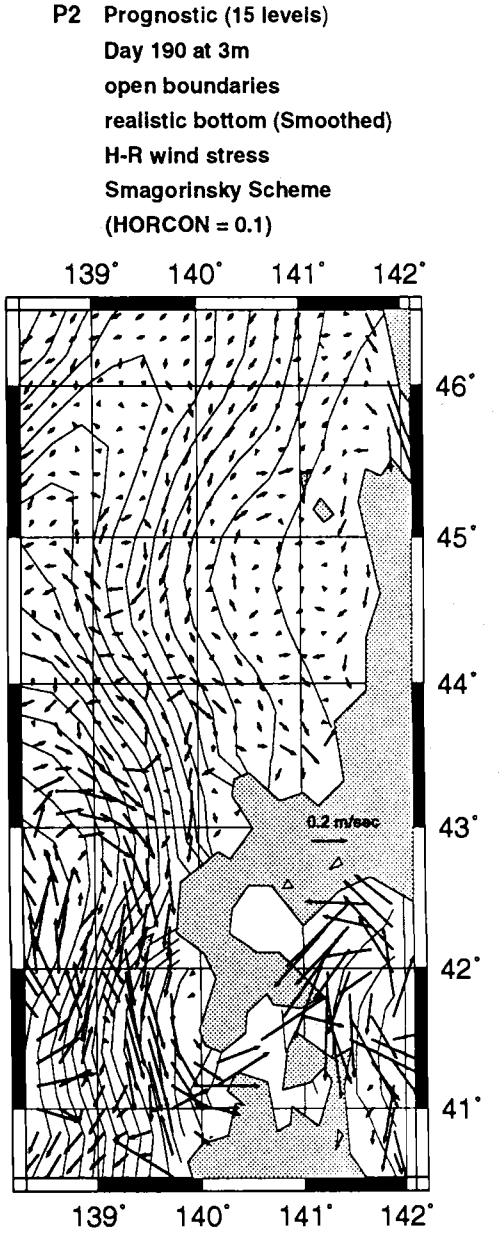

Fig. 4c. Surface currents for outflow subdomain - Day 190 of prognostic run..

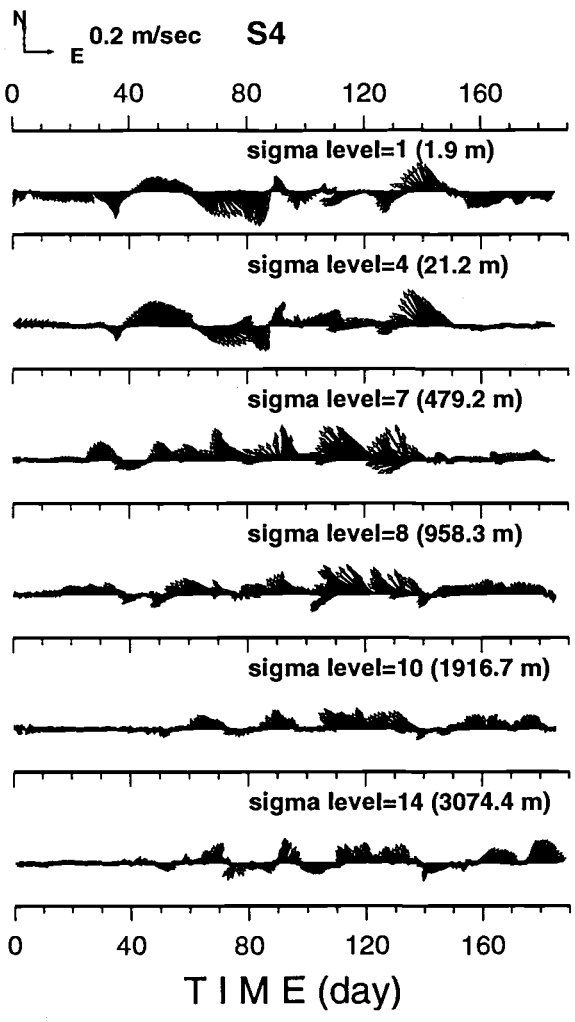

Fig. 5a. Time series of currents at selected levels - S4 (40.7N, 136.2E, water depth 3115 m).

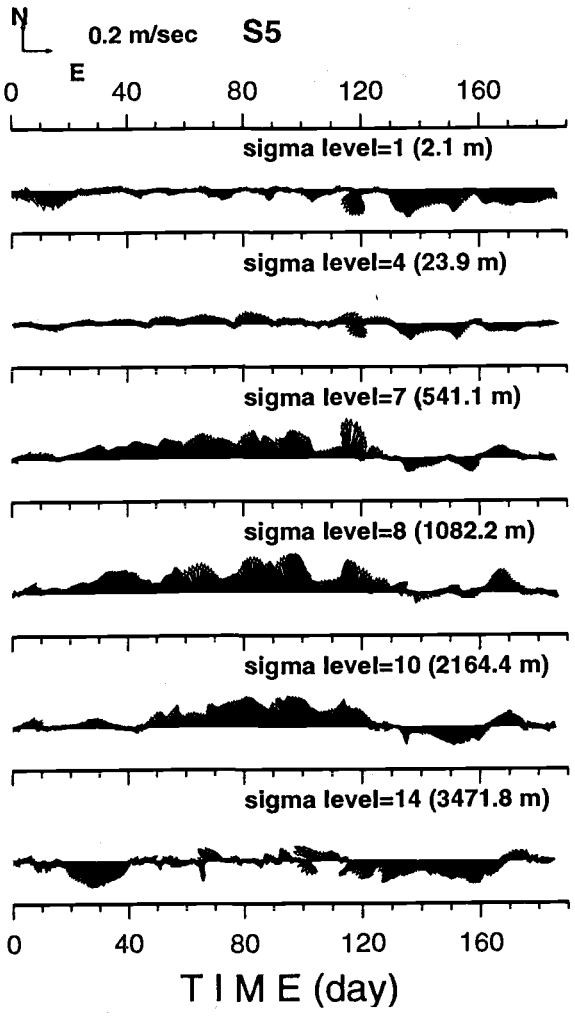

Fig. 5b. Time series of currents at selected levels - S5 (41.5N, 134.4E, water depth 3517 m).

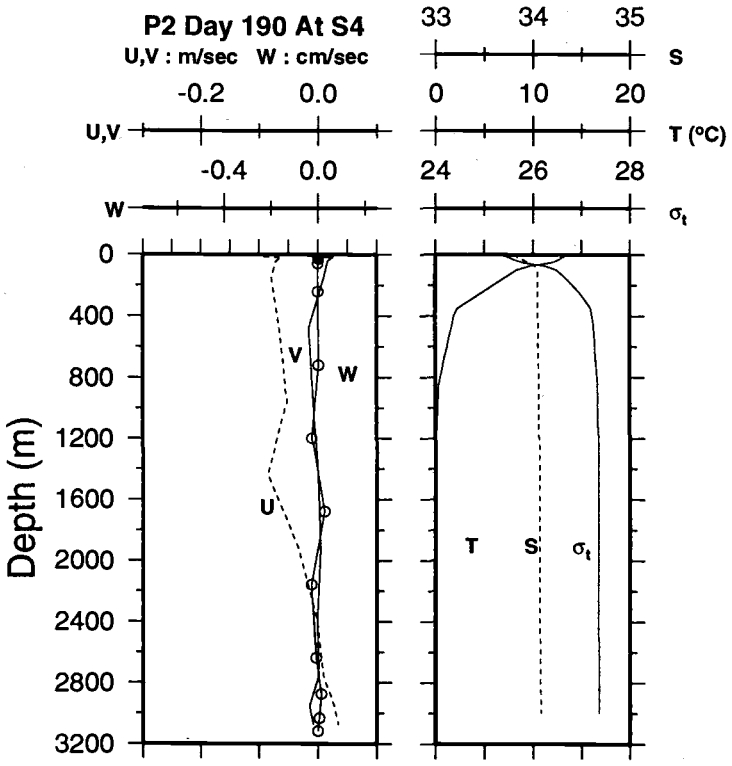

Fig. 6a. Vertical profiles of velocity components and temperature, salinity, and sigma-t at Day 190 - S4 (40.7N, 136.2E, water depth 3115 m).

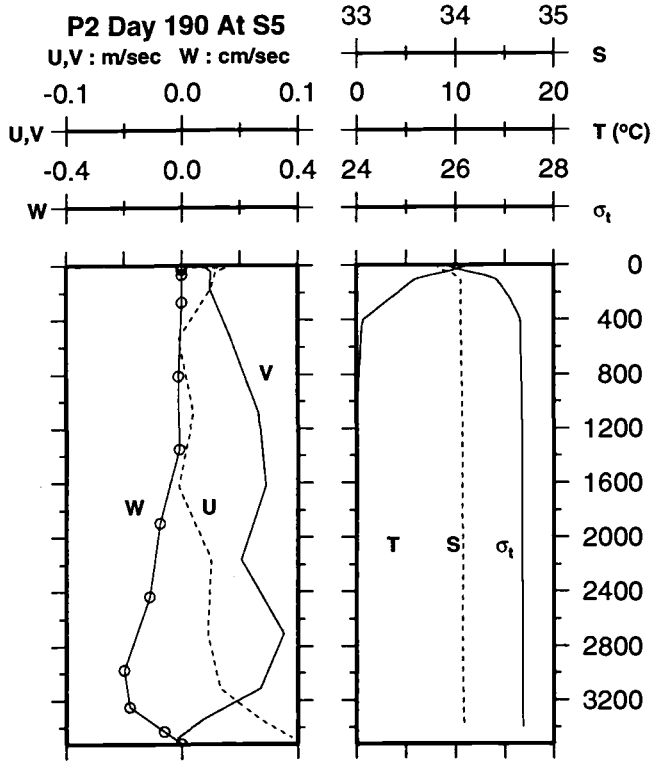

Fig. 6b. Vertical profiles of velocity components and temperature, salinity, and sigma-t at Day 190 - S5 (41.5N, 134.4E, water depth 3517 m).

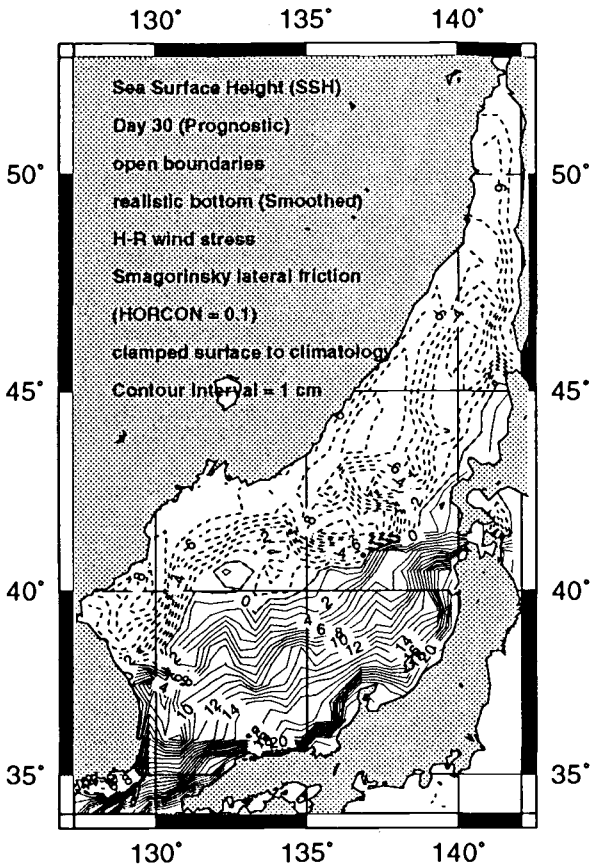

Fig. 7a. Sea Surface - sea surface height (cm) at Day 30 of prognostic run with surface clamping.

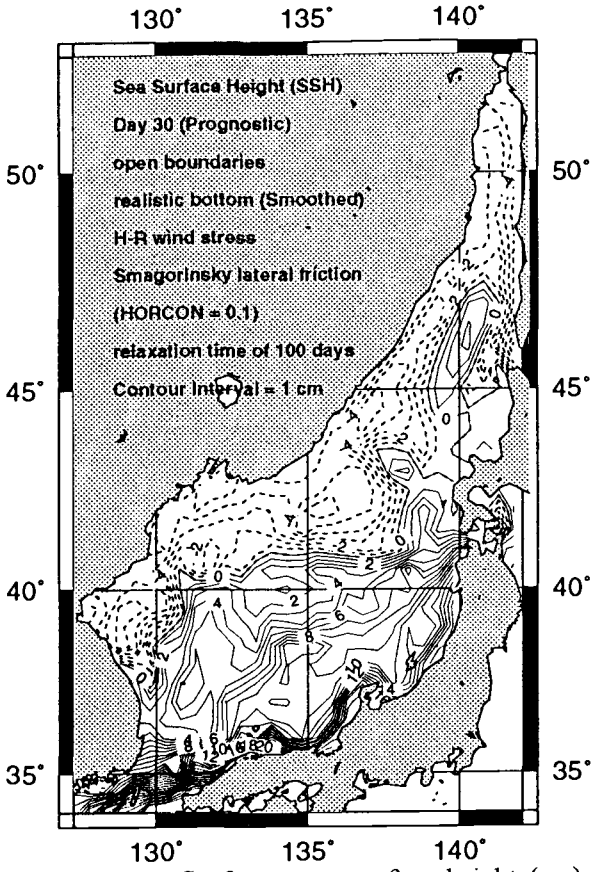

Fig. 7b. Sea Surface - sea surface height (cm) at Day 30 of prognostic run with surface relaxation time of 100 days.

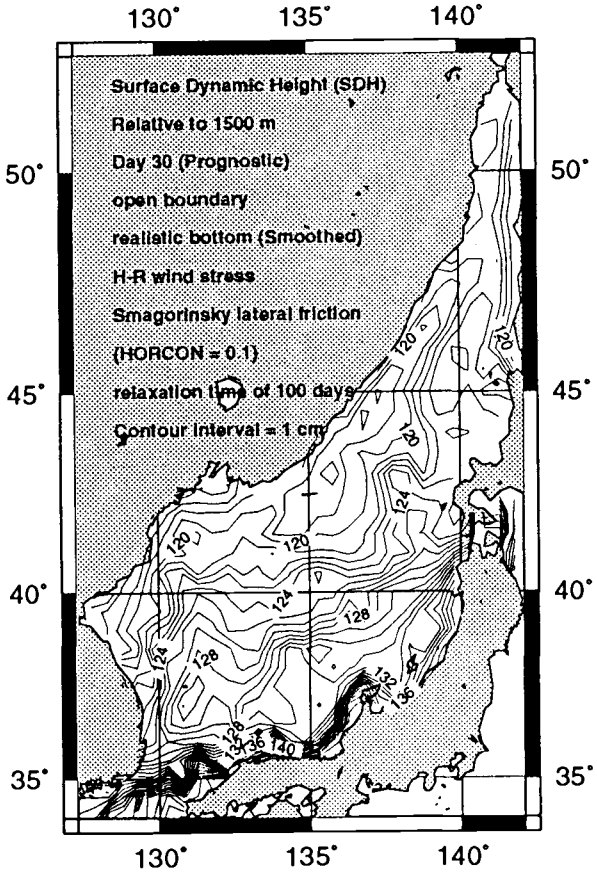

Fig. 7c. Sea Surface - surface dynamic height (cm) relative to 1500 m based on prognostic temperature and salinity fields at Day 30 of prognostic run with surface relaxation time of 100 days.

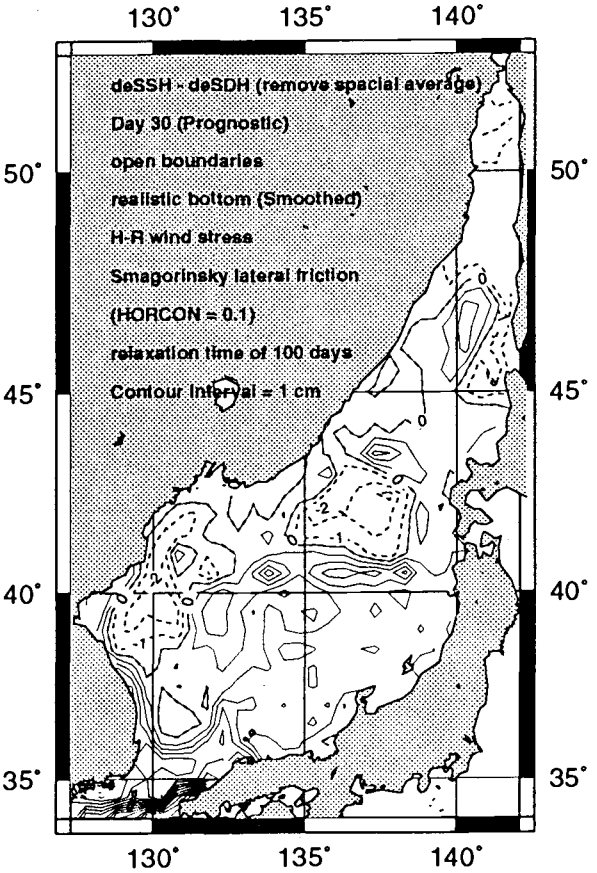

Fig. 7d. Sea Surface - difference field (cm) (i.e., Fig. 7a - 7b) at Day 30 of prognostic run with surface relaxation time of 100 days.

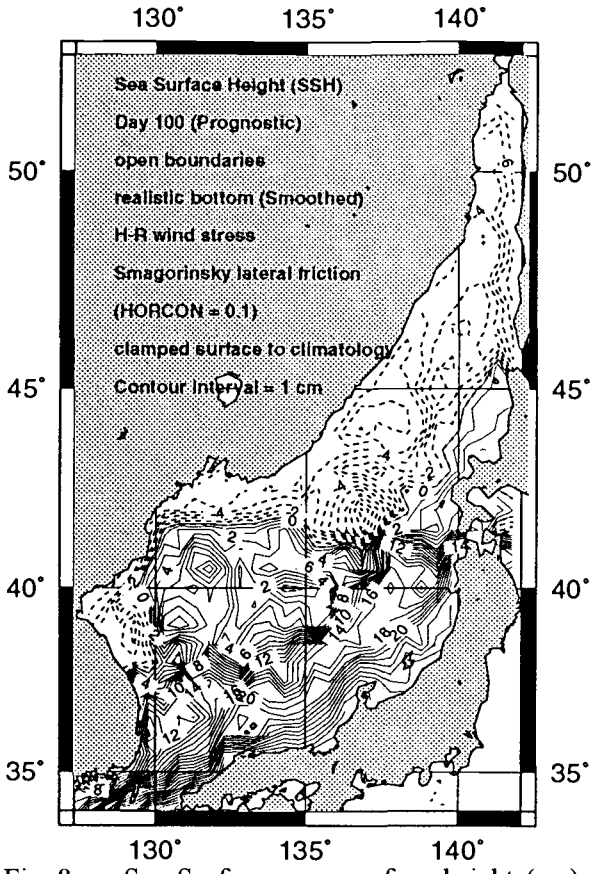

Fig. 8a. Sea Surface - sea surface height (cm) at Day 100 of prognostic run with surface clamping.

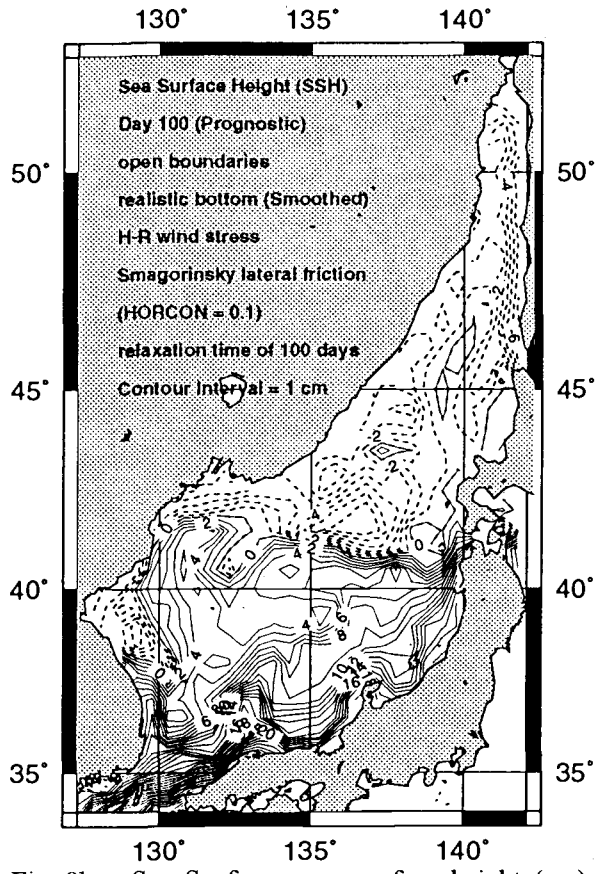

Fig. 8b. Sea Surface - sea surface height (cm) at Day 100 of prognostic run with surface relaxation time of 100 days.

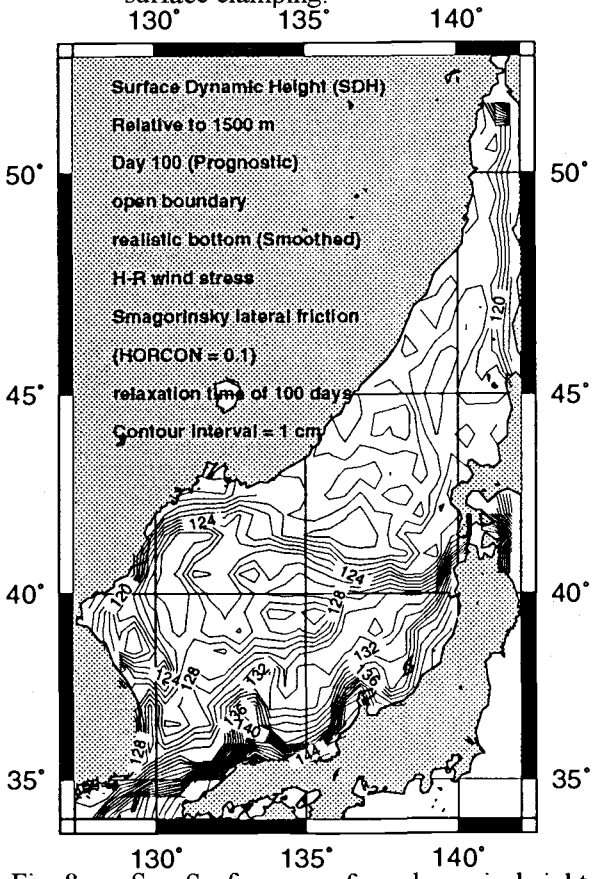

Fig. 8c. Sea Surface - surface dynamic height (cm) relative to 1500 m based on prognostic temperature and salinity fields at Day 100 of prognostic run with surface relaxation time of 100 days.

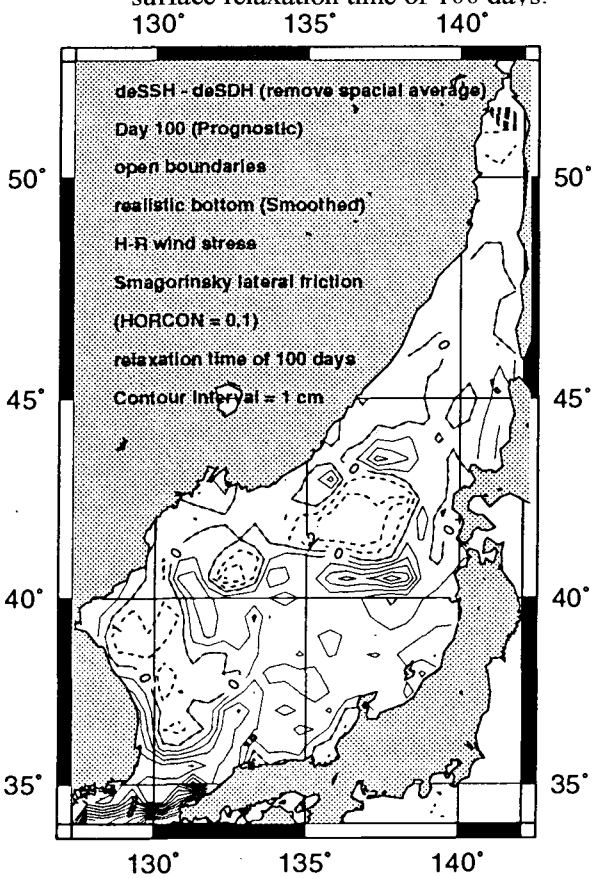

Fig. 8d. Sea Surface - difference field (cm) (i.e., Fig. 7a - 7b) at Day 100 of prognostic run with surface relaxation time of 100 days.

Influence of Ice Production on the Deep Water Formation in the Japan Sea

Lev P. YAKUNIN

Department of Oceanography, Far Eastern State University, Vladivostok, Russia

The main ice-forming areas in the Japan Sea are the Tatarsky Strait and Peter the Great Gulf. More than 90% of ice is produced in winter in the first region and this process occurs the most intensively in February. During that month ice covers 3, 6 and 11% of sea surface, respectively in a warm, temperate, and severe winter. At the same time ice volume changes from 2 to 6 cubic kilometers, with the average of 3 cubic kilometers. Ice is formed to the north off the Strait and, under the influence of wind and streams, moves to the south at an average speed of 11 miles a day. After 15-30 days it reaches the ice edge that is usually situated at 49°N. Further to the south ice starts breaking noticeably.

Assuming that the Tatarsky Strait is divided in two parts by 49°N and taking into account the thickness, concentration, hummock, and the speed of ice drift, we can estimate the amount of ice crossing a selected range:

$$V_i = A*L(h + \Delta h)v \quad \text{and} \quad \Delta h = 0.25T*h \tag{1}$$

where:

- V_i - ice volume, cubic kilometers;
- A - concentration level, decimals;
- L - width of the Strait at 49°N, kilometers;
- h - average ice thickness, kilometers;
- Δh - increase in ice thickness due to hummock, kilometers;
- T - level of hummock, /in 5-level scale/;
- v - speed of ice drift, kilometers per 10 days.

Based on a 26-year (1964-1989) data set we found that the volume of ice moved from north to south beyond 49°N during the "ice lifetime" varies from 12 to 53 cubic kilometers, with the average of 31 cubic kilometers. Martin et al (1972) reported the value of about 25 cubic kilometers a year for the volume of ice formed in 1988-1990, that is comparable with our calculations.

The amount of salt entering the water during the ice formation period can be computed by the simple formula:

$$S_s = \theta_i * V_i \ (S_{sw} - S_i) \tag{2}$$

where:

- S_s - amount of salt going into the water, tons;
- θ_i - density of ice, tons per cubic meter;
- V_i - ice volume, cubic kilometers;
- S_{sw} - salinity ($^0/_{00}$)of the surface-water;
- S_i - salinity ($^0/_{00}$) of ice.

Taking V_i from (1), θ_i = 0.9 tons m^{-3}, S_{sw} =32.5 °/$_{oo}$ and S_i =5 °/$_{oo}$ based on our measurements in the northern part of Tatarsky Strait and Sakhalin Gulf, we evaluated the annual numbers of S_s and the average value equal to 775*10^6 tons.

During the process of ice formation, only about 15% of salt remains in ice whereas the major part goes to increase salinity of the surface water and enables consecutive mixing. As a result, the surface water has T, S - indexes typical for the deep water of the Japan Sea. The volume of deep water formed due to ice production is given by following equation:

$$V_{dw} = \frac{S_s}{\theta_{dw} \cdot S_{dw} - \theta_{sw} \cdot S_{sw}} \qquad (3)$$

where:

V_{dw} - volume of deep water formed, cubic kilometers;
S_s - amount of salt brought into water (calculated by eq.2), tons;
θ_{dw} and θ_{sw} - density of deep and surface water, respectively, tons per cubic meter;
S_{dw} and S_{sw} - salinity of deep water and surface-water, respectively, (°/$_{oo}$).

In accordance with the characteristics of deep (S_{dw} = 34.08 °/$_{oo}$ and T_{dw} = 0.5°C) and surface (S_{sw} =32.5 °/$_{oo}$ and T_{sw} = -1.7°C) waters, the corresponding densities are equal to θ_{dw} = 1.02738 and θ_{sw} = 1.02614 tons per cubic meter (Oceanological Tables, 1975). Our further calculations demonstrated that for the period of observations the volume V_{dw} changes from 185 to 807 cubic kilometers, with the average value of 470 cubic kilometers (Fig. 1).

The amount of ice from other sources in the Japan Sea does not exceed 10% of the square and the volume of ice produced in the Tatarsky Strait. Therefore, in average the volume of deep water originated, because of ice formation, in the entire Japan Sea is under 550 cubic kilometers. This number accounts for less than 0.1% of the Sea volume and cannot significantly effect the hydrological properties of the Sea as a whole. Near the northwestern coast, within the shelf of Peter the Great Gulf and Tatarsky Strait, ice formation seems to have considerable influence on the thermohaline structure of water.

REFERENCES

Martin, S., E. Munoz, and R. Drucker. 1992. The Effect of Severe Storms on the Ice Cover of the Northern Tatarsky Strait. J. Geophys. Res. 97:17,753-17,764.

Oceanological Tables. 1975. Leningrad, Gidrometeoizdat. 477 p. (in Russian)

FIGURES

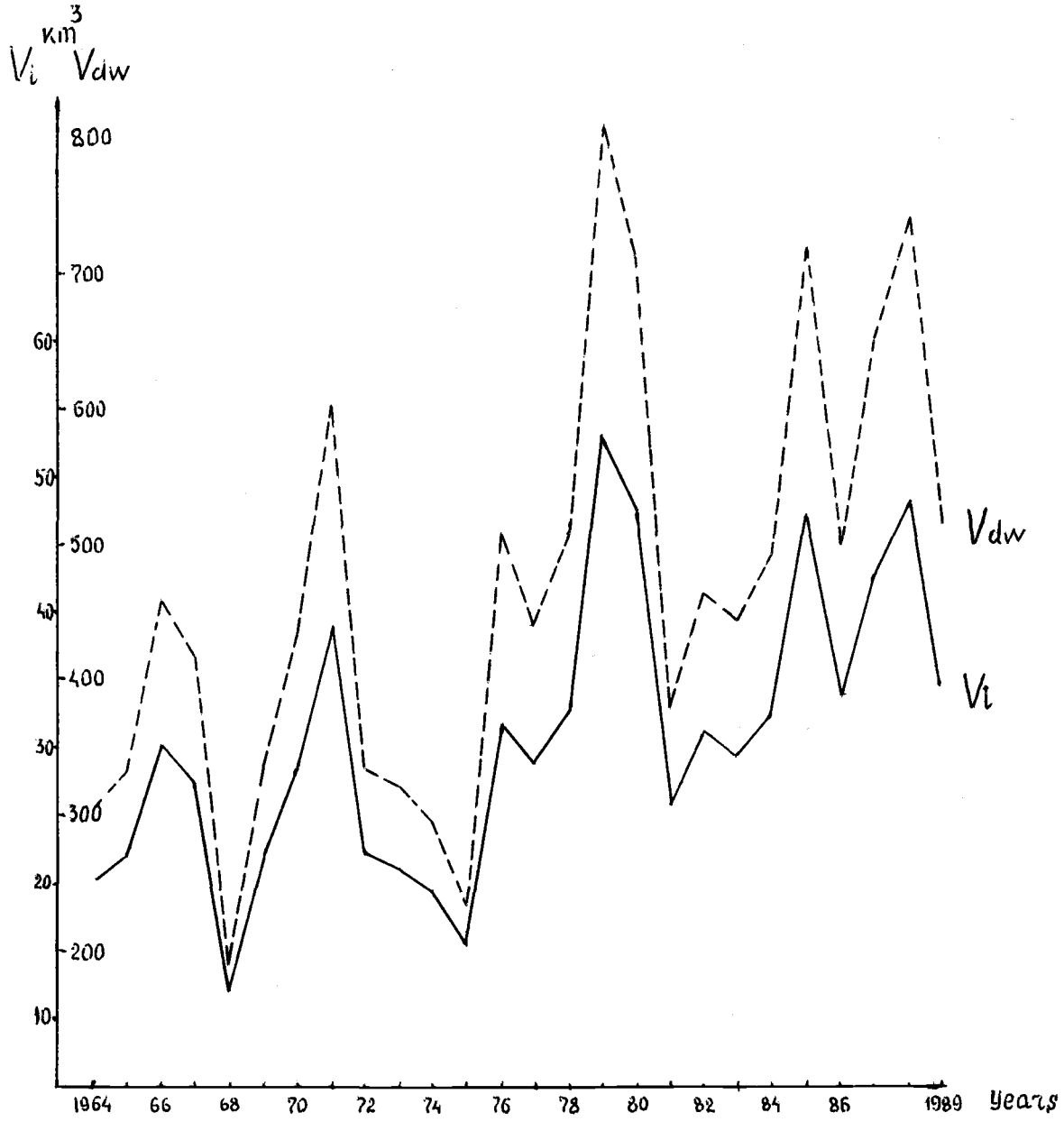

Fig. 1. Volume of ice (V_i) and deep water produced by ice formation (V_{dw}) in the Japan Sea.

II. SCIENTIFIC PAPERS SUBMITTED FROM SESSIONS

2. Fisheries and Biology Sessions

A. Communities of the Okhotsk Sea and adjacent waters: composition, structure and dynamics
B. Abundance, distribution, dynamics of the common fishes of the Okhotsk Sea
C. Salmon of the Okhotsk Sea: biology, abundance and stock identification

Exogenous Succession of the Southwestern Sakhalin Algal Communities

Lubov A. BALKONSKAYA

Sakhalin Research Institute of Fisheries & Oceanography
196, Komzomolskaya Street, Yuzhno-Sakhalinsk, Russia, 693016

The southwestern Sakhalin is a traditional harvesting region for *Laminaria japonica*. Recently, the commercial importance of this region decreased due to a reduction of the area occupied by algae. Shifts in species distribution have resulted in a change of the species mix from the past.

MATERIAL AND METHODS

Data was collected and processed using the method of Kalugina-Gutnick (1975). Photo surveys were carried out in 1965-1967, 1990, and the data was analyzed using VNIICAM (Sorokin and others, 1987). Algal samples were also collected by divers in 1963 (Sarochan, 1963), 1988-1944 (SakhTINRO, SakhNIRO).

RESULTS

Macrophytobenthos of southwest Sakhalin consists of 242 species, 41 species related to Chlorophyta, 70 to Phaeophyta, and 131 to Rhodophyta (Klochkova,1994). Macrophyte distribution depends on bottom type near the southwestern coast of Sakhalin where abrasion terraces or "benches", all without alluvium are found on the underwater shore slope. Bare rocky surfaces are zones of active hydrodynamic processes. Benches are found along all the southwestern coast of Sakhalin but interrupted by bays and inlets at river mouths where a thin layer of alluvium is observed. The southwestern littoral zone had little alluvium because the rivers and streams are small. Soils, mainly sand, which is moved some kilometres occurs near the Cape of Slepikovsky and the Cape of Lopatino.

Hydrological conditions of southwest Sakhalin littoral zone are generally determined by two currents, the West Sakhalin and the Tsushima. Waters of the Tsushima Current enter into the Tatar Strait around Moneron Island from the west and swung to the south along the coast into the La Perouse Strait. Waters of the Okhotsk Sea enter into the Japan Sea and move along the north coast creating a tidal current of cold-water near southwest Sakhalin (up to the Cape of Windis) (Budaeva, 1981).

The algae habitat is along the coast at depths of 0.5-15 m. Three algal communities, two three-strata, and one one-stratum were delineated. One community is located near Sadovniki-Gornozavodsk at depths of 0.5-1.5 m (Fig. 1). The upper stratum is large brown algae (*Laminaria japonica*, *Laminaria cichorioides*, *Costaria costata*, *Cystoseira crassipes*). *Laminaria japonica* is the dominant species in both biomass (2,000 g/sq.m in avarage) and in the frequency of occurrence. This community was named *Laminaria japonica*. The species most common to the middle stratum are *Dichloria viridis*, *Rhodymenia pertusa*, *Tichocarpus crinitus*, *Ptilota filicina*, *Chondrus pinnulatus*, *Ulva fenestata*, *Monostroma grevillei* and others. The algae which dominates the lower stratum are *Bossiela cretacea*, *Corallina filifermis* and cortical algae of genus *Melobesia*. For more than a year 30 species of macrophytes were found in this community.

A second community was located near Gornozavodsk, the Cape of Krilyon at depths of 1-10 m. It contains many-stratum and differs from the first area as *Alaria marginata* and *Laminaria angustata*. *Laminaria japonica* appeared in the upper stratum. Alaria marginata is not the most abundant but we called this community Alaria. The middle and lower stratum species structure is similar to the first community.

A third community was delineated as one-stratum composed of red corallina algae of species *Corallina*, *Bossiela*, *Melobesia* and *Lithothamnion* which we called the *Corallina* community. This community is located in the littoral zone near the village Sadovniki-Town Nevelskb but deeper in the water than the *Laminaria* community at depths of 2-10 m.

Analysis of data from the southwest Sakhalin near the village of Sadovniki-town Nevelsk indicats that exogenous succession occurred. The *Laminaria* community which only occurs in the most shallow part of bench at depths of 0.5-1.5 m was replaced by Corallina. This change is clearly seen in Fig. 2 where the algae distribution at the villages Yablochnoye-Antonovo is shown. Limits of the *Laminaria* distribution were determined with great precision. Table 1 shows the reduced distribution of *Laminaria* in the zone.

Laminaria japonica is locate on the tops of ridges where spring ice can cutoff the second year thallus. This causes *Laminaria japonica* to have a one-year cycle which can adversily affect the stock state as the biomass of one-year plants is smaller than second year plants. The horizontal distribution of succession rapidly takes place in a southerly direction. In 1994 succession occurred near Sadovniki-Kalinino and in 1995 the southern limit of the Corallina community reached Nevelsk (Fig. 3).

Succession also occurs near southwest Sakhalin which could have been caused by changes in the Tsushima Current found by Komaki (1988). If this hypothesis is true, the *Corallina* species movement along the coast will continue to the south up to the Cape of Windis. Another possible explanation for the succession could be the presence of dense accumulations of urchins (Nabata and others, 1992). Near Sadovniki-town Nevelsk the urchin (*Strongylocentrotus intermedius*) is mainly phytophagous. Last year, the reproduction of *Laminaria japonica* likely exceeded the algae consumed by urchins. The most dense urchin accumulations aree at 1-5 m in the *Corallina* community and these urchins are feeding on Corallinaceae. The succession may have been caused by the intensive use of concrete to develop 12% of the shoreline of the village Sadovniki-town Nevelsk. The direct influence of concrete on the development of algae has not studied however.

REFERENCES

Budaeva, V.D., V.G. Makarov, and S.N. Bulgakov. 1981. Circulation of waters in the Tatar Strait and its seasonal change Tr. DVNII. 83:35-44.

Kalugina-Gutnick, A.A. 1975. Phytobenthos of the Black Sea. K. Naukova dumka. 245 p.

Klochkova, N.G. 1994. Annotative bibliography on marine algae-macro- phytes of the Tatar Strait. V. Dalnauka. 108 p.

Komaki, T. 1988. Fluctuations of water temperature and changes in content of nutrient salts in waters of the Hokkaido Island. Tr. of the Institute Vak-kanai hokuseigakuen. p 257 - 269.

Nabata, S., E. Abe, and M. Kakiuti. 1992. About ISOYAKE conditions near the town Taysey-te, the southwestern part of Hokkaido. Hokusuisi kenho. p.14.

Sarochan, V.F. 1963. Biology of Laminaria japonica near the southwest coast of Sakhalin. Izv. TINRO. 49:115-135.

Sorokin, A.Z., B.I. Vanukhin, E.I. Kildushevsky, and D.S. Gurevich. 1987. Methodical guide of marine macrophytes landscape drawing a map and estimation of their stock with the help of aerophotosurveys. Murmansk PINRO. 134 p.

TABLES AND FIGURES

Table 1. Changes in the Laminaria community near Yablochnoye-Antonovo (sk.m).

Year	1965	1990	1995
Square	184300	95300	61000

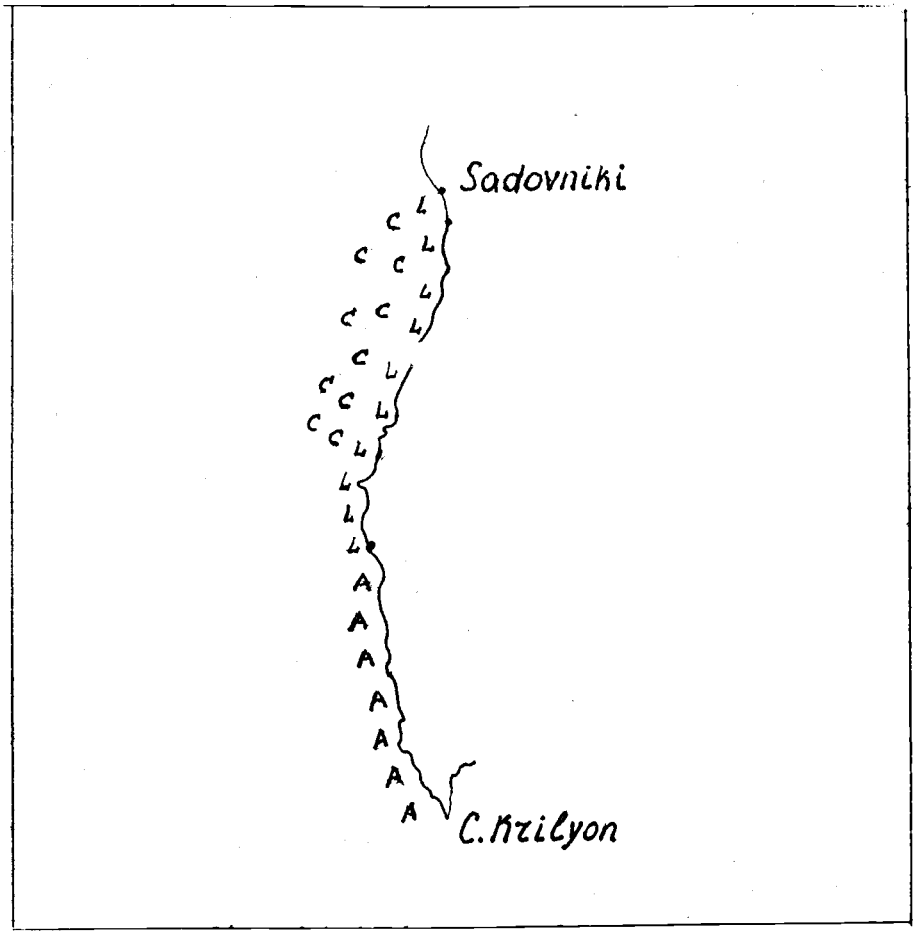

Fig.1. Scheme of algae association distribution in the area of the village Sadovniki- the Cape of Krilyon.
L- Laminaria association, A - Alaria association, C - Corallina association

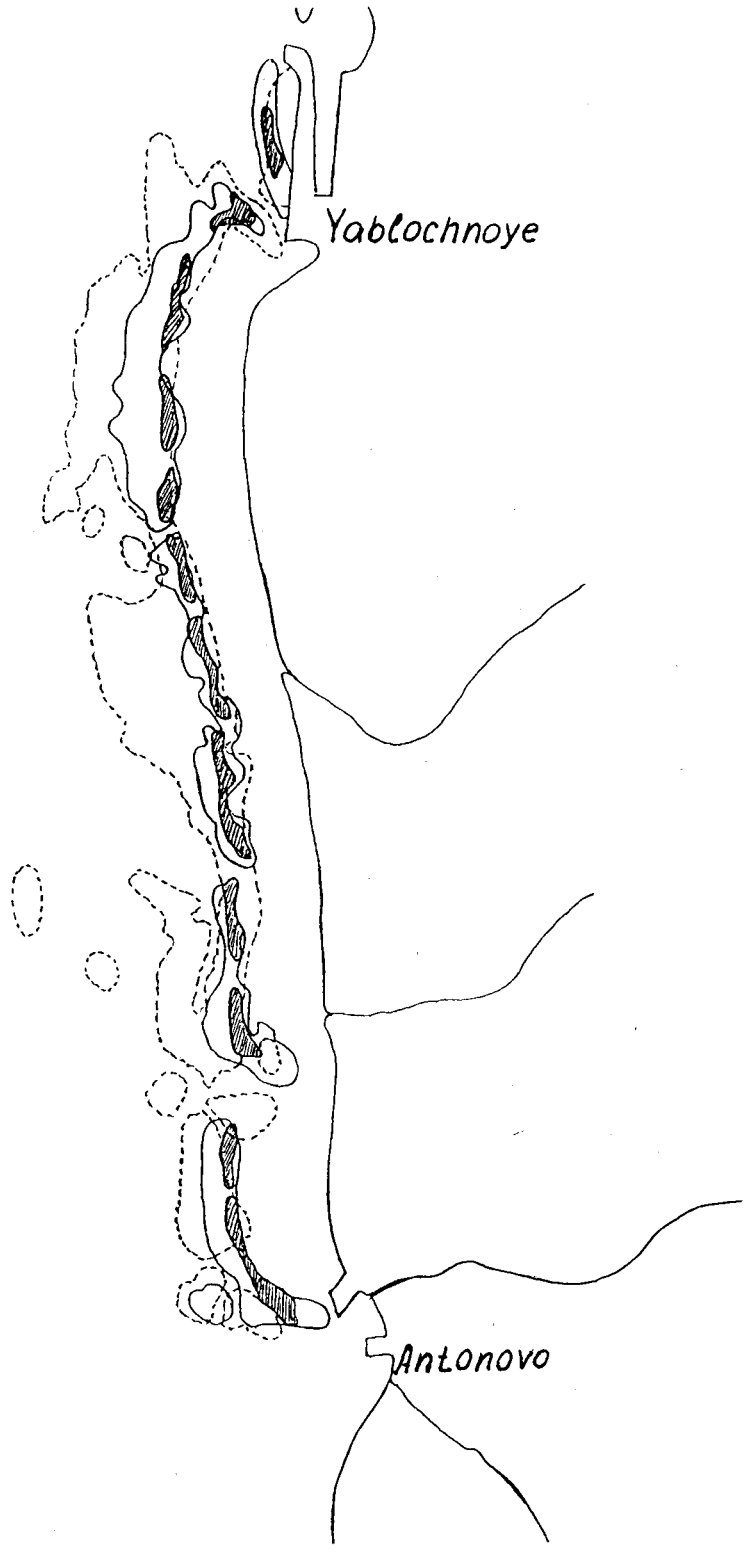

Fig.2. Map-scheme of Laminaria association area change in the region of the villages Yablochnoye-Antonovo from 1965 to 1995.
---- - 1965
____ - 1990
///// - 1995

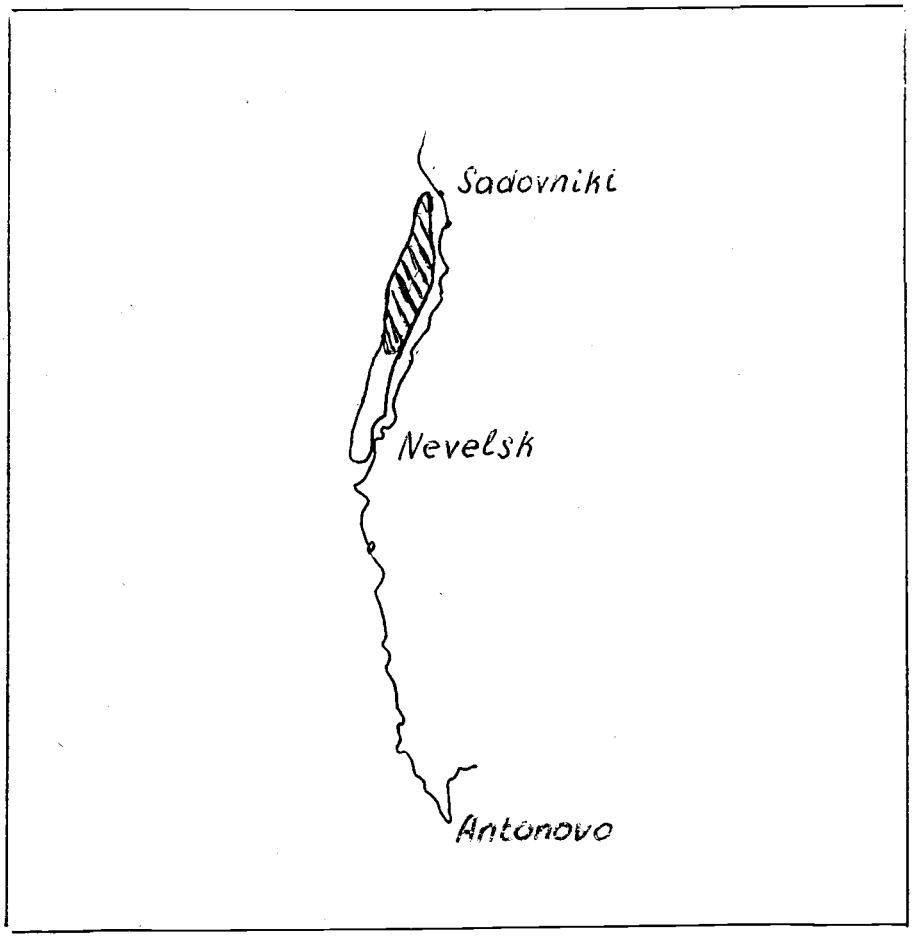

Fig.3. Scheme of Corallina association in the region of the village Sadovniki - Nevelsk in 1994-1995.
///// - 1994
—— - 1995

Characteristics of Pelagic and Benthic Communities on the North Sakhalin Island Shelf

Tatyana A. BELAN, Yelena V. OLEYNIK, Alexander V. TKALIN and Tat'yana S. LISHAVSKAYA

Far Eastern Regional Hydrometeorological Research Institute (FERHRI)
Vladivostok, Russia

INTRODUCTION

Sakhalin Island shelf is an area where a number of fisheries for bottom and pelagic species occur. The region also has a great potential for oil and gas exploitation and needs to have an ecological monitoring system developed to monitor exploration and production to prevent possible negative effects on marine organisms. Five expeditions to the North Sakhalin Island shelf have been carried out by FERHRI scientists in 1990, 1991 and 1994. Background data on pollutant concentrations and the characteristics of the benthos and phyto and zooplankton were collected (Tkalin, 1993; Tkalin and Belan, 1993).

Phytoplankton samples were collected from the surface layer and zooplankton was sampled from the bottom to surface during the daytime using a large Jeday net. Two benthos samples were taken at each station using a Van-Veen grab (0.11 m^2) or modified Petersen grab (0.25 m^2).

PHYTO AND ZOOPLANKTON

In 1990-1991, twenty four species of diatoms and flagellates were collected; 23 species are typical of marine waters and one (*Glenodinium pilula*) of brackish waters. The spatial distribution of phytoplankton is not uniform. In 1990, the maximum values of phytoplankton biomass and abundance (7,907 mg/m^3 and 454,500 ind/l) are in the northern part of study area and minimum values (262 mg/m^3 and 7,700 ind./l) are at the southern periphery. In 1991, high values of biomass and density of phytoplankton are in the northern part of study area (1,046 mg/m^3 and 22,100 ind/l) as well as in the south (2,082 mg/m^3, 16,600 ind/l). In 1990 and 1991, the diatom *Nitzshia seriata* is dominant (biomass) in the northern periphery and the flagellates *Protoperidinium granii* and *Gyrodinium lacryma* are dominant in the southern part of study area.

Zooplankton in the study area is mainly copepods (up to 88% from total abundance). The biomass and abundance of zooplankton decreases from the north to the south. In 1990, maximum values are about 1,660 mg/m^3 and 17,789 ind/m^3 and the minimum values are about 745 mg/m^3 and 11,315 ind/m^3 respectively. In 1991, the spatial distribution and abundance of zooplankton is the same as in 1990 but the seston biomass was three times lower.

In general the status of the plankton community is considered to be normal except for an area where the zooplankton is affected by an oil spill that caused a reduction of more than 40% of plankton (B.M. Borisov, personal communication).

BENTHOS

Benthos samples were collected along the North Sakhalin Island shelf in 1990-1991 and in 1994. In 1990 and 1991, the highest biomass (1,600 g/m$^{2)}$ is in the northern part of study area, with the average biomass being more than 500 g/m^2. The sea urchin *Echinarachnius parma* (*Echinodermata*) is the most abundant. Minimum values of biomass (13 g/m^2) were detected in the southern part of study area where *Polychaeta* and *Actiniaria* dominated. In general *Echinodermata* and *Bivalvia* are the most abundant (biomass) in the investigated area.

In 1994, benthos samples were collected from four polygons along the North Sakhalin Island shelf (Table 1). Data on the distribution of the benthos biomass are presented in Table 2. Polygon A is situated in the Sakhalin Bay, close to the Amur River mouth and the average biomass is 56 g/m^2. *Echinodermata* is absent except for *Stegophiura brachyactis* (*Ophiuroidea*) and the *Crustacea*, *Polychaeta* and *Bivalvia* are the most abundant (Table 3). Macrobenthic fauna is typical of brackish waters.

Polygons B, C and D were situated along the Northeast Sakhalin Island shelf. The biomass in polygon B ranged from 300 to 8,000 g/m^2 with an average of more than 1,300 g/m^2. Sea urchin *Echinarachnius parma* are the most abundant (Table 3). At some stations *E. parma* biomass exceeds 1,000 g/m^2 and at one station reached 8,000 g/m^2 (abundance 360 ind/m^2). The average biomass in polygon C exceeded 1,500 g/m^2, varying from 298 to 2,700 g/m^2. *E. parma* is dominant at all stations in this area comprising of up to 80% of the total benthos biomass (Table 3). At some stations the density of *E. parma* abundance and biomass reached 280 ind/m^2 and biomass 3,000 g/m^2 respectively. The average biomass in polygon D was 732 g/m^2. Sea urchin *E. parma* is dominant, but the percentage of the total biomass and frequency of occurrence decreased to 75% and 85% respectively (Table 3). The percentage of the *Bivalvia* increased to 13% and the mollusc *Tridonta borealis borealis* dominated at two stations.

CONCLUSION

Several expeditions were carried out in 1990-1991 and in 1994 to determine the abundance of species on the Sakhalin Island shelf. Data collected of benthos and phyto and zooplankton along the shelf off North Sakhalin Island before commercial oil and gas extraction shows high productivity and variability of pelagic and bottom communities. Continuous ecological monitoring during the exploitation of mineral resources is required to determine if negative changes in the marine environment quality occurs in order to take remedial action if necessary.

REFERENCES

Tkalin, A.V. 1993. Background pollution characteristics of the NE Sakhalin Island shelf. Marine Pollution Bulletin. 26 (12):704-705.

Tkalin, A.V., and T.A. Belan. 1993. Background ecological conditions of the NE Sakhalin Island shelf. Ocean Research. 15 (2):169-176.

TABLES AND FIGURES

Table 1. Polygons along the north shelf of Sakhalin Island.

Polygon	Latitude (center)	Longitude (center)	Average depth, m	Number of stations
A	52°58'	142°19'	25	10
B	52°55'	143°52'	67	20
C	52°31'	144°04'	83	15
D	52°26'	143°41'	32	13

Table 2. Benthos biomass in the study areas (g/m^2).

Polygon	n	min	max	X	(S_{n-1})
A	10	< 1	134	56	(50)
B	20	300	8248	1339	(1809)
C	15	298	2700	1503	(744)
D	13	24	2656	732	(701)

Table 3. Average biomass of benthos (g/m^2) and the percent of total biomass.

	Polygons			
Benthos	A	B	C	D
Actiniaria	< 1 (< 1)	50 (4)	57 (4)	43 (6)
Bivalvia	10 (18)	------	99 (7)	93 (13)
Crustacea	16 (29)	31 (2)	31 (2)	35 (5)
Echinoidea	------	1146 (86)	1195 (80)	552 (75)
Gastropoda	7 (12)	8 (< 1)	20 (1)	1 (< 1)
Ophiuroidea	7 (12)	------	44 (3)	1 (< 1)
Polychaeta	15 (27)	15 (1)	19 (1)	8 (1)

Fishery and Oceanographic Database of Okhotsk Sea

Lev N. BOCHAROV, Vladimir K. OZYORIN

Pacific Fishery and Research Centre (TINRO-Centre)

The specific feature of resource research and especially in commercial fishery forecasting is that field work costs are augmented by the processing of data from commercial and unexploited stocks. The requirement for providing marine resource data to researchers includes the following:

- planning, organizing and carrying out the vessel cruises;
- collecting data to allow the short and long term forecasting of stocks abundance;
- creating a data base management system for storing, assembling and processing oceanographic and biological data that can be easily used;
- developing programs to provide analytical and forecasting ability;
- preparing data for analysis and for monthly, quarterly and annual forecasts and for other practical recommendations.

These requirements are inter related to form a linear sequence of events; a sequential method for solving problems is a necessity for developing the technology for complex research on ocean bio-resources. It is possible to solve a number of questions using specialized computer systems developed for keeping the data with access channels and using the technical and research potentiality of staff to analyze the data. The data base should be available at all times for the data processing and analyses and "friendly" programs for complex data analyses should be available. These programs should allow for simple adaptation to new data and methods, etc. Thus, it should be possible to use an interactive process where a researcher can obtain current information quickly, process and present the data in a convenient form, make formal and expert analysis and repeat any stage of the data processing using new data etc. This paper deals with the state of data management and processing capability for the Okhotsk Sea resources. Bioproductivity of the Okhotsk Sea is at a high level from analysis of the data from long-term investigations carried out by TINRO research cruises.

By the early 1980s the monitoring of fishery resources were well developed by TINRO. The exploratory stage of investigating the North and South Pacific Ocean from Arctic to Antarctic was completed and the qualitative and quantitative composition of commercial fishing became the central activity. The main purpose of research is to focus on the establishment of rational fishing practices by the fishing fleet. A system of regular surveys was introduced to monitor pollock, herring, halibut, crabs and other species in the Okhotsk Sea.

The ecosystem investigations of 1980s in the Okhotsk Sea developed a better understanding of the biocenosis, food availability and the interaction of fishery resources. Since 1965, more than 160 cruises in the Okhotsk Sea contribute to the development of a large database that is available for analysis. The long-term monitoring data make it possible to better understand the dynamic processes which occur in the Okhotsk Sea and to estimate the influence of fishing pressure on the dynamic processes and to look at the effects of climate change, etc. Moreover, retrospective analysis of the data has become more important recently, due to funding shortages.

From early 1981 all data have been saved in a single format in the appropriate database. The most common formats are:

- trawl log
- specimen
- length frequency
- hydrological

A large amount of data is kept in the database as shown in Fig. 3. One data base deals with the distribution of hydrological stations in the northwest parts of Pacific ocean and adjacent seas and another with the coincident distribution of research trawls in Okhotsk Sea. More than 50,000 trawl logs were collected from esearch cruises; data on the results of biological analysis of 110,000 species; 7,000 samples of general analysis (one sample consists of 100-200 species) and more than 52,000 hydrological stations are held in the Okhotsk Sea database. The distribution of the biological data on fished species is shown in Table 1 and the distribution of monthly hydrological observations are shown in Table 2.

Fisheries statistics are collected in a special database. Monitoring of commercial fishing is ensured by a special automatic system for data collected from 60-80% of the commercial fleet. The captains provide daily information about the fishing operation. The monitoring of fishing has been in place for 12 years and it has resulted in the development of a unique data base on the main fishing areas. Data from 400,000 fishing trips dealing with fishing for pollack, cod, halibut and herring are kept in the database which include catches and other parameters for all areas. The Software allows analysis of each parameter for all fishing areas and to study the changes of the parameters with time, analyze stock density effects and solve a number of other problems related to the fishery. Since 1960, the data on catches have been kept in the database as annual observations. The database can be used to solve simple questions with unrestricted selection of time and space scales to complex analysis of population state.

The following analyses are the most popular: analysis of the cartography of unstudied parameters, contouring the size-mass frequency distributions using the annual data, calculating the climatic norms according to definite squares and calculating anomalies using different characteristics. The best result of our work is the creation of a Fishing Areas Catalogue. The Catalogue includes more than 400 fishing charts of the main areas and parameters of Okhotsk Sea. The Catalogue can be used, not only by scientists, but by captains of fishing vessels. Using fish distribution charts on board of vessels can allow captains to fish more effectively by selecting the best fishing grounds to improve catches while saving time and fuel. The creation of a Catalogue of Far Eastern Seas is possible using data available for all fish species from each research cruise. The surveys are often carried out through international cooperation by combining the efforts of scientists from interested countries to include their information sources, computer techniques, funding and printing facilities.

The information available on computers could be doubled if data collected in the 1960-80s period is added to the current data base. Our plans, for the near future, are to increase our efforts to put this data on the computer. In conclusion, it should be noted that developing the fishery biological database continues to be an ongoing process.

TABLES AND FIGURES

Species	Quantity of trawl logs	Quantity of specimen forms	Quantity of length frequency forms
Pollack	9274	70733	4408
Cod	3216	1690	153
Navaga	2152	2725	160
Herring	1694	4472	251
Flounder	14090	5649	920
Pacific Salmon	982	1819	36
Greenling	1240	1880	42
Halibut	4348	13687	427
Capelin	1269	2504	130
Saury	9	67	3
Mackerel	23	600	2
Goby	11710	1470	76
Sardine	277	5102	159
Smelt	1170	50	35
Rockfish	1690	-	34
Sea Bream	4	-	-
Jack Mackerel	10	-	-

Table 1. Distribution of biological data, collected during the trips of scientific and commercial vessels (Okhotsk Sea).

Depth (m)	MONTH												Number of measurments
	1	2	3	4	5	6	7	8	9	10	11	12	
0	801	1021	1184	2375	3720	7923	9545	10409	6390	4503	2269	1467	51607
	259	429	408	961	2218	5318	6724	7693	4172	2896	1644	1082	33798
100	443	646	684	1017	1741	4009	4157	4103	2723	2147	1293	973	23936
	185	337	303	462	1395	3228	3289	3083	1845	1471	1048	879	17525
200	240	447	492	528	1023	2638	2361	2215	1536	1190	766	644	14080
	129	283	260	313	863	2343	1905	1700	1119	866	663	585	11029
500	74	106	119	115	449	1015	980	920	478	571	279	242	5348
	73	96	113	108	415	953	852	740	353	455	268	243	4668
1000	39	7	48	36	155	439	320	286	132	187	167	121	1936
	42	7	47	68	155	317	303	262	116	160	159	115	1751
1500	23	3	27	11	73	207	96	158	51	68	56	75	846
	23	3	25	23	72	200	95	122	51	63	48	59	784
2000	10	-	7	1	46	134	27	39	14	33	30	37	378
	10	-	5	2	44	122	24	37	15	33	27	29	348
3000	-	-	-	-	17	32	8	10	2	16	4	8	97
	-	-	-	1	17	31	8	10	1	16	5	8	97

Table 2. Distribution of hydrological observations in Okhotsk Sea.

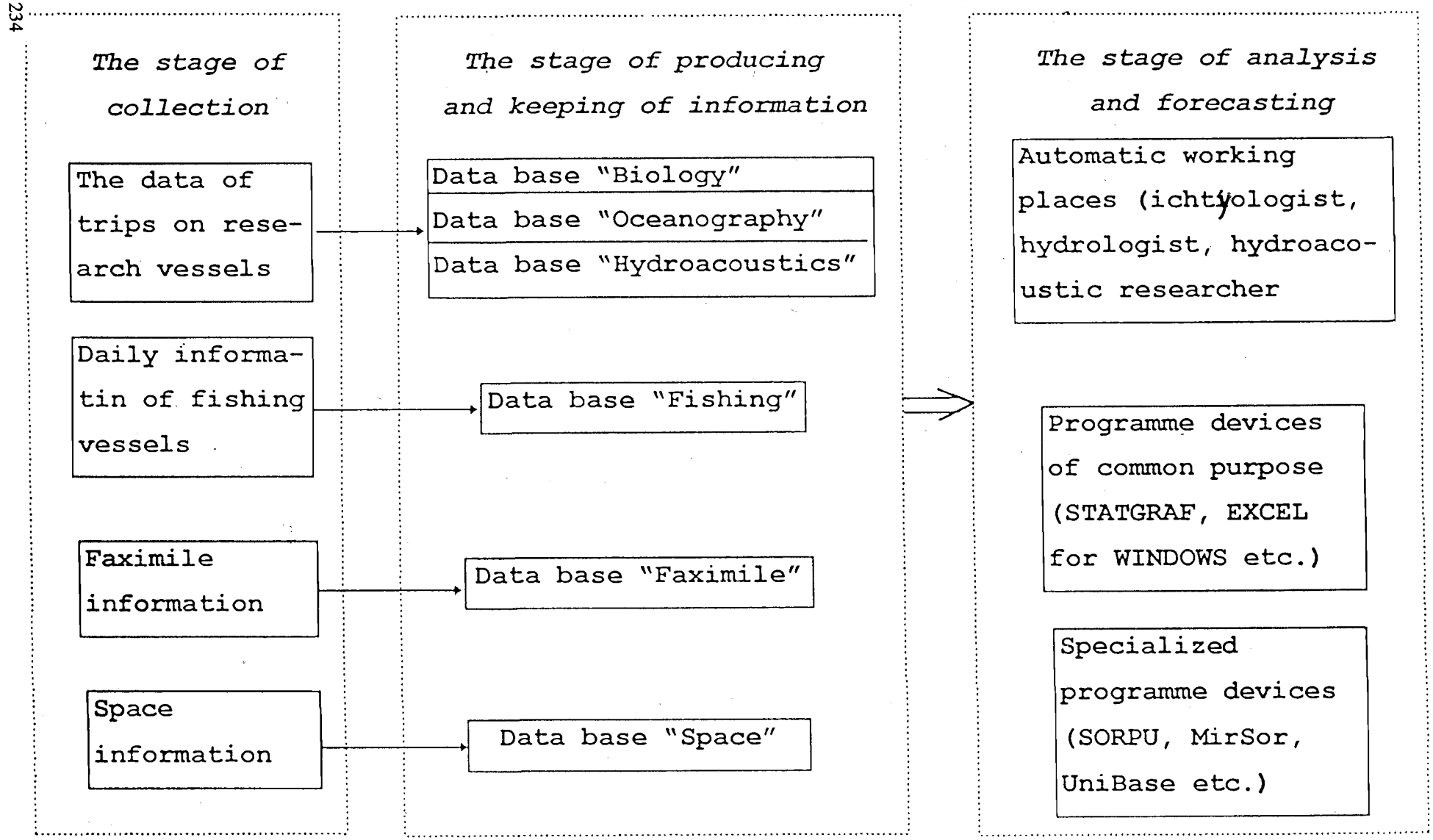

Fig. 1. The main stages of information technology (TINRO).

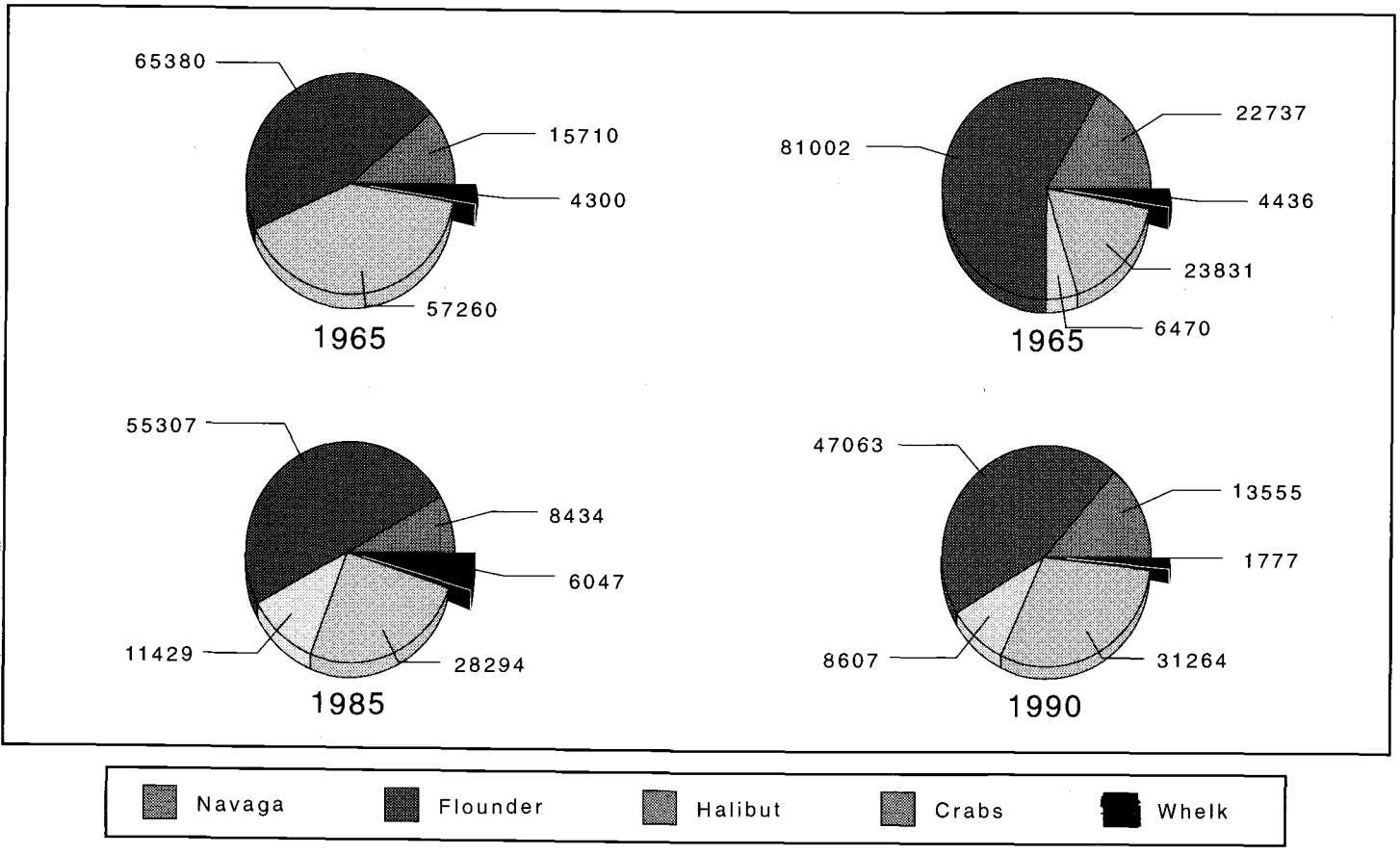

Fig. 2. Dynamics of catch structure of the main groundfish in tons.

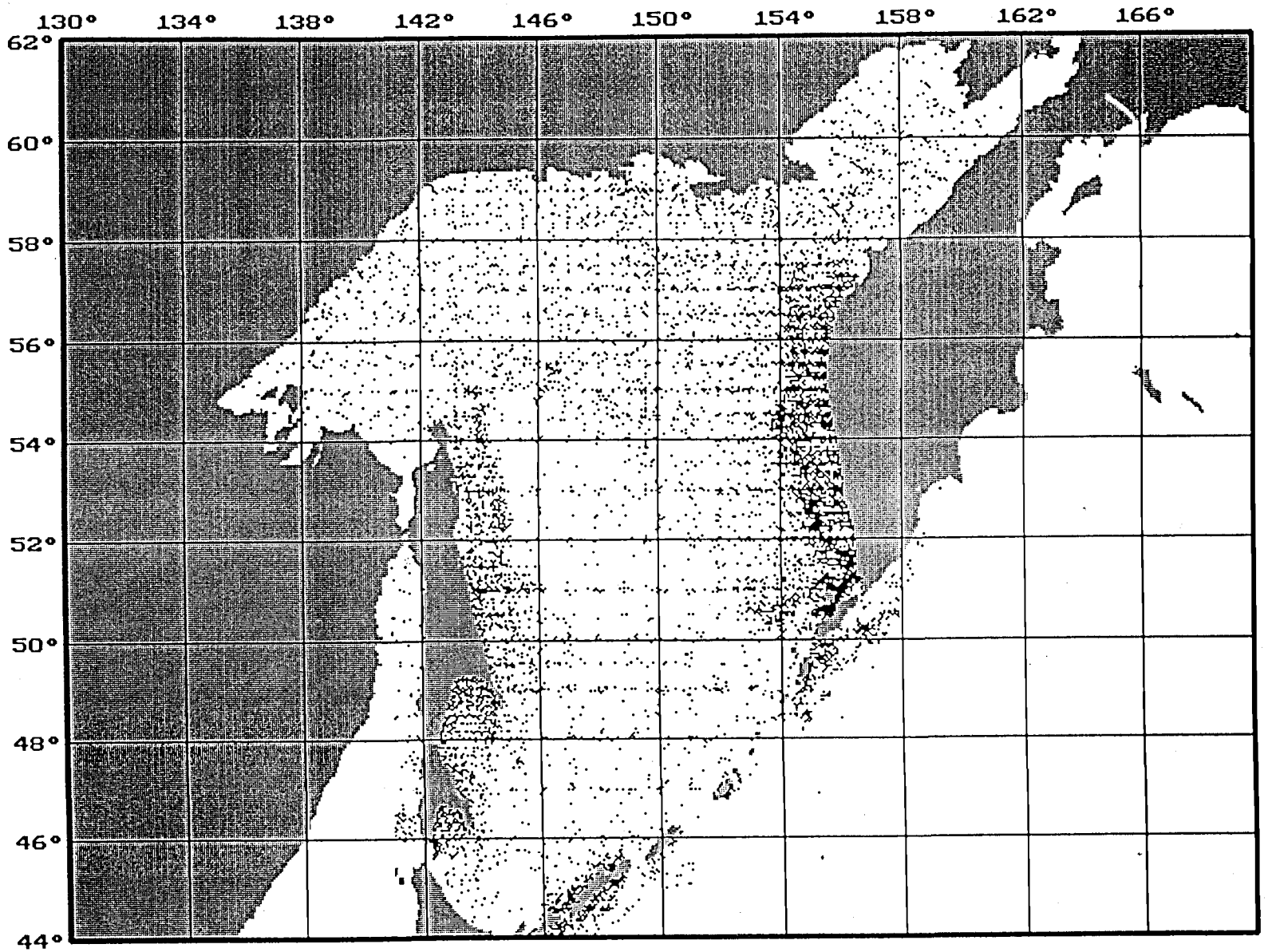

Fig. 3. Locations of research trawlings (1980-1994).

Interannual Dynamics of the Epipelagic Ichthyocen Structure in the Okhotsk Sea

Victor V. LAPKO

Pacific Research Fisheries Centre (TINRO-Centre)

From the beginning of the 1990s, the oceanography changes in the northern Pacific due to changes in the level of water exchange between the Okhotsk Sea and Pacific Ocean and, consequently, the sea current intensity. The abundance of common species changes and these fluctuations differs from the long-term interannual variability. The present time period is interpreted as "cold" similar to the 1940-60s cold period (Shuntov et al.1996).

Climate change in the Sea of Okhotsk is thought to have resulted from a long-term change of atmospheric circulation over the northern Pacific and a decrease in the intensity of water exchange between Okhotsk Sea and Pacific Ocean. The West Kamchatka and East Sakhalin Currents which indicate water inflow and outflow are weaker than in the previous ten years. The influence of the cold dichothermal layer becomes more apparent as a consequence of the decrease in the warm Pacific water inflow. Taking into consideration this reasoning, the present period is thought to be cold and the impact on the epipelagic fish community was found to be as follows:

1. the walleye pollock abundance decreases 2-3 times;
2. the herring abundance increases 4-5 times;
3. subtropical fishes such as pacific sardine and anchovy discontinue migrating into the southern Okhotsk Sea in summer;
4. the abundance of the pacific salmon increases over the last two years.

Increases in abundance of some fish species did not compensate for the decreases in walleye-pollock, thus, the total fish biomass in the epipelagic layer is still approximately 1.5 times lower (Table 1). A number of studies have been carried out on changes in the nekton composition but little is known about changes in the community structural. Data collected during the last combined surveys allow estimates of the total consumption of fish, the composition of food and the long-term dynamics.

The epipelagic fish community of the Okhotsk Sea consists of walleye-pollock (about 6.0 mln.t), herring (2.5 mln.t), capelin (0.08 mln.t), salmon (pink and chum, 0.48 mln.t) and northern smoothtongue (deep-sea smelt 1.2 mln.t). In comparison with the 1980s the main changes in the fish community composition occurs due to a decrease in abundance of walleye pollock while the herring increases. In previous years, walleye pollock in the southern deep basin is about 1.5-2.0 mln.t in the summer. Subtropical fishes such as sardine and anchovy stopped migrating to the southern Okhotsk Sea. Salmon and northern smoothtongue are the only abundant species there. The total fish biomass in the epipelagic layer, in the southern Okhotsk Sea, decreases approximately 2-3 times. In the northern Okhotsk Sea, the total fish biomass decreases insignificantly (15-20%) because both walleye-pollock and herring remain comparatively abundant. Therefore, fish distribution in the epipelagic layer increases northward relative to the long-term trends in species abundance.

The data show that the species composition has significantly changed and total fish daily diet decreases insignificantly from 568 th.t to 511 th.t in comparison with the 1980s (Fig. 1). Euphausiids decrease from 57 to 28% due to T.longipes, while amphipods increase from 7.5 to 17.3%, pteropods

from 0.8 to 9.2%, and copepods and forage fish stay at about the same level of abundance. The walleye pollock share of food resources stays stable while the capelin share increases two times and the mesopelagic fishes decreases six times. Other hydrobionts consume less than 1% of the total available food. Such changes in the total diet are due to the affect of fluctuations of key species in both the plankton and nekton. Thus, the trophic structure including fish distribution throughout Okhotsk Sea is influenced by the oceanographic conditions. Further, Walleye pollock eat about 80% of the total daily diet in the 1980s. Currently, in summer, walleye-pollock and herring consume almost equal amounts 48 and 44% respectively (Fig. 2). Although the condition of each species differs, as herring had a higher ration value of about 9% of body weight in comparison with about 4% for pollock.

CONCLUSION

Currently, walleye-pollock and herring are key nekton species utilizing most of the organic matter in the epipelagic layer of Okhotsk Sea, though the walleye pollock abundance has declined considerably. Taking into account that these two species are more abundant in the northern Okhotsk Sea, availability determines the total diet composition. In comparison with the 1980s, the total consumption decreases insignificantly throughout the whole epipelagic layer of the Okhotsk Sea, but recently a difference between the north and south appears to be because of the northward shift of fish species biomass. Though the total fish biomass in the epipelagic layer decreases by about 1.5 times, the quantity of organic material passing through fish remains almost the same.

REFERENCES

Shuntov, V.P., E.P. Dulepova, V.I. Radchenko, and V.V. Lapko. 1996. New data about communities of plankton and nekton of the Far-Eastern Seas in connection with climate-oceanological reorganization. Fisheries Oceanography. vol.5. N 1. (in press)

TABLES AND FIGURES

Table 1. Biomass of common fishes (thousand tonnes / %) in epipelagic layer (0-200 m) in Okhotsk Sea in summer

	1980-s		1993 - 95	
Walleye pollock	11300	78.3	6000	58.4
Herring	500	3.5	2500	24.4
Deep-sea smelt	2457	17.0	1200	11.7
Salmon	150	1.0	480	4.7
Capelin	15	0.1	80	0.8
Total	14422		10260	
Concentration, tonnes per km^2	9.6		6.8	

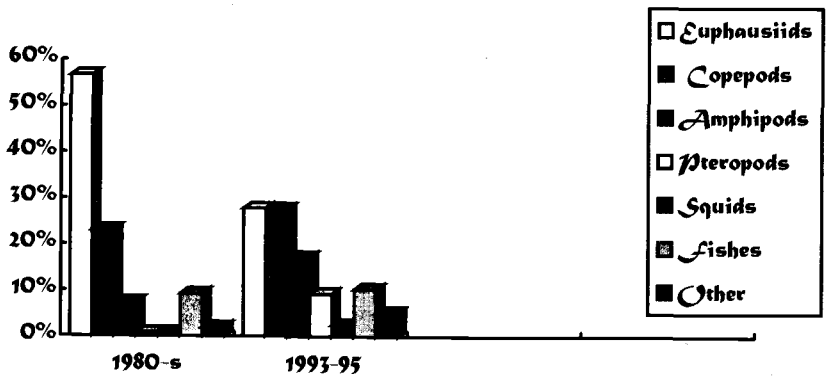

Fig. 1. Composition of total daily diet of all fishes in epipelagic layer of Okhotsk Sea in summer.

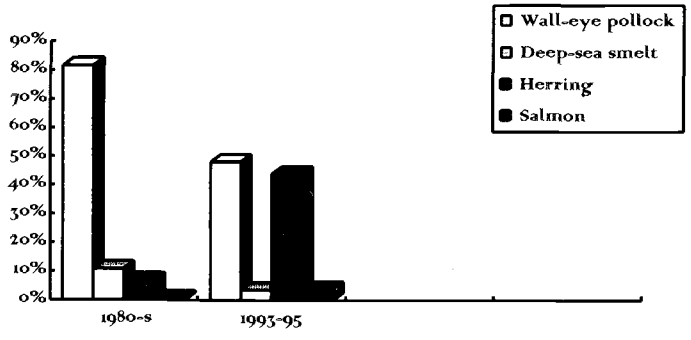

Fig. 2. The shares of common consumers in the total daily diet.

Quantitative Seasonal and Year-to-Year Changes of Phytoplankton in the Okhotsk Sea and off Kuril Area of the Pacific

Valentina I. LAPSHINA

Pacific Scientific Research Fisheries Centre (TINRO-centre)
4, Shevchenko Alley, Vladivostok, 690600, Russia

Data from 1353 Jady plankton net samples collected over 4 years from the upper layer of the Okhotsk Sea and adjacent Pacific Ocean areas were analysed (Fig. 1). The net is made of kapron with a mesh size of 0.168 mm and mouth diameter 37 cm. Tows were carried out in the 0-50 m and 0-200 m (bottom) levels. Phytoplankton was separated from zooplankton by a set of sieves ("Recomendations...",1984). The data were averaged by 1-degree squares and biostatistical areas (Fig. 1) (Volkov, 1986; Shuntov et al., 1993). The organisms sampled were separated into the different genera for analysis.

During the period of the investigation diatom algae are the most abundant. The "bloom" is caused by intensive development of *Chaetoceros* and *Thalassiothrix*. *Peridinium* is noted as single cells.

In 1993, three overlapping surveys are carried out by 3 vessels to estimate seasonal phytoplankton distribution (Fig. 2) and biomass (Tables 2, 3 & 4). Anomalous oceanographic condition were found due to a lack of water influx into the Okhotsk sea through the northern Kuril Straits (Shuntov, 1994), which causes sea surface temperatures of 9-10 degrees, 1-1.5 degrees lower than in 1991.

In area 13-a (above shelf water of the central and southern Kuril Islands), the phytoplankton abundance within the 50 m layer is the richest. The average phytoplankton biomass for all three surveys is at a maximum in the area and concentrations increase 4.2 times between July and August from 1,242-4,980-5,250 mg/m^3. The total phytoplankton concentration in the area increases from 4.6-18.3-19.3 bln.t. The same is observed in area 12 where the biomass of plankton during the second survey is 1.7 times higher than the first (2,050 and 1,242 mg/m^3). At the same time the quantity of silicon in both areas decreases from 10-20 to 5-6 mg-at./l and phosphates from 0.8-1.0 to 0.2-0.4 mkg-at/l. The difference in phytoplankton biomass between areas is most evident in the third survey. For instance, in areas 10 and 11 phytoplankton is almost non existent, in area 12, it is more than 1,000 mg/m^3 and in area 13 more than 5,000 mg/m^3.

In the Pacific, maximum biomass of phytoplankton occurs during the second survey (7,320, 8,152 and 5,800 mg/m^3) but the average biomass gradually increases between July and August, from the first survey to the third from 819 to 1,390 and to 1,470 mg/m^3.

In 1993, the biomass of phytoplankton in the Okhotsk sea and in the Pacific is 2-5 times higher than in other years.

In conclusion, the distribution of plankton is patchy which is caused by the complex oceanographic conditions. The highest biomass of phytoplankton is in areas above the shelf and in upwelling zones. The data confirms that the Sakhalin-Kuril region continues to be a highly productive area. Seasonal Bogorovs index varies from 0 to 4,540, thus, the plankton community appears to be in a different stage of seasonal succession in different parts of the region from spring to mid-summer.

Changes in abundance continues from April through to September - October depending on environmental condition in the main part of the Okhotsk Sea.

REFERENCES

Kusmorskaya, A.I. 1940. Seasonal changes of plankton of Okhotsk Sea. Bull. MOIP. biology. 49:155-170.

Recommendations on express-processing of net plankton in the sea. 1984. Vladivostok, TINRO. 31 p.

Smirnova, L.I. 1955. Phytoplankton of Okhotsk Sea and off Kuril area. Tr. IOAN the USSR. 30:3-51.

Shuntov, V.P., V.I. Radchenko, V.I. Chuchukalo, A. Ya. Efimkin, N.A. Kuznetsova, V.V. Lapko, Ya. N. Poltev, I.A. Senchenko. 1993. Content of necton communities in upper epipelagial of Sakhalin-Kuril region during salmons anadromous migrations. Biol. of sea. 4:32-43.

Shuntov, V.P. 1994. Characters of anadromous migrations of Asia pink salmon in 1993. Fish. econ. 2:34-38.

Volkov, A.F. 1986. The state of food base of the main commercial objects of the Okhotsk Sea in autumn period. Gadidae of the Far-Eastern Seas. Vladivostok, TINRO. p.132-133.

TABLES AND FIGURES

Table 1. Samples collected.

R/S	Year	Month	Number of samples in layer		
			200 - 0 m	50 - 0 m	Total
1. "Mlechny put"	1988	VI - VIII	187	-	187
2. "Pr. Levanidov", "Pr. Kaganovsky"	1991	VII - VIII	181	-	181
3. "Pr. Kaganovsky", "Novouljanovsk"	1992	VII - VIII	216	212	428
4. "Pr. Kizevetter"	1993	VII - VIII	35	36	71
"TINRO"	1993	VII - VIII	107	119	226
"Pr. Soldatov"	1993	VII - VIII	131	129	260
Total:			857	496	1353

Table 2. Biomass of phytoplankton in different areas of Sakhalin-Kuril region, July 1 - 28, 1993.

Area	Number of stat.	Square, t. km^2	Layer 50 - 0 m			Layer 200 - 0 m		
			Biomass, mg/m^3	Biomass, t/km^2	Stocks, thous. t	Biomass, mg/m^3	Biomass, t/km^2	Stocks, thous. t
Okhotsk Sea								
8	7	35.0	106	5.3	185.5	48	9.6	336.0
9	15	121.0	695	34.8	4210.8	157	31.4	3799.4
10	9	35.0	1580	79.0	2765.0	556	99.0	3465.0
11	8	56.0	49	2.5	140.0	22	2.7	151.2
12	15	154.0	1242	62.1	9563.4	349	69.8	10749.2
13[a]	14	73.5	1242	62.1	4564.4	396	79.2	5821.2
13[b]	3	24.5	104	5.2	127.4	41	8.2	200.9
Total:	71	499.0	717	35.9	21505.0	224	42.8	24522.9
Pacific Ocean								
7	27	150.0	1189	59.5	8925.0	465	90.7	13605.0
8	31	242.0	609	30.5	7381.0	170	34.0	8228.0
8[a]	8	83.0	176	8.8	730.4	37	7.4	614.2
9	8	38.5	1951	97.6	3757.6	523	95.7	3684.5
10	13	135.0	171	8.6	1161.0	68	13.6	1836.0
Total:	87	649.0	819	41.0	21955.0	253	48.3	27967.7

Table 3. Biomass of phytoplankton in different areas of Sakhalin-Kuril region, July 20 - August 7, 1993.

Area	Number of Stations	Square t. km^2	Layer 50 - 0 m			Layer 200 - 0 m		
			Biomass, mg/m^3	Biomass, t/km^2	Stocks thousand t	Biomass mg/m^3	Biomass t/km^2	Stocks thousand. t
Okhotsk Sea								
9	22	170.0	476	23.8	4046.0	174	34.8	5916.0
10	9	35.0	1071	53.6	1876.0	556	98.4	3444.0
11	8	56.0	49	2.5	140.0	22	2.7	151.2
12	22	154.0	2050	102.5	15785.0	692	138.4	21313.6
13[a]	10	73.5	4981	249.1	18308.9	2313	462.6	34001.1
13[b]	6	24.5	71	3.6	88.0	28	5.4	132.3
Total:	77	513.0	1450	72.5	40243.9	631	123.7	64958.2
Pacific Ocean								
7	14	150.0	1107	55.4	8310.0	317	63.4	9510.0
9	11	38.5	2912	145.6	5605.6	827	148.0	5698.0
10	3	40.0	150	7.5	47.5	39	7.8	312.0
Total:	28	228.5	1390	69.5	13963.1	394	73.1	15520.0

Table 4. Biomass of phytoplankton in different areas of Sakhalin-Kuril region, August 2 - 17, 1993.

Area	Number of stat.	Square, t. km^2	Layer 50 - 0 m			Layer 200 - 0 m		
			Biomass, mg/m^3	Biomass, t/km^2	Stocks, thous. t	Biomass, mg/m^3	Biomass, t/km^2	Stocks, thous. t
Okhotsk Sea								
9	9	170.0	507	25.4	4318.0	149	29.8	5066.0
10	7	35.0	+	+	+	24	3.8	133.0
11	9	56.0	1	0.1	5.6	17	1.2	67.2
12	14	154.0	1118	55.9	8608.6	632	126.4	19465.6
13[a]	13	73.5	5250	262.5	19293.8	2001	400.2	29414.7
13[b]	4	24.5	87	4.4	107.8	39	7.8	191.1
Total:	56	513.0	1161	58.0	32333.8	477	94.9	54337.6
Pacific Ocean								
7	13	150.0	1977	98.9	14827.5	669	133.8	20070.0
9	8	38.5	962	48.1	1851.9	624	124.8	4804.8
Total:	21	188.5	1470	73.5	16679.4	647	129.3	24874.8

Table 5. Interannual changes of biomass (mg/m^3) of phytoplankton in Sakhalin-Kuril region during summer. Layer 200 (bottom) - 0 m.

Area	Years			
	1988	1991	1992	1993
Okhotsk Sea				
1	140	-	-	-
2	3	-	39	-
3	41	-	-	-
4	588	-	-	-
5	126	-	10	-
6	37	200	14	-
7	20	925	35	-
8	+	415	5	-
9	423	210	5	160
10	95	22	135	379
11	103	35	45	20
12	275	176	30	558
13[a]	401	207	113	1570
13[b]	401	-	-	-
Total:	173	247	93	444
Square: thousand km^2	1502	690	864	513
Stocks, billion t	69.1	28.3	5.0	65.0
Pacific Ocean				
7	-	510	109	484
8	-	114	-	-
9	-	55	64	658
10	-	309	80	54
Total:	-	247	84	431
Square: thousand km^2	-	527	236	229
Stocks, billion t	-	22.7	3.6	15.5

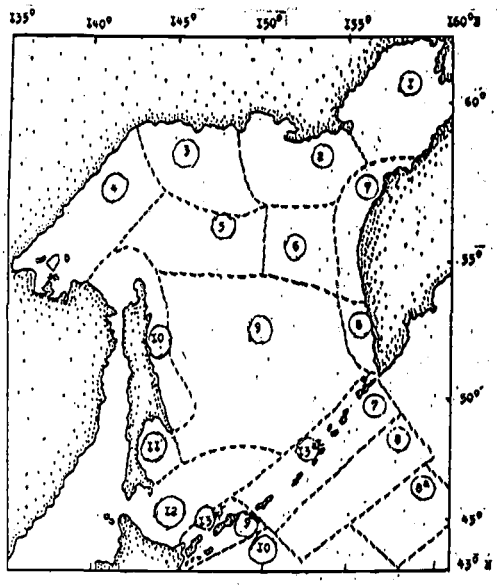

Fig. 1. Biostatical areas of Okhotsk Sea and adjacent waters to Pacific.

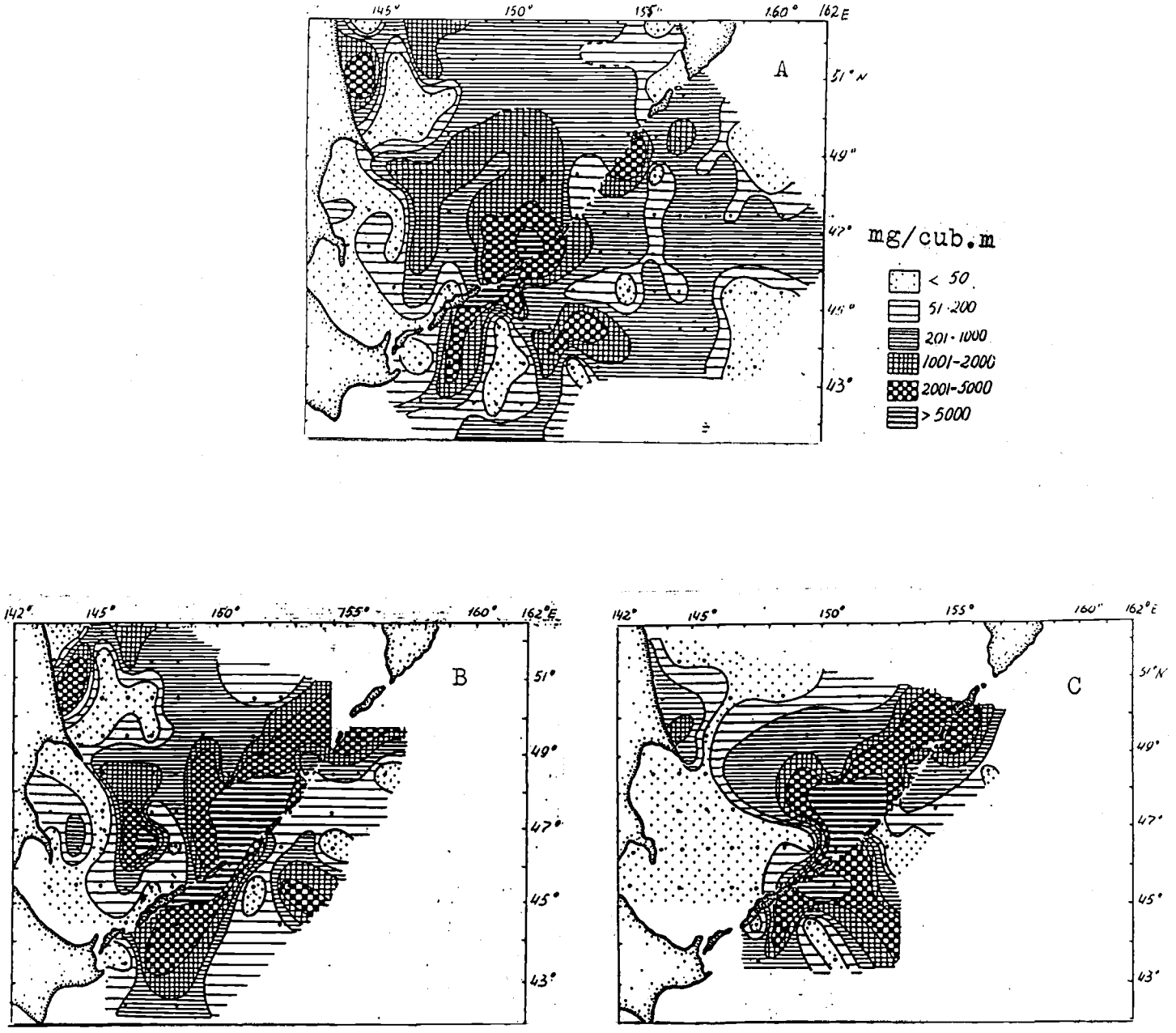

Fig. 2. Distribution of biomass of net phytoplankton (mg/cub.m) of Sakhalin-Kuril region in summer 1993. Layer 50-0 m.

A - first survey (July 1-28) B - second survey (July 20 - August 7)
C - third survey (August 1-17)

Biological Productivity in Anomalous Mercury Conditions (Northern Part of Okhotsk Sea)

Lyudmila N. LUCHSHEVA

Pacific Scientific Institute of Fisheries and Oceanography (TINRO)
4 Shevchenko Alley, Vladivostok, Russia. 690600

In August 1993 (24th cruise of the R/V " Alexander Nesmeyanov") the contents of mercury in the water, plankton and bottom sediments in some regions of the Okhotsk Sea were investigated. The research was conducted on the western Kamchatka shelf at the entrance to Shelikhov Bay and in the Tauisky Sakhalin region. Mercury is estimated using cold vapor atomic absorption spectrophotometry (Hatch and Ott, 1968). The mercury level in the sea water is determined following Virtsavs et al., 1974 and Mercury ..., 1979. The determination of mercury in plankton and bottom sediments is based on using standard methods (Oradovsky, 1977; GOST ..., 1986).

Analysis of the data indicates that mercury in the upper layer of the water column is rather homogeneous and the concentration ranges from 0.000 to 0.042 mcg/l (average 0.019 mcg/l) (Fig. 1). The relatively low mercury content of the water is observed in all regions. The upper microlayer of water had 1.6 times the mercury content of the lower layer (Fig. 2). The maximum concentration of mercury (0.070 mcg/l) is found in the entrance to Shelikhov Bay. Abnormally high concentrations of mercury (0.600 mcg/l) is found in the bottom layer of water of the entrance to Shelikhov Bay which was 6 times more than in marine fisheries waters (The collection ..., 1991) (Fig. 3).

In the bottom sediments, the concentrations of mercury ranges from 0.006 to 0.028 mcg/g of dry mass in association with the granulometric composition. The concentrations of mercury in plankton ranges from 0.036 to 0.121 mcg/g of dry mass. In the high mercury concentration 1 m bottom layer of water, similar increases in the concentration of mercury is found associated with bottom sediments and plankton.

The data suggest that a spatial mercury anomaly coincids with the location of a strong cyclonic eddy of the Jamsky current moving out from Shelikhov Bay. The surface waters are to a high degree satiated with oxygen (up to 138%) as a result of the high biomass of the diatom *Thalassiosira*. This diatom has the highest mitotic index for the area.

The maximum concentrations of organic carbon, carbohydrates, organic and mineral forms of biogenic elements are also found in the region. The maximum amount of chlorophyll "a" and abnormally high values of primary production are observed. The maximum biomasses of bacteria and infusoria and a large amount of zooplankton (99% of it were larvae of crab) are found along with large amounts of pollock. The size of algae and zooplankton are unusually large. Similarly, hydrological and hydrochemical conditions are observed over the Kashevarov Bank where the mercury content in the water is low. Upwelling of cold bottom waters are enriched by the biogenic elements which are in higher concentrations than in the entrance to Shelikhov Bay but the biological productivity is lower.

High biological productivity is found in areas where there is upwelling to the surface as the bottom waters are enriched with nutrients. In these zones, high biomass of phytoplankton and zooplankton occur along with fish species who feed on the plankton (Natarov, 1966).

In the region between the Tauisky Gulf and the entrance to Shelikhov Bay an inter-structural hydrological front is formed as a result of the interaction between the two currents which move in opposite directions (Chernyavsky, 1970). In the narrow zone between the flood, the upwelling of cold deep nutrient rich waters occurs. The constant exchange of nutrients produces an intensive, long development period of phytoplankton and a large accumulation of zooplankton in the entrance to Shelikhov Bay (Afanasyev, 1981). Most of the herring stocks and pollock stocks in Okhotsk Sea are found in the region. A number of studies have found that this area has an extraordinary high stable biological productivity (Kotlyar, 1970; Chernyavsky, 1970).

A very high abundance and biomass but simplification in the complexity marine organisms can be found in a polluted environment. The hyper development of some species and the decrease of species composition are a reaction to extremely high levels of nutrients and high levels of pollutants that favors only some species. Organisms living near volcanic activity on the sea-bottom where high levels some chemicals (including mercury) can cause a decrease of biological activity and reproduction (Tarasov et al., 1985).

Some levels of mercury may increase the length of hydrobionts life, stimulate their activity and cause strengthening of exchange processes (Weis et al., 1985; Weis et al., 1987). Natural selection may cause some organisms, that live in high concentrations of mercury, to become more resistant to pollution stress (Baker et al., 1985). The above experiment shows that the interaction of natural geochemical anomalies as well as antropogenic influences may cause an adaptation of populations of hydrobionts to allow them to live in a polluted environment.

REFERENCES

Afanasyev, N.N. 1981. Characteristics of macroplankton (Okhotsk Sea). Izvestiya TINRO. 105:56-60.

Baker, R., B. Lavie, and E. Nevo. 1985. Natural selection for resistance to mercury pollution. Experientia. 41(5):697-699.

Chernyavsky, V.I. 1970. Hydrological front of northern part of Okhotsk Sea. Izvestiya, TINRO. 71:3-11.

Chernyavsky, V.I. 1970. The causes of high biological productivity (northern part of Okhotsk Sea). Izvestya, TINRO. 71:13-22.

GOST 26927-86. 1986. Raw material and food. The methods of mercury determination. Edit. of standards, Moscow. p.14-18.

Hatch, W.R., and W.L. Ott. 1968. Determination of submicrogramme quantities of mercury by atomic absorption spectrophotometry. Anal. Chem. 40(14):2085-2087.

Kotlyar, L.K. 1970. Regularities of development and quantitative distribution of zooplankton as feeding base of herring in northeastern part (Okhotsk Sea). Izvestiya, TINRO. 71:59-73.

Mercury Analysis Working Party of BITC. 1979. Standartisation of methods for the determination of traces mercury. Anal. Chim. Acta. 109:209-228.

Natarov, V.V., and E.I. Chyorny. 1966. The formation of high biological productivity zones (Pacific ocean). Trudy, VNIRO. 9:4-9.

Oradovsky, S.L. 1977. The manual on chemical analysis methods of marine waters. Hydrometeoisdat, Leningrad. 208 p.

Tarasov, V.G., M.V. Propp, L.N. Propp, and other. 1985. Hydrothermal features and specific water ecosystem in Kraterny Bay (Kuril Islands). DVNTS AN USSR, Vladivostok. 30 p.

The collection of sanitary and hygienic standards and methods of control of dangerous substances in the objects of environment. 1991. The centre of ecology, Moscow. 370 p.

Virtsavs, M.V., O.E. Veveris, and Y.A. Bankovsky. 1974. The application of thiooxin for concentration of heavy metals by co-precipitation. II all-union conf. on concentration of metal in analit. chem. Moscow. 202-203.

Weis, J.S., P. Weis, M. Renna, and S. Vaidya. 1985. Search for a physiological component of methylmercury tolerance in the mummichog, Fundulus heteroclitus. Marine pollut. and physiol. Recent adv. Univ. of South Carolina Press, Columbia. 309-326.

Weis, J.S., M. Renna, S. Vaidya, and P. Weis. 1987. Mercury tolerance in killifish: A stage specific phenomenon. *In* Oceanographic Processes in Marine Pollution. V.1. Biological processes and Wasters in the Ocean Florida, Krieger Publishing Co.

FIGURES

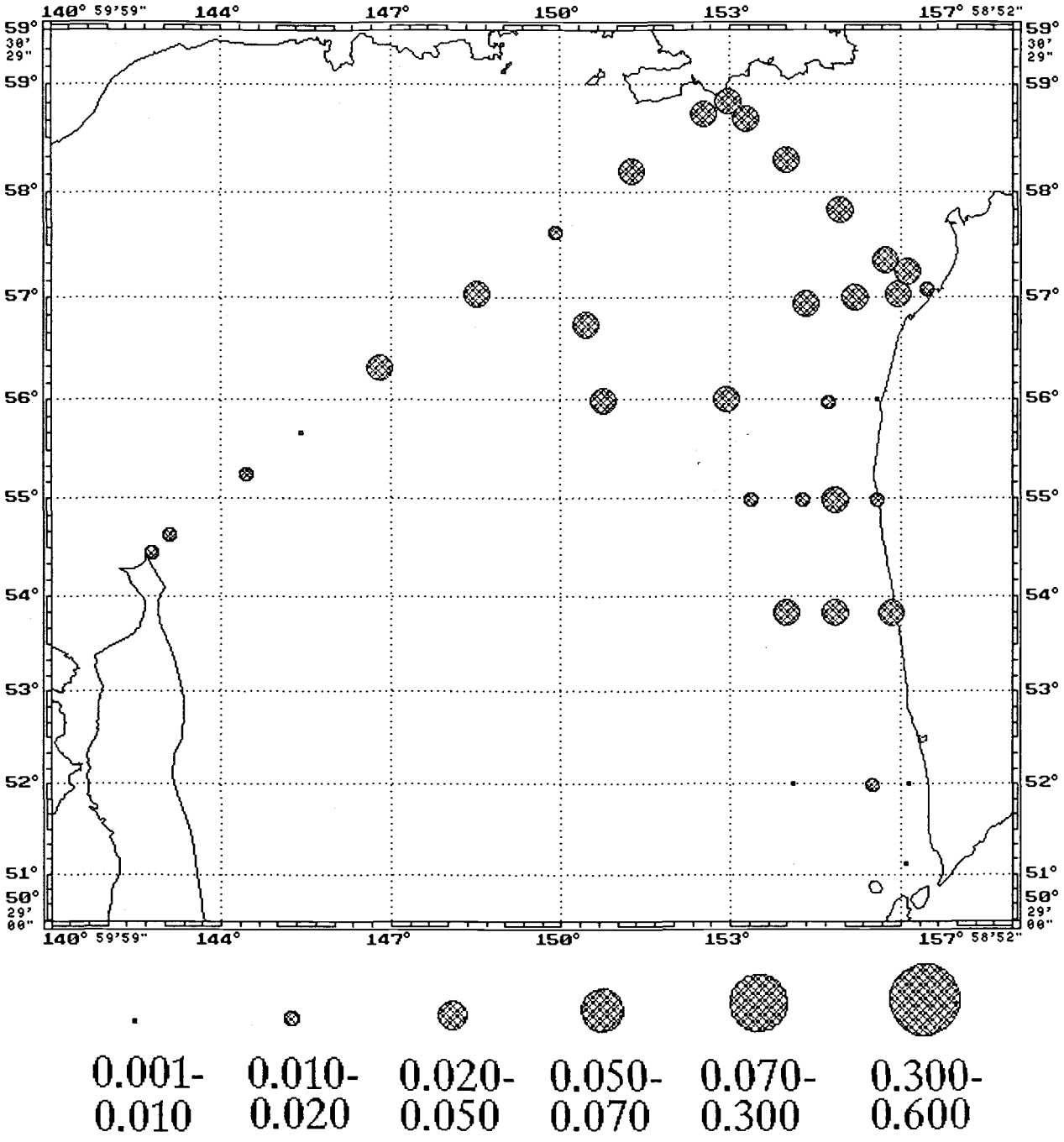

Fig. 1. Distribution of mercury concentrations (mcg/l) in the surface layer of water.

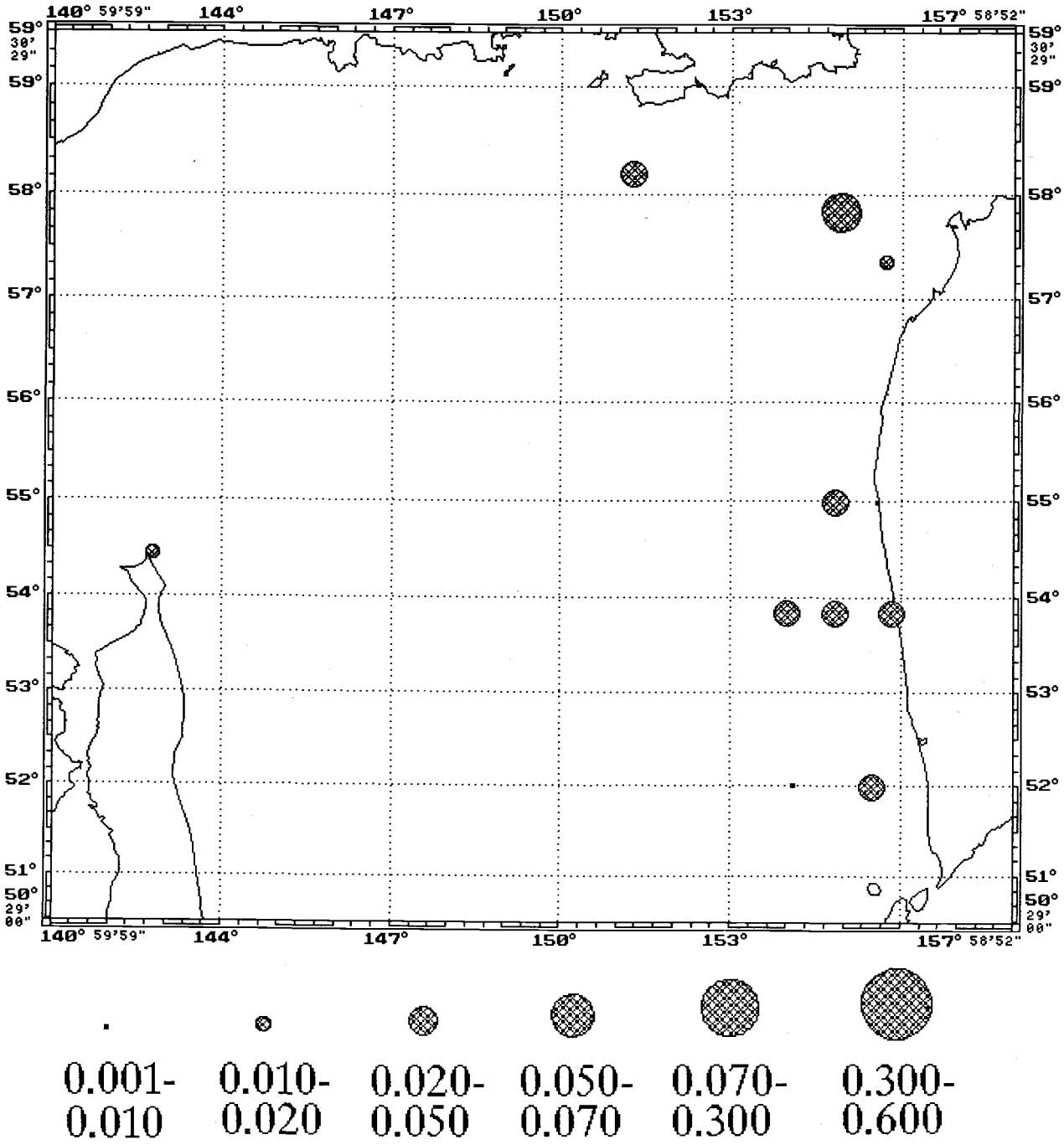

Fig. 2. Distribution of mercury concentrations (mcg/1) in the upper microlayer of water.

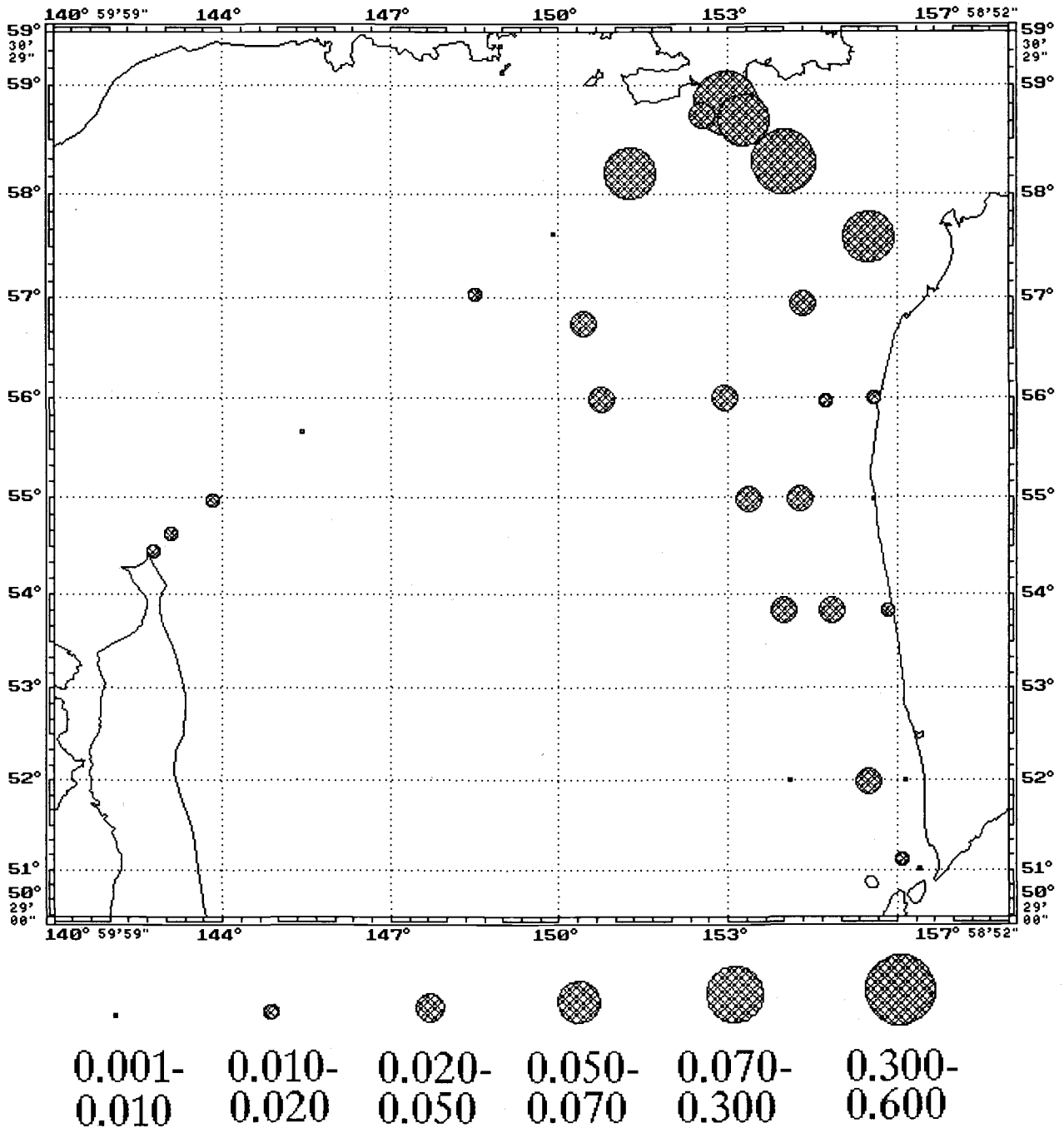

Fig. 3. Distribution of mercury concentrations (mcg/1) in the ground layer of water.

Origin of Hydrocarbons in the Ecosystem of Coastal Region of the Okhotsk Sea

Inna A. NEMIROVSKAYA

Institute of Oceanology, Russian Academy of Sciences, Moscow, Russia

The industrial development of oil and gas deposits at the Okhotsk Sea shelf has been started recently. Authentic information about distribution and origin of hydrocarbons (HC) is necessary to evaluate both the oil and gas development prospects and ecological rates setting of anthropogenic pressure on marine environment.

Our study included investigations of the concentration and composition distribution of dissolved and particulate aliphatic hydrocarbons (AHC) and polycyclic aromatic hydrocarbons (PAHC) in the surface waters and bottom sediments. The observations were carried out near the Kuril Islands, along the east coast of the Okhotsk Sea, in the Gulf of Sakhalin and on the N.E. Sakhalin Island shelf in August 1993 aboard the R/V *Academic Alexander Nesmeyanov* (cruise AN24). The last two areas were surveyed repeatedly during the 23rd cruise of the R/V *Academic Mikhail Lavrentev* in the fall of 1994. The purpose of this research is to establish the background characteristics and level of petrogenic hydrocarbons in these coastal zones.

The average concentration of dissolved aliphatic HC in surface waters collected from different regions of the Okhotsk Sea varied within a relatively narrow range: from 15 to 19 μg/1 in summer, 1993, and from 21 to 33 μg/1 in autumn, 1994; the degree of enrichment in the surface microlayer (ML) changed from 1.2 to 6.6 (Table). As have been shown earlier (Tkalin, 1993) the HC content in the water column and bottom sediments is not very high and comparable with the other regions of the N.W. Pacific. Along the N.E. Sakhalin Island shelf, the average AHC concentrations were from 9 to 15 μg/l in different seasons, with maximum value of 44 μg/1. The state of the benthic and pelagic environments appeared to be normal except for the area affected by a local oil spill.

The mean level of dissolved PAHC in the surface coastal waters was 8 μg/1, with the degree of their enrichment in the ML from 2 to 3. Naphthalene and fluoranthene dominated in PAHC composition whereas pyrene and benzo(a)pyrene remained minor components.

These data probably represent the background concentrations for the Okhotsk Sea. The removal from the coast in the offshore direction and from the river-sea boundary in the Gulf of Sakhalin did not significantly affect the distribution of dissolved HC, but their suspended (particulate) form. The distribution pattern of alkanes in waters near the Kuril Islands and the eastern shelf of the Okhotsk Sea indicated the natural origin of HC with various ratio of autochthonous and allochthonous components.

Bottom sediments in the coastal regions of the Okhotsk Sea are characterized by low concentrations of aliphatic HC in comparison with less productive aquatories. In the surface layer of the bottom sediments the average content of AHC changed from 3.8 to 19.6 μg/g (calculated on dry weight) and represented from 0.07 to 0.80% of organic carbon (C_{org})

whereas the average PAHC content varied from 2.2 to 43.1 μg/g and from 0.3 to 14.3×10^{-4}% in C_{org}. These values remained within the range of concentration (1.5 to 52 μg/g) found in bottom sediments of the Bering Sea by Venkatesan and Kaplan (1982). The reported concentrations of HC can be explained by comparatively low organic matter contents in the sediments which, in turn, can be related to the short vegetative period of diatom algae, as well as to the rapid biogenic decomposition of particulate organic matter dominated by proteins and carbohydrates (Romankevich, 1984). It is apparent that biological production of the region and lithology of sediments influence the distribution and composition of hydrocarbons.

In summer 1993 along the N.E. Sakhalin Island shelf (in the region of oil deposits) the aliphatic HC concentration in surface waters exceeded the background level sevenfold (on average), and the PAHC content surpassed the background level by 19. The bottom sediments indicated an increased portion of hydrocarbons in organic matter and a varied HC distribution pattern. In autumn 1994, in the Gulf of Sakhalin concentrations over 50 μg/1 were observed in surface as well as in near bottom waters.

The spatial distribution of hydrocarbons and the distribution pattern of alkanes in some samples suggest the existence of a local source of petroleum pollution on the Sakhalin Island shelf. However, comparison of the abnormal chromatograms of alkanes from water and bottom sediments in this area with chromatograms of the Sakhalin petroleum indicates some basic differences. Even if the Sakhalin petroleum is subjected to weathering (such as would occur 30 days after a spill on marine waters), alkanes C_{17} - C_{18} will dominate in the low molecular area (Mishukov et al., 1987). According to our chromatograms the homologous compounds up to C_{23} were practical absent.

Therefore, it is more likely that there is an endogenous source of the abnormal hydrocarbon concentrations in the bottom core (such as fluid flow). These data were obtained from the marginal regions which are connected with oil and gas-fields. They are restricted to very small areas (<1 m^2) with a limited depth of oil stratum bedding and with favorable tectonic and lithology situations (Venkatesan and Kaplan, 1982; Nesterova and Nemirovskaya, 1988). The analysis of fluid hydrocarbons has shown a high degree of similarity with crude oil and the HC composition observed in the bottom sediments.

On the other hand, migration of small quantities of low molecular hydrocarbons from the bottom core with fluid fluxes can promote intensive development of bacterial communities. This can lead not only to the appearance of the oil oxidizing bacteria, but also the bacteria which re-synthesize the high molecular alkanes, as was discovered in bottom water samples collected from the Bering Sea (Nesterova and Nemirovskaya, 1988).

It is quite likely that a natural distillation of petroleum in fluid fluxes takes place in deep water layers along the Sakhalin shelf, causing the selective accumulation of high molecular hydrocarbons. The transition of the transformed HC from the bottom sediments to the water column in shallow areas results in their accumulation in the surface waters. This assumption is supported by the similarity of alkanes distribution patterns in water and bottom sediments, as well as by high concentrations of PAHC at specific stations of this region.

Apparently, the ecosystem of the Okhotsk Sea can endure these natural fluxes of petroleum hydrocarbons, as evidenced by the background concentration and composition of HC in the South Sakhalin Island shelf. In addition, there is a high natural rate of the hydrocarbon biodegradation (mean value 540 μg/1 per day), reflecting a high assimilative capacity for petroleum hydrocarbons (Anikiev et al., 1992).

REFERENCES

Anikiev, V.V., M.N. Mansurov, and G.N. Moiseyevsky. 1992. Physical, chemical and bacterial destruction of oil on the shelf of Okhotsk and Japan Seas, p. 241-255. *In* V.I. Ilyichev and Anikiev [ed.] Oceanic and Anthropogenic Controls of Life in the Pacific Ocean. Kiuwer Academic Publishers, Netherlands.

Mishukov, V.F., O.V. Abramova, A.G. Zelenina, and M.N. Mansurov. 1987. The environmental fate of Sakhalin crude oil. Proc. 3-rd Pacific school on marine geology, geophysics and geochemistry, Part 2. Vladivostok. p. 168-173. (in Russian)

Nesterova, M.P., and I.A. Nemirovskaya. 1988. Surface pollution of the Pacific Ocean by petrochemicals. Geojournal. 16:29-34.

Romankevich, E.A. 1984. Geochemistry of Organic Matter in the Ocean. Springer-Verlag, Berlin. 334 p.

Tkalin, A.V. 1993. Background pollution characteristics of the N.E. Sakhalin Island shelf. Mar. Pollut. Bull. 26:704-705.

Venkatesan, M.J., and J.R. Kaplan. 1982. Distribution and transport of hydrocarbons in surface sediments of the Alaskan Outer Continental Shelf. Geochim. Cosmochim. Acta. 46:2135-2149.

TABLES

Table 1. Concentration of dissolved hydrocarbons in the Okhotsk Sea

Region	Depth	number of samples	aliphatic HC, μg l^{-1}			PAH, ng l^{-1}		
			mean	ranges	σ	mean	range	σ
			Summer 1993					
Kurily	ML	27	44	18-108	22	15	20-14	10
Islands	surface	42	15	6-40	5	6	3-8	2
Eastern Okhotsk Sea Shelf	ML	11	37	30-55	10	12	8-15	4
	surface	24	18	12-23	3	6	2-8	3
Okhotsk	ML	2		16-34		-	-	-
Sea	surface	9	18	11-23	3	5	2-8	2
Gulf of Sakhalin	surface	16	16	6-23	4	9	4-15	5
East Sakhalin Shelf north part	ML	1	-	574	-	-	5032	-
	surface	14	202	15-2172	548	145	8-338	214
south part	surface	10	19	11-26	5	12	6-14	5
			Autumn, 1994					
Gulf of	surface	11	33	13-60	17	10	5-18	8
Sakhalin	near bottom	8	28	12-75	20	9	4-17	7
Northeast	surface	17	21	9-33	5	9	5-13	8
shelf of Sakhalin Island	near bottom	18	19	12-29	5	9	6-17	9

Elements of the Pacific South Kuril Area Ecosystem

Tatyana A. SHATILINA

Pacific Research Fisheries Centre (TINRO-Centre)
4, Shevchenko Alley, Vladivostok, 690600, Russia

ABSTRACT

This paper examines the interannual variability of water temperature and atmospheric circulation as well as their effect on the distribution of plankton, saury and sardine. In cold years (1980-1988), the abundant growth of phytoplankton was observed to negatively affect saury entering the area because of the florescence but affected sardine positively as it feeds heavily on phytoplankton. "Warm" years (1970-1979) were characterized by low plankton biomass and rich saury abundance.

INTRODUCTION

Recently (1960-1994), Northwest Pacific saury catches fluctuated up and down while in 1976-1988 sardine catches underwent a period of increase followed by a decline. In 1960-1969 there was a periods of medium and small catches of saury in the South Kuril Area (SKA), while in 1970-1979 catches were large and from 1980-1988 catches were extremely poor for saury but good for sardine. Factors that affect growth and abundance of saury and sardines are water temperature and the state and distribution of plankton that is the main food of pelagic fish and squid. In turn, the production of these species are affected by the variability of atmospheric circulation.

METHODS AND MATERIALS

The atmospheric circulation over the Far-East can be analyzed from meridional and zonal forms of circulation and types of synoptic processes. These processes can be followed from the atlas for 1949-1985 (Kalachicova and Nikolayeva, 1985). The atlas includes atmospheric circulation from Ilyinsky (W, C, E, Z) as well as types of atmospheric processes (W, M, E, S). Using the atlas, the anomalies of atmospheric circulation (in days) and of ground synoptic process types from May to August, 1978-1985 can be accounted for.

W - western, E - eastern, C - central, M - mixed, Z - zonal, S - southern.

To estimate the long-term variability of the water thermal regime in the SKA, data from the coastal hydrometeorological stations for 1961-1989 was used. Decadal data on water temperature distribution near the sea surface and at a depth of 50 m as well as data on plankton within a layer of 0 to 100 m for seven years (July through September 1979-1981, 1983, 1984, 1987 and 1988) were analyzed.

RESULTS

In accordance with the earlier findings of Bokhan et al (1989), the area is divided into five sites associated with the heterogeneity of the water masses and of plankton distribution: Site 1; the South

Kuril shallows, Site 2; coastal waters adjacent to the Pacific shores of Iturup Island; Site 4; Southwestern Pacific and Site 5, Southeastern Pacific (Fig. 1).

From the August distribution of plankton in different years for different sites it is evident that there were differences in the plankton biomass distribution (Table 1). High value of plankton biomass for the years is observed northeast of the coastal waters of Iturup Island and Friz Strait. The smallest values of plankton biomass are observed in the South Kuril shallows and in the ocean .

The interannual variations of plankton biomass over the area was significant. In coastal waters of Iturup Island and Friz Strait, the plankton biomass is 1,000 to 7,000 mg/cub.m early in August 1981, and 200 to 1,000 mg/cub.m in August 1978-79.

It is well known that June is the last month of phytoplankton development and August is a period of the majority of zooplankton development. The maximum zooplankton development came, as a rule, 1.5-2 months after the completion of phytoplankton development in a boreal area (Kun,1985). We observed an extension of plankton productivity cycle except in August 1978-79 when plankton development was typical and fit the "biological summer" concept.

The variations in plankton distribution was reflected in the saury and sardines fishery conditions in the SKA. 1978 and 1979 were characterized by good saury catches (50,000-70,000 t), whereas in 1980-1988 there were extremely poor (0-10,000 t). At the same time the 1980s were marked by good catches of Pacific Sardine (250,000-300,000 t). The different responses of saury and sardine to plankton distribution can be explained by differences in their nutrition. Saury avoided areas of good phytoplankton development by migrating far from the South Kuril Islands into the ocean, northeast to the Central Kuril. The sardine diet included a wide variety of both zooplankton and phytoplankton as was observed in the 1980s (Kun, Shatilina, 1989).

To determine thermal conditions in the SKA, water temperature variation profiles of the surface and at the 50 m level were developed. An extremely warm year occurred at all sites in 1978. By early August the water temperature on the coastal of Iturup Island and Friz Strait was 11 and 13°C, being 5-10°C in 1980, 1981, 1987 and 1988 (Fig. 2). At the two ocean sites an abnormally high water temperature of 22°C occurred early in August 1984 and the lowest temperature was 13°C in 1980. In the South Kuril shallows, water temperature was 14-17°C. Late in July 1979 the water temperature was 10°C but rose to 16°C by mid August. In the 1980s the water temperature remained below 15°C.

Fig. 3 shows average monthly water temperature anomalies at the Kurilsk and Yuzhno-Kurilsk hydrometeorological stations in the summer. Two cold periods occurred, the first cold was observed from 1963 through 1971 and the second from 1980 to 1988. The temperature began to rise in August 1989 and continues to the present.

Variations in the seasonal and interannual plankton biomass were observed in relation to water temperature variations at all the sites of the SKA. The highest values of plankton biomass (phytoplankton bloom) are observed in cold waters of Iturup Island and near Friz Strait (Table 1). The least values of biomass is observed in the South Kuril shallow waters and at the ocean sites. In cold years, in coastal waters of Iturup Island and Friz Strait, the plankton is characterized by a late biological spring (extension of biological processes in plankton).

Table 2 shows the data of anomalies in types of bottom processes in 1978-1984. In the years when water temperature in the coastal waters of SKA is above normal, processes of the western type dominated over the Sea of Okhotsk and the South Kuril Islands. Thus, in July 1978, the western-type process comprised 25 days and in August 1979 it was 16 days. The high western-type process, with cyclone activity dominates the Far-Eastern sea and a high pressure field observed in the Northwest Pacific provides a transfer of warm air in the area of the Sea of Okhotsk and the Kuril Islands. In

years of low temperature in coastal waters of Kunashir and Iturup, a southern-type process is intensified providing cold northeastern air masses.

Table 3 represents the data of anomalies of circulation forms by Iliinskiy (1965). From these data, in 1978, zonal circulation dominates with a high-altitude frontal zone (HFZ) being located to the north of 40°N. In 1979, a western-type form dominated in the 1980s reiteration of the C and W forms became important. In May 1983 and 1984 the Z form reiteration is elevated but the HFZ was located to the south of 40°N. In June and July of 1984 and 1985 the reiteration of the high altitude depression is abnormally elevated over the Sea of Okhotsk and caused the intensification of an arctic invasions. In 1980 the C form reiteration was abnormally high which was related to the intensification of the Okhotsk invasion.

DISCUSSION

A cold type of thermal regime, and therefore an abundant development of plankton depends on the frequency and intensity of cold arctic invasions. Warm types are formed when zonal processes are intensified causing quick development of plankton.

One of the ways of determining SKA food availability is by forecasting water temperature which depends on atmospheric processes.

REFERENCES

Bokhan, L.N., and V.V. Nadtochy. 1989. Interannual dynamics of plankton distribution in the South Kuril area. Results of research on short-term forecasting of fishery conditions in the Far-East. Vladivostok, TINRO.

Bokhan, L.N., and T.A. Shatilina. 1989. Particularities of mesoplankton distribution in the South Kuril area in August 1980. Results of research on short-term forecasting of fishery conditions in the Far-East. Vladivostok, TINRO.

Kalachikova, V.S., and E.V. Nikolayeva. 1985. Calendar of circulation forms over the northern hemisphere, of circulation forms and synoptical processes types over Eastern Asia for 1949-1984. Vladivostok. 58 p.

Kun, M.S. 1975. Zooplankton of the Far-Eastern seas. M. Pishchevaya promyshlennost. 148 p.

Kun, M.S. 1985. Long-standing variabilities of productive zones forming in the area of subarctic front of Northwestern Pacific. *In* coll.: Biological basis of fishery developing of oceanic open areas. M. Nauka. p. 166-174.

Iliinskiy, O.K. 1965. The practice of the main form definition of atmosphere circulation over the Far East. Proc. Tr. Dal'nevost. Nauchno-issledovat. Gidrometeorolog. Inst. 20:26-45.

TABLES AND FIGURES

Table 1. Average values of plankton biomass (mg/cub.m) in the South-Kuril Area of the Pacific Ocean in the mid-August 1978-1988.

Year	I South Kuril I shallow I waters	Waters of the Iturup Island	Waters of the Friz Strait	Southwestern ocean area	Southeastern ocean area
	I 1	2	3	4	5
1978	I 500	500	200	700	200
1979	I 195	1148	1076		657
1980	I 639	2678	1103	1373	441
1983	I 284	1723	1121	1170	448
1984	I 749	1823	3448		
1987	I 717	1102	793		427
1988	I 1175	1082	1008		878

Table 2. Anomalies of bottom processes, western- (w) and southern (s) types in 1978-1984.

Month	1978		1979		1980		1981		1982		1983		1984	
	w	s	w	s	w	s	w	s	w	s	w	s	w	s
June	4	-7	8	-6	12	-13	-4	-4	6	-5	-5	6	4	-7
July	21	-15	-2	-5	-8	2	3	3	1	-3	5	-4	-2	8
August	8	-10	17	-10	-6	1	-4	11	6	5	6	5	9	-1

Table 3. Anomalies of atmospheric circulation forms in June 1978-1985.

Form	I 1987	1979	1980	1981	1982	1983	1984	1985
Zonal (Z)	I 2	-1	-8	4	0	4	-4	-3
Mixed (M)	I 4	3	2	-2	-3	-3	5	7
Eastern (E)	I -2	0	-2	-1	-3	1	5	3
Western (W)	I 5	4	-1	1	-3	3	1	-2
Central (C)	I -7	-5	8	-2	2	-3	-8	-8

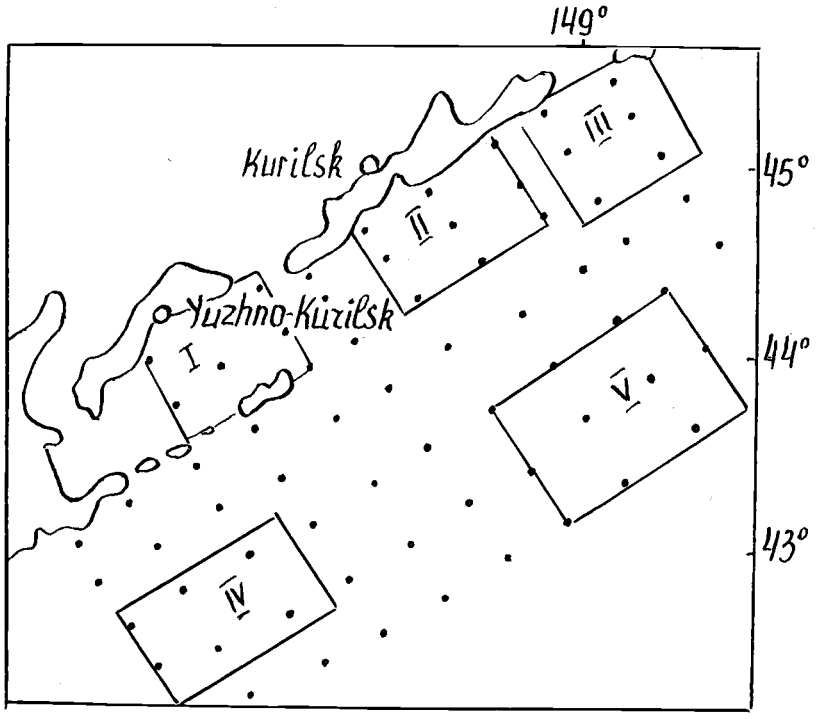

Fig. 1. The plot of the surveys according to the program "Poligon".

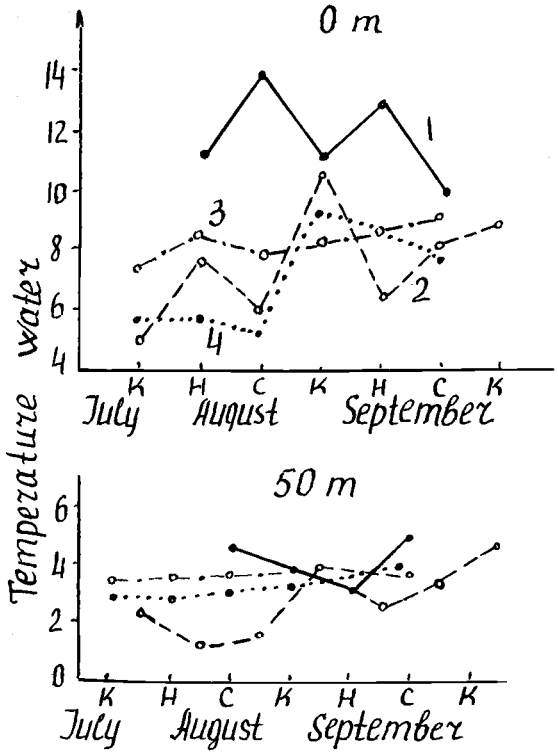

Fig. 2. Seasonal variability temperature water of the Friz Strait.

1 - 1978 2 - 1980 3 - 1984 4 - 1988

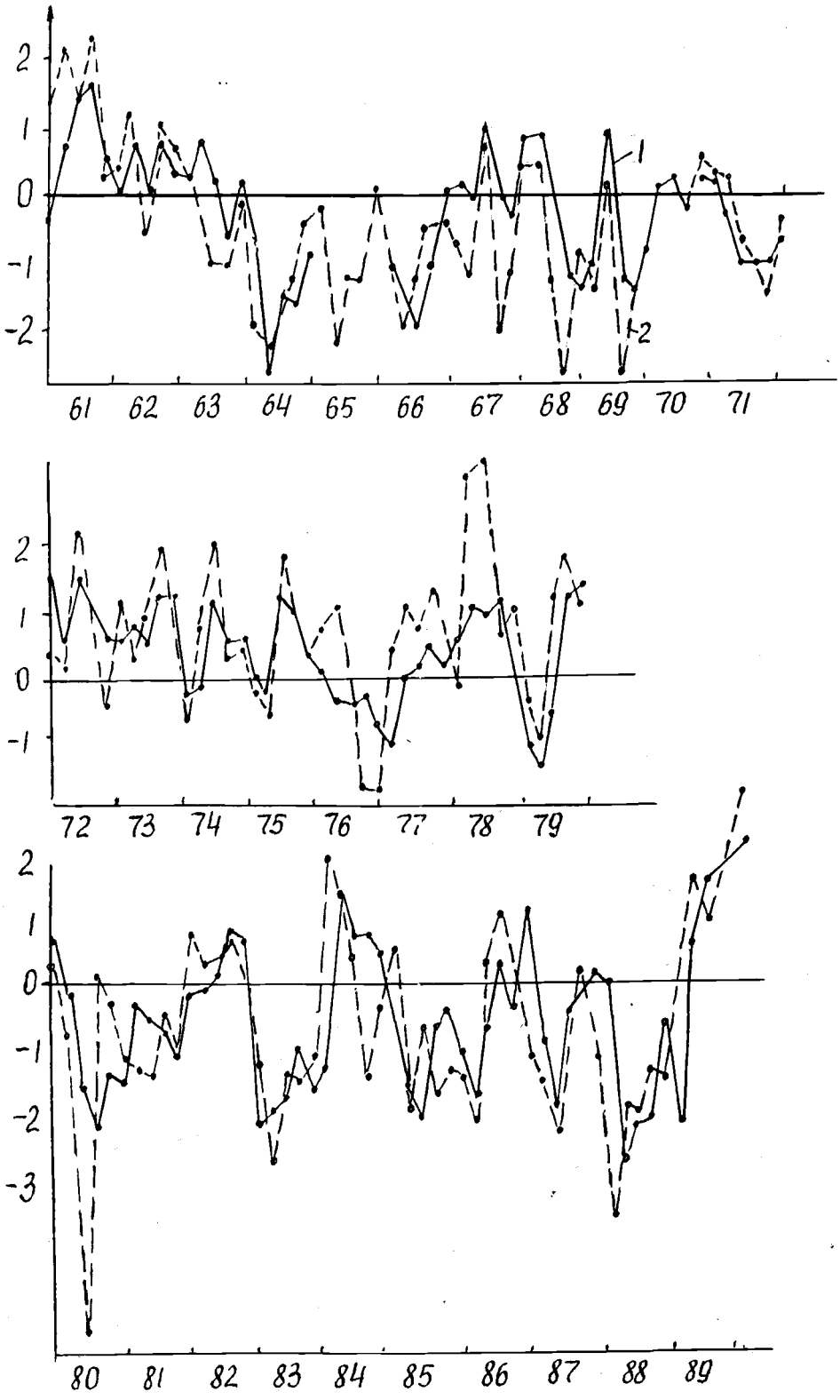

Fig. 3. Anomalies of temperature water in the South Kuril (SKA) in June-October, 1961-1990

1 - HMS Yuzhno-Kurilsk 2 - HMS Kurilsk

Biota of the Okhotsk Sea: Structure of Communities, the Interannual Dynamics and Current Status

Vyacheslav P. SHUNTOV, Yelena P. DULEPOVA

Laboratory of Biocenology, Pacific Research Center, Vladivostok, 690600 Russia

The biological resources of the Okhotsk Sea are of great importance to the Russian fishery. The size of the biological resources is related to the high productivity and lead to increased research activity on behalf of fishermen. Unfortunately, only TINRO has been engaged in regular research on the biological resources of the area and these studies are a summarization of a number of papers including reviews (Shuntov, 1985; Shuntov and Dulepova, 1993; Shuntov et al.,1993). This paper focuses on the characteristics of the biota during the 1990s. In order to evaluate the long-term dynamics in the biological phenomena a comparison of the new information with data of the previous year is necessary. These data were obtained from combined surveys conducted between 1980-1990 and from the literature.

In 1980, the relative stability of the composition and structure of the Okhotsk Sea communities and the biomass and production of major groups of hydrobionts is evident (Table 1). Based on these data, the energy balance requirements are calculated and diagrams of the partitioning of the energy flow between the different levels within the Okhotsk Sea ecosystem have been constructed (Fig. 1). The results are approximate and can be only considered as one of a number of possible variants.

The exchange of energy between the different levels of the food web cannot be explained unless the detritus cycle is included. The energy obtained from dead organic substance exceed by 1.5 times that from direct consumption of primary production. The greatest flow of energy passes through the bacteria and protozoa which are consumed by zooplankton and non-predatory zoo-benthos (Fig. 1). The energetic expenditure of bacterial plankton and protozoa exceed 85% of total respiration of all heterotrophs of the Okhotsk Sea ecosystem.

The non-predatory zooplankton mainly consist of copepods and euphausids (third in importance) which are a major energetic reserve for other higher trophic levels. Over 10% of the total energy flow and heterotrophic production is dependent on this link. The predatory zooplankton consume up to 65% of the energy and non-predatory zoobenthos, nekton and nektobenthos also depend on this component of the foodweb. Twenty five percent of the production of non-predatory zooplankton, which became part of the detritus component, replenish the energy reserve of the ecosystem from which the consumption by non-predatory zooplankton is more than two times. Predatory zooplankton consume 27% detritus in their diet. The rest of the ecosystem components are less important in utilizing detritus although they contribute a considerable share of their production to the cycle.

The demersal fauna (predatory and non-predatory benthos, nektobenthos) of the Okhotsk Sea consume slightly more than 1% of the total energy flow. These components of the ecosystem subsist, mainly, on microflora of the sediments, detritus , protozoa and bacterial plankton, although the pelagic animals are part of the nekton benthos ration, the greater part is consumed by demersal fishes and crabs (bentophags and predators) (Dulepova and Borets,1994). Taking into consideration fishing effects, the transformation of the demersal fauna production into detritus is much higher than for

zooplankton: non-predatory, zoobenthos more than 40%, predatory zoobenthos more than 80% and nektobenthos more 50%. Thus, a considerable part of the production of the ecosystem components (20 to 63%) is not utilized and turns into detritus but a lesser amount of organic substance goes to detritus than is consumed. The Ohkotsk Sea produces excess detritus which is related to the high level of phytopankton and protozoa production.

In the early 1990s, a climatic change took place in the pelagic zone of the Far-Eastern Seas analogous to a period from 1940s-1960 as changes from 1970-1980s is analogous to a period from 1920-1930s (Shuntov, 1993; Shuntov et al.,1993). In the 1990s, the pelagic community was considered to be in transition.

ZOOPLANKTON COMMUNITIES

Data on zooplankton for 1980-1990s was mainly only available from the southern Okhotsk Sea (Tables 1-2). In the early 1990s, the number of predatory plankton and euphausids increased but the number of copepods declined. The decline of the plankton communities in the early 1990s was likely from high concentrations of plankton feeding pollock and sardine. In 1994, the biomass of euphausids remained high and the biomass of copepods increased as the number of sagittas decreased. These changes were related to the beginning of the stabilization of the composition and structure of the plankton community under new conditions.

The plankton community of West Kamchatka was quite different to other areas of the Okhotsk Sea due to a pronounced reduction of the biomass of pollock, the most important plankton feeding fish. In 1994, the number of predatory plankton in Kamchatka waters was maximum but the levels remained high (Table 3). Such a high level of predatory plankton was abnormal in communities and was likely the result of decreased predation. It was likely that the process of succession occurred as was found in the southern part of Sea. New information about the Okhotsk Sea plankton also supported the conclusion that the plankton community was in a transition but the reorganization occurred at different rates in different areas.

NEKTON COMMUNITIES

In 1993, simultaneous to the decreased sardine and pollock biomass in the southern Okhotsk Sea, there was an increase of squids abundance which was unexpected (Table 4). In 1994, the biomass and abundance of the fish concentrations increased due to the increased number chum and pink salmon which came into the Okhotsk Sea for part of the year. In the southern part of pelagic zone there was no change in the number of some epipelagic fish after the pollack and sardine decreased. It was thought that herring from Sakhalin, anchovy, saury, arabesque, greeling and squids might have replaced the pollock. At the present time, changes in abundance of fish species in the north Okhotsk Sea is no longer synchronous (Table 5). In 1994, for the first time, more than one third of the fish biomass in the epipelagic zone was herring.

DEMERSAL ICHTIYOCENOSIS

Most populations of demersal fishes and invertebrates which were reduced by fishing in the 1950s-1960s, began to recover due to better management measures in allocating the catch (Shuntov, 1985). In the early 1980s, when fish and crab stocks grew, the production of the benthos was evidently under-exploited by fishes and invertebrates (Table 6). It was concluded that benthos stocks would further increase (Dulepova and Borets, 1990). In the late 1980s, the biomass of demersal fish

and crab on the West Kamchatka shelf increased approximately two times (Dulepova and Borets,1994). As a consequence, the consumption of benthos organisms approached the value of production (trophic capacity) if one considers that not all the benthos organisms were food for fish and crab. In this case under moderate fishing, such a situation can, evidently, be indefinitely continued.

FISHING

By the early 1960, the total catch in the Okhotsk Sea reached approximately 1 mln tons (Fig. 2). Herring, flatfish, salmon and crab were the most common species in the catch. In the second half of the 1960s, the volume of the catch of salmon and flatfish decreased but the catch of herring and, especially, pollock increased. The pollock became the most abundant of the species caught of all the fish species taken together. After the 200 mile fishing zone was introduced the access of foreign fleets to Russian waters was limited and the catch in the Okhotsk Sea decreased by approximately two times. By the mid-1980s, the Russian fishery had increased and stocks increased as a consequence of raising the natural reproduction efficiency as well as relaxation of the fishing pressure in the second half of the 1970s, the total catch in the Okhotsk Sea reached 2.6 mln. t., almost the 1975 level. This increase was related to the increased pollock catch and, to lesser degree, from other stocks which were, at the time, at a good level (salmon, cod, flatfish, crab).

In the early 1990s, fishery conditions worsened in most of areas of the Russian economic zone. In the Okhosk Sea, the catch remained stable until 1993 when the level declined from a maximum of 2.5-2.6 mln. tons to the present reduction of the catch by approximately 0.5 mln. t which was largely related to decreased pollock abundance. It is not inconceivable that the lost income from the pollock fishery can not be replaced by other species such as herring, cod, flat fishes, safron cod, crab, capelin and other species. Total catch in the Okhotsk Sea could be maintained at about 2 mln. t or somewhat higher if an increase of the Gizhigin and Sakhalin herring stocks were to take place. The Okhotsk Sea and adjacent waters will remain a major fishing area of Russia.

The research described in this publication was funded partly by Grant N N49300 from the International Science Foundation and the Government of Russia.

REFERENCES

Dulepova E.P., and L.A. Borets. 1990. Composition, trophic structure and productivity of the demersal communities in the Okhotsk Sea. Izvestia TINRO. 111:39-49.

Dulepova E.P., and L.A. Borets. 1994. Productivity and trophic relation between elements of demersal communities on the West Kamchatka shelf. Biologia morya. 20(5):359-364.

Shuntov V.P. 1984. Biological resources of the Okhotsk Sea. Agropromizdat, Moscow. 224 p.

Shuntov V.P. 1994. Once again on the problem of global warming and its impact on the Far-Eastern Seas biota. Vestnik DVO. 20:436-442.

Shuntov V.P., and E.P. Dulepova. 1993. Biological balance, present state of biological and fish productivities of the Okhotsk Sea ecosystem and elements of its functioning. (Gidrometeorologia and Hydrochemistry of Seas. Sea of Okhotsk). St.Peterburg: Gidrometeouzdat, 9(2):81-93.

Shuntov V.P., A.F. Volkov, O.S. Temnykh, and E.P. Dulepova. 1993. Alaska pollack in the ecosystems of the Far-Eastern Seas. TINRO, Vladivostok. 426 p.

TABLES AND FIGURES

Table 1. Elements of annual energetic balance (kkal/sq.m) of the Okhotsk Sea ecosystem.

Elements	Biomass	Production		K	K_2	U	Elements of energetic balance				
	mln.tons	mln.tons	g/sq.m.	kkal/g			P	A	C	R	F
Phytoplankton	-	15,100	9,450	0.7	-	-	6,615	-	-	-	-
Bacterioplankton	-	5,200	3,307	1	0.32	-	3,307	10,334	10,334	7,027	-
Protozoa	-	2,100	1,350	0.9	0.55	0.6	1,215	994	2,209	3,618	1,472
Non-predatory zooplankton	314	2,520	1,678	0.7	0.4	0.6	1,174	2,235	4,891	1,761	1,965
Predatory zooplankton	115	480	320	0.8	0.35	0.8	256	731	914	535	205
Non-predatory zoobenthos	208.6	318	201	0.3	0.3	0.5	60.3	201	402	141	201
Predatory zoobenthos	21.4	22.1	14	0.3	0.3	0.5	4.2	14	28	9.8	14
Pelagic fishes	31.5	1.7	9.9	1	0.3	0.8	9.9	33	41.3	23.1	8.3
Demersal fishes	3.5	1.7	1.08	1	0.2	0.7	1.08	5.4	6.8	4.3	1.4
Demersal invertebrates	1.5	0.5	0.32	0.5	0.35	0.8	0.158	0.45	0.56	0.58	0.2
Squids	2	7	4.4	0.8	0.35	0.8	3.5	10	12.5	6.5	2.5
Marine birds	0.012	0.004	0.003	1	0.15	0.8	0.003	0.02	0.025	0.017	0.005
Mammals	0.5	0.1	0.07	1	0.15	0.8	0.07	0.47	0.58	0.4	0.1

Note: K - calorific value
K_2 - net growth efficiency
U - digestion efficiency
P - annual production
A - assimilated part of annual ration
C - annual ration
R - respiration
F - non-assimilated part of annual ration

Table 2. Biomass (g/sq.m) of dimensional fraction of zooplankton in the epipelagical of the southern part of Okhotsk Sea (to south of 51°N) during summer in 1980-1990s.

Dimensional groups of plankton (fractions)	1986	1987	1988	1991	1992	1993	1994
Small	8.4	35.0	26.0	19.0	17.5	9.8	15.1
Middle	20.0	18.6	40.0	10.1	25.0	20.0	12.5
Large (macroplankton)	208.9	122.8	194.8	144.8	186.9	178.8	188.2
Total	237.3	176.4	260.8	173.9	229.4	208.6	215.8

Table 3. Biomass (g/sq.m) of major groups of macroplankton in the epipelagical of the southern part of Okhotsk sea (to south of 51°N) during summer in 1980-1990s.

Groups	1986	1987	1988	1991	1992	1993	1994
Euphausids	48.0	34.0	26.7	77.8	23.7	76.8	77.9
Copepods	120.0	53.0	113.7	31.2	52.0	26.6	63.4
Hyperiids	11.4	4.4	4.9	5.1	18.2	12.2	13.1
Saggitas	28.0	24.1	45.8	29.5	87.6	53.0	32.6
Other	1.5	7.3	3.7	1.2	5.4	10.2	1.2
Total	208.9	122.8	194.8	144.8	186.9	178.8	188.2

Table 4. Biomass (g/sq.m) and production (g/sq.m) of zooplanktonal fraction of predatory plankton (%) in the West Kamchatka Area in summer, 1980-1990s.

Indices	1986	1987	1988	1991	1992	1993	1994
	to the north 54 N						
Total biomass	278	243	532	80	183	-	315
Fraction of predatory zooplankton	15.5	22.6	19.6	23.0	31.0	-	42.0
Production of unpredatory zooplankton	1591	990	2699	472	501	-	533
Production of predatory zooplankton	121	171	372	61	222	-	501
	to the south of 54 N						
Total biomass	212	136	235	198	252	220	340
Fraction of predatory plankton	21.0	32.0	32.0	41.0	26.0	27.0	56.0
Production of unpredatory plankton	654	348	481	486	645	442	726
Production of predatory zooplankton	120	123	293	284	264	186	717

Table 5. Density of nekton (t/sq.m) in the upper epipelagical (0-50m) in Okhotsk Sea (to the south of 53°N) in 1990s).

Nekton groups	1991	1992	1993	1994
Fishes	1.70	1.76	1.0	1.29
Squids	0.10	0.06	0.16	0.08

Table 6. Biomass (thousand tons) and ratio (%) of fishes in the epipelagial of the northeastern part of Okhotsk Sea in September-October 1994.

Species and groups	Thousand tons	%
Salmons	40	0.63
Alaska pollack	3336	52.70
Herring	2276	35.90
Capellin	79	1.22
Spiny lumpfishes	18	0.30
Smooth-tonque	517	8.20
Other mesopelagic fishes	25	0.39
Sakhalin flounder	23	0.36
Other fishes	19	0.30
All fishes	6333	100.0

Table 7. Biomass and production (mln.tons) of the demersal fishes and invertebrates on the West Kamchatka shelf in 1980s (Dulepova and Borets; 1990,1994).

Index	The early 1980s	The late 1980s
Biomass of:		
Fishes	0.82	1.9
king crab	0.3	0.5
predatory benthos	3.1	3.1
unpedatory benthos	17.1	17.1
Production of benthos	27.0	27.0
Consumpion of benthos by fishes and predatory invertebrates	16.0	22.0

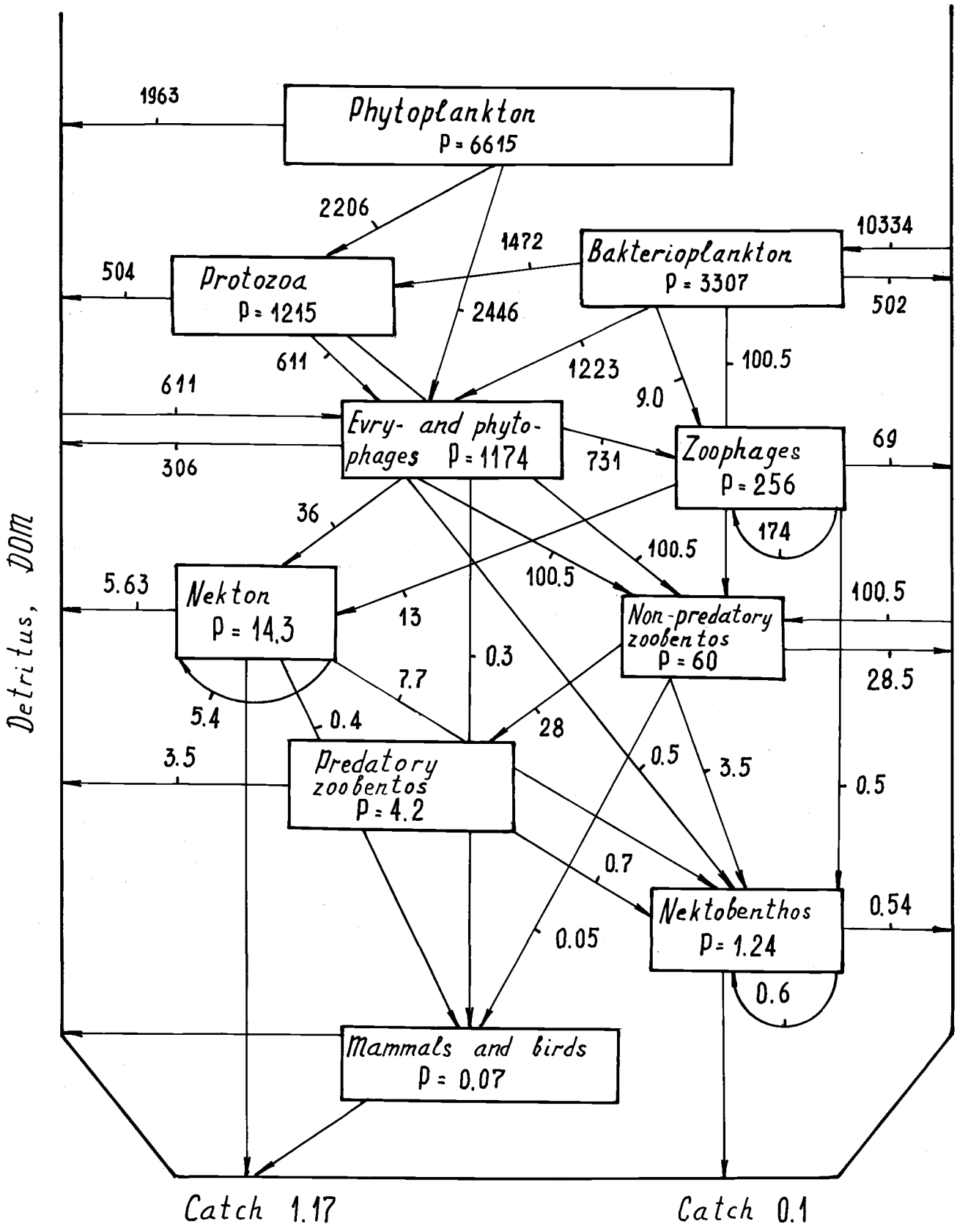

Fig. 1. Scheme of the substance flows (mln.t) in the Okhotsk Sea ecosystem in 1980s.

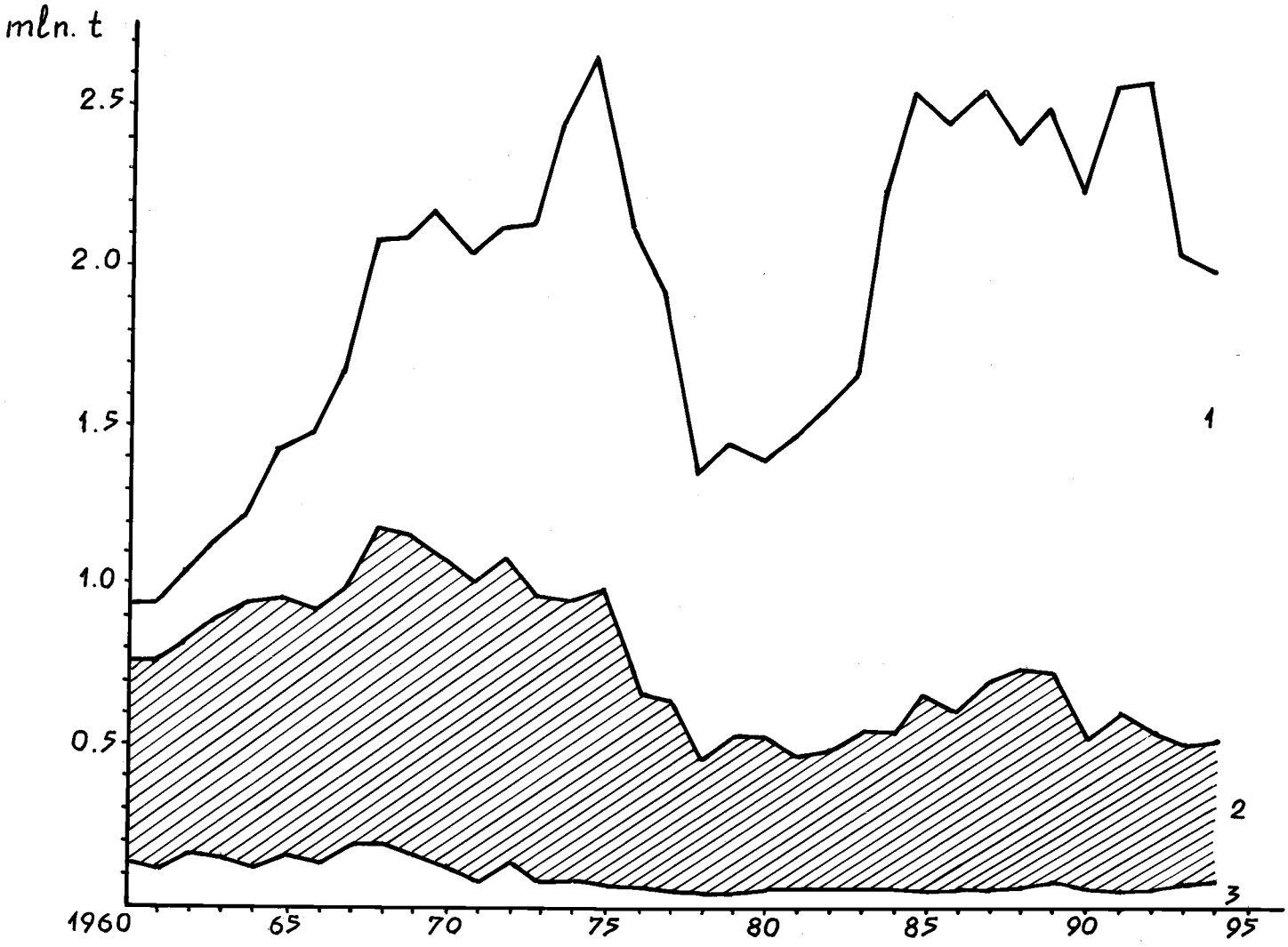

Fig. 2. Dynamic of catching (mln.t) of fish and other objects in the Okhotsk Sea after 1960.

1 - Alaska pollock 2 - other fishes 3 - other objects

Influence of some Abiotic Factors on Spatial Population Dynamics of the West Kamchatka Flounders (*Pleuronectidae*)

Yuri P. DIAKOV

Kamchatka Fisheries and Oceanography Research Institute Naberezhnaya
18 Petropavlovsk-Kamchatskii, 683002 Russia

Flounders, inhabiting the waters of West Kamchatka are currently the most important commercial species. The total catch increased from 30 to 55 thousand tons in an unregulated fishery. The commercial species of flounders, except halibut, are yellowfin sole, Alaska plaice, Sakhalin flounder, longhead dab, flathead sole, starry flounder and rock sole. Often inhabiting in the same regions, these species form a complex group. Various interspecific relationships and common biological features are tipical for the group.

The dynamic characteristics of flounder populations (distribution, migrations) are explored by many investigatiors (Moiseev, 1953; Polutov, 1958; Fadeev, 1971, 1987). This study estimates the influence of dynamic factors on fish distribution and migration on the annual cycle.

Two aspects of distribution of the above species are considered in the paper:

1. To define the influence of population density of each species on depth and temperature in different seasons, and to recognize the influence of these factors on fish distribution.
2. To determine the degree of habit coincidence of flounder which will give the opportunity to explore their interspecific competition. The results allow estimates of directed catch for certain species and to develop methods to determine commercial aggregations.

MATERIALS AND METHODS

Samples were collected by a bottom trawl survey on the shelf of West Kamchatka in 1973-1990. About 1,200 trawls samples were collected during the period. To ascertain population density, fish catch per unit effort is transformed into a relative number. The number is represented as the percent of the total catch per effort in a certain month and a year. Later a corresponding average value for each month for the years of the survey is estimated. The information obtained was used to characterize fish aggregation density in connection with three factors: depth (interval - 20 metres), temperature of water on the bottom (interval - 0.5°C) and latitude (interval - 15`).

RESULTS AND DISCUSSION

The distribution of West Kamchatka flounder in the seasonal cycle is typical of the distribution within limits of the depth and the temperature of water on the bottom. All flounder species examined were mostly concentraded at depths of 90 to 250 metres in winter (January-February) and in the shallows from 20 to 160 metres in spring due to seasonal migrations from deep waters to shoal waters. Quite different optimum temperature conditions for most of the West Kamchatka species are found during three time periods: winter-spring (January-May), summer (June-July) and summer-autumn (August-September). Four relatively stable periods of flounder distribution are found with various

combination of bathymetric and thermic conditions. These periods are as follows: winter (January-February), spring (April-May), summer (June-July) and summer-autumn period (August-September).

Analysis of the data indicate that there are common and specific features of flounder distribution for various species. Regular bathymetric distribution in different seasons is typical for flatfishes examined, except for the deepwater and cold water species: Sakhalin flounder and flathead sole. In winter, the flounders density decreases gradually with the depth. The nature of the relationship resembles a normal distribution. The dependence of population density on depth changes sharply in spring-summer, summer and summer-autumn periods. The most fish aggregations are marked on the shallows and decrease gradually as the depth increases (Figs. 1 (1, 2, 4, 6, 7)). Sakhalin flounder and flathead sole did not show variations of bathymetric distribution in various seasons. Flathead sole population density change a bit but it is independent of the season and depth (Figs. 1 (5)). Sakhalin flounder extend their range of depth in summer-autumn period which is typical for the species(Figs. 1 (3)).

West Kamchatka flounders population density varies greatly in different seasons with the water temperature on the bottom. In winter and in spring, all species form the most dense aggregations in 0 - +1°C water temperature. In summer, when the water warms, flounders are found in a broader thermic range and did not appear to prefer any particular temperature. Coldwater species, Sakhalin flounder and flathead sole, however, prefer waters of -1 - +2°C (Fig. 2).

The distribution of most West Kamchatka flatfish is related to depth during spring migration. In April-May the variation of flatfish density aggregations is closely related to the bathymetric gradient. In winter as well as in summer and summer-autumn the depth affects flatfish distribution the least. This is more typical for the three shallow species: longhead dab, yellowfin sole and Alaska plaice, and less for deep water species: Sakhalin flounder and flathead sole. The dependence of aggregation density on depth is not marked for Sakhalin flounder and flathead sole. Rock sole and starry flounder did not aggregate with depth gradient in winter but are found to do so in summer.

The temperature influence on West Kamchatka flatfish population density for four species: yellowfin sole, longhead dab, flathead sole and starry flounder is defined by the temperature layer on the bottom in winter and during spring migration. The dependence of flatfish distribution on the temperature for Alaska plaice, Sakhalin flounder and rock sole greatly increases during spring months compared with the winter period. The influence of temperature on flatfish distribution decreases sharply for the summer months as catches are similar throughout the temperature range. Thus, the results indicate that West Kamchatka flatfish distribution is influenced by the variability of habitat conditions observed. If the formation of flatfish concentrations is mainly dependent on water temperature in the home range in winter and during spring migration, the role of depth increases greatly as it defines fish distribution and the distance traveled.

During summer feeding the influence of the depth and water temperature, in particular, decreases. Probably fish distribution and behaviour is more related to the of food supply abundance and distribution.

Cluster analysis is used to determine the degree of habit competition among the different species during the year. Each row of fish population density distribution is compared separately to all other rows, depending on the depth, water temperature and latitude. In order to obtain quantative values for the degree of habit coincidence, methods developed by Zhivotovsky are used to analyze morphometric characters. The pair-group method by Baily (1970) is used to determine the population habit coincidence.

Based on the analysis of the data there are three flatfish ecological nitches relative to the habit conditions using a hierarchic approach (Fig. 3). Shallow and warm water species occupy one nitche: yellowfin sole, longhead dab, Alaska plaice and starry flounder. The yellowfin sole and longhead dab which belong to the genus Limanda are closely ecologically related (Fig. 3 (1)). The other nitche includes the deep sea and cold water species: Sakhalin flounder and flathead sole (Fig. 3 (2)). And, finally, the third group is represent by rock sole (Fig. 3 (3)). Deep but limited aggregations of rock sole are found on the southwest Kamchatka shelf. Rock sole is seldom found north to 53°N.

Assuming all flounder species occupy a specific ecological nitche, then indirect evidence of the competition between them can be considered. Likely strong competition occurs among species from the same or close nitches than for species from desperate nitches. The most adaptable species will increase in this case oppressing the other ecologically similar species. Yellowfin sole is the most abundant flatfish in the first group (Fig. 3), and longhead dab which is ecologically similar is not very abundant. Alaska place and starry flounder are not abundant though they are more abundant than longhead dab.

In the second group, Sakhalin flounder is abundant on the shelf while flathead sole abundance is in deeper water. And finally, rock sole form a separate group of high abundance in the southwest Kamchatka coast as evidenced from commercial exploitation.

REFERENCES

Beily, N. 1970. Mathematics in biology and medicine. M: Mir. 326 p. (in Russian)

Zhivotovsky, L.A. 1979. Population similarity measure for polymorphic characters. Journ. of Gen. Biol. 4:587-602. (in Russian)

Moiseev, P.A. 1953. The cod and flounders of Far-East Seas. Izv. TINRO. 15:1-288. (in Russian)

Polutov, I.A. 1958. Stock condition and fishery of Yellowfin sole at the West Coast of Kamchatka. Techn.-econ. bull. of Kamchatka Sovnarkhoz. 2-3:8-12. (in Russian)

Fadeev, N.S. 1971. Biology and fishery of Pacific flounders. Vladivostok. 100 p. (in Russian)

Fadeev, N.S. 1987. North-Pacific flounders. M: Agropromizdat. 176 p. (in Russian)

Masuda, H., K. Amaoka, C. Araga, T. Uyeno, and T. Yoshino. 1984. The Fishes of the Japanese Archipelago. Tokai University press. Text - 456 p., Plate - 378 p.

FIGURES

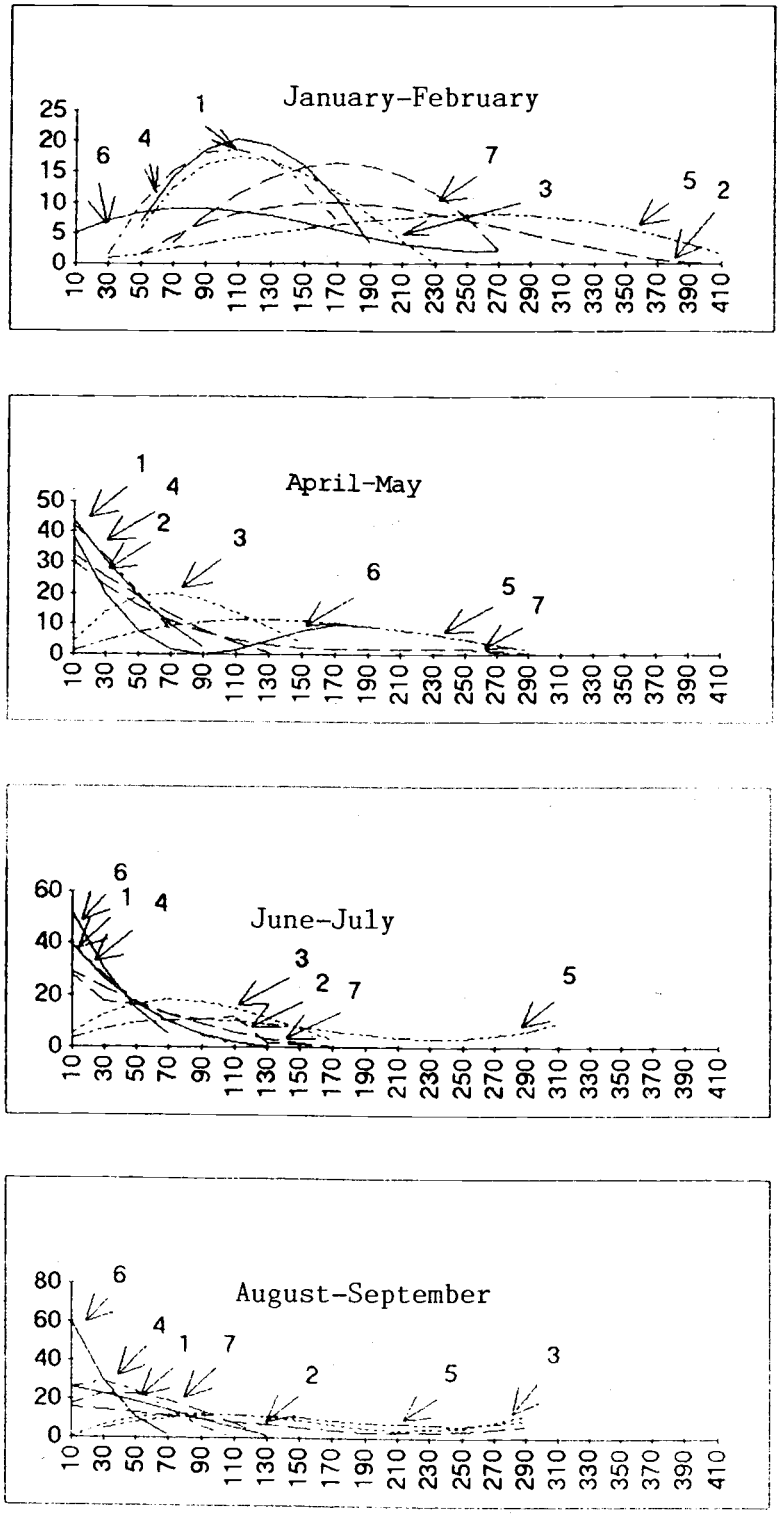

Fig. 1. Density dependence of flounder populations on depth.
1 - yellowfin sole 2 - Alaska plaice 3 - Sakhalin flounder 4 - longhead dab
5 - flathead sole 6 - starry flounder 7 - rock sole

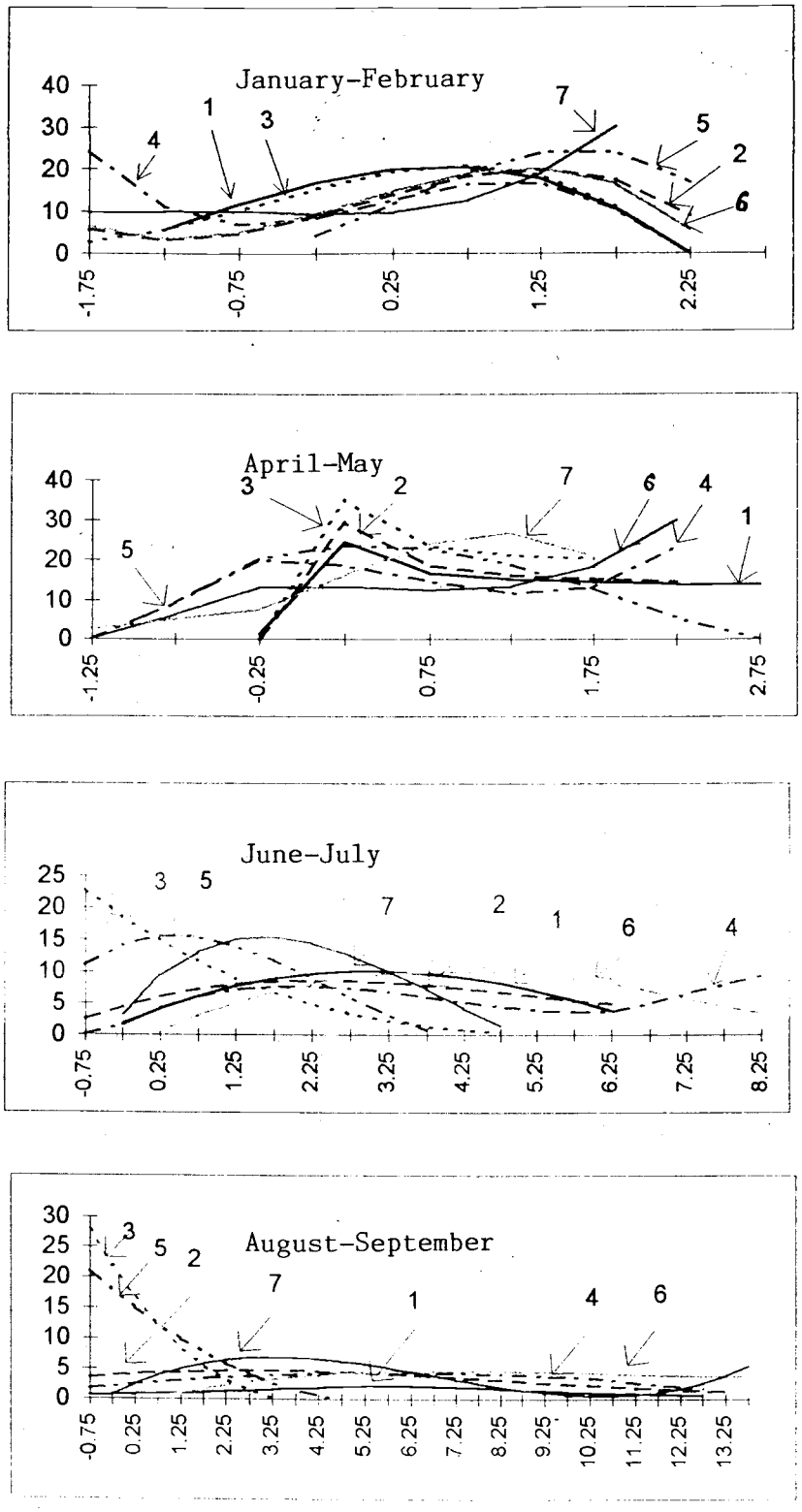

Fig. 2. Density dependence of flounder populations on water temperature.
1 - yellowfin sole 2 - Alaska plaice 3 - Sakhalin flounder 4 - longhead dab
5 - flathead sole 6 - starry flounder 7 - rock sole

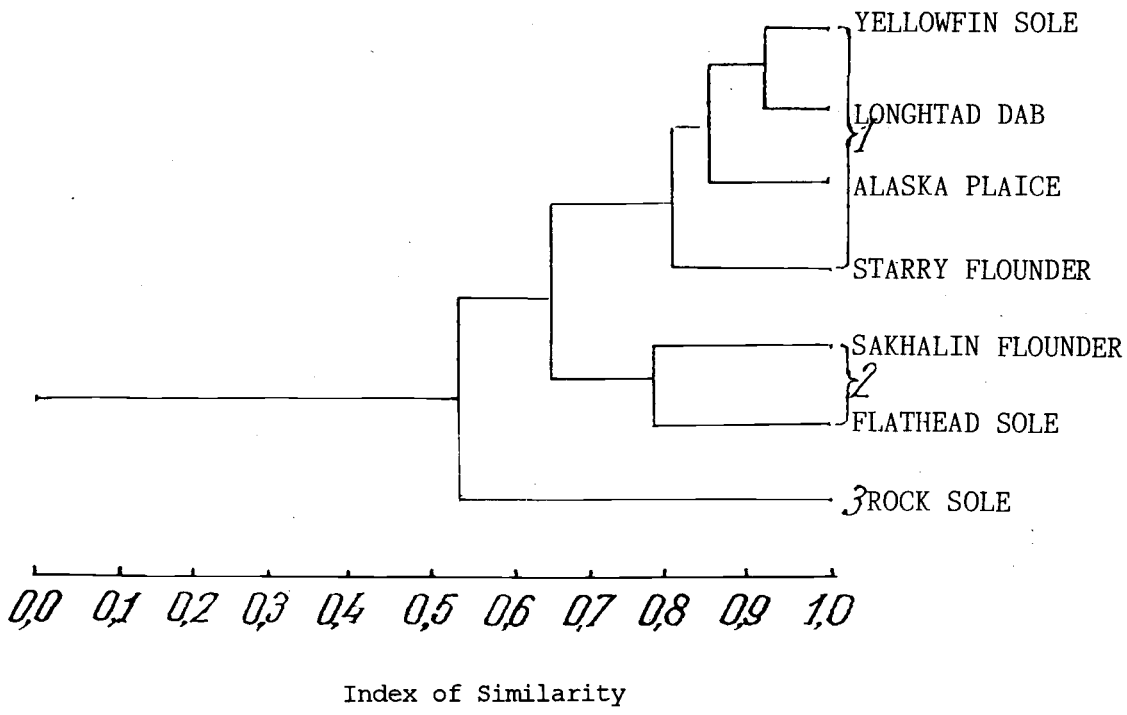

Fig. 3. The cluster of area similarity of flounders' population.

An Examination of Age Estimates of Walleye Pollock (*Theragra chalcogramma*) from the Sea of Okhotsk using the Burnt Otolith Method and Implications for Stock Assessment and Management

Gordon A. McFARLANE[1], Richard J. BEAMISH[1] and Larisa M. ZVERKOVA[2]

[1] Pacific Biological Station, Dept. of Fisheries and Oceans, Nanaimo, B.C., Canada. V9R 5K6
[2] Sakhalin Regional Institute of Fisheries and Oceanography, Yuzhno-Sakhalinsk, 693016, Russia

ABSTRACT

In a previous study the first two authors examined age determination structures of walleye pollock, *Theragra chalcogramma*, from five stocks in the Northeast Pacific Ocean. We found that the burnt otolith section method consistently produced older age estimates. In this report we used this method to age walleye pollock sampled from the Sea of Okhotsk, and compared these results with ages estimated for the same fish using the otolith surface method. We also discuss how these estimates change our understanding of a number of biological parameters used in stock assessment, and also discuss the ecological implications.

INTRODUCTION

Up until the early 1980s age determination methodology was considered routine and accurate for aging all fish in a population. Unfortunately, few of these methods were validated. In 1983, the first two authors published a study which reviewed the accuracy of methods used to provide fish ages for fisheries stock assessment and management (Beamish and McFarlane 1983). The study was intended to emphasize the complexity of producing accurate ages and to discuss the consequences to assessments and management of relying on ages of uncertain accuracy. We found that in general fish were being underaged and that these age estimates had a substantial impact on estimates of growth and mortality that strongly influenced the development of management strategies.

In 1989 McFarlane and Beamish (1990) examined a number of structures which had been used to estimate the age of walleye pollock (*Theragra chalcogramma*) in the Northeast Pacific Ocean to determine, on a stock basis, which structure produced the most consistent pattern of growth and the most obvious annuli. In 1990, we extended this study to walleye pollock in the Sea of Okhotsk. The purpose of this report is to briefly review the results of our examination of age-determination structures from pollock in the Northeast Pacific Ocean, present the results of our examination of otolith surface and otolith cross-sections (burnt otolith method) from pollock from the Sea of Okhotsk, and comment on the implications for stock assessment and management of these stocks.

METHODS

A sample of 160 pollock was collected by trawl from the Sea of Okhotsk (off northeastern Sakhalin) in July, 1990. Each fish was measured for fork length and sex was determined. Paired sagitta otoliths were collected from each fish. Unfortunately, scales were not collected from these fish. Ages were estimated using both the surface and burnt cross section. Criteria for annulus identification are presented in Chilton

and Beamish (1982). In general, an otolith surface can be aged by immersing the otolith in water on a black background and examining it with a dissecting microscope using reflected light. Some otoliths have a cloudy or chalky surface inhibiting the identification of the growth zones. These zones may be made slightly more distinct by rapidly dipping the otolith in a weak solution of HCI (usually 20%) before placing it in the water.

Otolith cross sections are aged by breaking the otolith dorso-ventrally through the nucleus and burning one of the broken surfaces in an alcohol flame and painting the burnt surface with non-toxic mineral oil to enhance the contrast between growth zones. The annulus was defined as the translucent zone or the zone of slower growth that appeared as a dark zone under reflected light.

RESULTS AND DISCUSSION

McFarlane and Beamish (1990) indicated that the most appropriate structure or method or both for age determination may vary among stocks. Pectoral fin-ray sections, otolith surfaces and burnt otolith sections are all suitable structures for stocks consisting of mainly younger fish.

Annuli on scales from all areas appeared to be distinct. However, ages estimated from scales were similar to ages determined from other structures only for the youngest fish. For most stocks, the burnt otolith section consistently produced older age fish. For example, for pollock from the Aleutian area and the international waters of the Bering Sea (Donut Hole), more annuli were identified on the burnt otolith section (Figs. 1 & 2) than on other structures. All four methods produced different age compositions (Figs. 3a & b), which resulted in different estimates of length at age, growth and mortality (McFarlane and Beamish 1990).

For the Sea of Okhotsk stock, a similar pattern was found. The burnt otolith sections consistently produced older ages than ages estimated using the otolith surface method (Fig. 4) when older fish were present in the sample. For example, when the fish is young (Figs. 4a & b), both methods produce the same estimates, however as the fish ages, and growth of the fish is reduced, otolith growth occurs almost exclusively on the ventral surface of the otolith (Figs. 4d, f & h) resulting in a thickening of the otolith.

In order to identify the annuli, the otolith must be sectioned (broken) and burnt. As with the other stocks (McFarlane and Beamish 1990), the two methods produced different age compositions (Fig. 5) and growth curves (Fig. 6).

We recognize that the age estimates for pollock have not been proven to be accurate. However, we applied the same age determination criteria to the burnt sections of pollock as we applied to other species such as rockfish and sablefish. The older ages for those species have been shown to be correct (Bennett et al. 1982; Leaman and Nagtegaal 1987; McFarlane and Beamish 1995). In our study and in other studies comparing otolith surface and section readings (reviewed in Beamish and McFarlane 1987) it was shown that otolith burnt sections do produce older age estimates than otolith surface readings.

Accurate age estimates are important for determining a number of biological parameters used in our assessment models. In particular, accurate age estimates are required to determine growth, mortality rates and identify strong year classes. If this small sample is considered representative of Sea of Okhotsk pollock, then the natural mortality estimate from this area is lower than determined using the otolith surface ages. Ensuring accurate age determination is also important in identifying and measuring the strength of year classes of the stock. Misidentification of strong year classes would lead to a misunderstanding of the precesses which regulate a population, particularly the importance of environmental factors.

We would like to conclude this report with a few thoughts on the "ecological" consequences of understanding the population dynamics of a population. For example, what is the effect of truncating the age

distribution of a population? What are the long-term implications. If many individuals in the population would actually live to 25 or 30 years in an unfished stock then there had to be an advantage to a population having these old fish around ... clearly related to environment.

In an earlier paper we hypothesized that the length of life was related to the longest period of unfavourable conditions that the species encountered. Just the fact that pollock can live this old means there were such environmentally unfavourable periods. If this is true then our management strategies must consider that at some point these environmental conditions leading to poor survival of pollock will reoccur. If we truncate the age structure then we are becoming the agents of natural selection - and we are selecting for fish that optimize their survival under heavy fishing pressure as opposed to natural selection which selects for survival of the species in an environment that has extreme fluctuations in the physical or biological conditions.

What happens to these "truncated" stocks when the extreme environmental changes occur. Notice we said when, not if. It is inevitable that these changes will occur. We believe that accurate ages of walleye pollock will indicate that in general our management of fisheries must be conservative both because mortality rates are lower (stocks less productive) and there needs to be enough fish to survive periods of poor conditions.

REFERENCES

Beamish, R.J., and G.A. McFarlane. 1983. The forgotten requirement for age validation in fisheries biology. Trans. Am. Fish. Soc. 112:735-743.

Beamish, R.J., and G.A. McFarlane. 1987. Current trends in age determination methods, p.15-42. *In* R.C. Summerfelt and G.E. Hall [ed.] Age and growth of fish. Iowa State University Press, Ames, Iowa.

Bennett, J.T., G.W. Boehlert, and K.K. Turekian. 1982. Confirmation of longevity in *Sebastes diploproa* (Pisces: Scorpaenidae) from $^{210}Ph/^{226}$ Ra measurements in otoliths. Marine Biology. 71:209-215.

Chilton, D.E., and R.J. Beamish. 1982. Age determination methods for fishes studied by the groundfish program at the Pacific Biological Station. Can. Spec. Publ. Fish. Aquat. Sci. 60, 102 p.

Leaman, B.M., and D.A. Nagtegaal. 1987. Age validation and revised natural mortality rate for yellowtail rockfish. Trans. Am. Fish. Soc. 116:171-175.

McFarlane, G.A., and R.J. Beamish. 1990. an examination of age determination structures of walleye pollock (*Theragra chalcogramma*) from five stocks in the Northeast Pacific Ocean, p.37-56. *In* L.L. Low [ed.]. Proceedings of the Symposium on Application of Stock Assessment Techniques to Gadids. International North Pacific Fisheries Commission Bulletin 50.

McFarlane, G.A., and R.J. Beamish. 1995. Validation of the otolith x-section method of age determination for sablefish using O.T.C. p.319-370. *In* D.H. Secor, J.M. Dean, and S.E. Campana [ed.] Recent developments in fish otolith research. Univ. South Carolina Press, Columbia, South Carolina.

FIGURES

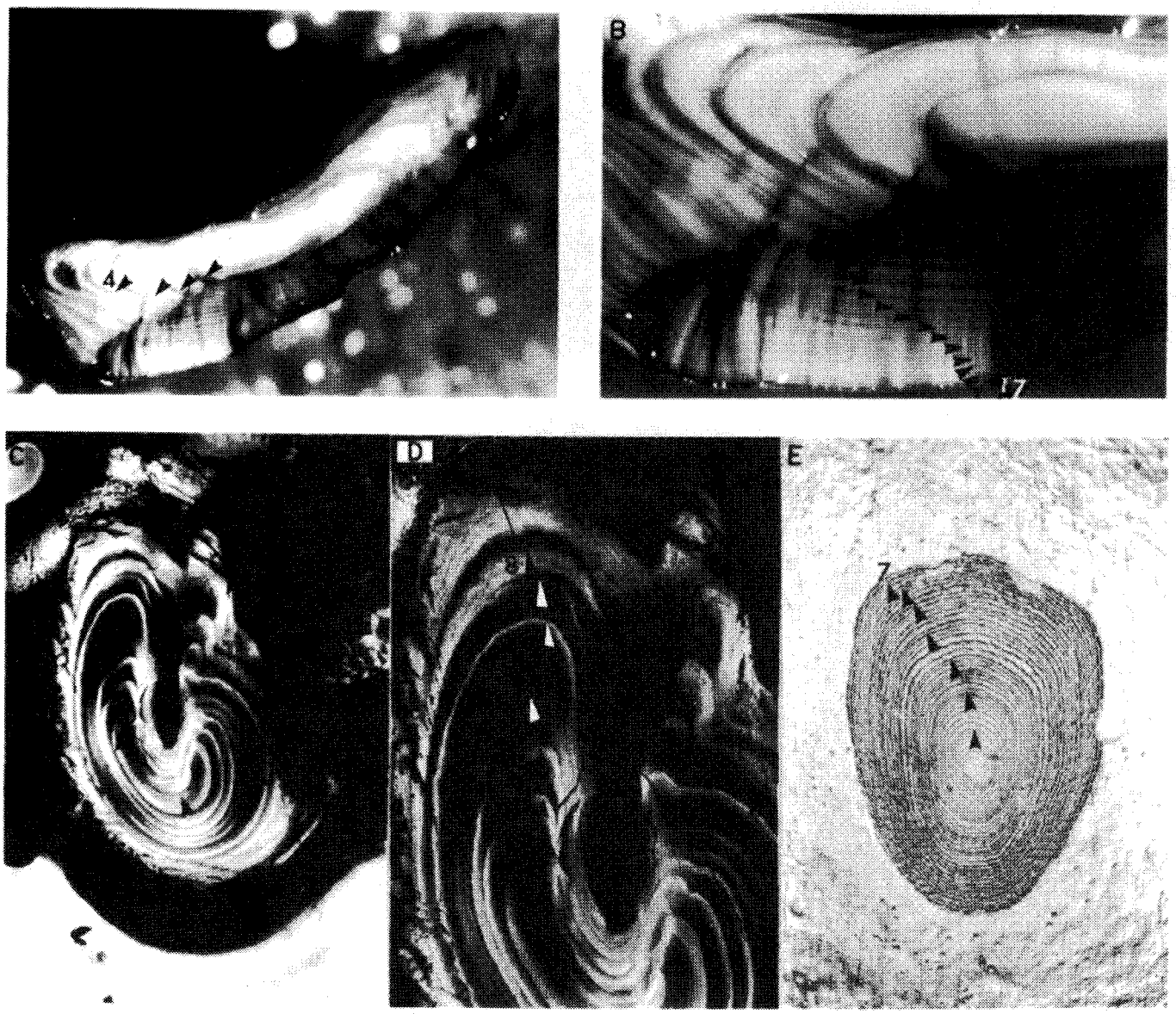

Fig. 1. Structures used for age determination collected from a 49 cm walleye pollock captured in the eastern Bering Sea (Aleutian area). A and B: Burnt otolith section showing 17 annuli. C and D: Pectoral fin ray showing 8 annuli and a large area between 8th annulus and the edge where annuli could not be identified. E: Scale showing 7 annuli. The otolith surface age was 10+.

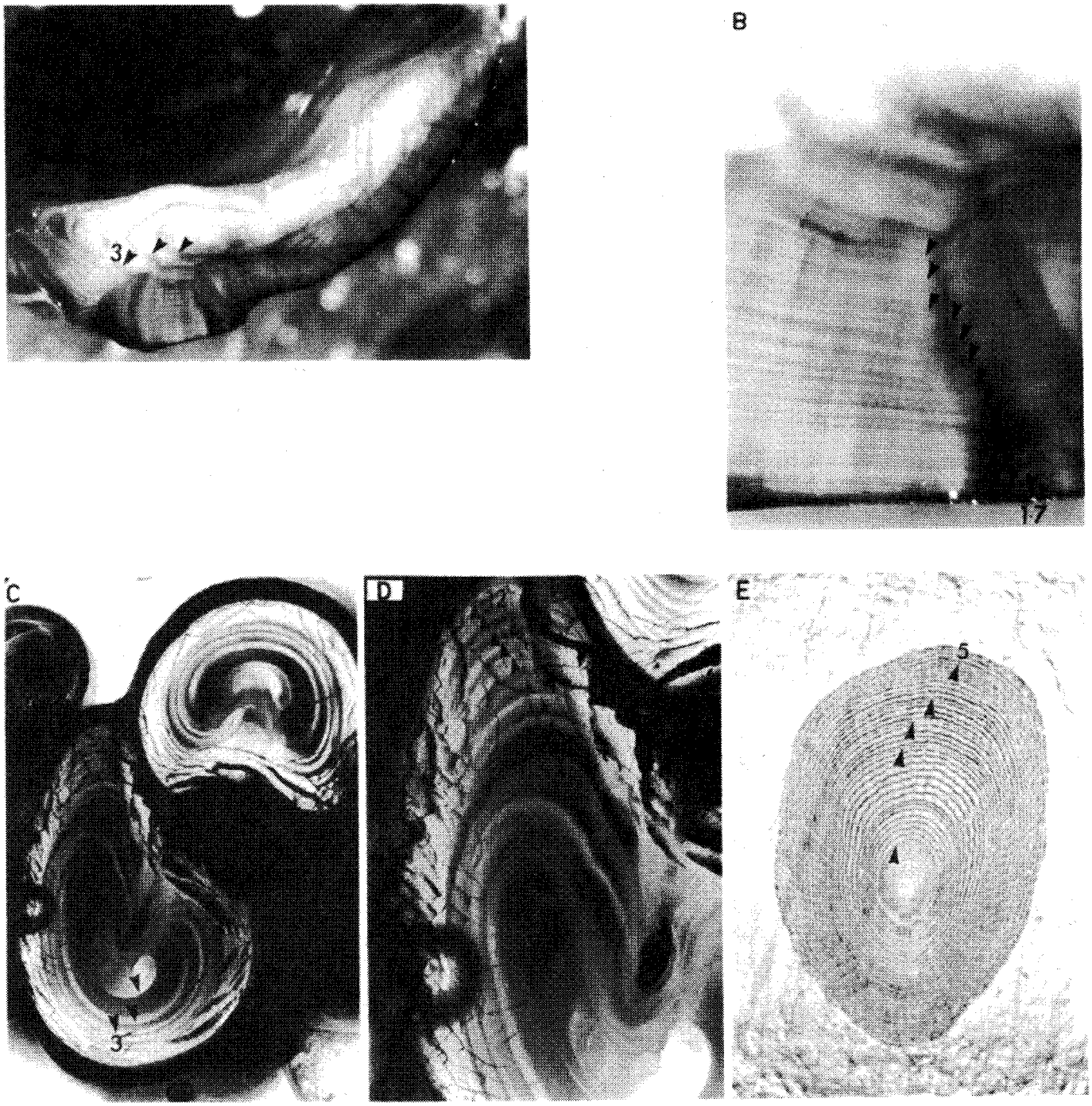

Fig. 2. Structures used for age determination collected from a 50 cm walleye pollock captured in the international waters of the Bering Sea (Donut Hole). A and B: Burnt otolith section showing 17 annuli. C and D: Pectoral fin-ray section showing 12 annuli. E: Scale showing 5 annuli. The otolith surface age was 11+.

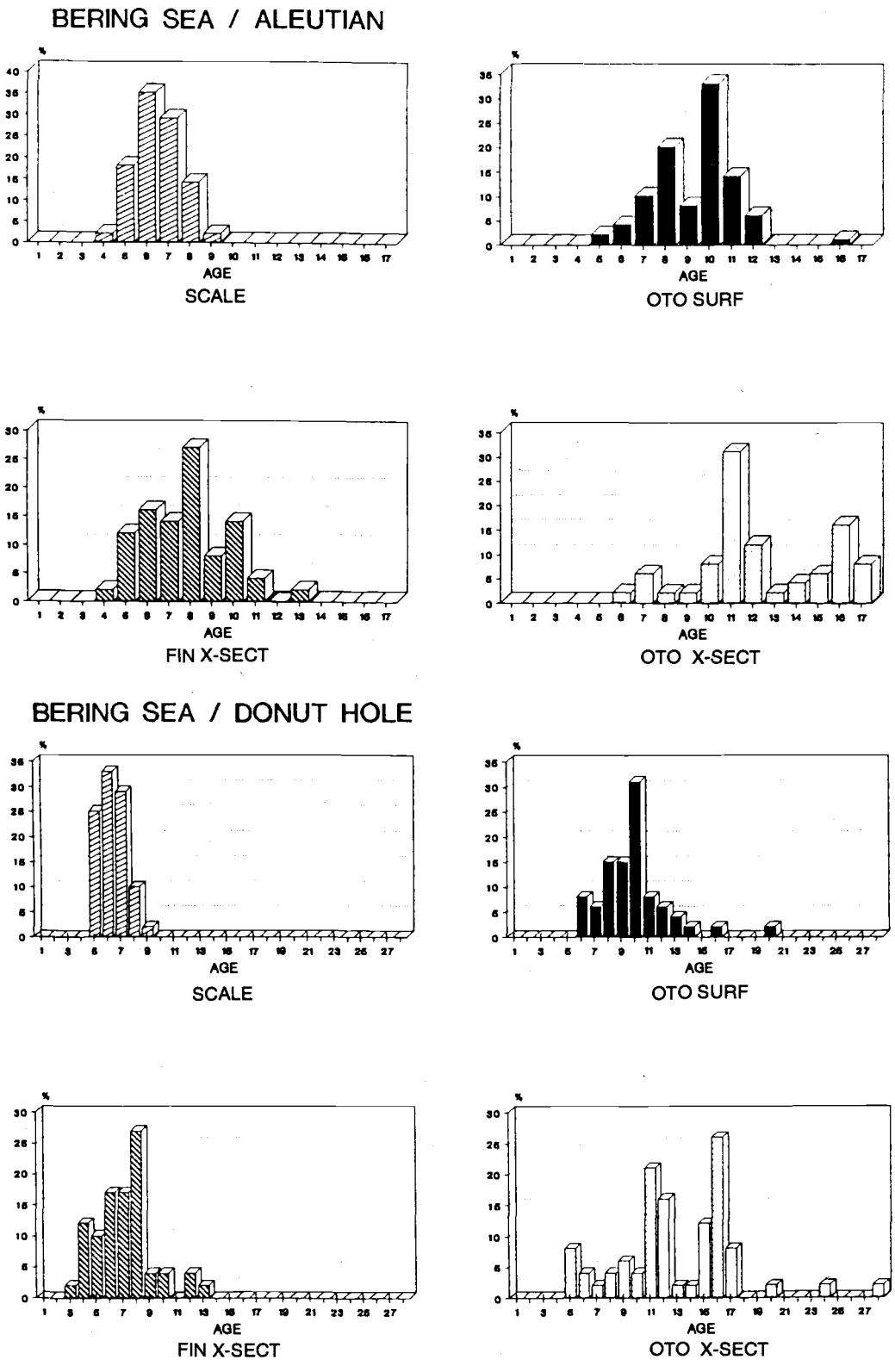

Fig. 3. Age compositions produced using the four ageing methods for the Bering Sea (Aleutian) area and the Bering Sea (Donut Hole) stocks.

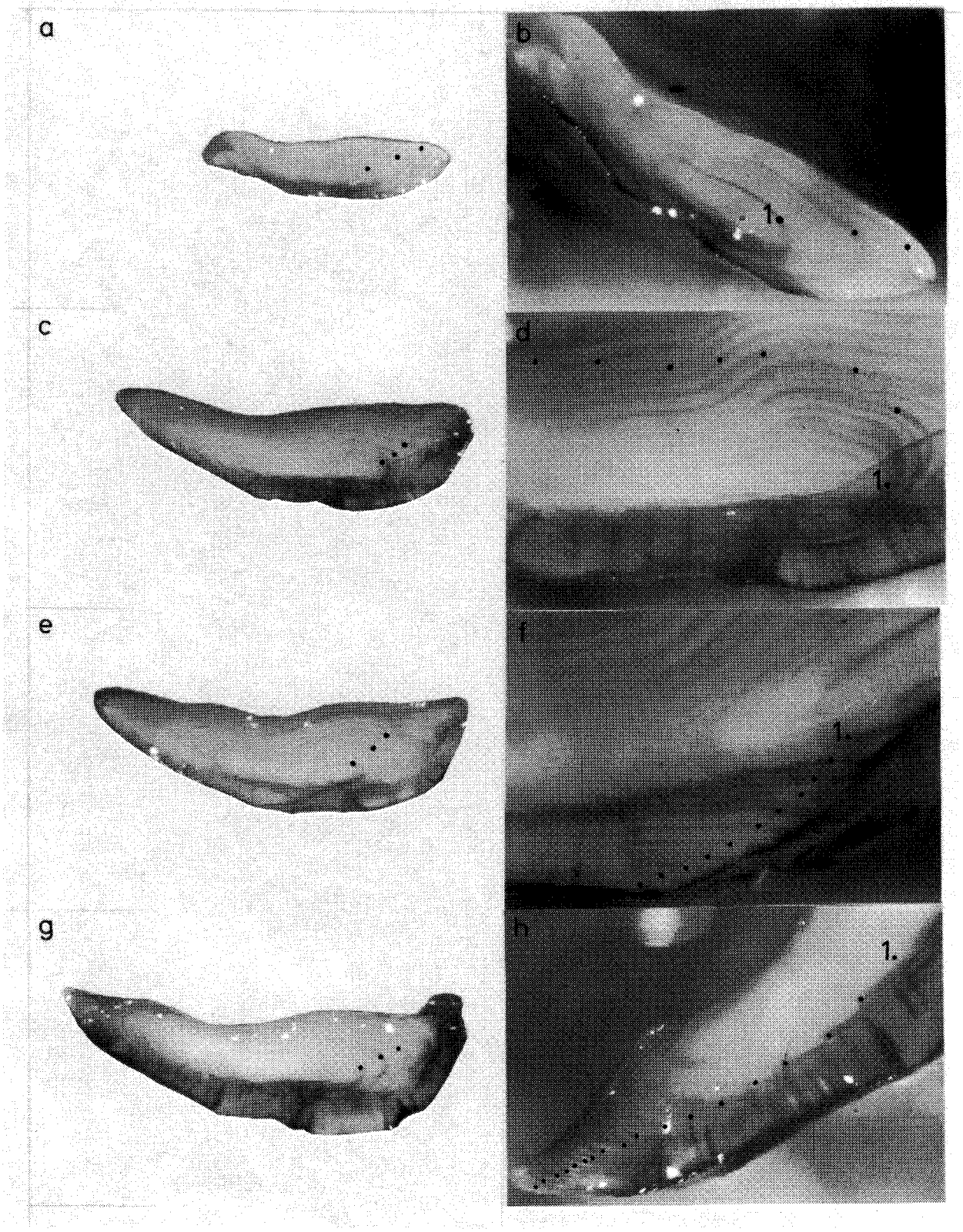

Fig. 4. Otolith burnt sections for walleye captured in the Sea of Okhotsk in July 1990. A and B: A 30 cm male showing 3 annuli, otolith surface age was also 3+. C and D: A 46 cm female showing 8 annuli, otolith surface age was 6+. E and F: A 53 cm male showing 11 annuli, otolith surface age as >3+ (difficult to interpret). G and H: A 57 cm female showing 18 annuli, otolith surface age was >5+ (difficult to interpret).

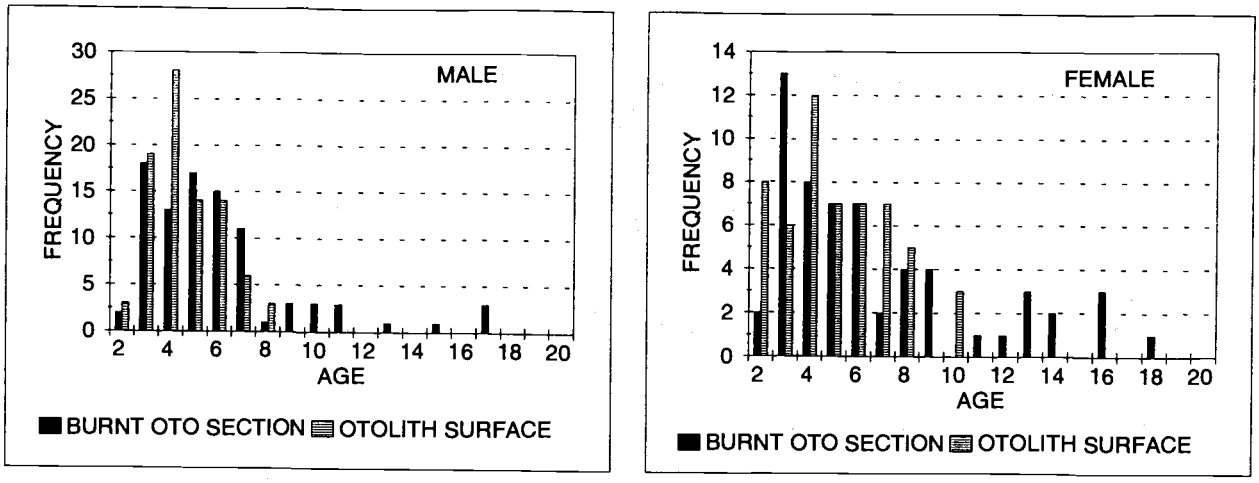

Fig. 5. Age compositions produced for Sea of Okhotsk walleye pollock using the burnt otolith section method and otolith surface method.

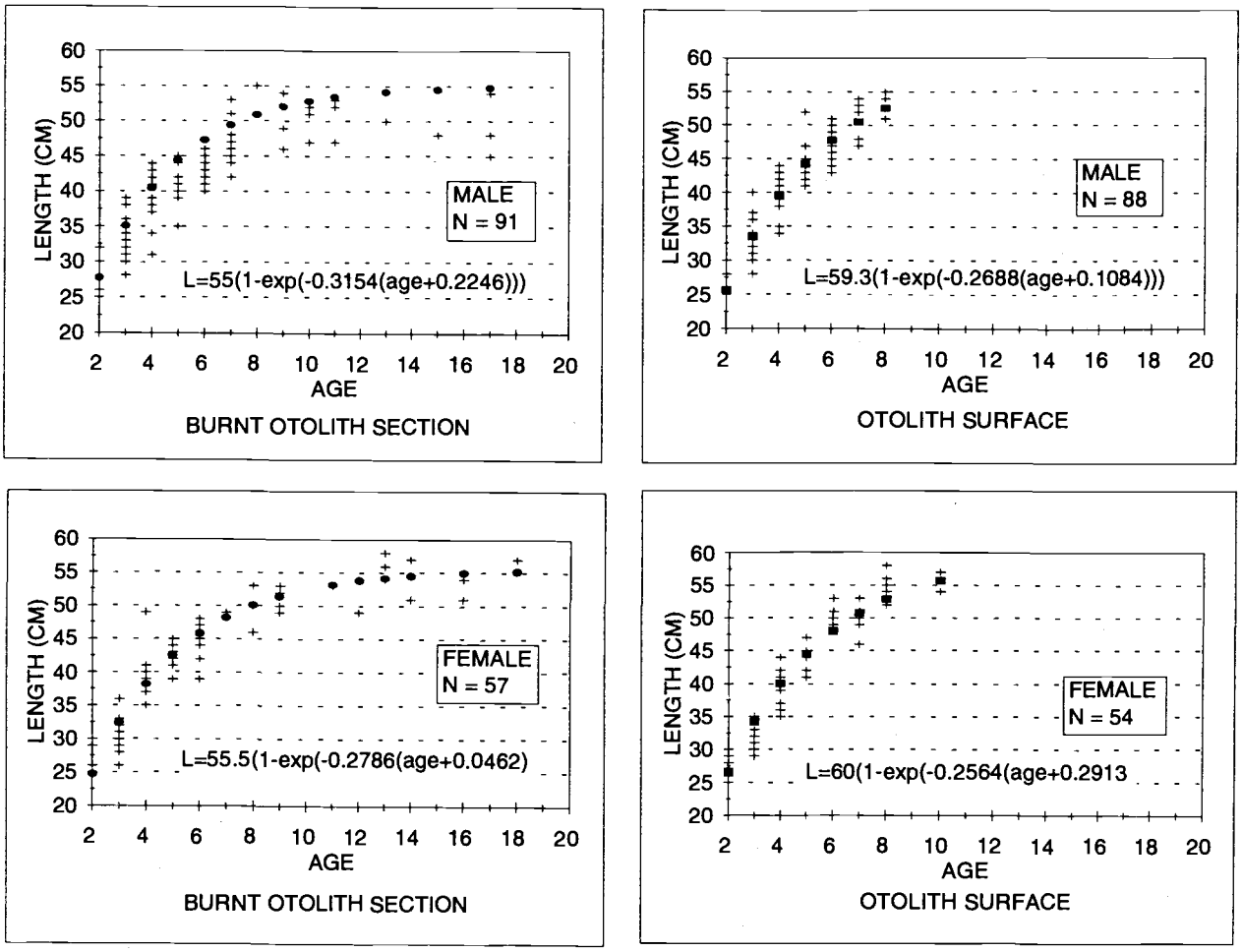

Fig. 6. Growth curves for male (upper panel) and female (lower panel) walleye pollock from the Sea of Okhotsk produced using the burnt otolith section method and the otolith surface method.

Migration of Greenland Turbot (*Reinhardtius hippoglossoides*) in the Okhotsk Sea

Larisa P. NIKOLENKO

Pacific Research Fisheries Centre (TINRO-Centre), Vladivostok, Russia

The Sea of Okhotsk Greenland turbot annual catch has been 15-19 thousand tons since 1976. The ecology of the species is not well understood, particular, the distribution of larvae and young up to three years old and during the pelagic phase. This information would be useful to better manage the fishery. This paper presents an analysis of ichthyoplankton survey data from surveys in 1984-1987, pelagical surveys 1985-1993 and botton surveys 1963-1993.

The analysis showed that Greenland turbot with mature gonads (stages IV-V, V, V-VI) occurred along the continental slope of western Kamchatka, northern Okhotsk Sea and northeastern Sakhalin. The most intensive spawning occurred in TINRO basin, where catches were 10-25 per hour trawled but some catches exceeded 50 (Fig. 1A). The Lebed trough and Tinro basin are import for commercial fishing which was confirmed by data collected by scientific observers on fishing vessels in October-November, 1985. Almost all spawning was concentrated in these two areas (Fig. 1B). The northeast Sakhalin slope is of secondary importance, where some catches reached 25 per hour trawled but the majority of catches did not exceed 10. In other areas, spawning individuals were rare from 1 to 10 per hour.

Larvae of Greenland turbot from 17 to 24.2 mm were caught in the epipelagic zone. The larvae were distributed over the north of the Sea of Okhotsk and some specimens were collected near the Kuril Islands (Fig. 2). High concentrations were found in the TINRO basin and near the northeastern Sakhalin coast.

Twelve to 15 cm fingerlings were caught while trawling from 0-60 m above the 60 to 190 m depth. There was a significant difference in the distribution of larvae and fingerlings. Fingerlings were found in Terpeniya Bay, Shelikhov Bay and adjacent waters as well as the nearshore of southwest Kamchatka (Fig. 3). The highest catches of 7-8 cm (100 or more) specimens were in Shelikhov Bay and adjacent shelf waters of northwest Kamchatka. In waters adjacent to southeast Sakhalin, fingerlings were rare, less than 10 per trawl.

The distribution of larvae and fingerlings was related to the main currents of the Sea of Okhotsk. Larvae from TINRO basin were carried by the current along the continental slope of northwest Kamchatka (the north branch of the West Kamchatka current) to Shelikhov Bay (Markina and Chernyavskyi, 1984). The origin of the Sakhalin fingerlings was probably from mixed eggs and larvae carried by the middle current from the northern part of the Sea of Okhotsk to northeast Sakhalin where they were picked up by the East Sakhalin current to join with local larvae in the South Bay of Islands.

All areas in the Sea of Okhotsk, where larvae and fingerlings were found, were regions of high biological productivity(Chernyavskyi et al., 1981; Markina and Chernyavskyi 1984; Shuntov et. al 1993). Some drift to other areas also occurred as catches of larvae and fingerlings were obtained near Kuril and Shantar Islands.

Greenland turbot yearlings were from 14-23 cm. At one year old they usually settled to the bottom in the Bering Sea and on the shelf of East Kamchatka. In the Sea of Okhotsk, good catches of 18-20 cm Turbot were caught in a pelagic trawl at depths of from 64 to 210 m at the same location as fingerling. Yearlings occurred in the pelagic zone of Shelikhov Bay where catches reach 25-50 per hour trawled but were less than 25 near southeast Sakhalin (Fig. 4). Older specimens moved in an anticlockwise direction in Shelikhov Bay and there was an appearance of some yearlings in Tauiskiy Bay and adjacent waters.

Not more than 5 per hour trawled of 1+ individuals occurred along the shelf of the north part of the Sea of Okhotsk and they were distributed over a broader area compared to the fingerlings. They also occurred along the shelf of Tauiskiy and adjacent waters on shelf and upper continental slope of TINRO basin and the northwest shore of Kamchatka.

In contrast to the northern areas, the number of fingerlings in the pelagic zone near Sakhalin decreased significantly and the majority of 1+ settled to the bottom of Terpeniya Bay and adjacent areas of the East Sakhalin shelf.

In general, the eggs and larvae drifted in the West Kamchatka Current toward Shelikhov Bay. Probably the concentration of young fish near southern Sakhalin had the same origin. Eggs and the larvae also drifted to the northeast Sakhalin coast in the Middle Current, and local larvae were carried by the East Sakhalin Current into Southern Bay of Islands where they eventually settled to the bottom.

Kelp, coral and balanus prevent bottom trawl surveys in Shelikhov Bay. Nevertheless, judging from the stable and dense concentrations of larvae and juveniles up to age 2 in the northeast area and in pelagic zone of Shelikhov Bay it can be theorized that part of the Okhotsk Greenland turbot settle in this Bay. The northeast area was favourable for development of the young because there are numerous gyres and upwellings and it is a zone of high biological productivity during the larval drift period along the northwest Kamchatka shore. A vast gyre in Shelikov Bay prevent juveniles from being carried to less productive areas before they settle to the bottom. The northern shelf within the Sea of Okhotsk provides good condition for a gradual transition of Greenland turbot from shallow to the deep depth as they grow older.

REFERENCES

Chernyavskyi, V.I., V.A. Bobrov, and N.N. Afanasyev. 1981. The major productive areas of the Okhotsk Sea. Izvesttiya TINRO. 105:20-25.

Markina, N.P., and V.I. Chernyavskyi. 1994. Quantitative distribution of plankton and benthos in the Okhotsk Sea. Izvesttiya TINRO. 109:109-119.

Shuntov, V.P., A.F. Volkov, O.S. Temnykh, and E.P. Dulepova. 1993. Walleye pollok in the ecosystems of the far-eastern seas. TINRO. 424 p.

FIGURES

Fig. 1. Distribution of catches of spawning Greenland turbot on the continental slope of the Okhotsk Sea.
A - data of surveys 1977-1987 years,
B - commercial catches in October 1985. Boundaries of the fisheries area are shown by dotted line. See figure 3 for the explanations.

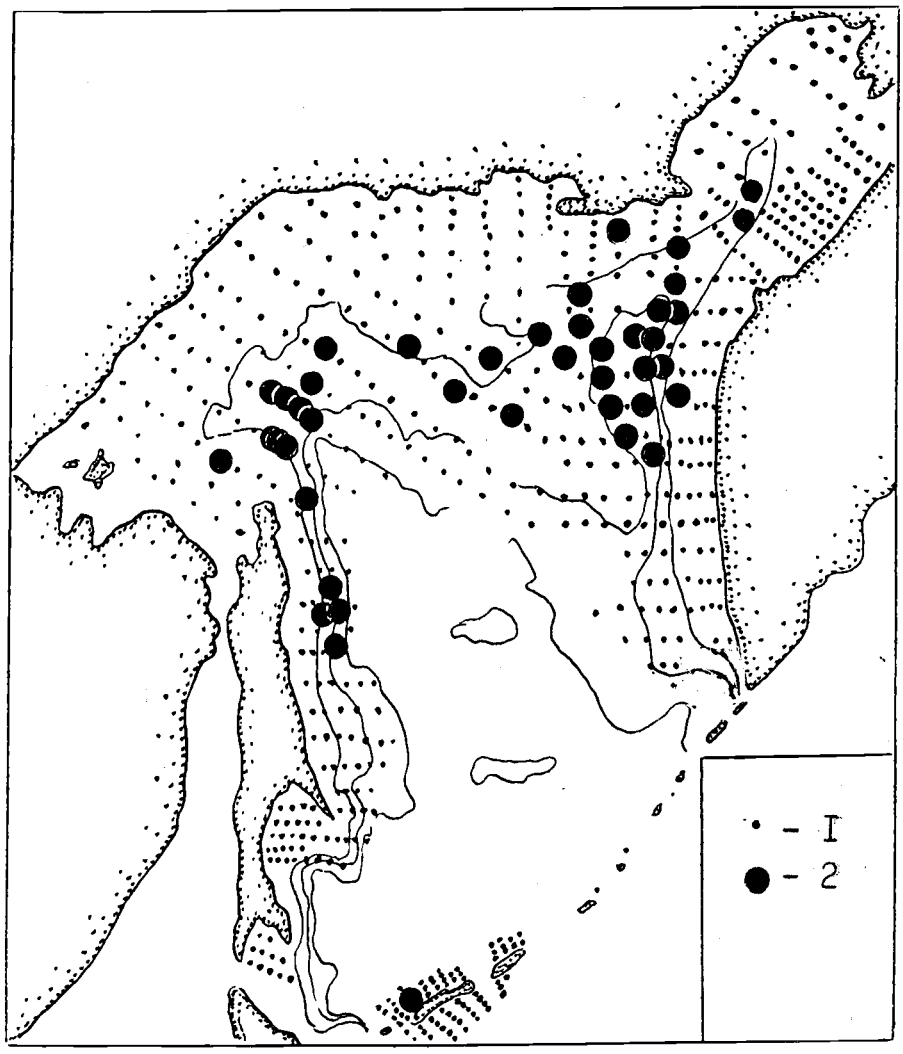

Fig. 2. Ichtyoplankton surveys in Okhotsk Sea 0-200 m in 1984-1988 (1 - stations) and catches of the Greenland turbot larvae (2). All catches from 1 to 5 specimens.

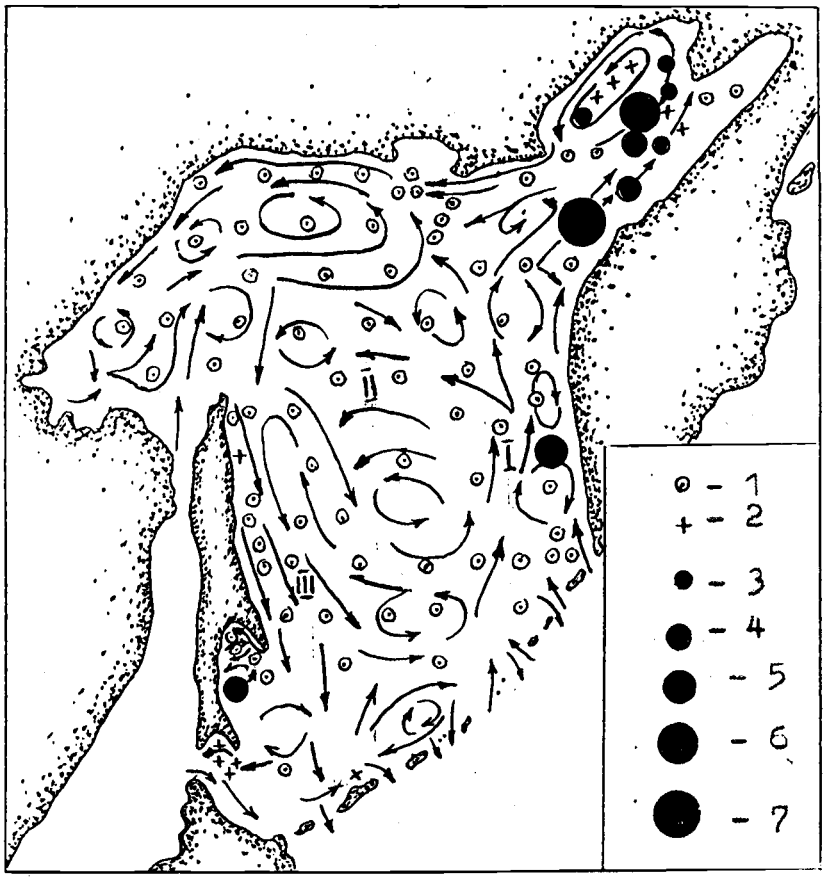

Fig. 3. Distribution of the Greenland turbot at age 0+ from the pelagic catches in the Okhotsk Sea in 1985-1992.

1 - no catch;
2 - 1-5;
3 - 6-10;
4 - 11-25;
5 - 26-50;
6 - 51-100;
7 - more than 100 specimens per hour trawling.

Arrow mark the main currents: I - Western Kamtchatka, II - Middle, III - Eastern Sakhalin.

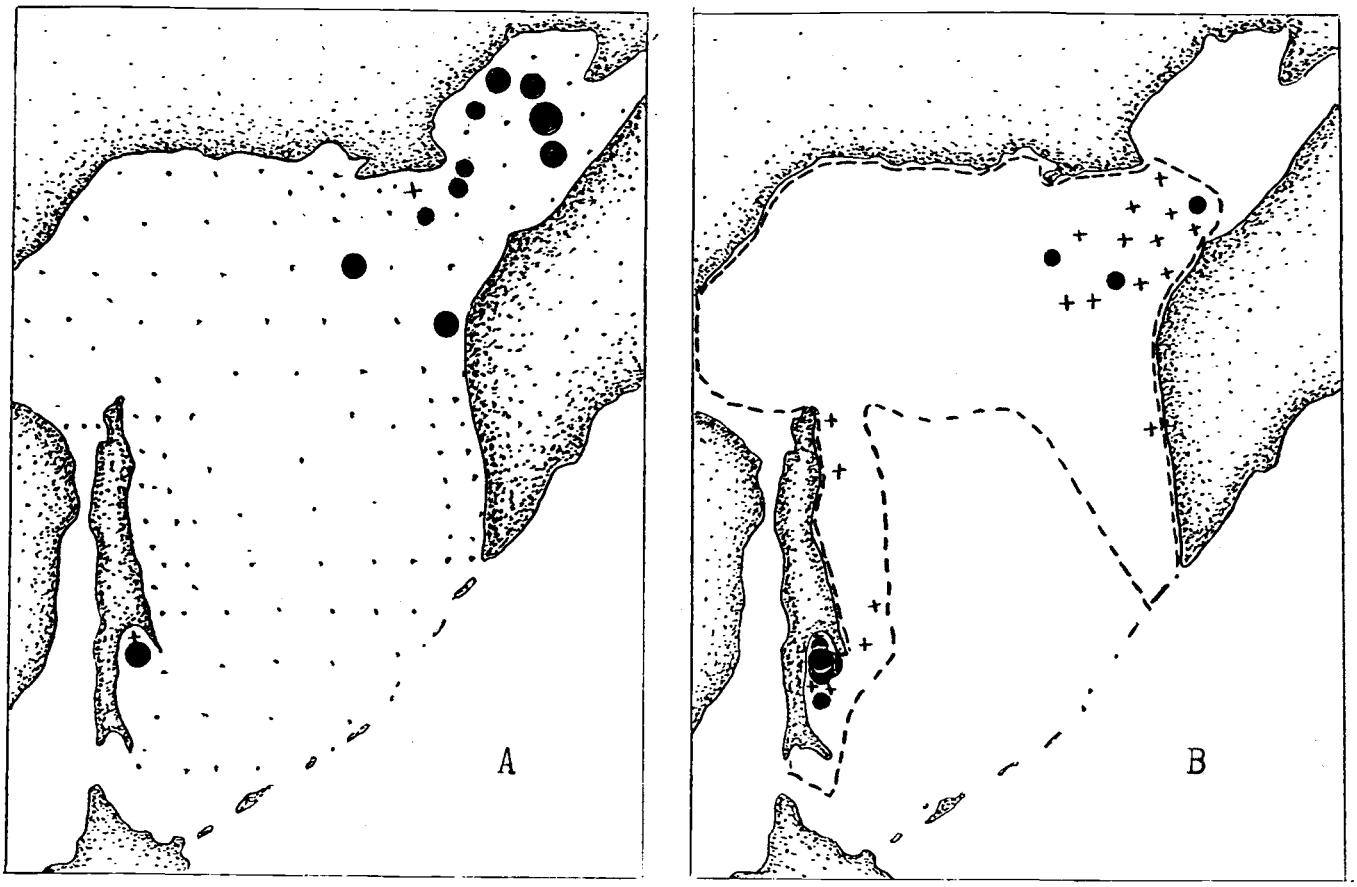

Fig. 4. Distribution of catches of the Greenland turbot at age 1+ in the Okhotsk Sea, judjing pelagic in 1985-1993 (A) and bottom in 1963-1993 (B) trawlings. Boundaries of the investigated area are shown by dotted line. See Fig. 3 for the explanations.

Fisheries Impact on the Sakhalin-Hokkaido Herring Population

Galina M. PUSHNIKOVA

Sakhalin Regional Research Institute of Fisheries and Oceanography (SakhNIRO)
196, Komsomolskaya st., Yuzhno-Sakhalinsk, 693016 Russia

For several decades the Sakhalin-Hokkaido herring *Clupea Pallasi* has attracted attention of fishery scientists because of the commercial exploitation potential from the population where annual cumulative catch reached a high of 1 mln t., a greater annual yield than any other Far-East population. At the same time, other regional populations such as Sakhalin-Hokkaido declined. Birman (1973) indicated that an increase in the Sakhalin-Hokkaido herring abundance should have been expected in the 1970s but actually only the 1973 yearclass was good. Sokolovsky (1985) predicted stock increases during the 1980s but only the 1983 yearclass was good although it proved to be lower than the 1973 yearclass. Therefore in the 1970-80s the abundance of the Sakhalin-Hokkaido herring population remained at extremely low levels. Conservation measures such as, stopping fishing for spawning and immature fish, introducing a commercial fish size limit and full closure of the fishery for a five-year period did not produce an increase in the stock. Thus, understanding the reasons causing the declines in abundance and ways to stabilize and increase abundance of the herring would help manage the fishery. In this paper, the author attempts to propose possible solutions by establishing reasons for regulating the herring fishery.

Data on the annual Sakhalin-Hokkaido herring catches for a period 1921-1992 together with information on the age composition, yearclass strength and stock levels are analyzed. The long time series of data allows a review of abundance fluctuations which indicates three abundance related periods in the Sakhalin-Hokkaido population as follows:

1. Before 1950 during a period of the high abundance year-classes varies from 201.5 bln in 1939 to 1.8 bln in 1949 with average 28.3 bln.
2. 1951-1960 a sharp abundance decline occurs (transitional stage) from 5.4 bln in 1953 to 0.3 bln in 1960 with average of 1.9 bln fish.
3. 1961-1992 the population remains in a depressed state. Yearclass strength varies from 4.7 bln in 1973 to 0.05 bln in 1985 with average of 0.8 bln fish.

During 1949-1951, 1953-1956, 1958, 1961 several bln individuals were produced but lower abundances occur in 1965, 1970; 1972-1973 (Fig. 1). In the years that followed only the 1983 yearclass is high (2.85 bln). In the other years extremely low abundance levels (tens of millions individuals) are observed.

The stock level declines from the early 1950s to the present is from fishing and poor yearclass production (Fig. 1). It is interesting to note that the occurrence of a few good year-classes did not prevent the stock from continuing to decline. The stock has not shown any attempt to recover and has remained in a depressed state for a long time. For each of the three abundance-related periods, the Sakhalin-Hokkaido population, mean stock abundance and catches are calculated for several age groups as follows:

1. In the periods of high abundance, the exploitation rates of cohorts 3 to 9 years old constituted 5.35% for the age 3, 7.8% for the age 4, 9.6% for age 5, 10.9% for age 6, 11.2% for age 7, 16.2% for age 8 and 39.0% for age 9 (Fig. 2).
2. During the reduced abundance period, the exploitation rate of 3 years olds increases to 39.2%, for 4, 5, 6 and 7s; 35.5%, 26.8%; 16.3 and 22.4% respectively. The exploitation rate of 8 and 9 year olds decreases to 14.7 and 13.7% respectively. The fishery appears to be concentrating on fish 3-5 years old during maturation .
3. Exploitation rates during low stock abundance for 3 to 9 year olds is similar to that observed during the decline; 34.3% for age 3, 39.7% for age 4, 44.2% for age 5, 23.1% for age 6, 6.0% for age 7, 2.9% for age 8 and 0.9% for age 9.

During normal stock abundance levels, commercial catches are dominated by individuals of older age (that might have participated in spawning at least 4 times) groups, while in periods of abundance decline catches are dominated by immature and first maturing fish. While the stock was depressed, the 1973 and 1983 year-classes are relatively high and the 1974 and 1980 are at low levels. The first two year-classes are exploited at 75.7% for 1973 for the 3 year olds and 56% for 1983 (Fig. 3). Exploitation rate for 4, 5 and 6 year olds for both years are 51-52, 25-44.5, and 21.6-25.6% respectively. Catch during the low 1974 and 1980 stock abundance also tends to be concentrated on young immature fish before they are able to breed. The stock has been harvested by both Japan and Russia. During the last 16 years, the Russian catch varies between 0.7-4.3 th. t, while the Japanese catch varies from 1.4 to 72.4 th. t (Fig. 4). The average annual exploitation rate is 14.5 and 85.5 % respectively. The Russian fishery focuses on feeding concentrations and the Japanese on over wintering and pre-spawning fish. In the initial years of the fisheries, Japan caught much more than Russia, especially of high abundance year-classes (Probatov, 1954). For example, a total catch for the 1983 brood year constituted 614 mln individuals, with Japanese portion amounting to 92.2% or 559.8 individuals. The catch of the Japanese fleet in 1986 was 73% or 408.7 mln of younger than 3 years old (Fig. 5). In 1987 the Japanese fishermen took 83.7 mln individuals of the same yearclass. Therefore, about 88% of the total catch of the 1983 yearclass were taken by the Japanese fleet during maturation period, which greatly reduces the reproductive potential of the parent stock (Fig. 5).

The lack of spawners on the Sakhalin-Hokkaido grounds has been discussed (Kachina, 1974, 1981; Pushnikova, 1981, 1994) including meetings of different levels and meetings between Russian and Japan. Russian scientists proposed a closure of the fishery to allow the population to increase but the proposal was not accepted by representatives from Japan. The eggs surveys conducted in 1970, 1980 and 1990s, reveal that 90% (and in some years even more) of the traditional Sakhalin-Hokkaido population spawning grounds is not visited by spawners even though the substrate is ideal (good algae and eel grass). No herring eggs were found in traditional areas where major spawning usually occurs. Spawn was observed at smaller spawning sites that were difficult to find (Fridland, 1951).

Based on a study to determine an appropriate parent progeny ratio, it is estimated that an optimum parental stock abundance for the population should be 3 bln individuals (Pushnikova, 1994). The estimated spawning stock strength from 1968 to 1976 varies between 0.04 and 0.35 bln fish about 15 times lower than the optimum level for the stock. If the current fishing strategy is continued on these stocks, the abundance will likely continue to drop. This is supported by the abundance decline, poor yearclass strength and no spawning on traditional spawning grounds and extremely low spawner abundance. To prevent this continuing decline the parent stocks should be stabilized and provide for favorable conditions to allow the stock to increase, thus, a closure of the fishery for both Russia and Japan should occur.

REFERENCES

Birman, I.B. 1973. Helio - Hydrobiological relation as a basis for long-term forecasts of commercial fish stocks (with reference to salmon and herring). Problems of ichthyology. 13(1):23-37.

Kachina, T.F. 1974. Stock, state and fishing adjustment of Pacific herring. Rybnoye Khoziaystvo. 1:9-11.

Kachina, T.F. 1981. Herring of the west part of the Bering Sea. Moscow, Legkaya and pischevaya prom. 120 p.

Fridlyand, I.G. 1951. Reproduction of herring near the southwest coast of Sakhalin. Izv. TINRO. 35:105-145.

Probatov, A.N. 1954. Distribution and abundance of spawning herring near the Japan Sea east coast. Izv. TINRO. 39:21-58.

Pushnikova, G.M. 1981. On the condition of stocks and age of optimum exploitation of Sakhalin-Hokkaido herring. Izv. TINRO. 105:79-84.

Pushnikova, G.M. 1994. Sakhalin-Hokkaido herring stock status and the ways to stabilize their abundance. Collective papers of SakhTINRO. 1:47-56.

Sokolovsky, A.S., and S.I. Glebova. 1985. Long-term fluctuations of Sakhalin-Hokkaido herring abundance. Collective papers of TINRO "Herring of the North Pacific Ocean". p. 3-12.

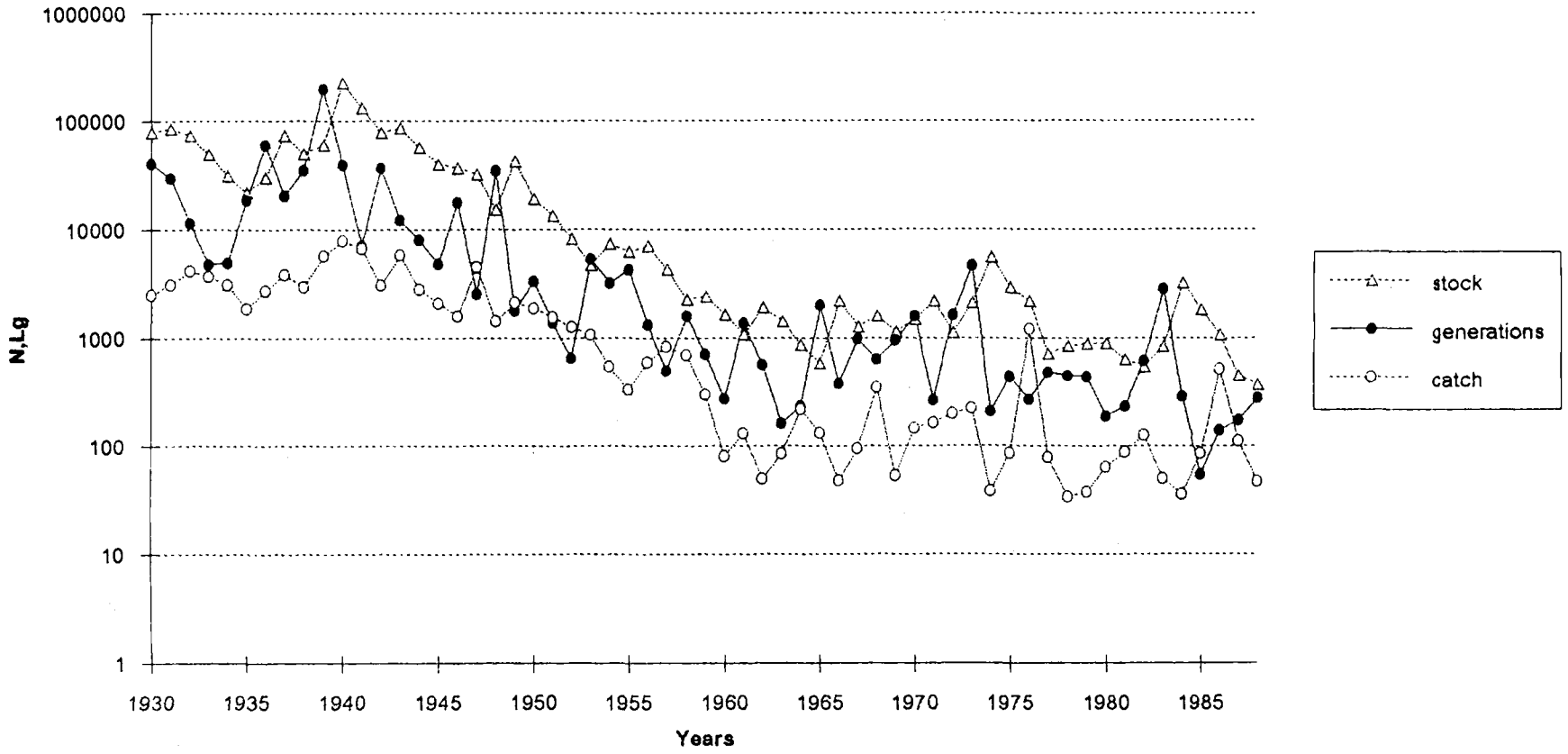

Fig. 1. Stock, generations and catch values (N) of the Sakhalin-Hokkaido herring in 1930-1990.

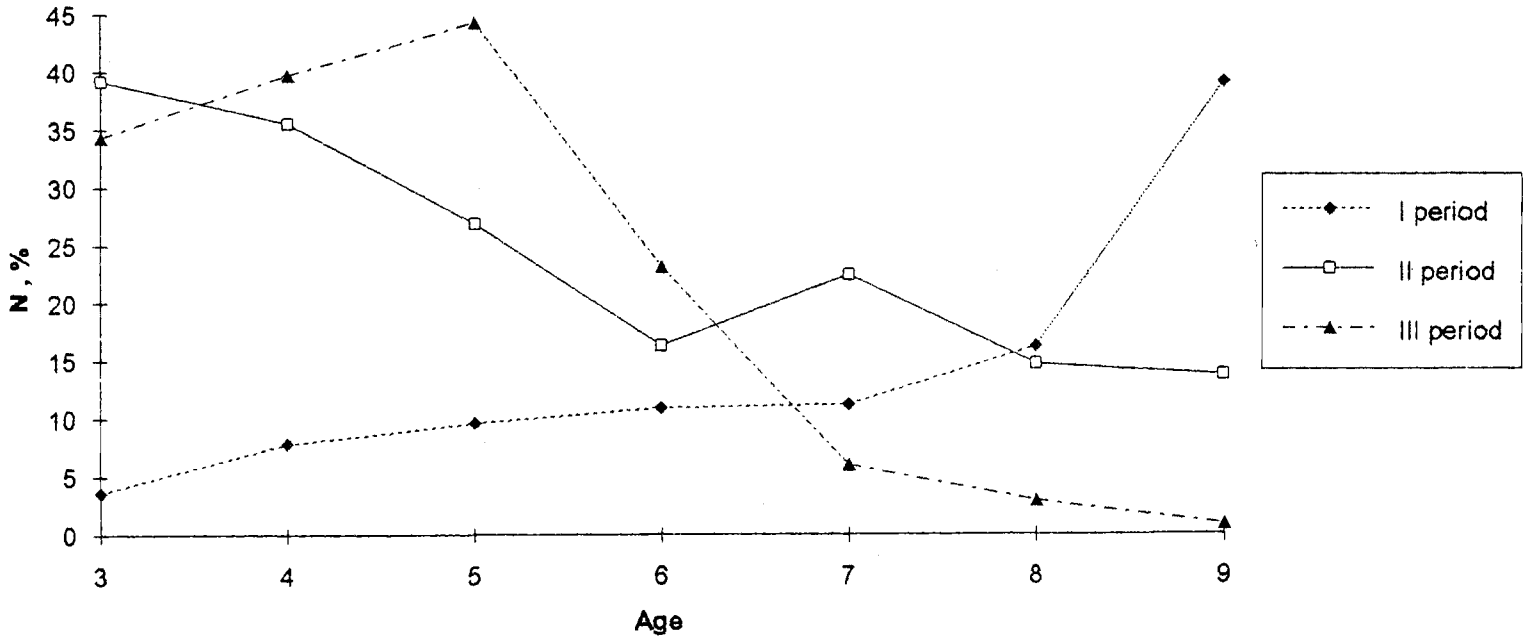

Fig. 2. Age composition of the Sakhalin-Hokkaido herring population in catches for three periods.

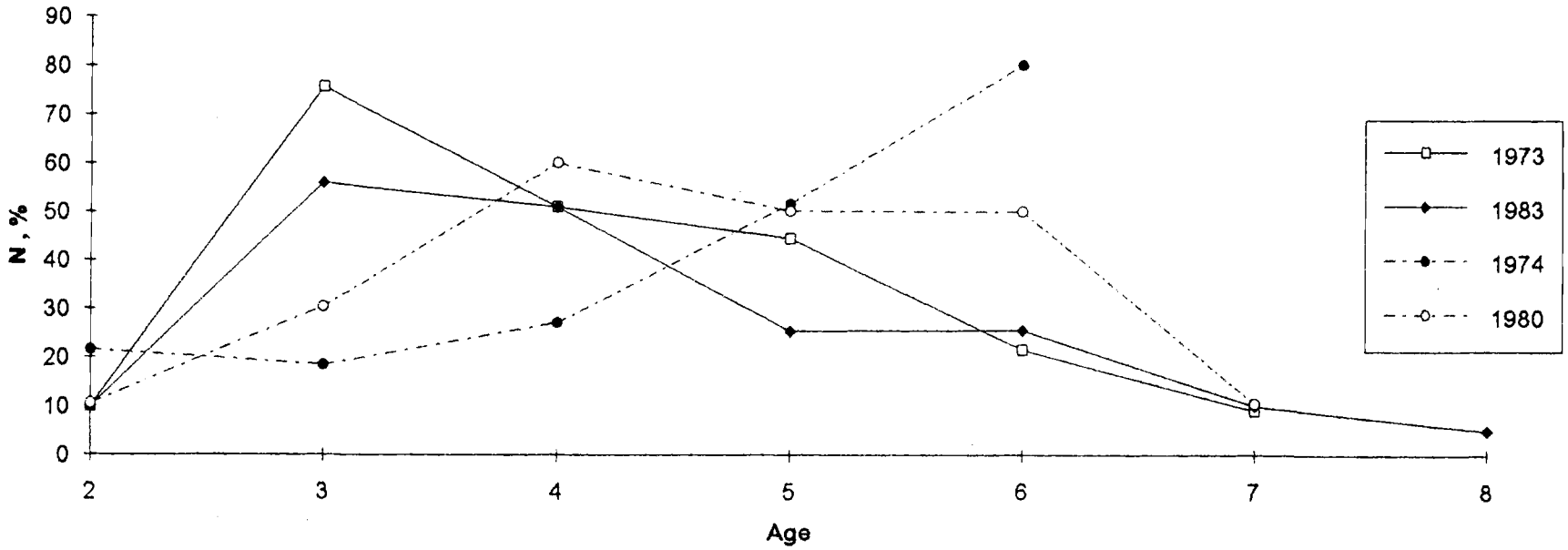

Fig. 3. Catch dynamics of Sakhalin-Hokkaido herring for 1973, 1983, 1974, 1980 generations.

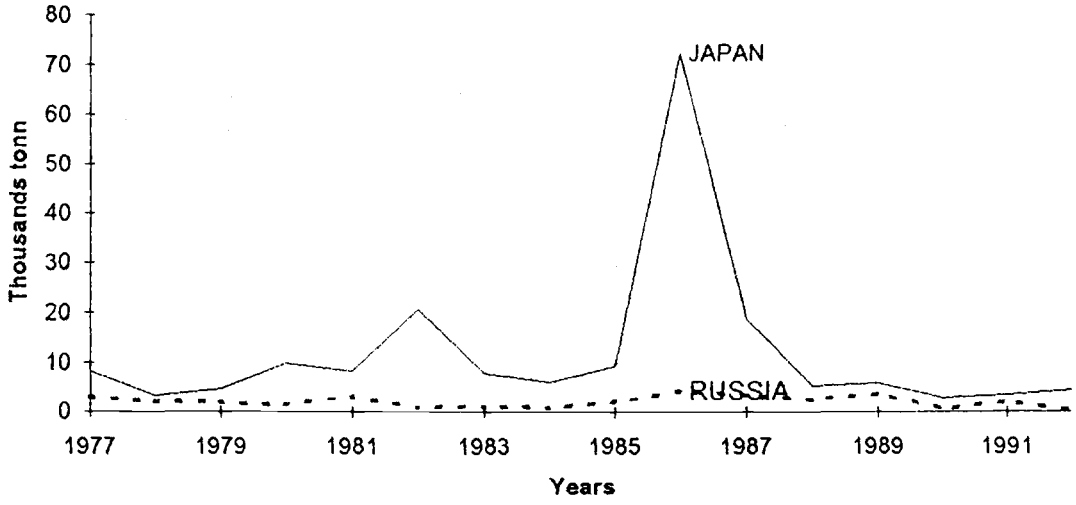

Fig. 4. Sakhalin-Hokkaido herring catch by Russia and Japan in 1977-1992.

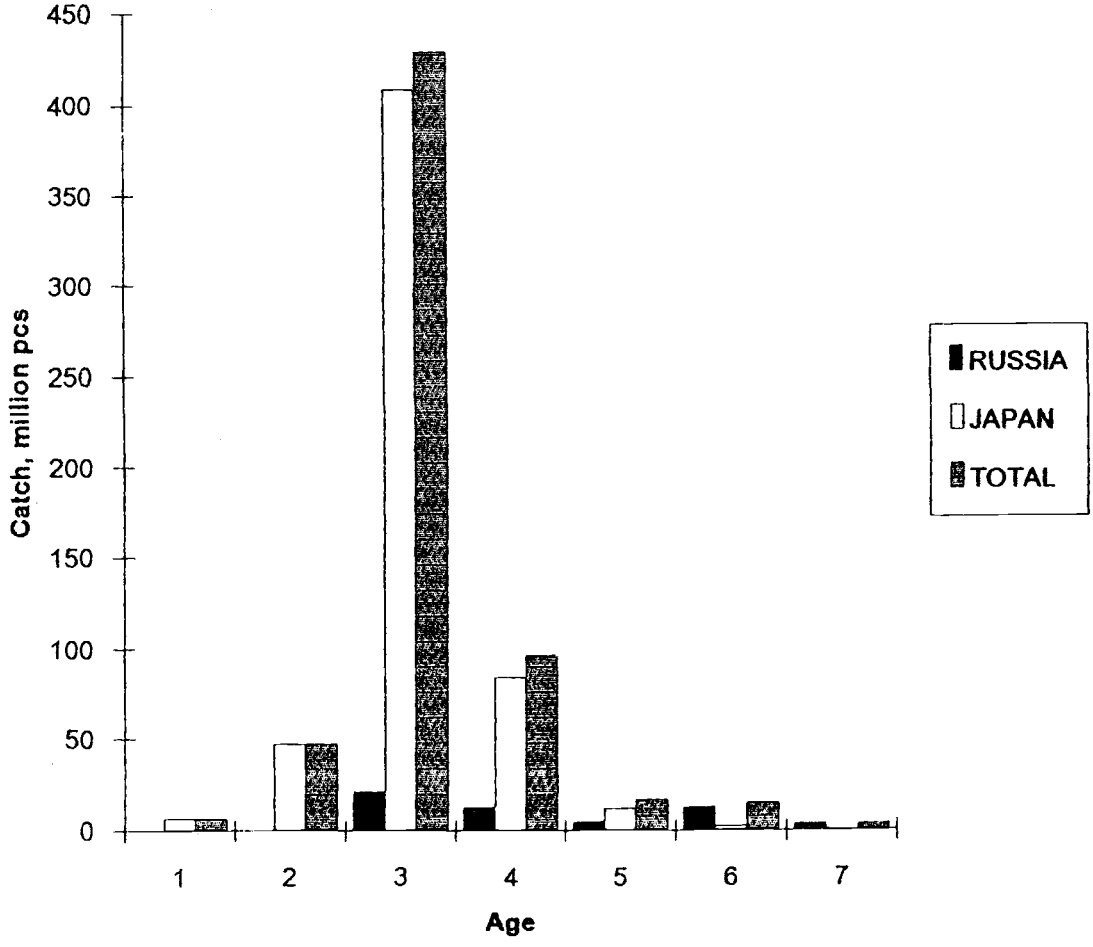

Fig. 5. 1983 generation catch.

Is Pollock Overfished?

Vidar G. WESPESTAD

Alaska Fisheries Science Center
7600 Sandpoint Way NE, Seattle, WA 98115, U.S.A.

Is pollock overfished?, is a question often asked by fisheries and conservation groups. The primary motivation has been the growth in the harvest by U.S. vessels, and the entry of large amounts of pollock on the international market from the Far East. The appearance of Russian pollock in the international market along with large catches from international waters in the Bering and Okhotsk Seas has increased concern over the long term health of the pollock resources. Conservationist point to pollock fisheries as a possible cause of declines in the abundance of sea lions and sea bird populations for which pollock is an important food. The recent history of exploitation and stock declines and collapses in North Atlantic cod populations has also caused conservation groups to question the management and condition of pollock in the North Pacific.

Catch relative to exploitable biomass has been relatively low for the major North Pacific pollock stocks. Comparing the level of exploitation of eastern Bering Sea pollock to the major cod stocks of the North Atlantic for the period 1964-1990, it can be seen that the level of exploitation was about 20% for pollock, while Atlantic cod stocks were fished at a much higher level (Fig. 1). The northeast Arctic cod of the Barents Sea was closed to fishing in the early 1990s and recovered due to the fortuitous occurrence of a very strong year-class. The Northern cod of eastern Canada collapsed recently following an extended period of over harvest and has caused economic hardship to the Newfoundland fishing community. The North Sea cod is likely the next stock to collapse, since the fishery now operates on age 2 fish, of which about 75% are harvested. Iceland is attempting to reduce cod harvest this year and has made sharp reductions in cod quotas hoping that controls will prevent a stock collapse similar to Canada and Norway.

Why compare walleye pollock to Atlantic cod? Primarily, because they are ecological equivalents, being the dominant gadid species and having similar behaviors. Fig. 1 clearly shows that, in gadids, that exploitation in excess of 50% is not sustainable. The question is what is the safe level of fishing for pollock and other members of the cod family.

The abundance of pollock is controlled by recruitment variation. In the eastern Bering Sea the largest year-class (18 billion fish at age 3) was 11 times greater than the weakest year-class, 1.6 billion at age 3. Eastern Bering Sea recruitment is best fitted to a Ricker spawner-recruit function, which is logical for pollock because cannibalism by adult pollock is a major factor influencing recruitment (Fig. 2). Temperature is also important, and warm years usually produce strong year-classes and cold years, weak ones. Variation in recruitment produces variation in stock biomass which can be quite strong in pollock as shown in Fig. 3 for the eastern Bering Sea and other stocks. What is interesting is the similarities between the Okhotsk Sea and eastern Bering Sea. In both the 1978 year-class was strong and more recently the 1989. The apparent similarity of biomass trends between the two areas suggests the influence of broad scale climatic factors. Perhaps further study of this phenomenon will produce some insight in underlying causes of recruitment variation. Since 1977, pollock harvest in the eastern Bering Sea has been kept to under 1.5 million t including discarded catch. Can this harvest be sustained?

To examine the question, I have been modeling the population dynamics of the stock along with different fishing patterns. The primary variable is recruitment. I incorporated recruitment in the model as a Ricker model with log normal error to reflect the natural variation observed in the history of the stock. One result of the model with fishing at the $F_{0.1}$ level, which is the F that results in a yield per recruit that is 10% that obtained from the first increment of fishing effort, shows the recruitment trend is similar to the trend observed (Fig. 4). The important point is that fishing at the $F_{0.1}$ level produces catches on average that are greater than recent year averages, and the biomass does not fall below 4 million t--the lowest level observed in the stock (Fig. 4 lower panel). Fishing at $F_{0.1}$ equals an F of 0.31, an exploitation of around 20%. The maximum level of harvest is at F=0.43 which 28% exploitation. Fishing at levels beyond a 28% exploitation rate results in overfishing and reduced long-term yield.

The long-term yield from the fishery is greater than currently taken and the biomass is near the long-term average. My conclusion is that eastern Bering Sea pollock is not overfished and catches near the current level can be sustained without any problem. Model results indicate that any exploitation below 28% does not impact the productivity of the pollock resource. Similar results have been obtained for Northeast Arctic cod, which suggests a 30% exploitation rate may be a maximal exploitation rate for gadids. The best exploitation policy for eastern Bering Sea pollock may be to fix catch in the range 1.3-1.5 million t for economic reasons, and not allow the fishery to grow beyond this level, thus avoiding having to reduce quotas at times of stock decreases, which given the recent crises in the Atlantic cod stocks, are apparently difficult to do.

FIGURES

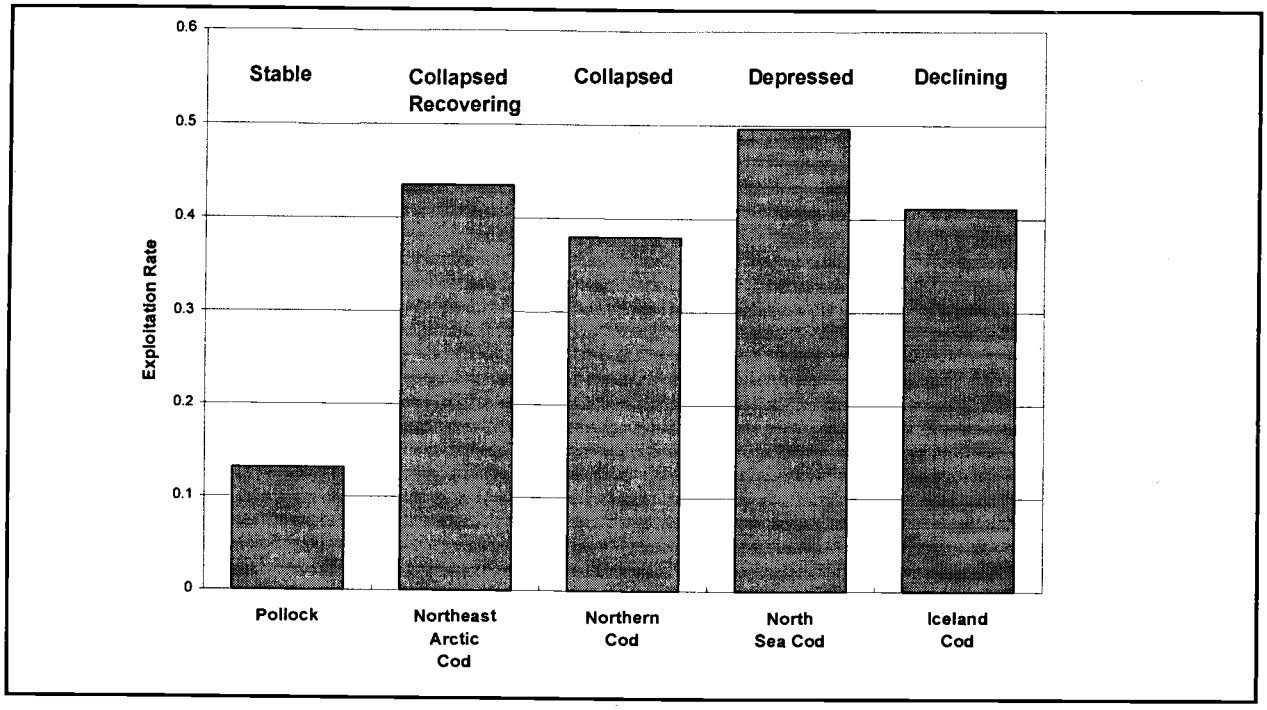

Fig. 1. Comparison of exploitation rates on eastern Bering Sea walleye pollock to exploitation rates on the major Atlantic cod stocks, 1964-1992.

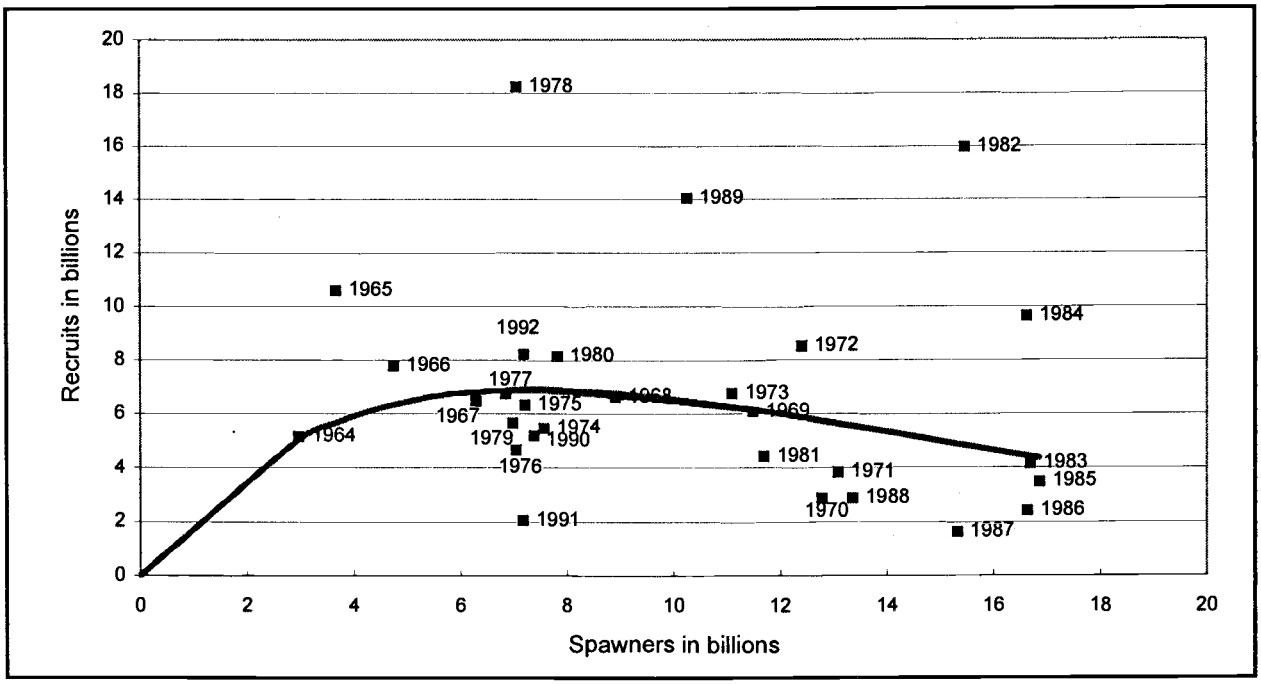

Fig. 2. Spawner-recruit relationship for eastern Bering Sea walleye pollock, 1964-1992 year-classes.

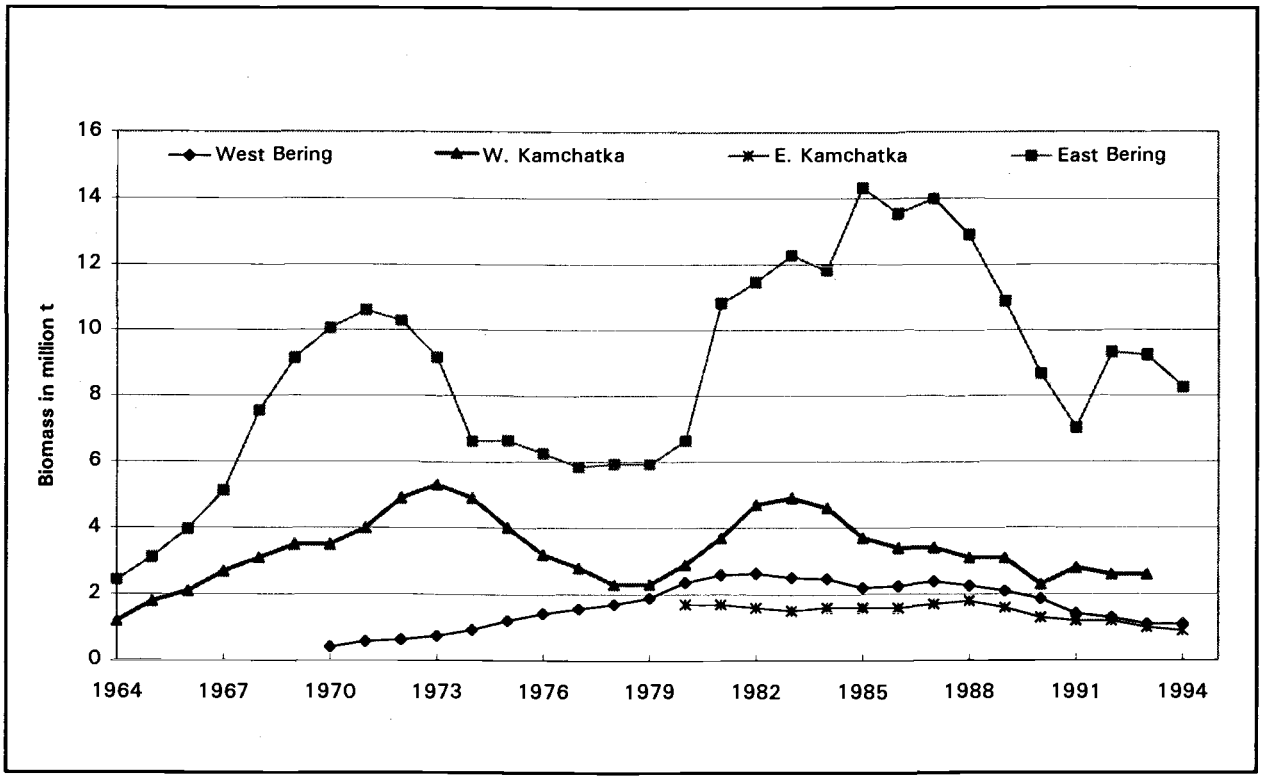

Fig. 3. Biomass trend of major walleye pollock stocks, 1964-1994.

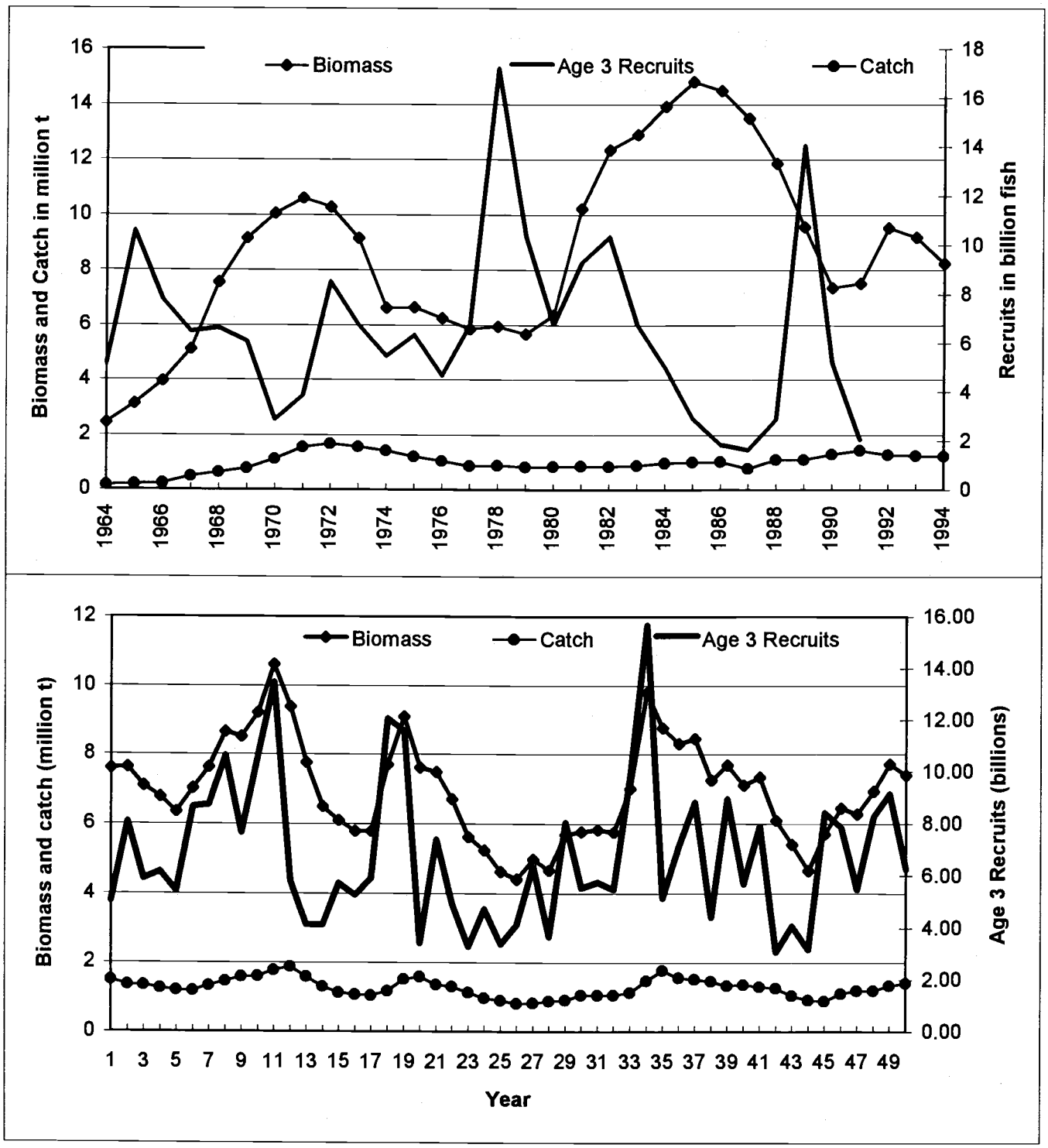

Fig. 4. Top panel: catch, biomass, and recruitment trend observed for eastern Bering Sea walleye pollock, 1964-1994. Bottom panel: a 50-year simulation of eastern Bering Sea walleye pollock catch, biomass and recruitment based on F=0.31 and a Ricker recruitment function incorporating log normal error.

Epipelagic Far Eastern Sardine of the Okhotsk Sea

Vladimir A. BELYAEV, Alexander Yu. ZHIGALIN

TINRO, Vladivostok

The far eastern sardine was one of the most abundant species in northwest Pacific in the 1970-1980 period. The distribution and migration patterns changed from earlier times (Kenya, 1981).

The maximum abundance of sardine during the feeding period (summer-autumn) migrates into the south part of the Okhotsk Sea from the Pacific following the warm waters from the Japan Sea and Soya Current. During the high sardine abundance levels, the Russian fishing fleet concentrated their effort on catching the species. Landings first occurred in 1977, however, the most successful fisheries were after 1984. The fishery usually occurs from June to October as was observed in 1988 when a maximum catch of 241,300 ton occurred (Fig. 1).

There are two main regions where sardines are caught in the Okhotsk Sea, near the Okhotsk Sea coast of the Kuril Islands and in the southern Okhotsk Sea near Sakhalin (Fig. 1). The sardine distribution in these two regions are usually distinct but in October 1985 they were continuous (Fig. 1.ii). Catches in the Okhotsk Sea are thought to have come from two different populations. A Pacific population that came through Kuril Straits to feed adjacent to the Kuril Islands, and a population from the Japan Sea entering into the Okhotsk Sea through Laperuza Strait, near Sakhalin. Sardines which fed near Sakhalin are from the Japan Sea population (Shvidkiy and Levada, 1987). Surveys indicate that the catch near the Kuril Islands was fish from the Pacific population near Sakhalin, a significant part of catch was from the Japan Sea population. The annual biomass was calculated for Sardines distributed near to Hokkaido, southern Kuril Islands (Pacific part) and in the Okhotsk Sea. Based on these estimates we assume that, in the summer-autumn period, up to 25% of the Pacific population migrates into the Okhotsk Sea.

The biomass of the Pacific sardine population during maximum abundance is estimated to be about 30 million tons which is comparable to the biomass of walleye pollock in the Northwest Pacific.

The sardine biomass in the Okhotsk Sea is calculated based on data that include the month, catch, catch per boat day and catch per effort (on one seine net haul). The analysis is standardized based on methods used by the Laboratory of Fish Resources from Kuroshio (Abakumov, 1993). The sardine biomass is estimated from 1985 to 1991. There is insufficient data for the earlier period since 1977. Biomass in the area of the fishery increases from 320 thousand tons to 1,200 thousand tons (Fig. 2). The total biomass is 3-4 millions tons as the fishery covered only small part of the distribution (Fig. 3). These data appear to indicate that sardine is the dominate species in the southern part of the Okhotsk Sea.

The total size of the sardine population has an influence on the epipelagic ecosystem of the Okhotsk Sea. It is one of the rare species that feeds on phytoplankton in this area (Kun, 1975). Sardine consume some zooplankton but the greatest portion of their diet consists of phytoplankton (Table 1). An estimate the quantity of food consumed by the sardine from data from the middle 1980's is used as an estimate of the biomass from the earlier period is poor. The food eaten during the day changes from 4 to 6% in the Japanese Sea, southern Kuril Islands and Hokkaido regions. Unfortunately, data on the ration of the sardine from the Okhotsk Sea is not available. The necessary

food required during maximum abundance of the sardine is estimated to be about 8 million tons (Fig. 2). If the real biomass of the sardine is three times higher the volume of food consumed, it would be 16-24 million tons.

The efficiency of food utilization by sardines from the southern part of the Okhotsk Sea is evaluated by Dulepova (1991) who found that the sardine has a significant influence on abundance and biomass of phyto- and zooplankton.

The existence of competition for food between sardine and other species is evaluated. For example, the food similarity between sardine and walleye pollock is from 20 to 30% overlap in various regions. Highest overlap is in the southern Kuril Islands (juvenile walleye pollock and adult sardine). It should be noted that there is an independent population of the walleye pollock in the southern part of the Okhotsk Sea called the Sakhalin-Hokkaido population. Most years competition for food resources between sardine and walleye pollock is relatively small except during the high abundance of the sardine in a middle of the 1980's. It should also be noted that the catch of walleye pollock in this region has decreased in comparison with the 1970's.

The increase of the populations of sardine in the 1980's in comparison with the end of 1970's is more than 500-1,000 times. At the same time the vital space of the walleye pollock in the southern part of the Okhotsk Sea is reduced.

CONCLUSION

During high abundance, the far eastern sardine population expands into the coldwater ecosystem of the Okhotsk Sea. At the same time, the increase in abundance creates an intensive fishery which is comparable to the dominant species of the coldwater complex (for example, walleye pollock). The influence of the sardine on the ecosystem of the Okhotsk Sea is found to be as follows:

1. the sardine consumes a great amount of zoo and phytoplankton which impacts on their abundance;
2. the sardine competes for food resources with other fish in the summer-autumn period;
3. the sardine serves as food for predatory fish, bird and marine mammals;
4. the abundance of the sardine is so great that it occupies a large part of the southern Okhotsk Sea;
5. other subtropical fishes (saury, anchovy, the common mackerel) also influence the ecosystem of the Okhotsk Sea in summer-autumn.

REFERENCES

Abakumov, A.I. 1993. Management and optimization in models of maintained population. Vladivostok, "Dalnauka". 129 p. (in Russian)

Dulepova, E.P. 1991. Plankton resources of the Okhotsk Sea and their use by fish. Ecology of the sea. 37:1-7. (in Russian)

Lapshina, V.I., I.I. Stepanenko, and O.E. Muraviova. 1990. Feeding of the Japan Sea sardine and some aspects it trofical connections. Dep. In VNIERX, 10(228):1-54. (in Russian)

Kun, M.S. 1975. Zooplankton of the Far-Eastern seas. Moscov., Pishevaya promishlennost. 148 p. (in Russian)

Chuchukalo, V.I., A.J. Efimkin, and V.V. Lapko. 1995. Feeding of some species of the planktofeeding fish in the Okhotsk Sea. Marine biology. 21(2):132-136. (in Russian)

Shvidkiy, G.V., and T.E. Levada. 1987. About origin of the sardine in Okhotsk Sea congestion. Rybnoe hoziyastvo. 9:27-28. (in Russian)

TABLES AND FIGURES

Table 1. Seasonal changes of food of the sardine (June - September).

Species	Months			
	VI	VII	VIII	IX
Calanus plumchrus	12.1	1.0	---	---
Calanus cristatus	1.2	---	---	---
Metridia lucens	8.7	1.6	2.5	---
Oithona varia	0.2	0.3	1.1	---
Paracalanus parvus	---	---	3.7	0.7
Parathemisto japonicus	2.1	2.5	1.7	---
Euphausiacea varia	---	0.8	9.6	---
Centropages nemurrica	---	---	---	1.5
Oikopleura diocca	---	---	---	0.6
Chaetognatha	---	---	---	0.4
Phytoplancton + Tintinnidae	73.9	91.3	74.8	90.7
Other	1.4	2.5	6.6	6.1

Table 2. The food of various fish species in the summer of 1985 (by Lapshina, 1990).

	Capelin	Walleye pollock	Greenling	Pacific herring	Sardine	Pink salmon
Capelin	---	17.0	9.4	18.1	13.4	1.9
Walleye pollock	17.0	---	31.7	26.1	22.9	5.1
Greenling	9.4	31.7	---	34.9	3.5	14.1
Pacific herring	18.1	26.1	34.9	---	17.1	6.7
Sardine	13.4	22.9	3.5	17.1	---	32.9
Pink salmon	1.9	5.1	14.1	6.7	32.9	---

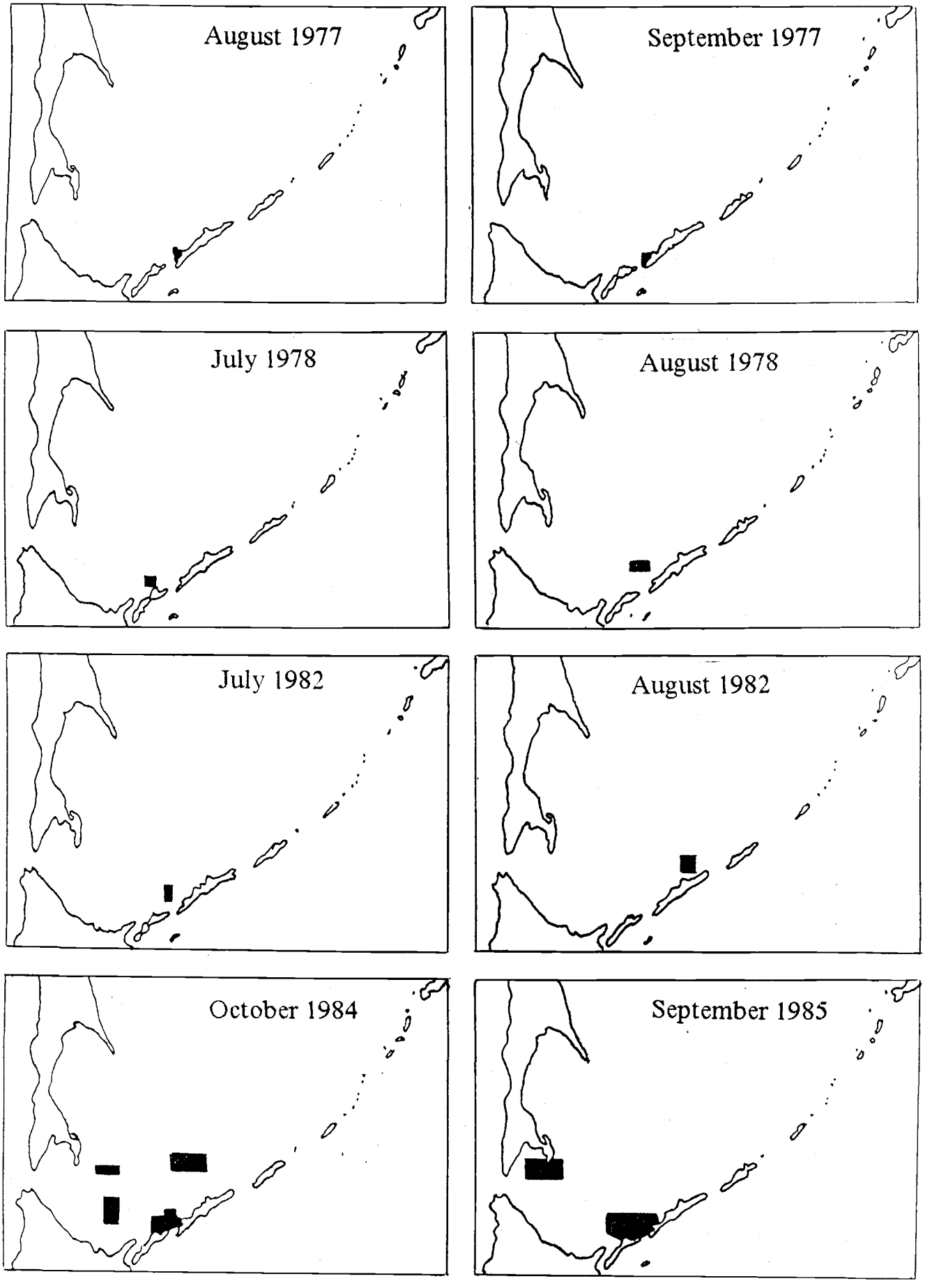

Fig. 1 (i). Fishing grounds of the sardine in the Okhotsk Sea.

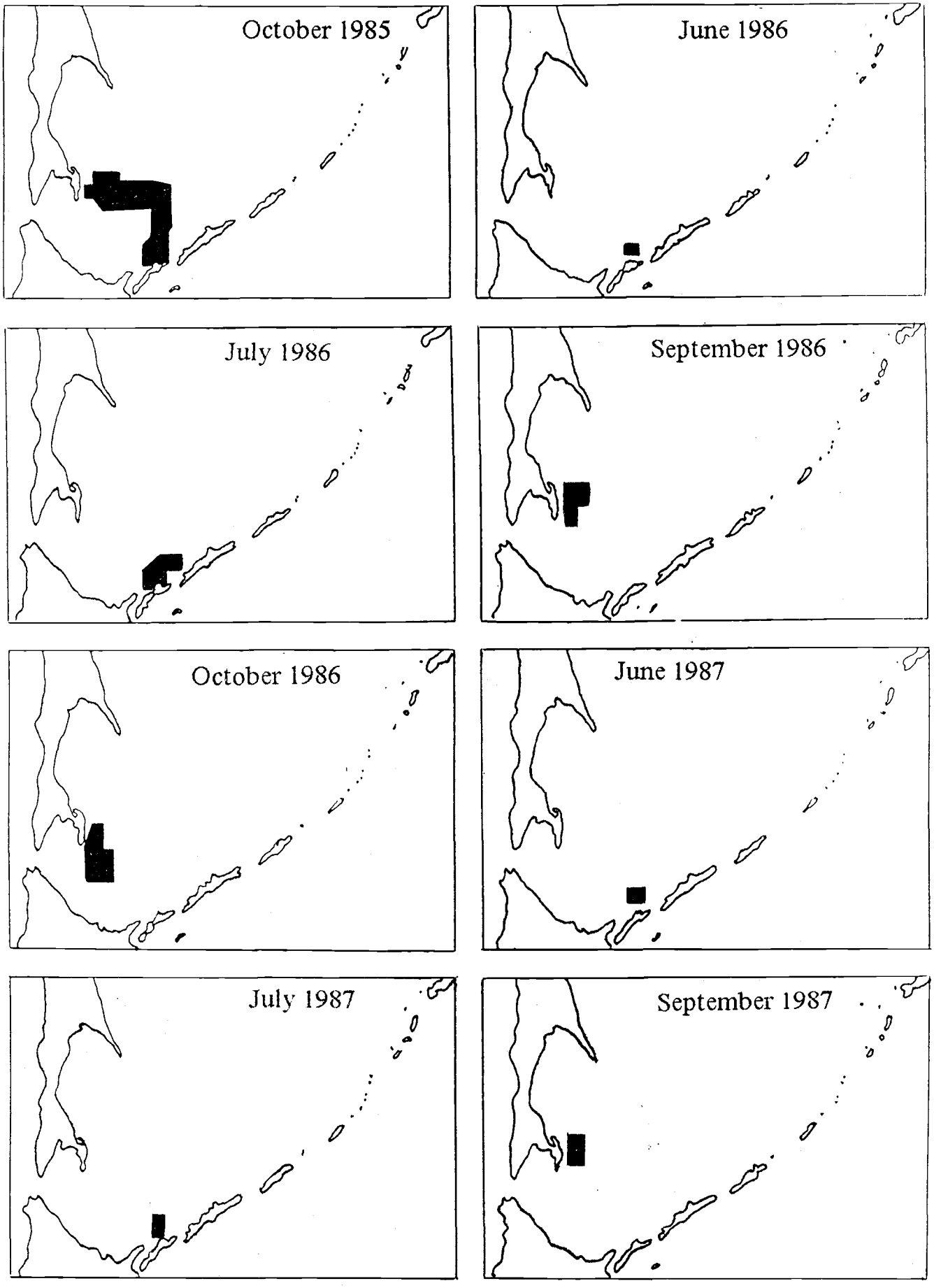
October 1985
June 1986
July 1986
September 1986
October 1986
June 1987
July 1987
September 1987

Fig. 1 (ii).

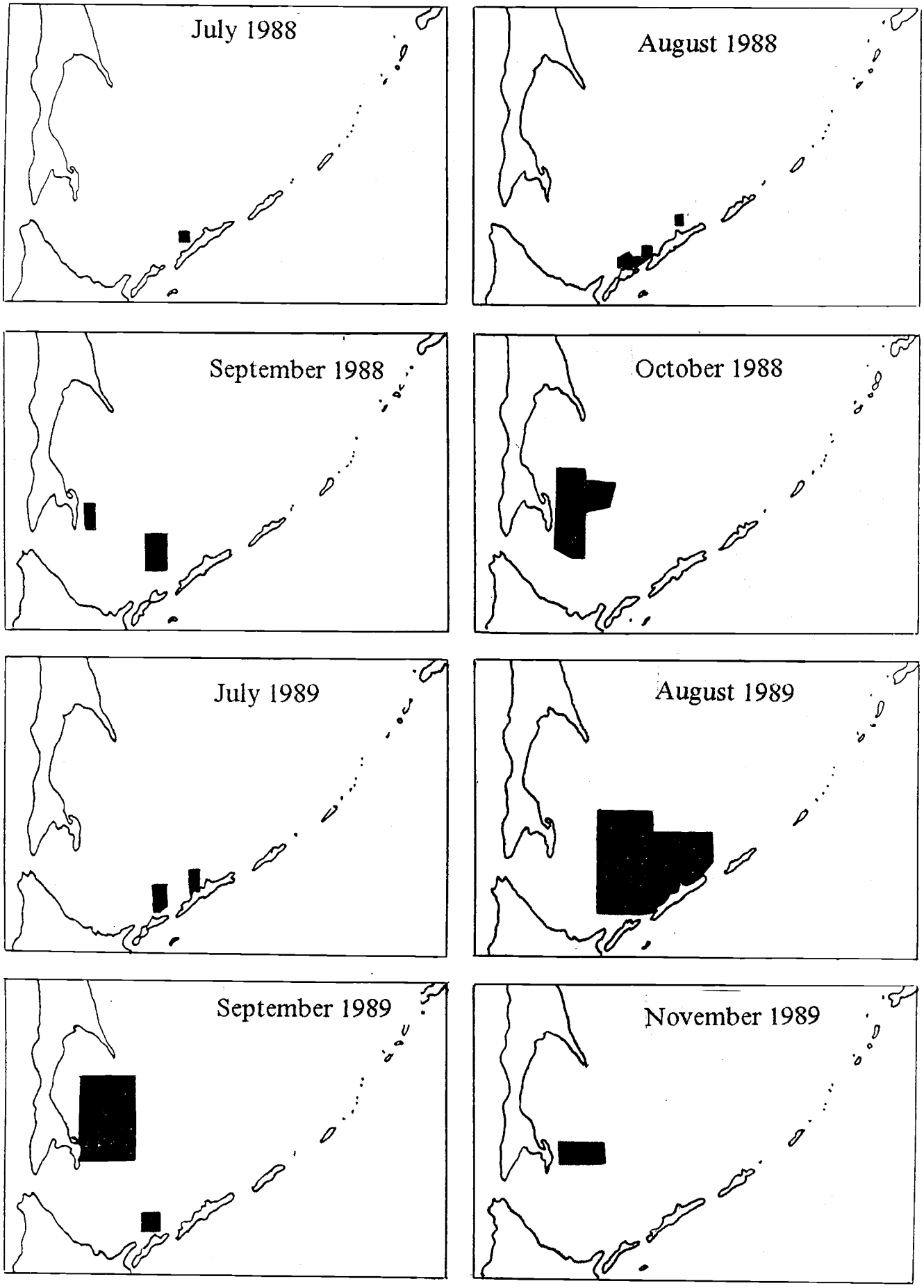
July 1988
August 1988
September 1988
October 1988
July 1989
August 1989
September 1989
November 1989

Fig. 1 (iii).

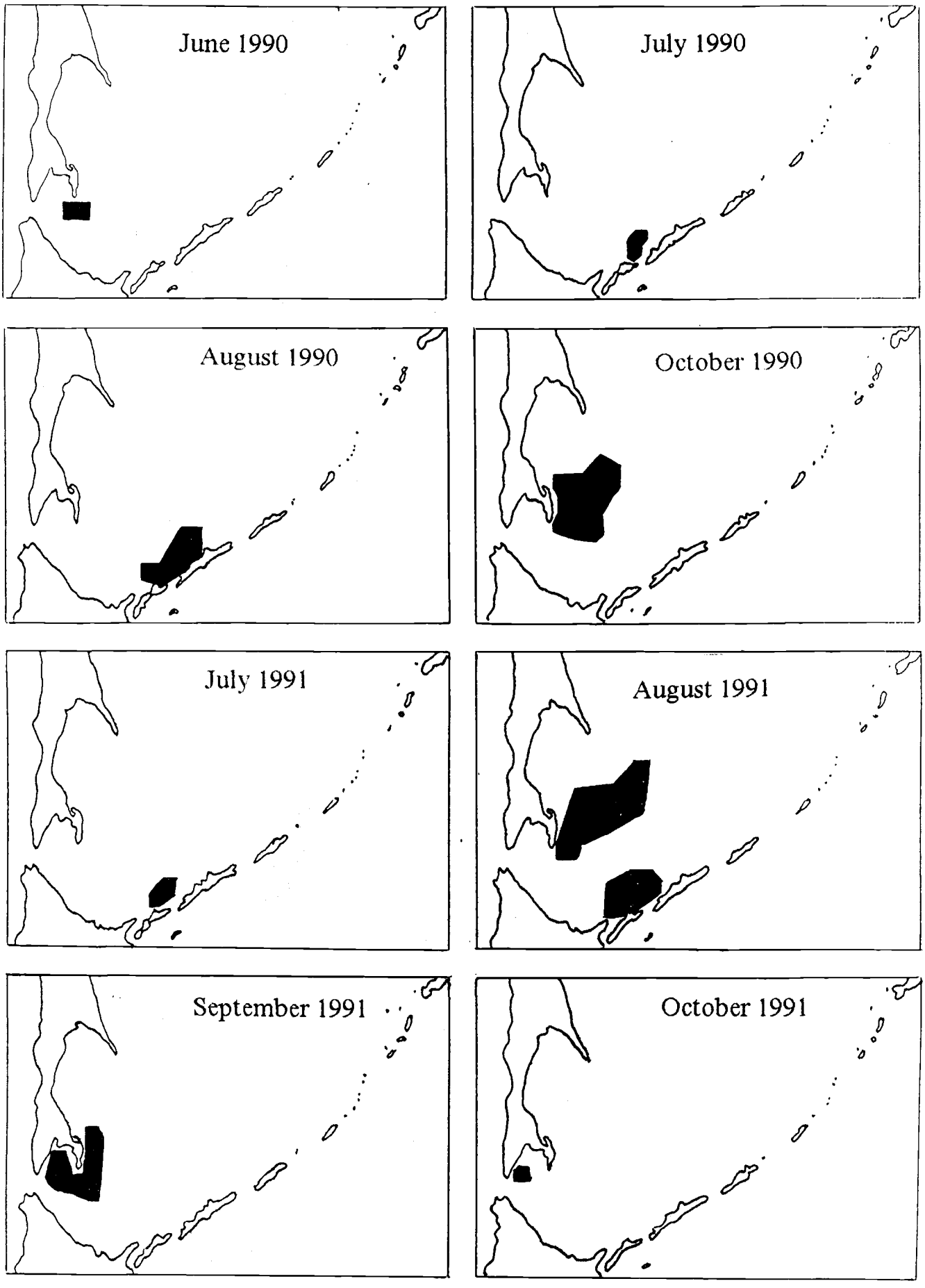
June 1990
July 1990
August 1990
October 1990
July 1991
August 1991
September 1991
October 1991

Fig. 1 (iv).

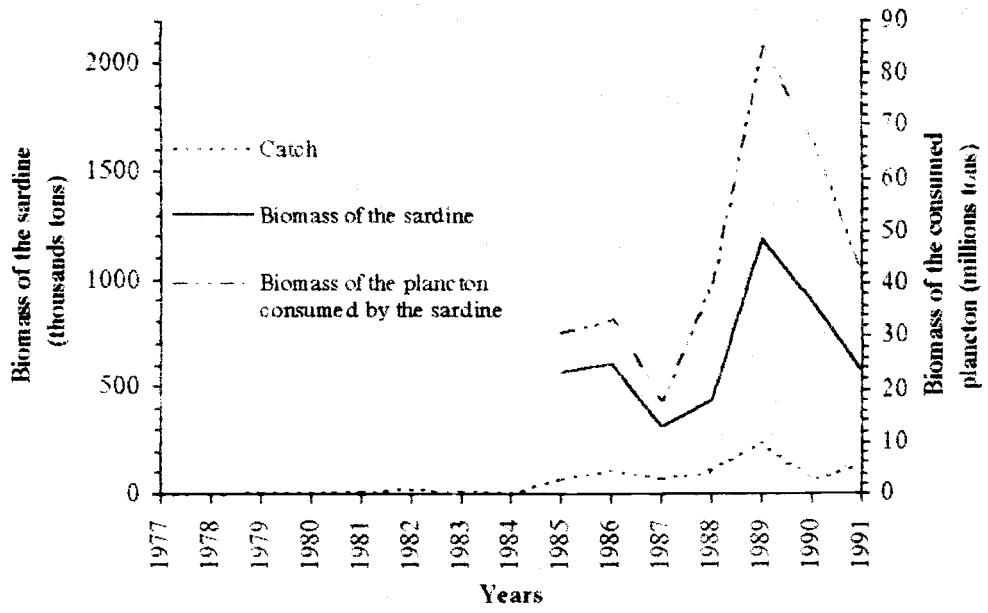

Fig. 2. Catch and biomass of the sardine in the Okhotsk Sea and biomass of the plancton consumed by the sardine.

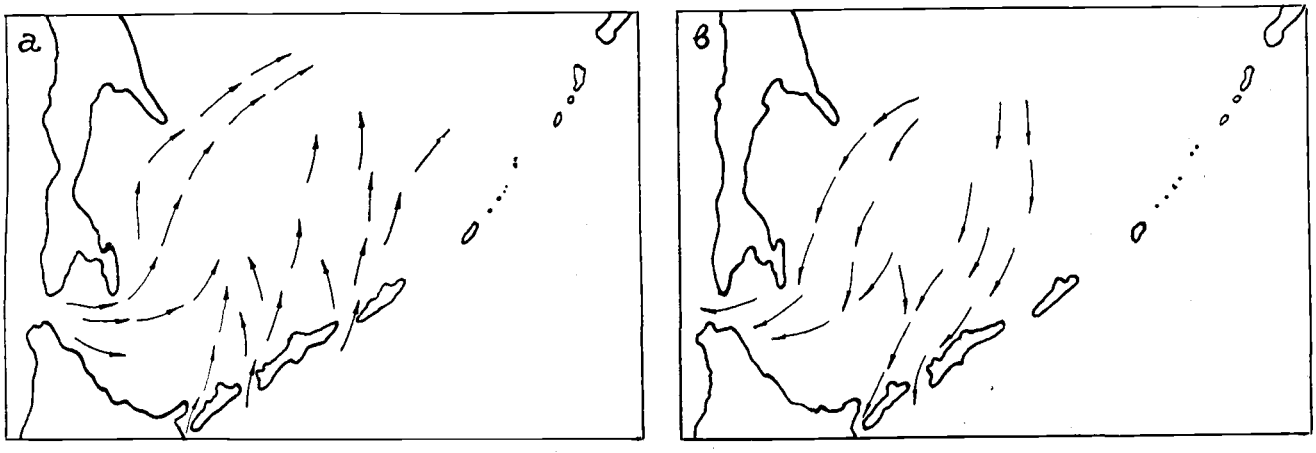

Fig. 3. Migration routes of the sardine in the Okhotsk Sea.
a - northward migration; b - southward migration.

A Preliminary Report on Stock Status and Productive Capacity of Horsehair Crab *Erimacrus Isenbeckii* (Brandt) in the South Kuril Strait

Yuri E. BREGMAN[1], Victor V. PUSHNIKOV[2], Lyudmila G. SEDOVA[1] and Vladimir Ph. IVANOV[2]

[1] Pacific Scientific Research Fisheries Center (TINRO-center), 4 Shevchenko Alley, Vladivostok, 690000, Russia.

[2] Sakhalin Research Institute of Fisheries & Oceanography (SakhNIRO), 196 Komsomolskaya St., Yuzhno-Sakhalinsk, 693016, Russia.

Developing a new stock exploitation plan for a horsehair crab fishery in the South Kuril Strait is difficult without having knowledge about the abundance and productive capacity including measurements of the population structure, growth rates and longevity.

In this paper analysis of data by crab groups to present some productive characteristics of horsehair crab stock state using catch effort and size structure is attempted.

THE MATERIAL AND METHODS

Samples were collected using a standard truncated cone shape trap, with bottom ring diameter of 103 cm, upper ring diameter of 54 cm, height of 50 cm and mesh size of 60 mm, set in the central part of the strait between Kunashir and Shikotan Islands at depths of 52-78 m. Fresh-frozen pollock was used as bait in traps that were fished for one to two days. Vernier calipers (precision of ±0.1 mm) were used to measure the largest width (W) and length (l) of the carpace. Stock age structure is determined by the size of animals using probability paper (Harding, 1949) and known size-age from North Hokkaido horsehair crab (Abe, 1977, 1982, 1984 - cit. by Abe, 1992). Histograms indicate that the size step is 1 mm. Group growth is calculated using Bertalanffy equations because of the good correspondence between the modal values of W at age of t years.

Samples were collected from July-September. Ten samples of individuals of different sexes were collected before and after molting. Samples NN 1, 5, 8, 10 were gathered in 1991, NN 2, 3, 4, 6, 7, 9 in 1994. The number of crabs caught in the samples were 3060, 3063, 888, 1169, 3012, 1148, 1265, 903, 1781 and 652, respectively.

RESULTS AND DISCUSSION

In July, 85-87% of the individuals had soft or semi-hard carpace due to molting and by the end of September 30% had a hard carpace. Most of the catches (82-92%) consist of males with carapace width of 35-122 mm and 50-70% were commercial size ($W > 80$ mm). The average weights of individuals was 490-520 g. Females size varied between 41-102 mm. Moulting is complete by the end of August when 50% of the individuals are fertilized and their reproductive orifice are sealed indicating the success of mating.

The average catch effort ($\bar{y}$) in all groups (commercial males, commercial males and females) increases up to the second week of August to 3.07 individuals, for large males at a depth of approximately 70 m, then decreases rapidly. Values $\bar{y}$ of commercial groups are 1.49, 1.36, 0.8 and 1.08 individuals in 1991, 1992, 1993 and 1994, respectively indicating a stock decrease during the period. Unfortunately, this conclusion cannot be confirmed because correct official statistics are not available. At the same time, a horsehair crab stock decrease was observed in the neighboring area along the north coastal of Hokkaido, where catches dropped from the beginning of the 60s to 2-3 thousands tons (Abe, 1992).

Bearing in mind postmoulting growth of body size, the estimate of the modal values W for individuals of each sex and physiological state were the same in different samples so they are combined to calculate the corresponding average values (Table 1). The horsehair crab reproduction period is lengthy (Abe,1992), and settling was found to be polymodal (Fig.1) which makes comparison of the age modes difficult. Thus, Abe's size-age method is used: males and females up to the second year moult grow similar; at the sixth instar (one year) the average carapace length is 20.4 mm; at the ninth instar (two years) 46.4 mm; male growth increases reaching 59.1, 73.3, 88.2, 103.5, 117.5 mm, at age 3, 4, 5-6, 7-8, 9-10 years at instars NN 10-14; female growth is 55.9, 65.8, 74.1 mm at age 3-5, 6-8, 9-11, 12-14 years at instars NN 10-13, respectively. We calculate the theoretical relationship to determine lengths in widths:

for males:

if $l < 75$ mm, $W = 0.93l$,
if $l > 75$ mm, $W = 0.886l + 3.465$ (original data),

for females: $W = 0.95l - 0.1$ (Kawakami, 1934 - cit. by Abe,1992).

It appears, that male carapace widths are 19, 43.1, 55, 68.4, 81.6, 95.1, 107.6 mm at age 1, 2, 3, 4, 5-6, 7-8, 9-10 years, and female are 19.3, 44, 51.6, 62.4, 70.3, 79.7 mm at age 1, 2, 3-5, 6-8, 9-11, 12-14 years, respectively. The following measure of average values of modes: 54.5, 68.8, 81.4, 95.2, 107.4 mm and 51.7, 63.4, 70.2, 81.2 closely correspond to the theoretical figures (Table 1). On the bases of these modes the curves of linear growth were constructed (Fig. 2). Up to the age of 3 years females grow very fast and then by about 50 mm width their growth rate slows significantly, which corresponds to the beginning of first maturity (Abe, 1992).

The equations of horsehair crab linear growth are as follows:

$$W_t = 135 \cdot \left(1 - e^{-0.1823t}\right) \quad \text{for males,}$$

$$W_t = 112.23 - 60.5 \cdot e^{-0.2087 \cdot (\tau - 1.333)} \quad \text{for females aged 4 or more years,}$$

where:

W_t - carapace width at age t (years);
135, 112.23 - definitive width sizes (W_∞), mm;
0.1823 year^{-1} and 0.2087 year^{-3} - constants of growth;
t - conventional age equal to $t/3$;
1.333 - conventional zero age for $t_0 = 4$ years;
$60.5 = W_\infty - W_0$, where $W_0 = 51.7$ mm.

The following theoretical values correspond to given equations: for males at age 1, 2, 3 ... 9 years, sizes are 22.5, 41.2, 56.9, 69.9, 80.7, 89.8 (conventionally), 97.3, 103.6 (conventionally), 108.8 mm; for females at age 4, 7, 10, 13, 16 years, 51.7, 63.1, 72.3, 79.9, 86 mm respectively.

Approximation correctness is estimated in the Fig. 2 from calculated sizes. Thus, the biggest horsehair crab male found is 152 mm length and for females 117 mm (Abe, 1992) which corresponds to approximately 138 and 111 mm width.

The average maximal theoretical crab age ($W_{max} = 0.95W_{\infty}$), was 16.4 year for males and about 37 years (!) for females. Such great longevity is theoretically due to the low rates of female growth. The real figures are likely lower due of strong fishing press.

The characteristics of growth for horsehair crab in the South Kuril Strait is identical to the populations off the coast of North Hokkaido; growth rates of mature females are very low which theoretically indicates greater longevity; for the last 4 years the catches decreases for the level of effort observed which could indicate that the stocks are over harvested.

REFERENCES

Abe, K. 1992. Important crab resources inhabiting Hokkaido waters. Mar.Behav.Phisiol. 21:153-183.

Harding, J.P. 1949. The use probability paper for graphical analysis of polymodal frequency distributions. J. Mar. Biol. Assoc. U.K., 28:141-153.

Table 1. The modal carapace widths (mm) of horsehair crabs from different samples.

N	Males before moulting					Males after moulting				Females before moulting			Females after moulting
N	Samples` numbers					Samples` numbers				Samples` numbers			Samples` numbers
	1	2	3	4	$\overline{m}$	5	6	7	$\overline{m}$	8	9	$\overline{m}$	10
1			48.3 (1.1)*		≈48.3						47.8 (3.1)	≈47.8	
2			54.5 (2.5)		≈54.5						51.7 (0.7)	≈51.7	
3	60.7 (1.1)		60.5 (1.8)		60.6	63 (1.3)			≈63	57 (1.1)	56.5 (3)	56.7	57.6 (0.6)
4	65(0.8)		65.2 (2.4)		65.4					60 (1.0)	60.3 (1.5)	60.1	61.3 (1.6)
5	68.5(1.1)	68.5 (3.0)	70 (1.4)	68.2 (1.6)	68.8	67.9 (1.6)	68.2 (1.3)		68	63.3 (1.3)	63.5 (1.0)	63.4	64 (1.2)
6	72.2-76.5 (1.9-2.2)	73.8 (2.3)	74.2 (1.7)	74.1 (2.7)	74.1	72.2-76.5 (1.3-1.7)	72.5-76.9 (1.6-2)		74.5	66.6 (1.6)	66 (1.0)	66.3	67.5 (1.2)
7		79 (2.2)	79.3 (2.80)	77.8 (1.7)	78.7	80 (0.7)	80.3 (0.7)		80.1	70 (1.7)	70.5 (1.8)	70.2	70.2 (0.9)
8	81.3(1.2)		81.9 (1.1)	81.2 (1.4)	81.4	83 (1.2)	82.8 (1.5)	82.5 (1.6)	82.8	71.9 (1.3)		71.9	72.8 (1.1)
9	84.7(1.4)	84(1.8)	85.5 (1.2)	85 (1.4)	84.8	85.8 (1.3)	86 (1.6)	87.5 (1.9)	86.4	75 (0.9)	73.7 (1.0)	74.3	75.8 (0.9)
10	88.4(1.3)	87.9(1.5)	88.6 (1.1)	88.5 (1.6)	88.3	89.5 (1.3)	89.5 (1.2)	91.2 (1.4)	90	77.9 (1.0)	76.7 (0.4)	77.3	78.3 (1.0)
11	91.5(1.2)	91.4(2.1)	91.4 (0.9)	91 (1.0)	91.3	92.5 (1.3)	93.2 (1.5)	94.7 (1.3)	93.4	81.3 (0.7)	81 (1.0)	81.2	81.8 (0.8)
12	95.4(1.7)	95.5(1.0)	94-96 (0.5-0.7)	95 (1.4)	95.2	95.7 (1.4)	95.8 (1.3)	97.3 (0.9)	96.3	83 (0.6)		83	84.4 (0.6)
13	99.3(2.0)	99(1.25)	98 (0.8)	99 (2.0)	98.8	99.3 (1.1)	100 (1.0)	100.5 (2.0)	99.9	85.7 (0.5)			87.3 (1.1)
14	103.5(1.5)	103(1.2)	100.5 (0.7)	102.3 (0.9)	102.3	102.5 (1.1)		≈102.5					
15	106.2-108.6 (0.8-1.3)				≈107.4	105.4-108.7 (1.0-1.2)		≈107					

*- The standard deviations (δ) are given in the brackets.

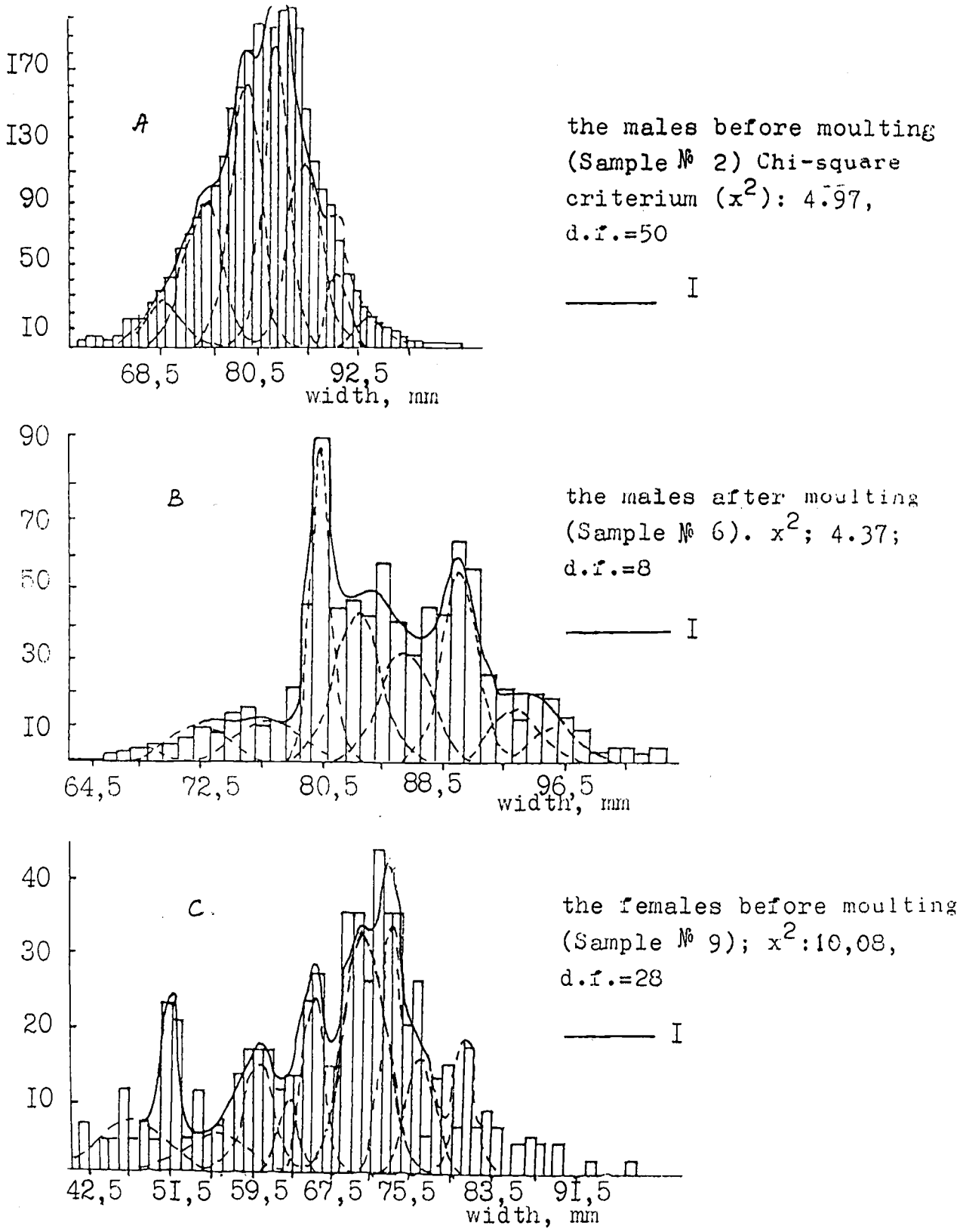

Fig. 1. Some examples of size-age structures of horsehair crab population in the South-Kuril Strait, July-September, 1994. Caraspace widths (mm) and frequencies (exempl.) are laid out on absciss and ordinate axes accordingly. I - lines, summing the normal distribution curves.

A - the males before moulting (Sample No. 2); chi-square criterium (χ^2):4.97; d.f. = 50

B - the males after moulting (Sample No. 6); χ^2:4.37; d.f. = 8

C - the females before moulting (Sample No. 9); χ^2:10.08; d.f. = 28

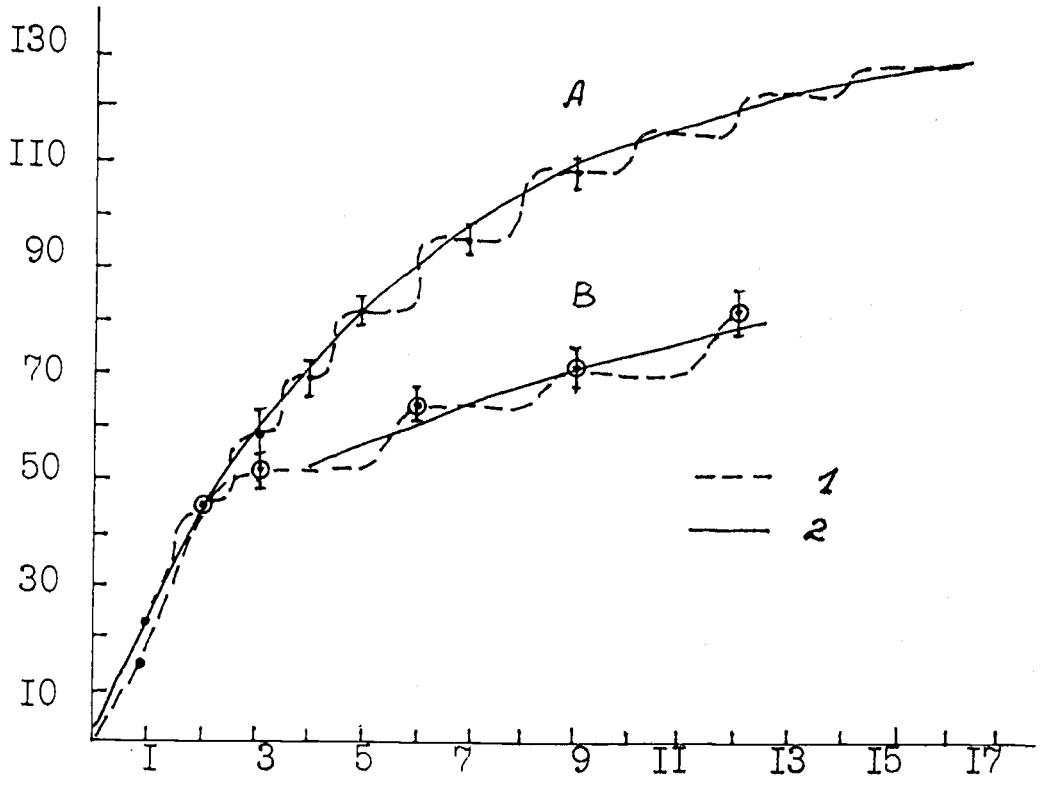

Fig. 2. The group linear growth of horsehair crabs (by Abe, 1992 with alterations).
A - the males
B - the females
1 - the real growth curves
2 - an approximation by growth equations.
Ages (years) and carapace widths (mm) are depicted on abscissa and ordinate axes accordingly.

Mezoplankton Distribution in the West Japan Sea

Natalia T. DOLGANOVA

Pacific Research Fisheries Centre (TINRO-Centre)
4, Shevchenko Alley, Vladivostok, 690600, Russia

Species composition and biomass distribution of mezoplankton in the western Japan Sea from 0-100 m are evaluated from data obtained from two surveys during April-May in 1989 and 1990. Samples were collected using a Jady plankton net (mouth square 0.1 sq. m., mesh size 0.168 mm, rising velocity 0.5 m/s). Phytoplankton biomass is estimated from the net samples. Zooplankton is divided into three size fractions and fishing efficiency is used to calculate their biomass ("Recommendations", 1984; Volkov, 1986). The distribution of plankton is considered in four specific water mass regions which had been defined by temperature salinity analysis:

I. - Primorye Current zone,
II. - subarctic zone,
III.- Polar front between region II and IV zone(Fig. 1),
IV.- subtropic zone.

A phytoplankton "bloom" of 50 to 500 mg/cub.m occurred in April from southwest to northeast. The species of genera *Coscinodiscus, Chaetoceros, Thallasiosira, Ceratium* are dominant. The "bloom" ended in late May when the biomass decreases to 50 mg/cub.m. Patches of high phytoplankton biomass (200-500 mg/cub.m) occur in the Primorye Current zone and in an area known for it's high productivity (Kun, 1984; Markina and Cherniavsky, 1985) (Fig. 2). In spring plankton accumulates in the upper 0-100 m layer (Zenkevich, 1963; Vinogradov, 1968). Zooplankton in Japan Sea is characterized by the highest biomass in spring (Kun, 1975; Markina and Cherniavsky, 1985; Volkov, Chuchukalo 1986; Lapshina et.al., 1990). The mean total biomass of zooplankton is about 1,000 mg/cub.m in April-May of both years. The total stock of plankton in the upper 100-m layer is estimated as 120 t/sq. km in 1989 and 140 t/sq. km in 1990. The ratio between size fractions in 1989-1990 is equal though the total biomass in 1990 is higher. The high numbers of the small zooplankton fraction (1.5 mm organisms were 100-360 mg/cub.m or almost 40% of total biomass) testifies to the reproductive success. The middle fraction biomass is formed by large numbers (Figs. 3 and 4).

A boreal complex was found to be present in the mezoplankton. This complex is composed of *Parasagitta elegans, Neocalanus plumchrus, Neocalanus cristatus, Eucalanus bungii, Metridia pacifica, Oithona similis, Oncaea borealis, Pseudocalanus minutus, Thysanoessa longipes, Euphausia pacifica* and others. Some are homogeneously distributed, while others are concentrated creating a large biomass in certain regions (Figs. 5 and 6). *Copepoda* dominated in all the sampled areas. *N. plumchrus and M. pacifica* constitute the maximal biomass but *O. similis* and *P. minutus* are the most numerous. All stages of maturity of these animals are present but the young are the most abundant.

The biomass of certain groups of zooplankton dominate in each of the four regions: *Copepoda* are the most abundant (84%) in the subarctic zone; followed by *Amphipoda* and *Chaetognatha* (each about 20%) in region II; *Euphausiacea (Thysanoessa longipes)* and *Chaetognatha* dominate in the Polar front, and they are observed to be the most significant species because of the faunae mixture; *Chaetognatha* and *Euphausia pacifica* dominate in the subtropic zone. The ratio of the main groups of

zooplankton and size at maturity correspond to the rate of plankton community succession in a particular water mass.

The day night cycle led to a change in the ratio of size fractions and the abundance of some groups (Table 1). There are such active migrants such as *Euphausia, Amphipoda* and *Chaetognatha.*

Diurnal migration coefficients are 3.0-10.0. They are specifically for *Copepoda*: *Metridia pacifica* 3.0 (adults) and 1.5 (copepodites III-IV); *N. cristatus* 5.0, *Pareuchaeta japonica* 6.0, *Gaidius variabilis* 8.0. Small *Copepoda, O. similis, P. minutus, O. borealis* concentrations did not change considerably throughout the maturity stages during the day/night cycle.

REFERENCES

Kun, M.S. 1975. Zooplankton of Far-Eastern Seas. Moscow: Pischev.promyshlen. 149 p.

Kun, M.S. 1984. A possibility of long-term forecasting of plankton succession in the zone of subarctic front in the Northwest Pacific. Izv. TINRO. 109:41-50.

Lapshina, V.I., O.E. Muravyava, and I.G. Stepanenko. 1990. Seasonal and interannual fluctuations of quantitative characteristics of net plankton from economical zone of USSR and PDRK. Izv. TINRO. 111:133-145.

Markina, N.P., and V.I. Cherniavsky. 1985. Quantitative distribution of phyto-,zooplankton and conditions of formation the productive zones in the Japan Sea. Izv. TINRO. 110:129-138.

Recommendations on express-processing of net plankton in the sea. 1984. Vladivostok: TINRO. 31 p.

Zenkevich, L.A. 1963. Biology of the USSR seas. AS USSR. M. 739 p.

Volkov, A.F. 1986. The state of food base of the main commencial objects of the Okhotsk Sea in autumn period, p. 122-133. *In* Gadidae of the Far-Eastern Seas, Vladivostok: TINRO.

Volkov, A.F., and V.I. Chuchukalo. 1985. Seasonal dynamics of mezoplankton in the Japan Sea (on the studies of TINRO in 1949-1969), p. 140-146. *In* Clupediae of north part of the Pacific Ocean. Vladivostok: TINRO.

Vinogradov, M.E. 1968. Vertical distribution of oceanic zooplankton. Science. M. 319 p.

TABLES AND FIGURES

Table 1. Distribution of zooplankton in different regions in the Japan Sea.

Date	Reg.	Daily Time	SF	MF	LF	Total	Main groups of plankton				
							Cope-poda	Amphi-poda	Eupha-usiida	Chae-togn.	Et. all
1989	I	D	357/45	61/ 7	380/48	798	664/83	78/10	4/ +	28/ 4	24/ 3
	I	N	359/45	151/19	281/36	791	662/84	34/ 4	8/ 1	47/ 6	40/ 5
	II	D	375/46	63/ 8	371/46	809	516/64	141/17	68/ 8	59/ 7	25/ 4
	II	N	140/21	37/ 5	492/74	669	275/41	174/26	78/12	137/20	5/ 1
	III	D	199/42	35/ 7	241/51	470	263/56	48/10	22/ 5	22 / 5	115/24
	III	N	120/34	37/11	191/55	348	191/55	95/27	9/ 3	22/ 6	31/ 9
	IV	D	100/45	15/ 7	107/48	222	122/55	14/ 6	7/ 3	10/ 6	69/31
	IV	N	179/36	47/ 9	272/55	498	270/54	98/20	112/22	4/ 1	14/ 3
1990	II	D	255/48	55/10	227/42	535	356/67	7/ 1	59/11	98/18	15/ 3
	II	N	362/27	61/ 5	896/68	1319	561/43	143/11	123/ 9	452/34	40/ 3
	III	D	181/46	50/13	160/41	391	258/66	13/ 3	19/ 5	88/23	13/ 3
	III	N	114/10	74/ 6	977/84	1165	337/29	194/17	318/27	315/27	1/ +
	IV	D	280/53	75/14	171/33	526	382/73	10/ 2	16/ 3	107/20	11/ 2
	IV	N	230/20	150/13	754/67	1134	567/50	158/14	142/13	247/22	20/11

Note: all entries in the table mg/m^3 / % of total biomass.
I - Primorye current ;
II - subarctic waters;
III - frontal zone;
IV - subtropic waters.

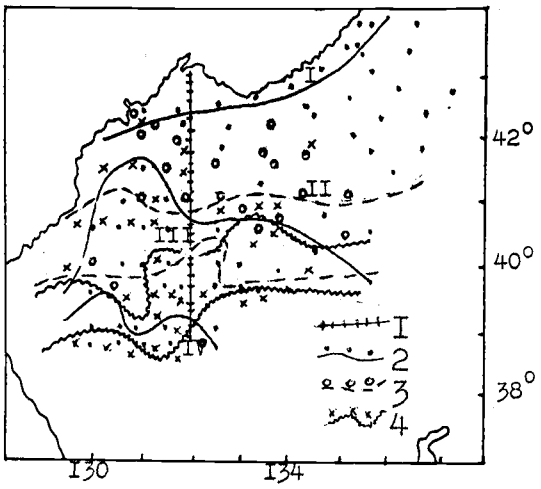

Fig. 1. Region of surveys

1. standard section
2. survey of 1989
3. first survey of 1990
4. second survey of 1990

I. zone of Primorye current
II. subarctic waters
III. frontal zone
IV. subtropic waters

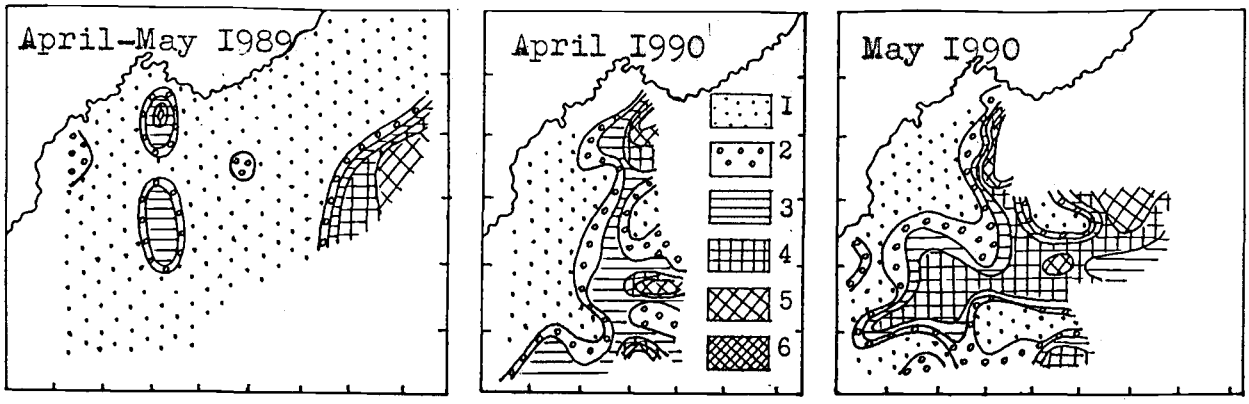

Fig. 2. Distribution of net phytoplankton biomass (mg/m^3)

1. less than 50
2. 50-100
3. 100-200
4. 200-500
5. 500-1,000
6. more than 1,000

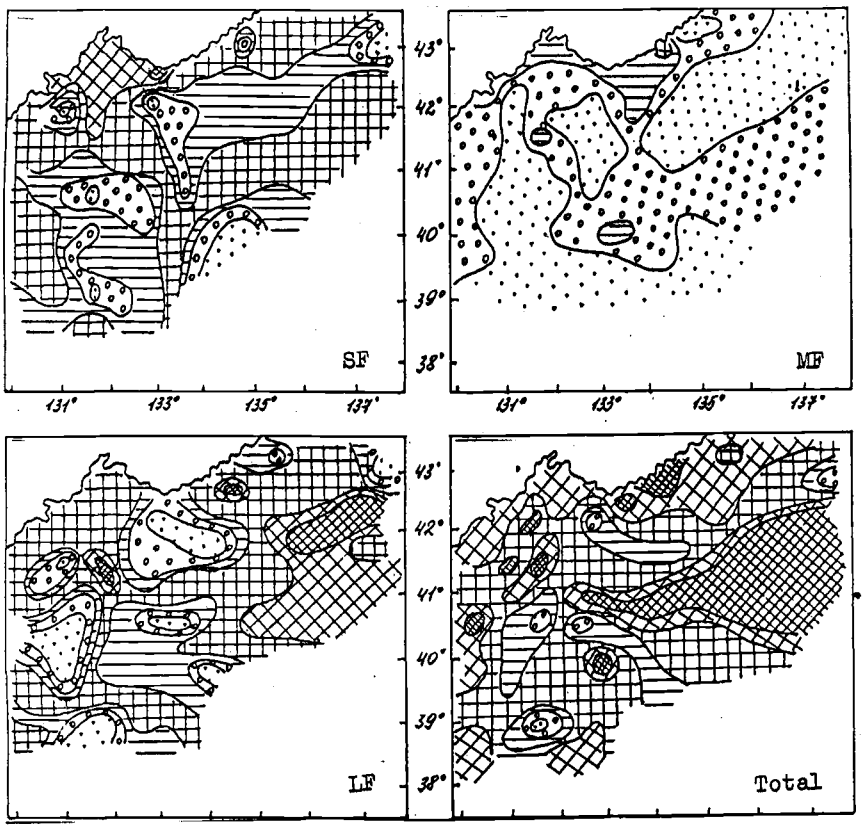

Fig. 3. Distribution of zooplankton biomass by three size fractions in 1989.

SF - small fraction (less than 1.5) MF - middle fraction (1.5-3.5)
LF - large fraction (more than 3.5 mm)

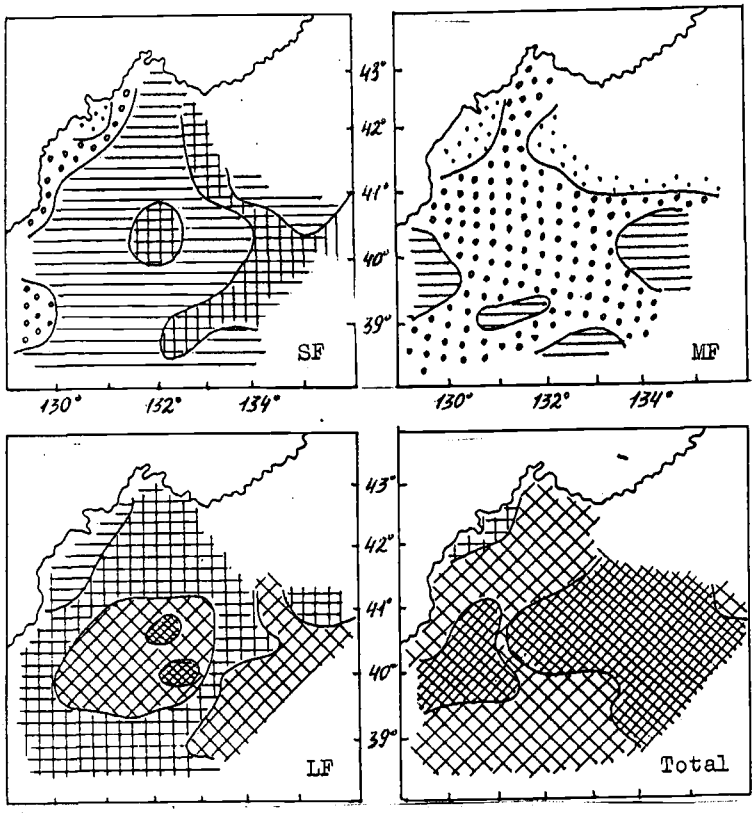

Fig. 4. Distribution of zooplankton biomass by three size fractions in 1990.

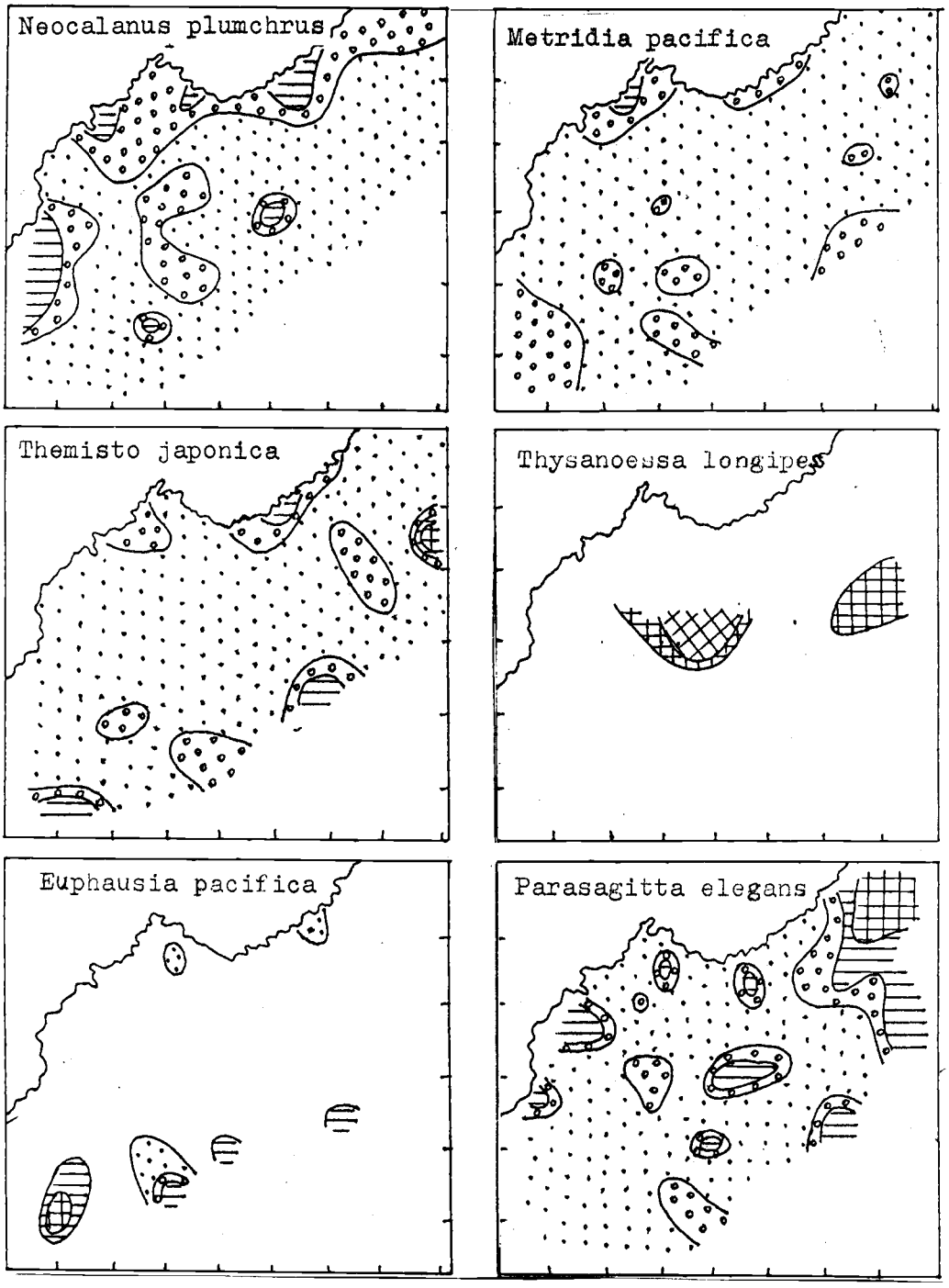

Fig. 5. Distribution of dominated species of zooplankton (mg/m^3) in 1989.

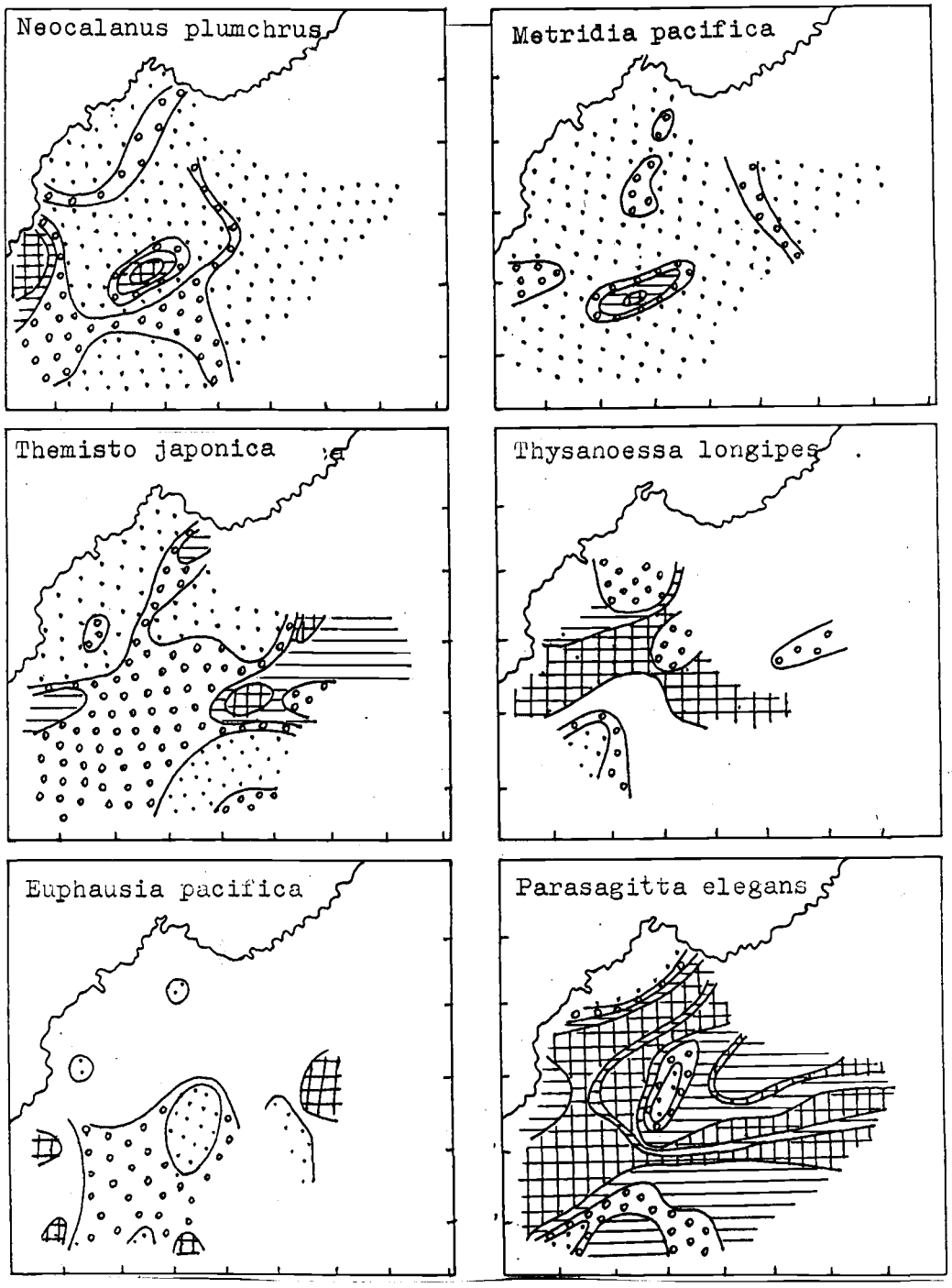

Fig. 6. Distribution of dominated species of zooplankton (mg/m^3) in 1990.

Application of Pink and Chum Salmon Genetic Baseline to Fishery Management

Vladimir V. EFREMOV[1], Richard L. WILMOT[2], Christine M. KONDZELA[2], Natalia V. VARNAVSKYA[3], Sharon L. HAWKINS[2] and Maria E. MALININA[4]

[1] Institute of Marine Biology, Vladivostok, 690041, Russia
[2] Auke Bay Laboratory NMFS, Juneau, AK 99801-8626, U.S.A.
[3] KamchatNIRO, Petropavlovsk-Kamchatsky, 683602, Russia
[4] TINRO, Vladivostok, 690600, Russia

The salmon form aggregations composed of numerous stocks during their marine portion of life. Identification of these stocks in mixtures has been a great problem in salmon management for fisheries agencies. The absence of the information on the stock composition results in either overharvest or over escapement.

One of the most informative methods for investigating stock structure is the electrophoretic analysis of protein variation. The method and its application began with developmental work by Utter and his associates at the National Marine Fisheries Service in the 1970's. This method has been used by several fisheries agencies in North America since the early 1980's and past results show that genetic stock identification (GSI) is a practical fisheries management tool (Grant et al., 1980; Milner et al., 1985; Utter et al., 1987; Shaklee et al., 1990; Wilmot et al., 1992).

Unfortunately, to date GSI analysis was almost never used for management purposes in Russia. Recently, the genetic baselines were constructed for Asian pink and chum salmon. These baselines cover main spawning regions of pink and chum in Asia ranging from Hokkaido to Anadyr river. Two goals of this work were:

1. to evaluate the accuracy and precision of stock composition estimates using computer simulations of baselines,
2. to estimate the stock-group contributions of the mixed fishery samples from the Sea of Okhotsk and the North Pacific Ocean via maximum likelihood method.

MATERIAL AND METHOD

Chum and even year pink salmon baselines (Auke Bay Laboratory NMFS) were used for computer simulations. Chum salmon baseline includes allozyme data for 30 loci and 33 stocks; even year pink salmon baseline - 24 loci and 21 stocks (Fig. 1 and Table 1). We attemped to obtain 100 adults whenever possible from each stock. Six hundred and twenty six pinks were collected in the Sea of Okhotsk and the North Pacific Ocean in 1994 during June-August by scientific vessels (Fig. 1).

Four tissues (muscle, liver, heart and eye) were taken from each fish for protein electrophoresis. Protein electrophoresis was conducted as described by Aebersold et al. (1987). Specific enzymes were stained according to Harris and Hopkinson (1976) and Aebersold et al. (1987).

Estimation of the mixture composition and a simulation of possible mixture scenarious for a given baselines were performed using the SPAM program (Gates, 1995).

RESULTS AND DISCUSSION

Simulated mixtures were used to evaluate the accuracy (bias) and precision (standard deviation) of the stock composition estimates. These hypothetical mixtures were generated using the baseline allele frequencies assuming Hardy-Weinberg equilibrium. First, we used a simulated mixture of 100% of the group and these simulations showed at least 87% accuracy for chum salmon and 83% for pink salmon (Tables 2 and 3). We also used mixtures where the contributions of each baselines stock-group to the simulated fishery mixture represented the stock compositions of likely mixed-stock fisheries. These simulations were performed to explore the effects of sample size on the accuracy and precision of the maximum likelihood estimates too. Our simulations revealed that chum and even year pink baselines can provide a reasonable estimates of regional contributions. The increase in sample size reduced the bias and standard deviations of the estimates (Tables 4 and 5).

Maximum likelihood were calculated for the samples collected from the Sea of Okhotsk and the North Pacific Ocean. The West Kamchatka region was the predominant group in all the estimates; its contribution ranged from 46% in the south part of the Sea of Okhotsk to 93% by the North Kuril Islands (Fig. 1 and Table 6).

The alaskan component was also fairly consistent in the Sea of Okhotsk near West Kamchatka ranging from 13% in the end of July up to 28% in the begining of August. These data contradict with tagging information (Takagi et al., 1981) and are needed to verify, but simulation showed that alaskan pinks can be identified with high accuracy and precision (Tables 2-5).

Computer simulations and mixed fishery analyses show the potentiality to use chum and pink salmon baselines for both management and studies of the marine migration. Our permanent challenge is to improve baselines, incorporating a new important stocks.

REFERENCES

Aebersold, P.B., G.A. Winans, D.J. Teel, G.B. Milner, and F.M. Utter. 1987. Manual for starch gel electrophoresis: a method for the detection of genetic variation. NOAA Tech. Rep. NMFS. 61:1-19.

Gates, R. 1995. SPAM. Statistics program for analysing mixtures. ADF&G, Anchorage, Alaska. 37 p.

Grant, W.S., G.B. Milner, P. Krasnovski, and F.M. Utter. 1980. Use of biochemical genetic variants for identification of sockeye salmon (*Oncorhynchus nerka*) stocks in Cook Inlet, Alaska. Can J.Fish.Aquat.Sci. 37:1236-1247.

Harris, H., and D.A. Hopkinson. 1976. Handbook of enzyme electrophoresis in human genetics. American Elsevier Publishing Co., New York.

Milner, G.B., D.J. Teel, F.M. Utter, and G.A. Winans. 1985. A genetic method of stock identification in mixed populations of Pacific salmon, Oncorhynchus spp. Mar.Fish.Rev. 47:1-8.

Shaklee, J.B., S.R. Phelps, and J. Salini. 1990. Analysis of fish stock structure and mixed-stock fisheries by the electrophoretic characterization of allelic isozymes, p.173-196. *In* D.H.Whitmore [ed.] Electrophoreticand isoelectric focusing techniques in fisheries management. CRC Press, Boca Raton, FL.

Takagi, K., K.V. Aro, A.C. Hartt, and M.B. Dell. 1981. Distribution and origin of pink salmon (Oncorhynchus gorbuscha) in offshore waters of the North Pacific Ocean. Int. North Pacific Fish. Comm. Bull. 40:1-195.

Utter, F., D. Teel., G. Milner, and D. McIsaac. 1987. Genetic estimates of stock composition of 1983 chinook salmon, Oncorhynchus tshawytscha, harvests off the Washington coast and the Columbia river. NMFS Fish.Bull. 85:13-23.

Wilmot, R.L., R.J. Everett, W.J. Spearman, and R. Baccus. 1992. Genetic stock identification of Yukon River chum and chinook salmon - 1987 to 1990. Prog. Rep. U.S. Fish. and Wildlife Service, Anchorage. AK. 132 p.

Winans, G.A., P.B. Aebersold, S. Urawa, and N.V. Varnavskaya. 1994. Determing continent of origin of chum salmon (Oncorhynchus keta) using genetic stock identification techniques: status of allozyme baseline in Asia. Can. J. Fish. Aquat. Sci. 51(Suppl. 1):95-113.

TABLES AND FIGURES

Table 1. Enzyme names, enzyme commision (EC) numbers and locus abbreviations for chum and pink salmon.

Enzyme name	EC No abbrev.	Locus	Chum	Pink
N-Acetil-b-glucosaminidase	3.2.1.30	bGLUA	+	-
Aconitate hydratase	4.2.1.3	sAH	+	-
		mAH-3,4	+	-
		mAH-3	-	+
		mAH-4	-	+
Adenosine deaminase	3.5.4.4	ADA-2	-	+
Alanine aminotransferase	2.6.1.2	ALAT	+	+
Aspartate aminotransferase	2.6.1.1	sAAT-1, 2	+	+
		sAAT-3	+	+
		mAAT-1	+	+
		mAAT-2	+	-
Creatine kinase	2.7.3.2	CKA-2	+	+
Dipeptidase	3.4.*.*	PEP-A	+	-
Esterase D	3.1.*.*	ESTD	+	-
Formaldehyde dehydrogenase	1.2.1.1	FDHG	-	+
Fumarate hydratase	4.2.1.2	FH	+	+
bGalactosidase	3.2.1.23	bGALA	+	-
Glucose-6-phospate isomerase	5.3.1.9	GPA-A	+	+
Glycerol-3-phosphate	1.1.1.8	G3PDH-1	-	+
dehydrogenase		G3PDH-2	+	-
Isocitrate dehydrogenase	1.1.1.42	sIDHP-2	+	-
		mIDHP-1	+	-
Lactate dehydrogenase	1.1.1.27	LDHA-1	+	+
		LDHB-1	-	+
		LDHB-2	+	+
Malate dehydrogenase	1.1.1.37	sMDHA-1,2	+	+
		sMDHB-1,2	+	+
Malic enzyme	1.1.1.40	sMEP-1	+	+
		mMEP-2	+	-
Mannose-6-phosphate isomerase	5.3.1.8	MPI	+	+
Phosphoglucomutase	5.4.2.2	PGM-1	+	-
		PGM-2	+	+
Phosphogluconate dehydrogenase	1.1.1.44	PGDH	+	+
Proline dipeptidase	3.4.13.9	PEPD-2	-	+
Triose-phosphate isomerase	5.3.1.1	TPI-3	+	-
		TPI-4	+	+
Tripeptidase	3.4.11.4	PEPB-1	+	+

Table 2. Simulation. Estimated contributions of chum salmon where each region comprises 100% of the mixture.

Region	Japan	Primorye	Sakhalin	Magadan	West Kamchatka	East Kamchatka
Japan	.9850	.0287	.0251	.0070	.0078	.0097
Primorye	.0013	.9482	.0098	.0017	.0004	.0012
Sakhalin	.0013	.0170	.9537	.0003	.0001	.0003
Magadan	.0010	.0002	.0005	.8761	.0255	.0225
West Kamchatka	.0044	.0008	.0033	.0630	.8808	.0900
East Kamchatka	.0041	.0008	.0039	.0408	.0821	.8716

Table 3. Simulation. Estimated contributions of pink salmon where each region comprises 100% of the mixture.

Region	Japan	Kuril Islands	Sakhalin	West Kamchatka	East Kamchatka	Alaska
Japan	.8317	.0648	.0522	.0153	.0017	.0056
Kuril Islands	.0279	.8338	.0023	.0042	.0015	.0041
Sakhalin	.1125	.0797	.9028	.0308	.0529	.0086
West Kamchatka	.0145	.0116	.0260	.8710	.0545	.0205
East Kamchatka	.0039	.0019	.0059	.0462	.8659	.0020
Alaska	.0085	.0081	.0102	.0310	.0226	.9583

Simulated sample size: 150. Number of resamplings: 100. Estimates not summing to 1.0000 are caused by randomly generated genotypes that cannot be explained by a randomly generated baseline.

Table 4. Simulation. Expected and estimated contributions of chum salmon for different sample sizes.

Region	Expected	Estimated N=150	Estimated N=50	Estimated N=25
Japan	.7000	.7064 (.0433)	.6866 (.0788)	.6552 (.1261)
Primorye	.0100	.0166 (.0173)	.0156 (.0250)	.0250 (.0430)
Sakhalin	.0800	.0753 (.0297)	.0705 (.0558)	.0687 (.0703)
Magadan	.0300	.0276 (.0285)	.0278 (.0379)	.0330 (.0553)
West Kamchatka	.0900	.0886 (.0404)	.0970 (.0669)	.1049 (.0815)
East Kamchatka	.0900	.0816 (.0395)	.0980 (.0650)	.1092 (.0987)

Table 5. Simulation. Expected and estimated contributions of pink salmon for different sample sizes.

Region	Expected	Estimated N=150	Estimated N=50	Estimated N=25
Japan	.0500	.0797 (.0697)	.0947 (.1003)	.0913 (.1191)
Kuril Islands	.1000	.0835 (.0679)	.0614 (.0720)	.0553 (.0972)
Sakhalin	.2500	.2400 (.1225)	.2381 (.1504)	.2865 (.1805)
West Kamchatka	.3000	.2892 (.0827)	.3054 (.1399)	.2594 (.1599)
East Kamchatka	.1000	.0953 (.0702)	.0873 (.0874)	.1043 (.1284)
Alaska	.2000	.2115 (.0673)	.2122 (.1043)	.2008 (.1311)

One standard deviation is in parenthesis. Number of resamplings: 100. Estimates not summing to 1.0000 are caused by randomly generated genotypes that cannot be explained by a randomly generated baseline.

Table 6. Mixed fishery analysis. Estimated contributions of pink salmon to the Sea of Okhotsk and the North Pacific Ocean test fishery in 1994.

Area	Japan	Kuril Islands	Sakhalin	West Kamch.	East Kamch.	Alaska
A	.0910 (.0879)	.0000 (.0000)	.4199 (.1645)	.4561 (.1548)	.0000 (.0000)	.0000 (.0000)
B1	.0001 (.0000)	.0000 (.0000)	.0000 (.0000)	.7874 (.0564)	.0649 (.0453)	.1263 (.0362)
B2	.0001 (.0000)	.0002 (.0000)	.0000 (.0000)	.6370 (.1363)	.0633 (.0952)	.2784 (.0902)
C	.0004 (.0001)	.0001 (.0001)	.0001 (.0000)	.9256 (.0619)	.0000 (.0000)	.0566 (.0619)

One standard deviation is in parenthesis.

Area A: Date of sampling - August 10. N = 92. Trawls 20 and 21 are summed.
Area B1: Date of sampling - July 17 - 27. N = 329. Trawls 27, 28, 36, 37, 43, 45, 51 and 55 are summed.
Area B2: Date of sampling - August 3-5. N = 143. Trawls 70, 73, 74 and 76 are summed.
Area C: Date of sampling - July 28-31. N=116. Trawls 59, 64 and 65 are summed.

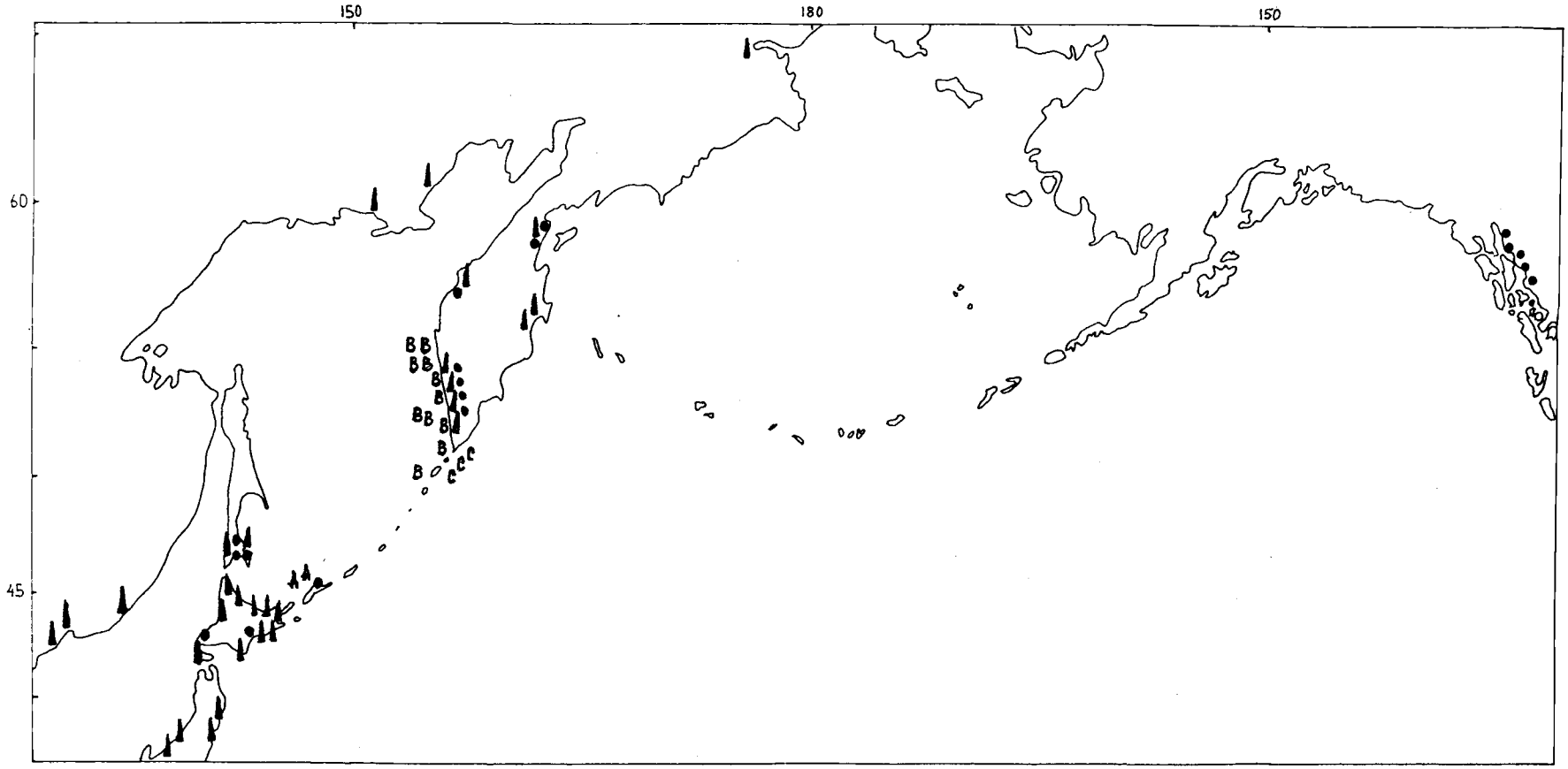

Fig. 1. Sampling sites for chum and pink salmon. Triangles show chum salmon baseline sites, circles show pink salmon baseline sites. Letters correspond to mixed fishery collection sites listed in Table 6. Japanese data were taken from Winans et al., 1994.

Strategy for Culture, Breeding and Numerous Dynamics of Sakhalin Salmon Populations

Vyacheslav N. IVANKOV and Valentina V. ANDREYEVA

Far-Eastern State University, Vladivostok, Russia

ABSTRACT

The marine littoral zone and the influence of hatchery produced salmon fry on the biocenose structure in South Sakhalin were studied. The littoral area is highly productive and had a complex community structure. The release of hatchery salmon fry influences a number of the components of littoral biocenose, particularly, the *Harpacticoida* which are the preferred food items of salmon fry upon entering the sea. In shallow waters, the competition for food by chum and pink salmon fry causes a deterioration of the habitat conditions for other species of fish, namely, pond smelt (*Hypomesus olidus*), Pacific sand lance (*Ammodytes personatus*) and the fry of plaice and Far-Eastern navaga etc. Salmon fry are also feed for carnivorous fishes such as kunscha (*Salvelinus leucomaenis*), rainbow Asiatic smelt and sculpins (Cottidae) etc and they compete for food with wild salmon fry which lead to increased mortality of the naturally bred fry.

INTRODUCTION

For ten years, the Chairman of Water Ecology and Sea Culture of Far-Eastern State University studied the conditions of salmon fry in regions influenced by hatchery production in the southwestern and eastern Sakhalin waters. There is an enormous shallows which is separated from the open sea by a stone ridge along the southwestern coast of Sakhalin. The warming and active aeration of waters in the area creates an intensive growth of aquatic vegetation producing favorable conditions for the reproduction of small invertebrates. Historically, a number of fish species inhabit the shallows and more recently young hatchery salmon have been introduced to feed as they move into the sea. The Department of Aquatic Ecology and Aquaculture has carried out research on wild communities and the impact of hatchery produced salmon on the coastal areas (Andreyeva et al., 1994).

MATERIALS AND METHODS

The investigations were carried out in different areas of southern Sakhalin from 1985 to 1991. Samples of plankton, benthos, epiphyton, and fish were collected during May-July, during 3-5 day periods. At the same time, 2 hr. diurnal observations were carried out in laboratory conditions. The temperature, salinity, oxygen content, water level, direction and strength of wind were measured.

RESULTS AND DISCUSSION

The salmon young feed on small invertebrates dwelling, in the water layers, on the vegetation and on the bottom surface layer. The community composition can be classified as plankton, benthos, and epiphyton as well as intermediate forms (planktobenthos). The most abundant groups in the study area are *Harpacticoida* and *Amphipoda*.

The data indicate that seasonal and interannual abundance changes occur for most animal groups but especially for *Harpacticoida* which are about 80-90% of the total biomass of plankton, epiphyton and meiobenthos. A maximum biomass of *Harpacticoida* (760 $sp.m^{-3}$) occurs in mid-May which then decreases and is replaced by other species (Fig. 1). Abundant spring species are also replaced by less abundant summer forms due to warm water formation (Fig. 2). Undoubtedly, the abundance of *Harpacticoida* depends on the amount eaten by the salmon young which are in high abundance at the end of May.

The plankton abundance (*Pseudocalanus minutus,Acartia clausi, Centropages abdominales, Oithona similis*, some larvae of *Polyhaeta*) is maximum during the flood tide except for *Eurytemora thompsoni* which increases during the falling tide. Daily rhythms were observed for other animals such as *Amphipoda, Harpacticoida, Isopoda, Ostracoda, Mysidacea*, however, the increased abundance in the water usually occurs during the night (Fig. 3). Diurnal fluctuations of abundance of these groups can be explained by changes in their activity during the day. According to some authors, the numbers and biomass of animals living in the bottom surface layer and on the vegetation increases in the water column at night (D'Amours, 1988; Walters, 1988). During this study, diurnal migrations vary among the different species but the number and biomass of *Harpacticoida* increases during the day. Animals with a pronounced daily migration into the water column are found to be more vulnerable to feeding young salmon and other fish. Young salmon mainly feed on *Harpacticoida, Amphipoda* and less often of *Polychaeta* and *Insecta* larvae. Daily changes in feeding intensity and food composition is typical for salmon young.

The food of the salmon young in the coastal marine areas consists of 14 groups of organisms, usually the size preference was a length of 0.5-2.5 mm. The food spectrum depends on the habitat type. In bays *Amphipoda* and *Harpacticoida* are 34.6 and 36.6% of the diet and in lagoons it is mainly *Polychaeta, Harpacticoida*, and *Amphipoda* to lesser extent. The food composition changes in May to large species of *Harpacticoida, Harpacticus uniremus* and species of *Thalestris* and *Dactylopodia*, whose size are 0.8 - 1.5 mm. In June smaller species are eaten such as *Tusbe* and *Scutellidium* which are 0.4-0.7 mm. The salmon young consume the maximum food at 1,200 in May and 1,400 in June. During the daily cycle *Harpacticoida* is the dominant species in May, *Amphipoda* and *Insecta* in June. The abundance of salmon fry had an influence on the abundance of the main components of the littoral biocenose, particularly, *Harpacticoida* due to heavy predation when leaving the river for the sea.

The salmon young near southwestern Sakhalin feed from the beginning of May to end of July. They are competitors with other of coastal fishes: silver smelt, sand lance, burnstickle as well as the young of Pacific navaga, flounders and other fish. Salmon fry are also food for carnivorous fishes of biocenose: kundscha (*Salvelinus leucomaenis*), rainbow Asiatic smelt, sculpins (*Cottidae*) etc. The salmon fry produced by hatcheries are competitors for food used by wild salmon fry which could lead to an increase in mortality of naturally spawned salmon fry (in rivers).

During feeding in the coastal marine areas (a month and a half on average), the young salmon consume up to 135 tons of food organisms daily which is estimated to be 30 mg day-1 per individual and approximately 80-100 million individuals aree released from the hatcheries of southwestern Sakhalin. The impact of hatchery salmon production changes food organism abundance and species, such as for Harpacticoida, Amphipoda, Polychaeta and others, during there migration to the sea. Food availability for a number of fish (smelt, flounder, sand lance, navaga and others) is also effected by the large hatchery production. From studies of the daily ration of fry and estimates of the optimal production of fry in this region about 3.5-11.5 million of fry would be optimum for the available littoral area of Kalinin.

The analysis of data show that the total production of Sakhalin hatcheries did not contribute to the low survival of fry and low recurrence of salmons. Rather the practice of releasing 20-30 million fry at one time from hatcheries impacts on survival. A better policy would be to release 2-4 million from the end of April to first part of May, 6-9 million from the middle of May and then reduce the output throughout June until the total production has been released. Additionally, it would be good practice organize the release by spreading it along the Sakhalin seashore.

REFERENCES

Andreyeva, V.V., V.N. Ivankov, N.V. Tyapkina. 1994. Biology and inhabiting conditions of the young of Pacific salmon in the coastal areas of southern Sakhalin, p. 8-9. Systematics, biology and biotechnics of hatching salmon, Sankt-Peterburg.

D'Amours, D. 1988. Vertical distribution and abundance of natant harpacticoid copepods on a vegetated tidalflat. Neth. J. Sea Res. 22:161-170.

Ivankov, V.N., V.V. Andreyeva, I.N. Volkov, and N.V. Mostovaya. 1990 About power and dynamics of discharging the salmon young from the hatcheries of Sakhalin, p.32-33. *In* Scientific and technical problems of marine culture in the country, Vladivostok.

Walters, K. 1988. Diel vertical migration of sediment associated meiofauna in subtropical sand and seagrass habitats. J. Exp. Mar. Biol. and Ecol. 117:169-186.

FIGURES

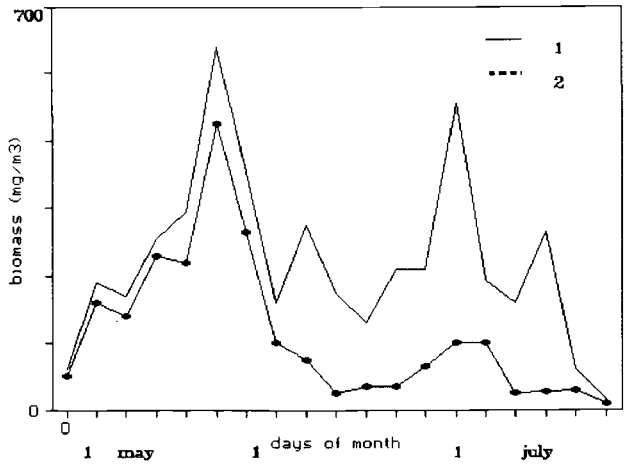

Fig. 1. Seasonal dynamics of biomass of plankton.
1 - total biomass 2 - biomass of Harpacticoida

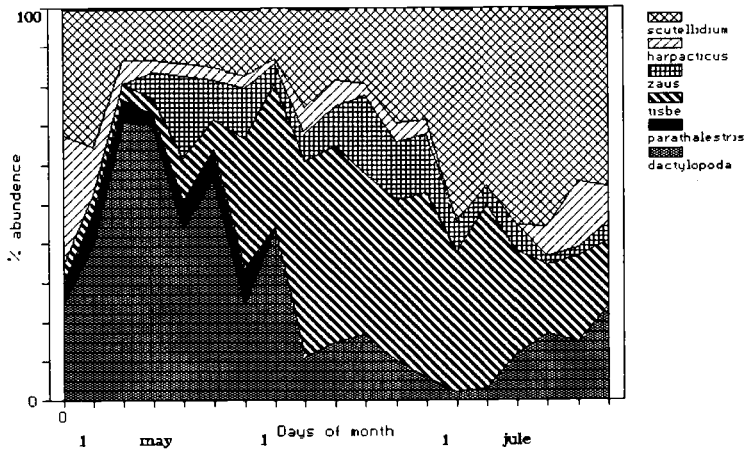

Fig. 2. Seasonal exchange of species composition of Harpacticoida in plankton.

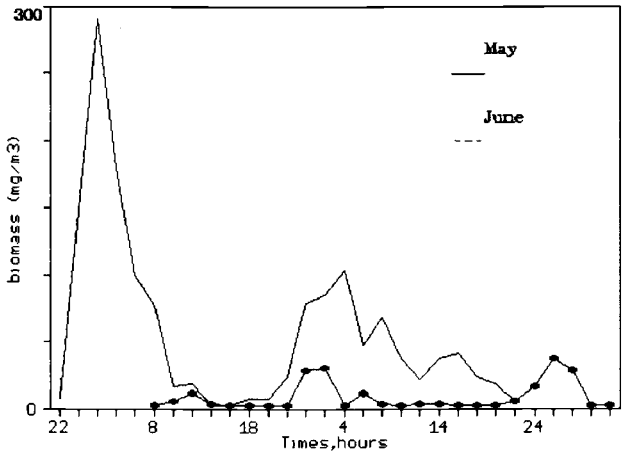

Fig. 3. Daily dynamics of abundance of Harpacticoida.

Primary Production in Sakhalin Shelf Waters

Alla M. KOVALEVSKAYA[1], Natalia I. SAVELYEVA[2] and Dmitry M. POLYAKOV[2]

[1] Pacific Institute of Bio-organic Chemistry FEB RAS
[2] Pacific Oceanological Institute FEB RAS

INTRODUCTION

The distribution and productivity of phytoplankton on the Sakhalin shelf varies in space and time depending on different physical forcing. The dominant physical effects on phytoplankton processes in this region are the strong seasonal changes in intensity of incoming solar radiation, wind direction and nutrients in the water.

This work examines primary production on petroleum deposits on the continental Sakhalin shelf at Chayvo, Arkutun-Dagi, Piltun and Sakhalin Bay. Development in these areas has started and the measurement of primary production can be used as an indication of the effects of chronic petroleum pollution and navigation on bioproductivity.

Productivity data were primarily collected from 27 stations located between 52° and 54° N and 142° and 144°E in depths not exceeding 90 m relative to the shelf waters.

METHODS

With some modifications, the primary production is measured according to Steeman Nielsen (1952). Photosynthesis is calculated by the incorporation of C^{14} in particles collected on 0.4 mkm Synpor filters. All samples are processed in 0.1 NHCl and analyzed with the help of the Delta-100 liquid scintillation counter. The fixing of carbon during the dark is determined in each experiment. The water is selected from different layers and incubated on the deck with neutral density filters to simulate the *in situ* radiation field. The fractional exposition of the same water samples are used to determine the daily production. In a special experiment C^{14} incorporation is very low at night compared to the usual radioactive background.

The curve of daily production of 1 m^3 of water is plotted on data of fractional expositions (by calculation of under peak square) to determine the daily production in the water column under 1 m^2. The coefficients for each daylight period are calculated to permit exposition at any time.

The Phytoplankton Primary Production on Petroleum Deposits of Continental Sakhalin Shelf

Two major natural parameters regulating the phytoplankton quantity and production in the ocean are light and nutrients, particularly, nitrogen. In the investigated region seasonal changes of solar radiation on the sea surface and nitrate concentrations are significant. The Sakhalin Bay nitrate concentration is very low, average 6 mM despite the Amur river discharge, much lower than in the open Okhotsk sea 15 mM, and Piltun deposit 18 mM (Tech. Report, 1992). The primary production is 0.33 gC/m^2 day, 0.8 gC/m^2 day and 2.4 gC/m^2 day respectively. The nitrate concentration is taken into account from the lower level of the photosynthesis zone to a depth not exceeding 50 m, since in the upper layers the concentrations are grazed and it would underestimate the initial conditions. In

August 1992 on the Piltun deposit the average value of primary production reaches 2.4 gC/m^2 day (maximum 5.56 gC/m^2 day), and in August 1993 it did not exceed 0.53 gC/m^2 day (Tech. Report, 1993). The comparison of primary production and nitrate concentration on stations with close coordinates indicate that nitrate contents are some times higher (Table 1). The 1994 primary production at the end of October during a shorter daylight period is compared to the longer daylight period of August 1993. The values of primary production varies from site to site: Chayvo the average primary production is 0.4 gC/m^2 day (maximum 0.65 gC/m^2 day); Arkutun-Dagi 1.24 gC/m^2 day (maximum 2.84 gC/m^2 day); Piltun 0.68 gC/m^2 day (maximum 1.4 gC/m^2 day) and in Sakhalin Bay 0.42 gC/m^2 day (maximum 1.21 gC/m^2day) (Fig. 1). The length of daylight is the major regulating parameter in the rate of phytoplankton production which explains the lower rate of photosynthesis on the Piltun stations, for example, 0.68 gC/m^2 day in October 1994 and 3.11 gC/m^2 day August 1992. Additionally, the role of the nutrient flux in the Okhotsk Sea euphotic zone should be taken into account as is shown in the nitrate example.

It is difficult to separate the different influences of these processes in determining primary production because they are closely related. Some regeneration of nitrogen in the eutrophic waters is caused by zooplankton and microzooplankton metabolism. The greatest phytoplankton biomass and rate of primary production is from the nitrate flux from upwelling (Eppley and Peterson, 1979; Dortch and Postel, 1989). While photosynthetic radiation defines the rate of primary production *in situ*, the rate of dissolved nitrogen production is responsible for high primary production in the upwelling zone. As a rule, a combination of the solar radiation and nitrate flux provides higher levels of primary production in summer.

The arrangement of the deposits and the distribution of primary production is shown in Fig. 1. The lowest primary production is observed on Chayvo, the highest on Arcutun-Dagi, and on other two sites the values are similar and intermediate. The change of the primary production on Chayvo is possibly connected to sampling conditions (the stormy weather causes the top and bottom water layers to mix in the shallow depths) as is evident from the vertical distribution of primary production in different layers. The maximum primary production which usually occurs near surface or just below does not occur at nearly all the stations. A similar distribution is observed on the very shallow Sakhalin Bay (maximal depth 22 m) deposit. The value of primary production is reasonably high 1.21 gC/m^2 day. The deposit is near the Amur river influence and the water structure is characterized by the upper quasi-homogenous layer to 10-15 m. It is reflected in the homogeneous vertical primary production structure. The lowest daily production, which did not exceed 0.2 gC/m^2 day, is observed in strong current. Thus the non-uniformity in primary production (from 1.21 to 0.15 gC/m^2 day) is connected to the hydrodynamic processes in this region.

At deep-water sites, there is a more ordered vertical distribution of primary production (Piltun deposit, maximum depth 63 m, and Arcutun-Dagi maximum depth 90 m). At the Arcutun-Dagi site, the photosynthetic zone ceases at 90 m while in summer months of 1993 it is 40 m (Tech. Report, 1993) and 60 m in 1979 (Eppley and Peterson, 1979).

Within the limits of each site, the variability of primary production is (particularly at Arcutun-Dagi deposit) from 2.84 gC/m^2 day to 0.09 gC/m^2 day. Such a mosaic, within the limits of the small area, testifies to the complexity of the photosynthesis process. The high primary production of waters at the study site indicates the possible problems that could occur from future industrial development. Primary production is sensitive to pollution, as is found for the toxic compounds of drilling muds which suppress photosynthesis (Tech. Report, 1993). As phytoplankton is the primary unit in the trophic food web, it is not hard determine possible consequence to the system of a toxic event. Therefore, primary production measurement can be used as main indicator of environmental conditions and to select harmless drilling mud.

The relationship between primary production in the water column and surface phytoplankton pigment biomass was investigated for the purpose of the determining the opportunities of using pigment concentration for predicting primary production (Eppley et al., 1985; Perry, 1986). It is shown that the biomass variability defines many, but far from all factors of primary production. Thus, the primary production method of research on photosynthesis gives the best representation of bioproductivity of the ocean. The method permits the simulation of any conditions *in situ.* In particular, the influence of various additives on primary production can be produced for guidance in areas where industrial development is planned.

REFERENCES

Steeman-Nielsen, E. 1952. The use of radioactive carbon (^{14}C) for measuring organic production in the sea. J. Cons. Int. Explor. Mer. 18:117-140.

Technological report about work in 23 cruise R/V "Academik A.Nesmeyanov", v.4. 1992.

Technological report about work in 24 cruise R/V "Academik A.Nesmeyanov", v.3, 4. 1993.

Eppley, R.W., and B.J. Peterson. 1979. Particulate Organic Matter Flux and Plankton New Production in the Deep Ocean. Nature. 282:677-680.

Dortch, Q., and J.R. Postel. 1989. Phytoplankton and nitrogen interactions, p.139-174. *In* M.L. Landry and B.M. Hickey [ed.] Coastal Oceanography of Washington and Oregon. Elsevier, Amsterdam, Neth.

Eppley, R.W., E. Stewart, M.R. Abbot, and U. Heyman. 1985. Estimating Ocean Primary Production from Satellite Chlorophyll: Introduction to Regional Differences and Statistics for the Southern California Right. J. Plankton Res. 7:57-70.

Perry, M.J. 1986. Assessing Marine Primary Production from Space. Bioscience. 36:461-466.

TABLES AND FIGURES

Table 1. The comparison of nitratcontents and primary production (PP) on stations of Piltun deposit in August 1992 and 1993.

Year	NO_3 mM	PP gC/m^2 day
1992, 7, August	14.18	1.17
1993, 14, August	8.43	0.53
1992, 7, August	19.03	2.33
1993, 14, August	5.01	0.15

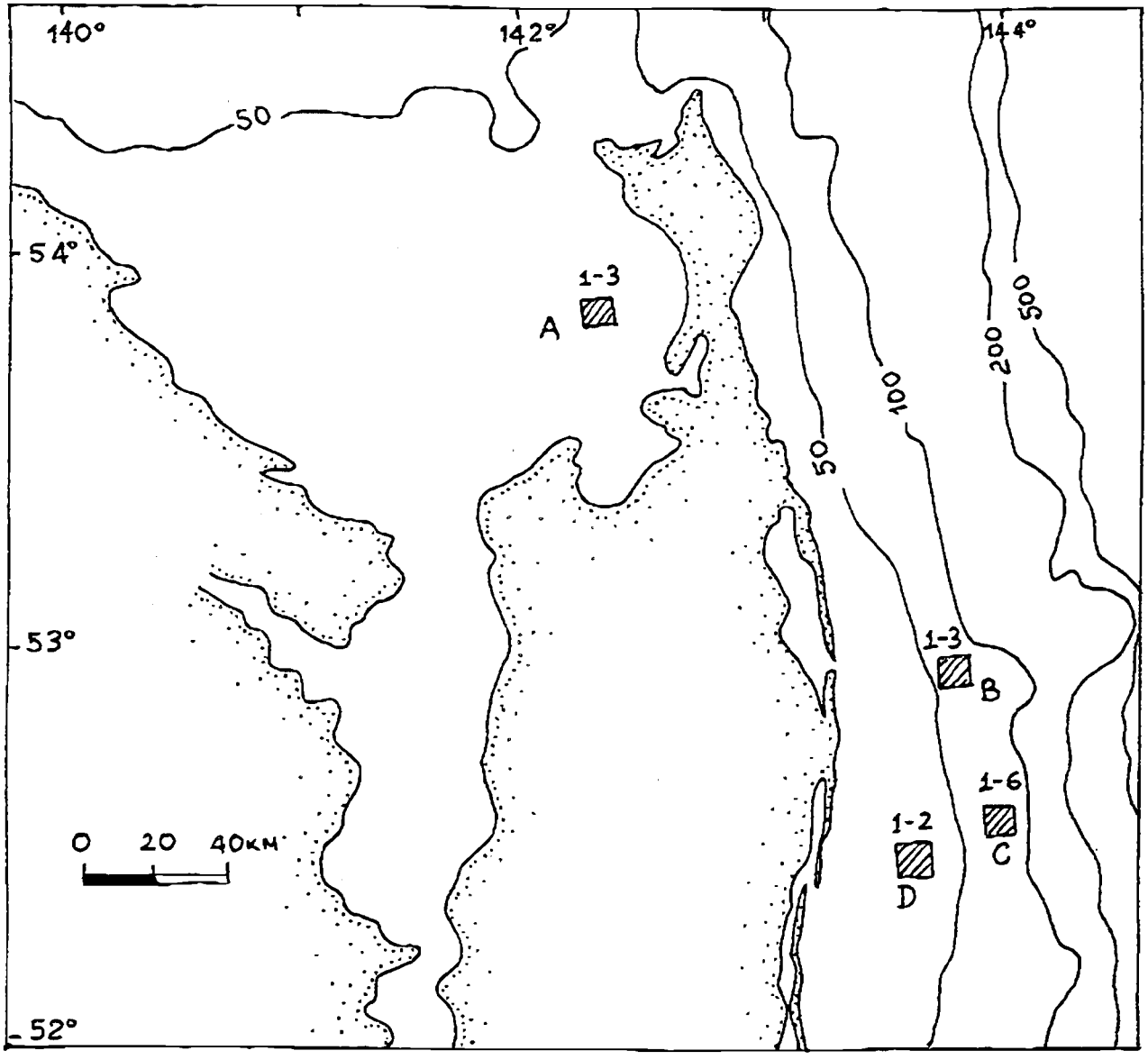

Fig.1. Map of Primary Production in Sakhalin Shelf Waters.
A - Sakhalin Bay, B - Piltun, C - Arcutun-Dagi, D - Chaivo.
The numbers indicate ranges in measured rates of PP, gC/m^2 : day: 1 - 0.500; 2 - 0.501-1.000; 3 - 1.001-1.500; 4 - 1.501-2.000; 5 - 2.001-2.500; 6 - 2.501-3.000.

Some Reasons for Resource Reduction of *Laminaria Japonica* (Primorye Region)

Tatyana N. KRUPNOVA

Pacific Research of Fisheries and Oceanography (TINRO)
4, Shevchenko Alley, Vladivostok, 690600, Russia

At the present time, the resources of *Laminaria japonica* are significantly reduced in three regions of the Primorye (north, middle and south). Surveys from recent years show that in a large area there are no commercial fids or they are in a depressed state. This lead to a 1991 closure of harvesting of *Laminaria japonica* to allow the stocks to rebuild. To determine the possible causes of the problem, analysis of growth, biological characteristics, climate and oceanographical condition were studied.

All three regions occur in the Prymorsky cold current. In the north the conditions are the most favorable for *Laminaria japonica* (many biogenes and low water temperature). In the South Primory region conditions are less favorable as there are less biogens and the temperature is higher (Fig. 1).

North Primorye the plants grow to a larger size and mass and the volume of sporogenesis tissue is greater than in the South Primorye. For example, in North Primorye one plant weighed 1,000 g and the coefficient of sporogenesis tissue K was 0.7 on a thallus. In the south region plants of *Laminaria japonica* weigh 600 g and the K was 0.5. In the middle region the weight is 800 g and K is 0.6 (Fig. 2). These proportions remained relatively stable in the three regions except for one year in the last 7-8 years when a weakening of the Prymorsky cold current resulted in less growth. For example, in 1981, in the north one plant weighed 800 g and K was 0.6; in the middle one plant weighed 500 g and K was 0.3; in the south one plant weighed 300 g and K was 0.2.

During the reproductive cycle in the fall, after zoospores are released to settle and sprout the temperature is found to fluctuate from 3°C-14°C which causes the destruction of gametophytes (Fig. 3). Thus, in these years the reduction of sporogenesis tissue causes the death of zoospores that are already formed. In the north and middle regions, cold waters results in low growth of rhizoids and zoospores are unable to attach to the substrate (Fig. 3). All these facts influence the yield of future years.

Commercial harvesting of *Laminaria* in Russia is undertaken by divers who only remove the plant material leaving the rhizoids to grow another year. In the years of reduced productivitiy, commercial harvesting of *Laminaria* should be stopped. At least harvesting should be stopped in the north and middle regions when the cold current causes low productivity. Taking into consideration all these facts there is an opportunity to use a new method for forecasting *Laminaria* yield and developing better management strategies for harvesting the plant.

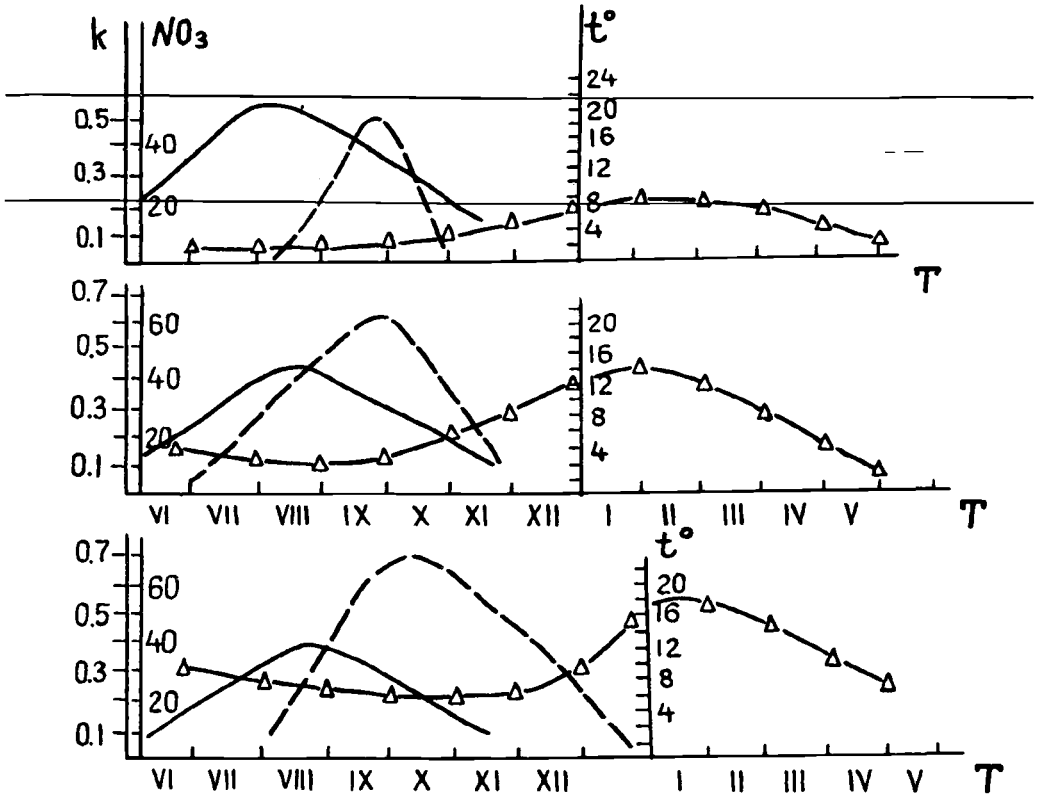

Fig. 1. Mean parameters from Middle Region.

—— temperature (t°C)

- - - coefficient of covering of thallus by sporogenesis tissue (K)

-Δ- NO_3 (mkg/l)

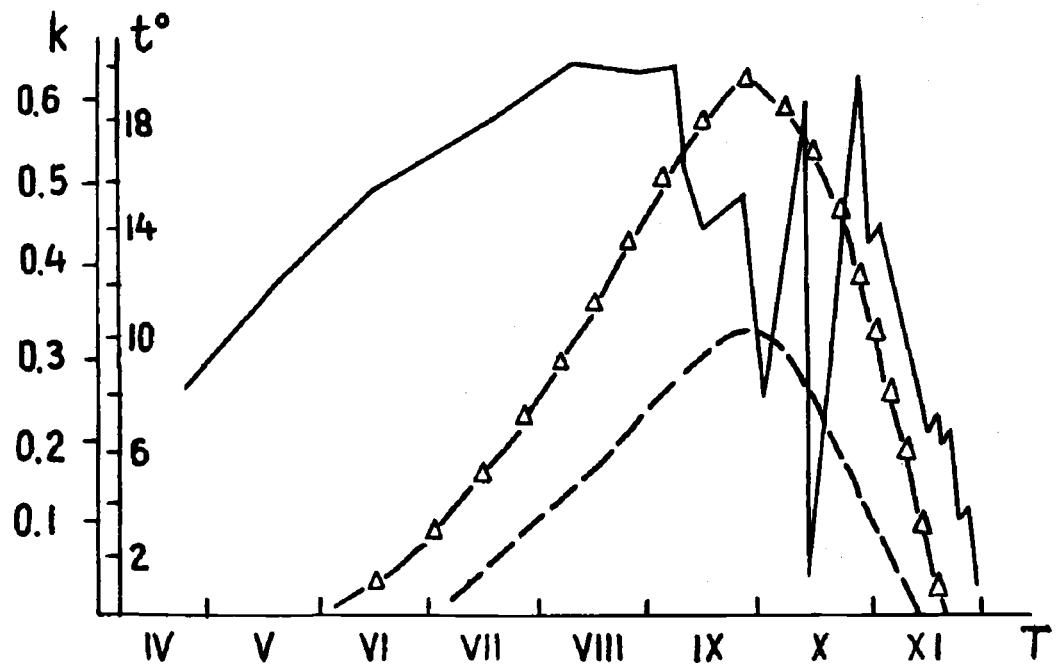

Fig. 2. Temperature of water and coefficient (K) of thallus covered by sporogenesis tissue in 1981 in Middle Primorye.

——— temperature of water (t°C)
- Δ - coefficient of thallus covered by sporogenesis tissue over many years (K)
------ coefficient of thallus covered by sporogenesis tissue in 1981 (K)

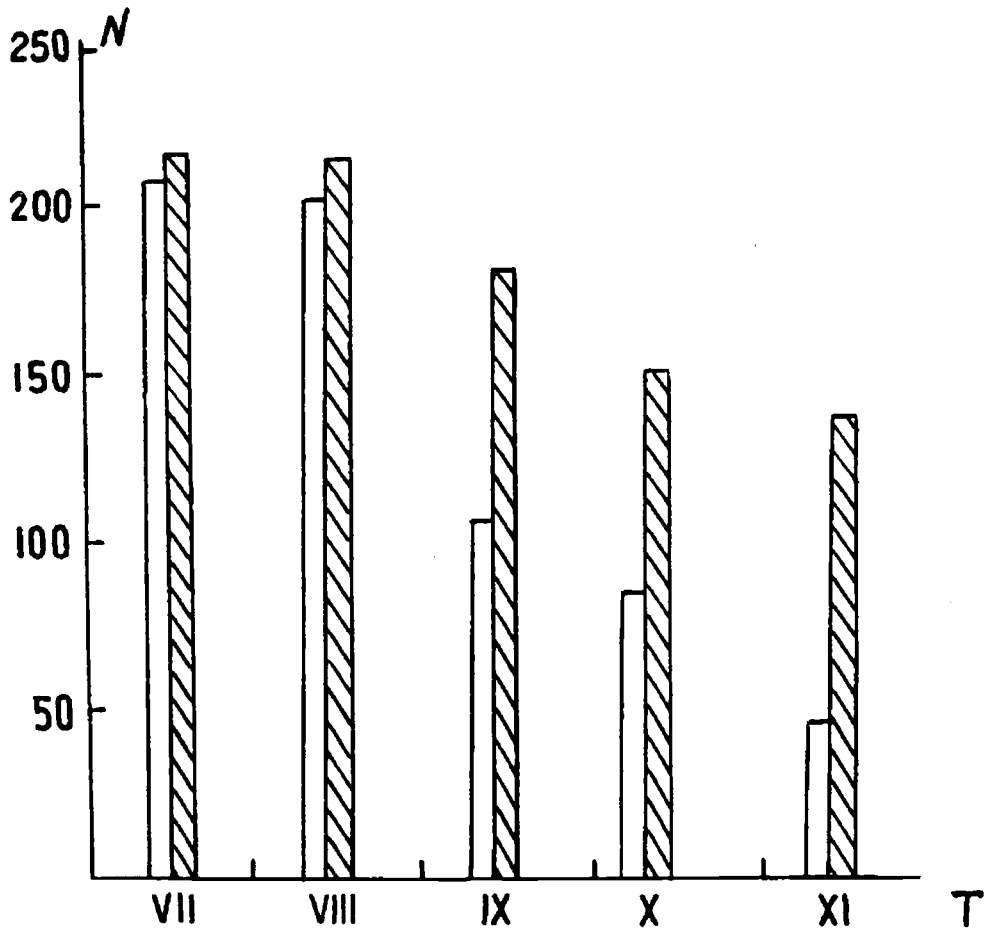

Fig. 3. Proportion between existing Laminaria plants and new rhizoides attaching to the substrate.

plants
rhizoides

Mercury in Bottom Sediments of the Northeastern Okhotsk Sea

Lyudmila N. LUCHSHEVA, Anatoliy I. BOTSUL

Pacific Scientific Institute of Fisheries and Oceanography (TINRO)
Pacific Oceanological Institute (POI)

To delineate the problem of monitoring mercury in the marine environment, data is needed at the ecosystem level. For example, data from bottom sediments are of great importance because they serve to locate where the long-term storage of mercury occurs, which potentially can be reintroduced into the environment (Hiroshi et al., 1989). In bottom sediments, mercury is transformed by microbiological activity into a highly toxic methyl-mercuric form which can cause serious ecological disturbances when incorporated into biota and *vice versa* (Akagi et al., 1979). Reasonable mercury levels in the bottom sediments can serve as an indicator of both anthropogenic (waste drain waters, aerosols, toxic waste burials, etc.) and natural (the seepage from the interior along deep faults, ore oxidation zones, disseminated cinnabar deposits) sources in the ocean.

The quantitative estimation of the extent of bottom pollution by mercury was determined using the flame atomic absorption spectroscopy method (Hatch and Ott, 1968) from bottom sediment probe samples collected on the R/V "Acad. A.Nesmeyanov" (24th Cruise) in 1993. The grain-size composition of bottom sediments was determined using the pipette method for estimation of the correlation between the mercury contents and the structural sedimentary types (Petelin, 1967). A map of the sediment type distribution has been plotted on the basis of grain-size analysis data (see Fig. 1). The most coarse-grained sediments (fine psammites) occur within the zone of intensive water-mass movements in the nearshore region off the west coast of Kamchatka near the Shelikhov Sound neck where the intra-structural hydrological front is characterized by high biological efficiency (Chernyavskiy, 1970). Aleurites and pelites are laid at greater depths where the dynamic activity causes the accumulation of finely dispersed sediments.

Bottom sediment mercury concentrations vary from 0.006 till 0.028 mcg/g of the dried mass. The lowest mercury content (0.006 mcg/g) is found in psammites that may be connected with their weak adsorption properties and with the intensive washout. At increasing depth, growth and particle size decreases and the mercury concentration increases up to 0.028 mcg/g due to the high metal adsorption capacity of the aleuritic fraction of bottom sediments (Duzzin et al., 1988).

When mercury concentrations in bottom sediments of our region are compared with the background values to determine a criterion for a quantitative pollution level estimation based on the relative mercury ground accumulation coefficient. For the Shelikhov Sound neck region, the coefficient varies from 2 to 4 units. The mercury content excess (relative to the background content) is a factor of 2-4 in the bottom sediments which was assigned to a category of sediments enriched with mercury. It should be noted that it was only this area where we observe elevated mercury concentrations in the near-bottom water layer. The high level is likely due to natural mercury fluid seepage from the deep earth crust. The mercury transfer is usually effected by alkaline sulfide solution or from organic compounds incorporated into the carbon bearing gases. The mercury transfer can also be in a vapour phase (Ozerova and Pikovskiy, 1982).

The tectonics data for the Okhotsk Sea region indicates that the Shelikhov Sound area is characterized by folded deformations in the earth crust. These deformations are caused by deep seated

faults (Gnibidenko and Khvedchuk, 1982). Tectonic movements along the faults are caused by active processes within the earth crust and upper mantle and by mantle differentiation. As a whole, our data shows that the mercury content values for the bottom sediments (laid within the anomalous mercury concentration zone in the near-bottom layer) are not high enough to cause environmental contamination. It was assumed that the mercury entering into the near-bottom water layer is in a vapor form. As the result of the high water agitation observed, the mercury transfer processes is presumably dominated by the mercury settling to the bottom surface. Thus, the undesirable action of the toxicant to biota tends to be diminished.

The data suggested development of a monitoring system for mercury contamination in the marine environment and for setting estimation criteria in waters and bottom sediments.

REFERENCES

Akagi, H., D.C. Mortimer, and D.R. Miller. 1979. Mercury methylation and partition in aquatic systems. Bull. Environ. Contam. Toxic. 23:372-376.

Chernyavskiy, V.I. 1970. Hydrological front in the northern part of the Okhotsk Sea. Izvestiya, TINRO (Proceedings of Pacific Institute of Fishing Culture and Oceanography). 71:3-11. (in Russian)

Duzzin, B., B. Panoni, and R. Donazzolo. 1988. Macroinvertebrate communities and sediments as pollution indicators for heavy metals in the River Adige (Italy). Water Res. 22(11):1353-1363.

Gnibidenko, G.S., and I.I. Khvedchuk. 1982. The main features of the tectonics of the Okhotsk Sea. The Geological Structure of the Okhotsk Sea Region. Vladivostok, Edition of the Pacific Branch of the Academy of Sciences of the USSR. 3-25. (in Russian)

Hatch, W.R., and W.L. Ott. 1968. Determination of submicrogramme quantities of mercury by atomic absorption spectrophotometry. Anal. Chem. 40(14):2085-2087.

Hiroshi, N., V. Masayuki, S. Masayuki, and M. Sadaaki. 1989. Mercury pollution in Tokuyama Bay. 4th Symp. Sediment/Water Interact., Melbourne, 1989. Hydrobiologia. 176/177:197-271.

Ozerova, N.A., and Yu. I. Pikovskiy. 1982. Mercury in hydrocarbon gases. Geochemistry of Ore Formation Processes. Moscow, Nauka (Science). p. 102-136. (in Russian)

Petelin, V.P. 1967. Grain-Size Analysis of Sea Bottom Sediments. Moscow, Nauka (Science). 126 p.

FIGURES

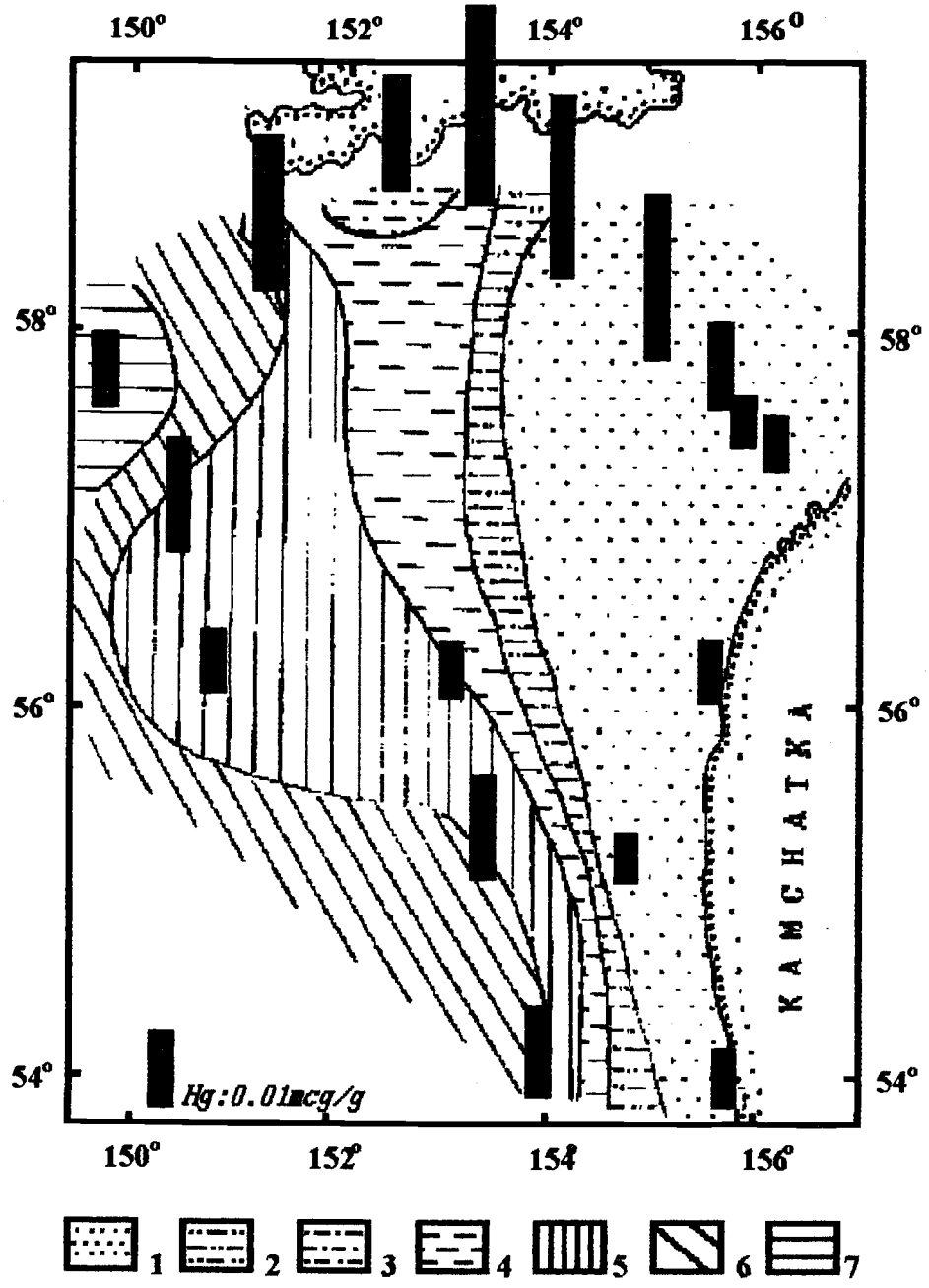

Fig. 1. Mercury distribution in bottom sediments of the North-Eastern part of the Okhotsk Sea:

1 - fine-grained psammites
2 - aleuritic psammites
3 - psammitic aleurites
4 - aleurites
5 - pelitic aleurites
6 - aleuritic pelites
7 - pelites

Lectins and Glycosidases from Marine Macro and Micro-organisms of Japan and Okhotsk Seas

Pavel A. LUK'YANOV, Natalia I. BELOGORTSEVA, Alexander A. BULGAKOV, Alexander A. KURIKA and Olga D. NOVIKOVA

Pacific Institute of Bio-Organic Chemistry
Far Eastern Branch of Russian Academy of Sciences, Vladivostok, Russia

ABSTRACT

Carbohydrate binding proteins and carbohydrases are widely used in glycobiology and biotechnology. In our laboratory galactose specific lectins were isolated from marine invertebrates of the Japan Sea from the mussel *Crenomytilus grayanus* and the marine worm *Chaetopterus variopedatus*. The peculiar lectin obtained from hemolymph of crab *Erimacrus isenbecki* showed affinity to sialic acids and N-acetyl-aminosugars. The lectins were found to bind Ehrlich carcinoma cells and the humane and animal erythrocytes in various manners. The reaction of agglutination was inhibited by such glycoproteins as mucin, fetuin, alpha-1-acid glycoprotein. The mannose specific lectin isolated from the celomic fluid of the marine cucumber *Stichopus japonicus* was shown to interact with high mannose "hybrid type" glycoproteins.

To search for producers of beta-N-acetyl-D-glucosaminidase, chitinase and carrageenase, the screening was carried out using marine bacteria from the Kuril Islands. The low-molecular weight of kappa- and lambda-carrageenans with potential antiviral activity were obtained by fermentolysis of natural polysaccharides. In a preparative scale, Chitobiose and chitotetraose were isolated after chitin degradation with a crude enzyme from marine bacteria KMM B-07. These substances are useful intermediates in technology of biologically active substances.

INTRODUCTION

The screening of genetic sources as tools for marine carbohydrate biotechnology is a problem of modern oceanography. The lectins from plants are very well known (Kilpatrick, et al. 1991; Gabius and Gabius. 1993). Recently, researchers are being directed to marine organisms (Renwrantz, 1986; Pavlenko et. al., 1990; Hatakeyama et. al., 1993). Special attention is being directed to substances (oncoprecipitins) which may bind with human oncofetal antigens (Pavlenko et. al., 1990; Moroz et. al., 1993). The isolated lectins and oncoprecipitins will be useful for diagnosis and therapy of cancer.

RESULTS AND DISCUSSIONS

Carbohydrases are useful tools for bioglycans structure investigation and the preparation of various biologically active substances. A chitinase, N-acetyl-beta-D-glucosaminidase, kappa- and lambda-carrageenases were obtained from some marine microorganisms. The following lectins and carbohydrases were isolated from marine invertebrates and microorganisms of Japan and Okhotsk Seas.

Lectin of the mussel *Crenomytilus grayanus* (CGL)

CGL was isolated from the mussel body using extraction of the mussel homogenate with saline solution followed by centrifugation and fractionation of the mixture obtained by affinity chromatography on the hydrolyzed Sepharose 6B or on Lactosyl-Sepharose 4B to yield the purified lectin.

Using HPLC on TSK G2000SW column or gel filtration on Sephadex G-75 column, the average molar weight was determined to be 36 kDa. A desegregation of the lectin was observed in the presence of 2-mercaptoethanol. CGL treated with 2-mercaptoethanol was subjected to sodium dodecyl sulfate-polyacrylamide gel electrophoresis (SDS-PAGE) to show a single band of 18 kDa. These data demonstrated that the mussel lectin appears to consist of two sub-units.

CGL was found to possess an agglutinating activity in relation to the human erythrocytes (ABO), sheep erythrocytes and Ehrlch's carcinoma cells. The highest agglutination titer was observed with the trypsinized human erythrocytes to reach up to maximum value for blood group B. A maintenance of agglutinability in the wide range of pH-values (2.5-10.0) indicated an occurrence of reversible alterations in the protein molecule. An inhibition of hemagglutination was achieved with galactose and derivatives of alpha-D-galactoside demonstrated alpha-D-galactose specificity of CGL. A peculiarity of the mussel lectin was thermo-stability of the molecule. CGL was found to maintain agglutination at an elevated temperature of up to 60C.

Lectin of the marine worm *Chaetopterus variopedatus* (CVL)

CVL was isolated from fresh marine worms *C. variopedatus* collected in the sublittoral zone of Bay of Peter the Great in the Japan Sea. Marine animals harvested were homogenized and subjected to extraction with a saline solution followed by precipitation with ammonium sulphate. The fraction obtained was shown to possess a hemagglutinating activity. Hemagglutination was inhibited with galactose and lactose. In this connection, a purification of CVL was achieved using affinity chromatography on lactosyl-Sepharose 4B followed by elution of the lectin with an aqueous solutions of galactose. The CVL obtained showed a single band on SDS-PAGE with a molar weight ca. 30 kDa. SDS-PAGE of CVL in the presence of 2-mercaptoethanol showed the same single band demonstrating the absence of disulfide bridges in the lectin. CVL was found to agglutinate all types of the human erythrocytes. The sheep and rabbit erythrocytes were also agglutinated with CVL. A treatment of erythrocytes with trypsin was shown to enhance hemagglutinating activity of CVL. In addition, a high titer of agglutination of the cells of Ehrlich's sarcoma was observed.

An alteration of pH-values of the buffer solutes demonstrated that specific activity of CVL was maintained in a range of pH 5-9. CVL showed a maximal activity at pH 8. An elevation of temperature of CVL solutes failed to substantially reduce specific activity up to 40C. A significant lost of activity occurred on heating at higher temperature. CVL was found to become inactive completely at 50C.

The minimal concentrations of various monosaccharides, oligosaccharides and glycoproteins require to completely inhibit agglutinating activity of CVL were determined. The galactose showed a maximal inhibitory activity among monosaccharides investigated. The inhibition of CVL with N-acetyl-D-galactosamine was substantially lower than that with galactose. The inhibitory activity of D-fucose and D-galacturonic acid reduced 3 and 4 fold respectively in comparison with that of D-galactose. This phenomenon indicated certain participation of the C5-C6 region of sugar in binding the lectin. An inhibitory ability of lactose was found to be equal to that of methyl beta-D-galactopyranoside. Lactose showed the most inhibition in comparison to raffinose and melibiose.

These data were possibly connected with an anomeric configuration of the galactose residue in the oligosaccharides as follows: beta-galactosyl residue involved in lactose while raffinose and melibiose contained alpha-galactosyl residues.

Mucin, fetuin and alpha-1-acid glycoprotein were found to be effective inhibitors of hemagglutination. It is noteworthy that desialylation of fetuin and alpha-1-acid glycoprotein was accompanied by a substantial increase of inhibitory activity while the desialylated mucin showed the same inhibition as the parent glycoprotein. As is known, the neuraminic acid residues occurred at C-6 of the subterminal galactose residue in mucin while C-3 atom was additionally involved in linkages with the neuraminic acid residues in both the other glycoproteins. This phenomenon demonstrated that the hydroxyl group at C-6 failed to influence binding the galactose residues of glycoproteins with CVL while hydroxyl group at C-3 appeared to be very significant for binding glycoproteins with the lectin. CVL was found to possess a substantial agglutinating activity in relation to the tumour cells due to oncofetal antigens involved in tumour cells which are known to contain regions which resemble those of mucin (Mikheyskaya et al, 1995).

The crab *Erimacrus isenbeckii* lectin (EIL)

A very interesting lectin was isolated from the hemolymph of crab *E.isenbeckii* (EIL) using affinity chromatography on bovine serum mucin-agarose column in the presence of Ca-ions. Elution of EIL was achieved with 0.5M GlcNAc in Tris-HCl buffer in the absence of Ca-ions. The EIL fraction was subjected to chromatography on a column with DEAE-Toyopearl 650M to obtain a purified lectin.

SDS-PAGE showed a single band of 70 kDa in the presence or absence of 2-mercaptoethanol thus indicating the occurrence of a single subunit. Homogenecity of EIL was confirmed by immunodiffusion against antiserum obtained by immunization of rabbits with a purified hemolymph of the crab. EIL was shown to represent glycoprotein which contained 2% sugars. An absence of amino acid residues contained S-atom was a peculiarity of the lectin.

EIL was found to agglutinate the human A, B, O erythrocytes. More high agglutinability was observed in relation to erythrocytes digested with trypsin. The sugar specificity of the lectin was elucidated using inhibition of EIL-hemagglutination with various sugars. The lectin agglutinability was inhibited with aminosugars (GlcNAc, GalNAc), with N-acetyl neuraminic acid (NANA) and glycoproteins which contain NANA residues (mucin, fetuin et. al.). In addition, uronic acids (GlcUA, GalUA) and KDO (2-keto-3-deoxy-octonic acid)-containing lipopolysaccharides were found to inhibit a hemagglutination of EIL.

Hemagglutinating activity of EIL was estimated to continue in the range of pH-values from 7 to 10. Activity was half a maximum at pH 6. EIL was shown to afford a precipitate at pH-values less than 4. EIL showed thermostability at the interval of temperature from 4 up to 40C. Its agglutinability was completely maintained at 37C for 30 min. Half an activity was observed at 50C. Activity was shown to disappear completely at 60C for 10 min. EIL was shown to represent Ca dependent protein similar to lectins from other species of crabs. The agglutination activity of EIL was completely lost after dialysis with a buffer containing EDTA. An addition of Ca-ions led to restoration of hemagglutination of EIL.

The marine cucumber *Stichopus japonicus* lectin (SJL-M)

SLJ-M was found in celomic fluids of *S. japonicus* by affinity chromatography on mannan-Sepharose 4B. Lectin agglutinated human group 0 and rabbit erythrocytes. The hemagglutination was

inhibited by yeast mannan from Saccharomyces cerevisiae and extra cellular mannan from Vibrio flavialis.

Two other lectins described early from cucumber's body have specificity to galactose (Hatakeyama et al, 1993). Such variability of the carbohydrate binding molecules to one organism is convincing that the Ocean might possibly be a good source of genetic information.

The mannose-binding proteins have various physiological activity and participate actively in the homeostasis and the defense of macroorganisms (Ohta et al, 1994; Nermes et al, 1995).

Carrageenases from marine microorganisms

The search for the enzymes which specifically degrade carrageenan (sulphatated galactan from red alga) is urgent because of its low molecular weight it is used in cosmetics and medicine. (Akagawa-Matsushita et al, 1992; Luk'yanov et al, 1995). The screening of carrageenases bacterial producers were carried out among epibiotic microorganisms of Rodophitae and microbes from various species of decomposed red algae as result of accessing 20 bacterial cultures capable of growing on solid kappa-carrageenan medium. Four strains had the highest enzyme production. The enzyme secretion was observed to be maximal in the period between 21 and 30 hours from start of bacterial growth in a 0.5% carrageenan medium.

Crude enzymes were obtained from the 25 h cultural medium of the most promising strains (KMM SW-4f, KMM 12-3, KMM 10-32). The enzymes purified by 40-70% (NH4)2SO4 precipitation with following gel chromatography had a specific activity of 10-20 units per mg protein which were determined by color reaction of reducing carbohydrates with 2, 3, 5-triphenyltetrasolium chloride with 0.25% carrageenans as substrate. The enzyme preparation was shown to be cryo-stable (after freezing-thawing it lost only 15% activity) and to have pH-optimum in the range of 5.5-7.0.

The isolated enzyme hydrolyzed kappa-carrageenan as it was shown by the decrease of polysaccharide solution viscosity and gel permeation chromatography. Low molecular weight carrageenan had molecular mass of 30-50 kDa.

Chitinase and beta-N-acetyl-D-glucosaminidase (NAGase) from bacteria

The complex of enzymes which hydrolyzes chitin (poly- beta-(1,4)-N-acetyl-D-glucosaminide) in living organisms consists of chitinase and (or) NAGase [ ]. The chitinase degrades polysaccharide to chitobiose, NAGase to N-acetyl-D-glucosamine. These compounds of polysaccharide fermentolysis are useful in biotechnology for synthesis of various biologically active substances. The high chitooligosaccharides are essentially interesting as substrates for lysozyme and syntons for preparation of glycolipids with immunostimulating activity.

The perspective bacterial strains (32) were found by the screening of more 200 chitinolytic strains from a Collection of Marine Microorganism (Pacific Institute of Bio-Organic Chemistry, FEB RAS, Vladivostok). Six of them had only chitinase activity. An enzymatic preparation was obtained from KMM B-07 culture by 40-70% (NH4)2SO4 precipitation. The chitobiose (37% from chitin), chitotetraose (8%) and chitohexaose (1.5%) were prepared by polysaccharide fermentolysis using this enzymatic preparation in a preparative scale.

Thus, it has been shown that the Ocean is a rich source of carbohydrate-binding and polysaccharide-hydrolyzing molecules as described above. The lectins isolated will be investigated for there diagnostic significance in use for oncological diseases.

REFERENCES

Akagawa-Matsushita, M., M. Matsuo, K. Yamasato. 1992. Alteromonas atlantica sp. nov. and Alteromonas carrageenovora sp. nov., bacteria that decompose algal polysaccharides. Int. J. Syst. Bacteriol. 42:621-627.

Gabius, H.J., and S. Gabius [ed.] 1993. Lectins and Glycobiology. Springer-Verlag, Berlin. 521 p.

Hatakeyama, T., T. Himeshima, A. Komatsu, and N. Yamasaki. 1993. Purification and characterization of two lectins from the sea cucumber Stichopus japonicus. Biosci. Biotech. Biochem. 57:1736-1739.

Kilpatrick, D.C., E. van Driessche, and T.C. Bog-Hansen [ed.] 1991. Lectin Reviews. Sigma Chemical Co., Sant Louis. 1:1-218.

Luk'yanov, P.A., O.D. Novikova, V.V. Mikhailov, O.I. Nedashkovskaya, T.F. Solov„yeva, and Yu. S. Ovodov. 1994. Carrageenanolitic activity of bacterial strains assitiated with red alga of the Kuril Islands region. Biologia Morya. 20:472-473.

Mikheyskaya, L.V., E.U. Evtushenko, R.G. Ovodova, N.I. Belogortseva, and Yu. S. Ovodov, 1995. Isolation and characterization of a new beta-galactose specific lectin from sea worm Chaetopterus variopedatus. Carbohydrate Chemistry. 275:193-200.

Moroz, S.V., A.V. Kurika, and A.F. Pavlenko. 1993. Oncoprecipitins a novel type of natural substances and oncofetal antigens. Pure & appl. chem. 65:1253-1264.

Nermes, M., J. Savolainen, and O. Kortekangas-Savolainen. 1995. Nitrocellulose-RAST analysis of allergenic cross reactivity of Candida albicans and Saccharomyces cerevisiae mannans. Int. Arch. Allergy Immunol. 106:118-123.

Ohta, M., and T. Kawasaki. 1994. Complement-dependent citotoxic activity of serum mannan-binding protein towards mammalian cells with surface-exposed high-mannose type glycans. Glycoconjugate J. 11:304-308.

Pavlenko, A.F., A.V. Kurika, I.V. Chicalovets, and Y.S. Ovodov. 1990. Oncoprecipitins from Marine-Invertebrates Are Glycoproteins with a Higher Specificity to Carcinoembryonic Antigen. Tumor Biology. 11:137-144.

Renwrantz, L. 1986. Lectins in molluscs and arthropods: their occurrence, origin and roles in immunity, p.81-90. *In* A.M. Lackie [ed.] Immune mechanisms in invertebrates vectors. Oxford.

PCR-Fingerprinting of Mitochondrial Genome of Chum Salmon, *Oncorhynchus Keta*

Boris A. MALYARCHUK[1], Olga A. RADCHENKO[1,2], Miroslava V. DERENKO, Andrey G. LAPINSKI[1,2] and Leonid L. SOLOVENCHUK[1,2]

[1] Institute of Biological Problems of the North, Far-East Division, Russian Academy of Sciences, Magadan, Russia, 685010
[2] International Pedagogical University, Magadan, Russia, 685000

Among existing approaches, the analysis of mitochondrial DNA (mtDNA) polymorphism seems to be the most feasible for the genetic marking of populations and separate stocks of Pacific salmon. However, the restriction endonuclease analysis of whole mtDNA from chum salmon (*Oncorhynchus keta Walb.*) and coho salmon (*O. kisutch Malb.*) as well as of its fragments, amplified by polymerase chain reaction (PCR) demonstrates the low level of intraspecific variability in these species of salmon (Ginatulina et al., 1988; Cronin et al., 1993). The use of the expensive direct sequencing for the mass screening and identification of populations, stocks and individuals is cumbersome.

The DNA fingerprinting technique (Wright, 1993) seems to be more useful but not less informative, including the recent approaches for the analysis of mtDNA polymorphisms as based on the PCH with a single primer (SP) PCR (Derenko and Malyarchuk, 1994), and low-stringency (LS) SP-PCR (Pena et al., 1994). The LSSP-PCR of the human mtDNA results in the set of PCR-products, whose quantity and distribution pattern depends on the type, quantity and character of mutational events in the studied DNA segment (Pena et al., 1994).

In this paper we present the results of LSSP-PCR fingerprinting of mtDNA genome of chum salmon which enable genetic identification at an individual level. This level partly includes the family due to the matrilinear inheritance of mtDNA (Avise and Lanchman, 1983) and maternally akin individuals possess the identical mitochondrial genomes.

MATERIALS AND METHODS

Standard methods were used to isolate the mtDNA from salmon muscle. The fragments from the control region of mtDNA (about 1,300 bp long) are amplified with the primers L15926 and H651 using conditions described by Kocher et al. (1989). The PCR products are isolated from the gel of LNP agarose (BioRad) and reamplified, using some modifications in the process, with the L15926 primer under LSSP-PCR conditions as described by Pena et al. (1994). The reaction mixture contains Taq-buffer (according to Hertzberg et al., 1989), dNTPs, 15 ng of DNA template, 48 pN of primer and 2.5U of Taq DNA polymerase. DNA is amplified under 35 two-phase cycles (1 min at 93° and 1 min at 30°). LSSP-PCR products are fractionated in 5 % polyacrylamide gel and stained by silver (Brandt et al., 1992).

The fragments of 5-ended cytochrome b gene region 375 bp long are amplified with the B1 and B2 primers (Kocher et al., 1989). Restriction analysis of cytochrome b gene of chum salmon is performed using restriction endonucleases AluI, HaeIII, HinfI, MspI, and RsaI from MBI Fermentas,

Lithuania. LSSP-PCR fingerprinting of products of the first PCR round is performed using the B1 primer. The PCR and analysis conditions are identical to those described above for the mtDNA control region.

The mathematical analysis of data include the construction of binary matrix where the columns correspond to the individuals and lines to the found segments with 1 and 0 elements according to the presence or absence of segmentation, respectively. Distinction coefficients (D) are calculated by dividing the number of segments which differ in the compared individuals by the sum of all segments found.

RESULTS AND DISCUSSION

The feasibility of a single primer PCR (LSSP-PCR technique) for the analysis of intraspecific variability of mtDNA control region was recently demonstrated for humans (Pena et al., 1994) and fur seal (author's unpublished data). This technique results in a set of fragments of mtDNA which is specific for species and individuals. The employment of the method described above for the analysis of mtDNA control region allows the identification of several samples of chum salmon and coho salmon. These results were unexpected since the non-coding regions of mtDNA in vertebrates possess a marked structural closeness, being significantly variable (Cantatore and Saccone, 1987).

The information about the variability of coding regions of a genome whose evolution more corresponds to a neutrally selective one is of consequence in the case of evolutionary and population genetic studies. In this case the character of accumulation of genome changes during molecular evolution looks to reflect the sequence of evolutionary changes in individuals, populations, species etc. The cytochrome b (cyt b) gene of mtDNA is among such regions whose polymorphisms are used in the phylogenetic studies in animals (Irwin et al., 1991). This protein (cyt b) has a rather conservative aminoacid sequence but the nucleotide sequence of the responsible gene possesses both intraspecific and higher range variations. The RFLP analysis reveals the mitochondrial genomes of such salmons as chum salmon and coho salmon have a somewhat low polymorphism thus making a genetic analysis difficult (Ginatulina et al., 1988; Cronin et al., 1993). Thus, we attempt to estimate the variability of evolutionary conservative cytb gene of chum salmon by means of PCR-fingerprinting.

We formerly demonstrate the low variability of cyt b gene of chum salmon by RFLP (Radchenko and Malyarchuk, 1995). One half of the sampled fish are characterized by 5A mitotype and the remainder by 5B mitotype. In this paper we use ILSSP-PCR fingerprinting to assess the variability of cytb gene in four chum salmon fish (sampled in Yana river, Magadan region). The RFLP shows these salmons to have 5A mitotype (samples Nl and N2) and 5B mitotype (N3 and N4). The LSSP-PCR spectra is characterized by a significant band variability. The number of bands sized (1,800 - 80 bp) per sample varies between 20 and 24. The individual differences in the number, position and intensive bands dominate in the LSSP-PCR spectra. The pair comparison of spectra show the variation in the number of common bands is 10 to 17. The samples Nl and N2 which had common 5A mitotype also shows the greatest similarity in LSSP-PCR spectra (D=0.652). However the samples N3 and N4 which also belong to a common mitotype 5B had fingerprints differing (D=0.74) from the pairs N2-N3 and Nl-N3 (D=0.733 and 0.724 respectively).

Our results point out the existence of a rather high level of diversity of cyt b gene in chum salmon which could not be proven by RFLP. LSSP-PCR-fingerprinting which has a higher resolving ability could, evidently, be recommended for studies in the micro-differentiation of populations as well as for separate stocks of salmon. This approach allows estimation of the real levels of genetic

variability in populations and it is hoped to enable the elaboration of techniques for marking populations according to LSSP-PCB spectra and estimating the degree of kinship of populations.

ACKNOWLEDGMENTS

This work was supported by grant from the Russian State Scientific and Technical Program "Biological diversity".

REFERENCES

Avise, J.C., and R.A. Lanchman 1983. Polymorphism of mitochondrial DNA in populations of higher animals / Evolution of genes and proteins, p.147-164. *In* M. Nei, R.K.Koehn [ed.] Sanderland: Sinauer.

Brandt, B., V. Greger, and D. Yandell. 1992. A simple and nonradioactive method for the Rbl.20 DNA polymorphism in the retinoblastoma gene. Amer. J. Hum. Genet. 51:1450-1451.

Cantatore, P., and C. Saccone. 1987. Organization, structure and evolution of mammalian mitochondrial genomes. Internat. Rev. Cytol. 108:149-208.

Cronin, N.A., W.J. Spearman, and R.L. Wilmot. 1993. Mitochonclrial DNA variation in chinook salmon (Oncorhynchus tshawytscha) and chum salmon (O.keta) detected by restriction enzyme analysis of polymerase chain reaction (PCR) products. Can. J. Fish. Aquat. Sci. 50(4):708-715.

Derenko, N.V., and B.A. Malyarchuk. 1994. Single-primer PCR amplification of segments of the main noncoding region of human mitochondrial DNA. Huss. J. Genet. 30(11):1329-1331.

Ginatulina, L.K., S.V. Shed'ko, I.I. Miroshnichenko, and A.A. Ginatulin. 1988. Sequence divergence in mitochondrial DNA from the pacific salmons. J. Evol. Biochem. Physiol. 24(4):477-483. (in Russian)

Hertzberg, M., K.N.P. Mickleson, and S.W. Serjeantson. 1989. An Asian-specific 9-bp deletion of mitochondrial DNA is frequently found in Polynesians. Amer. J. Human Genet. 44:504-510.

Irwin, D.M., T.D. Kocher, and A.C. Wilson. 1991. Evolution of the cytochrome b gene of mammals. J. Mol. Evol. 32:128-144.

Kocher, T.D., W.K. Thomas, and A. Meyer. 1989. Dynamics of mitochondrial DNA evolution in mammals: amplification and sequencing with conserved primers. Proc. Nat. Acad. Sci. USA. 86:6196-6200.

Pena, S.D.J., G. Barr eto, and A.R. Vago. 1994. Sequence-specific "gene signature" can be obtained by PCR with single specific primers at low stringency. Proc. Natl. Acad. Sci. USA. 91:1946-1949.

Radchenko, O.A., and B.A. Malyarchuk. 1995. Restriction analysis of the cytochrom b gene in chum salmon coho coho salmon / Idea, hypothesis, search. Magadan: Internat. Pedagog. Univ. Press. (in press) (in Russian)

Wright, J.M. 1993. DNA fingerprinting of fishes / Biochemistry and molecular biology of fishes. Hochachka and Mommsen [ed.] V. 2/3. V. 5/-91.

Chaos and Relaxation in Dynamics of the Pink Salmon (*Oncorhynchus Gorbuscha*) Returns for Two Regions

Alexander A. MIKHEEV

Sakhalin Regional Research Institute of Fisheries and Oceanography (SakhNIRO)
196, Komsomolskaya st., Yuzhno-Sakhalinsk. 693016 Russia

INTRODUCTION

"... Simple non-linear systems do not necessarily possess the simple dynamics properties".
Robert May. 1991

At present, the ecology of Oncorhynchus gorbuscha has been well studied (Birman, 1985). Pink salmon live in the freshwater for a very short period and migrate great distances in the ocean. Pink salmon tagging indicate that the frequency and the range of deviation from native rivers when returning to spawn is inversely related (Maksimovich, 1991). It seems quite reasonable to propose, that migration fluctuations are produced by the environment and represent system noise in nature. Consequently, there is some probable pink salmons population structure fluctuation. The strays join existing stocks to form new stocks without contradiction of the concept of fluctuation (Glubokovsky and Jivotovsky, 1986) and local (Ivankov, 1993) stocks, compete with strays from other stocks. This would mean that there is a statistical relationship of returns to different spawning sites.

We emphasise that the length of life of pink salmon has been determined with enough precision. The pink salmon hatch and leave for the ocean to return to spawn and die. This results in a chain of generations that do not overlap in time, but with strict reciprocal correspondence. It may be said that nature displays a biological model of known mathematical formulation: discreet mapping of a segment of the real straight line onto itself (Haken, 1985; Shuster, 1988; Ahromeeva et al., 1992; Sharkovsky, 1964; May, 1976; Feigenbaum, 1979).

Correspondence of mapping as a model of a natural prototype in many respects will be determined by the mapping parameters. It is assumed, that the most generalised demographic parameters, that reflect the biological state of a population, are reproduction and carrying capacity (Odum, 1975).

Reproduction integrates such characteristics as mortality, fertility and sex in pink salmon. These characteristics depend on a great number of factors, where the change in the scale of the time period is much less than the length of the reproductive cycle. Examples of the main groups of such factors are: weather, sea and river waters state, currents, anthropogenous activity and predation. Eventually changes in combinations of these factors take place that are specific to a region. As a result, local spatial fluctuations of the habitat appear. As solitary fluctuations are weekly forecast, it is more advisable to regard them as stochastic noise. Noise is present in almost all natural processes (Haken, 1985; Shuster, 1988; Ahromeeva et al., 1992). The influence of fluctuations on discrete mapping is analysed in general (Haken, 1985; Shuster, 1988; Wull et al., 1984) and in a particular case of disturbance of reproduction by white noise (Rabinovitch and Thieberger, 1988).

The scale of carrying capacity change corresponds to the scale of climatic change. Climate as a global factor is displayed in a similar way for different stock reproduction. Birman (1985) and Chigirinsky (1993) advanced and substantiated the thesis of a correlative connection between long-term pink salmon abundance and global climate variations. The role of climatic epoches in marine ecosystems was analysed by V.P. Shuntov (1993).

Taking into account the existing problems of forecasting pink salmon spawning abundance, it is necessary to study, in general, the role and contribution of external factors in affecting returns.

RESEARCH METHODS

The influence of the environment on the abundance of pink salmon spawning returns is studied using a simple model based on '"logistic" mapping of real straight line segments (May, 1976) with perturbed parameters. Reproduction is subjected to accidental non-correlative fluctuations and the carrying capacity changed quasi-periodically following global climatic variations. The model used was:

$$(1) \qquad x_n = X_n / K_n, \delta \le x_n \le \Delta, n = 0,1,\ldots,N,$$

$$(2) \qquad x_{n+1} = \begin{cases} (K_n / K_{n+1})(r+\varepsilon_n)x_n(1-x_n), & \text{if } \delta \le x_n < 1, \\ \delta, & \text{if } 1 \le x_n \le \Delta, \end{cases}$$

$$(3) \qquad K_n = K + s_x \sum_{m=1}^{3} \sin(\pi n / T_m + \varphi_m),$$

where controlling parameters $r>0$ and $K>0$ characterise pure reproduction and carrying capacity, respectively. X_n is a return number; x_n belongs to a segment of the real positive number $[\delta, \Delta]$, where Δ is the greatest of numbers x_n, $n = \overline{0,N}$; the n index of year return and discreteness of one iteration corresponds to a two years period. The quantity ε_n is white noise with parameters **0** and σ; s_x is the standard deviation of abundance during N years; T_m is a period and φ_m a phase of harmonic with index **m** in the trend of carrying capacity changes; π=3.14... . Periods, T_m, m=1, 2, 3, are equal to 11, 22, and 45 years, respectively, and phases $\varphi_1=1.2\pi$, $\varphi_2=0.5\pi$ and $\varphi_3=1.6\pi$ are selected so, that maximums will lie in the neighbourhood of 1989 (Shuntov, 1993). Shifts of the process with respect to adjacent generations is accomplished by changing the index **n** by half of the iteration step. A small parameter δ corresponds to the number of individuals, labile to the most unfavourable changes of the external environment. The equations (1) - (3) set a stochastic process, known as a Marcov chain (Rabinovitch and Thieberger, 1988).

The simulation process consists of setting an initial value of x_0 from actual time series and reconstruction of the model time series according to x_0 by the set parameters **r**, **K**, σ, δ of model (1) - (3). The model is tested on time series of pink salmon abundance returns of "even" and "odd" yearclasses (Birman, 1985) in two regions for the period 1970 - 1993. Location of regions with respect to each other is shown in the Fig. 1. For each model iteration the correlation coefficient **R** and standard deviation s relative to actual series are calculated. For every combination of parameters (**r**, **K**, σ, δ) 100 iterations took place, by which a frequency spectrum **f(R)** is produced. The position of the extreme right mode of spectrum serves as a criterion of model quality. That combination of

parameters is considered to be the best, by which the quality criterion approaches the maximum value $\mathbf{R_{max}}$. The last iteration is calculated by the gradient descent method (Bundy, 1988).

Using mode values, cross tabulations of **R** and **s**, the discriminating signs for parameters formally stood out in the form of couples (**R, s**). All outputs received in the process of modelling are classified with the help of discriminate analysis. Properties of return dynamics are studied comparing probability appearance characteristics of corresponding class, number, size, distribution and fluctuation in the time period for each output. The known characteristics of discrete mapping with noise were used.

RESULTS AND DISCUSSION

Results of parameter identification are presented in Table 1. The sensitivity of quality criterion $\mathbf{R_{max}}$ to the estimates of parameters (for exception of rather arbitrary parameter δ) appear to be an order higher for even year generations.

The spectrum **f(R)** for optimum the combination of parameters by region and generations are shown in the Fig. 2. The quantity $\mathbf{R_{max}}$ corresponds to the position of the extreme right line of all spectrums. Otherwise, the most similar output appears to be the most probable. By the figure one can compare the output with the actual dynamics for every region.

We note, that optimum values of **r** and σ form couples equal for the generations of the same eveness independently of the region. In Fig. 3 theoretical distributions of r are shown for even and odd year generations, respectively. The upper 99% percentile in these generations is practically the same and equal to $r_{0.99} = r_f = 4.5$. Thus, every couple (r, σ) is determined by the equality $r + 3\sigma = r_f$.

Of 1,000 outputs modelled by optimum parameters, there are five classes with peculiar values of **R** and **s** for every region and generation. For example, in Fig. 4 the classes for odd-year generations of Region 1 are shown. Visually comparing the morphometry of typical points of the discriminating output allows the setting of each class of output to possess a specific stable fluctuation distribution which makes a specific generalised image of the output dynamic class pattern. We point out the signs of the chosen classes and probability of their appearance: class with signs **(R, s)**=(0.75; 0.28) has probability 0.13; **(R, s)**=(0.65;0.32)-0.14; (0.55;0.28)-0.30; (0.55;0.32)-0.30; class (0.45;0.38)-0.13. Stability of patterns indicate the natural development and relation of fluctuations. Of the known properties of logistic mapping, it follows that the rate of fluctuation growth is higher for the value of perturbed reproduction $(r + \varepsilon_n)$. Fluctuations of the order σx_n are distributed accidentally and homogeneously in the time period. Global fluctuations of the order $K+3s_x$ have a periodicity of the climatic trend and taking into account the rate of growth are distributed in the time period by secluded groups of one to two "splashes".

We discuss output values for **r** and σ. The high individual fertility of pink salmon is considered to be 2,000 eggs (Birman, 1985). If it is assumed that the sex ratio is close to 1:1 and for every thousands eggs, 5 spawners return, then $r_f = 2{,}000 \times 0.5 \times 0.005 = 5$. This is not a bad correspondence allowing interpretation of r_f as a species reproductive maximum and equality $r + 3\sigma = r_f$ finds the meaning. On the other hand pink salmon population density regulation of reproduction is connected with the heterogeneous conditions for maturing and surviving and interspecies competition for the best habitat conditions (Birman, 1985). Thus the reproduction **r** of generations of low abundance will be greater, and the variability of reproduction σ smaller and their relationship is determined by the equality for r_f, cited above. Will the obtained correspondence values of **r** and σ to

theoretical distributions of reproductions for generations with different level of abundance (Fig. 3) be greatly strengthened, if it is possible to find an explanation of the fact that values of **r** appear to be equal for generations of the same eveness, independent of the region? Such explanation is found in the properties of logistic mapping (Haken, 1985; Shuster, 1988; Ahromeeva et al., 1992; Sharkovsky, 1964; May, 1976; Feigenbaum, 1979; Wull et al., 1984; Rabinovitch and Thieberger, 1988). A parameter **r** change leads to the consequent replacement of the dynamic types of quantity x_n. At **r** = 2.5, the value of x_n approaches a non-zero equilibrium, at **r** = 3.25 periodic oscillations appear in the dynamics, at **r** = 3.25 the number of harmonics begins to redouble to the chaos which appears at **r** = 4.0. The theoretical basis of the universality of bifurcation of values **r** is given by M. Feigenbaum (1979) (Feigenbaum, 1979), and the considered scenario of transition from equilibrium to chaos bears his name. Rabinovitch and Thieberger (1988) indicate that the influence of white noise on reproduction **r** in logistic mapping supports the scenario of Feigenbaum. Evidently any change of **K** is a simple transformation of the scale in the mapping, and also it cannot change the Feigenbaum scenario.

If the model represents nature, then when the density of spawning change is due to density regulation, there must be a transition from one type of dynamics to another according to Feigenbaum's scenario. Formally, we call this phenomenon the capability of pink salmon to adapt. Close location of r to bifurcation values speaks in favour of the existence of factors connected with abundance that at low level change chaotically and at high level relax after external influence on the equilibrium state. So, pink salmon generations with stable high abundance tend to depress fluctuations from outside, whereas generations with stable low abundance show the capability to increase fluctuations within. Such behaviour follows the reproductive strategy, the aim of which is to keep up the stock to an abundance level as high as possible for a specific region. In suitable external conditions, the strategy is able to lead to "dominant" generation replacement (Birman, 1985).

The presence of chaos and non-linearity in pink salmon returns indicated the problem of forecasting which can not be solved within the frameworks of traditional approaches. Discussing these problems is beyond the scope of this paper. May (1991) has worked out the non-linear dynamics of chaos forecasting and suggests the algorithm for a solution (May, 1991).

REFERENCES

Ahromeeva, T.S., S.P. Kurdumov, G.G. Malinetsky, and A.A. Samarsky. 1992. Non-stationary structures and diffusion chaos. M. Nauka. 544 p.

Birman, I.B. 1985. Sea period of life and questions of Pacific salmon stock dynamics. M. Agropromizdat. 208 p.

Bundy, B. 1988. Methods of optimization. Introductive course. M. Radio and svjaz. 128 p.

Chigirinsky, A.I. 1993. Global natural factors, fishing and abundance of Pacific salmon. Journal Rybnoye khozajstvo. 2:9-22.

Feigenbaum, M.J. 1979. The universal metric properties of nonlinear transformations. J. Stat. Phys. 21(6):669-706.

Glubokovsky, M.K., and L.A. Jivotovsky. 1986. Population structure of pink salmon: the system of fluctuating stocks. Journal Biologia morya. 2:39-44.

Haken, G. 1985. Sinergetica. Hierarchies of instabilities in selforganizing systems and structures. M. Mir. 419 p.

Ivankov, V.N. 1993. Population organization of Pacific salmon with short fresh-water period of life. Journal Voprosy ikhtiologii. 33(1):78-83.

Maksimovich, A.A. 1991. Pacific salmon: legends and facts. Journal Priroda. 10:40-47.

May, R.M. 1976. Simple mathematical models with very complicated dynamics. Nature. 261(5560):459-467.

May, R.M. 1991. Le chaos en biologie. La Recherche. 22(232):588-594, 597-598.

Odum, E. 1975. Basis of ecology. M. Mir. 740 p.

Rabinovitch, A., and R. Thieberger. 1988. Biological population obeying a stochastically perturbed logistic difference equation. J. Theor. Biol. 131(4):509-514.

Sharkovsky, A.N. 1964. Coexistence of cycles of persistent transformation of straight line onto itself. Ukr. math. Journal. 26(1):61-71.

Shuntov, V.P. 1993. Once more about the problem of global rise in temperature and its influence on biota of Far-East seas. Journal Rybnoye khozajstvo. 6:39-41.

Shuster, G. 1988. Determined chaos. Introduction. M. Mir. 240 p.

Wull, E.B., Ya. G. Sinay, and K.M. Khanin. 1984. Universality of Feigenbaum and thermodynamics formalism. Journal Uspekhi math. nauk. 39(3):3-37.

TABLES AND FIGURES

Table 1. Optimum values of parameters of model (1) - (3) and criterion of quality $\mathbf{R_{max}}$ by level of significance $\alpha < 0.01$, corresponding to them.

Parameters values	Even year generations		Odd year generations	
	Region 1	Region 2	Region 3	Region 4
r	4.15 ± 0.01*	4.15 ± 0.01	2.70 ± 0.15	2.70 ± 0.15
σ	0.10 ± 0.05	0.10 ± 0.05	0.60 ± 0.30	0.60 ± 0.30
K	30.00 ± 0.10	10.70 ± 0.01	30.00 ± 2.50	20.00 ± 0.50
δ	≤ 0.01	≤ 0.01	≤ 0.01	≤ 0.01
$\mathbf{R_{max}}$	0.90	0.85	0.80	0.85
$\mathbf{f(R_{max})}$, %	42	45	50	45

* range in which right mode in spectrum **f (R)** is maximum.

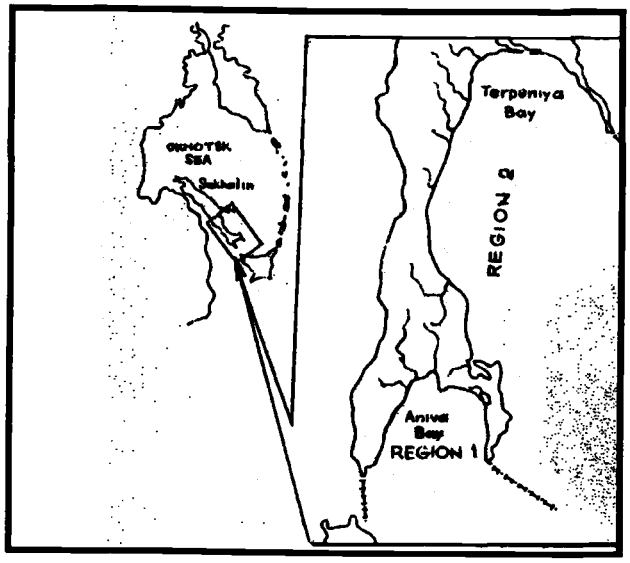

Fig. 1. The map-scheme of regions of pink salmon reproduction.

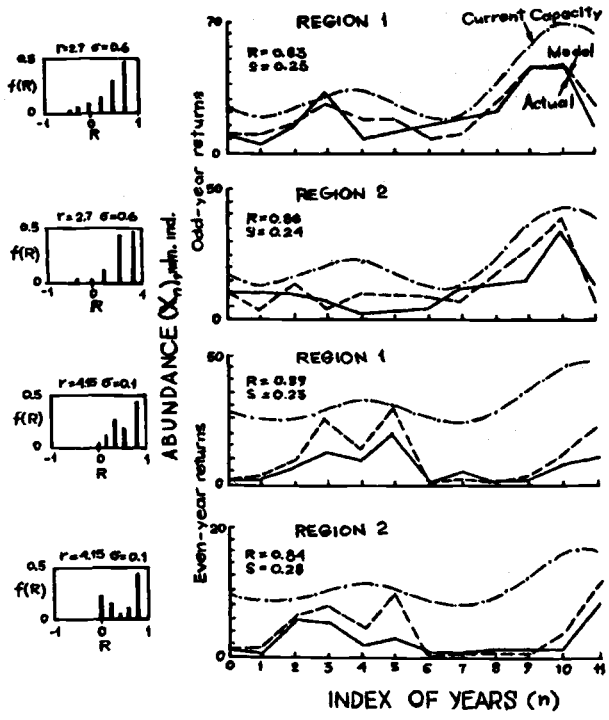

Fig. 2. Spectrums **f(R)** for optimal set of parameters of model (1)-(3) and model realizations with correlations $\mathbf{R_{max}}$ against the background of actual return dynamics by generations and regions for the period of 1970-1993 years.

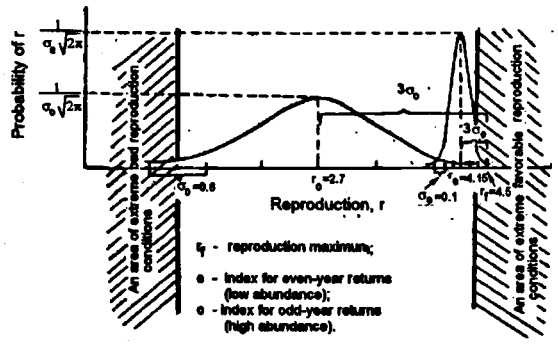

Fig. 3. Theoretical functions of parameter r distribution for generations with high and low abundance.

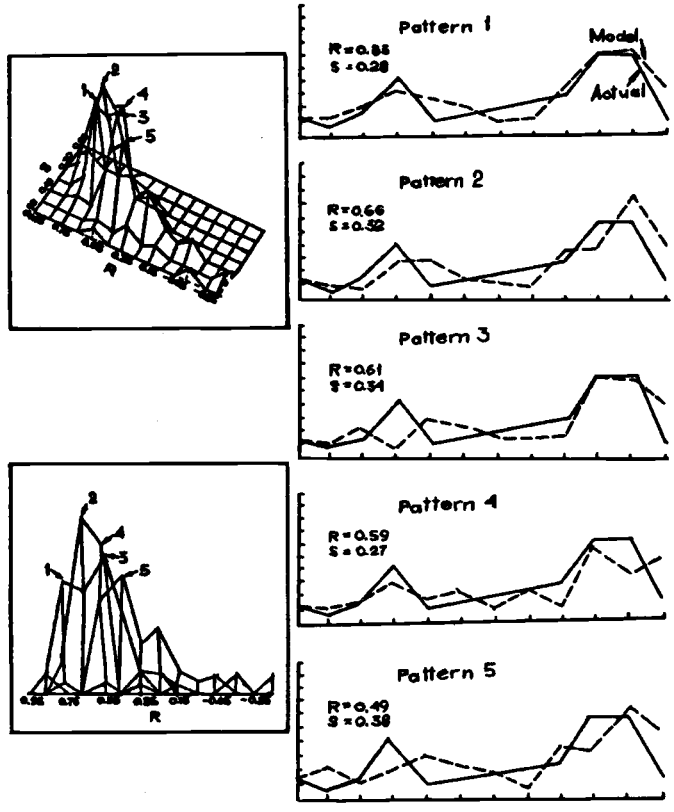

Fig. 4. Cross-tabulation of **R** and **s** with chosen model classes (**R**, **s**) and corresponding patterns for odd-year generation of the Region 1.

Fish-Culture of Pacific Salmons Increases the Number of Heredity Defects

Yuri A. MITROFANOV and Larisa N. LESNIKOVA

Pacific Oceanological Institute
Far-Eastern Branch of Russian Academy of Sciences , Vladivostok

It is known that fish-culture decreases the salmon qualitative indices (Bardach et al., 1976). Natural fertilization is very important to maintain genetic diversity, however, fish-breeders ignore the importance of natural selection during artificial fertilization. Mutation pressure has permanent effects on populations, therefore, various heredity defects can cause large defects (death, abnormal larvae) and/or small defects which will be described in this paper. Gamete selection can be used to eliminate defects. Sperm selection is more promising than egg selection because males produce numerous quantities (hundreds of billions) of sperms (Smirnov, 1975). The aim of this work is to investigate the influence of the artificial fertilization of eggs on changes in Pacific salmon survival, ratio of males to females, fluctuating asymmetric growth rates and so on.

MATERIALS AND METHODS

Hatchery fertilization techniques of chum *Oncorhynchus keta*, pink *O. gorbuscha* and chinook *O. tshawytcha* salmon were investigated in 1985-1992 in the Sakhalin Primorskiy region and Kamchatka. Egg fertilization by the dry method is used for the control groups as well as some embryos and small fry are also observed as a second control group. In the experiments on sperm selection, treatments are performed that prohibit fertilization of eggs by defective sperms.

RESULTS

The data indicated that different individuals can contain different levels of defective genes. Generally, week individuals of chum and pink salmon did not matured until the end of spawning season these individuals are thought to have a greater number of defective genes.

The dry method of fertilization provides an equal opportunity for all sperms to fertilize an egg. The quality of fertilized eggs from late maturing males produce a poor quality of progeny. A significant amount of dead embryos and dead fry along with an increase in the of ratio of males were observed. Sperm selection (SS) results in a decrease of these indices (Tables 1 and 2). Apparently, salmons which have more gene defects grow slower and therefore they become matured later. If the sperms of late spawning males are selected against by sperm selection the quality indices of progeny is improved (Tables 1 and 2).

The use of SS from early maturing males reduces the number of dead embryos (Tables 4 and 5) and increases the of sizes and weight of fry of chum (Table 3).

Fluctuating body asymmetry (FA) of chum is found to indicate the presence of significant small genetic errors during development. The number of body spots along the sides of fry is not an important feature, however, when the level of spots FA is high, the gill raker FA is significantly reduced and the pores FA on pre operculum is the least high (Table 5). The indices of FA of progeny

without SS is even lower than those of wild chum. The decrease of FA took place with the decrease progeny mortality and numbers of males. All these indices appear to reflect a process of reduction in the number of defective genes in progeny without SS.

The indices of FA indicates an increase in small gene errors during development. The FA indices are more sensitive than the other methods that we used. For instance, mortality because sperm selection also decreases the FA in progeny of early spawning salmons (Table 5). SS decreases the number of males too. According to Geodakyan (1987) the high number of males used is an index of the extent of population degeneration. It corresponds to the summarized data of FA change from our work. The FA decreases when male numbers decreases.

The method of sperm selection is also important to reproductive success for chinook *O. tshawytcha* of Kamchatka. The experiments are carried out using wild individuals from late spawning fish. The life history of chinook differs from other Pacific salmons as this salmon spawns in rapidly moving rivers waters and the sperm is more active than those of chum and pink salmon. Using the dry method of fertilization of chinook eggs (control) significantly decreases the of number of females (33.4%) which leads to an equal number of females and males. Thus, sperm selection leads to a decrease in the level of fluctuation asymmetry.

The connection of FA with viability and heredity of Salmon gairdneri is described in radiation ginogenesis experiments (Leary et al., 1985).

The SS method prevents the exposure of chum fry to unfavorable factors found in the environment such as oxygen deficiency. The SS influence on FA growth rate increases resistance to unfavorable factors from the environment which increases the number of females. We suppose that all these changes of features are based on small heredity defects in genes.

We suppose it to be important to discuss the differences of salmons of one population at the end and in beginning of spawning. N. Kulikova (1983) studied early and late spawning *Salmo gairdneri*. The survival of progeny from the late maturing females decrease to 63% fecundity (1,890 eggs) and the number of cells with chromosomes aberrations increases up to 23%. The progeny of females of early maturity is distinguished by high level of survival (87%) and fecundity (3,050 eggs) and also a decrease in the number of cells with chromosome aberrations (9%). Low levels chromosome aberrations is an important positive index. It shows stability of the heredity process. Thus, the early maturing Atlantic salmons produce more viable progeny.

CONCLUSIONS

1. Fertilization by late spawning male salmon using the dry method of fertilization of eggs leads to a significant high level of heredity defects in the progeny.
2. The method of sperm selection decreases the amount of large and small defects in the salmon produced and in the number males produced.

REFERENCES

Bardach, J.E., J.H. Ryther, and W.O. McLarney. 1976. Aquaculture. The Farming and Husbandry of Freshwater and Marine organisms. Wiley Intersience, a division of John Wiley & SonS, Inc. New-York London-Sydney-Toronto. 290 p.

Geodakyan, V.A., 1987. Evolution logic of sex differentiation in phylogeneze and onthogeneze: Doctoral thesis. Institute of biology of development of name of N.K. Koltcov. Moscow. 39 p. (in Russian)

Kulikova, N.I. 1983. The structure of artificial reproducing populations of Salmo gairdneri. Morphology, structure of population and problems of rational using of salmon fishes. Leningrad, Nauka. p.114-115. (in Russian)

Leary, R.F., F.W. Allendorf, K.L. Knudsen, and G.H. Thorgaard. 1985. Heterozygosity and developmental stability in gynogenetic diploid and triploid rainbow trout. Heredity. 54(2):219-225.

Smirnov, A.I., 1975. Biology, reproduction and development of Pacific salmons. Moscow State University. Moscow. 336 p. (in Russian)

TABLES AND FIGURES

Table 1. Mortality of progeny and number of females (late spawning pink salmon *O. gorbuscha*).

NN	variants	fertilized eggs,	mortality, %	% of females,
1	Control	843	43.4±2.2	44.6±1.5
2	SS	860	11.2±2.5	60.0±1.6
3	Control of factory	405	31.7±1.4	-

Table 2. Mortality of progeny (late spawning chum *O. keta*).

NN	variants	fertilized eggs,	mortality,
7	Control	3,120	30.1±1.1
8	SS	2,490	12.9±0.7

Table 3. Weight and size of fries of chum *O. keta*.

NN	variants	weight, mg size, cm	5-th month fries	6-th month fries
21	Control	mg	366.4±4.90	453.4±8.40
		cm	3.5±0.01	3.8±0.01
20	SS	mg	398.8±4.90	475.9±8.60
		cm	3.6±0.01	3.8±0.02
17	Control	mg	324.1±10.50	403.2±13.50
		cm	3.3±0.02	3.6±0.03
19	SS	mg	383.0±6.20	646.1±20.90
		cm	3.5±0.02	4.0±0.04

Table 4. Mortality of progeny and number of females (early spawning pink salmon *O. gorbuscha*).

NN	variantsfertilized eggs, number		mortality, %	number of females, %
5	Control	431	9.7±1.2	45.5±1.0
6	SS	752	5.8±1.0	65.5±1.1

Table 5. Changes of the indices chum after sperm selection (early spawning chum *O. keta*).

NN	Variant	Fertilized eggs, number fry,	Dead embryos, larvae, %	Fluctuating Spots, %	asymmetry Pores, %	Gill rakers, %	Number of females, %
17	Control	1392	6.7±1.2	143.0±0.3	21.3±0.3	36.9±0.2	43.7±0.3
19	SS	2092	4.1±0.8	84.0±2.4	9.9±0.1	18.8±0.1	58.3±0.2
21	Control	817	4.2±0.8	132.0±6.2	11.8±0.3	18.1±0.4	54.5±0.4
20	SS	920	2.5±0.2	103.2±1.2	10.3±0.1	13.0±0.1	55.6±0.2
	Wild	-	-	122.5±3.2	21.3±0.1	35.7±0.2	52.2±0.2

Abundance of Young Halibut along the West Kamchatka Shelf in 1982-1992

Larisa P. NIKOLENKO

Pacific Research Fisheries Centre (TINRO), Vladivostok, Russia

The Sea of Okhotsk is a marginal habitat for Pacific halibut, thus, it is less abundant than in the Bering sea and Pacific waters where a specialized fishery occurs. In the past, Sea of Okhotsk Pacific halibut have not been targeted for special investigation. There is some biological data but information on abundance has not been available. The Sea of Okhotsk halibut occurs all along the shelf on the upper continental slope but relatively stable accumulations were only observed on the West Kamchatka shelf. Data collected by expeditions for fishes (other than halibut) and invertebrates were analyzed keeping in mind that the sampling scheme may not have been appropriate for use in determining halibut abundance.

Abundance calculations were made using the method of squares (Aksyutina, 1968), adjusted for a trawl efficiency coefficient of 0.4.

30-85 cm individuals at age 4+ - 9+ were 80-95% of the catch by longline and trawl (Table 1). Thus, the West Kamchatka shelf appears to be a region for young Pacific halibut feeding migration in the Sea of Okhotsk. In 1982 the estimated abundance was 1.7 mln. and by 1989 it increased to 13.1 mln., while distribution increased three times from 3,149 to 9,163 sq.mile (Table 2, Fig. 1). At the same time, the abundance of halibut in the Pacific waters of Kamchatka increased (Bakkala, 1993; Kodolov et al., 1994). The increases in both areas may have been due to a shift in abundance and distribution throughout the region as a result of better conditions for halibut. From the early 90s western Kamchatka halibut abundance decreased to 6.5 mln by 1992 and the distribution also decreased in the area.

It is difficult to determine what were the causes of the fluctuations from the data available. However, a comparison 1989 and 1993 length frequencies from trawl catches indicated a decrease in the 50-70 cm length category from 63.6 to 39.9% of the total. On this evidence, it can be proposed that in the early 90s there was a decrease in survival and a shift in the distribution from the mid-80s. Without direct evidence, however, it is difficult to know if there has actually been a shift in survival and distribution of Okhotsk halibut. Large individuals were mainly found near the Kuril Islands, along the West Kamchatka slope, in the north area of Sea of Okhotsk and eastern Sakhalin areas. Gill nets and trawls used to catch turbot, crab traps and the cod long-lines were likely responsible for removing halibut but the available data are poor. Thus, it is difficult to determine shifts in the migration of young halibut off West Kamchatka.

REFERENCES

Aksyutina, Z.M. 1968. Elements of mathematical evaluation of observation results in biological and fisheries studies. Moskow, Pischevaya promyshlennost. 288 p.

Bakkala, R.G. 1993. Structure and Historical Changts in the Ground fish Complex of the Eastern Bering Sea. U.S. Dep. Commer., NOAA Tech. Rep. NMFS 114, 91 p.

Kodolov, L.S., T.I. Susina, and S.P. Matvejchuk. 1994. Stock Assessment of the Pacific Halibut (Hippoglossus stenolepis) in the northwestern Bering Sea. International symposium on north pacific flatfish. Abstract. p.33-34. University of Alaska Fairbanks, Anchorage, Alaska Sea Grand College Program.

Novikov, N.P. 1974. Commercial fishes of the North Pacific continen tal slope. Moskow, Pischevaya promyshlennost. 308 p.

TABLES AND FIGURES

Table 1. Size composition of Pacific Halibut of the Sea of Okhotsk in 1962-1968 (by Novikov, 1974), 1989 and 1991.

Year	Length, cm																				
	30	35	40	45	50	55	60	65	70	75	80	85	90	95	100	105	110	115	120-150	N	M
1962-1968 trawl	1.3	3.8	14.0	21.9	15.3	10.2	6.4	1.3	5.2	10.2	2.6	-	2.6	2.6	1.3	-	-	1.3		49	59.6
1989 trawl summer		1.3	8.9	15.2	19.0	20.2	12.7	5.1	6.3	3.8	1.3	2.5	1.3	-	-	1.3	1.3			79	54.2
1991 long line summer		0.6	2.0	11.7	23.9	24.2	16.2	12.0	6.0	1.4	0.6	0.6	0.3	0.3	0.3					351	58.6
1993 trawl spring	1.0	8.2	26.7	20.1	10.3	12.3	8.9	5.1	3.4	1.9	1.1	0.4	0.1	0.2	0.1	-	0.1	-	0.2	6272	51.7

Table 2. Change of abundance and distribution of young Pacific halibut along the West Kamchatka shelf in 1982-1992.

Year	1982 July-Sept.	1983 April-May	1986 July	1988 May-July	1989 May-June	1990 January-March	1992 June-August
Abundance mln/sp.	1.7	0.5	7.4	4.0	13.1	8.7	6.5
Investigated area, sq.mile	14,000	10,800	14,200	14,400	15,500	11,900	12,900
including catches	3149	2129	8476	5644	9163	7109	6541
density, thous. sp/sq.mile	0.12	0.05	0.52	0.28	0.85	0.73	0.5

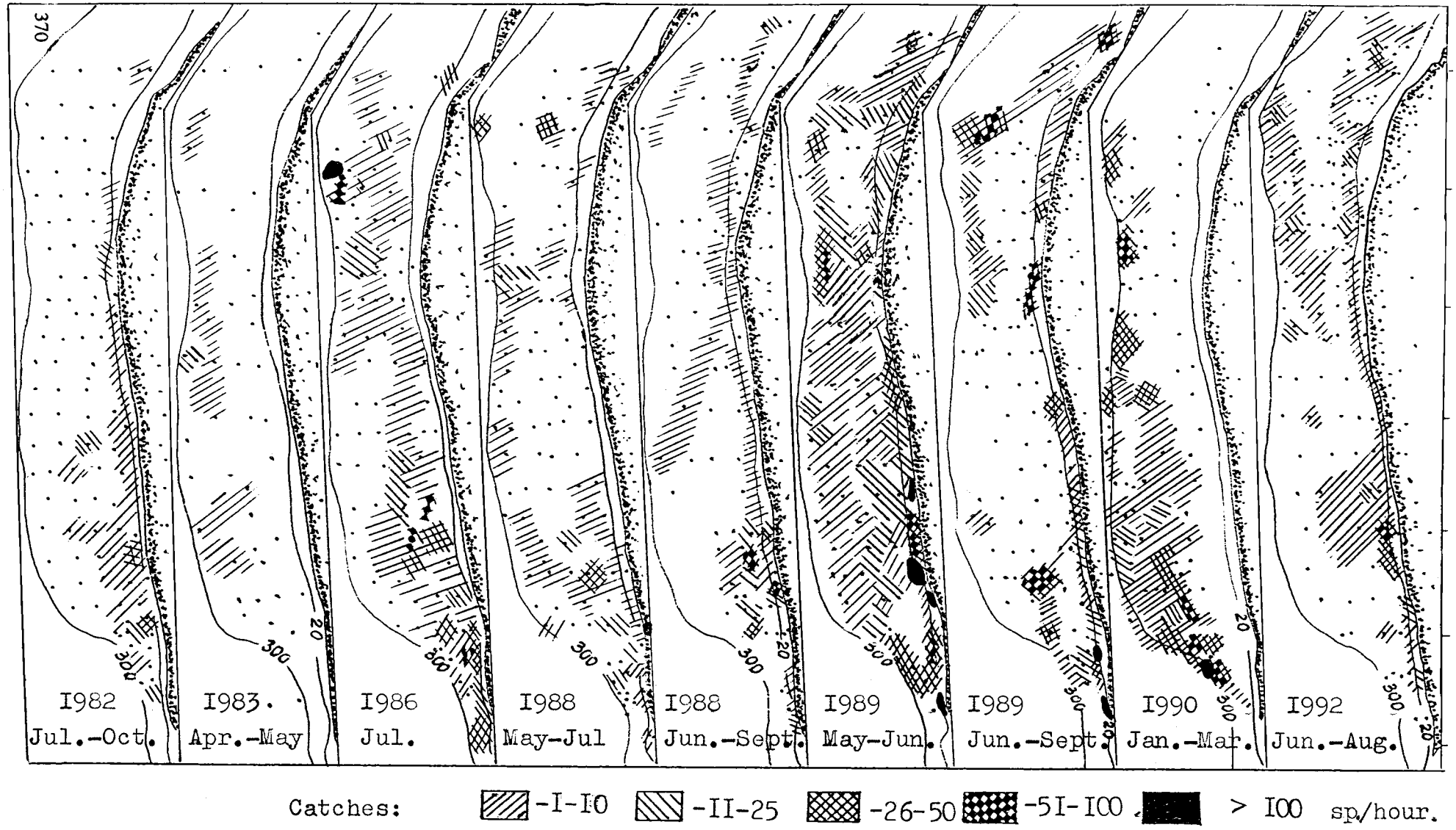

Fig. 1. Distribution of young Pacific halibut on the shelf of western Kamchatka in 1982-1992, specimens per hour trawling.

Living Conditions of Golden King Crab *Lithodes aequispina* in the Okhotsk Sea and near the Kuril Islands

Sergey A. NIZYAEV

Sakhalin Research Institute of Fisheries & Oceanography (SakhNIRO)
196, Komsomolskaya Street, Yuzhno-Sakhalinsk, Russia. 693016

In 1968 fishery information on golden king crab became available from Japanese vessels under a special pot fishery contract in the central part of the Okhotsk Sea (55°- 56°N, 147°-150°E). The first TINRO research on this crab on the continent slope of West Kamchatka was in August-September 1969 when a trawl survey was carried out at depths of 250-850 m to collect information on the biology, distribution and commercial importance of golden king crab (Rodin, 1970). Further investigations in the Northeast Okhotsk Sea were carried out in 1972, 1973, 1975-1977 but they did not focus on the golden king crab. In the spring-summer of 1989, an extensive trawl survey of the Okhotsk Sea to a depth of 2,000 m was carried out, except for the zone adjacent to the Kuril Islands. For the first time samples were collected of golden king crab over the continental slope throughout the Okhotsk Sea (Nizyaev, 1992). In 1991 a survey for golden king crab stocks in the Kuril Islands was undertaken using commercial crab vessels equipped with deep-water pots. Thus, directed research on golden king crab in Okhotsk Sea only started in the last 5-7 years but was limited to depths less than 200-300 m. There are always a number of difficulties with developing an investigation on the biology of a species where samples were collected from 200-600 m. and until recently crab pots were the main gear used by commercial fisheries and research. The pots are a highly size selective and some biological measurements are difficult to obtain unless the catching methods are modified to overcome the problem.

MATERIALS AND METHODS

Data were collected during trawl and pot surveys in the Okhotsk Sea from 1989-1994. Samples were collected using a 48-m trawl towed at 3 knots for one hour and by modified standard American trapezium pots of 175x175 cm in base, 90x90 cm in upper edge and 80 cm in height. Analysis of the data was according to "Guidance of studies of the Far-East Seas commercial Decapoda" (1979).

RESULTS AND DISCUSSIONS

From the 1989 trawl survey golden king crab was caught near West Kamchatka and to the west along the north coast of the Sea of Okhotsk to 142°30' E (Fig. 1). A high percent of crab was also caught by commercial nets for halibut near Northeast Sakhalin. Trawl catches of commercial crab averaged 10-20 per trawl. Crab caught from a stock discovered by trawling on Kashevarov bank averaged from 21 to 35 per pot. As a whole, the distribution of golden king crab in the open part of the Okhotsk Sea was similar from West Kamchatka to East Sakhalin except along 152°E where females and small males were absent and catches of commercial males did not exceed 1-2 per trawl.

In the area of Kuril Islands golden king crab was distributed all along all the ridge and near a group of islands. The greatest concentrations were found near the islands of Shiashkotan, Ushishir, Simushir and Iturup. Pot catches of commercial crab were 25-35 per pot.

The spatial structure of golden king crab was generally associated with local reproductive groups. Distribution of non commercial males and mature females was more local than that of commercial males. Non commercial males (of small size) were usually found near breeding areas in association with juvenile females the group that tended to migrate the least of all size groups. Mature females concentrated in high densities together with mature males. Some of the mature males located with the females took part in spawning while another assemblage of males were located in the outlying area of the female assemblage representing a reproductive potential.

Differences between golden king crab living conditions in the open part of the Okhotsk Sea and near the Kuril Islands were determined, mainly, from non-biological factors. With rare exception, the open area of the Okhotsk Sea is a plateau without sharp changes in depth allowing migration over long distances between different groups resulting in a mixing of genetic material. The Kuril Islands area on the other hand has sharp changes in depth on the bottom resulting in groups being isolated by restricting movement and the exchange of genetic material.

The genetic link between groups can also be kept up through larvae transport. Larvae of such crab species such as red king crab (Paralithodes camtschatica) and blue king crab (P. platypus) drift in the surface layer of the sea where they are dependant of surface currents. Golden king crab larvae behaviour is thought to be different by many authors. Somerton (1981) compared the developed yolk sac of Lithodes couesi (a close relative of golden king crab) with the red king crab larvae and expressed doubt of the necessity of Lithodes couesi larvae to migrate to the photic zone. Somerton and Otto (1986) advanced the hypothesis that the large size of golden king crab larvae in contrast to red king crab larvae allow them to go without food for longer periods and feed on large organisms. In the early stages of larvae development golden king crab may be lecythotrophic feeders resulting in a demersal type of existence, while shallow living shelf species larvae are planctotrophic. This idea is confirmed from the behaviour of the larvae of the deep-water crabs of genus Lithodidae which have not been found in the plancton layer, while larvae of red and blue king crab have been found in large numbers in the sea surface layer (Hoffman, 1968; Kurata, 1964; Marukawa, 1933; Takeuchi, 1962). In the Kuril Islands there is almost complete lack of crabs that have planktotrophic larvae. This is thought to be related to the powerful currents which could carry the larvae away from areas where they could settle to the bottom. Golden king crab is common to these areas which suggests that larvae development is independent surface currents. Thus, in the Kuril Islands the golden king crab is isolated by the topography and through larval drift limiting genetic exchange compared to the stocks living in the open part of the Okhotsk Sea.

High concentrations of crab on small isolated areas near the Kuril Islands may produce high catches per effort but lead to a false impression about the size of the stocks. Intensive harvesting would result in a sudden reduction of catch rate and it would take years to recover the lost biomass. On the plateau near the Shiashkotan and Lovushka Islands the average catches per effort decreased from 28 to 9 per pot over three years and the mode of males decreased from 210 for 175 mm carapace width. Lower harvest rates by adjusting commercial pressure on isolated stocks that are not connected need to be implemented to prevent over fishing and to allow recovery of stocks that have already been over exploited. Stocks in the open Okhotsk Sea remain more stable unless fishing pressure becomes to great for the rate of replacement of the stock biomass.

REFERENCES

Guidance of studies of the Far-East Seas commercial Decapoda. 1979. Vladivostok: TINRO. 59 p.

Hoffman, E.G. 1968. Description of laboratory-reared larvae of Paralithodes platypus. J. Fish. Res. Board Can. 25:439-455.

Kurata, H. 1964. Larvae of decapod Crustacea of Hokkaido. Lithodidae, (Anomura). Ibid. 21:9-14.

Marukawa, H. 1933. Biology and fishery research on Japanese king crab Paralithodes camtschatica. J. Imper. Fish. Exper. Sta. - Tokyo. p.1-152.

Nizyaev, S.A. 1992. Distribution and abundance of deep-water crabs in the Sea of Okhotsk. Promyslovo-biologicheskie issledovania morskikh bespozvonochnykh. - M. VNIRO. p.26-37.

Rodin, V.E. 1970. New data about golden king crab. Rybnoe Khozaistvo. [1] 6:11-13.

Somerton, D.A. 1981. Contribution to the life history of the deep-sea king crab, Lithodes couesi, in the Gulf of Alaska. Fish. Bul. 79([1] 2):259-269.

Somerton, D.A., and R.S. Otto. 1986. Distribution and reproductive biology of the golden king crab, Lithodes aequispina, in the eastern Bering sea. Fish. Bul. 84([1] 3):571-584.

Takeuchi, I. 1962. On the distribution of zoeae larvae of king crab, Paralithodes camtschatica, in the southeastern Bering sea in 1960. Bul. Hok. Reg. Fish. Res. Lab. 24:163-170.

FIGURES

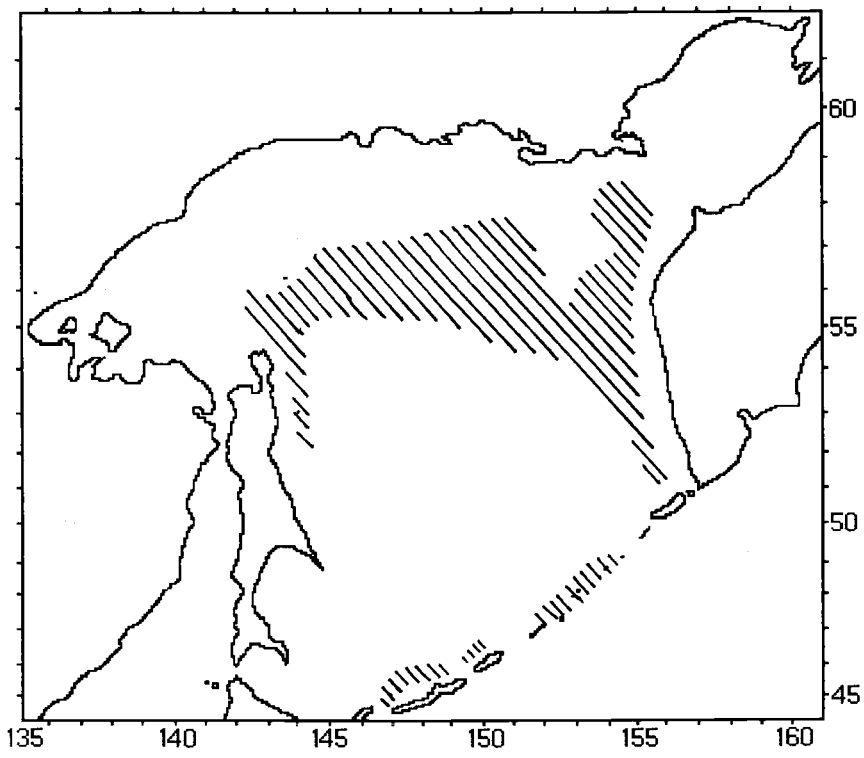

Fig. 1. Distribution of golden king crab in the Okhotsk Sea.

Settlements of Japanese Scallop in Reid Pallada Bay (Sea of Japan)

Ludmila A. POZDNYAKOVA and Alla V. SILINA

Institute of Marine Biology
Far-East Branch of Russian Academy of Sciences, Vladivostok 690041, Russia

INTRODUCTION

Reid Pallada Bay (northwestern part of Possjet Bay of the Sea of Japan) is the major scallop cultivation area in eastern Russia. The cultivation of the scallop *Mizuhopecten yessoensis* (Jay) involves collection of spat, spat rearing in nursery-cages for one year and the transfer of juveniles to the bottom culture sites for 2-3 years until they are an acceptable size (100 mm)(Belogrudov, 1986). Usually cultured juveniles are seeded in low density natural scallop populations. Over the last 20 years, cultured scallop in the bight of Reid Pallada Bay have replaced native populations. The purpose of this study was to delineate the stocks, the percentage of cultured and natural individuals, age and size composition and to compare the growth rates of seeded and natural scallops at six sites in Reid Pallada Bay.

MATERIALS AND METHODS

A Scuba survey of Reid Pallada Bay was undertaken along transects perpendicular to the coast line to 15 m depth. The number of natural and introduced scallops were counted in a 1 m wide band or in a 1 m frame, depending on the settlement density. To determine the growth, size and age structure of population 106-500 individuals were collected.

The shell height, wet weight, tissue weight and adductor muscle weight were determined. The age and linear growth of each scallop were determined from the microsculpture of the surface of the upper valve (Silina, 1978). The same method was used to reconstruct the individual linear growth of each scallop and to estimate the mean growth of scallops from each site. Scallops seeded into natural settlements were distinguished from the natural individuals by the presence of a noticeable mark in the elementary growth ring of the microsculpture in the upper valve surface which was caused during transport and seeding on the bottom. The year of transfer to the grounds of each scallops was determined from their age. The growth of cultured scallops in different years was compared with resident individuals.

RESULTS

All sites had an irregular strip like distribution of scallops with density 0.1-7.0 (in the main 0.5-5.0) per m. This was considerably higher than in natural settlements due to seeding to increase profits. The scallop shell height was 30-165 mm (1-12 years old) (Table 1) but the size and age distributions of the seeded scallops were differed from natural scallop. The maximum age in each population was found to occur in the cultured scallops but cultured scallops were smaller at age than resident (Table 2). The highest growth rates were in the northwest part of Reid Pallada Bay and in

Temp Bay, where they reached the commercial size at 3 years old. On the other studied sites scallops reached the harvest size at 4. The total number and weight of scallops on all six sites (127 hectares) was about 1,200,000 individuals weighing 240 tons. During August 1990 the estimated harvestable biomass was about 98.1 tons total weight and 17.8 t muscle weight.

DISCUSSION

An irregular strip like distribution was characteristic for cultured scallops in the study sites due to the method of seeding. Cultured scallops had a smaller shell height than the resident individuals of the same age (about one year) at the time of transfer, which was due to slower growth of juveniles in the nursery cages during the first year. After transfer the scallops need time for adaptation to new conditions and for regeneration of the growing edge of the shell which was usually broken during transportation to the grounds. The resulting difference in shell height usually remains throughout life (Pozdnyakova and Silina, 1993; Pozdnyakova et al. 1992; Silina et al. 1994). The growth rate of cultured scallop in the studied sites of Possjet Bay was slower than in most other areas of Peter the Great Bay (Silina and Pozdnyakova, 1986; Silina, 1990; Silina et al. 1994). The high water temperature (16 to 26 C) in July-September is thought to inhibit growth (Silina, 1983; Silina and Pozdnyakova, 1986) which means the scallops were not harvest size until about 4 years old.

The number of the resident scallops before introducing cultivated juveniles was small at five of the sites studied. The encouragement of natural scallop settlement on the bottom of Possjet Bay enhances productivity of commercial beds and there is good production of spat for artificial collection and rearing in nurse-cages for later seeding. This reduces the need for cultivation and transportation to the grounds which reduces the expenses as well as the adaptation after seeding.

REFERENCES

Belogrudov, E.A. 1986. Cultivation, p.203-208. *In* P.A. Motavkin [ed.] The Japanese scallop *Mizuhopecten yessoensis* (Jay). Far-East Science Centre, Academy of the USSR: Vladivostok, USSR. (in Russian, with English abstract and contents)

Pozdnyakova, L.A. and A.V. Silina. 1993. Population structure and growth in the sea scallop *Mizuhopecten yessoensis* in Vladimir Bay, Sea of Japan. Sov. J. Marine Biology. 19:131-135.

Silina, A.V. 1978. Determination of age and growth rate of Yezo scallop by the sculpture of its shell surface *Mizuhopecten yessoensis*. Sov. J. Marine Biology. 4:827-836.

Silina, A.V. 1983. Effect of temperature on linear growth of the Japanese scallop. Ecologija. 5:86-89. (in Russian)

Silina, A.V. and L.A. Pozdnyakova. 1986. Growth, p.144-165. *In* P.A. Motavkin [ed.] The Japanese scallop *Mizuhopecten yessoensis* (Jay). Far-East Science Centre, Academy of the USSR, Vladivostok, USSR. (in Russian, with English abstract and contents)

Silina, A.V. 1990. Selection of regions and breeding sites of Yezo scallop at the coast of Maritime Territory. Sov. J. Marine Biology. 5:283-286.

Silina, A.V., Ju.Ja Latypov, and L.A. Pozdnyakova. 1994. Japanese scallop cultivation on the bottom. Rybnoye Khozyaistvo. 3:41-42. (in Russian)

TABLES

Table 1. Composition of Japanese scallop Mizuhopecten yessoensis settlements in Reid Pallada Bay (Sea of Japan).

Sites	Age, years	Shell height, mm	Stock, thousand of individuals	Percentage of cultured scallops
Astafjev Cape	1-9	45-165	1.2	20.6
Between Astafiev Cape and Temp Bight	2-4	84-109	220.0	89.9
Temp Bight	2-6	88-131	1.5	48.8
Klykov Bight	2-8	77-154	500.0	87.5
Mininosok Bight	1-12	61-143	117.3	74.5
Northwestern part of Reid Pallada Bay	1-7	30-162	360.0	42.5

Table 2. Size and weight of Japanese scallop Mizuhopecten yessoensis in Reid Pallada Bay (Sea of Japan).

Sites	Age, years	Shell height, mm		Wet weight, g	
		natural	cultured	natural	cultured
Astafjev Cape	2	81.3±3.0	65.4±4.2	49.8±4.4	33.8±4.6
	3	98.3±3.2	-	99.8±5.6	-
	4	112.8±3.0	-	162.5±5.3	-
Between Astafie Cape and Temp Bight	2	84.2±5.6	-	52.7±12.4	-
	4	109.0±4.9	107.2±1.2	125.0±17.3	113.8±6.1
Temp Bight	2	88.2±3.9	-	74.1±9.5	-
	3	108.8±3.8	103.1±5.2	130.0±26.7	125.2±21.7
	4	116.0±4.1	118.2±3.3	-	195.7±26.7
Klykov Bight	4	109.8±4.8	100.2±1.9	119.3±5.4	103.9±12.0
Mininosok Bight	2	88.6±7.2	74.0±3.4	-	40.7±4.4
	3	103.5±2.7	96.8±1.9	84.1±6.2	-
	4	105.7±3.9	111.8±3.1	112.0+12.5	128.4±12.4
Northwestern part of Reid Pallada Bay	2	90.1±3.4	87.1±3.9	78.4±4.6	79.8±9.5
	3	108.7±2.3	103.3±2.0	-	129.8±5.3
	4	119.3±3.3	-	201.5±21.3	-

Data are shown as mean ± s.e.m.

Features of the Southwest Okhotsk Sea Herring

Galina M. PUSHNIKOVA

Sakhalin Research Institute of Fisheries and Oceanography (SakhNIRO)
196, Komsomolskaya st., Yuzhno-Sakhalinsk, 693016 Russia)

A number of independent herring populations with different levels of abundance, in the Far-East Seas, are in the process of changing (Svetovidov, 1952). Herring inhabiting Sakhalin waters differ from others because they have a more complex intraspecies structure (Frolov, 1950; Rumyantsev, 1967; Pushnikova and Rybnikova, 1991). Some authors have studied the population structure and tried to separate populations into groups using a number of ecological features. Frolov (1964) concluded from morphological characters that there are two groups of herring in Sakhalin waters; marine (Sakhalin-Hokkaido) and lake. Rumyantsev (1967) studied herring scale structure and came to conclusion that there are ocean, marine and lagoon groups. Other researchers (Sokolov, 1962; Drujinin, 1963) denied the existence of any groups of herring other than the Sakhalin-Hokkaido. Japanese researchers suggest two groups, oceanic and local herring and to separate local herring into lake and neritic herring (Iizuka and Morita, 1991).

This paper examines data on herring, inhabiting the southwest Okhotsk Sea along the Sakhalin coast and the Tatar Strait. Analysis of morphometric, biological and biochemical parameters suggest the presence of herring populations in the area of Sakhalin-Hokkaido, Terpeniya bay, Aniva bay, Sakhalin bay, Northeast Sakhalin coast bays, De-Kustry bay, Tunaycha lake, Nevskoye lake and Ainskoye lake (Pushnikova et al., 1987; Rybnikova, 1987; Zverkova et al., 1991). The data indicate that Sakhalin-Hokkaido herring differ from others by the greatest number of parameters and the stock occupies the largest area. Lake populations are characterized by the smallest number of parameters and smallest occupied area. The two groups differ from each other by the rate of growth, sex maturity, fecundity, location in waters of a different hydrochemical structure. Fish of other populations had intermediate biological and ecological parameters. Thus, biological and ecological parameters allowed the separation of the population into oceanic, local and lake.

The largest annual catch from the oceanic herring was one million tons, local populations 12 thousand tons and lake 200 tons (Table 1). Catches were reduced to 0.9, 0.08 and 0.001 thousand tons when the stocks decreased.

The maximum age of the different groups of herring are: oceanic 18, local 11 and lake 9. The longest body length is: oceanic 44 cm, local 32 cm and lake 29 cm. Recently, the abundance of the oceanic herring (largest stock) has been greatly depressed and the maturity age of all herring groups has been reduced to 2. Oceanic herring usually mature at 4, local at 3 and lake at 2 when the stocks are not depressed (Table 2).

Lake herring have the lowest rate of growth rate of all the groups(Fig. 1). The body length of 1 year olds was: lake 8 cm, local 10 cm, oceanic a little more than 12 cm. The maximum difference of body length at age 1 was 4 cm between oceanic and lake herring. This difference reaches 7cm at 4-years old and 10 cm at 8. For example, data on Sakhalin-Hokkaido herring (oceanic), on De-Kastry herring (local) and Tunaycha Lake herring (lake) are presented in Fig. 1.

Eighty percent of the lake group herring mature by 13.0 cm and mature local and oceanic groups of herring appear in small numbers by 19 cm when all the lake group was already mature (Fig. 2). Eighty percent of the local group is mature by 20 cm and 80% of the oceanic by 24 cm. The body length increased by 6 cm from the beginning to 100% maturity for lake and local herring but oceanic did not fully mature for 8 cm. The maturity rate of oceanic herring is slow in comparison with other groups. The slow rate of oceanic herring maturity compared to the other groups is, evidentely, an illustration of the deep intrastructure transformations that has happened in the Sakhalin-Hokkaido herring over the 40 year depressed period.

Fecundity data were different between the three herring groups. The average number of eggs of 19-25 cm lake group females was the highest among individuals this size group(Fig. 3). Further, with increasing of body length and fecundity of the same size groups of oceanic herring grows at a great rate, practically along the straight line at an angle about 60° to absciss axis. At the same time, the increase in the rate of lake herring fecundity is lower. When body length reaches 28 cm and more lake herring has the lowest number of eggs per female. The greatest fecundity oceanic herring is more, than 120 thousands eggs (body length - 35 cm), for local a little more than 60 thousands eggs (body length - 31 cm) and for lake herring less than 50 thousands eggs (body length - 29 cm).

The number of eggs per oceanic female is higher at all ages compared to local and lake herring (Fig. 4). Fecundity of local herring at 2 years old (the beginning of maturity for this groups) is lower compared to the lake group (2 years old is the age of greatest maturity). Further fecundity of the same age group of local herring increases and during the period of ontogenesis exceeds the index values of the lake herring.

The winter and spawning conditions of herring greatly differs among the three groups. Oceanic and local groups over winter in the open sea near the slope and slope areas, at 150-300 m depth. Lake herring over winter in lakes where the salinity does not exceed 12‰. Oceanic herring spawning takes place in open littoral areas, at depths of 1.0-10.0 m, mainly, on sea plants and brown algae. Salinity on the spawning grounds changes from 24.8 to 33.7‰. Local herring spawning occurs on open littoral areas, in bays, creeks and lagoons at depths of 0.5-4.0 m on sea grass, brown and red algae. Water salinity on the spawning grounds varies from 9.9 to 33.2‰. Lake herring spawn at sea, in low salinity which vary from 9.0 to 21.4‰ in the immediate neighbourhood of channels mouths joining lakes in the sea at depths of 1.0-2.0 m on sea grass and brown algae.

The oceanic group of herring inhabit the North Japan Sea, south and middle parts of the Okhotsk Sea and Pacific waters adjoining the South Kuril Island and Hokkaido at different stages of ontogenesis (Rumyantsev and Frolov et al., 1958). Local herring did not make extensive migrations as the Sakhalin-Hokkaido group but remain in De-Kastry, Aniva bays, Terpeniya, Sakhalin and bays and lagoons of the northeast coast of Sakhalin (Nabil, Nyivo, Chaivo, Piltun). Lake herring did not make extensive migrations and differ from other groups by feeding in open sea areas and returning to lakes in the winter. Herring populations of lakes Tunaycha, Nevskoye, Ainskoye form the lake groups.

REFERENCES

Druzhinin, A.D. 1963. Results of herring tagging in Sakhalin waters for 1956 - 1960. Izv. TINRO. 49:65-94.

Frolov, A.I. 1950. Local forms of Sakhalin herring. Izv. TINRO. 32:65-71.

Frolov, A.I. 1964. Morphological characteristics of herring in Sakhalin waters. Izv. TINRO. 55:39-53.

Pushnikova, G.M., V.V. Pushnikov, and I.G. Rybnikova. 1987. On intraspecies structure of herring in Sakhalin shelf for the period of stock depression. Coll. repr. "Results of researches on the questions of rational use and preservation of water, land and biological resources of Sakhalin and Kuril Islands". Yuzhno-Sakhalinsk. p. 111-113.

Pushnikova, G.M., and I.G. Rybnikova. 1991. On herring population structure of Northwest Pacific. Coll. repr. "Rational use of the Pacific Ocean biological resources". Vladivostok. p. 169-170.

Rumyantsev, A.I., A.I. Frolov. et al. 1958. Migrations and distribution of herring in Sakhalin waters. M. VNIRO. 48 p.

Rumyantsev, A.I. 1967. Methods used for estimation of stocks and forcasting of possible commercial fish catches in Sakhalin waters. Tr. VNIRO. 62:107-121.

Rybnikova, I.G. 1987. Results of the population-genetic studies of the Pacific herring Clupea pallasi Val. Coll. repr. "Genetic researches of marine hydrobiontes". M. p. 94-107.

Sokolov, V.A. 1962. Racial belonging of herring fry in the Aniva Bay. Vopr. Ikht. 2(22):73-78.

Svetovidov, A.N. 1952. Fauna of the USSR. Fishes. M. - L., A.N. USSR. 2(1):331 p.

Zverkova, L.M., G.M. Pushnikova, et al. 1991. Results of research of marine commercial fish populations in Sakhalin - Kuril area. Yuzhno-Sakhalinsk: SakhTINRO, 50 p. Dep. in VNITI 20.05.91, N 1154 - px91.

TABLES AND FIGURES

Table 1. Historical catches of ecological herring groups.

Ecological Groups	Catches, thousand t.	
	max	min
OCEANIC	1000	0.9
LOCAL	12	0.08
LAKE	0.2	0.001

Table 2. Biological parameters of the ecological herring groups.

Ecological Groups	Age limit	Length, cm		Age of sexual maturity	
		max	model	beginning	mass
OCEANIC	18	44	26 - 29	2	4
LOCAL	11	32	23 - 26	2	3
LAKE	9	29	18 - 21	2	2

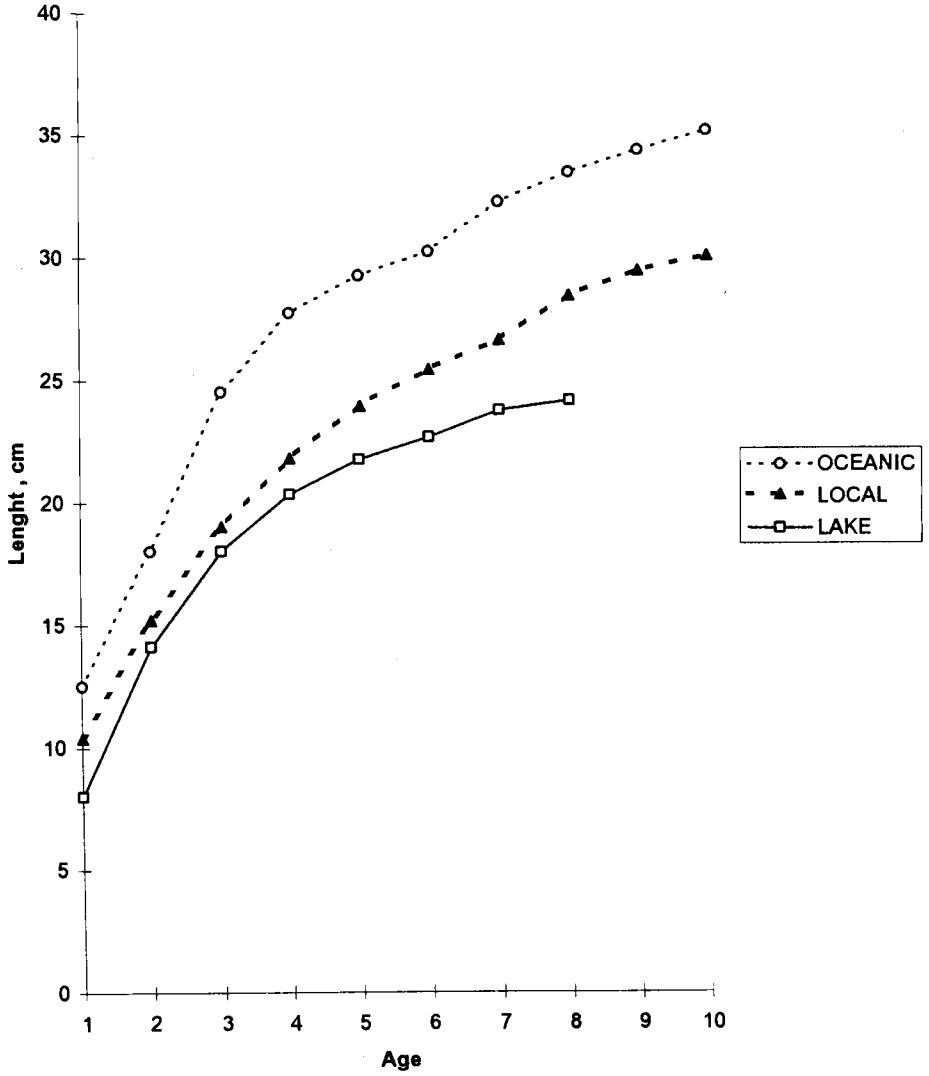

Fig. 1. Herring growth.

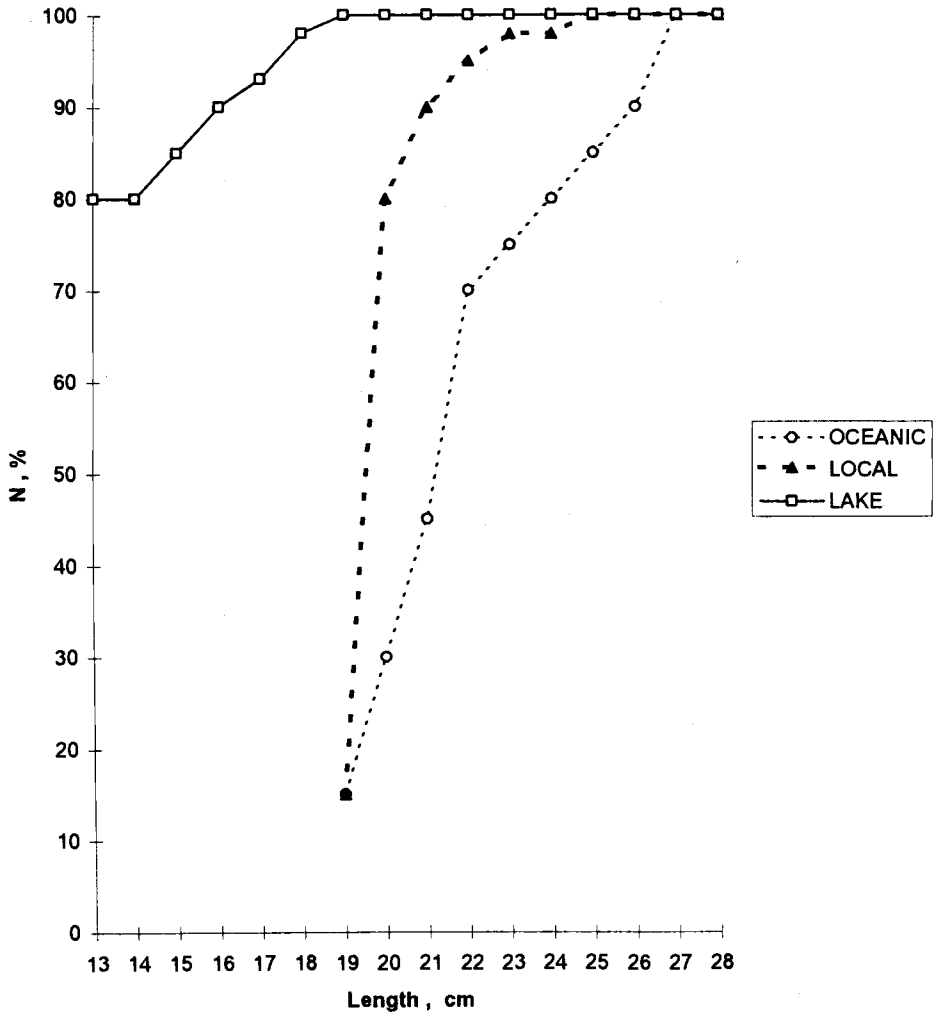

Fig. 2. Maturity rate of the herring.

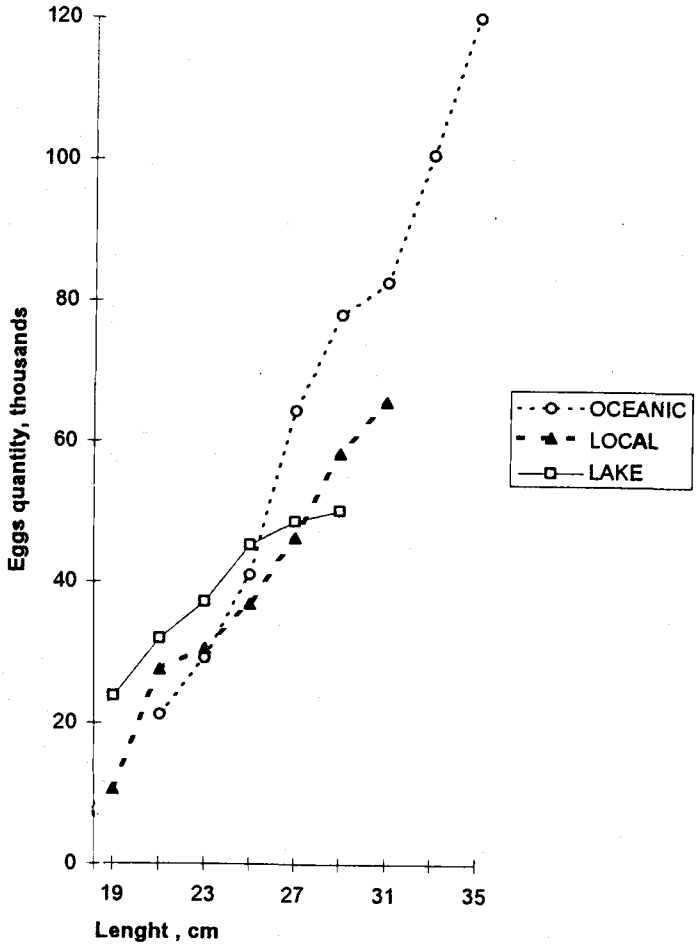

Fig. 3 Herring fecundity.

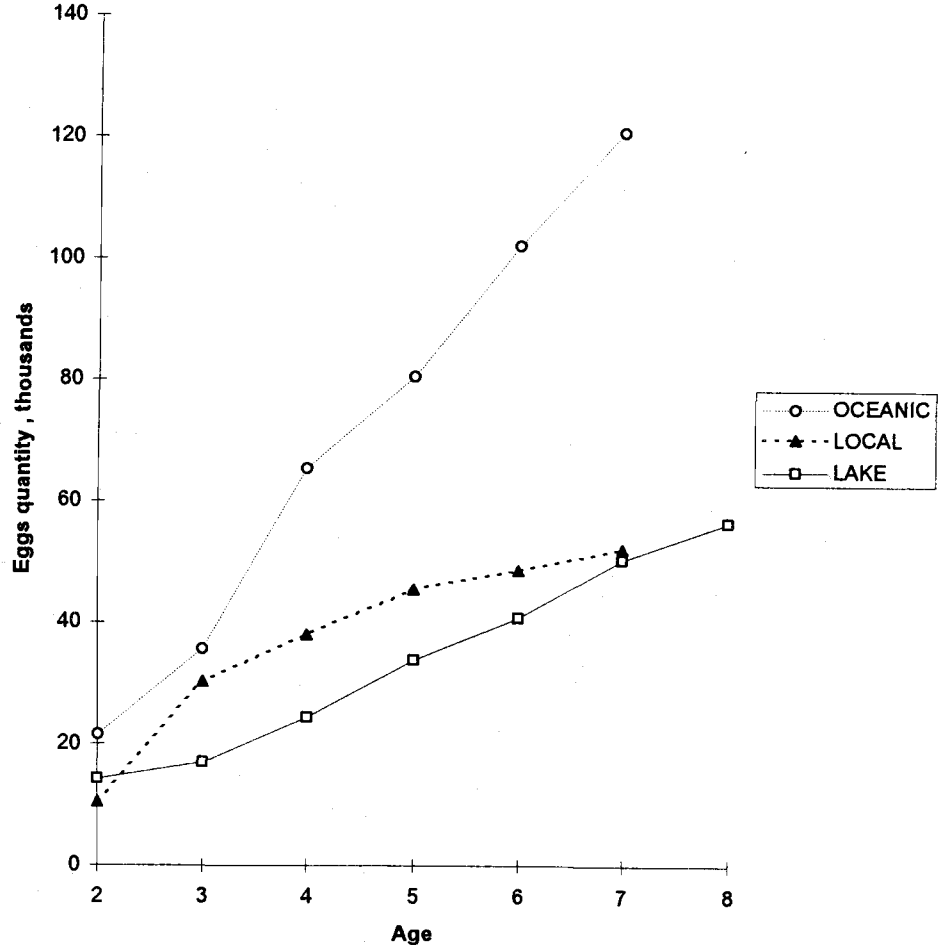

Fig. 4. Herring fecundity.

Present State of the Okhotsk Herring Stock and Fisheries Outlook

Vladimir I. RADCHENKO and Igor I. GLEBOV

Laboratory of Applied Biocenology of the Pacific Research Fisheries Center (TINRO-Center), Vladivostok, 690600, Russia

Pacific herring was one of major fisheries developed during the initial period of the Russian marine fisheries in the Far-East in the early 1950s. The Sea of Okhotsk the herring fishery has been based on two large stocks: Okhotsk and Gizhiginsky-Kamchatkan. Catch of Gizhiginsky-Kamchatkan herring quickly increased to the highest possible level and has sharply decreased since 1960s. The Okhotsk herring were the subject of large scale fisheries until the second half of the 1970s. By 1963 the annual catch by Soviet fishermen was in excess of 200 thousand tones and by 1968-1969 reached a peak of 417.9-424.4 th. t. The combined Russian and foreign catch was about 600 th. t. During this period, herring contribute 42.7-45.0% of fish production caught by the USSR in the Sea of Okhotsk (Shuntov, 1985).

The development of a large scale herring fishery stimulated the formation of the national marine fishing fleet in the Far-East. Historically, it has played an important role in Russian fisheries management strategy in the Pacific Basin. Planned increases in fish catch, resulted in the decline of herring stocks as well as for other traditional species (salmon, flounders, etc.) caught in the coastal areas and shelf, which caused a movement to fish walleye pollock. The presence of a powerful fishing fleet resulted in a shift of fishing efforts to the resources of the continental slope and offshore waters. This strategy was caused by an additional stimulus with the introduction of the 200-miles economic zone by most countries of Pacific region in 1978. In the mid 1980s, the walleye pollock became the most important fishery in Russian and in the world (Gershanovich et al., 1990).

An analysis of the stock dynamics of herring and walleye pollock, the two most abundant fish species of Far-Eastern Seas pelagic zone, reveals that an increase in abundance of one coincides with a decrease in abundance in the other (Shuntov, 1986, 1991; Naumenko et al., 1990). By the early 1990s, North Pacific walleye pollock biomass decreased, particularly, in the northern area from 20-25 to 6 mln. tons in the Bering Sea pelagic zone and from 14 to 5 mln. tons in the North Sea of Okhotsk. The cause of this significant decrease was periodic global climatic oceanographic change in the pelagic ecosystems of the Far-Eastern Seas, as well as, a corresponding change in the structure of the hydrobiont communities and the number of dominant fish species (Shuntov et al., 1993).

The majority of the herring populations throughout the Pacific region increased in abundance from the early 1990s. There is evidence of increases in herring stocks inhabiting the Gulf of Alaska and waters of British Columbia (Collie, Spencer, 1993; Schweigert et al., 1993). Data from a survey of the Korfa-Karaginsky herring stock in 1993, in the west Bering Sea, indicates a increase of about two times compared to the second half of the 1980s. Analysis indicate 286 thousand tons of herring occur within the shelf at depths more than 50 m. and 120 mln. fingerlings were found in the Karaginsky Bay. If in 1986-1987 the ratios of the numbers of walleye pollock to herring fingerlings were from 100:1 to 25:1 then in December 1993 it was 2:1. Data collected in fall of 1994 indicates that the ichthyofauna in the eastern Olyutorsky Bay was predominantly small herring (fork length 13.6-27.0 cm), about 37% of the estimated fish biomass while the walleye pollock was 29%.

From data collected in the eastern Bering Sea groundfish surveys, the estimated herring by-catch in 1988 as compared with that in the early 1980s increases by three times (Bakkala 1993). These data are mainly related to the herring from the Bristol Bay sub-population being about 80% of total numbers in the eastern Bering Sea. Some indirect data also provides evidences of the growth of this stock. In July 1992, a large group of herring (modal group of 32-33 cm) arrived in the Russian economic zone north of 58°N. The walleye pollock fishing fleet caught up to 60 tones per hour of which the catches sometimes contain up to 60% herring as by-catch. The herring are also distributed in open waters of the Aleutian Basin up to 100 miles off the shelf. In the fall of 1994, a similar large mass of herring was found by the r/v "Shursha" in Anadyr Bay. In the 1980s, the abundance and migration pattern of the East Bering Sea herring is less pronounced and the distribution is limited to the northern shelf. The abundance in the western Bering Sea did not exceed 35 mln. fish and the biomass was 8 th. tons or 2.5-3.0% of Korfa-Karaginsky herring.

Assessments of the Okhotsk herring stock were accepted until recently. The results of epipelagic ecosystem studies in the Sea of Okhotsk in 1984-1990 indicate a biomass in the order of 1 mln. tons (Shuntov et al., 1993) and herring are concentrated on the northern shelf. A recent assessment by scientists from the Magadan Branch of TINRO recommends a catch of 100 th. tons for the Okhotsk herring (Yolkin, 1988). In the early 1990s, there was an expansion of the feeding area of the Okhotsk herring to the south of West Kamchatka and north of Sakhalin. In November-December of 1993, herring biomass is estimated at 2.5 mln. tons by the volume method from a trawl macro-survey by the r/v "Professor Kaganovsky". However, the location of the survey area and the density of echo-records and catches (which is characteristic of hibernating herring) provides grounds for doubt of the estimation. In March-April of 1994, the trawler "Novokotovsk"(a small area 1.34 thousand sq. km) caught 45-160 tons (average for 24 trawls was 11.8 tons per hour) while surveying for walleye pollock. The average density of herring within the grounds is estimated to be 66.8 tones per sq.km and the biomass about 90 thousand tons. The boundary of herring concentrations is to the south, where herring is not found south of 57°N and to the southeast where catches are 2 tones per hour in TINRO Basin. In August 1994, when dispersed herring are feeding in the North Okhotsk Sea the r/v "Professor Levanidov" operating mainly to the south of 54°N caught up to 10 tones per hour to the northeast of Sakhalin, in an area where, in the 1970s-1980s, feeding herring was not typical (Yolkin, 1988).

The most complete information on the stock status, age composition and distribution of Okhotsk herring during active feeding migrations was collected from 498 thousand sq. km including 57 stations during a 25 day cruise of the r/v "TINRO" in September-October of 1994. A comprehensive survey of oceanographic conditions and the distribution of plankton, fish and squids was conducted. At each deep-water station, surface trawls and stepped trawls within a layer of 50-280 m were carried out using a rope trawl RT 108/528 equipped with a fine mesh cod end of 6 to 30 mm. On the outer shelf (depths more than 100 m) one half hour trawls were carried out in the surface layer and in the layer of echo-recordings. Only surface trawls were carried out over the shallow shelf. The average fish density was quite high at 12.7 tones / sq. km (Table 1). More than 95% of the biomass is from three species; walleye pollock (52.7%), herring (36.0%) and northern smooth-tongue (8.2%). A pronounced reduction of the walleye pollock occurs from 75.0-84.3% of the biomass in the latter half of 1980s and an increase of the herring is found from 3.5-9.7% (Shuntov et al., 1993). The herring biomass is greater than that of other fish species within the 0-50 m depth zone as well as in the coastal zone (Table 1). Herring were quite widely distributed in the North Sea of Okhotsk during the survey; 80.7% of 53 trawls on 46 stations contained herring. The major concentrations of herring occurs in the shelf zone of the northern part of the investigated area (Fig. 1). 99.3% of the herring biomass was concentrated in regions Nos. 1, 2 and 5 including 60.1% in Tauisky where the fishing fleet caught herring located to the south of the mouth of Tauisky inlet. The density was 92 tones per sq. km, on

average, in an area of 4.3 sq. km. The catch from that station was 52.5 tones of 24-32 cm in length. In region Nos. 6 and 7 the herring were dispersed (echo-records) and catches were not more than 90 kg per hour.

Size composition of herring varies insignificantly in the different areas. The 25-28 cm length group predominate: 62.4 - 94.3% of total numbers in the regions which average 85.2% over all. The modal length class is 27 cm: 28.3-53.7% which average 52.1% (Table 2). The average length of herring varies insignificantly from 26.2 to 26.8 cm with mean 26.7 cm. The Gizhiginsky- Kamchatkan herring are longer, 35 cm versus 33 cm for Okhotsk herring. The portion of fish greater than 28 cm is 18.3% in the Shelikhov Bay and 11.8% in the Tauisky region. The proportion of small herring in the Shelikhov Bay is more than in the Tauisky region: 13.4 % versus 0.4% for fish length less than 24 cm. The feeding grounds for fingerlings and maturing Okhotsk herring is in the Ayan-Shantar area and Sakhalin Bay.

Herring fingerlings were also caught in trawls in Gizhiginsk Inlet (up to 10.8 kg per hour) and at the coastal stations from Tolstoi Cape to Alevin Cape (single specimens). The length varies from 7.5-10 cm (some specimens reach 12 cm) with mean 8.74 cm (weight was 5.8 g) in large catches. In small catches the fingerlings vary from 5 to 7.3 cm. The low level of fingerlings in the Tauisky region may have been caused by commercial fishing which may have caused the biomass and numbers of herring fingerlings to be underestimated; 16.7 mln. for the Okhotsk stock and 0.2 mln. for Gizhiginsky-Kamchatkan. The herring biomass is calculated both by the areal method and from echo-records. Similar estimations have been obtained; approximately 1.9-2.0 mln. tons for Okhotsk and 0.27- 0.30 mln. tons for Gizhiginsky-Kamchatkan.

Based on the estimates of mature Okhotsk herring biomass, it is recommended that the quota could be increased during the herring feeding period because in early October, in the area of dense echo-records (55.2 thousand sq. km), a biomass of 715 thousand tons was estimated which would allow a fishery of 200 thousand tons without damage to the stock. A part of the herring stock is dispersed and another part is outside the range of the survey in a third (Okhotsk-Lisyansk) region serving as a "reserve". Based on the Okhotsk herring maturing by 5 years old, the age composition of the catch (Table 3) shows the spawning stock of about 1.5 mln. tons.

Herring spawning usually occurs in the coastal bays and inlets. The spawning success sharply decreases with a high density of spawners as was evidenced by the low hatching rate of larvae at high spawning density. Tyurnin (1980), concludes that a stock over 1 mln. tons requires more extensive use of available resources.

Based on data available, the recommended catch, in 1994, was increased to 120 th. tons for the Okhotsk herring stock. However, in the late October, due to the low levels of catch, an unrestricted (including trawling) fishery for herring was permitted by the "Glavrybvod" (Department of fish stocks conservation of Russian Ministry of Fisheries). Unfortunately, the weather over the North Sea of Okhotsk is extremely bad in December which prevented fishing.

Forecasting the Okhotsk herring catches for 1995 and subsequent years is under discussion due to data from air flights on herring spawning grounds which was not provided in a timely manner. The estimated spawning biomass of herring in the late spring early summer of 1994 is 700 thousand tons which implies a low level of stock exploitation (10% level). About 70% of the mature herring abundance is from the 1988 yearclass which spawned for the first time in 1994. From marine survey data (Table 1) the 1989 yearclass will spawn at age 6+ in 1995 and their portion was 61.5% in the fall of 1994 with biomass of 980-1030 th. tons. The biomass of the 1988 yearclass (28.4% of the abundance) is estimated at 530-560 th. tons. Thus, a large part of the spawning stock of the Okhotsk herring is not accounted for on the spawning grounds in 1994.

High density of Okhotsk herring during the feeding and hibernation periods is determined by the appearance of two abundant cohorts that are smaller in length and weight at age than other year-classes. The average length of the herring spawners at the ages of 5+, 6+ and 7+ are 266, 277 and 287 mm respectively (Yolkin 1988). Samples of herring going to hibernate in the winter at five, six and seven are 254, 264 and 273 mm long, respectively. The fork length of 8+ herring, on the average, is 306 mm, close to the long-term average of 303 mm. A small numbers of fish 8+ could imply an increase in the rates of natural mortality of elder age groups due to density dependent factors. Similarly, a reduction in fecundity of Okhotsk herring (average number of eggs spawned by one female) might also be caused by density dependent factors (personal communication R.K. Farkhutdinov).

Another indication of the considerable growth of herring is the massive occurrence of adults in late October in the vicinity of the TINRO Basin and Kashevarov Bank. Yolkin (1988) observed that herring migrate to the North Sea of Okhotsk shelf by the middle of September. The expansion of populations of herring causes an expansion of the inhabited area boundaries for the period of high abundance (Timofeyev-Resovsky et al., 1973). The resources (space, food) of neighboring habitat (including open ocean) which are chiefly used by walleye pollock in 1980s, are an immediate reserve. In the most cases, an expansion of herring towards open waters occurs at the expense of feeding migrations of mature fish (Blaber 1991).

Detailed discussions of results obtained from a cruise in 1993-1994 allows the doubling of the Okhotsk herring catch for 1996 to 120 th. tons. One can understand the reasons for caution when reminded of the sharp reduction of the Okhotsk herring abundance in the second half of 1970s which is thought to be caused by over harvesting and non-registered catches from the driftnet fishery. At the same time, recent studies show that a natural decline of herring abundance caused by global climate change and oceanic conditions occurs during the same period (Shuntov, 1991; Radchenko, 1994). The increase in Okhotsk herring abundance, in the early 1990s, appears to have been the result of a shift in conditions from what is expected in the long-term. It should also be considered that, unlike the usual gradual abundance increases, declines from high levels are usually abrupt. Evidently, it is determined by the sharp increase of natural mortality rates for productive generations after approaching of the limiting age.

The sustainable exploitation of marine biological resources provides for the removal of excess production. The actions should be even more promptly taken to remove surplus biomass which could cause the degradation of feeding and spawning conditions and density-dependent and intraspecific mechanisms leading to population productivity reductions, late maturation and low viability of embryos, larvae, etc. The Okhotsk herring quota should be increased for 1995. In 1996-1997 a change from a conservative approach of setting catch limits to a more pragmatic approach would annually allow a harvest of not less than 200 thousand tons of Okhotsk herring.

REFERENCES

Bakkala, R.G. 1993. Structure and historical changes in the groundfish complex of the eastern Bering Sea. U.S. Dep. Comm. NOAA Tech. Rep. NMFS. 114:91 p.

Blaber, N.J.M. 1991. Deep sea, estuarine and freshwater fishes: Life history strategies and ecological boundaries. Sth. Afr. J. Aquat. Sci. 17(1-2):2-11.

Collie, J.S., and P.D. Spencer. Modeling shifts in fish stock abundance in the eastern North Pacific. Abst. of PICES Second Ann. Meet. October, 25-30. 1993. Seattle, Washington, U.S.A. p. 5-6.

Gershanovich, D.E., A.A. Elizarov, and V.V. Sapozhnikov. 1990. Bioproductivity of ocean. Moscow: Agropromizdat. 237 p. (in Russian)

Naumenko, N.I., P.A. Balykin, E.A. Naumenko, and E.R. Shaginyan. 1990. Long-term changes in pelagic fish community in the western Bering Sea. Izv. TINRO. 111:49-57. (in Russian)

Radchenko, V.I. 1994. Composition, structure and dynamics of nektonic communities of the Bering Sea epipelagial. Masters thesis. 03.00.10. Vladivostok, TINRO. 24 p. (in Russian)

Schweigert, J.F., V. Haist, and C. Fort. Stock assessment for British Columbia herring in 1992 and forecasts of the potential catch in 1993. Abst. of PICES Second Ann. Meet. October, 25-30, 1993. Seattle, Washington, U.S.A. p. 52.

Shuntov, V.P. 1985. Biological resources of the Sea of Okhotsk. Moscow, Agropromizdat. 224 p. (in Russian)

Shuntov, V.P. 1986. State of studing of long-term cyclic changes of fish abundance of Far-Eastern seas. Biol. morya. 3:3-14. (in Russian)

Shuntov, V.P. 1991. Is global warming ruinous for the Bering Sea biological resources? Rybnoye Khoziaystvo. 9:27-30. (in Russian)

Shuntov, V.P., A.F. Volkov, O.S. Temnykh, and E.P. Dulepova. 1993. Pollock in the Far-Eastern seas ecosystems. Vladivostok, TINRO. 426 p. (in Russian)

Timofeyev-Resovsky, N.V., A.V. Yablokov, and N.V. Glotov. 1973. Essay of theory of population. Moscow, Nauka. 277 p. (in Russian)

Tyurnin, B.V. 1980. On causes of declining of Okhotsk herring stock and methods of it reconstruction. Biol. morya. 2:69-74. (in Russian)

Yolkin, E.Y. 1988. Guide on searching of the Okhotsk herring concentrations with application of 10-days charts of occurrence frequency of their schools. Vladivostok, TINRO. 65 p. (in Russian)

TABLES AND FIGURES

Table 1. Density of fish biomass distribution (metric tones per sq. km) and portions (%) of dominant species in diverse regions of the northern Sea of Okhotsk, 14.09-8.10.94.

Region	Depth (m)	Area (sq.km)	Fish biomass density	Portions of dominant species			
				pollock	herring	capelin	smoothtongue
1	up to 100	63.9	3.3	16.1	64.1	19.0	-
	100 - 200	32.1	15.2	85.5	8.0	6.0	-
	>200, layer 0-50	4.0	0.08	75.9	-	-	-
	>200, layer 100-50	4.0	0.4	90.9	-	9.1	-
2	100 - 200	43.7	42.8	26.6	73.0	0.02	-
	>200, layer 0-50	18.3	0.26	21.6	76.6	-	-
	>200, layer 280-50	18.3	40.8	99.8	0.1	-	-
5	>200,layer 0-50	160	1.8	4.1	12.8	-	75.7
	>200, layer 200-50	160	11.0	59.7	38.8	-	0.1
6	>200, layer 0-50	120	0.4	36.8	21.3	-	7.1
	>200, layer 280-50	120	6.7	60.8	0.2	-	36.4
7	up to 100	32.5	0.4	17.5	-	37.8	-
	100 - 200	9.7	2.3	15.9	4.3	11.7	-
	>200, layer 0-50	13.8	0.4	24.8	32.2	0.9	-
	>200, layer 280-50	13.8	6.0	81.4	0.9	0.1	-

Remarks: limits and numbers of regions are traditionally given in practice of ecosystem research of TINRO: 1 - Shelikhov Bay; 2 - Tauisky region; 5 - Kashevarov bank and adjacent shelf; 6 - TINRO Basin; 7 - West-Kamchatkan shelf and continental slope northwards of 54°N.

Table 2. Length composition (%) of herring catches in the northern Sea of Okhotsk in September-October of 1994.

Regions	Fork length (cm)																			Mean
	17	18	19	20	21	22	23	24	25	26	27	28	29	30	31	32	33	34	N	length
1	-	-	+	0.9	4.3	3.3	4.8	6.0	20.6	28.3	13.5	5.1	2.5	2.7	3.6	1.2	1.5	1.7	16406	26.6
2	0.4	-	+	+	+	+	0.5	3.5	23.4	40.5	22.4	4.9	3.1	0.9	0.4	-	-	-	268590	26.6
5	-	-	-	-	-	-	+	2.0	22.3	51.9	20.3	3.0	0.5	+	+	+	-	-	25203	26.5
6	-	-	-	-	-	-	-	1.7	24.4	48.7	20.7	3.1	0.9	0.5	-	-	-	-	1059	26.6
7	-	-	-	-	-	-	0.1	7.0	39.9	37.3	12.8	2.1	0.6	0.1	0.1	-	-	-	1689	26.2
All:	0.4	-	+	0.1	0.2	0.2	0.7	3.6	23.2	40.7	21.7	4.7	2.8	0.9	0.5	0.1	0.1	0.1	312947	26.6

Table 3. Age composition of herring (%) in diverse regions of the Sea of Okhotsk.

Regions	Age							N
	2+	3+	4+	5+	6+	7+	8+	
1	-	1.0	22.2	49.9	17.9	7.6	1.4	16129
2	+	0.1	5.2	61.0	29.6	3.8	0.3	266255
5	-	-	3.1	74.4	22.5	-	-	24554
6+7	-	-	3.5	67.4	24.8	4.3	-	2738
All regions	+	0.2	5.9	61.5	28.4	3.7	0.3	309676

Distribution of the Barnacle *Balanus Rostratus Eurostratus* Near the Coasts of Primorye (Sea of Japan)

Alla V. SILINA and Ida I. OVSYANNIKOVA

Institute of Marine Biology
Far-East Branch of Russian Academy of Sciences, Vladivostok 690041, Russia

INTRODUCTION

Balanus rostratus eurostratus Bronch occurs subtidally near the Sakhalin coasts of the Sea of Japan not farther north than 50°N and near the Japanese coasts (Tarasov and Zevina, 1957). This species is long-lived and one of the largest barnacles. It can form a large biomass on a small base. It inhabits stones, boulders, rocks as well as the shells of mollusks including commercially important species (Ovsyannikova, 1989; Silina and Ovsyannikova, 1995). This species is often found to foul the water intakes of hydro-technical construction (Gorin, 1975; Brykov et al., 1980), but it never settles in a ship bilge (Tarasov and Zevina, 1957). Barnacle larvae are generally food for fish and adult individuals for invertebrates and birds. The data on the biology and distribution of *B. rostratus eurostratus* are extremely scanty and fragmentary.

The purpose of this study was to analyze the data (about 90% of total), including data from the literature, on the distribution of the species near the coasts of Primorye on the substrate (bottom and hydro-technical construction), attached to organisms and to the mobile Japanese scallop *Mizuhopecten yessoensis* to study the occurrence of species in terms of the time spent in an area with increasing anthropogenic pollution.

MATERIAL AND METHODS

The study of the distribution of the *B. rostratus eurostratus* was conducted from 1973 to 1995 near the south coast of Primorye (from the west coast of Possjet Bay and Furugelm Island to Nakhodka Bay) and northeast of Povorotny Cape to Vladimir Bay. Barnacles were sampled by scuba divers at a depth of 0-40 m (most often at 0-20 m).

Measurements of the carinorostrum diameter of the shell base and the shell height by the carina plate for adult individuals were done using a slide gage. Juveniles were measured under a binocular microscope. The weight of concretions (druses) and individuals were determined.

RESULTS

In the northwest part of the Sea of Japan, *B. rostratus eurostratus* is found only in Peter the Great Bay (Table 1). North of Povorotny Cape, recognized as a boundary between the north and west Japan Sea districts of the Manchuria biogeographic province, is devoid of this species (Table 2). Similarly, the species is not found west of Povorotny Cape in the open part of Peter the Great Bay where there are strong currents and a small amount of organic detritus on the bottom(Table 2). The barnacle is not found to foul vessels. *B. rostratus eurostratus* most often occurs in protected and semi-

protected bays, near capes of bays or near islands where currents or wave action is significant. It was found that the barnacle attaches to the grotto walls or in the shade of large boulders and rocks.

B. rostratus eurostratus is generally found in concretions consisting of several barnacle generations along with the mussel *Crenomytilus grayanus*, and *Modiolus kurilensis*. The oyster *Crassostria gigas* inhabiting Possjet, Amur, and Ussuri bays also occurs in the concretions. Such concretions are generally attached to boulders, rocks and at the base of stones and mollusc shells on muddy and sandy bottom. A concretion found in Vostok Bay of *B. rostratus eurostratus* weight 1,232 g. The concretions with mussels and oysters found in the vicinity of Peschany Cape in Amur Bay are 75 cm in diameter and weigh about 5 kg. In addition to natural substrates, B. *rostratus eurostratus* colonizes objects, such as buoys, barrels, anchor chains, piers, rubber, glass and on cultured mollusk shells. The barnacle usually appears on buoys in the first month of life. In Possjet Bay, B. *rostratus eurostratus* together with other organisms form a biomass fouling hydro-technical constructions . For instance in Vityaz Bay up to 65 kg per meter of which 21 kg is B. *rostratus eurostratus* are found fouling anchor chains. The mass of single individuals did not generally exceed 85 g. The shell base is no more than 65 g and the carina height did not exceed 65 mm.

The greatest biomass of *B. rostratus eurostratus* occurs in areas where domestic and industrial sewage is discharged, i.e., in areas with high organic material. Significant changes in the timing of settlement is observed in these areas. In Amur Bay, near the city of Vladivostok, with a million population, pollution is increasing and substantial changes have occurred to *B. rostratus eurostratus* and to the Japanese scallop. In 1982, only few individuals of *B. rostratus eurostratus* are encountered, whereas, by 1987 this species is dominant, having a biomass of up to 550 g and up to 180 specimens per scallop shell. After flourishing since 1990, *B. rostratus eurostratus* has declined. It should be noted that in the more open parts of Amur and Possjet bays, there is a gradual tendency for the bottom to become increasingly muddy. Under these conditions there is an increase in occurrence of B. *rostratus eurostratus* settling on Japanese scallop. On muddy bottom, the shell changed to lily-shaped and it grows higher and sometimes its carina reaches a height of 76 mm and the shell base is 48 mm.

DISCUSSION

This study confirms the presence of a boundary where there is a noticeable change of species composition in the area of Povorotny Cape. These findings do not agree with the suggestions made for bryozoans (Kubanin, 1981) and polychaetes (Bagaveeva, 1988) that the boundary lies farther north in the area of Sokolovskay Bay. North of Povorotny Cape the influence of the cold Primorskoe Current (from the northern part of the Sea of Japan) on the presents of the species is considerable. In the innermost parts of unprotected bays, the water temperature increases to over 17-18°C for a short time to allow spawning of B. *rostratus eurostratus* to take place (Korn, 1985). Evidently, the need for a fairly high temperature, for reproduction, prevents it from existing farther north.

B. rostratus eurostratus forms large concretions on its own, on bivalve mollusks and on barnacles and serves to provide a refuge for other organisms. Seaweeds, bryozoans, hydroids, sea anemones, juvenile mollusks, other barnacle species and tubeworms attach themselves to the concretions. Between the "branches" of the concretions, polychaetes, various crustaceans, and nemertini are found. This increases the bioproductivity of polluted areas and enhances food for fish species. Barnacles and bivalves, being sestono-feeders favor clean water. At the same time, these aggregations can cause problems for mariculture installations and hydro-technical construction.

REFERENCES

Bagaveeva, E.V. 1988. Polychaetes of fouling of ships plying coasts in the northwestern part of the Sea of Japan. Sov. J. Mar. Biol. 14(3):143-147.

Brykov, V.A., V.S. Levin, I.I. Ovsynnikova, and N.I. Selin. 1980. Vertical distribution of mass species of fouling organisms on the anchor chain of the buoy in Vityaz Bay. Sov. J. Mar. Biol., 6(6):321-328.

Gorin, A.N. 1975. Fouling of hydro-technical installations of ports of the northwestern part of the Sea of Jaspan. *In* Fouling in the seas of Japan and Okhotsk. Vladivostok. p. 14-20. (in Russian)

Korn, O.M. 1985. The reproductive cycle of the barnacle Balanus rostratus in Peter the Great Bay, Sea of Japan. Sov. J. Mar. Biol. 11(3):144-152.

Kubanin, A.A. 1981. Species composition of sea bryozoans in fouling. *In* Fouling and bio-corrosion in water environment. Moscow. p. 18-39. (in Russian)

Ovsyannikova, I.I. 1989. Distribution of barnacles in shells of Yezo scallop grown in suspended culture. Sov. J. Mar. Biol. 15(4):288-292.

Silina, A.V., and I.I. Ovsyannikova. 1995. Long-term changes in a community of Japanese scallop and its epibionts in the polluted area of Amurskii Bay, Sea of Japan. Russian J. Mar. Biol. 21(1):54-60.

Tarasov, N.I., and G.B. Zevina. 1957. Barnacles of the seas of the USSR. Acad. Nauk SSSR, Moscow-Leningrad. 6(1):267 p. (in Russian)

TABLES

Table 1. Habitat of the barnacle *Balanus rostratus eurostratus* near the coasts of Primorye in the northwestern part of the Sea of Japan.

Areas	Biotope	Depth, m	Years of investigation
Possjet Bay			
Expeditziya Bight	M	6	1993
Novgorodskaya Bight	H	1	1970
Reid Pallada Bight	B,S	2-6	1962,1990-1992
Vityaz Bight	H,M,Sh	2-20	1974-1985
Amur Bay			
innermost part	O	1	1986
Screbtsova Island	B,M,O	4-8	1981
middle part			
western cost	B,M,S,Sh	4-15	1990-1995
eastern cost	S,H,Sh	1-6	1982-1995
open part	B	1-20	1973-1975
Slavyanski Bay			
Severnaya Bight	C,S	0-15	1985
Russki Islans	S	4	1994
Popova Island	B,S,C	6-15	1973-1995
Rejneke Island	B,S,M	4-8	1973-1994
Ussuri Bay			
Lazurnaya Bight	H,B,M,O	2-10	1974-1995
Tikhaya Bigh	B	1-2	1978
Vostok Bay	B,M	1-2	1973-1993
Nakhodka Bay	H	0-6	1970

B - stones, boulders, rocks; S - scallops; M - mussels; O - oysters; Sh - shells of other molluscs; H - hydrotechnical constractions; (piers, bouys, chains); C - maricultural cages.

Table 2. Areas in the northwestern Sea of Japan where *Balanus rostratus eurostrats* was not found.

Areas	Biotope	Depth, m	Years of investigation
Possjey Bay			
Furugelm Island	B,S,Sh,M	0-18	1973-1995
Gamov Cape	B,Sh	0-40	1979
Vityaz Bight	B,S	20-30	1979-1980
Alekseev Bihgt	B,S,Sh	10-17	1979-1980
Amur Bay			
Zolotoi Rog Bight	H	1-3	1970
Antipenko Island	B,S,Sh	6-15	1987-1990
Sibirtzeva Island	B,S,Sh	1-12	1987
Bolshoi Pelis Island	B,S,Sh	1-12	1987-1995
Stenina Island	B,S,Sh	6-18	1980
Anna Bay	S	4-12	1988-1992
Rifovaya Bay	B,S,Sh	0-10	1990-1992
Northward of Povorotny Cape			
Kaplunova Bay	B,S,Sh	1-15	1990
Usprniya Bay	B,S,Sh	0-22	1990
Olga Bay	B,S,Sh	0-20	1980
Vladimira Bay			
Severnaya Bight	B,S,Sh,C	1-16	1987-1990
Srednyaya Bight	B,S,Sh	0-12	1988-1990

B - stones, boulders, rocks; S - scallops; Sh - shells of other molluscs;
H - hydro-technical construction; (piers, bouys, chains); C - maricultural cages.

Dependence of Urchin *Strongylocentrotus Intermedius* Reproduction on Water Temperature

Galina I. VICTOROVSKAYA

Pacific Research Fishery Centre (TINRO)
4 Shevchenko Alley, Vladivostok, 690600 Russia

The sexual development and growth rate of urchins is, in many respects, determined by their environment and ecological factors. Temperature plays one of the most important roles in the complex of ecological factors regulating sexual activity of invertebrates (Korringa,1957; Milyakovsky, 1970; Kaufman, 1976; Wilson and Simons, 1985; Maru, 1985; Kasyanov, 1991; Hotimchenko, 1993). Reproduction responds to daily and seasonal temperature fluctuations and salinity is not considered as important (Mori, 1975; Yakovlev, 1976; Milyakovsky, 1981; Fretwel, 1987; Motavkine et al., 1990).

The purpose of work was to study the influence of the temperature on the reproductive process of gray urchins *Strongylocentus intermedius* inhabiting the coast of north Primorya (from Cape Gold to Cape Belkina).

MATERIAL AND METHODS

The object of the research was to collect samples by diving for gray urchins in their habitat from Cape Gold to Cape Belkina. The reproductive process is studied throughout the spring-summer-autumn during 1992-1993. The influence of temperature on gonad development is investigated using histology examination to determine the stage of ripeness and to compare this to a gonad index. The samples are fixed using 10% neutral formalin, filling with melted paraffin and 5 microns slides are prepared for viewing by washing with hematoxilin Arlih and aozin.

RESULTS AND DISCUSSIONS

Research of gray urchins gametogenesis inhabiting the coast of north Primorye indicate that water temperature is an important influence on the reproductive process, especial, in the formation eggs.

Growth and development of gametes is influenced by two time periods: the autumn when temperature of the water decreases and the spring when the temperature increases. The most active growth of gametes is observed at low positive but constantly rising temperature. During the winter, the low negative temperature prevents duplication and the main mass of sexual cells is reabsorbed.

Active growth of sexual cells is observed when the water begins to increase at the end of April beginning of May from Cape Gold to Cape Belkina (Fig. 1). Temperature of water did not exceed 1.5-2.5°C and the gonadal index values are from 1% up to 7-10% where cells are observed in the early stages of growth, "active gametogenesis" and "before spawing". Spawing males and females first appear in the region at the beginning of June. With increases in the temperature of water, the growth of sexual cells becomes more active. The most intensive growth is observed when the temperature of

the water is 4-8°C which is observed at northern sites from the end of May to the end of June. In this period, spawning females appear from the end of June to the beginning of July. The percent of the ripeness increases to 20. Spawning of the urchins, from Cape Gold to Cape Belkin, are from mid-July to mid-August. The maximum temperature during reproduction is 12-16°C. After spawning the eggs that remain in the gonads are reabsorbed and a 1.5 month period "of relative rest" occurs in which gonad physiological reorganization took place. When temperature decreases in the second half of September a new reproductive cycle begins with active growth of gametes. In autumn, different stages of reproductive growth of gametes is observed where the gonad index is from 1-10% and the percentage with ripe gonads reaches 60. In December, the low water temperature (up to 0°C) slows development of sexual cells. Temperature of approximately 0°C is critical for development of the gametes of gray urchins.

The development of invertebrate gonads depends on the water temperature and in particular the variation of the temperature during development determines when spawning occurs (Kaufman, 1977; Uki and Kikuchi, 1984). The water temperature is summed over the active period of sexual cell development. In the first phase of gametogenesis (autumn - winter), the degree days are summarized in intervals of 14. In the second phase, in the spring - summer, development of takes place from 0°C to spawning temperatures. Temperatures lower than 0°C cause re-absorption of cells, thus, zero is the critical temperature for gamete development. In the first phase, development of sexual cells of grey urchin requires 600-650 degree days (Fig. 2). In the second phase the effective temperature in this region increases development up to 800-850 degree days. In general, the development of sexual cells takes about 1,400-1,450 degree days.

It is necessary to emphasize that the sum of the effective temperature for development of sexual cells is constant and annual fluctuations in the spawning season depends on the seasonal changes of the water temperature(Yakovlev, 1976; Kasyanov, 1991). On northern plots, the peak spawning of urchins is the end of July beginning of August. Growth of larvae and spat settling generally occurs at a temperature of 15 - 18°C (Agatsuma et al., 1989; Kasyanov et al., 1983). At northern sites, the time to heat the water to the required temperature for urchin development to the larval stage compresses the spawning season. The importance water temperature in the process of development of sexual products is seen by the fact that urchins inhabiting areas on shoals, where the seasonal temperature rise occur earlier than at greater depths, spawn earlier (Milyakovsky, 1981; Kasyanov, 1991).

The dependence of urchin reproduction on other ecological factor and the external environment is a problem for further research.

REFERENCES

Agutsuma, et al. 1989. Seasonal larval occurrence and season of two sea urchin, Strongylocentrotus intermedius and S. Nudus, in southern Hokkaido. Sci. Rep. Hokkaido Fish. Expl. Stn. 33:9-20.

Fretwel, S.D. 1987. Food chain dynamics: the central theory of ecology?. Oikos. 50(3):291-301.

Hotimchenko, Y.S. 1993. Biology of duplication and regulation gametogenesis and spawning urchins. Ì. a Science. 168 p. (in Russian)

Kasyanov, V.L. 1991. Communication of terms of duplication two-folding molluscs and urchins with dynamics abiotic factors of environment in a gulf east of the Japanese Sea. Biol. The seas. 37:102-105. (in Russian)

Kasyanov, V.L. et al. 1983. Larvals marine of bivalve mollusc and urchins Ì. a Science. 214 p. (in Russian)

Kaufman, Z.S. 1976. Dependence gametogenesis marine bottom invertebrates from temperature of water. Gen. Biology. 37(6):912-916. (in Russian)

Korringa, P. 1957. Water temperature and breeding throughout the geographical range of Ostrea edulis. Annee biol. 33(1):2-6.

Maru, K. 1985. Ecological studies on the seed production of scallop, Patinopecten yessoensis (Jay). Idict. Mariv. Hokk. 27:1-53.

Milyakovsky, S.A. 1970. Dependence of duplication and spawning marine shoals bottom invertebrates from temperature of water. Col. IO ÀS USSR. 88:113-148. (in Russian)

Milyakovsky, S.A. 1981. Ecologia of duplication marine bentos. Ì. a Science. 90 p. (in Russian)

Mori, K. 1975. Seasonal variations in physiological activity of scallops under culture in the coastal waters Sanriku District, Japan, and a physiological approach of possible cause of their mass mortaliti. Bull. Mar. Biol. St. Asamushi. 2:59-79.

Motavkine, P.A. et al. 1990. Regulation of duplication and bio-technology of reception of sexual crates at two-folding molluscs. Ì. a Science. 216 p. (in Russian)

Uki, N., and S. Kikuchi. 1984. Regulation of maturation and spawning of an abalone, Haliotis (Gaastropoda) by external enviromental factors. Aquaculture. 39(1-4):247-461.

Wilson, J.N., and Y. Simons. 1985. Gametogenesis and breeding of Ostrea edulis on the west coast of Ireland. Aquaculture. 46:307-321.

Yakovlev, S.N. 1976. Seasons of duplication marine urchins Strongy locentrotus nudus and S. Intermedius in a gulf east of the Japanese Sea. Biol. Rec. gulf East. Vladivostok: FESC ÀS USSR. 5:136-142. (in Russian)

FIGURES

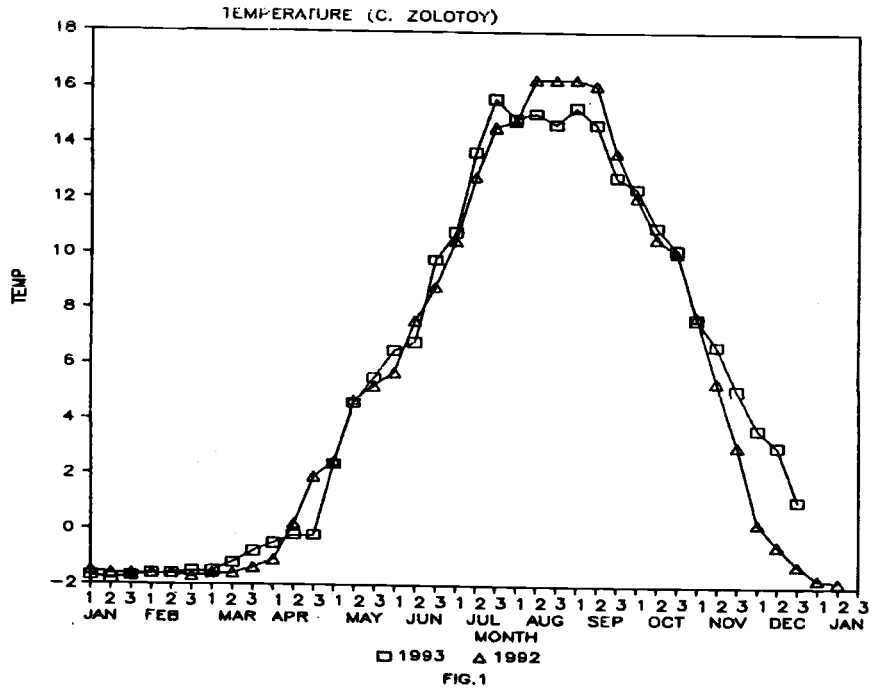

Fig. 1. Water temperature changes from Cape Gold to Cape Belkina.

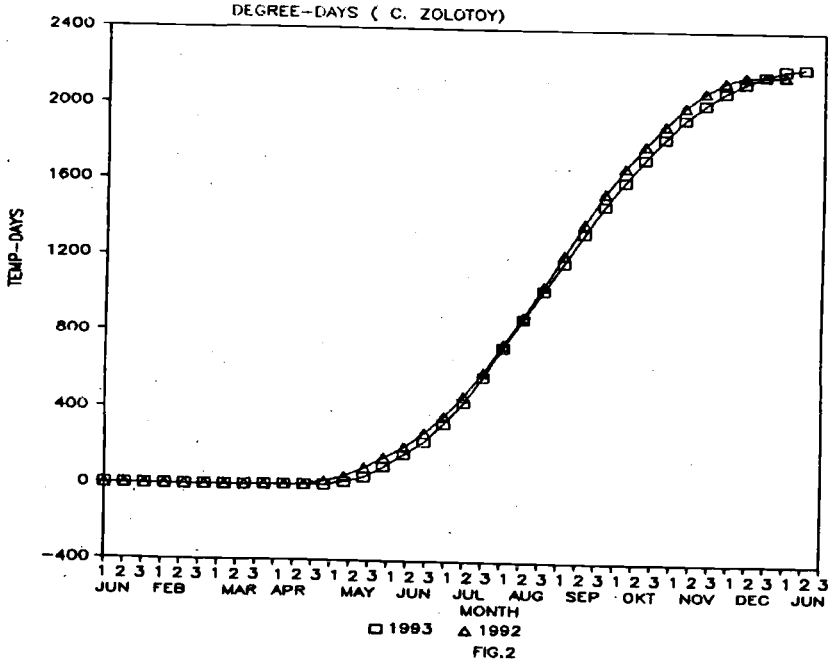

Fig. 2. Degree-days.

Feeding Habits of Pacific Salmon in the Sea of Okhotsk and in the Pacific Waters of the Kuril Islands in Summer 1993

Anatoly F. VOLKOV, Alexander Y. EFIMKIN, Valery I. CHUCHUKALO

Pacific Scientific Research Fisheries Centre (TINRO-centre)
4, Shevchenko Alley, Vladivostok, 690600, Russia

PINK SALMON

Pink salmon feeding in the Sea of Okhotsk was investigated. One-2 species predominate in the food of pink salmon (Synkova, 1951; Andrievskaya, 1957; Gorbatenko and Chuchukalo, 1989). Euphausiids are the predominated food item in the diet of pink except for West Kamchatka where hyperiids are the most important item eaten. Nekton proved to be a minor item and squid did not exceed 2% of the total food weight. Fish is also insignificant excepting near the Eastern Sakhalin, where it composed about 50% of the total weight of food eaten.

The Sea of Okhotsk plankton differ from Bering Sea and northwest Pacific by the high abundance of Euphausiids (Volkov, 1986; Shuntov et al., 1993). Feeding studies indicate that walleye pollock feed, mainly, on Euphausiids in the Sea of Okhotsk and copepods in Bering Sea. Similarly, the share of Euphausiids in the diet of salmon increases in the Okhotsk Sea, while the species composition of stomach content is simple. It is known, that many species of Euphausiids are unavailable to salmon because they descend to 100 m in the daytime and at twilight when most salmon are feeding (Volkov, 1994). In the summer of 1993, in the south Okhotsk Sea, common Euphausiids *Thysanoessa longipes* stay in patches of large mature specimen (from echo sounder tracings) in the epipelagic layer (0-50 m) during daytime. These crustacea, the most abundant among Euphausiids in the macroplankton are the main food of pink salmon.

In 1994, in almost all areas the stomach fullness of pink salmon was high. The species composition of food varies more in the Pacific waters of the Kuril Islands than in the Sea of Okhotsk. The nekton share in the diet is appreciably higher and Myctophids are the main item in the nekton, while squids are insignificant (up to 8%).

Euphausiids predominate in the diet near the Kuril Islands and *T.longipes* is the most numerous in the diet in the Okhotsk Sea but both *T.longipes* and *Euphausia pacifica* are abundant in the Pacific waters. The former in ocean ward areas and the latter in the waters adjacent to the Kuril Islands. A similar situation is observed in the plankton. The common hyperiids species *Parathemisto pacifica* is dominant in the food of salmon in all areas surveyed. The hyperiids are in the middle of the food group organisms but they are more common when stomach fullness was low. Fullness by hyperrids is higher (2.8-18.4%) among small fishes (40 -50 cm) and 3.0-7.6% for larger fish.

The proportion of pteropods in the diet of pink salmon is similar throughout the survey area. The highest share (14.4-33.7%) is observed over the deep water area where hyperiids are the most abundant in the plankton. Although the biomass of *Limacina helicina* is almost equal to *Clione limacina*, pink salmon prefer the former.

The Copepods *Calanus cristatus, C. plumchrus, Eucalanus bungii* and *Metridia pacifica* frequently occur but are insignificant in the stomachs, except for *C.cristatus* which is 2.4-10.8% of the stomach contents.

In general stomach fullness is lower in the ocean than in the Sea of Okhotsk.

CHUM SALMON

The composition and dominance of some species in the diet of chum are similar among all size groups (30-70 cm). Stomach fullness decreases with increasing body length. The nekton is a minor part of the food similar to pink salmon (Gorbatenko and Chuchukalo, 1989). Euphausiids *(T.longipes)* dominate in the diet of chum 59-78% and hyperiids constitute 15-30%. Pteropods, hyperiids and ctenophores are also present in increasing importance. *C. plumchrus* is significant among the copepods in the deep water zone.

In the Pacific waters of the Kuril Islands chum feeding is similar to the west Bering Sea and Pacific waters of Kamchatka. Pteropods such as *Clione* and *Limacina* are dominant in the diet and abundant in the plankton (6-13 and 5-12 mg/m^3 respectively) but the biomass is lower in most of Okhotsk Sea (0-6 mg/m^3). The pteropods in the chum's diet is an important part of the diet in summer of 1992 although it is lower than in 1993 (20-47%). Euphausiids (*T.longipes and E.pacifica*) and hyperiids (*P.pacifica*) are the second and third most abundant items in the plankton. Ctenophores (*Beroe cucumis*) sometimes exceed 50% of the stomach content wet weight. Jellyfish (mainly *Aglanta digitale*) also frequently occur but is insignificant in the total diet.

In general, the stomach fullness in the ocean is lower than in Okhotsk Sea.

We estimate the daily rate of chum and pink feeding using fullness, the share of empty and little filled stomaches and the fresh food in the stomach contents. Most pink had empty and half-empty stomaches from 00 to 7-8 a.m., when the least fullness is observed. The share of empty stomaches began to decrease after 9 a.m. The most fresh food occur from 1 p.m. to 00 o'clock. Chum salmon has a similar but lower daily rate of feeding. A classic daily rate of chum's feeding is established in the Bering Sea, where pteropods are the main food.

COHO AND CHINOOK SALMON

Data on the feeding behavior of these two species are sparse, so the average is calculated for south Okhotsk Sea and Pacific waters of the Kuril Islands. In 1993 the length of fishes range from 50 to 70 cm. Coho fed, mainly, on nekton (77-84%) but fish and squids are also found in fish from the Pacific Ocean and only fish in coho from the Okhotsk Sea. Euphausiids are also considerable (13-27%), while hyperiids and pteropods are scarce. Stomack fullness is high everywhere 146-181‰.

Chinook salmon stomaches often had little food or are empty. Nekton is the most common food item 67-70% (mainly fish) in the ocean and euphausiids, fish and squids are eaten in the Sea of Okhotsk.

It is interesting to note that small chinook (less than 30 cm) only fed on nekton in the Okhotsk Sea in the fall-winter period and no plankton is not found in their stomachs.

CONCLUSIONS

Owing to differences in the composition of plankton communities in the Okhotsk Sea and Pacific Ocean, some distinctive feeding behavior is observed in salmon. Species composition in the diet is similar for plankton but a diversity of other species dominate. During migration in summer (June-July) pink salmon actively feed on nekton (juveniles, small fishes and squids) and large

zooplankton (euphausiids, pteropods). Sometimes copepods are an appreciable (25-38%) amount of the food consumed. Euphausiids dominate in the pink diet in the Sea of Okhotsk, while the nekton is low. There is less euphausiids in the stomachs in Pacific waters of the Kuril Islands due to an increase of hyperiids and pteropods. Squids are insignificant in the total diet.

Chum feed, mainly, on euphausiids (*T.longipes*) in the Sea of Okhotsk and pteropods, hyperiids and nekton are a minor part of the food consumed (up to 25%). Pteropods, ctenophores and jelly-fishes dominate in the diet in Pacific waters, while euphausiids are a minor part of the food items.

Coho (50-70 cm) feed, mainly, on nekton (fish and squid). Chinook (50-70 cm) eat nekton (fishes) in Pacific waters of the Kuril Islands and euphausiids in the Sea of Okhotsk.

Copepods are a minor part of the salmon diet and the abundant chaethognaths are absent in the salmon diet.

REFERENCES

Andrievskaya, L.D. 1957. Summer migrations of the Pacific salmons and their feeding at the sea period of life. Izv. TINRO. 44:75-96.

Gorbatenko, K.M., and V.I. Chuchukalo. 1989. Feeding and daily rations of the Pacific salmons of Oncorhynchus genus in the Sea of Okhotsk at the summer-autumn period. Vopr. ikht. 29(3):456-464.

Shuntov, V.P., A.F. Volkov, O.S. Temnykh, and E.P. Dulepova. 1993. Walleye Pollock in Ecosystems of Far-Eastern Seas. TINRO, Vladivostok. 426 p.

Synkova, A.I. 1951. On feeding of the Pacific salmon in the Kamchatka waters. Izv. TINRO. 34:105-121.

Volkov, A.F. 1986. Nutritive base of the main commercial species of the Sea of Okhotsk in autumn, p.122-133. *In* Gadidae of the Far-Eastern seas. TINRO, Vladivostok.

Volkov, A.F. 1994. Features of Pink, Chum and Sockeye Salmon Feeding Habits during the Anadromous migration. Izv. TINRO. 116:128-136.

Okhotsk Sea Walleye Pollock Stock Status

Larisa M. ZVERKOVA, Georgy A. OKTYABRSKY

SakhNIRO, 196 Komsomolskaya st, Yuzhno - Sakhalinsk, 693016, Russia.

The stock status of the walleye pollock in the North Okhotsk Sea (to the north of 50°N) was analyzed using commercial fishery statistics and production models. Modelling of the catch enabled estimates of production parameters which were applied to concrete numerico-temporal conditions. The objective of this paper is to extend the previous study by Zverkova and Oktyabrsky (1994) using a longer time series and different assumptions. The time series and assumptions used in the previous study yielded an upper limit of the walleye pollock fishery stock at 7.4 mln. tons and the estimated maximum sustainable yield was 1.7 mln. tons for the optimum exploitation. The presented paper contains fewer limiting conditions than the previous one but still retains some model stability problems due to the short data time series.

MATERIAL AND METHODS

The walleye pollock found in the North Okhotsk Sea is relatively isolated and a single resource (Zverkova, 1993). The fishery has traditionally been conducted in the two regions. The first region is located in the eastern part of the sea and bounded by East Kamchatka and the North Kurils. The second region is located in the northwest part of the Okhotsk Sea and includes the area near Taui Inlet, Shelikhov's Bay and the highseas part of the Okhotsk sea, where largescale uncontrolled international fisheries are ongoing. Within the first region, fishing pressure has been a factor for approximately twenty years. The second region fishery, which began in 1981, developed into a large scale fishery by 1983. The fishery statistics used to run the model are summarized for the whole region starting from 1981. The cumulative walleye pollock catch for both the North Okhotsk Sea and the two fishery regions is shown in the Table 1.

The walleye fishery within the first region has always been more diversified than in the second region. The fleet fishing within the first region is by small, medium and large tonnage vessels and in the course of time the small vessels were replaced by more productive larger vessels as the medium tonnage fleet was updated. As these changes occurred, the walleye pollock resource became more available to the fishing fleet and catches were more representative of the effort expended. The medium tonnage fleet is used as a reference for the first region based on the significant impact they had on the total harvest. A hypothetical medium tonnage vessel is used to represent the fleet, ranging in characteristics from seiner-trawler to medium tonnage trawler. These vessel types proved to be the most productive in terms of walleye pollock harvesting and their unit effort is comparable with that of the large tonnage fleet. The walleye pollock fishery in the northern Okhotsk Sea has a seasonal cycle of catch and catch rates starting in November-December and finishing in April-May. The temporal distribution of catch per unit effort as corresponds to the efficiency of the fishery approximates a the convex function. However, due to the poor quality of the data and the need to consolidate it within one calendar year, it is assumed that the fishery efficiency is uniform during the fisheries season. For those years where we do not have annual data, average catch per unit effort is taken as the geometrical

mean for those months where data is available excluding the last month in the season. Fadeev and Smirnov, (1994) data from sources other than ours are used based on a uniform distribution.

The fishing effort that best describe efficiency of the reference medium tonnage vessel operation is catch per vessel day in the first region (Table 1). The standartization of the effort for a long time period would be a difficult task to solve, so it is assumed to be taken by the vessels of the seiner trawler and meduim tonnage trawler types.

The walleye pollock fishery in the second region is mainly by large refrigerator trawlers. Recently, the contribution of the medium tonnage fleet increased and has become dominant in the fishery. The catch of this fleet is more representative than the cumulative ones for the first region. The 1985-1992 time-series of the catch per unit effort for the second region is constructed based mainly on data taken from Programs ..., (1989). These data contain catch per unit effort obtained from the Russian large tonnage fleet in terms of tons per vessel day for the fishery. A hypothetical average vessel is developed combining the features of the large refrigerator and large autonomous freezer trawler types as a reference for the second region using vessel day as a unit of fishing effort.

Catch information from the high seas fishery is obtained partly from Li (1994). Since 1991, medium and large tonnage vessels have played a major role in the large-scale walleye pollock fishery. In 1991-1992, foreign vessels similar to the Russian large refrigerator trawlers and large autonomous refrigerator trawlers are used to calculate the averaged catch per unit effort. In 1994, due to the lack of data, the fishing efficiency in the high seas is assumed to be similar to that attained for the Russian large tonnage fleet in the second region. It is assumed that the whole catch was taken by the vessels of the reference type. Catch per unit effort by vessels of the reference type of vessel is shown in the Table 1.

Based on the assumptions for the walleye pollock fisheries in the two regions, a hypothetical fishing effort can be expressed as: $fi = Yi / Yf,i$ where i denotes the fishing regions. After summarizing the data for each region, the standartization is performed by the two methods:

$$\text{a) } Yf,st = Yf,1^{v1} \times Yf,2^{v2} \quad \text{and} \quad \text{b) } Yf,st = Yf,1^{1/2} \times Yf,2^{1/2}.$$

Where V1 and V2 are the mean values of the statistical weights for the fishing effort made by the reference vessels for the first and second regions, respectively. Expression "b" the geometrical means are given.

The aim of the study is to select a Production Model that would yield the best fit for the data series available. The models selected are Shaefer's model in linear $Yf = Yf(fe)$, and least square $Ye = Ye(f, f2)$, and $Ye = Ye(Yf, Y2f)$ versions and the generalised Fox model in two versions: $Yf = Yf(fn)$ and $Ye = Ye(f,fm)$. Estimated values are calculated using least square method, an approximation method by Kramer and the Shaefer method. The calculations are carried out using two software packages PROD (5) and ME202AUR (6).

The process of calculation and their results

The standardized values of fishery efforts: $f = Y / Yf$ are calculated based on the sum of catches for the two fishery regions and the standardized walleye pollock catches for the North Okhotsk Sea. Then the walleye pollock stock for the whole North Okhotsk Sea is calculated using the Production Models. Of the different modelling options the most acceptable results are obtained with $V1 = V2$ where catch per unit efforts and efforts are standardized according to version "b" above (Table 1) using the Shaefer Production model.

The input was the time-series 1981-1994 using the differential model versions:

$$Ye,t = Bt \times (1 - 0.1(6)Bt) \text{ mln T.}$$

Where Ye,t is the equilibrium catch; Bt the average biomass of the fishery portion of the walleye pollock stock for the year t; the maximum fishery biomass Bmax is taken as equal to 6 mln. tons, and instanteneous production increment rate (k) as 1 (year-1). Along with production parameters, the catchability q = 2.06*10-5 (vessel day {for the vessel of MLT type}-1) is calculated. Note that MLT means, a hypothetical vessel combining characteristics of both medium tonnage and large tonnage fleet on a 50-50 basis. An equation of equlibrium state or working model of Shaefer proper has the form:

$$Ye = 4.8 \text{ X } 104 \text{ Yf} - 389 \text{ Yf2.}$$

The equation yielded the following parameter values for the optimum exploitation: MSY (maximum sustainable yield) Yopt = 1.5 mln. tons, Yf, opt = 62 tons per vessel-day for MLT vessel type, fopt = 24 thousand vessel days for MLT vessel. Using q, we obtain the instanteous fishing mortality rate Fopt = 0.5 per year and the fish stock level Bopt= 3 mln tons.

The actual catch and that is obtained by the model and the theoretical mean values for the northern Okhotsk Sea walleye pollock stock for the period 1981-1994 are calculated by: Bi = Yi / Fi, where i represents a particular year (Fig. 1). Since 1984, actual catches exceed the sustainable yield and the stock has declined while catches for a number of years since have been near MSY with great deviations from it recorded in 1988 and 1990. The stock is underexploited for 11 years, according to Shaefer's model. In 1992, due to the international fisheries, the actual exploitation rate greatly exceeded MSY. The strength of the walleye pollock stock slightly exceeds the optimum level and that's why the pressure of the international fishery, exerted in 1992, left it at, the optimum level.

During the last two years the stock has remained at the optimum level and the harvest has been at the optimum exploitation. In view of this, it would be reasonable not to exceed the level of cumulative catch obtained by the nations fishing in the northern Okhotsk Sea so as not to overexploit the stock of walleye pollock and bring it below the optimum level.

REFERENCES

Fadeev, N.S., and A.V. Smirnov. 1994. Distribution, migration and the stock status of the northern Okhotsk Sea walleye pollock population. Scientific report, TINRO, Vladivostok. 10 p.

Kuznetsov, S., A. Khalileev, et al. 1989. MEZ0ZAUR - A system for time series analysis. M. CEMI with Academy of Science of Russia.

Li, Y. 1994. General stock status of the Okhotsk Sea walleye pollock. Report, Vladivostok TINRO. 40 p.

Programs for stock prediction, G.A. Oktyabrsky [ed.] 1989 A manual. Vladivostok TINRO. 80 p.

Zverkova, L. 1993. The study of the reproduction features and status of stock of the Okhotsk sea walleye pollock population. Scient. reports of Hokk. fish. exp. stat. 42:191-195.

Zverkova, L.M., and G.A. Oktyabrsky. 1994. Stock dynamics of the walleye pollock population inhabiting the norhhern Okhotsk Sea (to the north of 500) and fishery prospects. Published in collected volume Fishery studies in the Sakhalin-Kurile Islands Area, SakhNIRO. 110 p.

TABLES AND FIGURES

Table 1. Fishery data from walleye pollock harvested in the northern Okhotsk Sea.

Years	Ya	Yf,1,m	Yf,2,l	Yf^	fg	Y1	Y2
1981	583.1	78.2	75.1	76.6	7.61	481.5	101.6
1982	710.7	96.5	71.8	83.2	8.54	572.1	138.6
1983	811.7	117.1	80	96.8	8.39	704.4	107.3
1984	1391.1	99.9	84.7	92	15.12	935	456.1
1985	1437.1	96.6	84.6	90.4	15.90	975.4	461.7
1986	1439	87.7	97.6	92.5	15.55	693.2	745.8
1987	1514.6	81.5	86.5	84	18.04	786.1	728.5
1988	1241.1	81.6	90.2	85.8	14.47	646.4	594.7
1989	1375.7	62.8	84.9	73	18.84	691.2	684.5
1990	1263	67.5	86.2	76.3	16.56	446.6	816.4
1991	1514	69.3	73.6	71.4	21.20	573	941
1992	1964.9	59.1	75.1	66.6	29.50	760.2	1204.7
1993	1591.4	60.9	71.9	66.1	24.05	827	764.4
1994	1411.7	71.2	64.8	67.9	20.78	695.7	716

Where:

Ya - total annual catch: Y1 and Y2 total annual catch for each region in thousands of tons.

Yf,1,m - the catches per unit effort by the Russian medium tonnage fleet in Y1 and Yf,2,l, large tonnage fleet in Y2 in tons per vessel day.

Yf^ - mean geometrical catch per unit effort in tons per vessel day.

fg - cumulative fishing effort by hypothetically averaged vessel with mean geometrical unit effort expressed in thousands of vessel days.

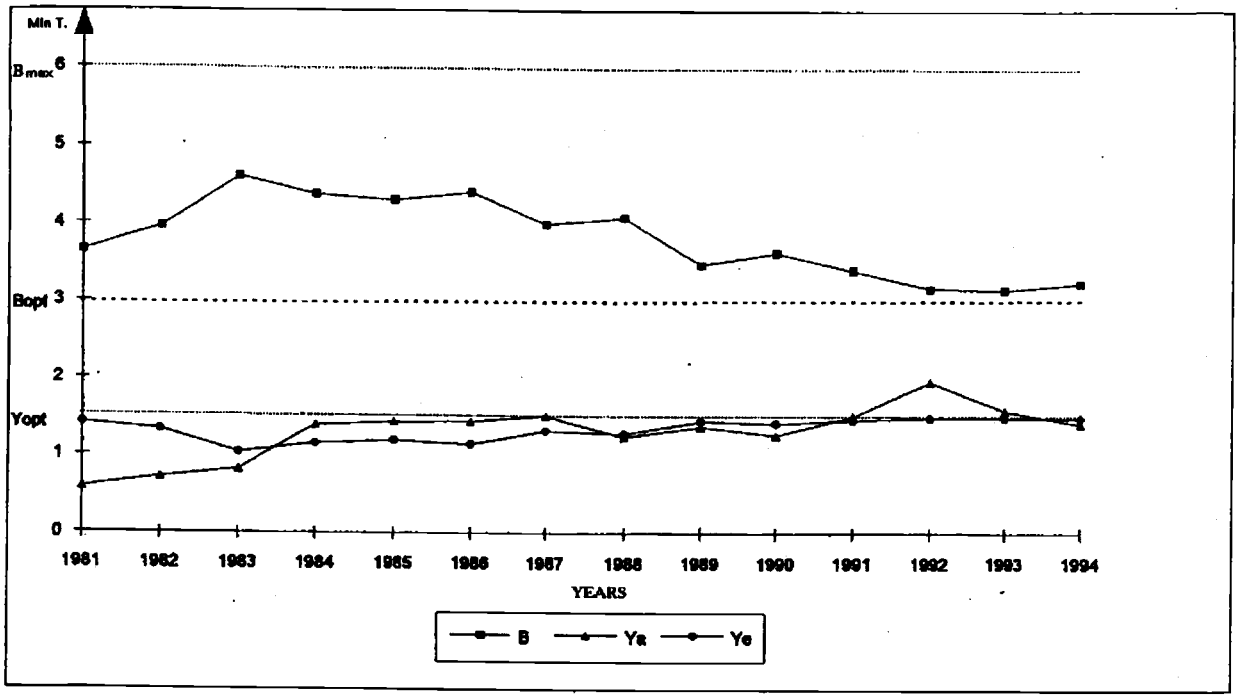

Fig. 1. Okhotsk Sea walleye pollock catches: Ya - cumulative catch for the northern Okhotsk Sea; Ye - equilibrium catch; B - biomass of the stock for 1981-1994 shown with respect to optimum catch levels (Y opt) and optimum stock (B opt); maximum stock biomass - B_{max}.

Water Soluble Polysaccharides of some Far-Eastern Seaweeds

Tatyana N. ZVYAGINTSEVA, Elena V. SUNDUKOVA, Natalia M. SHEVCHENKO and Ludmila A. ELYAKOVA

Pacific Institute of Bioorganic Chemistry
Far-Eastern Branch of the Academy of Sciences of Russia, Vladivostok, Russia

Seaweeds contain a large number of different polysaccharides that are of interest to mankind. These substances perform a broad spectrum of functions in seaweeds. They serve as energy resources, take part in the formation of cell walls, of outer capsules and in the internal matrix and cause selective cation absorption. The water extracts obtained from seaweeds and polysaccharides isolated from these extracts were shown to possess immunomodulatory and anti-tumor activities and to be able to bind some heavy metals, etc. (Colwell, 1985). These polysaccharides have enabled scientists to develop modern biotechnology tools and techniques (Reen, 1993). Although the results of many studies ascribe different physiological properties to these polysaccharides few can be found in the literature and few, if any, have ever reached commercial importance.

The abundant supply of algae and the large variety of their species make it possible to exploit the Russian Far-Eastern seas algae on an industrial scale. The main regions for commercial seaweed harvesting are the coasts of Primorye, Sakhalin Island and South Kurile Islands (Kizevetter et al., 1981).

Laminarans, fucoidans and alginic acids are the main polysaccharides of brown seaweeds. Their contents vary from 50 to 80% of alga dry weight. During seaweeds processing, these valuable water-soluble polysaccharides are waste despite the fact that they are widely used in the food industry and in medicine.

Term "laminaran" describes a group of the reserve, water-soluble 1→3; 1→6-β-D-glucans with low molecular mass isolated from seaweeds of Phaeophyta. Laminarans from different sources are well known to vary considerably in both content, and structure (Zvyagintseva et al., 1994). The study of 1, 3-β-D-glucanases and their substrates 1→3-β-D-glucans are explained by the direct participation of these substances in animals and plant immunity.

Fucoidans are the sulfated polysaccharides composed mainly of α-1→2 or α-1→3-linked L-fucose residues and they can also contain residues of galactose, mannose, xylose, and glucuronic acid. Fucoidans are nontoxic polyelectrolytes. They can be used like alginic acids for heavy metal binding or, like dextran sulfate for HIV infection treatment (McClure et al., 1992), etc.

The purpose of this study is to investigate the content and structure of laminaran and fucoidan collected from the most widely distributed Far-Eastern seaweeds: brown algae *Laminaria cichorioides, L.gurjanovae, L.digitata, L.japonica, Fucus evanescens*, and grass *Zostera*. Recently, a simple method for separation and isolation of 1→3; 1→6-β-D-glucans and fucoidans was developed in our laboratory. It allows the isolation of laminarans from very dilute solutions and to effectively separate them from fucoidan. A sample from dry powdered alga fronds is successively extracted with cold (t° ~20-25°C) and hot (t° ~70-80°C) water and the resultant extracts are separately subjected to hydrophobic chromatography. Structures of the laminarans and fucoidans isolated are studied using specific enzymes, and by means of gel-filtration, IR-, mass- and ^{13}C-n.m.r. spectroscopy, by

methylation analysis, and other standard methods of carbohydrate chemistry. The monosaccharide contents of these glycans are determined by means of carbohydrate analyzer after the complete acid hydrolysis.

The yield of polysaccharides from seaweeds appreciated concerning the dry weight of fatless frond (Table 1). The laminaran content varies from species to species and depends on the season. The greatest quantities accumulate in *Laminaria cichorioides* in the autumn.

The ^{13}C-n.m.r spectra of polysaccharide fractions provide evidence of the presence of 1→3; 1→6-β-D-glucans in almost all except for the hot extract fraction from *L.gurjanovae*, representing a linear 1→3-β-D-glucan (Table 2). The signal in the substituted C-1 (around 103.0 p.p.m.) and C-3 (85.0-87.0 p.p.m.) regions are complex for the majority of glucans and indicate their branched structures (Table 2).

All glucan fractions are treated with exo-(1→3)-β-D-glucanase from *Eulota maakii*. This enzyme produces D-glucose upon sequential hydrolysis of laminaran from the non-reducing end circumventing the β-(1→6)-linkages as they appear at the terminal end and attacks the adjacent β-(1→3)-linkages liberating gentiobiose. The molar ratio of gentiobiose to glucose estimated during enzymatic hydrolysis reflects the degree and localization of the glucan branching. Enzymatic hydrolysis products are analyzed by h.p.l.c. Besides the contents of 1,3-β- and 1,6-β-linked glucose residues are determined by methylation analysis and by ^{13}C-n.m.r. spectroscopy. The findings indicate that laminarans from the alga studied differ considerably in the ratio of 1, 3-β-linked glucose residues to 1, 6-β-ones (from 2:1 to 49:1) (Table 3).

The laminarans under study are also found to differ considerably in molecular mass reaching, in some cases, the value of about 50 kDa (Table 3, laminarans isolated from *Laminaria digitata* and *Zostera*).

All glucans under study are optically active and have negative rotation except for laminaran II from *Zostera* (Table 3). The water solution rotates in the polarization plane to the right but the solution in 0.05 M sodium hydroxide is optically inactive. This observation indicates that laminaran II from *Zostera* probably has an ordered triple-helical structure in neutral solutions.

So, neutral polysaccharides from the brown alga examined aree mainly 1→3; 1→6-β-D-glucans which differ considerably in the degree of branching, molecular-weight distribution, the value of specific rotation, the availability to enzymatic hydrolysis.

All seaweeds studied also contained a considerable quantities of fucoidan (Table 1). Fucoidans were the high sulfated heteropolysaccharides: IR-spectra showed characteristic absorption-peak at 842 cm^{-1}. Their molecular masses varies in a wide range. IR- and ^{13}C-n.m.r. spectra of fucoidans isolated from different sources differed including their monosaccharide compositions (Tables 1 and 4). One of the fucoidan fractions isolated from *Fucus evanescens* involved attention due to the following peculiarities: L-fucose content is diminished, but galactose content is raised; mannose is absent, but the presence of unidentified monosaccharide X was noted.

Brown alga *Laminaria cichorioides* seems to be a rich source of laminaran, and *Fucus evanescens* contained the greatest quantity of fucoidans differing in their structures.

REFERENCES

Colwell, R.R. 1985. Polysaccharides for pharmaceutical and microbiological applications, p.363-376. *In* R.R. Colwell, E.R. Pariser, A.J. Sinskey [ed.] Biotechnology of Marine Polysaccharides. Washington-N.-Y.-London: Hemisphere Publ. Corporation.

Kizevetter, I.V., M.V. Sukhoveeva, and W.P. Shmel'kova. 1981. Industrial Marine Algae And Grasses From Far-Eastern Seas. Moscow Legkaya and Pyshchevaya Promyshlennost. 113 p.

Liu, X., and Y. Zhang. 1992. Fractionation, purification and determination of the structure of fucoidin in *Laminaria japonica* aresch. Acta Biochim. Biophys. Sinica. 24:297-302. (in Chinese)

Mcclure, M.O., J.P. Moore, D.F. Blanc, et al. 1992. Investigations into the mechanism by which sulfated polysaccharides inhibit HIV-infection in vitro. AIDS Research & Human Retroviruses. 8:19-26.

Reen, D.W. 1993. Medical and biotechnological applications of marine macroalgae polysaccharides, p.181-196. *In* D.H. Attaway, O.R. Zaborsky [ed.] Marine Biotechnology. N.-Y.: Plenum Press. Vol. 1.

Zvyagintseva, T.N., N.I. Shirokova, and L.A. Elyakova. 1994. The structures of laminarans from some brown algae. Bioorgan. Khimiya. 20:349-1358. (in Russian).

TABLES

Table 1. The contents and some characteristics of glycans isolated from different sources.

Source, glycan		Yield, % of dry weight	Monosaccharide content, %
Laminaria	laminaran	10-12	Glc
cichorioides	fucoidan	15	Glc (5); Xyl (-); Gal (18.7); Fuc (64); Man (4); Rha (1.5); X* (1)
(Troitsa Bay, Sea of Japan)			
Laminaria	laminaran I	4.5	Glc
gurjanovae	laminaran II	0.5	Glc
(Academiya Bay,	fucoidan	19	n.d.
Sea of Okhotsk)			
Laminaria	laminaran I	0.32	Glc
digitata	laminaran II	0.45	Glc
(Sea of Okhotsk,	laminaran III	0.08	Glc
near Magadan)	laminaran IV	0.78	Glc
fucoidan		n.d.	n.d.
Laminaria	laminaran	1.0	Glc
japonica	fucoidan	12	Glc (2); Xyl (5); Gal (31); Fuc (55); Man (-); Rha (3)
(Troitsa Bay, Sea of Japan)			
Fucus evanescens	laminaran	3	Glc
(Sea of Okhotsk, Kraternaya Bay)			
	fucoidan I	24	Glc (3); Xyl (2); Gal (13.1); Fuc (62); Man (3); Rha (2); X (1)
	fucoidan II	0.5	Glc (5); Xyl (9); Gal (23); Fuc (42); Man (-); Rha (5); X (13)
Zostera	laminaran I	0.61	Glc
(Sea of Japan,	laminaran II	0.087	Glc
Troitsa Bay)			

Table 2. The chemical shifts of the carbon atoms in ^{13}C-N.M.R.-spectra of laminarans obtained from different sources.

Source,	fraction	β-linkage type	carbon atom C1	C2	C3	C4	C5	C6
Laminaria cichorioides	laminaran	1→3	103.0	73.8	85.1	68.8	76.6	61.4
		1→3,6	103.3	74.1	85.6	70.3	75.2	69.4
		mannitol						63.8
L. gurjanovae	laminaran I	1→3	103.0	73.8	85.1	68.8	76.3	61.4
		1→3,6			85.6	70.3		
		mannitol						63.8
L. gurjanovae	laminaran II	1→3	103.0	73.8	85.1	68.8	76.6	61.4
		1→3,6				70.3	75.2	
		mannitol						63.8
Fucus evanescens	laminaran	1→3	103.0	73.8	85.1	68.8	76.6	61.4
		1→3,6	103.3	74.1	85.6	70.3	75.2	
		1→6	103.3	74.1	76.2	70.3	75.6	69.4
		mannitol						63.8
Zostera	laminaran I	1→3	103.6	74.3	85.8	69.4	76.8	61.9
Zostera	laminaran II	1→3	103.6	74.4	85.8	69.4	76.6	62.1
					86.2			
		1→3,6	103.9	74.9	77.1			69.8
		mannitol						64.2

Table 3. Some characteristics of laminarans isolated from different sources.

Source, glycan		Molecular-weight distribution, kDa	Contents of 1→6-linked Glc, %	Value of specific rotation, °
Laminaria cichorioides	laminaran	3-6	10	-12
Laminaria gurjanovae	laminaran I	3-4.5	2	n.d.
	laminaran II	5-50	10	n.d.
Laminaria digitata	laminaran I	35.5-45	0	-146.5[1] (0.07)[2]
	laminaran II	35.5-50	10	-18.9[1] (0.54)
	laminaran III	22.5-40	6.5	-60.6 (0.12)
Laminaria japonica	laminaran	4-5	10	n.d.
Fucus evanescens	laminaran	5-9	35	-44.3 (0.07)
Zostera	laminaran I	5-8	6	-19.6 (0.09)
	laminaran II	4-50	0.1	-26.3 (0.08)

1 - the optical rotation of solution was measured in 0.05 M NaOH;
2 - the laminaran concentration, %.

Table 4. The chemical shifts of the carbon atoms in ^{13}C-N.M.R.-spectra of fucoidans obtained from different sources.

Laminaria cichorioides	*Laminaria japonica*		*Fucus evanescens*	
		[6]	I	II
16.5	16.7	18.14	16.8	16.5
16.8	17.2	18.32	17.1	
17.1	17.3	18.46		
17.3				
	28.0		22.0	
62.1				62.6
				62.1
	64.3			66.4
67.2	68.2		68.5	67.8
67.8				68.2
68.2				
				69.5
	70.9			70.6
71.5	71.1	71.06	71.1	71.6
		71.39		
	72.4	72.35	72.5	
74.4	74.1	73.82		73.1
		74.42		73.6
		74.65		73.9
		74.86		74.3
		75.89		
		75.97		
	77.2			76.8
				77.0
				77.7
				78.4
79.9	79.0		79.0	
			79.5	
	81.0		83.2	
		95.18	94.67	98.2
			96.4	
			98.0	
99.1	101.0	99.19	99.8	99.8
			100.5	
			101.1	101.8
			102.1	104.4

II. SCIENTIFIC PAPERS SUBMITTED FROM SESSIONS

3. Biodiversity Program

A. Biodiversity of island ecosystems and seasides of the North Pacific

Productivity of Japanese Scallop *Patinopecten Yessoensis* (IAY) Culture in Posieta Bay (Sea of Japan)

Larissa A. GAYKO

Institute of Marine Biology, Far East Branch, Russian Academy of Sciences
Vladivostok, 690041, Russia.

ABSTRACT

Data collected over 14 years from Posieta Bay are analyzed to determine the relationship between the hydrometeorology and hydrobiological characters of scallops. The annual development cycle of cultivated Japanese scallop *Patinopecten yessoensis* (Jay) is delineated. The average water and air temperature, points of temperature transition over 0°C, sums of "heat" and variability of temperature for each period and the duration of ice cover is evaluated to determine the statistical significant predictors to provide schemes for increasing production.

INTRODUCTION

Climatology is used to explore the productivity of sea farms, in particular, scallop farms of Primorye. The intensive development of sea farming in the Primorye in recent years has created conditions where it is becoming very important to determine the productivity of the farms.

To predict the long-term productivity of scallops, one must study the hydrology (water temperature, salinity, ice cover, water mass stratification, and wave activity), meteorology (air temperature, direction and speed of wind, precipitation, and sunshine) and solar activity (Wolf number) effects on Japanese scallop and on the method of cultivation. The major aim of this study was evaluate possible hydrometeorological predictors to forecast the long-term impact on sea farm scallop productivity in the South Primorye.

This study is the first stage of our research. Mori (1975) produced the first paper on this topic which was and followed by studies of other scientists (Belogrudov and Skokleneva, 1983; Belogrudov, 1986; Kucheryavenko, 1986; Gabayev, 1987).

MATERIAL AND METHODS

The area of the study was the Experimental Sea Base "Posieta" where bivalve mollusks have been cultivating since 1970. Hydrometeorological Station (HMS) "Posieta" observations are used from data that has been collected since 1931 (Fig. 1). All culture operations from the production of spat to commercial production are performed in natural conditions. From 1970-74 scallop spat is collected using shells and since 1975 a net consisting of an envelope and a filter is used. The net consists of 10 sacs attached one to another (Belogrudov, 1986). The timing of spat release is determined by the change in the gonadal index according to Ito et al. (1975). The sea surface water temperature, at Posieta HMS, was measured 4 times a day, air temperature 8 times a day, using standard procedures. The average daily temperature is used in the analysis. The duration of the ice

period is determined from the date of the first appearance of ice to the date of complete disappearance. The variability ratio is used to calculate water temperature as follows:

$$V = s * t^{-1} * 100\% \qquad (1)$$

The sum of "heat" for different periods of scallop development represents the sum of the daily averaged water temperatures throughout the period of observations.

RESULTS AND DISCUSSION

The analysis of data indicated that there are four annual development periods for cultivating scallops :

Period I - wintering(t_1);
Period II - a stable water temperature transition over 0°C to the beginning of spawning (t_2);
Period III - plankton development (t_3);
Period IV - beginning to full larvae settlement (t_4).

The duration of Period I (days) agrees with the ice period. Periods II, III and IV are calculated using the average daily water temperature, the provision of heat or "heat" sum and the coefficients of variation (Table 1). Correlation analysis indicates that scallop spat density is dependent on the following variables:

- duration of the ice period (t_1, days);
- duration of Period II;
- heat sum for Period II;
- variability of water temperature during spawning period (V, %).

The density is approximated by a linear regression (Table 2). Scallop spat density and ice period duration are the best correlates (inverse relationship) (Fig. 2). The medium and high values of spat density are recorded when spawning began but no earlier than the 19-22 June in 1976, 1977, 1979 and 1983. The negative effect of the water temperature variability during spawning on subsequent scallop spat density is due to the lack of the larvae's ability to adapt to sharp fluctuations. A rather stable water temperature (Period III) with V = 5.49% corresponds to the most productive year (1983). It is one third to two times as great as in other years (Table 1).

CONCLUSION

The data indicate that the duration of ice is the most significant hydrometeorological parameter. There is a linear dependency between the density of spat settlement and the following parameters: the period from stable water temperature transition over 0°C to the beginning of settlement, the stability of water temperature during spawning, and the sum of heat in the prespawning period. In the future these parameters will be use to project spat density.

REFERENCES

Belogrudov, E.A., and H.M. Skokleneva. 1983. Forecasting of the time of the collectors settlement and spat quantity of scallops, p.10-13. *In* V.G. Markovtsev [ed.] Mariculture in the Far-Eastern region. Vladivostok, TINRO. (in Russian)

Belogrudov, E.A., 1986. Cultivation, p.201-211. *In* P.A.Motavkin [ed.] Japanese scallop *Mizuhopecten yessoensis* (Jay). Institute of Marine Biology, Vladivostok, Far-East Science Centre, Academy of the USSR. (in Russian)

Gabaev, D.D. 1987b. Long-term forecast of spate of commercial species of bivalves setting on the collectors, p.99-100. *In* The 3 d All-Union Congress of Oceanologists, Abstracts, Ocean Biology Section, part 1. Leningrad, Arctic and Antarctic Research Institute. (in Russian)

Ito, S., H. Kanno, and K. Takahashi. 1975. Some problems on culture of the scallop in Mutsu bay. Bull. of the Mar. Biol. Stat. of asamushi. 15:89-100.

Kutcheryavenko, A.V., L.G. Makarova, N.N. Konovalova, G.V. Polycarpova. 1986. The state and prospects of mollusc culture in the Bay of Minonosok (the Gulf of Posjet), p.57-64. *In* V.G. Markovtsev [ed.] Mariculture in the Far-Eastern region. Vladivostok, TINRO. (in Russian)

Milekovsky, S.A. 1973. Speed of active movement of pelagic larvae of marine bottom invertebrates and their ability to regulate their vertical position. Mar. Biol. 23:11-17.

Mori, K. 1975. Seasonal variation in physiological activity of scallops under culture in the coastal waters, of Sanriku district, Japan, and a physiological approach of a possible cause of their mass mortaliky. Bull. of the Mar. Biol. Stat. of Asamushi. 15:59-79.

TABLES AND FIGURES

Table 1. Temperature conditions in different periods of scallop larval development.

Year	0°C - beginning of spawning				Beginning of spawning-beginning of settling				Beginning of settling-full settling			
	t_2 days	t °C	St °C	V %	t_3 days	t °C	S t °C	V %	t_4 days	t °C	S t °C	V %
1	2	3	4	5	6	7	8	9	10	11	12	13
1975	51	6.1	341.1	62.7	39	15.4	598.6	14.6	41	19.8	813.4	11.6
1976	69	5.2	360.9	74.4	26	15.4	401.4	11.4	24	17.9	429.6	9.9
1977	57	6.0	341.4	64.4	26	14.0	364.0	8.3	39	18.4	716.0	21.4
1978	53	5.0	263.4	59.5	31	13.5	418.5	9.4	29	19.0	550.1	9.9
1979	58	5.8	337.5	60.5	29	15.4	446.6	12.3	33	19.5	643.5	7.3
1980	55	5.1	278.8	62.5	29	14.8	430.3	13.8	27	18.7	504.1	7.7
1981	47	4.7	221.8	69.7	33	12.3	406.5	15.0	32	16.3	521.0	10.4
1982	61	5.3	323.3	69.2	29	13.1	379.9	16.3	32	19.7	628.8	9.2
1983	62	6.2	368.9	57.4	29	13.2	383.1	5.5	27	15.3	413.0	15.0
1984	42	5.5	229.3	65.7	24	13.8	331.4	12.7	34	19.2	652.8	9.2

Table 2. Parameters of linear regression.

No	Type of regression	a	b	R
1	2	3	4	5
1	r - duration of ice period (t_1, days)	5492.6	- 35.24	- 0.8182
2	r - duration of period from 0°C until spawning (t_2 ,days)	-781.24	20.82	0.565
3	r - sum of water temperatures from 0°C until spawning (°C)	-712.1	3.527	0.672
4	r - variability of water temperature during spawning (V,%)	1132.4	- 66.61	- 0.726

Note: The regression is of a type: $R = a + bx$, where r - scallop spat density, individuals/m^2, x - variables (factors), a and b - constants, R - correlation coefficient.

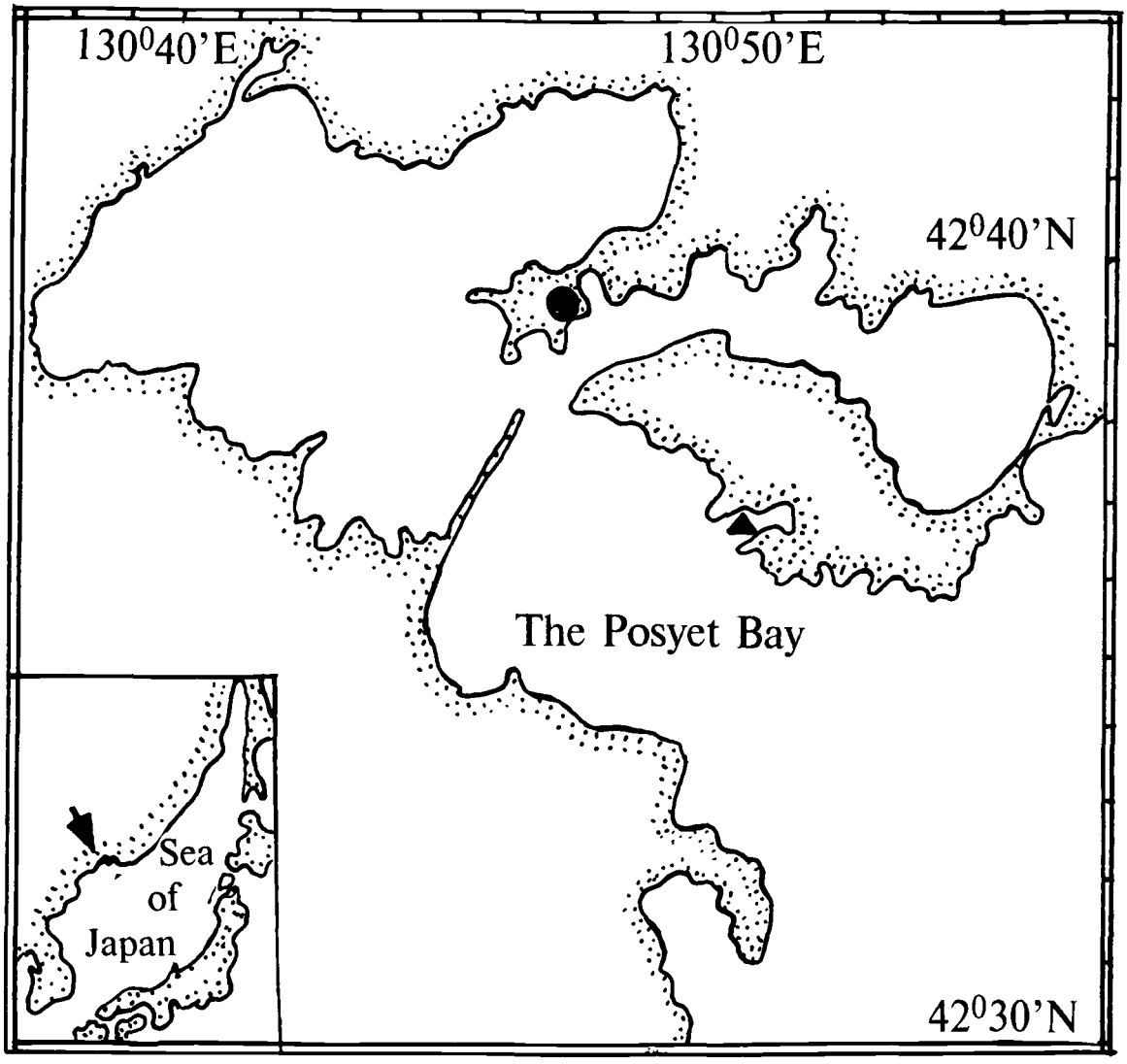

Fig. 1. The Posieta Bay.
● - position of Posieta Meteorological Station,
▲ - position of Experimental Mariculture Station.

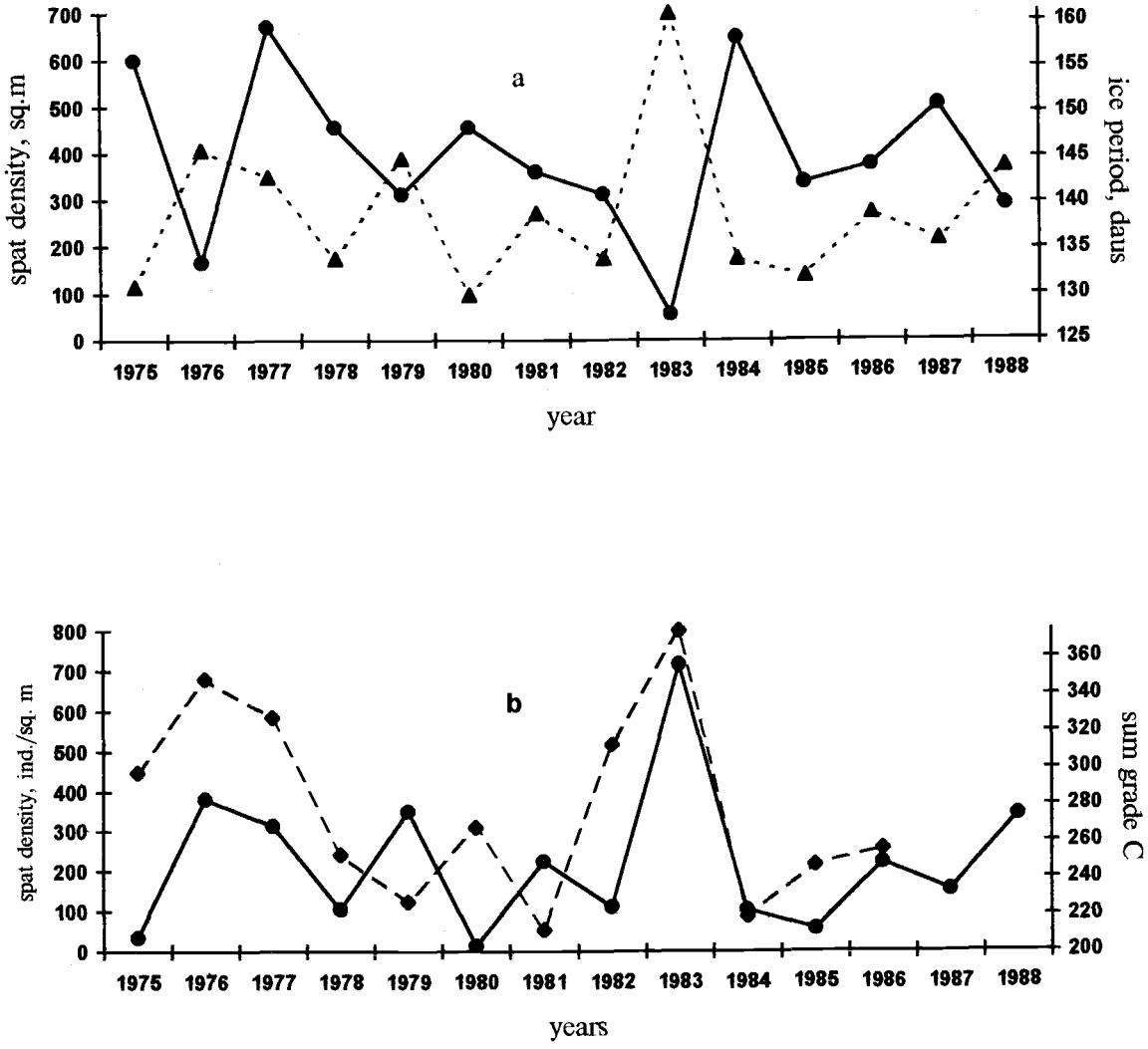

Fig. 2. Year-to-year dynamics of scallop spat density (ρ, individ/m^2) and hydrometeorological parameters in Posieta Bay:

a) ● - ρ, (1), ▲ - τ_1, duration of ice period, days (2),

b) ● - ρ, (1), ◆ - Σ, sum of "heat" from the date of water temperature rise over 0°C to the beginning of spawning, °C (2).

III. Appendices

1. List of Acronyms

ADCP	Acoustic Doppler Current Profiler
ALACE	Autonomous Lagrangian Circulation Explorer (float)
BIO	Biological Oceanography Committee
CCCC	Climate Change and Carrying Capacity
CREAMS	Circulation Research of the East Asian Marginal Seas
CTD	Conductivity, Temperature, Depth profiler
FEB RAS	Far East Branch of Academy of Sciences
FERHRI	Far East Hydrometeorological Research Institute
FIS	Fisheries Science Committee
ITSU	International Coordination Group for the Tsunami Warning System in the Pacific
IUGG	International Union of Geodesy and Geophysics
JEBAR	Joint Effect of the Baroclinicity and Bottom Relief
JFA	Japan Fisheries Agency
PICES	North Pacific Marine Science Organization
POC	Physical Oceanography and Climate Committee
POI	Pacific Oceanological Institute
RAFOS	Listening float (SOFAR spelled backwards)
Sakhalin NIRO	Sakhalin Research Institute of Fisheries and Oceanography
TCODE	Technical Committee on Data Exchange
TINRO	Pacific Research Institute of Fisheries and Oceanography

2. List of Participants

1.	Ablaev, A.G.	POI	Vladivostok
2.	Anikiev, V.V.	IO RAN	Moscow
3.	Aota, M.	Hokkaido University	Japan
4.	Azbukina, Z.M.	IBP	Vladivostok
5.	Bakunina, I.Y.	PIBOC	Vladivostok
6.	Barkalov, V.Y.	IBP	Vladivostok
7.	Bashmatchnikov, I.L.	St. Petersburg State Univ.	St. Petersburg
8.	Beamish, R.J.	Pacific Biological Station	Canada
9.	Belyaev ,V.A.	TINRO	Vladivostok
10.	Belan, T.A.	FERHRI	Vladivostok
11.	Bocharnikov, V.N.	PIG	Vladivostok
12.	Bocharov, L.N	TINRO	Vladivostok
13.	Bogdanov, K.T	SOI	Moscow
14.	Bruney, J.	Exxon Ventures	U.S.A.
15.	Biryukova, I.V.	TINRO	Vladivostok
16.	Bregman, Y.E.	TINRO	Vladivostok
17.	Brownell, R.L.	Southwest Fish. Science Center	U.S.A.
18.	Bulatov, N.V	TINRO	Vladivostok
19.	Bulanov, V.A.	Inst. of Marine Tech. Problem	Vladivostok
20.	Budaeva, V.D.	FERHRI	Vladivostok
21.	Bychkov, A.S.	POI	Vladivostok
22.	Cherbadgy, I.I.	IMB	Vladivostok
23.	Cheranyev, M.Y.	POI	Vladivostok
24.	Dashko, N.A.	FERHRI	Vladivostok
25.	Darnitskiy, V.B.	TINRO	Vladivostok
26.	Dolganova, N.T.	TINRO	Vladivostok
27.	Diakov, Y.P.	KamchatNIRO	P. Kamchatsky
28.	Diakov, B.S.	TINRO	Vladivostok
29.	Dulepova, E.P.	TINRO	Vladivostok
30.	Dzizyurov, V.D.	TINRO	Vladivostok
31.	Efremov, V.V.	IBM	Vladivostok
32.	Fadeev, N.S.	TINRO	Vladivostok
33.	Foux, V.R.	St. Petersburg State University	St. Petersburg
34.	Figurkin, A.L.	TINRO	Vladivostok
35.	Firsov, P.B.	FERHRI	Vladivostok
36.	Freeland, H.J.	Institute of Ocean Sciences	Canada
37.	Gayko, L.A.	IBM	Vladivostok
38.	Gladyshev, S.V.	POI	Vladivostok
39.	Glebova, S.Y.	TINRO	Vladivostok
40.	Goncharenko, I.A.	IACP	Vladivostok
41.	Gorbarenko, S.A.	POI	Vladivostok
42.	Herbeck, E.E.	IACP	Vladivostok
43.	Ignatova, N.K.	PIG	Vladivostok
44.	Ilynskiy, E.N.	TINRO	Vladivostok
45.	Ivanov, O.A.	TINRO	Vladivostok
46.	Ivankov, V.N.	Far East State University	Vladivostok
47.	Ivanova, A.A.	FETIFIE	Vladivostok

48.	Ivanov, V.V.	IMG & G	Y. Sakhalinsk
49.	Kashiwai, M.	Hokkaido Natl. Fish. Res. Inst.	Japan
50.	Karnaukhov, A.A.	POI	Vladivostok
51.	Kawasaki, Y.	Hokkaido Natl. Fish. Res. Inst.	Japan
52.	Keigwin, L.D.	Woods Hole Oceanogr. Inst.	U.S.A.
53.	Krupnova, T.N.	TINRO	Vladivostok
54.	Kim, G.Y.	Inst. Water & Ecolog. Problems	Khabarovsk
55.	Kilmatov, T.R.	POI	Vladivostok
56.	Kiselev, A.M.	PIG	Vladivostok
57.	Kozlov, V.F.	POI	Vladivostok
58.	Khrapchenkov, F.F.	POI	Vladivostok
59.	Khramushin, V.N.	SakhNIRO	Y. Sakhalinsk
60.	Kukharenko, L.A.	IMB	Vladivostok
61.	Kuzmin, V.A.	Green Cross	Vladivostok
62.	Lapko, V.V.	TINRO	Vladivostok
63.	Lapshina, V.I.	TINRO	Vladivostok
64.	Lee, J.C.	Pusan Fishery University	Korea
65.	Lebedev, G.A.	Arctic Antarctic Res. Inst.	St. Petersburg
66.	Lobanov, V.B.	POI	Vladivostok
67.	Luchin, V.A.	FERHRI	Vladivostok
68.	Luchsheva, L.N.	TINRO	Vladivostok
69.	Luk'yanov, P.A.	PIBOC	Vladivostok
70.	Martynov, A.V.	Computer Center SB RAS	Novosibirsk
71.	Manko, Y.I.	IBP	Vladivostok
72.	Makarov, V.G.	POI	Vladivostok
73.	Maximenko, N.A.	IO RAS	Moscow
74.	Moiseichenko, G.V.	TINRO	Vladivostok
75.	Moroz, V.V.	POI	Vladivostok
76.	Mooers, C.N.K.	University of Miami	U.S.A.
77.	Mikhailov, V.V.	PIBOC	Vladivostok
78.	Mikheev, A.A.	SakhNIRO	Y. Sakhalinsk
79.	Mitrofanov, Y.A.	POI	Vladivostok
80.	Mishukov, V.F.	POI	Vladivostok
81.	McFarlane, G.A.	Pacific Biological Station	Canada
82.	Muratov, L.F.	POI	Vladivostok
83.	Nagata, Y.	Mie University	Japan
84.	Nelezin, A.D.	FERHRI	Vladivostok
85.	Nikitin, A.A.	TINRO	Vladivostok
86.	Nishiyama, T.	Hokkaido Tokai University	Japan
87.	Nikolenko, L.P.	TINRO	Vladivostok
88.	Novikov, Y.V.	TINRO	Vladivostok
89.	Nor, A.V.	POI	Vladivostok
90.	Ono, S.	Hokkaiminyu Newspaper Co.	Japan
91.	Ozerin, V.K,	TINRO	Vladivostok
92.	Pack, V.V.	POI	Vladivostok
93.	Pestereva, N.	Far-Eastern State University	Vladivostok
94.	Petrov, A.G.	FERHRI	Vladivostok
95.	Polyakov, D.M.	POI	Vladivostok
96.	Pozdnyakova, L.A.	IMB	Vladivostok

97. Preobrazhenskaya, T.V.	IMB	Vladivostok
98. Preobrazhensky, B.V.	PIG	Vladivostok
99. Prelovsky, V.I.	PIG	Vladivostok
100. Probatova, N.S.	IBP	Vladivostok
101. Polomoshnov, A.M.	SOGI	Okha, Sakhalin
102. Polyakova, A.M.	POI	Vladivostok
103. Ponomarev, V.I.	POI	Vladivostok
104. Pischalnik, V.M.	SakhNIRO	Y. Sakhalinsk
105. Pushnikova, G.M.	CakhNIRO	Y. Sakhalinsk
106. Reznikov, B.I.	POI	Vladivostok
107. Riser, S.C.	University of Washington	U.S.A.
108. Ro, Y.J.	Chungnam Natl. University	Korea
109. Rogachev, K.A.	POI	Vladivostok
110. Rosly, Y.S.	Amur NIRO	Khabarovsk
111. Rykov, N.A.	FERHRI	Vladivostok
112. Salomatin, A.S.	POI	Vladivostok
113. Savelyeva, N.J.	POI	Vladivostok
114. Savin, A.	TINRO	Vladivostok
115. Sekine, Y.	Mie University	Japan
116. Semkin, B.I.	PIG	Vladivostok
117. Seledets, V.P.	PIG	Vladivostok
118. Skirina, I.F.	PIG	Vladivostok
119. Silina, A.V.	IMB	Vladivostok
120. Sosnin, V.A.	POI	Vladivostok
121. Sycheva, E.V.	IACP	Vladivostok
122. Shatilina, T.A.	TINRO	Vladivostok
123. Shevtsov, V.P.	POI	Vladivostok
124. Sundukova, E.V.	PIBOC	Vladivostok
125. Talley, L.D.	Scripps Inst. Oceanogr.	U.S.A.
126. Temnykh, O.S.	TINRO	Vladivostok
127. Tkalin, A.V.	FERHRI	Vladivostok
128. Tyukov, I.Y.	Far East State University	Vladivostok
129. Varlaty, E.P.	POI	Vladivostok
130. Varlamov, S.M.	FERHRI	Vladivostok
131. Vlasova, G.A.	POI	Vladivostok
132. Volkov, A.F.	TINRO	Vladivostok
133. Victorovskaya, G.I.	TINRO	Vladivostok
134. Vvedenskaya, T.L.	KamchatNIRO	P. Kamchatsky
135. Wang, A.T.	Exxon	U.S.A.
136. Wespested, V.G.	Alaska Fish. Science Center	U.S.A.
137. Wooster, W.S.	University of Washington	U.S.A.
138. Yakunin, L.P.	Far East State University	Vladivostok
139. Yurasov, G.I.	POI	Vladivostok
140. Zolotov, O.G.	Kamchat NIRO	P. Kamchatsky
141. Zvyagintseva, T.N.	PIBOC	Vladivostok
142. Zhabin, I.A.	POI	Vladivostok
143. Zhukova, N.V.	IMB	Vladivostok
144. Zuenko, Y.I.	TINRO	Vladivostok

HMSC
GC
781
.P5351
no.6

PICES Scientific Report No.6, 1996: Proceedings of the Workshop on the Okhatosk Sea and Adjacent Areas.
120012510190